EMERGING INFECTIOUS DISEASES®

U.S. CENTERS FOR DISEASE CONTROL AND PREVENTION

Vectors

July 2024

Possibly Agnolo Bronzino (1503–1572). *Allegorical Portrait of Dante* (16th Century). Oil on panel, 49 15/16 in × 47 1/4 in/126.9 cm × 120 cm. National Gallery of Art, Samuel H. Kress Collection. Washington, DC, United States. Open access image.

EMERGING INFECTIOUS DISEASES®

Emerging Infectious Diseases is published monthly by the Centers for Disease Control and Prevention, 1600 Clifton Rd NE, Mailstop H16-2, Atlanta, GA 30329-4018, USA. Telephone 404-639-1960; email, eideditor@cdc.gov

EMERGING INFECTIOUS DISEASES®

Vectors **July 2024**

On the Cover

Possibly Agnolo Bronzino (1503–1572). *Allegorical Portrait of Dante* (16th Century). Oil on panel, 49 15/16 in × 47 1/4 in/126.9 cm × 120 cm. National Gallery of Art, Samuel H. Kress Collection. Washington, DC, United States. Open access image.

About the Cover p. 1500

Perspective

Medscape EDUCATION ACTIVITY

Infectious Diseases and Clinical Xenotransplantation

Xenotransplantation requires gene-edited swine, novel immunosuppressive regimens, and infectious disease diagnostic tools.

J.A. Fishman, N.J. Mueller **1311**

Synopses

Looking Beyond the Lens of Crimean-Congo Hemorrhagic Fever in Africa

O.J. Okesanya et al. **1319**

Strategies to Enhance COVID-19 Vaccine Uptake among Prioritized Groups, Uganda — Lessons Learned and Recommendations for Future Research

D. Kiiza et al. **1326**

Research

Highly Pathogenic Avian Influenza A(H5N1) Clade 2.3.4.4b Virus Infection in Domestic Dairy Cattle and Cats, United States, 2024

E.R. Burrough et al. **1335**

Newly Recognized Spotted Fever Group *Rickettsia* as Cause of Severe Rocky Mountain Spotted Fever–Like Illness, Northern California, USA

W.S. Probert et al. **1344**

COVID-19 Death Determination Methods, Minnesota, USA, 2020–2022

L.J. Fess et al. **1352**

Sialic Acid Receptor Specificity in Mammary Gland of Dairy Cattle Infected with Highly Pathogenic Avian Influenza A(H5N1) Virus

R.K. Nelli et al. **1361**

Electronic Health Record Data for Lyme Disase Surveillance, Massachusetts, USA, 2017–2018

K. Nagavedu et al. **1374**

Prevalence of and Risk Factors for Post–COVID-19 Condition during Omicron BA.5–Dominant Wave, Japan

A. Iba et al. **1380**

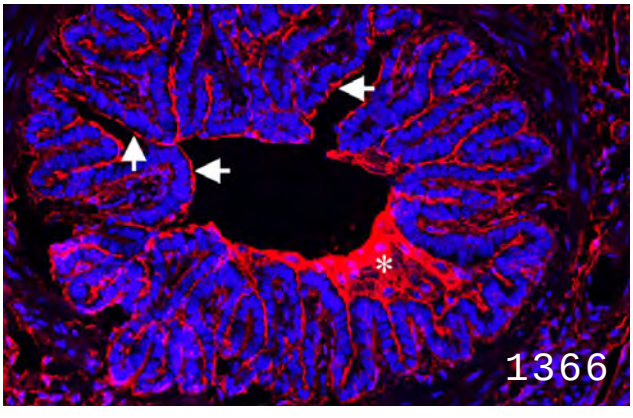

Engaging Communities in Emerging Infectious Disease Mitigation to Improve Public Health and Safety
M.E. Barak et al. **1390**

Dispatches

***Wuchereria bancrofti* Lymphatic Filariasis, Barrancabermeja, Colombia, 2023**
J.A. Suárez et al. **1398**

Treatment Outcomes for Tuberculosis Infection and Disease Among Persons Deprived of Liberty, Uganda, 2020
D. Lukoye et al. **1402**

Relapsed Mpox Keratitis, St. Louis, Missouri, USA
C. Pi et al. **1406**

Multicountry Spread of Influenza A(H1N1)pdm09 Viruses with Reduced Oseltamivir Inhibition, May 2023–February 2024
M.C. Patel et al. **1410**

Reemergence of Clade IIb–Associated Mpox, Germany, July–December 2023
P.E. Obermeier et al. **1416**

Risk for Donor-Derived Syphilis after Kidney Transplantation, China, 2007–2022
S. Yin et al. **1420**

EMERGING INFECTIOUS DISEASES®
July 2024

Avian Influenza A(H5N1) Virus Among Dairy Cattle, Texas, USA
J.U. Oguzie et al. **1425**

Vaccine Effectiveness against SARS-CoV-2 among Household Contacts during Omicron BA.2–Dominant Period, Japan
T. Ogata et al. **1430**

Alongshan Virus Infection in *Rangifer tarandus* Reindeer, Northeastern China
W. Xu et al. **1434**

Bluetongue Virus Serotype 3 and Schmallenberg Virus in Culicoides Biting Midges, Western Germany, 2023
A. Voigt et al. **1438**

Evidence of *Orientia* spp. Endemicity among Severe Infectious Disease Cohorts, Uganda
P.W. Blair et al. **1442**

Effect of Rodent Control Program on Incidence of Zoonotic Cutaneous Leishmaniasis, Iran
A. Abdoli et al. **1447**

Body Louse Pathogen Surveillance among Persons Experiencing Homelessness, Canada, 2020–2021
C. Boodman et al. **1450**

Orthohantaviruses in Misiones Province, Northeastern Argentina
M.V. Vadell et al. **1454**

***Rickettsia parkeri* Rickettsiosis in Kidney Transplant Recipient, North Carolina, USA, 2023**
G.M. Phadke et al. **1459**

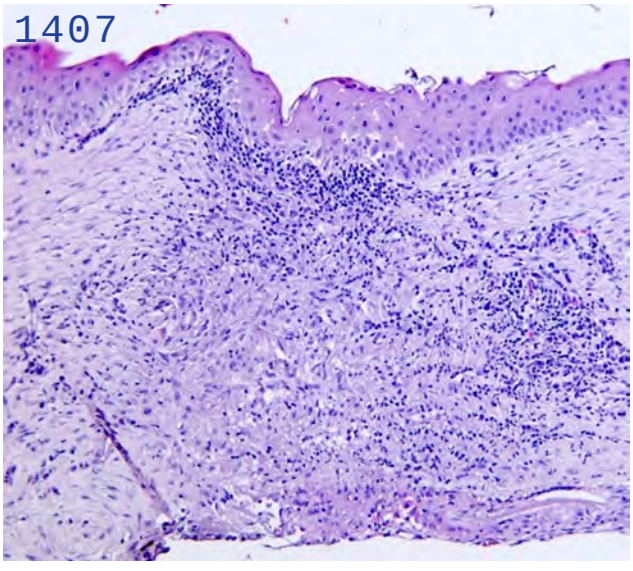

Rocky Mountain Spotted Fever Mimicking Multisystem Inflammatory Syndrome in Hospitalized Children, Sonora, Mexico
G. Álvarez-Hernández et al. **1463**

Molecular Confirmation of *Anopheles stephensi* Mosquitoes in the Al Hudaydah Governorate, Yemen, 2021 and 2022
M. Assada et al. **1467**

Acute Meningoencephalitis Associated with *Borrelia miyamotoi*, Minnesota, USA
J.M. Kubiak et al. **1472**

Research Letters

***Pasteurella bettyae* Infections in Men Who Have Sex with Men, France**
A. Li et al. **1475**

***Plasmodium vivax* Infections among Immigrants from China Traveling to the United States**
P. Khamly et al. **1477**

Emergence of Indigenous Dengue Fever, Niger, October 2023
H. Idé Amadou et al. **1479**

Large-Scale Outbreak of *Mycoplasma pneumoniae* Infection, Marseille, France, 2023–2024
S. Edouard et al. **1481**

Fatal Infection in Ferrets after Ocular Inoculation with Highly Pathogenic Avian Influenza A(H5N1) Virus
J.A. Belser et al. **1484**

Genomic Epidemiology of Large Blastomycosis Outbreak, Ontario, Canada, 2021
L.R. McTaggart et al. **1487**

EMERGING INFECTIOUS DISEASES®
July 2024

Serosurvey of Chikungunya Virus in Old World Fruit Bats, Senegal, 2020–2022
W.M. de Souza et al. **1490**

World Health Organization Enhanced Gonococcal Antimicrobial Surveillance Programme, Cambodia, 2023
V. Ouk et al. **1493**

Serosurvey of Blood Donors to Assess West Nile Virus Exposure, South-Central Spain
M. Frías et al. **1496**

Books and Media

Germ Theory: Medical Pioneers in Infectious Diseases, 2nd Edition
R.N Wofford **1488**

About the Cover

Poet, Politician, Exile, and Probable Malaria Victim
B. Breedlove **1501**

Corrections

Vol. 29, No. 7 **1498**
Funding information was missing in Novel Highly Pathogenic Avian Influenza A(H5N1) Clade 2.3.4.4b Virus in Wild Birds, South Korea

Vol. 28, No. 6 **1498**
An affiliation for the first author was missing in Lyme Disease, Anaplasmosis, and Babesiosis, Atlantic Canada.

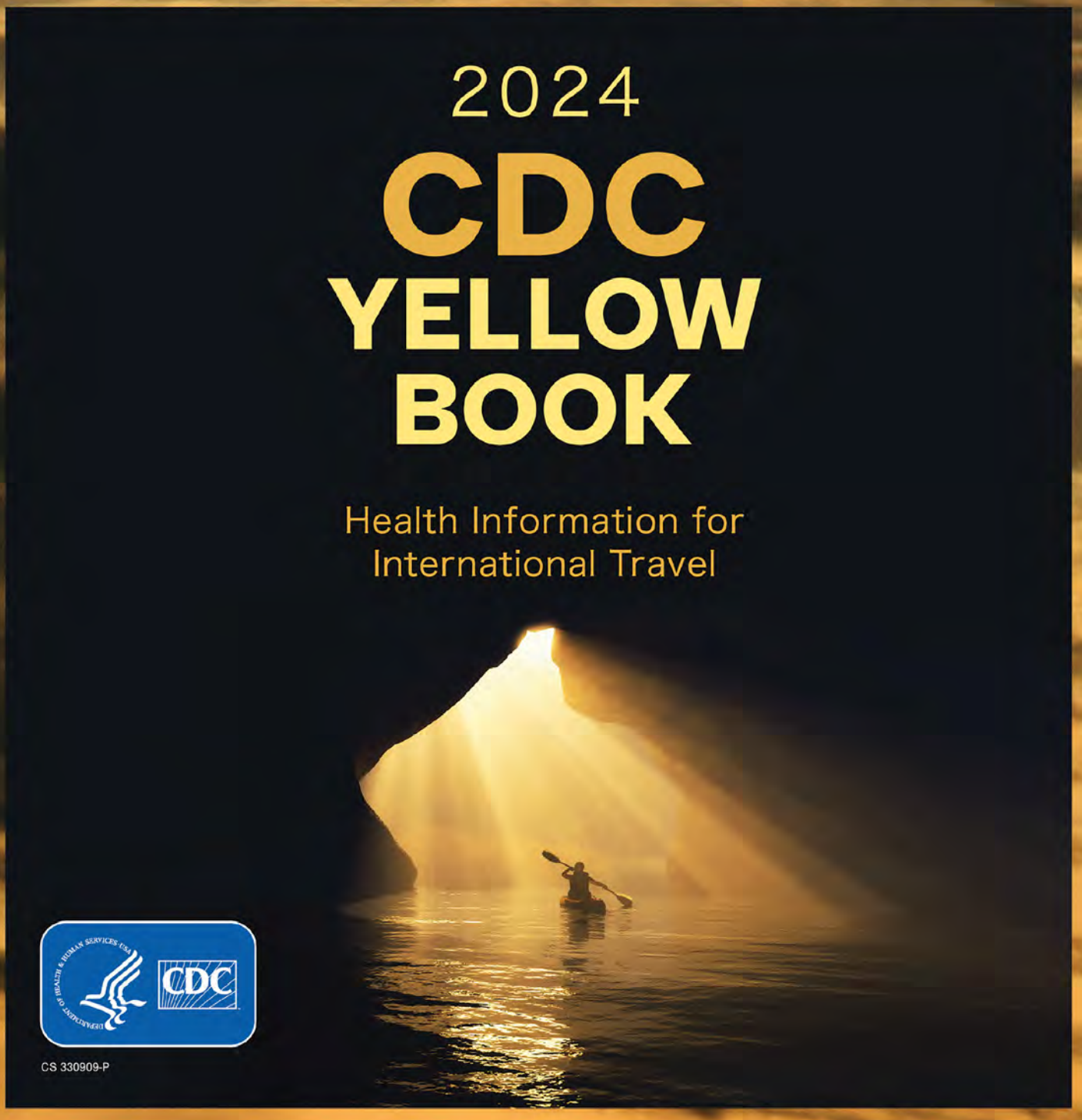

Launch of CDC Yellow Book 2024 – A Trusted Travel Medicine Resource

CDC is pleased to announce the launch of the CDC Yellow Book 2024. The CDC Yellow Book is a source of the U.S. Government's recommendations on travel medicine and has been a trusted resource among the travel medicine community for over 50 years. Healthcare professionals can use the print and digital versions to find the most up-to-date travel medicine information to better serve their patients' healthcare needs.

The CDC Yellow Book is available in print through Oxford University Press and online at www.cdc.gov/yellowbook.

Infectious Diseases and Clinical Xenotransplantation

Jay A. Fishman, Nicolas J. Mueller

Medscape CME Activity

In support of improving patient care, this activity has been planned and implemented by Medscape, LLC and Emerging Infectious Diseases. Medscape, LLC is jointly accredited with commendation by the Accreditation Council for Continuing Medical Education (ACCME), the Accreditation Council for Pharmacy Education (ACPE), and the American Nurses Credentialing Center (ANCC), to provide continuing education for the healthcare team.

Medscape, LLC designates this Journal-based CME activity for a maximum of 1.00 ***AMA PRA Category 1 Credit(s)™***. Physicians should claim only the credit commensurate with the extent of their participation in the activity.

Successful completion of this CME activity, which includes participation in the evaluation component, enables the participant to earn up to 1.0 MOC points in the American Board of Internal Medicine's (ABIM) Maintenance of Certification (MOC) program. Participants will earn MOC points equivalent to the amount of CME credits claimed for the activity. It is the CME activity provider's responsibility to submit participant completion information to ACCME for the purpose of granting ABIM MOC credit.

All other clinicians completing this activity will be issued a certificate of participation. To participate in this journal CME activity: (1) review the learning objectives and author disclosures; (2) study the education content; (3) take the post-test with a 75% minimum passing score and complete the evaluation at https://www.medscape.org/qna/processor/71951?showStandAlone=true&src=prt_jcme_eid_mscpedu; and (4) view/print certificate. For CME questions, see page 1503.

NOTE: It is Medscape's policy to avoid the use of Brand names in accredited activities. However, in an effort to be as clear as possible, trade names are used in this activity to distinguish between the mixtures and different tests. It is not meant to promote any particular product.

Release date: June 20, 2024; Expiration date: June 20, 2025

Learning Objectives

Upon completion of this activity, participants will be able to:

- Assess how swine are prepared as source animals for xenotransplantation
- Distinguish the most common potentially harmful organisms associated with xenotransplantation
- Compare viruses that may infect human and swine cells vs swine cells only
- Evaluate therapeutic interventions to reduce the risk for infectious complications of xenotransplantation

CME Editor

Dana C. Dolan, BS, Technical Writer/Editor, Emerging Infectious Diseases. *Disclosure: Dana C. Dolan, BS, has no relevant financial relationships.*

CME Author

Charles P. Vega, MD, Health Sciences Clinical Professor of Family Medicine, University of California, Irvine School of Medicine, Irvine, California. *Charles P. Vega, MD, has the following relevant financial relationships: consultant or advisor for Boehringer Ingelheim; GlaxoSmithKline.*

Authors

Jay A. Fishman, MD; Nicolas J. Mueller.

Author affiliations: Massachusetts General Hospital and Harvard Medical School, Boston, Massachusetts, USA (J.A. Fishman); University Hospital Zurich, University of Zurich, Switzerland (N.J. Mueller)

DOI: http://doi.org/10.3201/eid3007.240273

Xenotransplantation, transplantation into humans of vascularized organs or viable cells from nonhuman species, is a potential solution to shortages of transplantable human organs. Among challenges to application of clinical xenotransplantation are unknown risks of transmission of animal microbes to immunosuppressed recipients or the community. Experience in allotransplantation and in preclinical models suggests that viral infections are the greatest concern. Worldwide, the distribution of swine pathogens is heterogeneous and cannot be fully controlled by international agricultural regulations. It is possible to screen source animals for potential human pathogens before procuring organs in a manner not possible within the time available for surveillance testing in allotransplantation. Infection control measures require microbiological assays for surveillance of source animals and xenograft recipients and research into zoonotic potential of porcine organisms. Available data suggest that infectious risks of xenotransplantation are manageable and that clinical trials can advance with appropriate protocols for microbiological monitoring of source animals and recipients.

Xenotransplantation, the implantation of vascularized organs or viable cells from nonhuman species into humans, is under development to address the shortage of human organs for transplantation. Clinical xenotransplantation from swine has become more practical through advances in molecular biology (e.g., CRISPR manipulations) that have enabled the breeding of swine with advantageous immunologic traits coupled with newer immunosuppressive regimens (Figure; Appendix Table 1, https://wwwnc.cdc.gov/EID/article/30/7/24-0273-App1.pdf). Recent porcine cardiac and renal transplants survived for about 2 months in hosts with multiple comorbid conditions and who were not candidates for allotransplantation. Decedent xenografts of hearts and kidneys have been used to demonstrate fundamental functions and immune responses of porcine xenografts in human hosts. Prior experience with xenogeneic (pig, bovine) heart valves, tendons, and skin have generally been fixed or sterilized tissues not carrying viable cells. Regulatory guidelines exist for the clinical use of genetically modified animals but incompletely address microbiologic standards (*1*–*5*). Experience in allotransplantation indicates that the risk for xenosis or xenozoonosis (transmission of infection from animals to humans from viable cells of organs or cellular transplantation) is determined by epidemiologic exposure of source animals and human recipients, the net state of immunosuppression, and the underlying factors contributing to infectious risk, including the type, intensity, and duration of immunosuppression (*6*,*7*). In human allotransplantation, immunosuppression is largely standardized, the pattern of infections is predictable, and prophylactic regimens are standardized (*6*,*7*). Some infections are considered

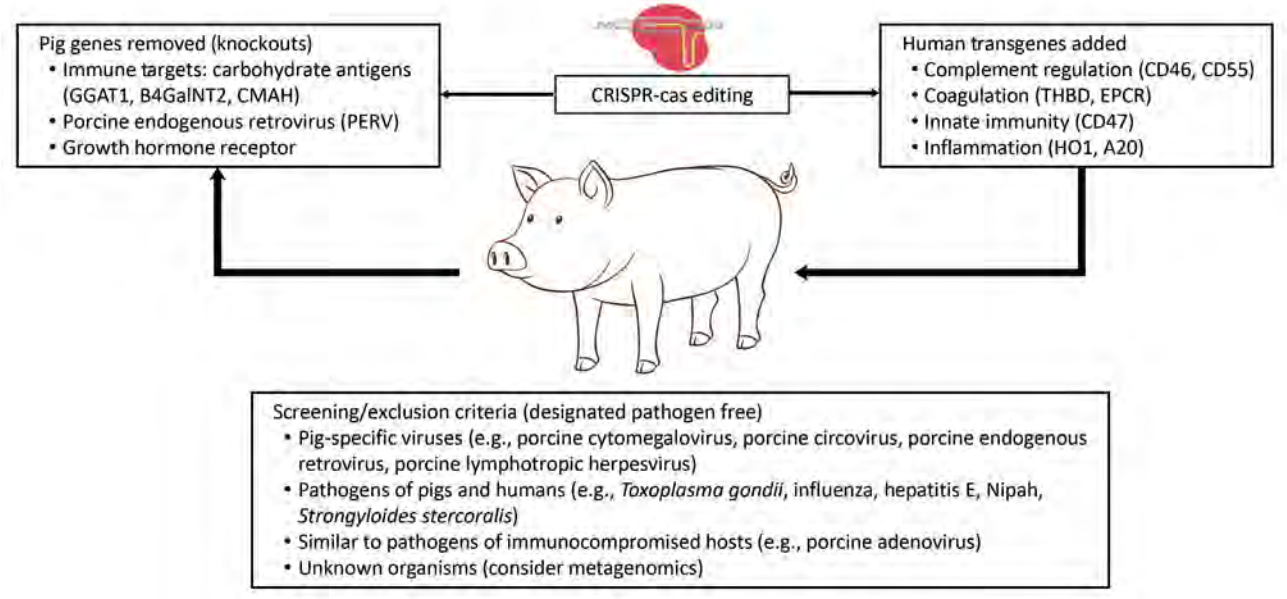

Figure. Advances in genetic engineering have led to the breeding of pigs with advantages in infection, immunology, coagulation, size, and inflammation. Breeding of source animals in biosecure facilities enables screening for potential pathogens. B4GalNT2, glycosyltransferase; CD46, human membrane cofactor protein; CD47, block SIRPα tyrosine phosphorylation; CD55, human decay-accelerating factor; CMAH, cytidine monophosphate-N-acetylneuraminic acid hydroxylase; EPCR, endothelial cell protein C receptor; GGAT1, α-1,3-glycosyltransferase; HO1, heme oxygenase-1; HA20, human A20; PERV, porcine endogenous retrovirus; THBD, human thrombomodulin gene.

routine (human cytomegalovirus [CMV], Epstein-Barr virus [EBV]); unexpected infections reflect excess immunosuppression, unusual exposures in the hospital or community, or donor organ–derived infections. Unexpected donor-derived infections are uncommon despite the urgency of screening, given time limitations for organ implantation (*8*,*9*). Data from microbiologic screening studies are often not available until after implantation.

Immunosuppressed xenograft recipients have potential exposure to microbes carried by xenografts as well as to community-derived exposures and reactivation of latent infections in the human host (*10*). The likelihood of infection caused by any specific organism is unknown, particularly without clinical trials or validated assays for pig-specific pathogens. A challenge and benefit of xenotransplantation is the ability to develop herds of animals free of potential pathogens; thus, developing serologic and molecular assays for use in swine herds and to monitor for infection in recipients is an important component of safety in clinical xenotransplantation.

Developing Swine as Source Animals for Clinical Xenotransplantation

Consensus does not exist around optimal screening paradigms for source animals and for monitoring of human recipients (Appendix Tables 2, 3). Effective prophylactic strategies require gaining clinical experience, identifying important pathogens, and studying antimicrobial efficacy for organisms from pigs (*10*,*11*). Veterinary guidance for pig health tracks common pathogens and requires screening of animal care providers and animals for infectious exposures. Animals determined specific pathogen–free (SPF) are generally screened for drug-resistant organisms, have limited routine use of antimicrobial agents, are vaccinated extensively, and receive sterile feed in biosecure facilities. Herds of swine for xenotransplantation are maintained in biosecure facilities and monitored routinely to exclude potential human pathogens; this practice is termed designated pathogen-free (DPF) status, a term adopted by regulatory authorities (*12*,*13*). This list of potential pathogens is based on experience in allotransplantation and preclinical xenotransplantation; it includes organisms that cause infection in immunocompromised persons (e.g., *Toxoplasma gondii*) or that are like those causing infection in transplant recipients (Appendix Table 2). Some porcine viruses have known zoonotic potential, including hepatitis E virus, influenza A virus (IAV), Japanese encephalitis virus, and Nipah virus. Pathogens known to be infectious in both pigs and humans (e.g., hepatitis E, influenza) merit monitoring and exclusion from breeding herds (*14*). Depending on the sensitivity of the assays used, organisms excluded from the breeding herd should not pose a threat to xenograft recipients. Pigs are rescreened at the time of organ procurement for xenotransplantation for known pathogens (Appendix Table 3). They are also screened by histopathology, by metagenomic sequencing for unknown organisms, and by routine blood and tissue cultures for bacteria or fungi; not all data are available at the time of procurement.

Immunosuppression for xenotransplantation in nonhuman primates and in recent human xenocardiac and xenokidney recipients has included costimulatory blockade by CD40 or CD154 monoclonal antibodies, mycophenylate mofetil, and T-cell (antithymocyte globulin), B-cell (CD20), and complement inhibition or depletion with perfusion solutions containing anti-inflammatory agents (*15*–*18*). Similar regimens in humans are associated with increased risk for infections from certain viruses (CMV, EBV, BK polyomavirus), *Pneumocystis* spp., *Toxoplasma* spp., and encapsulated bacteria (e.g., *Neisseria meningiditis* A and B).

Groenendaal et al. compiled a list of all known organisms infecting swine from the literature and sorted these based on pathogenicity for pigs and similarity to organisms causing infection in immunocompromised human hosts (*19*). The report identified 254 potential pathogens in pigs in the United States: 108 viruses, 75 bacteria, 59 parasites, 11 fungi and 1 prion; it did not include organisms potentially introduced during the procurement and transportation of organs intended for transplantation (*19*). The list includes organisms important to routine pig health status, pig pathogens, and potential human pathogens; clear distinction is not yet feasible given limited clinical experience (*19*). Most (≈130) pathogens are routinely excluded from biosecure pig-breeding facilities. The list supports development of risk mitigation strategies including requirements for biosecure breeding facilities, pathogen monitoring and exclusion, pharmaceutical treatment or vaccination, and genome editing; however, screening and monitoring for infection remained difficult.

Some viruses identified in preclinical pig-to-primate xenotransplantation appear to be species specific and do not infect human cells; those viruses include porcine cytomegalovirus, PCMV, and porcine circovirus. The viruses proliferate in xenografts in immunosuppressed nonhuman primates (NHP) and may cause graft dysfunction, graft rejection,

coagulopathy, or other syndromes (*20*–*23*). In baboon recipients of porcine heart and kidney xenografts, PCMV-infected pig cells and viral DNA are found in circulation despite ganciclovir prophylaxis. PCMV-infected porcine endothelial cells become activated to produce tissue factor, leading to systemic consumptive coagulopathy and accelerated renal xenograft rejection (*12*,*20*,*21*,*23*). PCMV can be excluded from pig colonies by caesarean delivery, early weaning, and biosecure isolation but is easily reintroduced (*24*–*26*). Those interventions inconsistently reduce transmission of porcine lymphotropic herpesvirus (PLHV) from sow to piglet (*25*,*27*). In a human recipient of a porcine cardiac xenograft, PCMV was detected by unbiased plasma microbial cell-free DNA testing despite negative molecular testing of nasal swab and buffy coat before organ procurement and ganciclovir prophylaxis (*28*,*29*). Those observations demonstrate the value of pig screening using serologic testing, nucleic acid testing (NAT), and other advanced techniques. Four species of porcine circovirus, 1–4, cause infection in swine; diverse clinical associations have been made between PCVs in swine. PCV2 and PCV3 disseminate with shed cells from cardiac xenografts in baboons; transmission to primate cells has not been demonstrated. No transmission of PCV was identified in a seropositive pig-to-human cardiac recipient (*28*).

The porcine endogenous retroviruses (PERV) have the theoretical capacity to integrate into the hosts' germline DNA causing insertional effects (*13*,*30*). PERV receptors for PERV-A and -B are ubiquitous in human cells (HuPAR-1 and HuPAR-2) (*31*). PERV-A and PERV-B can infect transformed human cells. PERV-C infects only pig cells. Receptor homologs in porcine cells are active while those in baboon appear inactive; baboons do not have PERV infection develop after xenotransplantation. Recombinant PERV-AC is a naturally occurring recombinant between PERV-A and -C and infects with greater efficiency than PERV-A into transformed human cells via the PERV-A receptor domain. PERV infection of humans exposed to porcine cells has not been reported. Various PERV mitigation strategies for source pigs include selective breeding of PERV-C–free pigs (which does not preclude recipient infection due to PERV-A or PERV-B), or genetic inactivation of the polymerase gene of PERV proviral elements using CRISPR-Cas9 (*32*).

Shifting Epidemiology of Organisms of Swine

Infectious disease management is a central component of the pork industry. Biosecurity precautions vary across breeding facilities; one precaution is the exclusion of birds, rodents, and amphibians. Strict regulations exist for the international movement of pigs, feed, and pork products. The intensification of animal agriculture, applying technological advances to allow increased density of animal rearing, has accounted for emergence of new zoonoses resulting from various practices including crowded housing, use of antibiotics, deforestation, and inadequate waste management and contributes to global warming (*33*). The spread of animal microbes to humans has increased with contacts between humans and wild or domesticated animal hosts in agriculture and markets (*33*–*35*). For example, the spread of HIV, SARS-CoV-2, Middle East respiratory syndrome virus, swine influenza virus, hepatitis E virus, and Japanese encephalitis virus was the result of contacts between animal reservoirs and humans (*36*–*38*). The need for constant review of pathogens that require surveillance in swine raised for clinical xenotransplantation is demonstrated by porcine circovirus type 4, which was not reported in the literature until 2019 but had been identified in epidemiologic studies of swine for more than a decade (*39*). Global warming and intensified pig farming in previous bat habitats may have contributed to the spread of Nipah virus to swine and farmers in Malaysia. Epidemiologically restricted pathogens of swine are likely to spread to new areas with global warming, economic development, and international travel and trade. Those pathogens may include many parasites, bacteria such as *Burkholderia* species and viruses such as Nipah, PCV4, lymphocytic choriomeningitis, and Japanese encephalitis. Worldwide, porcine organisms of concern with zoonotic potential are increasing; among those, use of antimicrobial agents is associated with increasing antimicrobial resistance. They include bacteria (*Salmonella*, *S. suis*, *S. aureus*, *Campylobacter*, *Mycobacteria*, *Brucella*, *Leptospira*, *E. coli*), parasites (*Trichinella*, *Toxoplasma*, *Trypanosoma*), and viruses (influenza, Nipah, Japanese encephalitis, Menangel) (*19*). Those pathogens merit surveillance in pig herds as their epidemiologic footprint expands. At the same time, biosecurity facilities have improved through experience and necessity in genetic manipulation and oocyte implantation, which may mitigate some of the challenges of maintenance of DPF status.

Microbiological Testing in the Human Recipient

The key elements of infection control are exclusion of potential pathogens from breeding herds (DPF status) and monitoring in xenograft recipients and

clinical staff (Appendix Table 3) (*11*,*30*,*40*,*41*). Although bacteria, fungi, and parasites can generally be identified in veterinary or clinical microbiologic labs by culture-based techniques, viruses require both serologic and NAT. Multiplexed PCRs against multiple viral targets have been reported for use in pigs (*42*). Pathogen-directed viral assays are not yet validated in humans; some assays may not be able to distinguish between similar porcine and human pathogens (*43*). Porcine retroviruses such as PERV AC have some unstable target sequences or variable tissue tropism and may require functional assays (e.g., reverse transcribed retrovirus on productively infected target cells), full sequence analysis, or in situ hybridization (*44*).

The availability of archived biospecimens from source pigs and recipients, and from persons with significant exposures to donor swine and recipients, will enable researchers to evaluate infections and possible donor-derived transmissions. Metagenomic or next-generation sequencing (NGS) approaches rely on available pathogen sequence data for analyzing sequences derived from animals or in preclinical or clinical recipients. As genetic databases for genomic and microbial sequences grow, retrospective analysis of stored clinical samples is feasible. Because infections are common in immunosuppressed allotransplant recipients, such techniques are also helpful for evaluating infectious syndromes for which a specific diagnosis cannot be established. NGS approaches are pathogen agnostic and may also detect colonizing species or replication-incompetent sequences of unclear clinical significance (*40*). Using a NGS approach is of particular interest for pathogen discovery in the context of xenotransplantation where knowledge of potential porcine pathogens is limited (*45*); the technology was instrumental in the discovery of several new viruses, some associated with human disease (*46*). Those data will also address concerns regarding potential spread of xenogeneic organisms to the general population.

Prevention and Surveillance of Infection in the Xenograft Recipient

After xenotransplantation, recipient surveillance must consider both swine and human pathogens (Appendix Table 3). Standard allotransplantation prophylactic regimens can be used for perioperative bacterial infections, herpesviruses, molds, *Toxoplasma gondii*, and *Pneumocystis jirovecii*. Novel immunosuppression regimens may alter the spectrum of opportunistic infections. Testing should be guided by knowledge of microbes not excluded from the breeding herd (e.g., PERV and PCMV status). Surveillance will require use of laboratory-developed assays or off-label use of available tests for more extensive pathogen discovery (e.g., NGS). Recent porcine-to-human cardiac and renal xenotransplants successfully used NGS for posttransplant surveillance (*28*). Biopsies used to monitor graft rejection should include microbial analysis using cultures, NGS, immunohistology, and electron microscopy for viral infections. Clinical trials should consider standard protocols for management of fevers or infectious syndromes in addition to routine screening during early periods. Treating graft rejection or infectious syndromes requires increased testing.

Porcine Antiviral Therapy Prophylaxis and Treatment

Strategies for prevention and treatment of potential viral infections in xenotransplantation, as for allotransplantation, include understanding of the antiviral susceptibilities of porcine viruses. Data on antiviral therapy for porcine viruses are limited (*41*). PCMV does not infect human cells but can provoke graft dysfunction and coagulopathy and will merit prophylaxis and therapy. PCMV has reduced susceptibility to acyclovir, ganciclovir, and foscarnet; ganciclovir prophylaxis at full treatment doses is inconsistently effective in vivo in immunosuppressed NHP xenograft recipients. Consistent with homology with human herpesvirus 6, the nephrotoxic agent cidofovir is more effective at therapeutic concentrations in vitro (*22*,*47*). Porcine lymphotropic herpesviruses (PLHV) 1, 2, and 3 have been associated with a lymphoproliferative disorder after experimental hematopoietic stem cell transplantation in pigs; the viruses are not a known to be pathogens in NHP or in humans, and no effective antiviral drugs exist. PLHV was not activated after xenotransplantation of various organs from swine infected with PLHV into nonhuman primates (*20*)

Regarding PERV, transmission was not identified in decedent recipients of renal xenografts for ≤72 hours or in recipients of PERV-C negative cardiac xenografts for ≤60 days; chimerism of cells infected with PERV-A or -B is expected. Retroviral transmission to xenograft recipients remains a concern (*28*,*48*,*49*). Antiretroviral drugs used to treat HIV-1, including reverse transcription inhibitors zidovudine, tenofovir, and adefovir, as well as the integrase inhibitors raltegravir and dolutegravir, can inhibit PERV. Nonnucleoside reverse transcriptase inhibitors (nevirapine) and protease inhibitors lack inhibitory activity for PERV. Should PERV therapy

or postexposure prophylaxis be required, combination antiretroviral therapy using integrase inhibitors and active nucleoside reverse transcriptase inhibitors would be recommended.

There are no specific treatments known for circoviruses PCV1–4; however, swine vaccination is available. Caesarean delivery and colostrum deprivation with use of NAT can prevent PCV transmission to piglets.

Infection Control in Clinical Xenotransplantation

As part of protocol development and the informed consent process, prospective xenograft recipients require education about infectious risks of xenotransplantation to themselves and potentially to social and sexual partners, of which data are limited. In the absence of PERV risk, standard universal precautions for xenograft recipients should be adequate to protect hospital staff and social contacts. No infections have been reported among veterinary staff, scientists, or surgeons participating in preclinical xenotransplant studies. As for any surgical procedure, the risk for exposure is greatest for operating room staff handling pig organs and fluids or via splash or needlestick injury. Standard surgical infection control practices should prevent such exposures. Given the unknowns, archiving baseline leukocyte and plasma samples could enable future investigations should infectious syndromes emerge in xenograft recipients. Additional samples can be obtained for documented exposures to bodily fluids or with undiagnosed infectious syndromes in xenograft recipients or surgical teams. General hospital care workers for xenotransplant recipients should not have risks of exposure beyond those prevented by universal precautions. Infection and infectious syndromes are common in immunosuppressed transplant recipients; recipients should follow isolation precautions based on the primary syndrome (e.g., for diarrhea or pneumonitis).

Occupational health service staff should be aware of xenotransplantation protocols for blood or body fluid exposure from source animals or xenotransplant recipients. In such situations, knowing the infectious status of the source pig and the recipient is invaluable. If the donor animal is PERV negative, postexposure retroviral prophylaxis should not be required. For PERV-positive donors, prophylaxis after needlestick exposure to porcine tissues recommends use of a reverse transcription inhibitor and integrase inhibitor. Testing should include NAT for swine-specific pathogens, as well as standard tests for HIV, hepatitis C and hepatitis B. Repeat NAT testing should be performed at regular intervals (e.g., 1, 3, and 6 months) after a blood or body fluid exposure. Plans for passive surveillance and active testing and treatment will be required for clinical trials; those plans should be developed in conjunction with Infection Control and Occupational Health groups. Informed consent may be required for acquiring and storing patient blood samples obtained from clinical care providers.

Because clinical experience is limited, infectious risks to close contacts of the xenotransplant recipient are not defined. The clinical trial design and consent process should address the benefits and feasibility of posttransplant surveillance of close contacts to inform blood sample archiving in advance of the procedure in the event of blood or body fluid exposure. As part of pretransplant education, the recipient and close contacts should be instructed to refrain from blood donation and unprotected sexual contacts; household members may be counseled to avoid sharing items that could be contaminated with blood. Education on potential risks to recipients, healthcare providers, and the general public includes ethical considerations for unknown hazards. The actual risk for infectious spread to the public is unknown; most potential pathogens are species specific. Active PERV can be excluded; recombination events should not occur without viral replication but cannot be completely excluded. With careful screening of source animals and monitoring of recipients for unknown as well as known microbes, the risk for xenogeneic spread to the public is very limited. Data from clinical trials will refine our understanding of disease transmission via xenotransplantation and will inform education for potential recipients and the public.

Conclusions

The risk for transmission of infection caused by novel pathogens in association with xenotransplantation is unknown. Microbiological screening of source animals may reduce infectious risk; however, unknown porcine pathogens with capacity to infect humans may exist and are unlikely to be identified in the absence of clinical trials. The effect of the activation of PCMV in 1 cardiac recipient demonstrated the importance of herd screening for xenotransplants (*28*). Studies in deceased recipients of kidneys and hearts have provided information on metabolic and immunologic aspects (e.g., role of innate immunity), but they have reported limited immunosuppression and are of limited durations (<2 months) and so are less informative regarding infectious risks (*50*). Infection control measures include storage of baseline blood samples from the

xenograft donor, persons involved in procurement and transplantation of pig organs, and serial monitoring of the recipient and close contacts for known and possible unknown pathogens. Assays, including metagenomics, for potential pig pathogens need to be developed and validated. Transparency is essential in microbiologic investigations performed in clinical xenotransplantation trials.

J.A.F. is a consultant to United Therapeutics, eGenesis, Makana, Elion, Jura, Well Medical, Kamada, CLD Inc, OM1, and Vertex Inc.

About the Author

Dr. Fishman is professor of medicine at Harvard Medical School, director of the Transplant Infectious Diseases Program at Massachusetts General Hospital, associate director of the MGH Transplant Center, and president-elect of the International Xenotransplantation Society. His primary research interests include managing infectious risk in allotransplantation and xenotransplantation and studied porcine cytomegalovirus and porcine endogenous retrovirus in preclinical models. Dr. Mueller is a transplant infectious diseases physician and head of the transplant center at the University Hospital Zurich and chairman of the Scientific Committee of the Swiss Transplant Cohort Study. His initial research focused on viral infections in animal models of allo- and xenotransplantation; more recently, his primary research focus has been the role of latent herpes virus infections in the immunocompromised host.

References

1. Hering BJ, Cozzi E, Spizzo T, Cowan PJ, Rayat GR, Cooper DK, et al. First update of the International Xenotransplantation Association consensus statement on conditions for undertaking clinical trials of porcine islet products in type 1 diabetes—executive summary. Xenotransplantation. 2016;23:3–13. https://doi.org/10.1111/xen.12231
2. Food and Drug Administration. Source animal, product, preclinical, and clinical issues concerning the use of xenotransplantation products in humans; guidance for industry. 2016 [cited 2024 May 24]. https://www.fda.gov/downloads/biologicsbloodvaccines/guidancecompliance-regulatoryinformation/guidances/xenotransplantation/ucm533036.pdf
3. Food and Drug Administration. PHS guideline on infectious disease issues in xenotransplantation. 66 F.R. 8120. 2001 [cited 2024 May 24]. https://www.federalregister.gov/documents/2001/01/29/01-2419/phs-guideline-on-infectious-disease-issues-in-xenotransplantation-availability
4. World Health Organization. Second WHO global consultation on regulatory requirements for xenotransplantation clinical trials. 2001 [cited 2024 May 24]. http://www.who.int/transplantation/xeno/report2nd_global_consultation_xtx.pdf
5. Hawthorne WJ, Cowan PJ, Bühler LH, Yi S, Bottino R, Pierson RN III, et al. Third WHO global consultation on regulatory requirements for xenotransplantation clinical trials, Changsha, Hunan, China, December 12–14, 2018. Xenotransplantation. 2019;26:e12513. https://doi.org/10.1111/xen.12513
6. Fishman JA. Infection in solid-organ transplant recipients. N Engl J Med. 2007;357:2601–14. https://doi.org/10.1056/NEJMra064928
7. Fishman JA. Infection in organ transplantation. Am J Transplant. 2017;17:856–79. https://doi.org/10.1111/ajt.14208
8. Fishman JA, Grossi PA. Donor-derived infection—the challenge for transplant safety. Nat Rev Nephrol. 2014;10:663–72. https://doi.org/10.1038/nrneph.2014.159
9. Fishman JA. Xenosis and xenotransplantation: addressing the infectious risks posed by an emerging technology. Kidney Int Suppl. 1997;58:S41–5.
10. Fishman JA. Risks of infectious disease in xenotransplantation. N Engl J Med. 2022;387:2258–67. https://doi.org/10.1056/NEJMra2207462
11. Nellore A, Walker J, Kahn MJ, Fishman JA. Moving xenotransplantation from bench to bedside: managing infectious risk. Transpl Infect Dis. 2022:e13909. https://doi.org/10.1111/tid.13909
12. Fishman JA. Infection in xenotransplantation. J Card Surg. 2001;16:363–73. https://doi.org/10.1111/j.1540-8191.2001.tb00536.x
13. Fishman JA, Patience C. Xenotransplantation: infectious risk revisited. Am J Transplant. 2004;4:1383–90. https://doi.org/10.1111/j.1600-6143.2004.00542.x
14. Denner J. Hepatitis E virus (HEV)—the future. Viruses. 2019;11:251. https://doi.org/10.3390/v11030251
15. Längin M, Mayr T, Reichart B, Michel S, Buchholz S, Guethoff S, et al. Consistent success in life-supporting porcine cardiac xenotransplantation. Nature. 2018;564:430–3. https://doi.org/10.1038/s41586-018-0765-z
16. Mohiuddin MM, Singh AK, Corcoran PC, Thomas ML III, Clark T, Lewis BG, et al. Chimeric 2C10R4 anti-CD40 antibody therapy is critical for long-term survival of GTKO.hCD46.hTBM pig-to-primate cardiac xenograft. Nat Commun. 2016;7:11138. https://doi.org/10.1038/ncomms11138
17. Ma D, Hirose T, Lassiter G, Sasaki H, Rosales I, Coe TM, et al. Kidney transplantation from triple-knockout pigs expressing multiple human proteins in cynomolgus macaques. Am J Transplant. 2022;22:46–57. https://doi.org/10.1111/ajt.16780
18. Firl DJ, Markmann JF. Measuring success in pig to non-human-primate renal xenotransplantation: Systematic review and comparative outcomes analysis of 1051 life-sustaining NHP renal allo- and xeno-transplants. Am J Transplant. 2022;22:1527–36. https://doi.org/10.1111/ajt.16994
19. Groenendaal H, Costard S, Ballard R, Bienhoff S, Challen DC, Dominguez BJ, et al. Expert opinion on the identification, risk assessment, and mitigation of microorganisms and parasites relevant to xenotransplantation products from pigs. Xenotransplantation. 2023;30:e12815. https://doi.org/10.1111/xen.12815
20. Mueller NJ, Barth RN, Yamamoto S, Kitamura H, Patience C, Yamada K, et al. Activation of cytomegalovirus in pig-to-primate organ xenotransplantation. J Virol. 2002;76:4734–40. https://doi.org/10.1128/JVI.76.10.4734-4740.2002
21. Gollackner B, Mueller NJ, Houser S, Qawi I, Soizic D, Knosalla C, et al. Porcine cytomegalovirus and coagulopathy in pig-to-primate xenotransplantation. Transplantation. 2003;75:1841–7. https://doi.org/10.1097/01.TP.0000065806.90840.C1

22. Mueller NJ, Sulling K, Gollackner B, Yamamoto S, Knosalla C, Wilkinson RA, et al. Reduced efficacy of ganciclovir against porcine and baboon cytomegalovirus in pig-to-baboon xenotransplantation. Am J Transplant. 2003; 3:1057–64. https://doi.org/10.1034/j.1600-6143.2003.00192.x
23. Mueller NJ, Kuwaki K, Dor FJ, Knosalla C, Gollackner B, Wilkinson RA, et al. Reduction of consumptive coagulopathy using porcine cytomegalovirus-free cardiac porcine grafts in pig-to-primate xenotransplantation. Transplantation. 2004;78:1449–53. https://doi.org/10.1097/01.TP.0000141361.68446.1F
24. Clark DA, Fryer JF, Tucker AW, McArdle PD, Hughes AE, Emery VC, et al. Porcine cytomegalovirus in pigs being bred for xenograft organs: progress towards control. Xenotransplantation. 2003;10:142–8. https://doi.org/10.1034/j.1399-3089.2003.01128.x
25. Mueller NJ, Kuwaki K, Knosalla C, Dor FJ, Gollackner B, Wilkinson RA, et al. Early weaning of piglets fails to exclude porcine lymphotropic herpesvirus. Xenotransplantation. 2005;12:59–62. https://doi.org/10.1111/j.1399-3089.2004.00196.x
26. Yamada K, Tasaki M, Sekijima M, Wilkinson RA, Villani V, Moran SG, et al. Porcine cytomegalovirus infection is associated with early rejection of kidney grafts in a pig to baboon xenotransplantation model. Transplantation. 2014;98:411–8. https://doi.org/10.1097/TP.0000000000000232
27. Denner J. Porcine lymphotropic herpesviruses (PLHVs) and xenotranplantation. Viruses. 2021;13:1072. https://doi.org/10.3390/v13061072
28. Griffith BP, Goerlich CE, Singh AK, Rothblatt M, Lau CL, Shah A, et al. Genetically modified porcine-to-human cardiac xenotransplantation. N Engl J Med. 2022;387:35–44. https://doi.org/10.1056/NEJMoa2201422
29. Fishman JA. Next-generation sequencing for identifying unknown pathogens in sentinel immunocompromised hosts. Emerg Infect Dis. 2023;29:431–2. https://doi.org/10.3201/eid2902.221829
30. Fishman JA. Infectious disease risks in xenotransplantation. Am J Transplant. 2018;18:1857–64. https://doi.org/10.1111/ajt.14725
31. Ericsson TA, Takeuchi Y, Templin C, Quinn G, Farhadian SF, Wood JC, et al. Identification of receptors for pig endogenous retrovirus. Proc Natl Acad Sci U S A. 2003;100:6759–64. https://doi.org/10.1073/pnas.1138025100
32. Niu D, Wei HJ, Lin L, George H, Wang T, Lee IH, et al. Inactivation of porcine endogenous retrovirus in pigs using CRISPR-Cas9. Science. 2017;357:1303–7. https://doi.org/10.1126/science.aan4187
33. Hayek MN. The infectious disease trap of animal agriculture. Sci Adv. 2022;8:eadd6681. https://doi.org/10.1126/sciadv.add6681
34. Linder A. Animal markets and zoonotic disease in the United States. 2023 [cited 2024 May 24]. https://animal.law.harvard.edu/wp-content/uploads/Animal-Markets-and-Zoonotic-Disease-in-the-United-States.pdf
35. VanderWaal K, Deen J. Global trends in infectious diseases of swine. Proc Natl Acad Sci U S A. 2018;115:11495–500. https://doi.org/10.1073/pnas.1806068115
36. Pavio N, Meng XJ, Renou C. Zoonotic hepatitis E: animal reservoirs and emerging risks. Vet Res. 2010;41:46. https://doi.org/10.1051/vetres/2010018
37. Lopez-Moreno G, Davies P, Yang M, Culhane MR, Corzo CA, Li C, et al. Evidence of influenza A infection and risk of transmission between pigs and farmworkers. Zoonoses Public Health. 2022;69:560–71. https://doi.org/10.1111/zph.12948
38. McLean RK, Graham SP. The pig as an amplifying host for new and emerging zoonotic viruses. One Health. 2022;14:100384. https://doi.org/10.1016/j.onehlt.2022.100384
39. Zhai SL, Lu SS, Wei WK, Lv DH, Wen XH, Zhai Q, et al. Reservoirs of porcine circoviruses: a mini review. Front Vet Sci. 2019;6:319. https://doi.org/10.3389/fvets.2019.00319
40. Fishman JA. Prevention of infection in xenotransplantation: designated pathogen-free swine in the safety equation. Xenotransplantation. 2020;27:e12595. https://doi.org/10.1111/xen.12595
41. Mehta SA, Saharia KK, Nellore A, Blumberg EA, Fishman JA. Infection and clinical xenotransplantation: guidance from the Infectious Disease Community of Practice of the American Society of Transplantation. Am J Transplant. 2023;23:309–15. https://doi.org/10.1016/j.ajt.2022.12.013
42. Hartline CB, Conner RL, James SH, Potter J, Gray E, Estrada J, et al. Xenotransplantation panel for the detection of infectious agents in pigs. Xenotransplantation. 2018;25:e12427. https://doi.org/10.1111/xen.12427
43. Fiebig U, Holzer A, Ivanusic D, Plotzki E, Hengel H, Neipel F, et al. Antibody cross-reactivity between porcine cytomegalovirus (PCMV) and human herpesvirus-6 (HHV-6). Viruses. 2017;9:317. https://doi.org/10.3390/v9110317
44. Kono K, Kataoka K, Yuan Y, Yusa K, Uchida K, Sato Y. A highly sensitive method for the detection of recombinant PERV-A/C env RNA using next generation sequencing technologies. Sci Rep. 2020;10:21935. https://doi.org/10.1038/s41598-020-78890-2
45. Santiago-Rodriguez TM, Hollister EB. Unraveling the viral dark matter through viral metagenomics. Front Immunol. 2022;13:1005107. https://doi.org/10.3389/ fimmu.2022.1005107
46. Li L, Kapoor A, Slikas B, Bamidele OS, Wang C, Shaukat S, et al. Multiple diverse circoviruses infect farm animals and are commonly found in human and chimpanzee feces. J Virol. 2010;84:1674–82. https://doi.org/10.1128/JVI.02109-09
47. Fryer JF, Griffiths PD, Fishman JA, Emery VC, Clark DA. Quantitation of porcine cytomegalovirus in pig tissues by PCR. J Clin Microbiol. 2001;39:1155–6. https://doi.org/10.1128/JCM.39.3.1155-1156.2001
48. Porrett PM, Orandi BJ, Kumar V, Houp J, Anderson D, Cozette Killian A, et al. First clinical-grade porcine kidney xenotransplant using a human decedent model. Am J Transplant. 2022;22:1037–53. https://doi.org/10.1111/ajt.16930
49. Montgomery RA, Stern JM, Lonze BE, Tatapudi VS, Mangiola M, Wu M, et al. Results of two cases of pig-to-human kidney xenotransplantation. N Engl J Med. 2022;386:1889–98. https://doi.org/10.1056/NEJMoa2120238
50. Loupy A, Goutaudier V, Giarraputo A, Mezine F, Morgand E, Robin B, et al. Immune response after pig-to-human kidney xenotransplantation: a multimodal phenotyping study. Lancet. 2023;402:1158–69. https://doi.org/10.1016/S0140-6736(23)01349-1

Address for correspondence: Jay Fishman, MGH Transplant Center, 55 Fruit St, Boston, MA 02114 USA; email: fishman.jay@mgh.harvard.edu

Looking Beyond the Lens of Crimean-Congo Hemorrhagic Fever in Africa

Olalekan John Okesanya,[1] Gbolahan Deji Olatunji, Emmanuel Kokori, Noah Olabode Olaleke, Olaniyi Abideen Adigun, Emery Manirambona, Don Eliseo Lucero-Prisno III

Crimean-Congo hemorrhagic fever (CCHF) is a lethal viral disease that has severe public health effects throughout Africa and a case fatality rate of 10%–40%. CCHF virus was first discovered in Crimea in 1944 and has since caused a substantial disease burden in Africa. The shortage of diagnostic tools, ineffective tick control efforts, slow adoption of preventive measures, and cultural hurdles to public education are among the problems associated with continued CCHF virus transmission. Progress in preventing virus spread is also hampered by the dearth of effective serodiagnostic testing for animals and absence of precise surveillance protocols. Intergovernmental coordination, creation of regional reference laboratories, multiinstitutional public education partnerships, investments in healthcare infrastructure, vaccine development, and a One Health approach are strategic methods for solving prevention challenges. Coordinated efforts and financial commitments are needed to combat Crimean-Congo hemorrhagic fever and improve all-around readiness for newly developing infectious illnesses in Africa.

Crimean-Congo hemorrhagic fever (CCHF) is caused by a tickborne virus belonging to the genus *Nairovirus* within the family Bunyaviridae. The disease was first observed among military personnel from the former Soviet Union who were stationed in Crimea during World War II (*1*), leading to the name Crimea hemorrhagic fever. Later, researchers discovered that the virus found in Crimea was the same as the Congo virus, which caused febrile illness in the Belgian Congo. Therefore, the virus was named Crimean-Congo hemorrhagic fever virus (CCHFV). The virus was identified after it was isolated from the blood and tissues of infected persons and intracerebral inoculation of suckling mice (*2*). Since its identification, CCHFV has been recognized as a major public health threat. Outbreaks have been reported across numerous countries, particularly in Africa, the Middle East, Asia, and parts of Europe (*1*,*2*).

CCHFV is transmitted to humans through tick bites, direct contact with the blood from an infected person, or contact with blood or tissue from infected livestock. Tickborne transmission typically occurs through the bite of hard-bodied *Hyalomma* ticks belonging to the family Ixodidae (*2*). However, >35 tick species, including several soft ticks from the family Argasidae, are carriers of CCHFV (*1*,*3*). Some of those ticks are carried across Europe and other areas by migratory birds following flight paths across continents. Among the tickborne viruses that affect humans, CCHFV has the broadest geographic distribution.

Persons at greatest risk for exposure to infected ticks are those who engage in outdoor activities, such as forest workers, farmers, soldiers, and hikers. Persons at greatest risk for exposure to the blood or tissue of infected livestock are veterinarians, farmers, shepherds, slaughterhouse employees, and butchers (*4*,*5*). CCHFV can also be transmitted through human-to-human sexual contact, intrafamily transmission, or aerosol-producing medical procedures (*6*,*7*) and other nosocomial routes. Household contacts of infected patients and healthcare personnel are at risk for exposure through contact with patient blood and secretions or needlesticks (*8*). CCHFV transmission is increased by climatic

Author affiliations: Neuropsychiatric Hospital Aro, Abeokuta, Nigeria (O.J. Okesanya, O.A. Adigun); University of Ilorin, Ilorin, Nigeria (G.D. Olatunji, E. Kokori); Kwara State University, Malete, Nigeria (N.O. Olaleke); Obafemi Awolowo University Teaching Hospital Complex, Ile-Ife, Nigeria (N.O. Olaleke); University of Rwanda, Kigali, Rwanda (E. Manirambona); London School of Hygiene and Tropical Medicine, London, UK (D.E. Lucero-Prisno III)

DOI: https://doi.org/10.3201/eid3007.230810

[1]Current affiliation: University of Thessaly, Volos, Greece.

and environmental changes, increased tick populations, livestock movement, and transport of virus-infected ticks by migratory birds (*9*).

The incubation period for CCHF can range from 9 days after a tick bite to 14 days after direct contact with the blood of an infected person or livestock (*3*). The disease progresses through 4 stages: incubation, prehemorrhagic, hemorrhagic, and convalescent stages. The prehemorrhagic stage is characterized by high fever, muscle pain, severe headaches, chills, nausea, vomiting, diarrhea, facial redness, and rash. As the disease advances, subcutaneous bleeding and hemorrhagic symptoms occur in various organs of the body. CCHF-positive patients often have low lymphocyte, monocyte, and neutrophil counts (*10*,*11*). The disease has a high case-fatality rate of 10%–40% (*1*).

Since the initial report of CCHF in Crimea in 1944, sporadic outbreaks of the disease have been reported intermittently in Europe, Asia, and Africa (*12*); the highest number of outbreaks have been reported in the former Soviet Union, Turkey, Iran, Bulgaria, China, and Africa (*13*,*14*). Although CCHF is mostly undiagnosed and unreported in Africa, the continent has a high CCHF disease burden; 62 cases and 17 deaths occurred in outbreaks during 2003–2018 (*10*). Africa has experienced several outbreaks with varying rates of cases and deaths in Uganda, Senegal, South Africa, and Mauritania (*10*). In a 2023 outbreak in Namibia, the index patient was reported to have exhibited symptoms on May 16 and died on May 18; CCHF was confirmed by an unspecified laboratory method (*15*). We describe the status of CCHF in Africa, challenges for its control, and recommendations to mitigate CCHFV spread.

CCHF Outbreaks in Africa

CCHF in Africa has likely been underestimated for decades because of shortcomings in surveillance (*16*). Through organized efforts between individual countries' health departments and international organizations, such as the Africa Centre for Disease Control and the World Health Organization, 19 nations in Africa have recorded CCHF cases in humans from January 1956, when the first cases were reported, through July 2020 (*17*,*18*). During that period, ≥494 cases and 115 fatalities were recorded (*16*). Incidence for most of those nations was calculated according to random sampling or serosurveys, methods that are not sufficient to confirm the initial identification of CCHF cases (*19*). CCHF cases are underestimated in Africa because of a lack of active zoonotic surveillance and a dearth of appropriate diagnostic tools (*19*,*20*).

South Africa and Uganda have reported an appreciable number of CCHF cases and deaths because they established robust surveillance systems, the Special Pathogen Unit of the National Institute of Communicable Diseases in South Africa and the Virus Research Institute in Uganda (*16*,*21*). However, Mozambique, Eswatini, Botswana, and Lesotho have recorded no cases (*22*,*23*), and Tanzania, South Sudan, Zimbabwe, and Kenya have only confirmed 1 case each. No other cases have been recorded in Burkina Faso since its first reported case in 1983 (*24*). If other nations had developed robust surveillance systems, such as those in South Africa and Uganda, more cases would likely have been detected (Figures 1, 2) (*25*).

Special Challenges Faced by Countries in Africa

Countries in Africa face special challenges in preventing and controlling CCHF. For example, those countries often lack efficient surveillance systems that are essential for early CCHF case detection and rapid outbreak response. Time delays from initial healthcare contact to diagnosis can lead to an increase in transmission (*26*). Patients have had to travel long distances to receive proper care (*15*,*27*). Insufficient collaboration between animal and human disease control sectors in Africa has posed a major obstacle to reducing outbreaks. In addition, the shortage of diagnostic laboratory kits for CCHF (particularly at the district level), the lack of accessible diagnostic facilities, inadequate laboratory capacities, and a shortage of trained laboratory personnel have hindered the diagnostic process and response efforts. Those problems have led to misdiagnosis, delayed treatment, and an increase in fatalities (*16*). Another problem has been poor tick control activities, especially during animal-gathering events. The absence of tick control initiatives has likely exacerbated outbreaks, particularly in rural areas where resources are scarce.

Countries in Africa face obstacles in adopting personal protective measures among persons at risk for CCHF, such as healthcare workers and livestock handlers. The limited availability of protective equipment impedes compliance with preventive measures (*28*). Another challenge is certain cultural beliefs that thwart disease prevention and promote mistrust and low health literacy, which have reduced community participation and cooperation (*26*). Other obstacles include the lack of suitable serodiagnostic tests for extensive animal testing, the absence of clear guidance for standardized surveillance in the animal health sector, and the costs associated with implementing routine testing and surveillance (*29*,*30*).

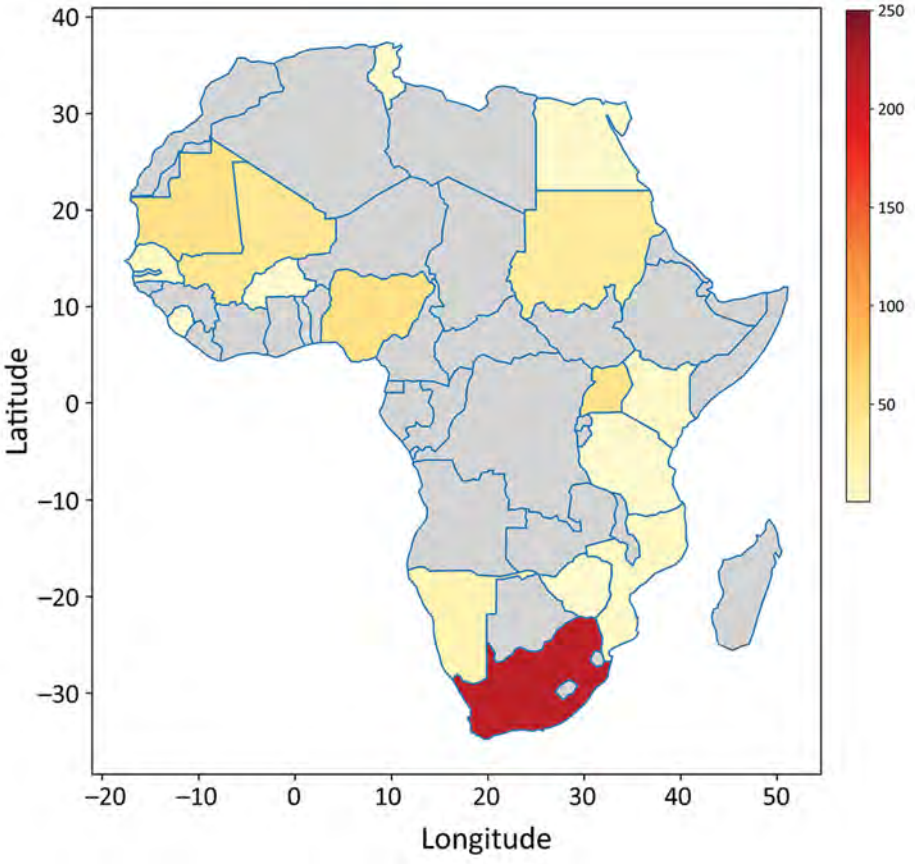

Figure 1. Distribution of Crimean-Congo hemorrhagic fever cases in Africa. Total numbers of CCHF cases were recorded by 19 nations in Africa during January 1956–July 2020. Colors in key indicate the number of confirmed cases in each country. Red indicates the highest number of cases occurred in South Africa. Gray indicates no cases were reported in those countries.

Recommendations for Africa

Intergovernmental Assistance and Cross-Organizational Alliances

To strengthen the response to CCHF in Africa, collaboration between governments and institutions at the regional and continental levels is crucial. Such collaborations should enable development of human and ecologic surveillance networks for CCHF across the continent (*16*). During CCHF outbreaks, countries that have diagnostic capabilities should offer rapid diagnostic support to countries that do not have them. The have and have-not countries should work collectively to establish surveillance networks to control outbreaks and create a more comprehensive understanding of CCHF epidemiology in Africa. Collaborative efforts should include active surveillance, testing ticks for CCHFV, and conducting serologic tests for animals and humans with suspected CCHFV infections (*31*–*33*).

Establishing Regional Reference Laboratories

The general lack of healthcare infrastructure in many countries in Africa poses challenges in investigating CCHF outbreaks, identifying cases promptly, isolating patients, and providing medical care. We recommend establishing regional reference laboratories in major geopolitical zones that are easily accessible by rural communities (*11*,*12*). Those laboratories should be equipped with standard diagnostic equipment that enable molecular assays, such as real-time PCR, which is the most accurate method of CCHF diagnosis; immunological assays, such as ELISA to identify specific IgG and IgM; and simple rapid tests. We also recommend enhancing other resources, such as laboratory diagnostic training plans for all health personnel, which could provide rapid diagnostic assistance during CCHF epidemics (*2*). Developing and using external quality assessment programs should be given top priority, and they should be used at the national or regional levels with the goals of increasing competence of medical specialists, standardizing diagnostic procedures, and guaranteeing the accuracy of CCHF test results (*34*,*35*). To enable effective diagnosis of CCHF by healthcare providers in Africa, we recommend external quality assessments and diagnostic evaluation methods, collaboration with international organizations, continual monitoring of diagnostic capabilities, and acquiring sufficient funds for those endeavors wherever possible (*36*). Better diagnostic capability

would help improve the capacity for timely detection and response to CCHF cases in Africa, which is a crucial component of patient management and CCHFV transmission prevention (*37*).

Multiinstitutional Collaboration for Public Education

Engaging communities in outbreak response activities, including education, risk communication, and behavioral change, is central to control CCHF outbreaks. Institutional collaboration in countries in Africa should prioritize public education on CCHFV transmission, including how the virus is transmitted and the importance of using personal protective equipment (PPE), when recommended. It is essential to provide appropriate PPE to persons at risk for CCHF, such as animal handlers and healthcare workers, and to educate them on how to use the PPE effectively while practicing good hygiene to prevent both community and nosocomial outbreaks (*38*). Collaborative efforts can contribute to reducing the spread of CCHFV and safeguarding public health by raising awareness and ensuring access to necessary protective gear (*39*).

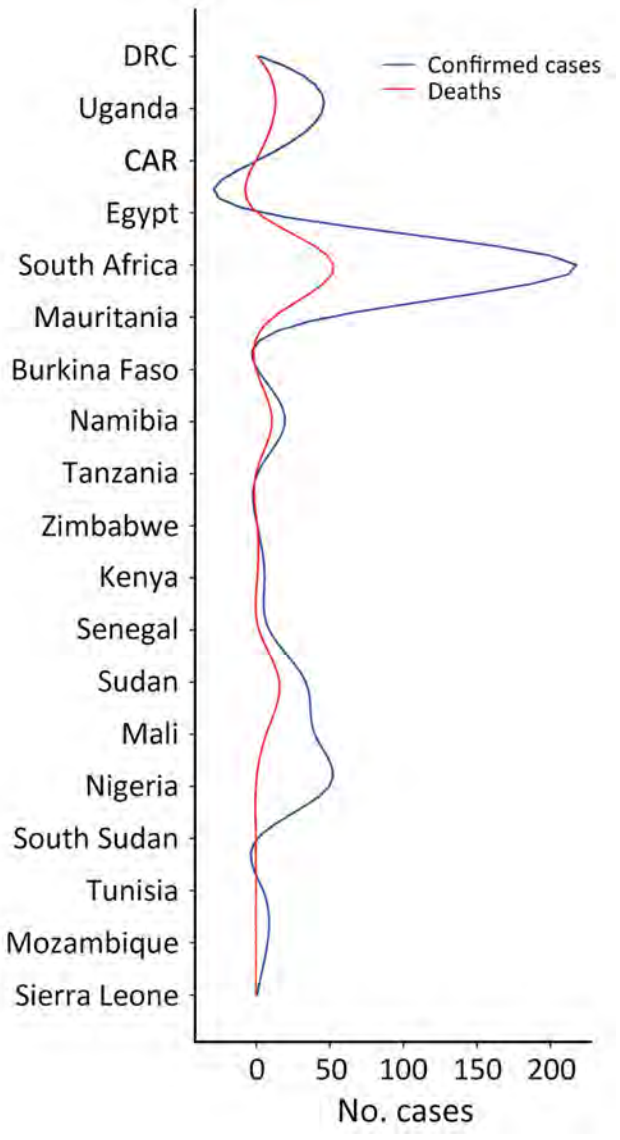

Figure 2. Number of Crimean-Congo hemorrhagic fever cases and related deaths in different countries within Africa. Total numbers of CCHF cases and deaths were recorded by 19 nations in Africa during January 1956–July 2020. CAR, Central African Republic; DRC, Democratic Republic of the Congo.

Investment in Public Health Infrastructure

Countries in Africa need to increase investments in public health infrastructure, such as by strengthening staff capacity, upgrading healthcare facilities, and establishing well-equipped laboratories. Improving training programs and raising awareness are needed to develop a skilled public health workforce that can respond effectively to epidemics (*40*). We recommend additional support for research projects across the continent to better understand the epidemiology and transmission dynamics of CCHF and to predict, prevent, and manage outbreaks (*39*). Further research is also needed to explore potential vaccines and evaluate the efficacy of treatment options, including ribavirin and other antiviral drugs.

Vaccines

CCHF is the most common tickborne viral disease infecting humans, calling for effective vaccines to prevent outbreaks and reduce transmission risks (*41*). Several vaccine options are being researched and developed with promising results. However, no widely accepted CCHF vaccines are available for humans or animals. Preclinical trials have shown promise for various vaccine candidates, including attenuated live virus vaccines, vectored vaccines (using virus vectors to deliver CCHFV antigens), and plant-expressed vaccines (producing CCHFV antigens in plants for vaccine delivery). Those options are being investigated to determine their efficacy and potential as preventive strategies against CCHF. To optimize CCHF vaccine efficacy and investigate other therapeutic approaches, comprehensive detailed research, including preclinical research, clinical trials, and continuous surveillance, is required (*42*). Since 1974, Bulgaria has used the Bulgarian vaccine, an inactivated vaccine made from the brain tissue of suckling mice infected with CCHFV (*43*). The vaccine is given subcutaneously, and persons ≥16 years of age need several booster doses. T-cell activity against CCHFV is strong after vaccination, but persons receiving

numerous doses also exhibit higher levels of IgG and interferon-secreting effector T cells (*43*,*44*). Neutralizing antibody levels in immunized persons are still insufficient even after booster shots. Despite being used domestically, the Bulgarian vaccine has not been approved globally because of safety concerns and the lack of controlled clinical efficacy trials (*41*), emphasizing the continuous need for further research on and development of CCHF vaccines. To address the genetic diversity of various CCHFV strains in vaccine development, it is essential to optimize vaccine formulations, evaluate dosing regimens, and identify immunogenic epitopes that confer robust and lasting immunity against CCHFV (*45*). Identifying those epitopes is critical for developing vaccines that can defend against CCHFV genetic variants (*15*). As previously described, inactivated vaccines produced from mouse brains have been used, but they are not widely available. Developing new mouse models that simulate human CCHF disease has proven to be beneficial in vaccine research (*46*). In addition to human immunization initiatives, veterinary vaccines for livestock have the potential to minimize exposure during animal handling and disrupt the tick-vector cycle. Despite continuous research, no animal vaccines are available on the market; however, the modified vaccinia virus Ankara glycoprotein GP vaccine is being tested in sheep, which represents an essential area of investigation (*3*,*29*,*47*).

One Health Approach

The World Health Organization introduced a One Health approach to improve coordination among livestock and agriculture professionals, veterinarians, and researchers. The approach brings together agriculture, environmental service, and veterinary service sectors to achieve better CCHF control and prevention and further development of preventive practices, research, and training in Africa (*48*). The One Health approach acknowledges the need for a comprehensive and interdisciplinary strategy to control CCHF epidemics in Africa (*49*).

Conclusions

CCHF imposes a substantial disease burden in Africa. Public education, tick control, infection prevention and control, and protection for persons conducting high-risk activities, such as livestock rearing and working in slaughterhouses, are essential in CCHF-endemic areas to protect populations at risk for CCHFV infection. In addition, developing reliable diagnostics, effective vaccines, and antiviral treatments is crucial for minimizing the burden of CCHF on patients and healthcare systems. Sustained commitment and cooperation among nations of Africa, regional organizations, and international partners that prioritize collaborative efforts, strengthen surveillance networks, and invest in public health infrastructure will safeguard public health and produce a continent better prepared to effectively respond to CCHF and other disease outbreaks.

About the Author

Mr. Okesanya is a medical laboratory scientist at the Neuropsychiatric Hospital Aro in Nigeria and is pursuing a degree in public health at the University of Thessaly, Volos, Greece. His research interests focus on infectious illnesses, public and global health, laboratory medicine, and medical microbiology.

References

1. Hawman DW, Feldmann H. Crimean-Congo haemorrhagic fever virus. Nat Rev Microbiol. 202321:463–77. https://doi.org/10.1038/s41579-023-00871-9
2. Appannanavar SB, Mishra B. An update on Crimean Congo hemorrhagic fever. J Glob Infect Dis. 2011;3:285–92. https://doi.org/10.4103/0974-777X.83537
3. Shahhosseini N, Wong G, Babuadze G, Camp JV, Ergonul O, Kobinger GP, et al. Crimean-Congo hemorrhagic fever virus in Asia, Africa and Europe. Microorganisms. 2021;9:1907. https://doi.org/10.3390/microorganisms9091907
4. Msimang V, Weyer J, le Roux C, Kemp A, Burt FJ, Tempia S, et al. Risk factors associated with exposure to Crimean-Congo haemorrhagic fever virus in animal workers and cattle, and molecular detection in ticks, South Africa. PLoS Negl Trop Dis. 2021;15:e0009384. https://doi.org/10.1371/journal.pntd.0009384
5. Balinandi S, Patel K, Ojwang J, Kyondo J, Mulei S, Tumusiime A, et al. Investigation of an isolated case of human Crimean-Congo hemorrhagic fever in Central Uganda, 2015. Int J Infect Dis. 2018;68:88–93. https://doi.org/10.1016/j.ijid.2018.01.013
6. Pshenichnaya NY, Nenadskaya SA. Probable Crimean-Congo hemorrhagic fever virus transmission occurred after aerosol-generating medical procedures in Russia: nosocomial cluster. Int J Infect Dis. 2015;33:120–2. https://doi.org/10.1016/j.ijid.2014.12.047
7. Pshenichnaya NY, Sydenko IS, Klinovaya EP, Romanova EB, Zhuravlev AS. Possible sexual transmission of Crimean-Congo hemorrhagic fever. Int J Infect Dis. 2016;45:109–11. PubMed https://doi.org/10.1016/j.ijid.2016.02.1008
8. Leblebicioglu H, Sunbul M, Guner R, Bodur H, Bulut C, Duygu F, et al. Healthcare-associated Crimean-Congo haemorrhagic fever in Turkey, 2002–2014: a multicentre retrospective cross-sectional study. Clin Microbiol Infect. 2016;22:387.e1–4. https://doi.org/10.1016/j.cmi.2015.11.024
9. Nuttall PA. Climate change impacts on ticks and tick-borne infections. Biologia. 2022;77:1503–12. https://doi.org/10.1007/s11756-021-00927-2
10. Africa Centres for Disease Control and Prevention. Crimean-Congo haemorrhagic fever [cited 2023 May 25]. https://africacdc.org/disease/crimean-congo-haemorrhagic-fever

11. Gürbüz E, Ekici A, Ünlü AH, Yılmaz H. Evaluation of seroprevalence and clinical and laboratory findings of patients admitted to health institutions in Gümüşhane with suspicion of Crimean-Congo hemorrhagic fever. Turk J Med Sci. 2021;51:1825–32. https://doi.org/10.3906/sag-2001-82
12. Elaldi N, Kaya S. Crimean-Congo hemorrhagic fever. J Microbiol Infect Dis. 2014;4:S1–9. https://doi.org/10.5799/ahinjs.02.2014.S1.0135
13. Fillâtre P, Revest M, Tattevin P. Crimean-Congo hemorrhagic fever: an update. Med Mal Infect. 2019;49:574–85. https://doi.org/10.1016/j.medmal.2019.09.005
14. Ak Ç, Ergönül Ö, Gönen M. A prospective prediction tool for understanding Crimean-Congo haemorrhagic fever dynamics in Turkey. Clin Microbiol Infect. 2020;26:123.e1–7. PubMed https://doi.org/10.1016/j.cmi.2019.05.006
15. University of Nebraska Medical Center Global Center for Health Security. Namibia confirms outbreak of Crimean-Congo hemorrhagic fever [cited 2024 May 10]. https://www.unmc.edu/healthsecurity/transmission/2023/05/23/namibia-confirms-outbreak-of-crimean-congo-hemorrhagic-fever
16. Temur AI, Kuhn JH, Pecor DB, Apanaskevich DA, Keshtkar-Jahromi M. Epidemiology of Crimean-Congo hemorrhagic fever (CCHF) in Africa—underestimated for decades. Am J Trop Med Hyg. 2021;104:1978–90. https://doi.org/10.4269/ajtmh.20-1413
17. Blair PW, Kuhn JH, Pecor DB, Apanaskevich DA, Kortepeter MG, Cardile AP, et al. An emerging biothreat: Crimean-Congo hemorrhagic fever virus in southern and western Asia. Am J Trop Med Hyg. 2019;100:16–23. https://doi.org/10.4269/ajtmh.18-0553
18. Hoogstraal H. The epidemiology of tick-borne Crimean-Congo hemorrhagic fever in Asia, Europe, and Africa. J Med Entomol. 1979;15:307–417. https://doi.org/10.1093/jmedent/15.4.307
19. Chauhan RP, Dessie ZG, Noreddin A, El Zowalaty ME. Systematic review of important viral diseases in Africa in light of the 'One Health' concept. Pathogens. 2020;9:301. https://doi.org/10.3390/pathogens9040301
20. Ergonul O, Whitehouse CA, editors. Crimean-Congo hemorrhagic fever: a global perspective. Dordrecht (the Netherlands): Springer; 2007.
21. Balinandi S, Whitmer S, Mulei S, Nyakarahuka L, Tumusiime A, Kyondo J, et al. Clinical and molecular epidemiology of Crimean-Congo hemorrhagic fever in humans in Uganda, 2013–2019. Am J Trop Med Hyg. 2021;106:88–98. PubMed https://doi.org/10.4269/ajtmh.21-0685
22. Apanaskevich DA, Horak IG. The genus *Hyalomma* Koch, 1844: v. re-evaluation of the taxonomic rank of taxa comprising the *H.* (*Euhyalomma*) *marginatum*koch complex of species (Acari: Ixodidae) with redescription of all parasitic stages and notes on biology. Int J Acarol. 2008;34:13–42. https://doi.org/10.1080/01647950808683704
23. Carmichael IH. Ticks from the African buffalo (*Syncerus-caffer*) in Ngamiland, Botswana. Onderstepoort J Vet Res. 1976;43:27–9.
24. Saluzzo JF, Digoutte JP, Cornet M, Baudon D, Roux J, Robert V. Isolation of Crimean-Congo haemorrhagic fever and Rift Valley fever viruses in Upper Volta. Lancet. 1984;323:1179. https://doi.org/10.1016/s0140-6736(84)91419-3
25. Kebede S, Duales S, Yokouide A, Alemu W. Trends of major disease outbreaks in the African region, 2003–2007. East Afr J Public Health. 2010;7:20–9. https://doi.org/10.4314/eajph.v7i1.64672
26. ayatilleke K. Challenges in implementing surveillance tools of high-income countries (HICs) in low middle income countries (LMICs). Curr Treat Options Infect Dis. 2020;12:191–201. https://doi.org/10.1007/s40506-020-00229-2
27. Reuters. Namibia declares outbreak of Crimean-Congo fever after patient dies [cited 2024 May 8]. https://www.reuters.com/world/africa/namibia-declares-outbreak-crimean-congo-fever-after-patient-dies-2023-05-23
28. Johansson M, Mysterud A, Flykt A. Livestock owners' worry and fear of tick-borne diseases. Parasit Vectors. 2020;13:331. https://doi.org/10.1186/s13071-020-04162-7
29. Mazzola LT, Kelly-Cirino C. Diagnostic tests for Crimean-Congo haemorrhagic fever: a widespread tickborne disease. BMJ Glob Health. 2019;4:e001114. https://doi.org/10.1136/bmjgh-2018-001114
30. Schüpbach G, Silva LC, Buzzell–Hatav A. Surveillance plan proposal for early detection of zoonotic pathogens in ruminants. EFSA Support Publ. 2023;20:7887E. https://doi.org/10.2903/sp.efsa.2023.EN-7887
31. Ul Ain Q, Saeed A, Larik EA, Ghafoor T, Khosa ZA, Ali A, et al. Evaluation of event based surveillance system of Crimean Congo haemorrhagic fever in Balochistan Pakistan, 2017. Glob Biosecurity. 2019;1:1–7. https://doi.org/10.31646/gbio.34
32. Al-Abri SS, Abaidani IA, Fazlalipour M, Mostafavi E, Leblebicioglu H, Pshenichnaya N, et al. Current status of Crimean-Congo haemorrhagic fever in the World Health Organization Eastern Mediterranean Region: issues, challenges, and future directions. Int J Infect Dis. 2017;58:82–9. https://doi.org/10.1016/j.ijid.2017.02.018
33. Aslam M, Abbas RZ, Alsayeqh A. Distribution pattern of Crimean–Congo hemorrhagic fever in Asia and the Middle East. Front Public Health. 2023;11:1093817. https://doi.org/10.3389/fpubh.2023.1093817
34. Montalvão SAL, Lowe A, Kitchen S. Advantages of external quality assessment-EQA programs. Haemophilia. 2022;28:679–86. https://doi.org/10.1111/hae.14562
35. Carter JY. External quality assessment in resource-limited countries. Biochem Med. 2017;27:97–109. https://doi.org/10.11613/BM.2017.013
36. Bartolini B, Gruber CE, Koopmans M, Avšič T, Bino S, Christova I, et al. Laboratory management of Crimean-Congo haemorrhagic fever virus infections: perspectives from two European networks. Euro Surveill. 2019;24:1800093. https://doi.org/10.2807/1560-7917.ES.2019.24.5.1800093
37. Oleribe OO, Momoh J, Uzochukwu BS, Mbofana F, Adebiyi A, Barbera T, et al. Identifying key challenges facing healthcare systems in Africa and potential solutions. Int J Gen Med. 2019;12:395–403. https://doi.org/10.2147/IJGM.S223882
38. Fletcher TE, Gulzhan A, Ahmeti S, Al-Abri SS, Asik Z, Atilla A, et al. Infection prevention and control practice for Crimean-Congo hemorrhagic fever—a multi-center cross-sectional survey in Eurasia. PLoS One. 2017;12:e0182315. PubMed https://doi.org/10.1371/journal.pone.0182315
39. Sorvillo TE, Rodriguez SE, Hudson P, Carey M, Rodriguez LL, Spiropoulou CF, et al. Towards a sustainable One Health approach to Crimean-Congo hemorrhagic fever prevention: focus areas and gaps in knowledge. Trop Med Infect Dis. 2020;5:113. https://doi.org/10.3390/tropicalmed5030113
40. Omosigho PO, Okesanya OJ, Olaleke NO, Eshun G, Lucero-Prisno DE 3rd. Multiple burden of infectious disease outbreaks: implications for Africa healthcare system. J Taibah Univ Med Sci. 2023;18:1446–8. https://doi.org/10.1016/j.jtumed.2023.06.004
41. Ahata B, Akçapınar GB. CCHFV vaccine development, current challenges, limitations, and future directions. Front

Immunol. 2023;14:1238882. https://doi.org/10.3389/fimmu.2023.1238882
42. Ozdarendeli A. Crimean-Congo hemorrhagic fever virus: progress in vaccine development. Diagnostics (Basel). 2023;13:2708. https://doi.org/10.3390/diagnostics13162708
43. Behboudi E, Kakavandi E, Hamidi-Sofiani V, Ebrahimian A, Shayestehpour M. Crimean-Congo hemorrhagic fever virus vaccine: past, present, and future. Rev Res Med Microbiol. 2022;33:109–16. https://doi.org/10.1097/MRM.0000000000000260
44. Mousavi-Jazi M, Karlberg H, Papa A, Christova I, Mirazimi A. Healthy individuals' immune response to the Bulgarian Crimean-Congo hemorrhagic fever virus vaccine. Vaccine. 2012;30:6225–9. https://doi.org/10.1016/j.vaccine.2012.08.003
45. Chen T, Ding Z, Lan J, Wong G. Advances and perspectives in the development of vaccines against highly pathogenic bunyaviruses. Front Cell Infect Microbiol. 2023;13:1174030. https://doi.org/10.3389/fcimb.2023.1174030
46. Dowall SD, Carroll MW, Hewson R. Development of vaccines against Crimean-Congo haemorrhagic fever virus. Vaccine. 2017;35:6015–23. https://doi.org/10.1016/j.vaccine.2017.05.031
47. Zhang Y, Ye F, Xia LX, Zhu LW, Kamara IL, Huang KQ, et al. Next-generation sequencing study of pathogens in serum from patients with febrile jaundice in Sierra Leone. Biomed Environ Sci. 2019;32:363–70. https://doi.org/10.3967/bes2019.048
48. Ferrinho P, Fronteira I. Developing One Health systems: a central role for the One Health workforce. Int J Environ Res Public Health. 2023;20:4704. https://doi.org/10.3390/ijerph20064704
49. Jafar U, Usman M, Ehsan M, Naveed A, Ayyan M, Cheema HA. The outbreak of Crimean-Congo hemorrhagic fever in Iraq—challenges and way forward. Ann Med Surg (Lond). 2022;81:104382. https://doi.org/10.1016/j.amsu.2022.104382

Address for correspondence: Gbolahan Deji Olatunji, Medicine and Surgery, PMB 1515, University of Ilorin, Ilorin 240101, Nigeria; email: gbolahanolatunji153@gmail.com

etymologia revisited

Picobirnavirus [pi-ko-burʹnə-viʺrəs]

Picobirnavirus, the recently recognized sole genus in the family *Picobirnaviridae*, is a small (*Pico*, Spanish for small), bisegmented (*bi*, Latin for two), double-stranded RNA virus. Picobirnaviruses were initially considered to be birna-like viruses, and the name was derived from birnavirus (bisegmented RNA), but the virions are much smaller (diameter 35 nm vs. 65 nm).

Picobirnaviruses are reported in gastroenteric and respiratory infections. These infections were first described in humans and black-footed pigmy rice rats in 1988. Thereafter, these infections have been reported in feces and intestinal contents from a wide variety of mammals with or without diarrhea, and in birds and reptiles worldwide.

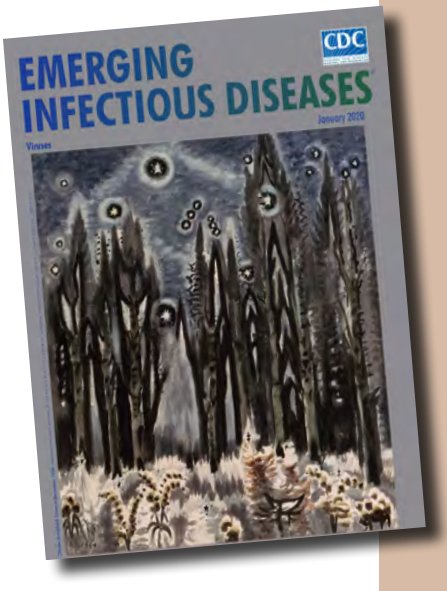

Originally published in January 2020

Sources

1. Delmas B, Attoui H, Ghosh S, Malik YS, Mundt E, Vakharia VN; ICTV Report Consortium. ICTV virus taxonomy profile: Picobirnaviridae. J Gen Virol. 2019;100:133–4. https://doi.org/10.1099/jgv.0.001186
2. Malik YS, Kumar N, Sharma K, Dhama K, Shabbir MZ, Ganesh B, et al. Epidemiology, phylogeny, and evolution of emerging enteric Picobirnaviruses of animal origin and their relationship to human strains. BioMed Res Int. 2014;2014:780752. https://doi.org/10.1155/2014/780752
3. Pereira HG, Flewett TH, Candeias JA, Barth OM. A virus with a bisegmented double-stranded RNA genome in rat (*Oryzomys nigripes*) intestines. J Gen Virol. 1988;69:2749–54. https://doi.org/10.1099/0022-1317-69-11-2749
4. Smits SL, van Leeuwen M, Schapendonk CM, Schürch AC, Bodewes R, Haagmans BL, et al. Picobirnaviruses in the human respiratory tract. Emerg Infect Dis. 2012;18:1539–40. https://doi.org/10.3201/eid1809.120507

https//wwwnc.cdc.gov/eid/article/26/1/et-2601_article

Strategies to Enhance COVID-19 Vaccine Uptake among Prioritized Groups, Uganda—Lessons Learned and Recommendations for Future Pandemics

Daniel Kiiza, Judith Nanyondo Semanda, Boneventure Brian Kawere, Claire Ajore, Christopher Kaliisa Wasswa, Andrew Kwiringira, Emmanuel Tumukugize, Joel Sserubidde, Nashiba Namyalo, Ronald Baker Wadria, Peter Mukiibi, Julie Kasule, Ivan Chemos, Acham Winfred Ruth, Ritah Atugonza, Flora Banage, Yvette Wibabara, Immaculate Ampaire, Alfred Driwale, Waverly Vosburgh, Lisa Nelson, Mohammed Lamorde, Amy Boore

COVID-19 vaccination was launched in March 2021 in Uganda and initially prioritized persons ≥50 years of age, persons with underlying conditions, healthcare workers, teachers, and security forces. However, uptake remained low 5 months after the program launch. Makerere University's Infectious Diseases Institute supported Uganda's Ministry of Health in optimizing COVID-19 vaccination uptake models by using point-of-care, place of worship, and place of work engagement and the Social Assistance Grant for Empowerment model in 47 of 135 districts in Uganda, where we trained influencers to support mobilization for vaccination outreach under each model. During July–December, vaccination rates increased significantly in targeted regions, from 92% to 130% for healthcare workers, 40% to 90% for teachers, 25% to 33% for security personnel, 6% to 15% for persons ≥50 years of age, and 6% to 11% for persons with underlying conditions. Our approach could be adopted in other targeted vaccination campaigns for future pandemics.

Globally, the COVID-19 pandemic resulted in >650 million infections and 6.5 million deaths during March 2020–December 2022 (*1*,*2*). Uganda recorded its first case of SARS-CoV-2 infection on March 21, 2020; as of January 20, 2023, Uganda had reported >170,000 cases and 3,630 deaths (*2*–*4*).

SARS-CoV-2 infections can have various clinical manifestations, ranging from asymptomatic infection to mild-to-severe and critical respiratory illnesses requiring hospitalization. Vulnerable populations, such as healthcare workers and persons with underlying conditions, immune dysfunction, or advanced age, are at increased risk for COVID-19, progression to severe disease, and death (*5*–*7*).

COVID-19 vaccination is critical in reducing severe disease and death in vulnerable populations while protecting health systems and enabling the relaxation of public health measures (*8*–*11*). More important, rapidly vaccinating high-priority groups is crucial for mitigating the effect of the pandemic, similar to emergency immunization response strategies applied during outbreaks of other vaccine-preventable disease (*12*).

In March 2021, the Ministry of Health in Uganda launched the National COVID-19 Vaccine Deployment Plan. Phase 1 targeted priority populations for vaccination, including healthcare workers, other essential workers (including security personnel and teachers), persons ≥50 years of age, and patients with underlying chronic medical conditions (*13*,*14*). This approach considered the heightened

Author affiliations: Makerere University Infectious Diseases Institute, Kampala, Uganda (D. Kiiza, J. Nanyondo Semanda, B.B. Kawere, C. Ajore, C.K. Wasswa, A. Kwiringira, N. Namyalo, R. Baker Wadria, P. Mukiibi, M. Lamorde); Mildmay Uganda, Kampala (E. Tumukugize, J. Sserubidde); Centers for Disease Control and Prevention, Atlanta, Georgia, USA (J. Kasule, F. Banage, Y. Wibabara, W. Vosburgh, L. Nelson, A. Boore); Rakai Health Sciences Program, Kalisizo, Uganda (I. Chemos); The AIDS Support Organization, Kampala (A.W. Ruth); Ministry of Health, Kampala (R. Atugonza, I. Ampaire, A. Driwale)

DOI: https://doi.org/10.3201/eid3007.231001

global demand for COVID-19 vaccine limiting availability and driving vaccine inequity to lower-income countries at the time and the disproportionate occurrence of severe COVID-19 disease and death in vulnerable groups in Uganda (*15*). As such, a phased vaccine deployment approach prioritizing vulnerable groups was crucial to maximize the public health gains from the rollout. However, 5 months into phase 1 rollout, COVID-19 vaccination coverage in those groups remained low (*16*,*17*).

To address this shortfall, the US Centers for Disease Control and Prevention (CDC) and the Infectious Diseases Institute (IDI) at Makerere University in Uganda implemented a project to support the Uganda Ministry of Health (MoH) through the Uganda National Expanded Program for Immunization (UNEPI) in accelerating vaccination uptake in high-priority groups. We describe strategies designed and deployed to enhance the COVID-19 vaccination uptake among prioritized groups.

Methods

Project Description Strategy and Context

IDI launched the COVID-19 vaccination project through its Global Health Security Department in July 2021 to increase COVID-19 vaccine uptake among national priority groups through national and subnational implementational support to MoH and UNEPI. The project recruited 3 officers and deployed them at MoH and UNEPI with distinct roles in supporting UNEPI in developing strategies for vaccine advocacy and vaccine safety and technical coordination of all subgranted partners in the regional implementation of vaccine service delivery support. With national-level coordination from the IDI, funding was provided to 4 organizations already receiving funding from the US President's Emergency Plan for AIDS Relief (PEPFAR) for the HIV Comprehensive Care Program through CDC. This funding was designated to support project implementation in 5 regions across 47 districts and 5 cities. The funded implementing partners and areas of coverage included IDI, reaching 12 districts and 1 city in the West Nile Region and the 1 district and 2 cities of Kampala (metropolitan district of Kampala) and Entebbe (metropolitan district of Wakiso); the Rakai Health Sciences Program, reaching 12 districts and 1 city in South Central (Southern Buganda) Region; the AIDS Support Organization (TASO), covering 10 districts of Teso Region and 4 districts of Southern Karamoja Region; and Mildmay Uganda, covering 8 districts in the North Central (Northern Buganda) Region.

Each implementing partner recruited ≥4 personnel, including a regional coordinator and data officers. The goal was to layer project implementation into the broader PEPFAR HIV Comprehensive Care Program, which employs a cluster approach with, on average, 4 clusters in each geographic region. MoH technical experts used the adapted version of the World Health Organization (WHO) online COVID Vaccination Training for Health Workers (https://openwho.org/courses/covid-19-vaccination-healthworkers-en) to train all regional implementing officers to ensure adequate support of government vaccination activities in the 47 supported districts and 5 cities. Furthermore, this effort was supplemented with supportive supervision visits from the national team to reinforce appropriate project implementation, link stakeholder groups to implementing partners, and roll out the developed vaccination models (Figure 1).

The project aimed to accelerate COVID-19 vaccination among priority populations by developing evidence-based strategies and models for vaccination uptake. We used guidance from the WHO Behavioral and Social Drivers of the Vaccination Framework (*18*) to inform our approach with interventions that included community engagement, dialogue-based approaches, interpersonal advocacy efforts, and targeted vaccination outreach.

Stakeholder Mapping and Engagement

In partnership with UNEPI, project technical personnel provided national-level assistance in mapping stakeholders associated with priority populations for phase 1 vaccination, engaging them through in-person and virtual teleconference meetings. We discussed the challenges of vaccination uptake among priority populations and brainstormed strategies to address these challenges, highlighting the stakeholders' role.

COVID-19 Vaccination Uptake Models

The strategies described informed the development of COVID-19 vaccination uptake models to accelerate vaccination among priority populations. As part of national-level technical support to the MoH and UNEPI, models were conceptualized and subsequently rolled out at the subnational level, collaborating with subgranted implementing partners in respective districts.

Point-of-Care Vaccination Model

Under this model, we selected high-volume health facilities with specialized clinics for chronic conditions such as HIV, diabetes, and cardiovascular disease.

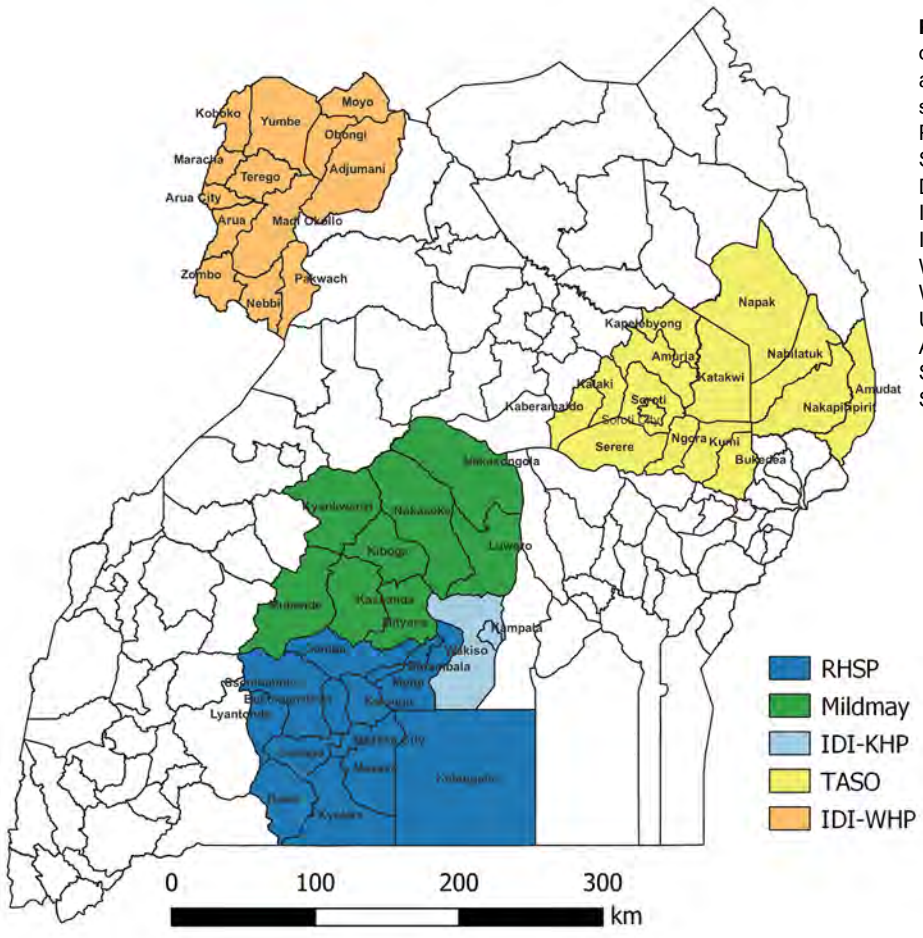

Figure 1. Regional implementation of COVID-19 vaccination project across 47 districts and 5 cities supported by the CDC–PEPFAR Program, Uganda, July 2021–September 2022. CDC, Centers for Diseases Control and Prevention; IDI-KHP; Infectious Diseases Institute–Kampala HIV Project; IDI-WHP, Infectious Diseases Institute–West Nile HIV Project; PEPFAR, US President's Emergency Plan for AIDS Relief; RHSP, Rakai Health Sciences Program; TASO, The AIDS Support Organization.

We identified healthcare workers and key influencers among patients in these clinics and trained them to be vaccination champions to support interpersonal mobilization for COVID-19 vaccination within the clinics. We distributed information, education, and communication (IEC) materials to assist with mobilization efforts. Furthermore, we built healthcare workers' capacity to screen and line-list eligible patients for COVID-19 vaccination. District vaccination teams were then linked to work closely with the vaccination champions to conduct targeted outreach on prespecified clinic days.

Place of Work Model

We identified corporate entities and their leaders and used virtual platforms to train the leaders and their staff members to be vaccination champions. During training sessions, we provided essential IEC materials and e-posters to support the interpersonal mobilization of leaders and staff members' family members and colleagues for COVID-19 vaccination. We then linked district vaccination teams to the corporate entities' management to conduct vaccination outreaches at the corporate headquarters or preferred locations, such as playgrounds and recreation centers.

Place of Worship Model

We identified places of worship and their leaders, including key influencers within the congregations, and trained them to be vaccination champions. We provided these persons with IEC materials to support interpersonal mobilization for vaccination. This effort was followed by linking vaccination teams to these places of worship to conduct outreach vaccination outreach after prayer.

Social Assistance Grant for Empowerment (SAGE) Model

The government of Uganda operates a social protection program offering quarterly stipends to persons ≥80 years of age. Those payments are administered at the subcounty level under district Community Development Officers' (CDO) oversight. We conducted training sessions for the CDOs and influential persons ≥80 years of age, appointing them to be vaccination champions to spearhead interpersonal mobilization efforts. Subsequently, we connected district

vaccination teams with the CDOs and vaccination champions to conduct targeted vaccination outreach near payment sites.

Development of the COVID-19 Vaccination Champions Toolkit

We trained the vaccination champions and key influencers identified for each model described by using the COVID-19 Vaccination Champions Toolkit (Appendix, https://wwwnc.cdc.gov/EID/article/30/7/23-1001-App1.pdf) for conducting interpersonal and social mobilization of their communities for vaccination. IDI supported MoH in developing the Vaccination Champion's toolkit, which consists of 3 modules. Module 1 provides an overview of COVID-19 basics, including information on transmission, prevention strategies, and identifying the most vulnerable persons requiring vaccination. Module 2, focused on vaccines, addresses safety concerns and guidelines for reporting adverse effects after immunization. Module 3 focuses on communication strategies related to vaccination, incorporating key insights from WHO's Behavioral and Social Drivers of the Vaccination Framework (*18*).

We developed the toolkit by adapting existing UNEPI COVID-19 vaccination training materials for healthcare workers for lay audiences, coopting WHO explainers on COVID-19 and vaccines (*19*), and tailoring the San Francisco Public Health Department and the University of California–San Francisco Vaccine Ambassador training program to the situation of Uganda (*20*). We convened a 1-day workshop on October 8, 2021, to adapt the drafted toolkit with key inputs from the MoH and UNEPI Advocacy and Risk Communication Department and a patient advocacy group, Community Health Advocacy and Information Network.

We used the mobile communication application WhatsApp as a virtual collaborative platform for sharing electronic IEC materials and updates on vaccine availability and vaccination locations with trained vaccination champions. In addition, we used the platform to counter the evolving misinformation and disinformation surrounding the COVID-19 vaccination program.

Data Management and Ethics Considerations

COVID-19 vaccination uptake was the outcome variable of interest, which we defined as the number of persons vaccinated with a certain dose of the vaccine in a certain period expressed as the proportion of a target population (*21*). We extracted aggregate COVID-19 vaccination uptake data, categorized by prioritized groups, from the District Health Information System 2.0 database. We transferred those data, devoid of unique identifier information, to a computer with restricted access. Subsequently, we used the data during March–December 2021 to generate vaccination uptake trend curves for prioritized groups in the PEPFAR-supported districts. This intervention was implemented in response to a public health emergency after receiving authorization from MoH's Office of the Director General of Health Services.

Results

Stakeholder Mapping and Engagement

We engaged 23/30 (77%) of the mapped stakeholders' groups in 6 in-person and 7 virtual meeting sessions. The initial meetings with stakeholders were mainly physical, intended to establish rapport, update stakeholders on the challenges of vaccination in the priority population, and discuss the role they can play. A total of 44 leaders of stakeholder groups participated in the physical meetings and the subsequent virtual meeting that involved training 1,333 members to be vaccination champions. Three of 6 of the initial engagements with the stakeholder leadership blended physical and virtual meetings.

Some of the engagements with the stakeholders lead to key outputs, such as mobilizing members for training as vaccination champions, piloting the models, engaging media to call to action priority populations for vaccination, and conducting targeted outreach of stakeholder members. Specifically, 3 stakeholders designated places of worship for targeted vaccination outreach campaigns (Watoto Ministries, Kakande Ministries, and Gadhafi Mosque). This process resulted in vaccinations from direct mobilization support from the stakeholders after the engagement with stakeholders targeting the key priority populations that are part of the stakeholder membership (Table 1; Figure 2).

COVID-19 Vaccination Uptake by Models

We assessed COVID-19 vaccination by vaccination model (Table 2). During the implementation period of September–December 2021, a total of 75,098 vulnerable priority persons were vaccinated through activities and outreach based on the models. All 4 models were piloted in Kampala, where all stakeholder engagements occurred and were hosted in the IDI and Kampala HIV Project operational region. Those models were subsequently rolled out to other implementing regions. We assessed the percentage of overall COVID-19 vaccinations attributable to each

Table 1. Engagement of stakeholders linked to the priority populations for COVID-19 vaccination, Uganda, July–September 2021

Category	Stakeholders engaged	Physical meeting	Virtual meetings
Healthcare workers	Uganda Medical and Dental Practitioners Council; Uganda Medical Association	9 members, including Uganda Medical and Dental Practitioners Council Registrar and Uganda Medical Association President	70 doctors; 380 infection prevention and control specialists
	Uganda Nurses and Midwives Councils; Uganda Nurses and Midwives Union (UNMU)	UNMU President and Uganda Nurses and Midwives Councils Registrar	56 national executive committee personnel to the UNMU and chairpersons countrywide
	Pharmacy Council; Pharmaceutical Society of Uganda; Allied Health Practitioners Council	15 members of the pharmacy council and Pharmaceutical Society of Uganda engaged in both virtual and physical session	80 pharmacists sensitized on COVID-19 vaccination
Teachers	Uganda National Teachers Union; Ministry of Education and Sports; Ministry of Local Government	Chairperson, commissioner, and permanent secretary	131 district education officers, 500 private school owners, private teachers association, faith-based schools
Security personnel	Uganda Peoples' Defense Forces; Uganda Police Force; Uganda Prison Services	5 personnel concerned with health and medical matters	
Persons ≥50 years of age	Ministry of Gender, Labour, and Social Development; members of parliament for persons ≥50 years of age; faith-based organizations	Supreme Mufti, church leadership, 3 members of parliament, and the state minister	47 members
Persons with underlying conditions	Community Health and Information Network; Uganda Diabetes Association; Uganda Heart Institute; Uganda Cancer Institute; Uganda AIDS Control Program; corporate entities (Stanbic Bank, UMEME Limited, Diamond Trust Bank)	17 members	

model: point-of-care, 11%; place of worship, 38%; place of work, 8%; and SAGE, 43%.

Phase 1 of the National COVID-19 Vaccine Deployment Plan aimed to vaccinate 4.8 million priority persons (150,000 healthcare workers, 550,000 teachers, 250,000 security personnel, 3,348,5000 persons ≥50 years of age, and 500,000 persons with underlying conditions). In July 2021, 5 months into the national COVID-19 vaccination roll-out in Uganda, national-level vaccination uptake among those groups (by receipt of first dose) stood at 94,684/150,000 (63.1%) for healthcare workers, 158,406/550,000 (29%) for teachers, 142,509/250,000 (57%) for security personnel, 276,736/ 3,384,000 (8%) for persons ≥50 years of age, and 25,361/500,000 (5.1%) for persons with underlying conditions. As of November 15, 2021, approximately 4 months into the implementation of project activities from inception in July 2021, vaccination uptake improved to 140,635 (93.8%) for healthcare workers, 376,555 (68.595%) for teachers, 161,491 (64.6%) for security personnel, 511,142 (15.3%) for persons ≥50 years of age, and 40,443 (8.1%) for persons with underlying conditions.

For programmatic tracking, the CDC–PEPFAR supported districts were assigned 72,225 healthcare workers, 264,825 teachers, 120,375 security personnel, 1,612,304 persons ≥50 years of age, and 240,750 persons with underlying conditions as target contributions to the overall national target for priority populations for phase 1. Three months after initiation of project activities in the CDC–PEPFAR supported districts, vaccination uptake improved from 66,561/72,225 (92%) to 93,889/72,225 (130%) for healthcare workers, 105,310/264,825 (40%) to 238,791/264,825 (90%) for teachers, 29,808/120,375 (25%) to 40,041/120,375 (33%) for security personnel, 100,788/1,612,304 (6%) to 235,439,1,612,304 (15%) for persons ≥50 years of age, and 14,878/240,750 (6%) to 26,134/240,750 (11%) for persons with underlying conditions.

By the close of 2021, a total of 115,737/72,225 (160%) healthcare workers, 285,369/264,825 (108%) teachers, 49,773/120,375 (41%) security personnel, 713,776/1,612,304 (44%) persons ≥50 years of age, and 47,892/240,750 (20%) persons with underlying conditions were vaccinated in CDC–PEPFAR supported districts. In terms of the percentage of vaccinations nationwide per target group, those regions contributed 115,737/153,673 (75%) of vaccinations among healthcare workers, 285,369/403,184 (71%) of vaccinations among teachers, 49,773/161,491 (31%) of vaccinations among security personnel, 713,776/1,314,706 (54%) of vaccinations among persons ≥50 years of age, and 47,892/47,555

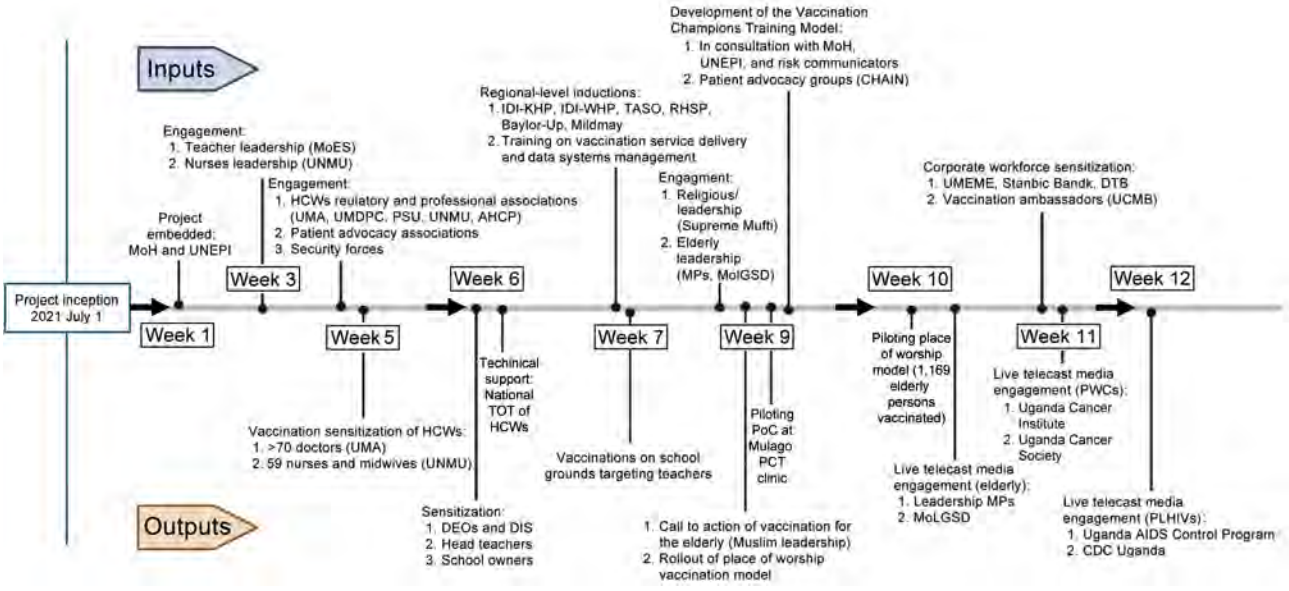

Figure 2. Timeline series of engagements and their respective outputs (starting July 1, 2021) within the first 12 weeks of the COVID-19 vaccination project, Uganda, July–September 2021. ACP, AIDS Control Program; AHPC, Allied Health Practitioners Council; CDC, US Centers for Disease Control and Prevention; CHAIN, Community Health and Information Network; DEOs, District Education Officers; DIS, District Inspector of School; DTB, Diamond Trust Bank; HCWs, healthcare workers; IDI-KHP, Infectious Diseases Institute–Kampala HIV Project; IDI-WHP, Infectious Diseases Institute–West Nile HIV Project; MoES, Ministry of Education and Sports; MoH, Ministry of Health; MoLGSD, Ministry of Gender, Labour, and Social Development; MPs, Members of Parliament; PCT, HIV Prevention Care and Treatment; PoC, point-of-care; PSU, Pharmacy Council, Pharmaceutical Society of Uganda; PWCs, persons with underlying conditions; RHSP, Rakai Health Sciences Program; TASO, The AIDS Support Organization; ToT, training of trainers; UCI, Uganda Cancer Institute; UCMB, Uganda Catholic Medical Bureau; UDA, Uganda Diabetes Association; UHI, Uganda Heart Institute; UMA, Uganda Medical Association; UMDPC, Uganda Medical and Dental Practitioners Council; UNEPI, Uganda National Expanded Program on Immunization; UNMC, Uganda Nurses and Midwives Councils; UNMU, Uganda Nurses and Midwives Union.

(101%) of vaccinations among persons with underlying conditions at the close of 2021 (Figure 3).

Discussion

Targeting priority populations for COVID-19 vaccination has been challenging globally, and countries in sub-Saharan Africa, including Uganda, are no exception (*22*–*25*). Despite government efforts to ensure COVID-19 vaccines are available to populations, practical issues, perceptions, and social processes within vulnerable target groups present access challenges that hinder achieving high vaccination coverage in these populations. Our study elucidates strategies for effectively targeting priority populations for COVID-19 vaccinations. We offer methodologic insights that are transferrable for the effective rollout of vaccination to future pandemics and outbreaks of other vaccine-preventable diseases with identifiable at-risk populations.

This project has demonstrated that stakeholder involvement is essential in planning and targeting vaccination efforts, particularly in the context of COVID-19 vaccination integration into routine healthcare service delivery, to effectively target vulnerable persons and close gaps between government agencies and communities (*26*,*27*). Community-based

Table 2. Contribution of vaccination models targeting priority groups for COVID-19 vaccination uptake in CDC–PEPFAR supported districts, Uganda, September–December 2021*

Vaccination model	CDC PEPFAR implementing partners					Total no. (%)
	IDI-KHP	IDI-WHP	Mildmay Uganda	TASO	RHSP	
Point-of-care	4,096	427	0	787	3,020	8,330 (11)
Place of worship	27,284	330	0	316	570	28,500 (38)
Place of work	2,711	1,000	0	1891	200	5,802 (8)
SAGE	694	13,731	1,808	16,233	0	32,466 (43)
Total	34,785	15,488	1,808	19,227	3,790	75,098 (100)

*CDC, Centers for Disease Control and Prevention; IDI-KHP, Infectious Diseases Institute–Kampala HIV Project; IDI-WHP, Infectious Diseases Institute–West Nile HIV Project; PEPFAR, US President's Emergency Plan for AIDS Relief; RHSP, Rakai Health Sciences Program; SAGE, Social Assistance Grant for Empowerment; TASO, The AIDS Support Organization.

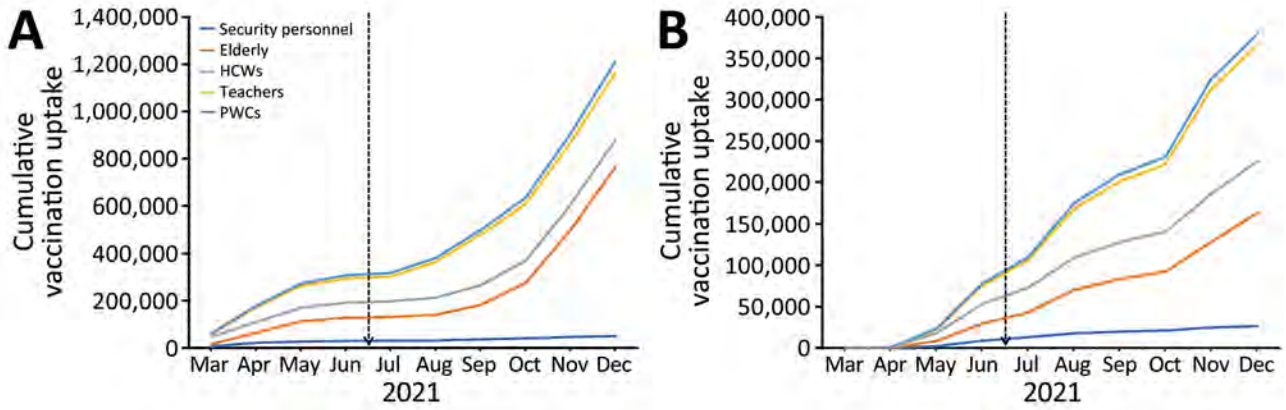

Figure 3. COVID-19 vaccination coverage among priority populations, by receipt of first (A) and second (B) dose, showing project inception date (vertical dashed line) and vaccine uptake trends among priority populations, Uganda, March–December 2021. HCWs, healthcare workers; PWCs, persons with underlying conditions.

stakeholders with ties to target populations play a critical role in fostering vaccination-related interpersonal mobilization. Moreover, local influencers can be mobilized to raise COVID-19 vaccination acceptance rates in priority populations as vaccination champions. Such influencers include religious leaders, community leaders, informed patients, and other notable community representatives. The strategies can be adapted for targeted vaccination campaigns to protect vulnerable populations from future pandemics. Studies have demonstrated that the engagement of influencers in developing and implementing vaccination strategies served to reduce misunderstandings and mistrust regarding COVID-19 vaccinations, rekindled community trust and vaccine confidence, and resulted in increased vaccination rates (*28*–*30*).

Using existing public health delivery platforms and community social structures in emergency response efforts can reinforce health systems' resilience to future pandemics. Our project demonstrates the potential of leveraging existing public health infrastructures, as observed with the involvement of the PEPFAR Comprehensive HIV Care Program and other community-based organizations linked to priority populations, to support COVID-19 vaccination efforts. During the past 2 decades, HIV programs have cultivated community structures and a strong presence that have earned trust within communities toward public health programs. Those established systems can serve as a solid foundation upon which other pandemic prevention preparedness and response efforts, such as COVID-19 vaccination, can build on (*31*–*33*). Such structures can enhance vaccine access and delivery, especially where community involvement is critical for mobilizing vulnerable populations.

This project also has implications for global health security responses, particularly in rapidly deploying medical countermeasures, such as vaccines, as a part of preparedness and response strategies during outbreaks (*33*). Those measures can be optimized to suit specific contexts to effectively deliver a successful rapid vaccination campaign as an emergency response targeting vulnerable populations. A cautious approach should be taken in integrating health security with HIV programming because this process might impede the effective delivery of HIV care services caused by the inevitable competition for resources. A crucial aspect to consider is efficient allocation of resources for each initiative to prevent overburdening either program. Integration efforts should prioritize the streamlining of resource allocations to ensure effectiveness.

We did not set out to independently assess the acceptability and feasibility of implementing various models, leaving room for future exploration. Similarly, evaluating interventions' effectiveness was not a primary objective, given the urgent public health crisis posed by the COVID-19 pandemic. Consequently, comparison groups were not established because of potential ethical concerns. However, retrospective investigation is now feasible, necessitating an independent evaluation study. Although we used District Health Information System 2.0 data to report COVID-19 vaccination uptake in supported districts, data backlog and completeness were beyond the project's control. Of note, targets for priority populations were based on estimates from the Uganda Bureau of Statistics and Ministry of Public Service, potentially leading to overperformance caused by underestimation, particularly among healthcare workers, because private sector estimates were not considered.

The vaccination models developed through stakeholder engagement increased COVID-19 vaccine uptake among prioritized groups in supported regions in Uganda. Embracing this approach as part of future pandemic prevention preparedness and response efforts holds promise for enhancing vaccination uptake. Moreover, we highlight the importance of stakeholder engagement in developing models to mobilize priority populations for COVID-19 vaccination, fostering collaboration, and building public confidence in vaccines between government agencies and the communities. Efforts to target persons in high-priority groups should continue to use these models in a tailored approach during the post–COVID-19 era as a critical stabilization and postrecovery strategy for MoH and UNEPI (*34*).

This project demonstrates that, by leveraging the PEPFAR platform, we effectively and expeditiously deployed vaccination, among other emergency public health interventions, by layering health security on earlier global health initiatives in HIV response. Therefore, we recommend that global health security programs consider adopting these strategies to bolster their resilience and effectively support vaccination programs as part of future pandemic prevention preparedness and response efforts. Such proactive measures will strengthen global health security and safeguard populations against emerging threats.

Acknowledgments

We thank the implementing partners and district local governments.

This project received funding and technical support from CDC's International Health Regulations project (grant no. GH000045) entitled "Strengthening Partnerships for Preparedness and Response in Uganda."

About the Author

Dr. Kiiza is a clinical pharmacologist and technical advisor (medical countermeasures) for the CDC-funded International Health Regulations Program at the Infectious Diseases Institute Makerere University. His research interests include clinical development and equitable access to medical countermeasures, including vaccines, in the health security space.

References

1. World Health Organization. Coronavirus disease (COVID-19) weekly epidemiological update and weekly operational update. 2021 [cited 2023 Jan 4]. https://www.who.int/emergencies/diseases/novel-coronavirus-2019/situation-reports
2. World Health Organization. COVID-19 confirmed cases and deaths. 2023 Jan 11 [cited 2023 Jan 12]. https://covid19.who.int
3. Ministry of Health Uganda. Coronavirus (pandemic) COVID-19. 2022 [cited 2022 Dec 21]. https://www.health.go.ug/covid
4. Ministry of Health Uganda. COVID-19 response info hub. 2021 [cited 2022 Dec 21]. https://covid19.gou.go.ug/statistics.html
5. Novida H, Soelistyo SA, Cahyani C, Siagian N, Hadi U, Pranoto A. Factors associated with disease severity of COVID19 in patients with type 2 diabetes mellitus. Biomed Rep. 2022;18:8. https://doi.org/10.3892/br.2022.1590
6. Mancilla-Galindo J, Kammar-García A, Martínez-Esteban A, Meza-Comparán HD, Mancilla-Ramírez J, Galindo-Sevilla N. COVID-19 patients with increasing age experience differential time to initial medical care and severity of symptoms. Epidemiol Infect. 2021;149:e230. https://doi.org/10.1017/S095026882100234X
7. Romero Starke K, Reissig D, Petereit-Haack G, Schmauder S, Nienhaus A, Seidler A. The isolated effect of age on the risk of COVID-19 severe outcomes: a systematic review with meta-analysis. BMJ Glob Health. 2021;6:e006434. https://doi.org/10.1136/bmjgh-2021-006434
8. Moghadas SM, Vilches TN, Zhang K, Wells CR, Shoukat A, Singer BH, et al. The impact of vaccination on coronavirus disease 2019 (COVID-19) outbreaks in the United States. Clin Infect Dis. 2021;73:2257–64.
9. Buratto A, Muttoni M, Wrzaczek S, Freiberger M. Should the COVID-19 lockdown be relaxed or intensified in case a vaccine becomes available? PLoS One. 2022;17:e0273557. https://doi.org/10.1371/journal.pone.0273557
10. Kaye AD, Okeagu CN, Pham AD, Silva RA, Hurley JJ, Arron BL, et al. Economic impact of COVID-19 pandemic on healthcare facilities and systems: international perspectives. Best Pract Res Clin Anaesthesiol. 2021;35:293–306. https://doi.org/10.1016/j.bpa.2020.11.009
11. World Health Organization. Strategy to achieve global COVID-19 vaccination by mid-2022. 2021 Sep 15 [cited 2023 Jan 20]. https://www.who.int/publications/m/item/strategy-to-achieve-global-covid-19-vaccination-by-mid-2022
12. Walldorf JA, Date KA, Sreenivasan N, Harris JB, Hyde TB. Lessons learned from emergency response vaccination efforts for cholera, typhoid, yellow fever, and Ebola. Emerg Infect Dis. 2017;23:S210–6. https://doi.org/10.3201/eid2313.170550
13. World Health Organization. Uganda receives 864,000 doses of COVID-19 vaccines. 2021 Mar 6 [cited 2022 Jan 20]. https://www.afro.who.int/news/uganda-receives-864000-doses-covid-19-vaccines
14. Ministry of Health Uganda. COVID-19 vaccine deployment plan. Phase 1: vaccination of persons at the highest risk of COVID-19 infections, severe disease and death. 2021 [cited 2022 Dec 21]. https://www.health.go.ug/cause/update-on-covid-19-vaccination-in-uganda
15. Kirenga B, Muttamba W, Kayongo A, Nsereko C, Siddharthan T, Lusiba J, et al. Characteristics and outcomes of admitted patients infected with SARS-CoV-2 in Uganda. BMJ Open Respir Res. 2020;7:e000646. https://doi.org/10.1136/bmjresp-2020-000646
16. Ministry of Health Uganda. UNEPI COVID vaccination updates. 2021 [cited 2022 Dec 21]. https://www.health.go.ug/cause/update-on-covid-19-vaccination-in-uganda
17. Uganda National Immunization Technical Advisory Group. Accelerating COVID-19 vaccine uptake in Uganda: updated recommendation to the Ministry of Health, Uganda.

Uganda National Academy of Science. 2021 Dec 9 [cited 2024 Mar 19]. https://www.nitag-resource.org/resources/accelerating-covid-19-vaccine-uptake-uganda
18. World Health Organization. Behavioural and social drivers of vaccination: tools and practical guidance for achieving high uptake. 2022 [cited 2023 Jan 12]. https://iris.who.int/handle/10665/354459
19. World Health Organization. Coronavirus disease (COVID-19): vaccines. 2022 May 17 [cited 2023 Apr 6]. https://www.who.int/emergencies/diseases/novel-coronavirus-2019/covid-19-vaccines/explainers
20. Marquez C, Kerkhoff AD, Naso J, Contreras MG, Castellanos Diaz E, Rojas S, et al. A multi-component, community-based strategy to facilitate COVID-19 vaccine uptake among Latinx populations: from theory to practice. PLoS One. 2021;16:e0257111. https://doi.org/10.1371/journal.pone.0257111
21. World Health Organization. Monitoring COVID-19 vaccination. Considerations for the collection and use of vaccination data: interim guidance. 2021 [cited 2024 Mar 19]. https://www.who.int/publications/i/item/monitoring-covid-19-vaccination-interim-guidance
22. Zola Matuvanga T, Doshi RH, Muya A, Cikomola A, Milabyo A, Nasaka P, et al. Challenges to COVID-19 vaccine introduction in the Democratic Republic of the Congo—a commentary. Hum Vaccin Immunother. 2022;18:2127272. https://doi.org/10.1080/21645515.2022.2127272
23. Nzaji MK, Kamenga JDD, Lungayo CL, Bene ACM, Meyou SF, Kapit AM, et al. Factors associated with COVID-19 vaccine uptake and hesitancy among healthcare workers in the Democratic Republic of the Congo. PLOS Glob Public Health. 2024;4:e0002772. https://doi.org/10.1371/journal.pgph.0002772
24. Muhindo R, Okoboi S, Kiragga A, King R, Arinaitwe WJ, Castelnuovo B. COVID-19 vaccine acceptability, and uptake among people living with HIV in Uganda. PLoS One. 2022;17:e0278692. https://doi.org/10.1371/journal.pone.0278692
25. Kabir Sulaiman S, Sale Musa M, Isma'il Tsiga-Ahmed F, Muhammad Dayyab F, Kabir Sulaiman A, Dabo B, et al.; SQuAD-HIV collaborators. COVID-19 vaccine hesitancy among people living with HIV in a low-resource setting: a multi-center study of prevalence, correlates and reasons. Vaccine. 2023;41:2476–84. https://doi.org/10.1016/j.vaccine.2023.02.056
26. Folayan MO, Brown B, Haire B, Babalola CP, Ndembi N. Considerations for stakeholder engagement and COVID-19 related clinical trials' conduct in sub-Saharan Africa. Developing World Bioeth. 2021;21:44–50. https://doi.org/10.1111/dewb.12283
27. Rabin BA, Cain KL, Watson P Jr, Oswald W, Laurent LC, Meadows AR, et al. Scaling and sustaining COVID-19 vaccination through meaningful community engagement and care coordination for underserved communities: hybrid type 3 effectiveness-implementation sequential multiple assignment randomized trial. Implement Sci. 2023;18:28. https://doi.org/10.1186/s13012-023-01283-2
28. Hausenkamph DS. Community mobilisation: a strategy to rebuild trust and promote vaccine uptake in sub-Saharan Africa. Where trust in governments is low, community leaders and informal influencers can be effective messengers for accurate health information. 2021 [cited 2022 Mar 23]. https://www.u4.no/blog/community-mobilisation-to-rebuild-trust-promote-vaccine-uptake-africa
29. Sullivan W. Championing health workers to lead vaccination efforts in Uganda. 2023 [cited 2023 Apr 26]. https://news.mit.edu/2023/championing-health-workers-lead-vaccination-efforts-uganda-0420
30. Ndejjo R, Chen N, Kabwama SN, Namale A, Wafula ST, Wanyana I, et al. Uptake of COVID-19 vaccines and associated factors among adults in Uganda: a cross-sectional survey. BMJ Open. 2023;13:e067377. https://doi.org/10.1136/bmjopen-2022-067377
31. Brault MA, Vermund SH, Aliyu MH, Omer SB, Clark D, Spiegelman D. Leveraging HIV care infrastructures for integrated chronic disease and pandemic management in sub-Saharan Africa. Int J Environ Res Public Health. 2021;18:10751. https://doi.org/10.3390/ijerph182010751
32. Collins C, Isbell MT, Ratevosian J, Beyrer C, Abdool Karim Q, Maleche A, et al. Build on HIV investments for future pandemic preparedness. BMJ Glob Health. 2021;6:e007980. https://doi.org/10.1136/bmjgh-2021-007980
33. Collins C, Isbell MT, Karim QA, Sohn AH, Beyrer C, Maleche A. Leveraging the HIV response to strengthen pandemic preparedness. PLOS Glob Public Health. 2023; 3:e0001511. https://doi.org/10.1371/journal.pgph.0001511
34. King P, Wanyana MW, Migisha R, Kadobera D, Kwesiga B, Claire B, et al. COVID-19 vaccine uptake and coverage, Uganda, 2021–2022. Uganda National Institute of Public Health Quarterly Epidemiological Bulletin. 2023 [cited 2024 Mar 19]. https://uniph.go.ug/covid-19-vaccine-uptake-and-coverage-uganda-2021-2022

Address for correspondence: Daniel Kiiza, Infectious Diseases Institute, Makerere University, PO Box 22418, Kampala, Uganda; email: dkiiza@idi.co.ug

Highly Pathogenic Avian Influenza A(H5N1) Clade 2.3.4.4b Virus Infection in Domestic Dairy Cattle and Cats, United States, 2024

Eric R. Burrough, Drew R. Magstadt, Barbara Petersen, Simon J. Timmermans, Phillip C. Gauger, Jianqiang Zhang, Chris Siepker, Marta Mainenti, Ganwu Li, Alexis C. Thompson, Patrick J. Gorden, Paul J. Plummer, Rodger Main

We report highly pathogenic avian influenza A(H5N1) virus in dairy cattle and cats in Kansas and Texas, United States, which reflects the continued spread of clade 2.3.4.4b viruses that entered the country in late 2021. Infected cattle experienced nonspecific illness, reduced feed intake and rumination, and an abrupt drop in milk production, but fatal systemic influenza infection developed in domestic cats fed raw (unpasteurized) colostrum and milk from affected cows. Cow-to-cow transmission appears to have occurred because infections were observed in cattle on Michigan, Idaho, and Ohio farms where avian influenza virus–infected cows were transported. Although the US Food and Drug Administration has indicated the commercial milk supply remains safe, the detection of influenza virus in unpasteurized bovine milk is a concern because of potential cross-species transmission. Continued surveillance of highly pathogenic avian influenza viruses in domestic production animals is needed to prevent cross-species and mammal-to-mammal transmission.

Highly pathogenic avian influenza (HPAI) viruses pose a threat to wild birds and poultry globally, and HPAI H5N1 viruses are of even greater concern because of their frequent spillover into mammals. In late 2021, the Eurasian strain of H5N1 (clade 2.3.4.4b) was detected in North America (*1*,*2*) and initiated an outbreak that continued into 2024. Spillover detections and deaths from this clade have been reported in both terrestrial and marine mammals in the United States (*3*,*4*). The detection of HPAI H5N1 clade 2.3.4.4b virus in severe cases of human disease in Ecuador (*5*) and Chile (*6*) raises further concerns regarding the pandemic potential of specific HPAI viruses.

In February 2024, veterinarians were alerted to a syndrome occurring in lactating dairy cattle in the panhandle region of northern Texas. Nonspecific illness accompanied by reduced feed intake and rumination and an abrupt drop in milk production developed in affected animals. The milk from most affected cows had a thickened, creamy yellow appearance similar to colostrum. On affected farms, incidence appeared to peak 4–6 days after the first animals were affected and then tapered off within 10–14 days; afterward, most animals were slowly returned to regular milking. Clinical signs were commonly reported in multiparous cows during middle to late lactation; ≈10%–15% illness and minimal death of cattle were observed on affected farms. Initial submissions of blood, urine, feces, milk, and nasal swab samples and postmortem tissues to regional diagnostic laboratories did not reveal a consistent, specific cause for reduced milk production. Milk cultures were often negative, and serum chemistry testing showed mildly increased aspartate aminotransferase, gamma-glutamyl transferase, creatinine kinase, and bilirubin values, whereas complete blood counts showed variable anemia and leukocytopenia.

In early March 2024, similar clinical cases were reported in dairy cattle in southwestern Kansas and northeastern New Mexico; deaths of wild birds and

Author affiliations: Iowa State University College of Veterinary Medicine, Ames, Iowa, USA (E.R. Burrough, D.R. Magstadt, P.C. Gauger, J. Zhang, C. Siepker, M. Mainenti, G. Li, P.J. Gorden, P.J. Plummer, R. Main); Sunrise Veterinary Service PLLC, Amarillo, Texas, USA (B. Petersen); Veterinary Research & Consulting Services LLC, Hays, Kansas, USA (S.J. Timmermans); Texas A&M Veterinary Medical Diagnostic Laboratory, College Station, Texas, USA (A.C. Thompson)

DOI: https://doi.org/10.3201/eid3007.240508

domestic cats were also observed within affected sites in the Texas panhandle. In ≥1 dairy farms in Texas, deaths occurred in domestic cats fed raw colostrum and milk from sick cows that were in the hospital parlor. Antemortem clinical signs in affected cats were depressed mental state, stiff body movements, ataxia, blindness, circling, and copious oculonasal discharge. Neurologic exams of affected cats revealed the absence of menace reflexes and pupillary light responses with a weak blink response.

On March 21, 2024, milk, serum, and fresh and fixed tissue samples from cattle located in affected dairies in Texas and 2 deceased cats from an affected Texas dairy farm were received at the Iowa State University Veterinary Diagnostic Laboratory (ISUVDL; Ames, IA, USA). The next day, similar sets of samples were received from cattle located in affected dairies in Kansas. Milk and tissue samples from cattle and tissue samples from the cats tested positive for influenza A virus (IAV) by screening PCR, which was confirmed and characterized as HPAI H5N1 virus by the US Department of Agriculture National Veterinary Services Laboratory. Detection led to an initial press release by the US Department of Agriculture Animal and Plant Health Inspection Service on March 25, 2024, confirming HPAI virus in dairy cattle (*7*). We report the characterizations performed at the ISUVDL for HPAI H5N1 viruses infecting cattle and cats in Kansas and Texas.

Materials and Methods

Milk samples (cases 2–5) and fresh and formalin-fixed tissues (cases 1, 3–5) from dairy cattle were received at the ISUVDL from Texas on March 21 and from Kansas on March 22, 2024. The cattle exhibited nonspecific illness and reduced lactation, as described previously. The tissue samples for diagnostic testing came from 3 cows that were euthanized and 3 that died naturally; all postmortem examinations were performed on the premises of affected farms.

The bodies of 2 adult domestic shorthaired cats from a north Texas dairy farm were received at the ISUVDL for a complete postmortem examination on March 21, 2024. The cats were found dead with no apparent signs of injury and were from a resident population of ≈24 domestic cats that had been fed milk from sick cows. Clinical disease in cows on that farm was first noted on March 16; the cats became sick on March 17, and several cats died in a cluster during March 19–20. In total, >50% of the cats at that dairy became ill and died. We collected cerebrum, cerebellum, eye, lung, heart, spleen, liver, lymph node, and kidney tissue samples from the cats and placed them in 10% neutral-buffered formalin for histopathology.

At ISUVDL, we trimmed, embedded in paraffin, and processed formalin-fixed tissues from affected cattle and cats for hematoxylin/eosin staining and histologic evaluation. For immunohistochemistry (IHC), we prepared 4-μm–thick sections from paraffin-embedded tissues, placed them on Superfrost Plus slides (VWR, https://www.vwr.com), and dried them for 20 minutes at 60°C. We used a Ventana Discovery Ultra IHC/ISH research platform (Roche, https://www.roche.com) for deparaffinization until and including counterstaining. We obtained all products except the primary antibody from Roche. Automated deparaffination was followed by enzymatic digestion with protease 1 for 8 minutes at 37°C and endogenous peroxidase blocking. We obtained the primary influenza A virus antibody from the hybridoma cell line H16-L10–4R5 (ATCC, https://www.atcc.org) and diluted at 1:100 in Discovery PSS diluent; we incubated sections with antibody for 32 minutes at room temperature. Next, we incubated the sections with a hapten-labeled conjugate, Discovery anti-mouse HQ, for 16 minutes at 37°C followed by a 16-minute incubation with the horseradish peroxidase conjugate, Discovery anti-HQ HRP. We used a ChromoMap DAB kit for antigen visualization, followed by counterstaining with hematoxylin and then bluing. Positive controls were sections of IAV-positive swine lung. Negative controls were sections of brain, lung, and eyes from cats not infected with IAV.

We diluted milk samples 1:3 vol/vol in phosphate buffered saline, pH 7.4 (Gibco/Thermo Fisher Scientific, https://www.thermofisher.com) by mixing 1 unit volume of milk and 3 unit volumes of phosphate buffered saline. We prepared 10% homogenates of mammary glands, brains, lungs, spleens, and lymph nodes in Earle's balanced salt solution (Sigma-Aldrich, https://www.sigmaaldrich.com). Processing was not necessary for ocular fluid, rumen content, or serum samples. After processing, we extracted samples according to a National Animal Health Laboratory Network (NAHLN) protocol that had 2 NAHLN-approved deviations for ISUVDL consisting of the MagMax Viral RNA Isolation Kit for 100 μL sample volumes and a Kingfisher Flex instrument (both Thermo Fisher Scientific).

We performed real-time reverse transcription PCR (rRT-PCR) by using an NAHLN-approved assay with 1 deviation, which was the VetMAX-Gold SIV Detection kit (Thermo Fisher Scientific), to screen for the presence of IAV RNA. We tested samples along with the VetMAX XENO Internal Positive Control to

monitor the possible presence of PCR inhibitors. Each rRT-PCR 96-well plate had 2 positive amplification controls, 2 negative amplification controls, 1 positive extraction control, and 1 negative extraction control. We ran the rRT-PCR on an ABI 7500 Fast thermocycler and analyzed data with Design and Analysis Software 2.7.0 (both Thermo Fisher Scientific). We considered samples with cycle threshold (Ct) values <40.0 to be positive for virus.

After the screening rRT-PCR, we analyzed IAV RNA–positive samples for the H5 subtype and H5 clade 2.3.4.4b by using the same RNA extraction and NAHLN-approved rRT-PCR protocols as described previously, according to standard operating procedures. We performed PCR on the ABI 7500 Fast thermocycler by using appropriate controls to detect H5-specific IAV. We considered samples with Ct values <40.0 to be positive for the IAV H5 subtype.

We conducted genomic sequencing of 2 milk samples from infected dairy cattle from Texas and 2 tissue samples (lung and brain) from cats that died at a different Texas dairy. We subjected the whole-genome sequencing data to bioinformatics analysis to assemble the 8 different IAV segment sequences according to previously described methods (*8*). We used the hemagglutinin (HA) and neuraminidase (NA) sequences for phylogenetic analysis. We obtained reference sequences for the HA and NA segments of IAV H5 clade 2.3.4.4 from publicly available databases, including GISAID (https://www.gisaid.org) and GenBank. We aligned the sequences by using MAFFT version 7.520 software (https://mafft.cbrc.jp/alignment/server/index.html) to create multiple sequence alignments for subsequent phylogenetic analysis. We used IQTree2 (https://github.com/iqtree/iqtree2) to construct the phylogenetic tree from the aligned sequences. The software was configured to automatically identify the optimal substitution model by using the ModelFinder Plus option, ensuring the selection of the most suitable model for the dataset and, thereby, improving the accuracy of the reconstructed tree. We visualized the resulting phylogenetic tree by using iTOL (https://itol.embl.de), a web-based platform for interactive tree exploration and annotation.

Results

Gross Lesions in Cows and Cats

All cows were in good body condition with adequate rumen fill and no external indications of disease. Postmortem examinations of the affected dairy cows revealed firm mammary glands typical of mastitis; however, mammary gland lesions were not consistent. Two cows that were acutely ill before postmortem examination had grossly normal milk and no abnormal mammary gland lesions. The gastrointestinal tract of some cows had small abomasal ulcers and shallow linear erosions of the intestines, but those observations were also not consistent in all animals. The colon contents were brown and sticky, suggesting moderate dehydration. The feces contained feed particles that appeared to have undergone minimal ruminal fermentation. The rumen contents had normal color and appearance but appeared to have undergone minimal fermentation.

The 2 adult cats (1 intact male, 1 intact female) received at the ISUVDL were in adequate body and postmortem condition. External examination was unremarkable. Mild hemorrhages were observed in the subcutaneous tissues over the dorsal skull, and multifocal meningeal hemorrhages were observed in the cerebrums of both cats. The gastrointestinal tracts were empty, and no other gross lesions were observed.

Microscopic Lesions in Cows and Cats

The chief microscopic lesion observed in affected cows was moderate acute multifocal neutrophilic mastitis (Figure 1); however, mammary glands were not received from every cow. Three cows had mild neutrophilic or lymphocytic hepatitis. Because they were adult cattle, other observed microscopic lesions (e.g., mild lymphoplasmacytic interstitial nephritis and mild to moderate lymphocytic abomasitis) were presumed to be nonspecific, age-related changes. We did not observe major lesions in the other evaluated tissues. We performed IHC for IAV antigen on all evaluated tissues; the only tissues with positive immunoreactivity were mastitic mammary glands from 2 cows that showed nuclear and cytoplasmic labeling of alveolar epithelial cells and cells within lumina (Figure 1) and multifocal germinal centers within a lymph node from 1 cow (Table 1).

Both cats had microscopic lesions consistent with severe systemic virus infection, including severe subacute multifocal necrotizing and lymphocytic meningoencephalitis with vasculitis and neuronal necrosis, moderate subacute multifocal necrotizing and lymphocytic interstitial pneumonia, moderate to severe subacute multifocal necrotizing and lymphohistiocytic myocarditis, and moderate subacute multifocal lymphoplasmacytic chorioretinitis with ganglion cell necrosis and attenuation of the internal plexiform and nuclear layers (Table 2; Figure 2). We performed IHC for IAV antigen on multiple tissues (brain, eye, lung, heart, spleen, liver, and kidney). We detected positive IAV immunoreactivity in brain (intracytoplasmic,

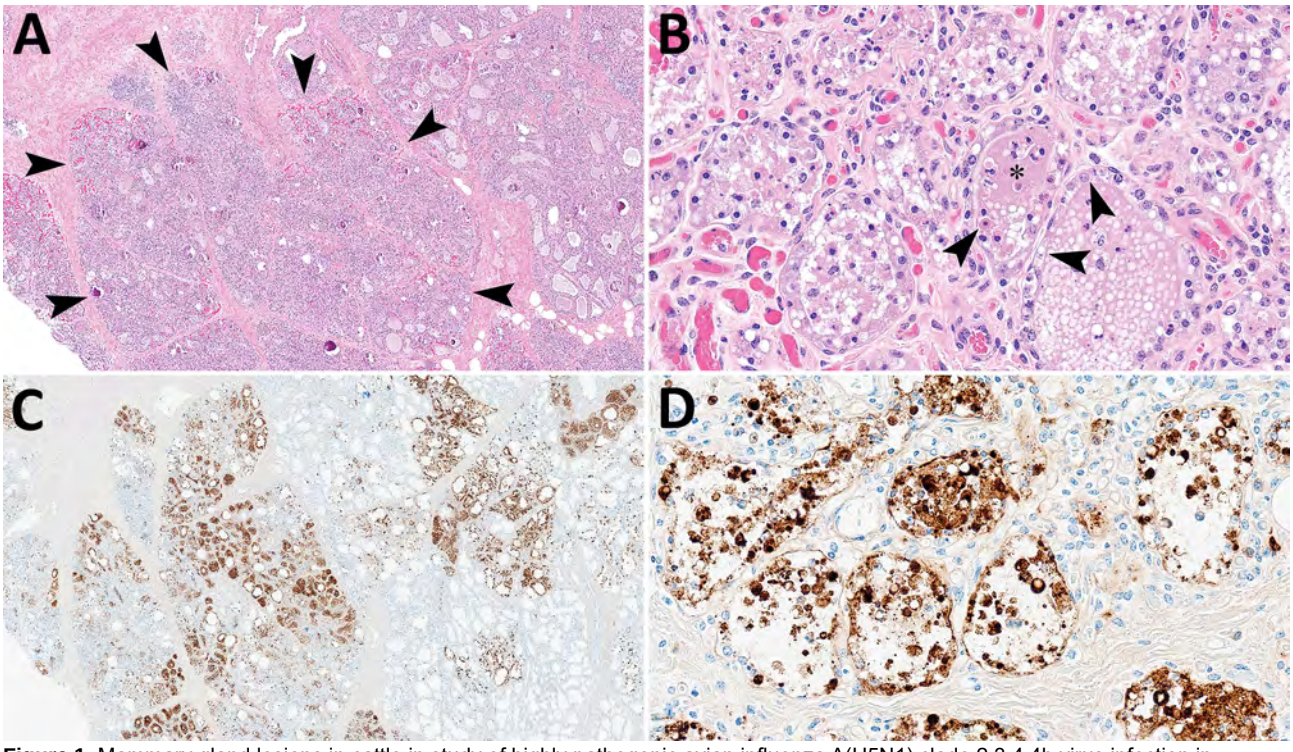

Figure 1. Mammary gland lesions in cattle in study of highly pathogenic avian influenza A(H5N1) clade 2.3.4.4b virus infection in domestic dairy cattle and cats, United States, 2024. A, B) Mammary gland tissue sections stained with hematoxylin and eosin. A) Arrowheads indicate segmental loss within open secretory mammary alveoli. Original magnification ×40. B) Arrowheads indicate epithelial degeneration and necrosis lining alveoli with intraluminal sloughing. Asterisk indicates intraluminal neutrophilic inflammation. Original magnification ×400. C, D) Mammary gland tissue sections stained by using avian influenza A immunohistochemistry. C) Brown staining indicates lobular distribution of avian influenza A virus. Original magnification ×40. D) Brown staining indicates strong nuclear and intracytoplasmic immunoreactivity of intact and sloughed epithelial cells within mammary alveoli. Original magnification ×400.

intranuclear, and axonal immunolabeling of neurons), lung, and heart, and multifocal and segmental immunoreactivity within all layers of the retina (Figure 2).

PCR Data from Cows and Cats

We tested various samples from 8 clinically affected mature dairy cows by IAV screening and H5 subtype-specific PCR (Table 3). Milk and mammary gland homogenates consistently showed low Ct values: 12.3–16.9 by IAV screening PCR, 17.6–23.1 by H5 subtype PCR, and 14.7–20.0 by H5 2.3.4.4 clade PCR (case 1, cow 1; case 2, cows 1 and 2; case 3, cow 1; and case 4, cow 1). We forwarded the samples to the National Veterinary Services Laboratory, which confirmed the virus was an HPAI H5N1 virus strain.

When they were available, we also tested tissue homogenates (e.g., lung, spleen, and lymph nodes), ocular fluid, and rumen contents from 6 cows by IAV and H5 subtype-specific PCR (Table 3). However, the PCR findings were not consistent. For example, the tissue homogenates and ocular fluid tested positive in some but not all cows. In case 5, cow 1, the milk sample tested negative by IAV screening PCR, but the spleen homogenate tested positive by IAV screening, H5 subtype, and H5 2.3.4.4 PCR. For 2 cows (case 3,

Table 1. Microscopic lesions observed in cattle in study of highly pathogenic avian influenza A(H5N1) clade 2.3.4.4b virus infection in domestic dairy cattle and cats, United States, 2024*

Case no.	Animal	US state	Suppurative mastitis	Hepatitis	Abomasitis	IAV-positive tissue†
1	Cow 1	Texas	++	+	+	Mammary gland
1	Cow 2	Texas	++	+	++	Mammary gland
3	Cow 1	Kansas	NA	+	+	NA
3	Cow 2	Kansas	NA	–	+	NA
4	Cow 1	Kansas	NA	–	NA	Lymph node
5	Cow 1	Kansas	NA	–	–	NA

*Avian influenza A(H5N1) virus was detected by using real-time reverse transcription PCR. IAV, influenza A virus; NA, not available; –, negative; +, scant lesions; ++, moderate lesions.
†Determined by immunohistochemistry.

Table 2. Microscopic lesions observed in cats in study of highly pathogenic avian influenza A(H5N1) clade 2.3.4.4b virus infection in domestic dairy cattle and cats, United States, 2024*

Case no.	Animal	US state	Encephalitis	Retinitis	Interstitial pneumonia	Necrotizing myocarditis	Vacuolar hepatopathy	IAV-positive tissues†
6	Cat 1	Texas	+++	–	++	++	+	Brain, lung, heart
6	Cat 2	Texas	+++	++	++	++	+	Brain, lung, heart

*Avian influenza A(H5N1) virus was detected by using real-time reverse transcription PCR. IAV, influenza A virus; –, negative; +, scant lesions; ++, moderate lesions; +++, severe lesions.
†Determined by immunohistochemistry.

cow 1; and case 4, cow 1) that had both milk and rumen contents available, both samples tested positive for IAV. Nevertheless, all IAV-positive nonmammary gland tissue homogenates, ocular fluid, and rumen contents had markedly elevated Ct values in contrast to the low Ct values for milk and mammary gland homogenate samples.

We tested brain and lung samples from the 2 cats (case 6, cats 1 and 2) by IAV screening and H5 subtype-specific PCR (Table 3). Both sample types were positive by IAV screening PCR; Ct values were 9.9–13.5 for brain and 17.4–24.4 for lung samples, indicating high amounts of virus nucleic acid in those samples. The H5 subtype and H5 2.3.4.4 PCR results were also positive for the brain and lung samples; Ct values were consistent with the IAV screening PCR (Table 3).

Phylogenetic Analyses

We assembled the sequences of all 8 segments of the HPAI viruses from both cow milk and cat tissue samples. We used the hemagglutinin (HA) and neuraminidase (NA) sequences specifically for phylogenetic analysis to delineate the clade of the HA gene and subtype of the NA gene.

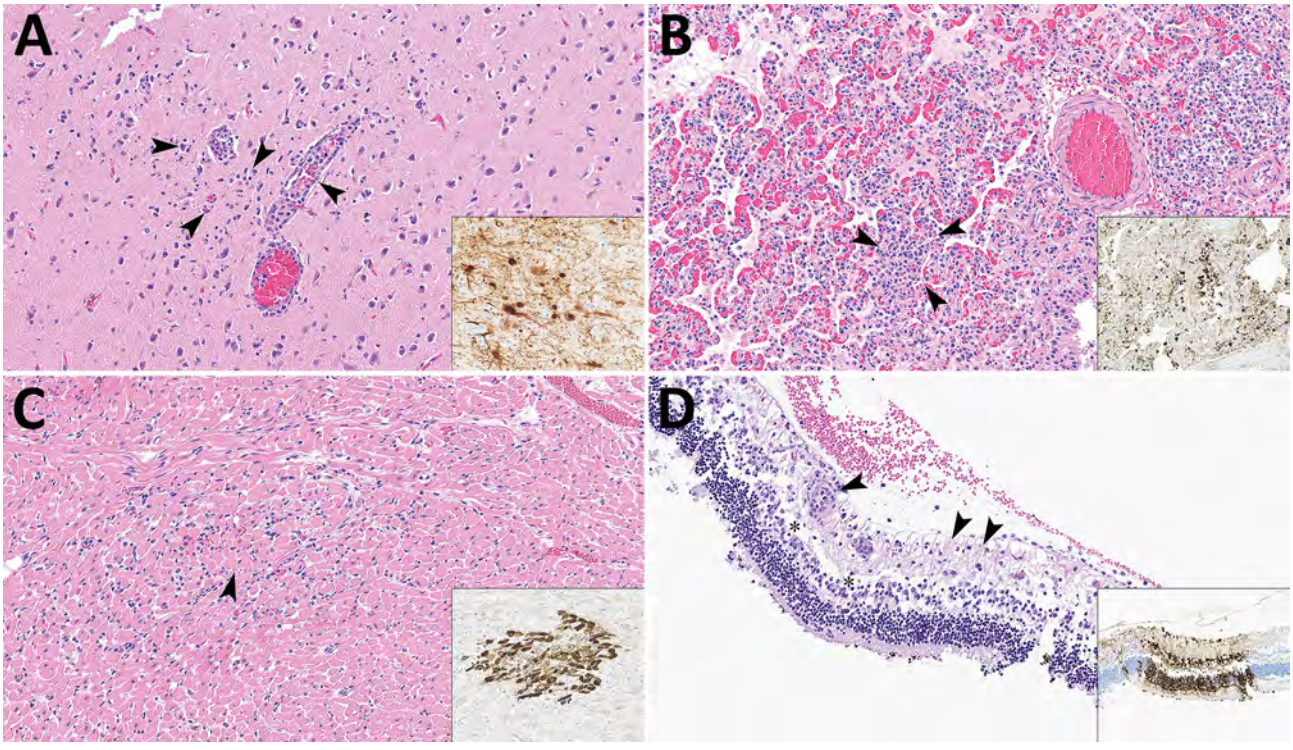

Figure 2. Lesions in cat tissues in study of highly pathogenic avian influenza A(H5N1) clade 2.3.4.4b virus infection in domestic dairy cattle and cats, United States, 2024. Tissue sections were stained with hematoxylin and eosin; insets show brown staining of avian influenza A viruses via immunohistochemistry by using the chromogen 3,3′-diaminobenzidine tetrahydrochloride. Original magnification ×200 for all images and insets. A) Section from cerebral tissue. Arrowheads show perivascular lymphocytic encephalitis, gliosis, and neuronal necrosis. Inset shows neurons. B) Section of lung tissue showing lymphocytic and fibrinous interstitial pneumonia with septal necrosis and alveolar edema; arrowheads indicate lymphocytes. Inset shows bronchiolar epithelium, necrotic cells, and intraseptal mononuclear cells. C) Section of heart tissue. Arrowhead shows interstitial lymphocytic myocarditis and focal peracute myocardial coagulative necrosis. Inset shows cardiomyocytes. D) Section of retinal tissue. Arrowheads show perivascular lymphocytic retinitis with segmental neuronal loss and rarefaction in the ganglion cell layer. Asterisks indicate attenuation of the inner plexiform and nuclear layers with artifactual retinal detachment. Insets shows all layers of the retina segmentally within affected areas have strong cytoplasmic and nuclear immunoreactivity to influenza A virus.

For HA gene analysis, both HA sequences derived from cow milk samples exhibited a high degree of similarity, sharing 99.88% nucleotide identity, whereas the 2 HA sequences from cat tissue samples showed complete identity at 100%. The HA sequences from the milk samples had 99.94% nucleotide identities with HA sequences from the cat tissues, resulting in a distinct subcluster comprising all 4 HA sequences, which clustered together with other H5N1 viruses belonging to clade 2.3.4.4b (Figure 3, https://wwwnc.cdc.gov/EID/article/30/7/24-0508-F3.htm). The HA sequences were deposited in GenBank (accession nos. PP599465 [case 2, cow 1], PP599473 [case 2, cow 2], PP692142 [case 6, cat 1], and PP692195 [case 6, cat 2]).

For NA gene analysis, the 2 NA sequences obtained from cow milk samples showed 99.93% nucleotide identity. Moreover, the NA sequences derived from the milk samples exhibited complete nucleotide identities (100%) with those from the cat tissues. The 4 NA sequences were grouped within the N1 subtype of HPAI viruses (Figure 4, https://wwwnc.cdc.gov/EID/article/30/7/24-0508-F4.htm). The NA sequences were deposited in GenBank (accession nos. PP599467 [case 2, cow 1], PP599475 [case 2, cow 2], PP692144 [case 6, cat 1], and PP692197 [case 6, cat 2]).

Discussion

This case series differs from most previous reports of IAV infection in bovids, which indicated cattle were inapparently infected or resistant to infection (*9*). We describe an H5N1 strain of IAV in dairy cattle that resulted in apparent systemic illness, reduced milk production, and abundant virus shedding in milk. The magnitude of this finding is further emphasized by the high death rate (≈50%) of cats on farm premises that were fed raw colostrum and milk from affected cows; clinical disease and lesions developed that were consistent with previous reports of H5N1 infection in cats presumably derived from consuming infected wild birds (*10*–*12*). Although exposure to and consumption of dead wild birds cannot be completely ruled out for the cats described in this report, the known consumption of unpasteurized milk and colostrum from infected cows and the high amount of virus nucleic acid within the milk make milk and colostrum consumption a likely route of exposure. Therefore, our findings

Table 3. PCR results from various specimens in study of highly pathogenic avian influenza A(H5N1) clade 2.3.4.4b virus infection in domestic dairy cattle and cats, United States, 2024*

				Ct values for IAV PCR							
Case no.	Animal	State	IAV PCR test	Milk	Mammary gland	Brain	Lung	Spleen	Lymph node	Ocular fluid	Rumen contents
1	Cow 1	Texas	IAV screen	NA	16.2	NA	≥40	NA	NA	NA	NA
			H5 subtype		17.9		NA				
			H5 2.3.4.4		17.8		NA				
1	Cow 2	Texas	IAV screen	NA	NA	NA	32.6	NA	NA	NA	NA
			H5 subtype				36.0				
			H5 2.3.4.4				34.8				
2	Cow 1	Texas	IAV screen	12.3	NA	NA	NA	NA	NA	NA	NA
			H5 subtype	18.8							
			H5 2.3.4.4	14.7							
2	Cow 2	Texas	IAV screen	13.1	NA	NA	NA	NA	NA	NA	NA
			H5 subtype	17.6							
			H5 2.3.4.4	15.1							
3	Cow 1	Kansas	IAV screen	15.2	NA	NA	≥40	≥40	≥40	29.0	31.0
			H5 subtype	19.5			NA	NA	NA	31.2	32.7
			H5 2.3.4.4	17.1			NA	NA	NA	30.9	32.2
3	Cow 2	Kansas	IAV screen	NA	NA	NA	≥40	≥40	NA	≥40	≥40
			H5 subtype				NA	NA		NA	NA
			H5 2.3.4.4				NA	NA		NA	NA
4	Cow 1	Kansas	IAV screen	16.9	NA	NA	33.0	≥40	31.2	≥40	29.4
			H5 subtype	23.1			≥40	NA	38.0	NA	32.4
			H5 2.3.4.4	20.0			≥40	NA	33.9	NA	31.1
5	Cow 1	Kansas	IAV screen	≥40	NA	NA	34.1	29.8	NA	NA	NA
			H5 subtype	NA			37.8	36.1			
			H5 2.3.4.4	NA			37.3	33.9			
6	Cat 1	Texas	IAV screen	NA	NA	9.9	17.4	NA	NA	NA	NA
			H5 subtype			10.7	16.5				
			H5 2.3.4.4			11.9	18.0				
6	Cat 2	Texas	IAV screen	NA	NA	13.5	24.4	NA	NA	NA	NA
			H5 subtype			14.0	23.8				
			H5 2.3.4.4			15.2	24.8				

*Ct values were obtained by using real-time reverse transcription PCR tests for influenza A viruses, the H5 subtype, and H5 clade 2.3.4.4 viruses. Ct, cycle threshold; H5, hemagglutinin 5; IAV, influenza A virus; NA, not available.

suggest cross-species mammal-to-mammal transmission of HPAI H5N1 virus and raise new concerns regarding the potential for virus spread within mammal populations. Horizontal transmission of HPAI H5N1 virus has been previously demonstrated in experimentally infected cats (*13*) and ferrets (*14*) and is suspected to account for large dieoffs observed during natural outbreaks in mink (*15*) and sea lions (*16*). Future experimental studies of HPAI H5N1 virus in dairy cattle should seek to confirm cross-species transmission to cats and potentially other mammals.

Clinical IAV infection in cattle has been infrequently reported in the published literature. The first report occurred in Japan in 1949, where a short course of disease with pyrexia, anorexia, nasal discharge, pneumonia, and decreased lactation developed in cattle (*17*). In 1997, a similar condition occurred in dairy cows in southwest England leading to a sporadic drop in milk production (*18*), and IAV seroconversion was later associated with reduced milk yield and respiratory disease (*19*–*21*). Rising antibody titers against human-origin influenza A viruses (H1N1 and H3N2) were later again reported in dairy cattle in England, which led to an acute fall in milk production during October 2005–March 2006 (*22*). Limited reports of IAV isolation from cattle exist; most reports occurred during the 1960s and 1970s in Hungary and in the former Soviet Union, where H3N2 was recovered from cattle experiencing respiratory disease (*9*,*23*). Direct detection of IAV in milk and the potential transmission from cattle to cats through feeding of unpasteurized milk has not been previously reported.

An IAV-associated drop in milk production in dairy cattle appears to have occurred during ≥4 distinct periods and within 3 widely separated geographic areas: 1949 in Japan (*17*), 1997–1998 and 2005–2006 in Europe (*19*,*21*), and 2024 in the United States (this report). The sporadic occurrence of clinical disease in dairy cattle worldwide might be the result of changes in subclinical infection rates and the presence or absence of sufficient baseline IAV antibodies in cattle to prevent infection. Milk IgG, lactoferrin, and conglutinin have also been suggested as host factors that might reduce susceptibility of bovids to IAV infection (*9*). Contemporary estimates of the seroprevalence of IAV antibodies in US cattle are not well described in the published literature. One retrospective serologic survey in the United States in the late 1990s showed 27% of serum samples had positive antibody titers and 31% had low-positive titers for IAV H1 subtype-specific antigen in cattle with no evidence of clinical infections (*24*). Antibody titers for H5 subtype-specific antigen have not been reported in US cattle.

The susceptibility of domestic cats to HPAI H5N1 is well-documented globally (*10*–*12*,*25*–*28*), and infection often results in neurologic signs in affected felids and other terrestrial mammals (*4*). Most cases in cats result from consuming infected wild birds or contaminated poultry products (*12*,*27*). The incubation period in cats is short; clinical disease is often observed 2–3 days after infection (*28*). Brain tissue has been suggested as the best diagnostic sample to confirm HPAI virus infection in cats (*10*), and our results support that finding. One unique finding in the cats from this report is the presence of blindness and microscopic lesions of chorioretinitis. Those results suggest that further investigation into potential ocular manifestations of HPAI H5N1 virus infection in cats might be warranted.

The genomic sequencing and subsequent analysis of clinical samples from both bovine and feline sources provided considerable insights. The HA and NA sequences derived from both bovine milk and cat tissue samples from different Texas farms had a notable degree of similarity. Those findings strongly suggest a shared origin for the viruses detected in the dairy cattle and cat tissues. Further research, case series investigations, and surveillance data are needed to better understand and inform measures to curtail the clinical effects, shedding, and spread of HPAI viruses among mammals. Although pasteurization of commercial milk mitigates risks for transmission to humans, a 2019 US consumer study showed that 4.4% of adults consumed raw milk ≥1 time during the previous year (*29*), indicating a need for public awareness of the potential presence of HPAI H5N1 viruses in raw milk.

Ingestion of feed contaminated with feces from wild birds infected with HPAI virus is presumed to be the most likely initial source of infection in the dairy farms. Although the exact source of the virus is unknown, migratory birds (Anseriformes and Charadriiformes) are likely sources because the Texas panhandle region lies in the Central Flyway, and those birds are the main natural reservoir for avian influenza viruses (*30*). HPAI H5N1 viruses are well adapted to domestic ducks and geese, and ducks appear to be a major reservoir (*31*); however, terns have also emerged as an important source of virus spread (*32*). The mode of transmission among infected cattle is also unknown; however, horizontal transmission has been suggested because disease developed in resident cattle herds in Michigan, Idaho, and Ohio farms that received infected cattle from the affected regions, and those cattle tested positive for HPAI H5N1 (*33*). Experimental studies are needed to decipher the transmission routes and

pathogenesis (e.g., replication sites and movement) of the virus within infected cattle.

In conclusion, we showed that dairy cattle are susceptible to infection with HPAI H5N1 virus and can shed virus in milk and, therefore, might potentially transmit infection to other mammals via unpasteurized milk. A reduction in milk production and vague systemic illness were the most commonly reported clinical signs in affected cows, but neurologic signs and death rapidly developed in affected domestic cats. HPAI virus infection should be considered in dairy cattle when an unexpected and unexplained abrupt drop in feed intake and milk production occurs and for cats when rapid onset of neurologic signs and blindness develop. The recurring nature of global HPAI H5N1 virus outbreaks and detection of spillover events in a broad host range is concerning and suggests increasing virus adaptation in mammals. Surveillance of HPAI viruses in domestic production animals, including cattle, is needed to elucidate influenza virus evolution and ecology and prevent cross-species transmission.

Acknowledgments

We thank the faculty and staff at the ISUVDL who contributed to the processing and analysis of clinical samples in this investigation, the veterinarians involved with clinical assessments at affected dairies and various conference calls in the days before diagnostic submissions that ultimately led to the detection of HPAI virus in the cattle, and the US Department of Agriculture National Veterinary Services Laboratory and NAHLN for their roles and assistance in providing their expertise, confirmatory diagnostic support, and communications surrounding the HPAI virus cases impacting lactating dairy cattle.

About the Author

Dr. Burrough is a professor and diagnostic pathologist at the Iowa State University College of Veterinary Medicine and Veterinary Diagnostic Laboratory. His research focuses on infectious diseases of livestock with an emphasis on swine.

References

1. Caliendo V, Lewis NS, Pohlmann A, Baillie SR, Banyard AC, Beer M, et al. Transatlantic spread of highly pathogenic avian influenza H5N1 by wild birds from Europe to North America in 2021. Sci Rep. 2022;12:11729. https://doi.org/10.1038/s41598-022-13447-z
2. Bevins SN, Shriner SA, Cumbee JC Jr, Dilione KE, Douglass KE, Ellis JW, et al. Intercontinental movement of highly pathogenic avian influenza A(H5N1) clade 2.3.4.4 virus to the United States, 2021. Emerg Infect Dis. 2022;28:1006–11. https://doi.org/10.3201/eid2805.220318
3. Puryear W, Sawatzki K, Hill N, Foss A, Stone JJ, Doughty L, et al. Highly pathogenic avian influenza A(H5N1) virus outbreak in New England seals, United States. Emerg Infect Dis. 2023;29:786–91. https://doi.org/10.3201/eid2904.221538
4. Elsmo EJ, Wünschmann A, Beckmen KB, Broughton-Neiswanger LE, Buckles EL, Ellis J, et al. Highly pathogenic avian influenza A(H5N1) virus clade 2.3.4.4b infections in wild terrestrial mammals, United States, 2022. Emerg Infect Dis. 2023;29:2451–60. https://doi.org/10.3201/eid2912.230464
5. Bruno A, Alfaro-Núñez A, de Mora D, Armas R, Olmedo M, Garcés J, et al. First case of human infection with highly pathogenic H5 avian influenza A virus in South America: a new zoonotic pandemic threat for 2023? J Travel Med. 2023;30:taad032. https://doi.org/10.1093/jtm/taad032
6. Pulit-Penaloza JA, Brock N, Belser JA, Sun X, Pappas C, Kieran TJ, et al. Highly pathogenic avian influenza A(H5N1) virus of clade 2.3.4.4b isolated from a human case in Chile causes fatal disease and transmits between co-housed ferrets. Emerg Microbes Infect. 2024 Mar 17 [Epub ahead of print]. https://doi.org/10.1080/22221751.2024.2332667
7. United States Department of Agriculture Animal and Plant Health Inspection Service. Federal and state veterinary, public health agencies share update on HPAI detection in Kansas, Texas dairy herds. 2024 [cited 2024 Mar 29]. https://www.aphis.usda.gov/news/agency-announcements/federal-state-veterinary-public-health-agencies-share-update-hpai
8. Sharma A, Zeller MA, Souza CK, Anderson TK, Vincent AL, Harmon K, et al. Characterization of a 2016–2017 human seasonal H3 influenza A virus spillover now endemic to U.S. swine. mSphere. 2022;7:e0080921. https://doi.org/10.1128/msphere.00809-21
9. Sreenivasan CC, Thomas M, Kaushik RS, Wang D, Li F. Influenza A in bovine species: a narrative literature review. Viruses. 2019;11:561. https://doi.org/10.3390/v11060561
10. Sillman SJ, Drozd M, Loy D, Harris SP. Naturally occurring highly pathogenic avian influenza virus H5N1 clade 2.3.4.4b infection in three domestic cats in North America during 2023. J Comp Pathol. 2023;205:17–23. https://doi.org/10.1016/j.jcpa.2023.07.001
11. Klopfleisch R, Wolf PU, Uhl W, Gerst S, Harder T, Starick E, et al. Distribution of lesions and antigen of highly pathogenic avian influenza virus A/Swan/Germany/R65/06 (H5N1) in domestic cats after presumptive infection by wild birds. Vet Pathol. 2007;44:261–8. https://doi.org/10.1354/vp.44-3-261
12. Keawcharoen J, Oraveerakul K, Kuiken T, Fouchier RAM, Amonsin A, Payungporn S, et al. Avian influenza H5N1 in tigers and leopards. Emerg Infect Dis. 2004;10:2189–91. https://doi.org/10.3201/eid1012.040759
13. Kuiken T, Rimmelzwaan G, van Riel D, van Amerongen G, Baars M, Fouchier R, et al. Avian H5N1 influenza in cats. Science. 2004;306:241. https://doi.org/10.1126/science.1102287
14. Herfst S, Schrauwen EJA, Linster M, Chutinimitkul S, de Wit E, Munster VJ, et al. Airborne transmission of influenza A/H5N1 virus between ferrets. Science. 2012;336:1534–41. https://doi.org/10.1126/science.1213362
15. Agüero M, Monne I, Sánchez A, Zecchin B, Fusaro A, Ruano MJ, et al. Highly pathogenic avian influenza A(H5N1) virus infection in farmed minks, Spain, October 2022. Euro Surveill. 2023;28:2300001. https://doi.org/10.2807/1560-7917.ES.2023.28.3.2300001
16. Leguia M, Garcia-Glaessner A, Muñoz-Saavedra B, Juarez D, Barrera P, Calvo-Mac C, et al. Highly pathogenic avian influenza A(H5N1) in marine mammals and seabirds in Peru. Nat Commun. 2023;14:5489. https://doi.org/10.1038/s41467-023-41182-0

17. Saito K. An outbreak of cattle influenza in Japan in the fall of 1949. J Am Vet Med Assoc. 1951;118:316–9.
18. Gunning RF, Pritchard GC. Unexplained sporadic milk drop in dairy cows. Vet Rec. 1997;140:488.
19. Brown IH, Crawshaw TR, Harris PA, Alexander DJ. Detection of antibodies to influenza A virus in cattle in association with respiratory disease and reduced milk yield. Vet Rec. 1998;143:637–8.
20. Crawshaw TR, Brown I. Bovine influenza. Vet Rec. 1998; 143:372.
21. Gunning RF, Brown IH, Crawshaw TR. Evidence of influenza A virus infection in dairy cows with sporadic milk drop syndrome. Vet Rec. 1999;145:556–7. https://doi.org/10.1136/vr.145.19.556
22. Crawshaw TR, Brown IH, Essen SC, Young SCL. Significant rising antibody titres to influenza A are associated with an acute reduction in milk yield in cattle. Vet J. 2008;178:98–102. https://doi.org/10.1016/j.tvjl.2007.07.022
23. Lopez JW, Woods GT. Influenza virus in ruminants: a review. Res Commun Chem Pathol Pharmacol. 1984;45:445–62.
24. Jones-Lang K, Ernst-Larson M, Lee B, Goyal SM, Bey R. Prevalence of influenza A virus (H1N1) antibodies in bovine sera. New Microbiol. 1998;21:153–60.
25. Briand FX, Souchaud F, Pierre I, Beven V, Hirchaud E, Hérault F, et al. Highly pathogenic avian influenza A(H5N1) clade 2.3.4.4b virus in domestic cat, France, 2022. Emerg Infect Dis. 2023;29:1696–8. https://doi.org/10.3201/eid2908.230188
26. Frymus T, Belák S, Egberink H, Hofmann-Lehmann R, Marsilio F, Addie DD, et al. Influenza virus infections in cats. Viruses. 2021;13:1435. https://doi.org/10.3390/v13081435
27. Songserm T, Amonsin A, Jam-on R, Sae-Heng N, Meemak N, Pariyothorn N, et al. Avian influenza H5N1 in naturally infected domestic cat. Emerg Infect Dis. 2006;12:681–3. https://doi.org/10.3201/eid1204.051396
28. Thiry E, Zicola A, Addie D, Egberink H, Hartmann K, Lutz H, et al. Highly pathogenic avian influenza H5N1 virus in cats and other carnivores. Vet Microbiol. 2007;122:25–31. https://doi.org/10.1016/j.vetmic.2006.12.021
29. Lando AM, Bazaco MC, Parker CC, Ferguson M. Characteristics of U.S. consumers reporting past year intake of raw (unpasteurized) milk: results from the 2016 Food Safety Survey and 2019 Food Safety and Nutrition Survey. J Food Prot. 2022;85:1036–43. https://doi.org/10.4315/JFP-21-407
30. Fourment M, Darling AE, Holmes EC. The impact of migratory flyways on the spread of avian influenza virus in North America. BMC Evol Biol. 2017;17:118. https://doi.org/10.1186/s12862-017-0965-4
31. Guan Y, Smith GJD. The emergence and diversification of panzootic H5N1 influenza viruses. Virus Res. 2013;178:35–43. https://doi.org/10.1016/j.virusres.2013.05.012
32. de Araújo AC, Silva LMN, Cho AY, Repenning M, Amgarten D, de Moraes AP, et al. Incursion of highly pathogenic avian influenza A(H5N1) clade 2.3.4.4b virus, Brazil, 2023. Emerg Infect Dis. 2024;30:619–21. https://doi.org/10.3201/eid3003.231157
33. American Veterinary Medical Association. States with HPAI-infected dairy cows grows to six. USDA provides guidance for veterinarians, producers on protecting cattle from the virus. 2024 [cited 2024 Apr 10]. https://www.avma.org/news/states-hpai-infected-dairy-cows-grows-six

Address for correspondence: Eric R. Burrough, Iowa State University Veterinary Diagnostic Laboratory, 1937 Christensen Dr, Ames, IA 50011, USA; email: burrough@iastate.edu

Newly Recognized Spotted Fever Group *Rickettsia* as Cause of Severe Rocky Mountain Spotted Fever–Like Illness, Northern California, USA

Will S. Probert, Monica P. Haw, Aran C. Nichol, Carol A. Glaser, Sarah Y. Park, Laura E. Campbell, Kavita K. Trivedi, Hannah Romo, Megan E.M. Saunders, Anne M. Kjemtrup, Kerry A. Padgett, Jill K. Hacker

The incidence of spotted fever group (SFG) rickettsioses in the United States has tripled since 2010. Rocky Mountain spotted fever, the most severe SFG rickettsiosis, is caused by *Rickettsia rickettsii*. The lack of species-specific confirmatory testing obfuscates the relative contribution of *R. rickettsii* and other SFG *Rickettsia* to this increase. We report a newly recognized rickettsial pathogen, *Rickettsia* sp. CA6269, as the cause of severe Rocky Mountain spotted fever–like illness in 2 case-patients residing in northern California. Multilocus sequence typing supported the recognition of this pathogen as a novel *Rickettsia* genotype most closely related to *R. rickettsii*. Cross-reactivity observed for an established molecular diagnostic test indicated that *Rickettsia* sp. CA6269 might be misidentified as *R. rickettsii*. We developed a *Rickettsia* sp. CA6269–specific real-time PCR to help resolve this diagnostic challenge and better characterize the spectrum of clinical disease and ecologic epidemiology of this pathogen.

Rickettsioses are undifferentiated febrile illnesses, often accompanied by myalgia and rash, that are caused by intracellular gram-negative bacteria of the genus *Rickettsia*. Spotted fever group (SFG) *Rickettsia* are transmitted through the bite of ticks or mites and are grouped together on the basis of antigenic and genetic similarities that distinguish this group from other *Rickettsia*, namely the typhus group. The incidence of SFG rickettsioses in the United States increased 3-fold from 2010 to 2018 (*1*). The SFG *Rickettsia* associated with human illness in the United States include the tickborne agents *R. rickettsii* (Rocky Mountain spotted fever [RMSF]), *R. parkeri* (*Rickettsia parkeri* rickettsiosis), and *Rickettsia* 364D (Pacific Coast tick fever [PCTF]) and the miteborne agent *R. akari* (rickettsialpox) (*1*,*2*). Among the SFG rickettsioses, RMSF is the most severe; its case-fatality rate is 5%–10% in the United States (*3*,*4*). Unfortunately, the relative contribution of *R. rickettsii* and other rickettsial agents to the increase in SFG rickettsioses is largely unknown because of the reliance on group-specific (SFG or typhus group) serologic testing and the lack of species-specific confirmatory testing (*1*,*5*).

In California, SFG rickettsioses are a reportable condition tracked for public health surveillance purposes. California has the lowest incidence of SFG rickettsioses among reporting states and averages only 11 probable and 1 confirmed SFG rickettsiosis cases annually (*1*,*6*,*7*). Only RMSF and PCTF are endemic to California (*7*). Ticks infected with *R. rickettsii* are extremely rare in California; only 1 infected *Dermacentor occidentalis* tick and 2 *Rhipicephalus sanguineus* ticks have been detected despite numerous environmental surveys (*7*). In contrast, *Rickettsia* 364D, a genetic near neighbor of *R. rickettsii*, is found in 2.1% of adult *D. occidentalis* ticks (*8*,*9*). PCTF was recognized in 2008 and is clinically less severe than RMSF (*10*). The presence of an inoculation eschar at the site of a tick bite and lack of a rash can be useful in differentiating PCTF from RMSF (*9*). Another genetic near neighbor of *R. rickettsii*, *Rickettsia* sp. CA6269, recently was reported

Author affiliations: California Department of Public Health, Richmond, California, USA (W.S. Probert, M.P. Haw, C.A. Glaser, H. Romo, M.E.M Saunders, K.A. Padgett, J.K. Hacker); Kaiser Permanente, Oakland, California, USA (A.C. Nichol); Karius, Redwood City, California, USA (S.Y. Park); Alameda County Public Health Department, San Leandro, California, USA (L.E. Campbell, K.K. Trivedi); California Department of Public Health, Sacramento, California, USA (A.M. Kjemtrup)

DOI: https://doi.org/10.3201/eid3007.231771

in rabbit ticks (*Haemaphysalis leporispalustris*) collected in Northern California (*11*). Multilocus sequence typing (MLST) of that strain revealed a novel genotype having sufficient sequence divergence from *R. rickettsii* to lead the investigators to propose a new species, *Candidatus* Rickettsia lanei. Here, we describe the clinical and epidemiologic features of severe RMSF-like illness in 2 patients in northern California who had disease onset dates separated by nearly 20 years and whose illness was caused by a newly identified SFG *Rickettsia*, *Rickettsia* sp. CA6269.

Materials And Methods

Clinical Specimens

Clinical specimens for confirmatory testing of suspected rickettsial diseases were submitted to the California Department of Public Health Viral and Rickettsial Disease Laboratory (CDPH-VRDL) for public health surveillance purposes and considered exempt from human subject regulations by the California Health and Human Services Agency Committee for the Protection of Human Subjects (project no. 2023-085). In addition to a plasma specimen from the initial case-patient, archival clinical specimens (serum or plasma) collected over the past 20 years from 8 confirmed SFG rickettsiosis case-patients were available for molecular characterization. SFG rickettsiosis cases were classified as confirmed for public health surveillance purposes on the basis of clinical and laboratory criteria (*12*).

Nucleic Acid Extraction and Real-time PCR

We extracted total nucleic acids using the NucliSENS easyMAG instrument (bioMérieux, https://www.biomerieux.com) with a serum or plasma input volume of 300 μL and a total nucleic acids output volume of 110 μL. We further concentrated total nucleic acids from case-patient 2 by 4-fold using the RNA Clean and Concentrator Kit (Zymo Research, https://www.zymoresearch.com).

We tested specimens for *Rickettsia* using a laboratory-developed triplex real-time reverse transcription PCR (rRT-PCR) targeting a *R. rickettsii*–specific 23S rRNA single-nucleotide polymorphism (SNP), a *R. typhi*–specific 23S rRNA SNP, and genus-specific regions of the 23S rRNA (Appendix, https://wwwnc.cdc.gov/EID/article/30/7/23-1771-App1.pdf). The assay was developed and the performance specifications established by the CDPH-VRDL as required under the Clinical Laboratory Improvement Amendments. A *R. rickettsii*–specific real-time PCR (rPCR) assay, RRi6, was performed as described by Kato et al. (*13*); the assay does not detect *Rickettsia* 364D (*14*).

MLST

We amplified and sequenced 6 target sequences, 23S rRNA, 16S rRNA, *gltA*, *ompA*, *ompB*, and *sca4* (Appendix); the last 5 of those targets correspond to the regions recommended for the gene sequence–based classification of *Rickettsia* (*15*). A commercial laboratory performed bidirectional Sanger sequencing (ELIM Biopharmaceuticals, https://elimbio.com). We performed sequence editing and assembly using Geneious Prime 2022.0.2 (https://www.geneious.com). Nucleotide BLAST searches of the National Center for Biotechnology Information (NCBI) nucleotide collection and whole-genome shotgun contigs databases (https://blast.ncbi.nlm.nih.gov) were performed to identify genetic near neighbors and facilitate phylogenetic analyses. We concatenated and aligned the 16S rRNA, *gltA*, *ompA*, *ompB*, and *sca4* sequences for validly named SFG *Rickettsia* species and constructed a maximum-likelihood phylogenetic tree using MEGA 10 (https://www.megasoftware.net). We measured the reliability of the resulting tree by bootstrap resampling using 1,000 replicates.

Tick Collection and Testing

We conducted field investigations at potential exposure sites by flagging vegetation and leaf litter for ticks. We identified tick species, sex, and life stages by examining morphologic features. For the 2023 case investigation, we processed adult ticks collected from Alameda and Contra Costa Counties for nucleic acid extraction using the DNeasy Blood and Tissue Kit (QIAGEN, https://www.qiagen.com). We screened tick nucleic acid extracts for *R. rickettsii* using the RRi6 assay. Ticks collected and identified from San Mateo and Marin Counties during the 2004 case investigation were screened for *R. rickettsii* DNA by the US Army Center for Health Promotion and Preventative Medicine–West.

Design and Development of a *Rickettsia* sp. CA6269 Real-Time PCR

We performed a nucleotide BLAST search using the *ompA* sequence from *Rickettsia* sp. CA6269 (GenBank accession no. JN990595) and downloaded and aligned selected sequences using the multiple sequence alignment tool. We selected regions of sequence divergence for primer and probe design using Primer-BLAST (https://www.ncbi.nlm.nih.gov/tools/primer-blast). We designed a 5′ exonuclease rPCR to amplify and detect a 146 bp region of *ompA*. The assay oligonucleotides were synthesized by Integrated DNA Technologies (https://www.idtdna.com). The 25-μL reaction mixture consisted

of RLompAF1 (5′-GGGCACTTGGTGTTCCTACA-3′) and RLompAR1 (5′-AAATGCCCAATTGTTTTGAG GAC-3′) primers at 500 nM, RLompAP1 (6FAM-CTAATGGTG/ZEN/ATCCTACTGGCG-3IABkFQ) probe at 100 nM, 1X Premix ExTaq (Probe qPCR) mix (Takara Biosciences, https://www.takarabio.com), and 5 μL of total nucleic acids. We performed amplification and fluorescence detection with the ABI 7500 FAST DX Sequence Detection System (ThermoFisher Scientific, https://www.thermofisher.com) using the fast mode and the following amplification conditions: 1 minute at 95°C, 45 cycles of 95°C for 3 seconds, and 60°C for 30 seconds. We assessed assay analytical specificity by using a panel of 37 total nucleic acid extracts from members of the order Rickettsiales (Appendix) and evaluated analytical sensitivity by using 10-fold serial dilutions of a quantified 156-bp gBlock gene fragment (Integrated DNA Technologies) spiked into nucleic acids from pooled human blood and tested in replicates of five. We defined the assay limit of detection as the smallest number of DNA copies detected per reaction for all 5 replicates.

Results

Case-Patient 1

The CDPH was notified of a suspected RMSF case involving a man with symptom onset in July 2023. The case-patient sought care at the emergency department (ED) with a 3-day history of influenza-like symptoms; he experienced fever, headaches, myalgias, arthralgias, malaise, loss of appetite, nonbloody diarrhea, and left-sided abdominal pain. Vital signs included temperature of 103°F (39.4°C), pulse of 96 beats/min, blood pressure of 116/71 mm Hg, and respiratory rate of 16 breaths/min. Lower left quadrant and suprapubic abdominal tenderness were noted upon physical examination. Of note, a rash was not observed. An antimicrobial regimen of ceftriaxone, metronidazole, and oral vancomycin was initiated, and the case-patient was hospitalized. The case-patient was transferred to the intensive care unit (ICU) on day 3 of hospitalization because of worsening hypoxemia, acidosis, encephalopathy, and seizures. Doxycycline was added to the treatment regimen on day 3 of hospitalization after an infectious diseases consultation that included rickettsial diseases in the differential diagnosis because of the severity of illness and clinical manifestations (Table 1).

Serologic testing for SFG *Rickettsia* by a commercial laboratory failed to detect a significant IgG titer in an acute serum specimen collected 5 days after symptom onset (Table 1). All blood cultures were negative. A laboratory diagnosis of rickettsial infection was initially made with the Karius Test, a microbial cell–free DNA (mcfDNA) metagenomic sequencing method (*16*). Sequencing of a plasma specimen collected 7 days after the onset of symptoms determined that *R. rickettsii* detected at 254,523 DNA molecules/microliter and *R. slovaca* detected at 97,653 DNA molecules/microliter were the best matches in the Karius Test genomic reference database. Serologic testing of a convalescent serum specimen, collected 105 days after symptom onset, demonstrated a significant IgG titer of >1:256 for SFG *Rickettsia*. The case-patient was discharged after being hospitalized for 22 days, including 11 days in the ICU, with a primary diagnosis of RMSF and secondary diagnoses of septic shock, acute kidney injury caused by acute tubular necrosis requiring intermittent hemodialysis, acute hypoxemic respiratory failure, encephalopathy, seizures, diarrhea, hyponatremia, abnormal liver enzymes, thrombocytopenia, supraventricular tachycardia, atrial fibrillation, and gangrene involving multiple digits on both hands.

The residual plasma specimen from mcfDNA sequencing was provided to the CDPH-VRDL for species-specific confirmatory testing. We tested total nucleic acids extracted from this sample with the triplex rRT-PCR that detects a *Rickettsia*-specific sequence, an *R. rickettsii*–specific SNP, and an *R. typhi*–specific SNP in the 23S rRNA. Unexpectedly, only the *Rickettsia* species target, and not the *R. rickettsii*–specific SNP, was detected (cycle threshold [Ct] value 24.9) (Table 2). Subsequent testing with the RRi6 assay detected DNA at a Ct value of 30.5 (Table 2). To address the discordant *R. rickettsii* test results for the triplex rRT-PCR and the RRi6 assay, we sequenced a 1,468-nt segment of the rickettsial 23S rRNA (GenBank accession no. OR600926). Comparative sequence analysis revealed a 2-nt difference from *Rickettsia* 364D and a 3- to 4-nt difference from *R. rickettsii*, including an alternate SNP allele for the rRT-PCR SNP target. We further assessed species relatedness using a MLST scheme established for the classification of *Rickettsia* (*15*). We amplified and sequenced a 1,408 nt segment of 16S rRNA, a 1,051 nt segment of *gltA*, a 587 nt segment of *ompA*, a 4,849 nt segment of *ompB*, and a 2,944 nt segment of *sca4* (GenBank accession nos. OR600927 and OR596747–50). Searches of the NCBI nucleotide databases revealed perfect sequence matches with *gltA* (290 nt) and *sca4* (673 nt), a single nucleotide insertion/deletion difference in *ompA* (471 nt), and a single SNP difference in *ompB* (758 nt) from *Rickettsia* sp. CA6269 (GenBank accession nos. JN990594–7) (*11*). MLST results indicated that the strain, designated CA23RL1, was nearly

Table 1. Clinical and laboratory features of *Rickettsia* sp. CA6269 infections in study of newly recognized SFG *Rickettsia* as cause of severe RMSF-like illness, northern California, USA*

Feature	Case-patient 1	Case-patient 2
Clinical		
Fever at hospital admission	Present, 103°F (39.4°C)	Present, 101.8°F (38.8°C)
Inoculation eschar	Absent	Absent
Rash	Absent	Present, maculopapular including palms
Myalgia	Present	Present
Headache	Present	Present
Nausea	Present	Present
Vomiting	Present	Present
Diarrhea	Present	Absent
Abdominal pain	Present	Absent
Acute kidney injury	Present	Absent
Photophobia	Present	Present
Altered mental status	Present	Present
Acute respiratory failure	Present	Present
Cutaneous necrosis and gangrene	Present	Absent
Coma	Present	Present
Days in intensive care unit	11	4
Days hospitalized	22	13
Laboratory†		
Serum sodium	Low (124 mEq/L)	Low (133 mEq/L)
Serum lactate dehydrogenase	High (421 U/L)	High (1,280 U/L)
Serum creatinine	High (1.44 mg/dL)	Unremarkable (1.0 mg/dL)
Serum bilirubin, total	High (2.3 mg/dL)	Unremarkable (0.6 mg/dL)
Aspartate transaminase	High (483 U/L)	High (268 U/L)
Alanine transaminase	High (323 U/L)	High (125 U/L)
CBC platelets	Low (45K/uL)	Low (80K/uL)
CBC leukocyte count	Unremarkable (4.5K/uL)	High (12.9K/uL)
CBC neutrophil percentage	Unremarkable (64%)	High (84%)
CSF glucose	NA	Unremarkable (69 mg/uL)
CSF protein	NA	High (147 mg/dL)
CSF leukocyte count	NA	High (9/uL)
SFG *Rickettsia* IgG titer (acute)	Unremarkable <1:128	Elevated (1:4,096)
SFG *Rickettsia* IgG titer (convalescent)	Elevated (>1:256)	Elevated (1:16,384)

*CBC, complete blood count; CSF, cerebral spinal fluid; NA, not applicable; RMSF, Rocky Mountain spotted fever; SFG, spotted fever group.
†Samples for the blood metabolic panel, CBC, and CSF analyses (case-patient 2 only) were collected on the day of hospital admission for case-patient 1 and 3 days after hospital admission for case-patient 2.

identical to *Rickettsia* sp. CA6269. In contrast, CA23RL1 displayed significant sequence divergence from *R. rickettsii* and *Rickettsia* 364D at each MLST target (Table 3). Phylogenetic analysis of concatenated sequences from validly named SFG *Rickettsia* demonstrated that CA23RL1 occupied a distinct branch and was most closely related to *R. rickettsii* (Figure).

The case-patient had not traveled outside of the San Francisco Bay area within 19 days of illness onset and did not recall a tick bite. The case-patient had played golf at 5 courses located in Alameda and Contra Costa Counties within 14 days of symptom onset, including the day symptoms began. Of note, the case-patient recalled entering vegetation to retrieve golf balls at several courses. Because that activity might have been a potential source of exposure to ticks, as follow-up we collected ticks from the 5 golf courses within 16–22 days (late July and early August) of illness onset. In all,

Table 2. Comparison of real-time PCR results for case-patient 1 and retrospective SFG rickettsiosis case-patients in study of newly recognized SFG *Rickettsia* as cause of severe RMSF-like illness, northern California, USA*

SFG rickettsiosis case-patient	Specimen type	Cycle threshold value, by test type				
		Triplex *Rickettsia* spp.	Triplex *R. rickettsii* SNP	Triplex *R. typhi* SNP	RRi6 *R. rickettsii*	*Rickettsia* sp. CA6269 *ompA*
1	Plasma	24.9	ND	ND	30.5	29.6
2	Serum	34.3	ND	ND	34.3	34.4
3	Plasma	23.3	25.2	ND	25.4	ND
4	Serum	30.3	27	ND	34	ND
5	Serum	32.8	30.2	ND	35	ND
6	Serum	32.2	32.8	ND	33.6	ND
7	Plasma	29.5	29.2	ND	33.3	ND
8	Serum	20.8	19.2	ND	25.1	ND
9	Plasma	28.6	27.3	ND	30.2	ND

*ND, not detected; RMSF, Rocky Mountain spotted fever; SFG, spotted fever group; SNP, single-nucleotide polymorphism.

Table 3. *Rickettsia* sp. CA23RL1 sequence similarity with *Rickettsia rickettsii* and *Rickettsia* 364D in study of newly recognized SFG *Rickettsia* as cause of severe RMSF-like illness, northern California, USA *

Rickettsia sp. CA23RL1 target sequence	*R. rickettsii* sequence similarity†	*Rickettsia* 364 sequence similarity‡
16S rRNA	99.7%	99.6%
gltA	99.2%	99.6%
ompA	96.8%	97.3%
ompB	98.6%	98.8%
sca4	98.6%	98.6%

*RMSF, Rocky Mountain spotted fever; SFG, spotted fever group.
†*Rickettsia rickettsii* strain Sheila Smith, GenBank accession no. CP000848.1.
‡*Rickettsia* 364D, GenBank accession no. CP003308.1.

197 adult ticks were collected and identified as either *D. occidentalis* (n = 135) or *D. similis* (n = 62). None of the ticks were infected with *R. rickettsii* or *Rickettsia* sp. CA6269 as determined by the RRi6 assay.

Case-Patient 2

We identified case-patient 2 through retrospective testing of 8 confirmed SFG rickettsiosis cases with the triplex rRT-PCR and RRi6 assays (Table 2). We detected *Rickettsia* spp. (Ct value 34.3), but not *R. rickettsii* or *R. typhi*, using the triplex rRT-PCR. The RRi6 assay detected rickettsial DNA (Ct value 34.3). Amplification and sequencing of a 397-nt segment of 23S rRNA (GenBank accession no. OR600925) by nested RT-PCR revealed an exact match to the 23S rRNA sequence determined for case-patient 1 and a 2- to 4-nt difference from *Rickettsia* 364D and *R. rickettsii*, supporting the identification of a second case of *Rickettsia* sp. CA6269 infection.

Case-patient 2, a male adult, was diagnosed with RMSF in 2004 on the basis of clinical features and a 4-fold increase in serologic titer to SFG *Rickettsia* in serum specimens collected 10 days apart (Table 1). Illness onset occurred in June; the case-patient sought care at the ED with a 5-day history of headaches, vomiting, photophobia, neck pain, and confusion. Upon initial examination, vital signs included a body temperature of

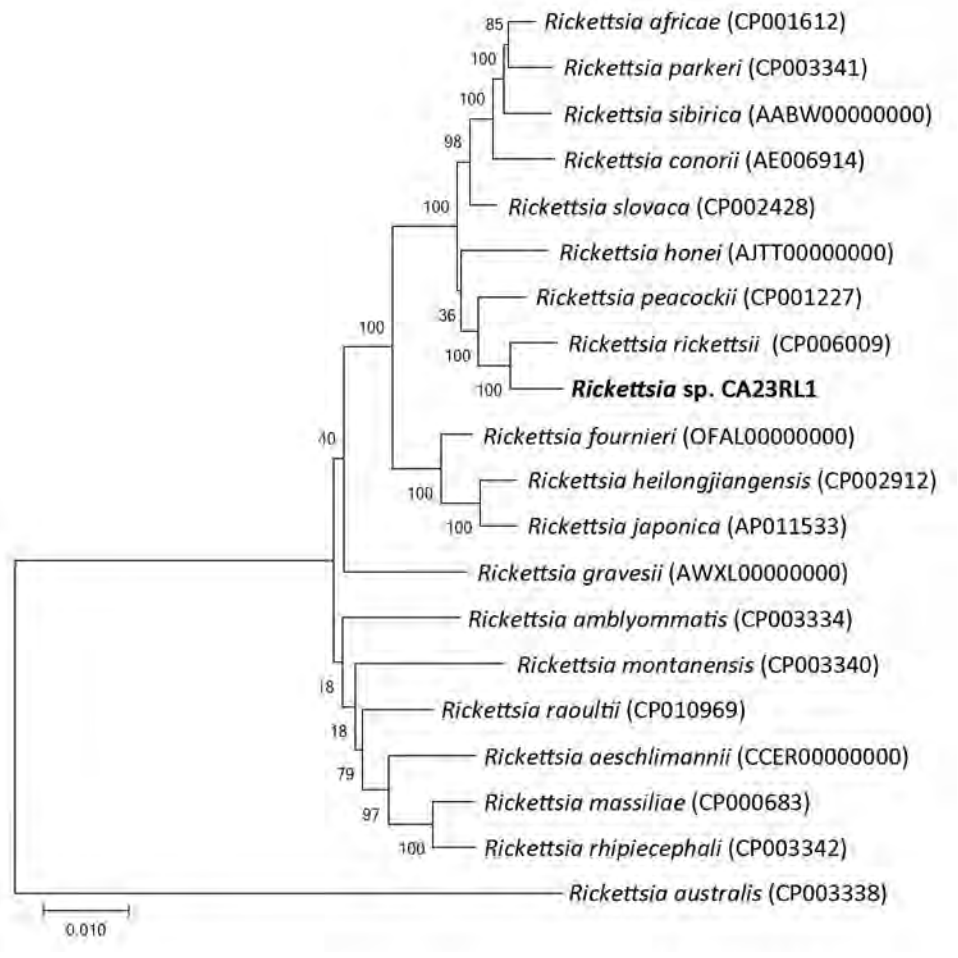

Figure. Maximum-likelihood phylogenetic tree of concatenated multilocus sequences in study of newly recognized spotted fever group *Rickettsia* as cause of severe Rocky Mountain spotted fever–like illness, northern California, USA. *Rickettsia* sp. CA23RL1 (bold text) occupies a distinct branch most closely related to *R. rickettsii*. *Rickettsia australis*, a transitional group *Rickettsia*, was included as an outgroup. Bootstrap values for 1,000 replicates are provided at each branch of the phylogenetic tree. GenBank accession numbers are provided in parentheses. Scale bar indicates evolutionary distance as measured by the number of substitutions per site.

101.8°F (38.8°C), pulse of 96 beats/min, blood pressure of 143/89 mm Hg, and respiratory rate of 20 breaths/min. Physical examination revealed mild nuchal rigidity, a maculopapular rash on the arms and legs, and leg edema. The case-patient was hospitalized on the basis of the ED assessment that included encephalitis, sepsis, hypoxemia, rash of unknown etiology, and chronic leg edema, and antimicrobial treatment with ceftriaxone, vancomycin, and acyclovir was initiated. On day 3 of hospitalization, the patient became hypoxic and comatose and was intubated and transferred to the ICU for 4 days. Doxycycline was added to the treatment regimen on day 3 of hospitalization after an infectious diseases consultation that included rickettsioses in the differential diagnosis on the basis of clinical manifestations and the patient's outdoor activities. Results of blood, CSF, urine, and sputum cultures were negative for significant pathogens. Serologic test results on day 10 of hospitalization indicated an IgG titer of 1:4,096 for SFG *Rickettsia*. After 13 days, the patient was discharged with a primary diagnosis of *Rickettsia* encephalitis.

The case-patient had not traveled outside the San Francisco Bay area during the 2 weeks before onset but had visited and camped at a county park and state beach in San Mateo County and a rural community in Marin County within that period. At the county park, he recalled finding a tick crawling on his body but not a tick bite. Field investigations at these locations conducted 30–40 days (July) after illness onset yielded 10 *D. occidentalis* ticks, 8 *D. similis* ticks, and 6 *Ixodes pacificus* ticks. Molecular testing of the *Dermacentor* spp. ticks did not detect *R. rickettsii*.

Rickettsia sp. CA6269–Specific Real-time PCR

After the sequence-based identification of *Rickettsia* sp. CA6269 infections, we developed an rPCR targeting genotype-specific regions of *ompA*. We did not observe assay cross-reactivity with nucleic acids from *Anaplasma phagocytophilum*, *Ehrlichia chaffeensis*, *Orientia tsutsugamushi*, and 14 *Rickettsia* species, including 10 *R. rickettsii* strains and 11 *Rickettsia* 364D strains (Appendix). The assay limit of detection was 1 copy of DNA per reaction. Of 9 SFG rickettsiosis case-patients tested, *Rickettsia* sp. CA6269 was detected only for case-patient 1 (Ct value 29.6) and case-patient 2 (Ct value 34.4) (Table 2). The remaining 7 case-patients were confirmed *R. rickettsii* infections on the basis of detection of the species-specific 23S rRNA SNP with the triplex rRT-PCR.

Discussion

We describe the clinical and epidemiologic features of 2 case-patients with RMSF-like illness attributed to a newly recognized rickettsial pathogen, *Rickettsia* sp. CA6269. The case-patients experienced severe clinical manifestations shared with RMSF, including acute kidney injury and respiratory failure, cutaneous necrosis and gangrene, and encephalitis. No unique clinical features were recognized in the 2 case-patients that would distinguish between infections caused by *Rickettsia* sp. CA6269 and *R. rickettsii*. Both patients likely acquired the infections locally during outdoor activities: in 1 case, golfing at courses with adjacent wildlands, and in the other case, visiting parks and camping. Although neither case-patient recalled being bitten by a tick, 1 case-patient had observed a tick crawling on his body. Nearly half of reported RMSF cases do not recall tick bites (*4*). These cases illustrate that clinicians should remain cognizant of SFG rickettsiosis in the differential diagnosis of undifferentiated febrile illnesses despite the lack of travel to areas of rickettsiosis endemicity and the absence of a recognized tick bite. Field investigations at locations of suspected exposure produced mostly *Dermacentor* spp. ticks and no *H. leporispalustris* ticks. Molecular testing of *Dermacentor* spp. ticks, established vectors of *R. rickettsii*, failed to detect *R. rickettsii* or *Rickettsia* sp. CA6269. Those potential locations of exposure will be the focus of future environmental investigations timed to better correlate with peak *H. leporispalustris* tick questing behavior.

Rickettsia sp. CA6269 was discovered during a survey of *H. leporispalustris* ticks collected in California for SFG *Rickettsia* (*11*). Of 234 ticks collected at the northern California site, 1 larval pool and 1 nymph produced a unique genotype, *Rickettsia* sp. CA6269. This unique genotype was not identified in the 179 ticks collected in southern California. The investigators proposed designating this novel *Rickettsia* as *Candidatus* R. lanei on the basis of results from an abbreviated MLST scheme. We have extended this work by sequencing the full-length regions originally proposed for the sequence-based classification of *Rickettsia* and established that *Rickettsia* sp. CA6269 meets the 2003 criteria for defining a new *Rickettsia* species (*15*). More recently, 2 genome sequence-based methods have been proposed for the classification of *Rickettsia* species (*17*,*18*). One method used genome sequence–based criteria aligned with the classic taxonomic analyses of bacteria to delineate *Rickettsia* into 9 species; nearly all SFG *Rickettsia* were classified as a single species (*17*). The other approach used genome sequence–based criteria that account for the unique phenotypic characteristics of rickettsiae and established phylogenetic relationships that were consistent with the current taxonomic classification of *Rickettsia* (*18*). That method displayed a strong correlation with MLST for *Rickettsia* classification. Despite the lack of updated consensus criteria for the taxonomic

classification of *Rickettsia* species, delineating *Rickettsia* sp. CA6269 as a strain or subspecies of *R. rickettsii* or a new species will benefit from isolating and cultivating strains, describing phenotypic characteristics including ecologic epidemiology, and determining whole-genome sequences.

Additional environmental studies are needed to investigate the geographic distribution, potential vectors, prevalence of infection, and reservoir hosts of *Rickettsia* sp. CA6269. The *H. leporispalustris* tick has been shown to be a maintenance vector of *R. rickettsii* and is distributed throughout the Americas from Alaska to Argentina (*19*,*20*). Adult *H. leporispalustris* ticks feed on rabbits and hares, whereas the nymph and larval stages feed on ground-frequenting birds and small rodents (*21*). Humans are rarely bitten by *H. leporispalustris*, indicating a limited role for this tick in transmitting SFG rickettsioses (*22*). Several surveys for *Rickettsia* infections in *H. leporispalustris* and rabbits have been conducted in California (*11*,*23*–*26*). In addition to the initial report of *Rickettsia* sp. CA6269, a further 2 studies have reported SFG *Rickettsia* detections in *H. leporispalustris*; 1 of those studies described the isolation of a *Rickettsia* antigenically related to *R. rickettsii* (*11*,*23*,*24*). Although likely rare, the case-patients described in this study might have encountered questing *H. leporispalustris* infected with *Rickettsia* sp. CA6269. Alternatively, *D. occidentalis*, a tick vector that more frequently bites humans and parasitizes a wide variety of mammals including lagomorphs, the preferred host of adult *H. leporispalustris*, might have been the source of *Rickettsia* sp. CA6269 transmission (*27*,*28*).

As with *R. rickettsii*, *Rickettsia* sp. CA6269 is likely a rarely encountered pathogen in California (*7*). After the initial detection of *Rickettsia* sp. CA6269, retrospective testing of 8 SFG rickettsiosis patient samples revealed a second case from nearly 20 years earlier. Nucleic acids from both cases lacked a *R. rickettsii*–specific 23S rRNA SNP but were detected with the RRi6 assay, indicating cross-reactivity of the RRi6 assay with *Rickettsia* sp. CA6269. The RRi6 assay was designed as *R. rickettsii*–specific on the basis of comparative genome analyses and targets a gene encoding a hypothetical protein absent in other rickettsial genomes including *Rickettsia* 364D (*13*,*14*). A homologue to this target sequence is likely present within the *Rickettsia* sp. CA6269 genome, creating the potential for misidentification of *Rickettsia* sp. CA6269 as *R. rickettsii* when using the RRi6 assay. To address this issue, we developed a *Rickettsia* sp. CA6269–specific rPCR assay that provides excellent analytical specificity and sensitivity. With more extensive performance characterization, this assay should prove useful for diagnostic testing and environmental screening of potential vectors and reservoir hosts of *Rickettsia* sp. CA6269.

In summary, we have identified *Rickettsia* sp. CA6269 as a causative agent of severe RMSF-like illness in California and have described an assay for its detection. The application of this new test, both prospectively and retrospectively, could identify additional cases, thereby leading to a better understanding of both the clinical spectrum of disease caused by *Rickettsia* sp. CA6269 and the relative contribution of this pathogen to the increasing incidence of SFG rickettsioses in the United States. In addition, the new test will enable environmental studies to define the ecologic epidemiology of this emerging pathogen.

Acknowledgments

We thank Chris Paddock and Joy Hecht for providing the *Rickettsiaceae* nucleic acids and thank Summer Adams, Alexa Quintana, Ricardo Berumen, Sabrina Gilliam, Brandon Stavig, Bianca Gonzaga, and Maria Salas for technical and medical records support. We would also like to thank Darvin Scott Smith for participating in the California Encephalitis Project and facilitating specimen submission. We also gratefully acknowledge Mary Joyce Pakingan and Erin Trent for tick extraction, Contra Costa Mosquito and Vector Control District for tick collection, and Alameda County Vector Control Services District for both tick collection and extraction efforts.

This work is funded in part by the Centers for Disease Control and Prevention Epidemiology and Laboratory Capacity for Infectious Diseases program (grant Number 5 NU50CK000539).

The findings and conclusions in this article are those of the author(s) and do not necessarily represent the views or opinions of the California Department of Public Health or the California Health and Human Services Agency.

About the Author

Dr. Probert is a research scientist with the Viral and Rickettsial Disease Laboratory of the California Department of Public Health. He is interested in the development of molecular diagnostic assays for the detection and genotyping of microbial pathogens.

References

1. Bishop A, Borski J, Wang HH, Donaldson TG, Michalk A, Montgomery A, et al. Increasing incidence of spotted fever group rickettsioses in the United States, 2010–2018. Vector Borne Zoonotic Dis. 2022;22:491–7. https://doi.org/10.1089/vbz.2022.0021
2. Blanton LS. The rickettsioses: a practical update. Infect Dis Clin North Am. 2019;33:213–29. https://doi.org/10.1016/j.idc.2018.10.010

3. Paddock CD, Finley RW, Wright CS, Robinson HN, Schrodt BJ, Lane CC, et al. *Rickettsia parkeri* rickettsiosis and its clinical distinction from Rocky Mountain spotted fever. Clin Infect Dis. 2008;47:1188–96. https://doi.org/10.1086/592254
4. Biggs HM, Behravesh CB, Bradley KK, Dahlgren FS, Drexler NA, Dumler JS, et al. Diagnosis and management of tickborne rickettsial diseases: Rocky Mountain spotted fever and other spotted fever group rickettsioses, ehrlichioses, and anaplasmosis—United States. MMWR Recomm Rep. 2016;65:1–44. https://doi.org/10.15585/mmwr.rr6502a1
5. Binder AM, Nichols Heitman K, Drexler NA. Diagnostic methods used to classify confirmed and probable cases of spotted fever rickettsioses—United States, 2010–2015. MMWR Morb Mortal Wkly Rep. 2019;68:243–6. https://doi.org/10.15585/mmwr.mm6810a3
6. California Department of Public Health. IDB yearly summaries of selected communicable diseases in California, 2013–2021 [cited 2023 Oct 20]. https://www.cdph.ca.gov/Programs/CID/DCDC/Pages/YearlySummSelectedGeneralCommDisinCA.aspx
7. Kjemtrup AM, Padgett K, Paddock CD, Messenger S, Hacker JK, Feiszli T, et al. A forty-year review of Rocky Mountain spotted fever cases in California shows clinical and epidemiologic changes. PLoS Negl Trop Dis. 2022;16:e0010738. https://doi.org/10.1371/journal.pntd.0010738
8. Paddock CD, Yoshimizu MH, Zambrano ML, Lane RS, Ryan BM, Espinosa A, et al. *Rickettsia* species isolated from *Dermacentor occidentalis* (Acari: Ixodidae) from California. J Med Entomol. 2018;55:1555–60. https://doi.org/10.1093/jme/tjy100
9. Padgett KA, Bonilla D, Eremeeva ME, Glaser C, Lane RS, Porse CC, et al. The Eco-epidemiology of Pacific coast tick fever in California. PLoS Negl Trop Dis. 2016;10:e0005020. https://doi.org/10.1371/journal.pntd.0005020
10. Shapiro MR, Fritz CL, Tait K, Paddock CD, Nicholson WL, Abramowicz KF, et al. *Rickettsia* 364D: a newly recognized cause of eschar-associated illness in California. Clin Infect Dis. 2010;50:541–8. 10.1086/649926 https://doi.org/10.1086/649926
11. Eremeeva ME, Weiner LM, Zambrano ML, Dasch GA, Hu R, Vilcins I, et al. Detection and characterization of a novel spotted fever group *Rickettsia* genotype in *Haemaphysalis leporispalustris* from California, USA. Ticks Tick Borne Dis. 2018;9:814–8. 10.1016/j.ttbdis.2018.02.023 https://doi.org/10.1016/j.ttbdis.2018.02.023
12. Centers for Disease Control and Prevention. Spotted fever rickettsioses (including Rocky Mountain spotted fever) (SFR, including RMSF) 2020 case definition [cited 2023 Oct 20]. https://ndc.services.cdc.gov/case-definitions/spotted-fever-rickettsiosis-2020
13. Kato CY, Chung IH, Robinson LK, Austin AL, Dasch GA, Massung RF. Assessment of real-time PCR assay for detection of *Rickettsia* spp. and *Rickettsia rickettsii* in banked clinical samples. J Clin Microbiol. 2013;51:314–7. https://doi.org/10.1128/JCM.01723-12
14. Denison AM, Amin BD, Nicholson WL, Paddock CD. Detection of *Rickettsia rickettsii, Rickettsia parkeri*, and *Rickettsia akari* in skin biopsy specimens using a multiplex real-time polymerase chain reaction assay. Clin Infect Dis. 2014;59:635–42. https://doi.org/10.1093/cid/ciu358
15. Fournier PE, Dumler JS, Greub G, Zhang J, Wu Y, Raoult D. Gene sequence-based criteria for identification of new *rickettsia* isolates and description of *Rickettsia heilongjiangensis* sp. nov. J Clin Microbiol. 2003;41:5456–65. https://doi.org/10.1128/JCM.41.12.5456-5465.2003
16. Blauwkamp TA, Thair S, Rosen MJ, Blair L, Lindner MS, Vilfan ID, et al. Analytical and clinical validation of a microbial cell-free DNA sequencing test for infectious disease. Nat Microbiol. 2019;4:663–74. https://doi.org/10.1038/s41564-018-0349-6
17. Chung M, Munro JB, Tettelin H, Dunning Hotopp JC. Using core genome alignments to assign bacterial species. mSystems. 2018;3:e00236–18. https://doi.org/10.1128/mSystems.00236-18
18. Diop A, El Karkouri K, Raoult D, Fournier PE. Genome sequence-based criteria for demarcation and definition of species in the genus *Rickettsia.* Int J Syst Evol Microbiol. 2020;70:1738–50. https://doi.org/10.1099/ijsem.0.003963
19. Freitas LH, Faccini JL, Labruna MB. Experimental infection of the rabbit tick, *Haemaphysalis leporispalustris*, with the bacterium *Rickettsia rickettsii*, and comparative biology of infected and uninfected tick lineages. Exp Appl Acarol. 2009;47:321–45. https://doi.org/10.1007/s10493-008-9220-4
20. Kohls GM. Records and new synonymy of new world *Haemaphysalis* ticks, with descriptions of the nymph and larva of *H. juxtakochi* Cooley. J Parasitol. 1960;46:355–61. https://doi.org/10.2307/3275499
21. Burgdorfer W. Ecology of tick vectors of American spotted fever. Bull World Health Organ. 1969;40:375–81.
22. Nieto NC, Porter WT, Wachara JC, Lowrey TJ, Martin L, Motyka PJ, et al. Using citizen science to describe the prevalence and distribution of tick bite and exposure to tick-borne diseases in the United States. PLoS One. 2018;13:e0199644. 10.1371/journal.pone.0199644 https://doi.org/10.1371/journal.pone.0199644
23. Lane RS, Emmons RW, Dondero DV, Nelson BC. Ecology of tick-borne agents in California. I. Spotted fever group rickettsiae. Am J Trop Med Hyg. 1981;30:239–52. 10.4269/ajtmh.1981.30.239 https://doi.org/10.4269/ajtmh.1981.30.239
24. Gurfield N, Grewal S, Doggett D, Ferran K, LaFreniere R. Detection of spotted fever group *Rickettsia* and *Borrelia burgdorferi* in San Diego County rabbit ticks. Proc Pap Annu Conf Mosq Vector Control Assoc Calif. 2011;79:25–6.
25. Roth T, Lane RS, Foley J. A molecular survey for *Francisella tularensis* and *Rickettsia* spp. in *Haemaphysalis leporispalustris* (Acari: Ixodidae) in northern California. J Med Entomol. 2017;54:492–5. https://doi.org/10.1093/jme/tjw202
26. Schmitz KM, Foley JE, Kasten RW, Chomel BB, Larsen RS. Prevalence of vector-borne bacterial pathogens in riparian brush rabbits (*Sylvilagus bachmani riparius*) and their ticks. J Wildl Dis. 2014;50:369–73. https://doi.org/10.7589/2012-11-292
27. Eisen L. Tick species infesting humans in the United States. Ticks Tick Borne Dis. 2022;13:102025. https://doi.org/10.1016/j.ttbdis.2022.102025
28. Lane RS, Burgdorfer W. Spirochetes in mammals and ticks (Acari: Ixodidae) from a focus of Lyme borreliosis in California. J Wildl Dis. 1988;24:1–9. https://doi.org/10.7589/0090-3558-24.1.1

Address for correspondence: Will Probert, California Department of Public Health, Viral and Rickettsial Disease Laboratory, 850 Marina Bay Pkwy, Richmond, CA, 94804, USA; email: will.probert@cdph.ca.gov

COVID-19 Death Determination Methods, Minnesota, USA, 2020–2022[1]

Lydia J. Fess, Ashley Fell, Siobhan O'Toole, Paige D'Heilly, Stacy Holzbauer, Leslie Kollmann, Amanda Markelz, Keeley Morris, Abbey Ruhland, Scott Seys, Elizabeth Schiffman, Haley Wienkes, Zachary Zirnhelt, Stephanie Meyer, Kathryn Como-Sabetti

Accurate and timely mortality surveillance is crucial for elucidating risk factors, particularly for emerging diseases. We compared use of COVID-19 keywords on death certificates alone to identify COVID-19 deaths in Minnesota, USA, during 2020–2022, with use of a standardized mortality definition incorporating additional clinical data. For analyses, we used likelihood ratio χ^2 and median 1-way tests. Death certificates alone identified 96% of COVID-19 deaths confirmed by the standardized definition and an additional 3% of deaths that had been classified as non–COVID-19 deaths by the standardized definition. Agreement between methods was ≥90% for most groups except children, although agreement among adults varied by demographics and location at death. Overall median time from death to filing of death certificate was 3 days; decedent characteristics and whether autopsy was performed varied. Death certificates are an efficient and timely source of COVID-19 mortality data when paired with SARS-CoV-2 testing data.

As of November 1, 2023, ≈1 million COVID-19 deaths have been reported in the United States (*1*) including >15,000 among Minnesota residents (*2*). The literature suggests that for the general population, COVID-19 death counts are probably underreported compared with excess mortality estimates (*3*–*8*) but may overrepresent White non-Hispanic and elderly populations (*9*). Extensive case-based mortality investigation is time and resource intensive, raising the question of how to balance accuracy, representativeness, and efficiency in a COVID-19 mortality surveillance system.

Author affiliations: Minnesota Department of Health, Saint Paul, Minnesota, USA (L.J. Fess, A. Fell, S. O'Toole, P. D'Heilly, S. Holzbauer, L. Kollmann, A. Markelz, K. Morris, A. Ruhland, S. Seys, E. Schiffman, H. Wienkes, Z. Zirnhelt, S. Meyer, K. Como-Sabetti); Centers for Disease Control and Prevention, Atlanta, Georgia, USA (S. Holzbauer)

DOI: https://doi.org/10.3201/eid3007.231522

Accurate and timely mortality surveillance is a crucial tool for elucidating risk factors for death and also provides information for public health response, including policies associated with risk mitigation and high-risk populations (e.g., long-term care facility residents). COVID-19 mortality estimation methods have strengths and weaknesses (*10*). Death certificates are limited by the accuracy and consistency of completion by medical certifiers and by the evolving knowledge of SARS-CoV-2 pathogeneses and contribution to death. Similarly, excess deaths are limited by uncertainty around baseline and reported data. Early in the pandemic, rapid dissemination of mortality counts from healthcare systems and community surveillance were crucial to the public health response (*11*). However, officially filed death certificates, although often slower, provide valuable data about disease severity and disparity of mortality burden, as well as data for response planning (*10*). When available, death certificates are a valuable source of data for mortality surveillance for COVID-19 and other diseases (e.g., influenza) (*12*) and can also be relatively timely with access to provisional (not yet finalized) death certificates. Although previous work has analyzed codes from the International Classification of Diseases, Tenth Revision (ICD-10) listed on death certificates to determine appropriateness of COVID-19 inclusion, literature comparing death certificates with other forms of COVID-19 surveillance is lacking (*13*).

National organizations such as the Council of State and Territorial Epidemiologists (CSTE) provide guidance for COVID-19–associated mortality designation (*14*); however, mortality surveillance methods

[1]Preliminary results from this analysis were presented at the Council of State and Territorial Epidemiologists annual conference; 2023 Jun 25–29; Salt Lake City, Utah, USA.

are determined primarily by individual jurisdictions and may differ. Early in the COVID-19 pandemic, Minnesota established a case investigation and death certificate–based mortality definition to enable systematic classification before the release of the first CSTE case definition.

To provide information for revisions to the state COVID-19–associated mortality definition, we evaluated the Minnesota Department of Health (MDH) COVID-19 mortality surveillance system. At the time of the analysis, Minnesota surveillance was more in-depth than the CSTE case definition and more robust than review of vital records alone, although it was more resource intensive. We sought to determine the effect of a more robust and resource-intensive case definition compared with the less resource-intensive case definition. To do so, we assessed the Minnesota surveillance system by calculating rates of agreement between COVID-19 deaths confirmed by the Minnesota standardized case definition and inclusion of COVID-19 on death certificates, as well as timeliness of death processing and reporting, throughout several years and phases of the pandemic. Our analysis was a surveillance evaluation of previously collected public health data obtained in accordance with Minnesota reportable disease statutes and is not subject to human subjects research review boards (National Archives and Records Administration, Title 45, Public Welfare, Code of Federal Regulations [annual edition] Sect. 46.102, Oct 1, 2020; and Minnesota Rules, 2018, Chapter 4605).

Methods

Study Population

Our study population included decedents with confirmed COVID-19 deaths, as defined by the Minnesota definition of COVID-19 mortality, and deaths that were determined to not meet the COVID-19 death definition but included COVID-19 keywords on the death certificate (non–COVID-19 deaths). We excluded confirmed COVID-19 deaths without an available death certificate (e.g., Minnesota residents who died out of state). All decedents were Minnesota residents who died March 19, 2020 (first COVID-19 death in Minnesota), through December 31, 2022.

COVID-19 Death Classification

Possible COVID-19 deaths were reported to MDH via provisional death certificates, by the MDH Unexplained Critical Illnesses and Deaths/Medical Examiner Infectious Deaths Surveillance (UNEX/MED-X) program (*15*,*16*), case interviews, laboratory results, and other sources including reports from providers, hospitals, long-term care facilities, and medical examiners. Death reports were linked with SARS-CoV-2 laboratory results reported to the Minnesota Electronic Disease Surveillance System and assessed by using the Minnesota COVID-19 mortality definition. Death certificates containing COVID-19 keywords (e.g., "COVID," "SARS," "coronavirus") were pulled daily from the Minnesota Registration and Certification database and reviewed. Keywords were used in place of ICD-10 codes to enable identification before the ICD coding process and to avoid potential coding errors.

A death met the Minnesota definition of a COVID-19 mortality if the decedent had a positive laboratory SARS-CoV-2 RNA PCR or antigen test result before or after death and ≥1 of the following: COVID-19 was listed in either part I or part II of the cause of death section of the death certificate, or clinical history or autopsy findings were consistent with COVID-19 in the absence of an alternative cause of death as evaluated by MDH staff during the mortality investigation process (Appendix, https://wwwnc.cdc.gov/EID/article/30/7/23-1522-App1.pdf). For our analysis, a confirmed COVID-19 death was a death that met the Minnesota definition of COVID-19 mortality.

We further investigated deaths that occurred within 30 days of a COVID-19 infection but did not indicate COVID-19 on the death certificate, deaths that included conditional language on the death certificate such as history of COVID, deaths that included COVID-19 on the death certificate but the positive SARS-CoV-2 specimen collection date was >1 year before death, and deaths that included COVID-19 on the death certificate but had a potential alternative cause of death. When necessary, we consulted additional information (e.g., medical records and autopsy reports) to determine if a death met the case definition. Data for confirmed COVID-19 deaths and all other death certificates with COVID-19 keywords were managed in a REDCap (Research Electronic Data Capture) database (*17*,*18*).

For analyses, we created the following groups: confirmed COVID-19 deaths with COVID-19 keywords listed on the death certificate (confirmed COVID-19 deaths with death certificate), confirmed COVID-19 deaths that were determined to meet the Minnesota definition of mortality but did not include COVID-19 on the death certificate (confirmed COVID-19 deaths without death certificate), and deaths that included COVID-19 on the death certificate but did not meet the Minnesota definition of COVID-19 mortality (ruled-out COVID-19 deaths).

We considered confirmed COVID-19 deaths with death certificate to have agreement between the Minnesota definition of COVID-19 mortality and the death certificate, and we considered confirmed COVID-19 deaths without death certificate and ruled-out deaths to have disagreement. We assessed timeliness of COVID-19 death investigations by calculating median number of days from date of death (DOD) to date of death certificate medical filing.

Analyses

To assess death certificate agreement with the Minnesota definition of COVID-19 mortality, we compared all confirmed COVID-19 deaths with death certificates with confirmed COVID-19 deaths without death certificates and ruled-out COVID-19 deaths. We reviewed ruled-out deaths for death certificate language before analysis. Death certificates that clearly indicated that COVID-19 did not contribute to death (e.g., "viral infection, not COVID" listed in part I or II of the death certificate) were excluded from analysis. We approximated death certificate accuracy as agreement between inclusion of COVID-19 on the death certificate as a primary or contributing cause of death and the Minnesota definition of COVID-19 mortality. To calculate rates of agreement, we generated a 2 × 2 table of COVID-19 mortality definition and inclusion of COVID-19 on the death certificate.

We analyzed all measures by sex, age group, race/ethnicity, Minnesota region of residence (Minneapolis/Saint Paul metropolitan area or greater Minnesota), living setting, location of death, variant era, hospitalization history, underlying health conditions, autopsy status (whether performed), and median days between symptom onset (or if unavailable, date of specimen with positive SARS-CoV-2 result) and death. We defined variant eras by the week(s) at which the COVID-19 variant or lineage accounted for ≥50% of sequenced samples in Minnesota. To analyze categorial variables, we used likelihood χ^2 or Fisher exact tests; for continuous variables, we used a median 1-way analysis. We conducted all analyses in SAS 9.4 (https://www.sas.com) and defined significance as $p<0.05$.

Results

Our analysis included 14,004 deaths among Minnesota residents: 13,591 confirmed COVID-19 deaths (13,108 confirmed COVID-19 deaths with death certificate and 483 confirmed COVID-19 deaths without death certificate) and 413 ruled-out COVID-19 deaths. We excluded 59 ruled-out deaths because of language that indicated that COVID-19 did not contribute to death. Confirmed COVID-19 deaths most often occurred in persons who were male (54%) and ≥80 years of age (53%) (Table 1). Most confirmed COVID-19 decedents were White non-Hispanic (87%), were from the Minneapolis/Saint Paul metropolitan area (52%), and lived in a private residence (51%). About 64% persons with confirmed death had a known COVID-19–associated hospitalization before death, and death occurred during hospitalization for 50%. Only 3% of confirmed COVID-19 decedents underwent an autopsy; 95% had ≥1 documented underlying condition. Many (49%) of the confirmed COVID-19 deaths occurred before Alpha variant predominance in Minnesota. Median time between symptom onset and death was 14.0 days (interquartile range [IQR] 8.0–25.0 days).

Timeliness of COVID-19 Death Processing

The median number of days between DOD and date of death certificate filing differed by sex, age, race/ethnicity, Minnesota region, living setting, location of death, hospitalization history, autopsy, variant era, and underlying conditions (Table 2). However, median time to death certificate filing did not exceed 7.5 days for any subgroup except decedents who underwent an autopsy (22 days) and decedents <18 years of age (40 days). Among decedents who did not undergo an autopsy, median time from DOD to death certificate filing was similar for those who were younger (<50 years, 4 days; <18 years, 2 days) and those who were ≥50 years of age (3 days). Median time from DOD to death certificate filing was longer for decedents who resided in an other setting (e.g., homeless shelter) (7.5 days) than for private or long-term care residents (3 days) (Table 2). Median time from DOD to death certificate filing was also longer for Asian/Pacific Islander and Black/African American decedents (6 days) than for White non-Hispanic decedents (3 days).

Death Certificate Agreement

Overall, death certificates accurately captured 96% (13,108) of Minnesota confirmed COVID-19 deaths (Table 3). Death certificates for 483 (4%) COVID-19 deaths confirmed by the Minnesota mortality definition did not include COVID-19 keywords, and an additional 413 (3%) death certificates listed COVID-19 as a cause of death but were classified as COVID-19 ruled-out deaths by the Minnesota mortality definition.

Agreement between the Minnesota definition of COVID-19 mortality and inclusion of COVID-19 on the death certificate varied by demographics and disease history but was >90% for all groups analyzed except

pediatric decedents (Appendix Table 1). Rate of agreement was highest for decedents who underwent an autopsy (98%), decedents with no underlying conditions (97%), and decedents who were identified as Asian/Pacific Islander (97%) (Appendix Table 1). Rate of agreement was lowest for pediatric decedents (<18 years of age) (74%), followed by decedents who died in congregate living (90%) and those with no known hospitalization history (90%). The median time from onset or positive specimen date to death was shorter for decedents with death certificate agreement (14.0 days, IQR 8.0–26.0 days) than for decedents with disagreement (19.0 days, IQR 6.0– 75.5 days).

Discussion

We found that death certificates are accurate and timely sources of COVID-19 mortality surveillance data in Minnesota. However, agreement between death certificates and the Minnesota definition of COVID-19 mortality, as well as timeliness of death certificate

Table 1. Patient demographic and disease history characteristics for COVID-19 deaths determined by using the Minnesota Department of Health case definition of COVID-19 mortality, March 19, 2020–December 31, 2022*

Patient characteristic	Total	Confirmed COVID-19 deaths	Ruled-out COVID-19 deaths
Sex			
M	7,518 (53.7)	7,336 (54.0)	182 (44.1)
F	6,486 (46.3)	6,255 (46.0)	231 (55.9)
Age, y			
0–17	19 (0.14)	14 (0.10)	5 (1.2)
18–49	561 (4.0)	529 (3.9)	32 (7.8)
50–59	920 (6.6)	903 (6.6)	17 (4.1)
60–69	1,921 (13.7)	1,883 (13.9)	38 (9.2)
70–79	3,176 (22.7)	3,098 (22.8)	78 (18.9)
≥80	7,407 (52.9)	7,164 (52.7)	243 (58.8)
Race/ethnicity			
American Indian/Alaska Native	241 (1.7)	232 (1.7)	9 (2.2)
Asian/Pacific Islander	517 (3.7)	512 (3.8)	5 (1.2)
Black/African American	686 (4.9)	668 (4.9)	18 (4.4)
Hispanic	353 (2.5)	341 (2.5)	12 (2.9)
Multiracial	62 (0.44)	60 (0.4)	2 (0.48)
Other or unknown	22 (0.16)	21 (0.2)	1 (0.24)
White non-Hispanic	12,123 (86.6)	11,757 (86.5)	366 (88.6)
Minnesota region			
Greater Minnesota	6,665 (47.6)	6,501 (47.8)	164 (39.7)
Minneapolis and Saint Paul metropolitan area	7,339 (52.4)	7,090 (52.2)	249 (60.3)
Living setting			
Private residence	7,018 (50.1)	6,880 (50.6)	138 (33.4)
Long-term care	6,916 (49.4)	6,645 (48.9)	271 (65.6)
Other†	70 (0.50)	66 (0.5)	4 (0.97)
Location of death			
Hospital inpatient	6,827 (48.8)	6,748 (49.7)	79 (19.1)
Congregate living	5,497 (39.3)	5,245 (38.6)	252 (61.0)
Other‡	1,680 (12.0)	1,598 (11.8)	82 (19.9)
Hospitalization history			
Hospitalized	8,860 (63.3)	8,657 (63.7)	203 (49.2)
No/unknown	5,144 (36.7)	4,934 (36.3)	210 (50.9)
Autopsy status			
Yes	343 (2.5)	343 (2.5)	0
No/unknown	13,661 (97.6)	13,248 (97.5)	413 (100.0)
Variant era			
Pre-Alpha	6,853 (48.9)	6,697 (49.3)	156 (37.8)
Alpha	857 (6.1)	778 (5.7)	79 (19.1)
Delta	2,851 (20.4)	2,799 (20.6)	52 (12.6)
Omicron BA.1	1,785 (12.8)	1,754 (12.9)	31 (7.5)
Omicron BA.2	335 (2.4)	314 (2.3)	21 (5.1)
Omicron BA.4/BA.5	1,323 (9.5)	1,249 (9.2)	74 (17.9)
Underlying conditions status			
Yes	13,300 (95.0)	12,921 (95.1)	379 (91.8)
No	192 (1.4)	188 (1.4)	4 (1.0)
Unknown	512 (3.7)	482 (3.6)	30 (7.3)
Median onset date to death (days, IQR)	15.0 (8.0–27.0)	14.0 (8.0–25.0)	82.0 (30.0–185.0)
Total	14,004	13,591 (97.1)	413 (3.0)

*Values are no. (%) except as indicated. IQR, interquartile range.
†Other includes sheltered and unsheltered homeless, jail/prison, dormitories, and other settings.
‡Other includes decedents who died at home, in the emergency department, or in other settings, such as at another private residence.

Table 2. Median days from date of death to filing of death certificate, by demographic and disease history characteristics, for confirmed COVID-19 deaths detected by using the Minnesota Department of Health COVID-19 mortality case definition, March 19, 2020–December 31, 2022*

Patient characteristic	No.	Days from date of death to death certificate filing, median (IQR)	p value
Sex			0.0002†
M	7,336	3 (2–6)	
F	6,255	3 (2–5)	
Age, y			<0.0001†
0–17	14	40 (4–95)	
18–49	529	6 (3–20)	
50–59	903	4 (2–7)	
60–69	1,883	4 (2–6)	
70–79	3,098	3 (2–5)	
≥80	7,164	3 (1–5)	
Race/ethnicity			<0.0001†
American Indian/Alaska Native	232	5 (3–7)	
Asian/Pacific Islander	512	6 (3–14)	
Black/African American	668	6 (3–13.5)	
Hispanic	341	4 (2–7)	
Multiracial	60	4 (2–8)	
Other or Unknown	21	4 (3–5)	
White, non-Hispanic	11,757	3 (2–5)	
Minnesota region			<0.0001†
Greater Minnesota	6,501	3 (1,–4)	
Minneapolis and Saint Paul metropolitan area	7,090	4 (2–6)	
Living setting			<0.0001†
Private residence	6,880	3 (2–6)	
Long-term care	6,645	3 (1–5)	
Other‡	66	7.5 (3–19)	
Location of death			<0.0001†
Hospital inpatient	6,748	3 (2–6)	
Congregate living	5,245	3 (1–5)	
Other§	1,598	4 (2–10)	
Hospitalization history			<0.0001†
Hospitalized	8,657	3 (2–5)	
No/unknown	4,934	3 (1–5)	
Autopsy status			<0.0001†
Yes	343	22 (5–45)	
No/unknown	13,248	3 (2–5)	
Variant era			<0.0001†
Pre-alpha	6,697	3 (2–5)	
Alpha	778	3 (2–5)	
Delta	2,799	3 (2–6)	
Omicron BA.1	1,754	3 (2–6)	
Omicron BA.2	314	3 (2–5)	
Omicron BA.4/5	1,249	3 (2–5)	
Underlying conditions			0.0038†
Yes	12,921	3 (2–5)	
No	188	4 (2–8)	
Unknown	482	3 (2–6)	
Total	13,591	3 (2–5)	

*Values are no. (%) except as indicated. IQR, interquartile range.
†Statistically significant at p = 0.05. p values are for median 1-way analysis.
‡Other includes sheltered and unsheltered homeless, jail/prison–dormitories, and other settings.
§Other includes decedents who died at home, in the emergency department, and in other settings, such as at another private residence.

filing, varied by certain demographics. In addition, access to provisional death certificates is a consistently expeditious method for obtaining reports of potential COVID-19–associated deaths.

In our analysis, median days between DOD and death certificate filing differed by multiple demographic and disease history variables. However, median time was within 8 days for most groups except those who underwent an autopsy (22 days) and pediatric decedents (40 days), enabling timely access to mortality data for public health insight. In addition, autopsies are rare, and delay is expected when they are performed. Median time from DOD to death certificate filing was longer for younger decedents (<50 years of age, particularly <18 years of age) than for those in older age groups, although the median time to death certificate filing for those who did not undergo autopsy was similar across age groups (<50

years, 4 days; <18 years, 2 days; ≥50 years, 3 days). Median time to death certificate filing was longer for those in Black, Indigenous, or People of Color (BIPOC) groups, potentially reflecting inequities in healthcare access or increased rates of autopsy (*19*–*22*).

Decedents with agreement between COVID-19 mortality definition and the death certificate were more likely to have a known hospitalization history or completed autopsy. Hospitalization and autopsy provide valuable information and context for both the health department and the certifier, probably contributing to greater agreement. That finding is consistent with a prior study in Olmsted County, Minnesota, that found higher rates of death certificate accuracy for coronary artery disease and an autopsy rate that was twice the national average (*23*).

Disagreement between the death certificate and the Minnesota mortality definition was more common among decedents <18 years of age, decedents who were White non-Hispanic, decedents who were long-term care residents, and decedents who died outside a hospital. The MDH UNEX/MED-X program investigates unexplained deaths of possible infectious etiology in addition to conducting population-based surveillance for deaths that may be associated with infectious disease(s) and are reported to Minnesota medical examiners (*15*,*16*). The program performs postmortem testing for an assortment of infectious diseases on a wide range of decedents, including medical examiner–investigated deaths that may have resulted from nonnatural causes. UNEX/MED-X identifies many young decedents, as well as many persons with incidental COVID-19 infection or nonnatural alternative causes of death (e.g., drug overdose), who may not have otherwise been identified by routine surveillance systems. Inclusion of COVID-19 as a contributing cause of death on the death certificate for young decedents with a nonnatural alternative cause of death probably explains the higher rate of disagreement among pediatric decedents. In contrast, BIPOC persons may be less likely to have a laboratory confirmed SARS-CoV-2 test result or to access healthcare for COVID-19 illnesses (*20*,*22*,*24*,*25*) and may therefore be more likely to be underreported in case surveillance, resulting in higher rates of death certificate agreement. BIPOC status has been associated with hospitalization risk (*26*–*31*), and non–English-speaking status and Black race have been associated with lower rates of SARS-CoV-2 testing (*32*,*33*).

Long-term care decedents were more likely to be considered both a confirmed COVID-19 death without death certificate and a ruled-out death when compared with private residents, resulting in a lower rate of agreement (Appendix Table 2). Those findings may result from multiple factors, including detection of mild or asymptomatic SARS-CoV-2 during facilitywide testing and complicated medical histories. Detection of mild or asymptomatic SARS-CoV-2 may increase the likelihood of COVID-19 being indicated on the death certificate in addition to an alternative cause of death. In addition, underlying health conditions (e.g., chronic obstructive pulmonary disease) are more prevalent in older and institutionalized populations (*34*), and such conditions can complicate cause-of-death determination. Residents may also be less likely to communicate subjective symptoms associated with COVID-19 infection or may exhibit signs not always associated with infection (e.g., falling more frequently). In addition, previous literature has found that death certificates overestimate death caused by coronary artery disease in certain demographic groups (*35*), particularly out-of-hospital deaths, which are common among long-term care residents (*36*). Other reports have found underestimates of Legionnaires' disease by death certificates and misattribution of death to underlying conditions or other illnesses because of nonspecific manifestations (*37*). It is reasonable to assume a similar phenomenon may occur among COVID-19 case-patients with complex medical histories, particularly if symptoms could be confused for those of an existing chronic condition (e.g., shortness of breath) or are unobservable (e.g., loss of sense of taste).

Overall, death certificates were generally in high agreement with case-based investigation using the Minnesota definition of COVID-19 mortality. Undercounting (missing confirmed COVID-19 deaths) was observed more often than overcounting (i.e., erroneously identifying a decedent as a COVID-19 death). Those results are consistent with the existing

Table 3. COVID-19 inclusion on the death certificate and the MDH case definition of COVID-19 mortality, March 19, 2020–December 31, 2022

COVID-19 inclusion status	Confirmed COVID-19 death using MDH COVID-19 mortality case definition	Non–COVID-19 death	Total
"COVID-19" on death certificate (death certificate comparison method)	13,108	413	13,521
"COVID-19" not on death certificate	483	0	483
Total	13,591	413	14,004

*MDH, Minnesota Department of Health.

literature (*3*–*7*). In our analysis, agreement ranged from 74% among pediatric decedents to 98% among those who underwent an autopsy; agreement was >90% for all groups except pediatric decedents. The small sample size for pediatric deaths complicates efforts to understand differences in characteristics. As more data become available, mortality surveillance systems should adapt as needed to better serve and identify special populations. Adaptations may include additional investigations into potential COVID-19 pediatric deaths (e.g., medical record review) to describe those deaths as accurately as possible.

Death certificates can be combined with case surveillance data (e.g., SARS-CoV-2 testing data) to form a robust COVID-19 mortality surveillance system. Misclassification of COVID-19 deaths is inevitable. Our analysis suggests that misclassification may skew toward underreporting and that some groups are more likely than others to be misclassified. Factors to consider when evaluating misclassification or cases missed by a surveillance system are racial and ethnic disparities in healthcare access, healthcare-seeking behavior, and infection and severe illness risk. For example, pediatric decedents may be overcounted because of intense scrutiny and comprehensive testing, and BIPOC persons may be undercounted because of lack of access to testing. Reliance on death certificates as a primary source of COVID-19–associated death reporting may serve as an accurate surveillance system, especially with limited public health resources. However, when available, public health entities should consider investing resources in more investigations for populations who may be more likely to be misclassified by death certificates, such as pediatric decedents and long-term care residents.

Among the limitations of our analysis, high reliance on the death certificates in the MDH COVID-19 death identification and determination process may skew results toward greater congruence between the death certificate and COVID-19 mortality definition. Although death certificates were an integral part of the Minnesota definition of COVID-19 mortality, we conducted further investigation for specified COVID-19 language, for deaths that occurred >1 year after a positive test result and for deaths that occurred within 30 days of a positive test result and did not have COVID-19 indicated on the death certificate. Therefore, our analysis compares a resource-intensive approach, including review of all available sources, with reliance on death certificate reporting alone. In addition, our analysis identified populations for which an intensive investigation was less likely to agree with the death certificate, which could have implications for future mortality surveillance and analysis.

The Minnesota definition of COVID-19 mortality underwent several revisions during the study period; specifically, a prior definition categorized deaths as probable if the decedent had undergone only antigen testing for SARS-CoV-2. However, probable and confirmed deaths were both still considered COVID-19 deaths and therefore did not affect the overall mortality reporting used for our analysis. In addition, resources to investigate deaths fluctuated throughout the pandemic, so it is possible that not all deaths underwent the same level of investigation. Because intensive investigations were used to rule out and rule in COVID-19 deaths, we expect that the net effect of resource differences over time would minimally affect our findings.

The Minnesota case definition was in place for several years from the beginning of the pandemic, resulting in consistent detailed data collection beyond the initial phase of intensive COVID-19 contact tracing and case investigations. Confirmed Minnesota COVID-19 deaths in our analysis are laboratory-confirmed COVID-19 cases. Documented inequities in access to COVID-19 testing (*32*,*33*,*38*) may have biased mortality and case surveillance. Access to (and use of) at-home tests, which are not reported to MDH or counted as laboratory-confirmed cases, has increased, particularly during the latter stages of the pandemic, and are probably used at different rates by different populations. The population of our analysis constitutes mostly White non-Hispanic persons in an upper Midwestern state with robust public health resources, including the UNEX/MED-X program, and thus, results may not be generalizable to other states. Variables assessed in our analysis may be correlated (e.g., long-term care residency and race/ethnicity), potentially affecting analysis outcomes and generalizability to states with different demographics. Future research may use regression models to explore the relationship between demographic and disease history variables.

Trained public health professionals in Minnesota evaluated death certificates for any mention of COVID-19 rather than searching for specific ICD codes or underlying causes of death, which enabled more timely death reporting and inclusion of language from the entire death certificate. That approach also avoided errors associated with incorrect identification of underlying cause of death on the death certificate, which previous research suggests may be common (*39*,*40*). Last, our analysis adds to the body of COVID-19 knowledge by evaluating a COVID-19

mortality surveillance approach for accuracy and timeliness, providing context for future mortality surveillance development and evaluation of emerging diseases in Minnesota and beyond.

In conclusion, we analyzed a large sample of possible COVID-19 deaths that were reviewed by using a standard case definition throughout several years of the COVID-19 pandemic. Comparisons of the Minnesota definition of COVID-19 mortality and inclusion of COVID-19 on the death certificate indicated that death certificates are an efficient and timely source of COVID-19 mortality data when paired with SARS-CoV-2 testing data and should be an integral part of COVID-19 mortality surveillance. Supplemental investigations may be warranted for key groups, such as pediatric decedents, as resources allow. Mortality surveillance is a vital aspect of disease surveillance, particularly during emergence of a new disease, and surveillance evaluations are needed to improve existing systems and prepare for the next public health challenge.

Acknowledgments

We acknowledge Ruth Lynfield, Richard Danila, Ellen Laine, Linnea Thorell, Greta Ciessau, the Minnesota Office of Vital Records, the Minnesota Public Health Laboratory, and the Emerging Infectious Disease Epidemiology and Response section at the Minnesota Department of Health for data collection and case definition development.

About the Author

Ms. Fess is an epidemiologist at the Minnesota Department of Health in Saint Paul. Her primary research interests include emerging infectious diseases, zoonotic and fungal diseases, and mortality surveillance.

References

1. Centers for Disease Control and Prevention. COVID Data Tracker [cited 2023 Mar 6]. https://covid.cdc.gov/covid-data-tracker
2. Minnesota Department of Health. Mortality (death) data: COVID-19 situation update [cited 2023 Mar 7]. https://www.health.state.mn.us/diseases/coronavirus/stats/death.html
3. Iuliano AD, Chang HH, Patel NN, Threlkel R, Kniss K, Reich J, et al. Estimating under-recognized COVID-19 deaths, United States, March 2020–May 2021 using an excess mortality modelling approach. Lancet Reg Health Am. 2021;1:100019.
4. Whittaker C, Walker PGT, Alhaffar M, Hamlet A, Djaafara BA, Ghani A, et al. Under-reporting of deaths limits our understanding of true burden of covid-19. BMJ. 2021;375:n2239. https://doi.org/10.1136/bmj.n2239
5. Wang H, Paulson KR, Pease SA, Watson S, Comfort H, Zheng P, et al.; COVID-19 Excess Mortality Collaborators. Estimating excess mortality due to the COVID-19 pandemic: a systematic analysis of COVID-19-related mortality, 2020–21. Lancet. 2022;399:1513–36. https://doi.org/10.1016/S0140-6736(21)02796-3
6. Weinberger DM, Chen J, Cohen T, Crawford FW, Mostashari F, Olson D, et al. Estimation of excess deaths associated with the COVID-19 pandemic in the United States, March to May 2020. JAMA Intern Med. 2020;180:1336–44. https://doi.org/10.1001/jamainternmed.2020.3391
7. Stokes AC, Lundberg DJ, Elo IT, Hempstead K, Bor J, Preston SH. COVID-19 and excess mortality in the United States: a county-level analysis. PLoS Med. 2021;18:e1003571. https://doi.org/10.1371/journal.pmed.1003571
8. Rivera R, Rosenbaum JE, Quispe W. Excess mortality in the United States during the first three months of the COVID-19 pandemic. Epidemiol Infect. 2020;148:e264. https://doi.org/10.1017/S0950268820002617
9. Aliseda-Alonso A, Lis SB, Lee A, Pond EN, Blauer B, Rutkow L, et al. The missing COVID-19 demographic data: a statewide analysis of COVID-19-related demographic data from local government sources and a comparison with federal public surveillance data. Am J Public Health. 2022;112:1161–9. https://doi.org/10.2105/AJPH.2022.306892
10. Kiang MV, Irizarry RA, Buckee CO, Balsari S. Every body counts: measuring mortality from the COVID-19 pandemic. Ann Intern Med. 2020;173:1004–7. https://doi.org/10.7326/M20-3100
11. Setel P, AbouZahr C, Atuheire EB, Bratschi M, Cercone E, Chinganya O, et al. Mortality surveillance during the COVID-19 pandemic. Bull World Health Organ. 2020;98:374. https://doi.org/10.2471/BLT.20.263194
12. Centers for Disease Control and Prevention. Influenza [cited 2023 Mar 9]. https://www.cdc.gov/nchs/fastats/flu.htm
13. Gundlapalli AV, Lavery AM, Boehmer TK, Beach MJ, Walke HT, Sutton PD, et al. Death certificate–based ICD-10 diagnosis codes for COVID-19 mortality surveillance—United States, January–December 2020. MMWR Morb Mortal Wkly Rep. 2021;70:523–7. https://doi.org/10.15585/mmwr.mm7014e2
14. Council of State and Territorial Epidemiologists. CSTE revised COVID-19-associated death classification guidance for public health surveillance programs [cited 2023 Mar 14]. https://preparedness.cste.org/wp-content/uploads/2022/12/CSTE-Revised-Classification-of-COVID-19-associated-Deaths.Final_.11.22.22.pdf
15. DeVries A, Lees C, Rainbow J, Lynfield R. Explaining the unexplained: identifying infectious causes of critical illness and death in Minnesota. Minn Med. 2008;91:34–6.
16. Minnesota Department of Health. Medical Examiner Infectious Deaths Surveillance Program (MED-X) [cited 2023 Mar 14]. https://www.health.state.mn.us/diseases/unex/me/index.html
17. Harris PA, Taylor R, Thielke R, Payne J, Gonzalez N, Conde JG. Research electronic data capture (REDCap)—a metadata-driven methodology and workflow process for providing translational research informatics support. J Biomed Inform. 2009;42:377–81. https://doi.org/10.1016/j.jbi.2008.08.010
18. Harris PA, Taylor R, Minor BL, Elliott V, Fernandez M, O'Neal L, et al.; REDCap Consortium. The REDCap Consortium: building an international community of software platform partners. J Biomed Inform. 2019;95:103208. https://doi.org/10.1016/j.jbi.2019.103208
19. Clay SL, Woodson MJ, Mazurek K, Antonio B. Racial disparities and COVID-19: exploring the relationship between race/ethnicity, personal factors, health access/affordability, and conditions associated with an increased

severity of COVID-19. Race Soc Probl. 2021;13:279–91. https://doi.org/10.1007/s12552-021-09320-9
20. Chunara R, Zhao Y, Chen J, Lawrence K, Testa PA, Nov O, et al. Telemedicine and healthcare disparities: a cohort study in a large healthcare system in New York City during COVID-19. J Am Med Inform Assoc. 2021;28:33–41. https://doi.org/10.1093/jamia/ocaa217
21. Gupta A, Premnath N, Kuo PL, Sedhom R, Brawley OW, Chino F. Assessment of racial differences in rates of autopsy in the US, 2008–2017. JAMA Intern Med. 2020;180:1123–4. https://doi.org/10.1001/jamainternmed.2020.2239
22. Firestone MJ, Thorell L, Kollmann L, Fess L, Ciessau G, Strain AK, et al.; UNEX Surveillance Team. Surveillance for unexplained deaths of possible infectious etiologies during the COVID-19 pandemic—Minnesota, 2020–2021. Public Health Rep. 2024;139:325–32. https://doi.org/10.1177/00333549231218283
23. Goraya TY, Jacobsen SJ, Belau PG, Weston SA, Kottke TE, Roger VL. Validation of death certificate diagnosis of out-of-hospital coronary heart disease deaths in Olmsted County, Minnesota. Mayo Clin Proc. 2000;75:681–7. https://doi.org/10.1016/S0025-6196(11)64613-2
24. Wu EL, Kumar RN, Moore WJ, Hall GT, Vysniauskaite I, Kim KA, et al. Disparities in COVID-19 monoclonal antibody delivery: a retrospective cohort study. J Gen Intern Med. 2022;37:2505–13. https://doi.org/10.1007/s11606-022-07603-4
25. Wiltz JL, Feehan AK, Molinari NM, Ladva CN, Truman BI, Hall J, et al. Racial and ethnic disparities in receipt of medications for treatment of COVID-19—United States, March 2020–August 2021. MMWR Morb Mortal Wkly Rep. 2022;71:96–102. https://doi.org/10.15585/mmwr.mm7103e1
26. Gu T, Mack JA, Salvatore M, Prabhu Sankar S, Valley TS, Singh K, et al. Characteristics associated with racial/ethnic disparities in COVID-19 outcomes in an academic health care system. JAMA Netw Open. 2020;3:e2025197. https://doi.org/10.1001/jamanetworkopen.2020.25197
27. Izzy S, Tahir Z, Cote DJ, Al Jarrah A, Roberts MB, Turbett S, et al. Characteristics and outcomes of Latinx patients with COVID-19 in comparison with other ethnic and racial groups. Open Forum Infect Dis. 2020;7:ofaa401.
28. Silver V, Chapple AG, Feibus AH, Beckford J, Halapin NA, Barua D, et al. Clinical characteristics and outcomes based on race of hospitalized patients with COVID-19 in a New Orleans cohort. Open Forum Infect Dis. 2020;7:ofaa339.
29. Azar KMJ, Shen Z, Romanelli RJ, Lockhart SH, Smits K, Robinson S, et al. Disparities in outcomes among COVID-19 patients in a large health care system in California. Health Aff (Millwood). 2020;39:1253–62. https://doi.org/10.1377/hlthaff.2020.00598
30. Killerby ME, Link-Gelles R, Haight SC, Schrodt CA, England L, Gomes DJ, et al.; CDC COVID-19 Response Clinical Team. Characteristics associated with hospitalization among patients with COVID-19—metropolitan Atlanta, Georgia, March–April 2020. MMWR Morb Mortal Wkly Rep. 2020;69:790–4. https://doi.org/10.15585/mmwr.mm6925e1
31. Muñoz-Price LS, Nattinger AB, Rivera F, Hanson R, Gmehlin CG, Perez A, et al. Racial disparities in incidence and outcomes among patients with COVID-19. JAMA Netw Open. 2020;3:e2021892. https://doi.org/10.1001/jamanetworkopen.2020.21892
32. Kim HN, Lan KF, Nkyekyer E, Neme S, Pierre-Louis M, Chew L, et al. Assessment of disparities in COVID-19 testing and infection across language groups in Seattle, Washington. JAMA Netw Open. 2020;3:e2021213. https://doi.org/10.1001/jamanetworkopen.2020.21213
33. Mody A, Pfeifauf K, Bradley C, Fox B, Hlatshwayo MG, Ross W, et al. Understanding drivers of coronavirus disease 2019 (COVID-19) racial disparities: a population-level analysis of COVID-19 testing among black and white populations. Clin Infect Dis. 2021;73:e2921–31. https://doi.org/10.1093/cid/ciaa1848
34. D'ascanio M, Innammorato M, Pasquariello L, Pizzirusso D, Guerrieri G, Castelli S, et al. Age is not the only risk factor in COVID-19: the role of comorbidities and of long staying in residential care homes. BMC Geriatr. 2021;21:63. https://doi.org/10.1186/s12877-021-02013-3
35. Coady SA, Sorlie PD, Cooper LS, Folsom AR, Rosamond WD, Conwill DE. Validation of death certificate diagnosis for coronary heart disease: the Atherosclerosis Risk in Communities (ARIC) Study. J Clin Epidemiol. 2001;54:40–50. https://doi.org/10.1016/S0895-4356(00)00272-9
36. Temkin-Greener H, Zheng NT, Xing J, Mukamel DB. Site of death among nursing home residents in the United States: changing patterns, 2003–2007. J Am Med Dir Assoc. 2013;14:741–8. https://doi.org/10.1016/j.jamda.2013.03.009
37. Tran OC, Lucero DE, Balter S, Fitzhenry R, Huynh M, Varma JK, et al. Sensitivity and positive predictive value of death certificate data among deaths caused by Legionnaires' disease in New York City, 2008–2013. Public Health Rep. 2018;133:578–83.
38. Lieberman-Cribbin W, Tuminello S, Flores RM, Taioli E. Disparities in COVID-19 testing and positivity in New York City. Am J Prev Med. 2020;59:326–32. https://doi.org/10.1016/j.amepre.2020.06.005
39. Dean S, Litzky L, Fuchs B, Cambor C. Assessing the accuracy of death certificate completion by physicians using the "death module": an academic institution's experience with an electronic death registration program. Am J Clin Pathol. 2012;138(suppl_2):A130. https://doi.org/10.1093/ajcp/138.suppl2.11
40. McGivern L, Shulman L, Carney JK, Shapiro S, Bundock E. Death certification errors and the effect on mortality statistics. Public Health Rep. 2017;132:669–75. https://doi.org/10.1177/0033354917736514

Address for correspondence: Lydia J. Fess, Minnesota Department of Health, Infectious Disease Epidemiology, Prevention, and Control, 625 Robert St N, Saint Paul, MN 55155, USA; email: lydia.fess@state.mn.us

Sialic Acid Receptor Specificity in Mammary Gland of Dairy Cattle Infected with Highly Pathogenic Avian Influenza A(H5N1) Virus

Rahul K. Nelli,[1] Tyler A. Harm,[1] Chris Siepker,[1] Jennifer M. Groeltz-Thrush, Brianna Jones, Ning-Chieh Twu, Ariel S. Nenninger, Drew R. Magstadt, Eric R. Burrough, Pablo E. Piñeyro, Marta Mainenti, Silvia Carnaccini, Paul J. Plummer, Todd M. Bell

In March 2024, the US Department of Agriculture's Animal and Plant Health Inspection Service reported detection of highly pathogenic avian influenza (HPAI) A(H5N1) virus in dairy cattle in the United States for the first time. One factor that determines susceptibility to HPAI H5N1 infection is the presence of specific virus receptors on host cells; however, little is known about the distribution of the sialic acid (SA) receptors in dairy cattle, particularly in mammary glands. We compared the distribution of SA receptors in the respiratory tract and mammary gland of dairy cattle naturally infected with HPAI H5N1. The respiratory and mammary glands of HPAI H5N1–infected dairy cattle are rich in SA, particularly avian influenza virus–specific SA α2,3-gal. Mammary gland tissues co-stained with sialic acids and influenza A virus nucleoprotein showed predominant co-localization with the virus and SA α2,3-gal. HPAI H5N1 exhibited epitheliotropism within the mammary gland, and we observed rare immunolabeling within macrophages.

The recent discovery that dairy cattle can be infected by highly pathogenic avian influenza (HPAI) virus of the H5N1 subtype (*1*,*2*), in combination with the virus's propensity to replicate in the mammary gland, has raised many questions and is causing fresh concerns about HPAI H5N1 spread (*3*). Detection of high levels of viral RNA in the milk during the acute stage of infection (*1*) has triggered public health alerts and premovement testing requirements (*4*), and has suggested the potential for the presence of the virus in unpasteurized milk.

HPAI H5N1 clade 2.3.4.4b virus was first detected in wild birds in the United States in late 2021 (*5*–*7*) and spread widely across North America (*7*,*8*). In early 2022, HPAI H5N1 virus began causing outbreaks in commercial and backyard poultry flocks. The US Department of Agriculture's Animal and Plant Health Inspection Service reported >6,400 cases in wild birds in 49 states and >790 backyard flocks in 47 states during January 2022–March 2023 (*7*). The widespread distribution of HPAI H5N1 virus eventually spilled into multiple mammal species within those areas, often presumably because of the consumption of infected wild birds (*8*). By the end of 2023, HPAI H5N1 had been reported in >20 different mammal species in the United States (*9*). Dairy cattle were affected in the spring of 2024, when multiple dairy herds were determined to be positive for HPAI H5N1 clade 2.3.4.4b virus (*1*,*2*). On the basis of genetic sequencing, this introduction into dairy cattle is thought to be from a wild bird source (*1*,*2*).

A major determinant of a virus-host range is receptor availability (*9*,*10*). Influenza A viruses (IAVs) use host sialic acids as their receptors for initial attachment and entry into the cells. Sialic acids (SAs) are a diverse group of 9-carbon carboxylated monosaccharides synthesized in animal species. IAVs from avian species have been shown to preferentially bind to SA receptors linked to galactose by an α2,3-galactose linkage (SA α2,3-gal). More specifically, IAVs from chickens preferentially bound to SA α2,3-gal-β (1–4)

Author affiliations: Iowa State University College of Veterinary Medicine, Ames, Iowa, USA (R.K. Nelli, T.A. Harm, C. Siepker, J.M. Groeltz-Thrush, B. Jones, N.-C. Twu, A.S. Nenninger, D.R. Magstadt, E.R. Burrough, P.E. Piñeyro, M. Mainenti, P.J. Plummer, T.M. Bell); University of Georgia, Athens, Georgia, USA (S. Carnaccini)

DOI: https://doi.org/10.3201/eid3007.240689

[1]These first authors contributed equally to this article.

N-acetylglucosamine (GlcNAc), whereas IAVs from ducks displayed a higher affinity for SA α2,3-gal-β (1–3) N-acetylgalactosamine (GalNAc) (*10*). IAVs originating from human and classical swine viruses prefer SA receptors with an α2,6-galactose linkage (SA α2,6-gal) (*10*–*14*). Various methods have been used to characterize the SA receptor distribution profiles among multiple host species. Plant lectin binding affinity toward SA is used to study SA distribution in animal tissues (*15*). Plant lectins from the species *Sambucus nigra* (SNA) are routinely used to detect α2,6-linked SA; *Maackia amurensis* lectin–I (MAL-I) is used to detect SA α2,3-gal-β (1–4) GlcNAc and *M. amurensis* lectin–II (MAL-II) to detect SA α2,3-gal-β (1–3) GalNAc.

We explored the presence and distribution of cellular and receptor factors that enable HPAI H5N1 virus infection in Holstein dairy cattle. The previously reported index cases highlighted a multifocal or segmental distribution of IAV within provided mammary gland samples (*1*). This type of distribution was of particular interest regarding potential binding sites within the lactiferous tree. Specifically, our study reports the expression and distribution of SA receptors using lectin histochemistry and viral binding assay in the bovine respiratory tract and mammary glands of dairy cattle that were affected with HPAI H5N1 clade 2.3.4.4b virus (A/dairy_cattle/Texas/24_009110). Our study seeks to uncover the underlying reasons behind the uncommon mammary gland infection by HPAI H5N1 virus.

Materials and Methods

Sample Collection

We used formalin-fixed and paraffin-embedded sections of trachea, lung, and mammary gland tissues, as well as milk in EDTA tubes, from 2 adult Holstein dairy cows in Texas, USA, diagnosed with HPAI H5N1 virus infection at the Iowa State University Veterinary Diagnostic Laboratory (Ames, IA, USA) on March 2024 (*1*). The cows reportedly exhibited a nonspecific illness, including reduced lactation and thickened, yellow milk with a similar appearance to colostrum. The diagnosis was based on detection of HPAI H5N1 IAV by real-time reverse transcription PCR (rRT-PCR) in the mammary gland and lung, as well as by detecting IAV nucleoprotein by immunohistochemistry in the mammary glands (*1*). In addition, we confirmed affected tissue sections to be positive for IAV matrix gene nucleic acid by RNAscope in situ hybridization assay (Appendix Figure 1, https://wwwnc.cdc.gov/EID/article/30/7/24-0689-App1.pdf). Testing of macroscopic and microscopic lesions, including IAV chromogenic immunohistochemistry and rRT-PCR, was previously described (*1*). The mammary glands from the cows had a multifocal lesion pattern, which enabled the dissection of affected and unaffected regions of the mammary gland. We used unaffected regions as control tissue. To be classified as unaffected, the sections could not have any inflammation or epithelial changes. In addition, unaffected sections were required to have a negative IAV immunohistochemistry result.

Cytologic Evaluation of Milk Sample

We used milk from EDTA tubes to make direct smears onto cytocentrifuged slides. We performed cytocentrifugation of milk by using a Shandon Cytospin3 (ThermoFisher Scientific, https://www.thermofisher.com) at 72 g for 10 minutes (low acceleration). We prepared air-dried slides and stained them with modified Wright stain on an automated stainer (Siemens Healthineers, https://www.siemens-healthineers.com). We determined differential cell counts under ×1,000 original magnification by counting 100 nucleated cells.

Fluorescently Labeled Dual Lectin and Immunochemistry Staining

We characterized mammary tissues for sialic acids by using an automated adaptation of a lectin histochemistry assay previously described (*16*) combined with influenza A nucleoprotein (IAV-Np) staining. We sectioned formalin-fixed, paraffin-embedded tissue sections of the bovine mammary gland at 4 μm with placement on Superfrost Plus slides (VWR International, https://www.vwr.com). We dried slides at 60°C for 20 minutes before deparaffinization and staining on the Ventana Discovery Ultra research platform (Roche Diagnostics, https://diagnostics.roche.com). We accomplished heat retrieval by using cell conditioning solution at 100°C for 24 minutes (Roche Diagnostics). We blocked slides with 1X Carbo-Free blocking solution (Vector Laboratories, https://vectorlabs.com) for 32 minutes, then used a Streptavidin/Biotin Blocking Kit (Vector Laboratories) with a separate application each of 12 minutes. We incubated the sections for 4 hours at room temperature with 1 of the 3 lectins (SNA, MAL-I, MAL-II) from Vector Laboratories at the specified concentrations (Appendix Table) (*17*), where SNA is specific for α2,6-gal/GalNAc, MAL-I is specific for N-linked or O-linked glycans with SAα2,3-gal-β (1–4) GlcNAc, and MAL-II is specific for O-linked glycans with SA α2,3-gal-β (1–3) GalNAc. After lectin incubation, we applied streptavidin conjugated with Alexa Fluor 647 (ThermoFisher Scientific) and incubated the sections for 2 hours at room temperature.

We performed immunostaining with IAV-Np by incubating sections with rabbit recombinant monoclonal anti-nucleoprotein for IAV labeled with DyLight 594 (Novus Biologicals, https://www.novusbio.com) for 4 hours at room temperature. We manually performed counterstaining and mounting with Prolong Gold antifade mountant with DAPI (ThermoFisher Scientific). Negative assay controls consisted of primary lectin or antibody omission. We evaluated nonspecific lectin labeling by using sialidase-A treated sections (Appendix). We performed positive lectin assay controls on porcine tissues because lectin labeling has been previously established (*17*). We also performed positive IAV-Np controls on porcine lung tissue with known IAV infection status (data not shown). We performed multicolor fluorescent staining by using lectin and IAV-Np assay to aid co-labeling.

We conducted multicolor immunofluorescent staining by using mouse monoclonal anti-human cytokeratin, Clone AE1/AE3 (Agilent Technologies, https://www.agilent.com), and rabbit monoclonal anti-ionized calcium binding adaptor molecule 1 (Iba1) (Abcam, https://www.abcam.com), along with the primary IAV-Np antibody previously described (Appendix Table). Modifications to this lectin-antibody procedure include heat retrieval with cell conditioning solution for 48 minutes at 100°C, replacing the lectin with an antibody incubation at 37°C (Iba1 at 60 minutes and cytokeratin at 32 minutes), as well as incubation of a Biotinylated Link from a Universal LSAB2 Kit (Agilent Technologies) for 1 hour before application of the streptavidin conjugate. We then examined slides and imaged them by using a BX-53 Olympus trinocular microscope equipped with an Olympus DP23 camera, Excelitas X-Cite mini+ compact illumination system, and CellSyns Dimension software.

Results

We selected retrospectively collected respiratory tract and mammary gland samples from 2 naturally infected lactating Holstein dairy cows with HPAI H5N1 virus infections for evaluation. The clinicopathologic manifestations, detection methods, and sequencing data pertaining to the dairy cows in this study have been previously reported (*1*,*2*).

In brief, the HPAI H5N1 virus–infected mammary gland had acute multifocal moderate mastitis with epithelial attenuation lining the secretory alveoli and interlobular ducts, as well as intraluminal neutrophilic inflammation (Figure 1, panel A, C). Immunohistochemistry for IAV-Np on the affected mammary gland showed intranuclear and intracytoplasmic immunoreactivity in alveolar and interlobular ductal epithelial cells (Figure 1, panel B, D). We examined the milk from the affected gland cytologically, which had not previously been reported. Routine cytologic assessment identified moderate to marked neutrophilic and mild macrophagic inflammation consistent with mastitis (Figure 1, panel E, F).

We considered the evaluation of bovine tissue distribution for SA α2–3 and SA α2–6 receptors to be warranted, given the detection of HPAI H5N1 virus and lesion development in the dairy cows. We evaluated the distribution of SA α2–3 and SA α2–6 receptors in the respiratory and mammary tissues from the cows through fluorescent and chromogenic-based lectin histochemistry.

Both fluorescent and chromogenic lectin histochemistry methodologies concur with the distribution of lectins (Table; Figures 2, 3). We only observed SNA labeling in goblet cells, submucosal glands, and intraepithelial and lamina proprial immune cells (suspected to be lymphocytes) of the trachea and bronchi (Figure 2; Figure 3, panels C, F). MAL-I and MAL-II labeling was multifocal, weak to moderate, apical, and membranous in the respiratory epithelium of the trachea (Figure 2; Figure 3, panels A, B). MAL-I and MAL-II labeling in the tracheal and bronchial goblet cells and submucosal glandular epithelial cells was intense, granular, and cytoplasmic (Figure 2; Figure 3, panels A, B, D, E). However, MAL-I and MAL-II labeling differed in the bronchial respiratory epithelium, where MAL-I labeling (Figure 2; Figure 3, panel D) was more diffuse, whereas MAL-II labeling (Figure 2; Figure 3, panel E) was multifocal. MAL-I (Figure 2; Figure 3, panels G, J) and MAL-II (Figure 2; Figure 3, panels H, K) labeling of the respiratory epithelium was similar in the bronchioles and alveoli, where labeling was diffuse.

In the mammary gland, MAL-II (Figure 4; Figure 5, panels C, D) and SNA (Figure 4; Figure 5, panels E, F) labeling were expressed in unaffected secretory alveoli. We only observed unaffected interlobular ducts to have SNA labeling (Figure 4; Figure 5, panel F) but observed no detectable MAL-I (Figure 4; Figure 5, panels A, B) or IAV-Np labeling in unaffected mammary gland sections. SNA labeling was moderate to intense, granular to fibrillary, membranous to cytoplasmic, and predominately apically located within the alveolar lining epithelium (Figure 4; Figure 5, panel E), and the expression was abundant in the epithelial cells lining the interlobular ducts (Figure 4; Figure 5, panel F). MAL-II labeling was intense, fibrillary, membranous, and exclusively apical (Figure 4; Figure 5, panel C), but we did not not observe MAL-II labeling in interlobular duct epithelium (Figure 4; Figure 5, panel D).

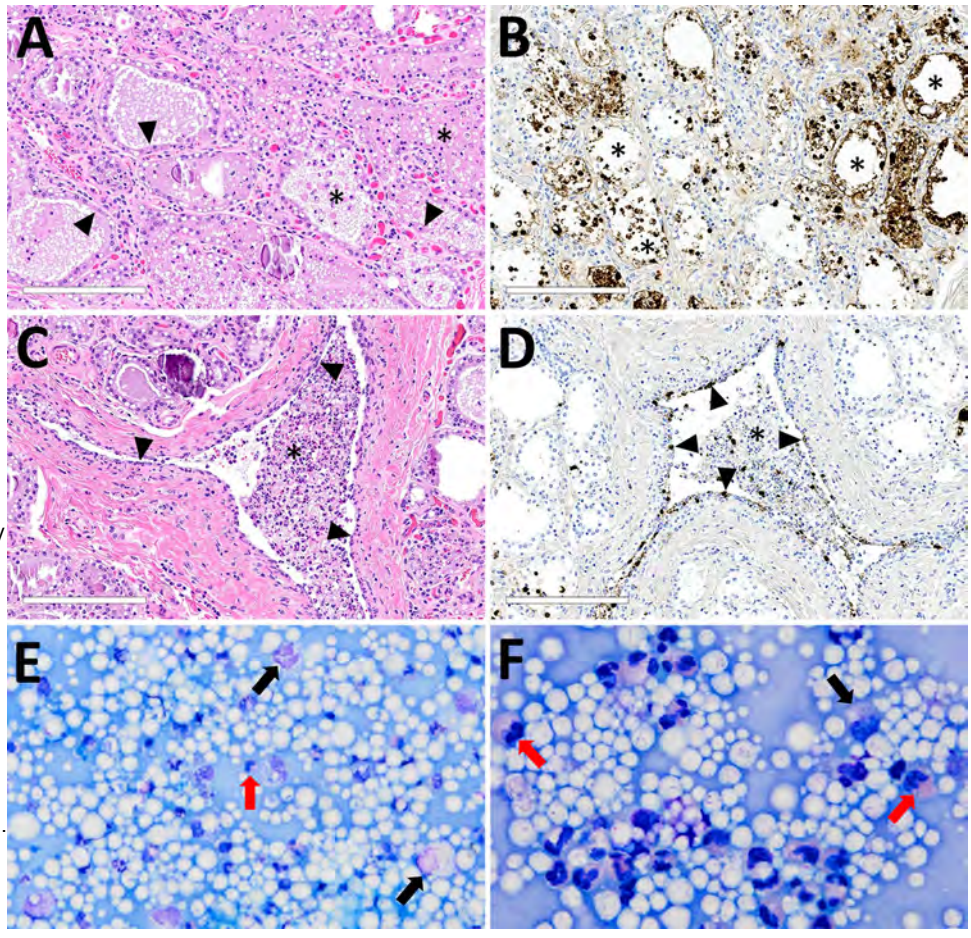

Figure 1. Microscopic mammary lesions of an index case in US dairy cattle naturally infected with highly pathogenic avian influenza A(H5N1) virus clade 2.3.4.4b. A) Mammary gland alveoli show epithelial attenuation and vacuolation (arrows), leading to degeneration with intraluminal sloughing and neutrophilic intraluminal inflammation (asterisk). Hematoxylin and eosin stain. B) Mammary glad alveoli show degenerative epithelial cells (asterisks) and strong intracytoplasmic and nuclear immunoreactivity to influenza A virus nucleoprotein. C) Cuboidal epithelium lining of the interlobular duct was markedly attenuated (arrowheads) with abundant intraluminal sloughing and neutrophilic inflammation (asterisk). Hematoxylin and eosin stain. D) Interlobular duct shows of attenuating and degenerative epithelium by intranuclear and cytoplasmic immunoreactivity (brown labeling) with immunopositive intraluminal debris and inflammation (asterisk). Scale bars indicate 200 μm. E, F) Modified Wright's stained representative cytology images of milk from a dairy cow with highly pathogenic avian influenza A(H5N1) virus infection, demonstrating moderate to marked neutrophilic inflammation (red arrows) with low numbers of vacuolated macrophages (black arrows) among large numbers of lipid vacuoles. A 100-cell count was performed, and nucleated cells were found to consist of 83% neutrophils, 12% macrophages, and 5% lymphocytes. Original magnifications ×500 for panel E and ×1,000 for panel F.

Overall, lectin histochemistry results within unaffected (i.e., respiratory tract and mammary gland) and affected (i.e., mammary gland) tissues closely mirrored fluorescent microscopic findings (Table). Not surprisingly, the sensitivity and localization of labeling with chromogenic, lectin-based assays were not as definitive as fluorescent labeling. We detected no MAL-I labeling in the mammary gland with lectin histochemistry.

As described previously, the HPAI H5N1 virus–infected mammary gland had multifocal acute moderate mastitis with prominent epithelial changes in the secretory alveoli and ducts with sloughed intraluminal

Table. Distribution of α2,3 and α2,6 receptors with influenza A virus nucleoprotein in the respiratory tract and mammary gland of US dairy cattle naturally infected with highly pathogenic avian influenza A(H5N1) virus*

Site	MAL-I	MAL-II	SNA	IAV-Np
Respiratory tract				
Tracheal epithelium	+ (mem, goblet)	+ (mem, goblet)	+/− (goblet)	–
Bronchial epithelium	+ (mem, goblet)	+ (mem, goblet)	–	–
Bronchiolar epithelium	+ (mem)	+ (mem)	–	–
Pneumocytes, alveolus	+ (mem)	+ (mem)	–	–
Mammary gland				
Glandular epithelium	–	+ (mem)	+ (mem)	+ (IN, IC)
Interlobular ductal epithelium	–	–	+ (mem)	+ (IN, IC)

*Goblet, goblet cells; IC, intracytoplasmic; IN, intranuclear; IAV-Np, influenza A virus nucleoprotein; MAL, *Maackia amurensis* lectin; mem, membranous; SNA, *Sambucus nigra* lectin; –, no labeling observed; +, positive labeling.
†α2,3-gal-β (1–4) N-acetylglucosamine.
‡α2,3-gal-β (1–3) N-acetylgalactosamine.
§α2,6-gal.

epithelial cells, macrophages, and neutrophils (Figure 6, panel A). We used pancytokeratin (epithelial marker) and Iba1 (macrophage marker) to evaluate the intracellular distribution of IAV-Np. We observed co-labeling of IAV-Np labeling with pan-cytokeratin in cells lining the secretory alveoli and interlobular ducts (Figure 6, panels B, C). IAV-Np labeling was more widely distributed and intense in the secretory alveolar epithelium than in the ductal epithelium. Some intraluminal cells within secretory alveoli and ducts had both intranuclear and cytoplasmic IAV-Np expression. Intraluminal cells are commonly labeled with pancytokeratin (sloughed epithelial cells) and rare Iba1-positive cells (macrophages) (Figure 6, panels B, D). Interstitial Iba1-labeled cells did not have IAV-Np co-labeling (Figure 6, panel D). We observed co-labeling with intranuclear IAV-Np labeling and MAL-II (Figure 7; Figure 8, panel C) and SNA (Figure 7; Figure 8, panel E) in epithelial cells lining the secretory alveoli. We observed only co-labeling with intranuclear IAV-Np labeling and SNA in the ductal epithelial cells (Figure 7; Figure 8, panel F), given that we did not observe MAL-II labeling in

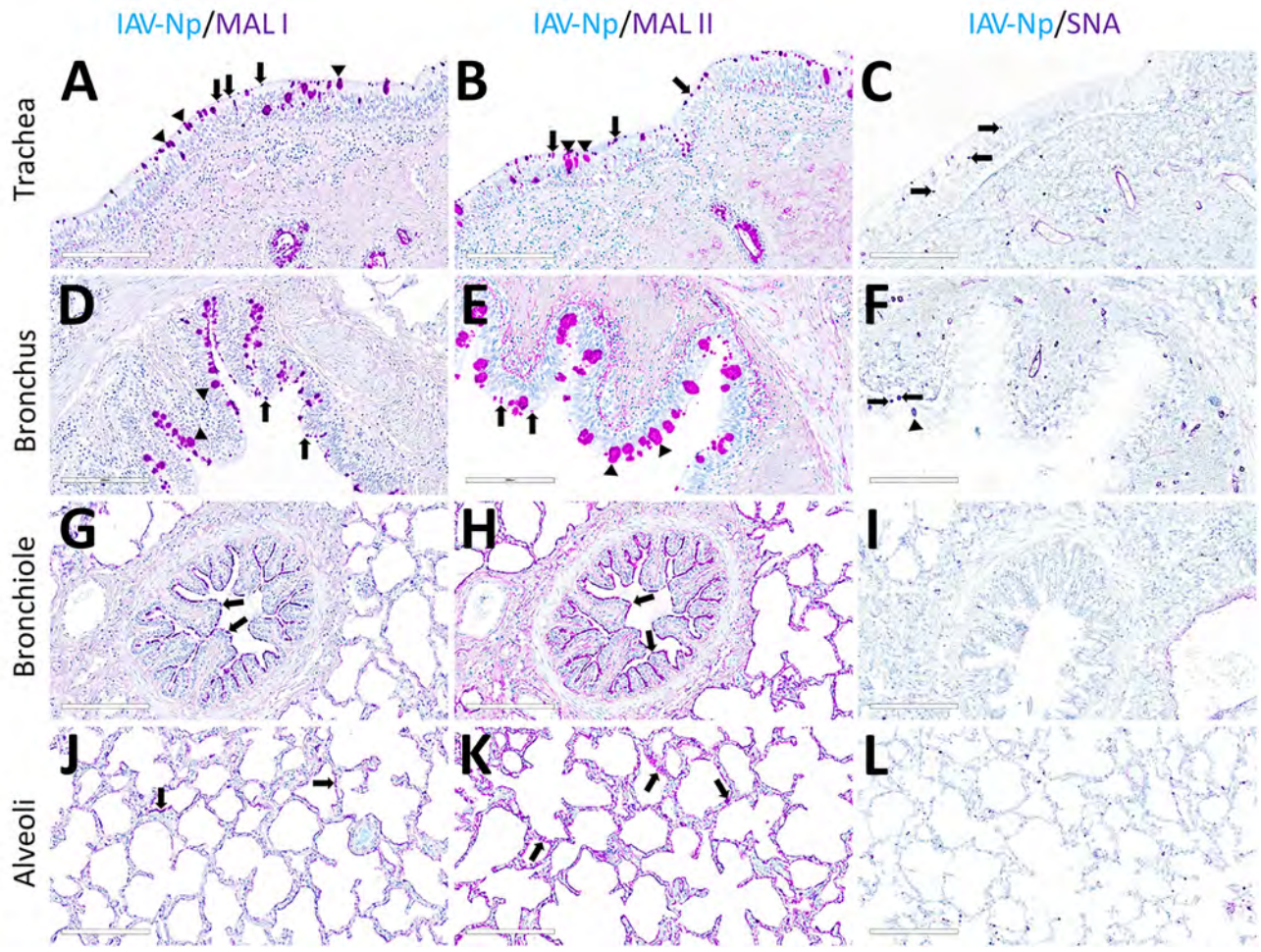

Figure 2. Respiratory tract tissues from a US dairy cow infected with highly pathogenic avian influenza A(H5N1) virus, showing IAV-Np (teal chromogen), individually duplexed with MAL-I (magenta chromogen), MAL-II (magenta chromogen), and SNA (magenta chromogen) using chromogenic staining. Representative images are shown for IAV-Np/MAL-I (A, D, G, J), IAV-Np/MAL-II (B, E, H, K), and IAV-Np/SNA (C, F, I, L) are shown. No IAV-Np was observed in the unaffected respiratory tissue sections. Intense granular to punctate labeling for MAL-I (A) and MAL-II (B) were observed within goblet cells (arrowheads), along the apical ciliated margin (arrows), and glands of the trachea. SNA labeling (C) was confined to intraepithelial round cells (arrows), endothelium, and glands of the trachea. Similar labeling for MAL-I (D) and MALII (E) was observed within the bronchial lumen within goblet cells (arrowheads) and along the apical cell margin (arrows). SNA (F) labeling was only observed in rare goblet cells (arrowheads) and lamina proprial round cells (arrows) in the bronchus. Bronchioles had diffuse, fine, fibrillary to apical membranous labeling (arrows) MAL-I (G) and MALII (H). No substantial labeling was detected within the mucosal epithelial cells of bronchioles with SNA (I). Diffuse, fine, apical membranous labeling of pneumocytes lining alveoli was observed with MAL-I (J) and MAL-II (K) (arrows). SNA (L) labeling within the alveolar portions of the lung was confined to endothelium and interstitial round cells. Scale bars indicate 200 μm. IAV-Np, influenza A virus nucleoprotein; MAL, *Maackia amurensis* lectin; SNA, *Sambucus nigra* lectin.

the ducts (Figure 7; Figure 8, panel D). MAL-I labeling could not be detected with IAV-Np because MAL-I labeling was not observed in the secretory alveoli or ducts (Figure 7; Figure 8, panels A, B).

Discussion

The presence of HPAI H5N1 virus in dairy cattle, more so in the mammary gland and milk, once again highlights the importance of IAV adaptability to

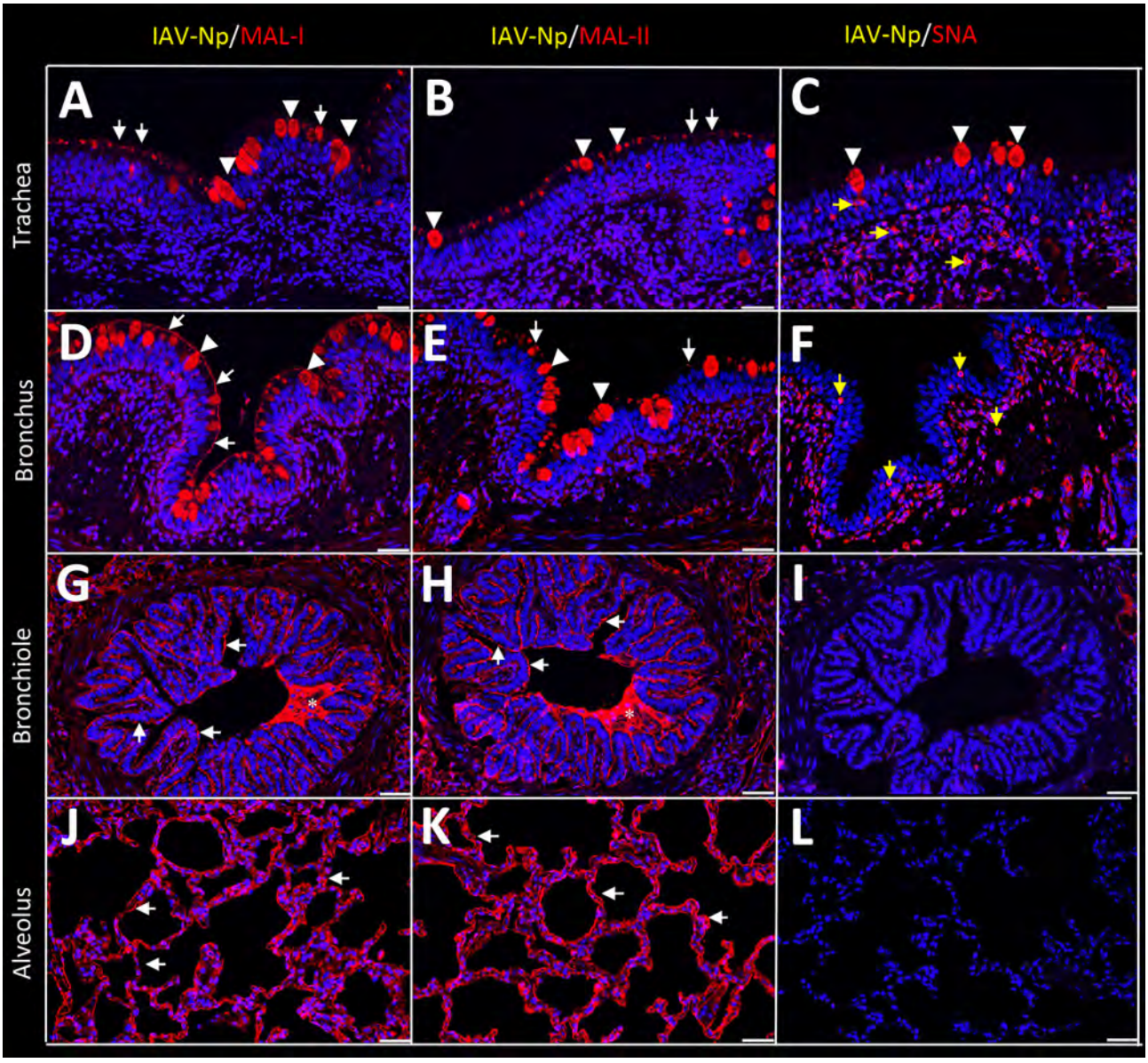

Figure 3. Respiratory tract tissues from a US dairy cow infected with highly pathogenic avian influenza A(H5N1) virus, labeled with IAV-Np (yellow pseudocolor, DyLight 594), individually duplexed with MAL-I (red pseudocolor, Alexa Fluor 647), MAL-II (red pseudocolor, Alexa Fluor 647), and SNA (red pseudocolor, Alexa Fluor 647) using fluorescent staining. Representative merged images are shown for IAV-Np and MAL-I (A, D, G, J), IAV-Np and MAL-II (B, E, H, K), and IAV-Np and SNA (C, F, I, L). IAV-Np labeling was not detected within the respiratory tissue sections. Intense, granular to punctate, cytoplasmic MAL-I, MAL-II, and SNA labeling was observed in goblet cells (arrowheads) and glands of the trachea (A–C). Similar goblet cell labeling (arrowheads) for MAL-I (D) and MAL-II (E) was observed in the bronchi with weak SNA labeling (F). Multifocal, moderate, fibrillar, apical, membranous MAL-I (A) and MAL-II (B) labeling (white arrows) was observed on the tracheal epithelium. The respiratory epithelium of the bronchi, bronchioles, and alveoli had diffuse, moderate to intense, apical, fibrillar MAL-I labeling (white arrows) (D, G, J). The respiratory epithelium of the bronchi had multifocal, moderate, fibrillar, apical MAL-II labeling (white arrows) (E). The respiratory epithelium of the bronchioles and alveoli had diffuse MAL-II labeling (white arrows) (H, K). Intraluminal secretory material (asterisks) in the bronchi and bronchioles were intensely labeled with MAL-I and MAL-II (G, H). Membranous, granular SNA labeling (yellow arrows) was observed in intraepithelial and lamina proprial round cells in the trachea and bronchi (C, F). Scale bars indicate 50 μm. IAV-Np, influenza A virus nucleoprotein; MAL, *Maackia amurensis* lectin; SNA, *Sambucus nigra* lectin.

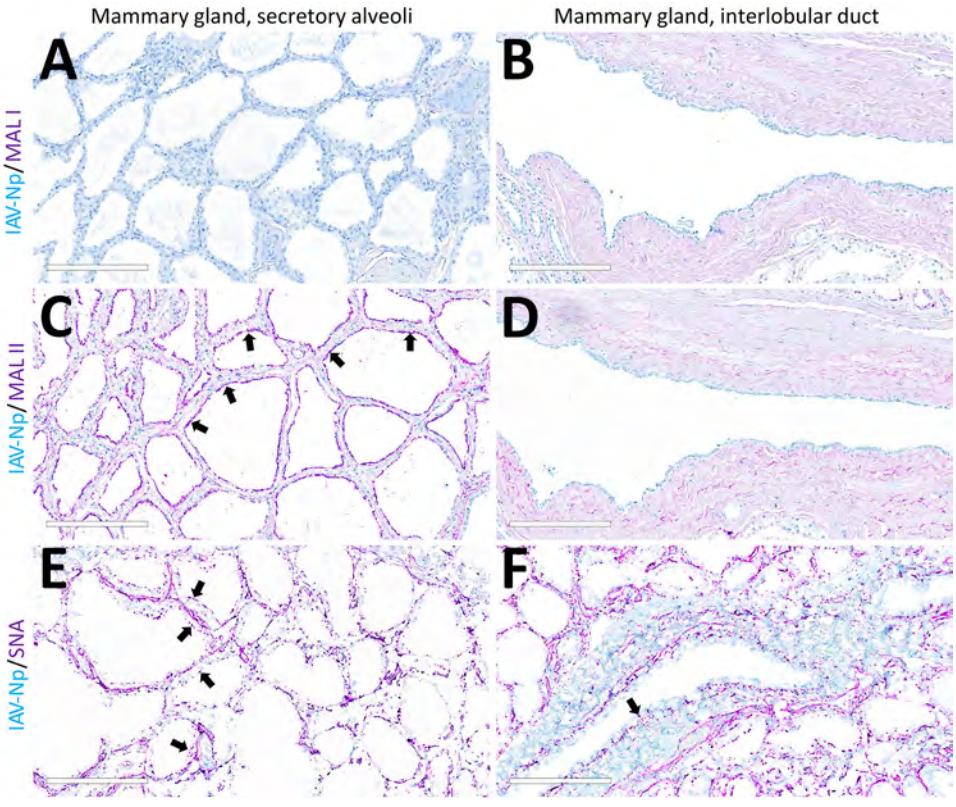

Figure 4. Unaffected region of the mammary gland from a US dairy cow infected with highly pathogenic avian influenza A(H5N1) virus, showing IAV-Np (teal chromogen), individually duplexed with MAL-I (magenta chromogen), MAL-II (magenta chromogen), and SNA (magenta chromogen) using chromogenic staining. Representative images of IAV-Np/MAL-I (A, B), IAV-Np/MAL-II (C, D), and IAV-Np/SNA (E, F) showing no IAV-Np labeling within unaffected mammary gland tissue sections. No MAL-I was detected in the mammary glandular (A) or interlobular duct epithelium (B). Within the alveolar gland epithelium, intense, granular, fibrillar labeling (arrows) of the apical portion labeling of MAL-II (C) was noted, with no epithelial labeling within the interlobular duct (D). Multifocal, strong, punctate, apical labeling (arrows) with SNA was observed within the mammary glandular epithelium (E). Scant apical labeling (arrow) was observed within the interlobular ductal epithelium with SNA (F). Scale bars indicate 200 μm. IAV-Np, influenza A virus nucleoprotein; MAL, *Maackia amurensis* lectin; SNA, *Sambucus nigra* lectin.

other nontraditional species and cross-species transmission. This finding reiterates the need for active IAV surveillance efforts in animal species. Like coronaviruses, IAVs have a broad host range involving avian and mammal species. RNA viruses are inherently error-prone, and infection of new host species gives the virus additional opportunities to replicate and subsequently mutate to be better adapt to novel hosts. Another contributing factor to the broad host range of IAV is the presence of virus SA receptors. Many RNA and DNA viruses, including SARS-CoV-2 (co-receptor), use SA as host receptors for initial attachment and entry into the cells (*18*).

In general, IAVs originating from humans and swine preferentially bind to SA linked to galactose through α2,6 linkage (*14*,*19*), whereas the IAVs of avian and equine species preferentially bind to SA linked to galactose through α2,3 linkage (*10*,*20*,*21*). The susceptibility of a host to IAV infection is determined by the type of SA receptor present on the host cell surface, along with other host factors. Previous studies indicated that the HPAI H5N1 virus preferentially binds to α2,3-linked SA receptors (*22*–*24*) and is expressed abundantly in avian upper airways and their gastrointestinal tracts (*20*,*21*). IAV strains established in mammals, particularly in humans and swine, exhibit a higher tropism or affinity for α2,6-linked SA receptors, which are predominantly expressed on the epithelial lining of their upper airways (*23*,*25*).

SAs are 9-carbon carboxylated monosaccharides synthesized in animals but not in plants (*26*,*27*). The most common forms of SAs are N-acetylneuraminic acid (Neu5Ac) or N-glycoloylneuraminic acid (Neu5Gc) (*26*). Although IAVs bind to both Neu5Ac and Neu5Gc, the role of Neu5Gc was reported to be nonfunctional (*28*,*29*). SAs are also a major component of milk (*30*). Cattle and goat milk predominantly contain Neu5Gc versus Neu5Ac, and their content decreases with the progression of the lactation stage (*31*,*32*).

Our study explores the expression and distribution of SAs in the respiratory tract and mammary glands of Holstein dairy cows naturally infected with HPAI H5N1 virus. The lectins such as SNA, MAL-I, and MAL-II used in this study specifically detect the Neu5Ac form of SA (*12*,*33*). Our findings suggest that SAs are widely expressed in these tissues with predominant SA α2,3-gal-β (1–3) GalNAc (MAL-II), followed by α2,6-linked SA (SNA) and SAα2,3-gal-β

(1–4) GlcNAc (MAL-I). However, the expression and distribution varied across tissues. The lectin binding specificity was further validated in a normal mammary gland of a biobanked slide, in which, after removing SAs (90%) by using sialidase A, lectin expression was negative, and so was low pathogenicity H5 virus binding affinity in those tissues (Appendix Figures 2–4). Although HPAI H5N1 and low pathogenicity avian influenza H5N9 viruses were of completely different clades, the findings suggest that no limitations would exist regarding receptor availability and distribution in the bovine mammary gland for IAVs to bind.

In the respiratory tract, the dairy cows expressed both SAα2,3-gal and SAα2,6-gal. Unlike in pigs and humans (*17*,*19*), the mammal-specific SAα2,6-gal in cattle is mainly confined to the subepithelial region of the trachea, occasionally in the goblet cells and subepithelial glands. The expression of SAα2,3-gal continued on the epithelium of bronchi to alveolar pneumocytes. The findings suggest that avian IAVs have the potential binding affinity to the bovine respiratory tract. In the mammary gland, both SA α2,3-gal-β (1–3) GalNAc (MAL-II) and SAα2,6-gal (SNA) were expressed, and co-localization was mainly observed in the alveolar gland and intralobular duct epithelium, whereas SA α2,3-gal-β (1–4) GlcNAc was minimal and confined to interstitial regions. Mammalian- and avian-origin IAVs might bind to cells in the mammary gland. Our findings were further supported by the co-localization of intranuclear and cytoplasmic IAV-Np of HPAI H5N1 virus in some intraluminal cells within secretory alveoli and ducts, suggesting possible virus replication.

The exact pathogenesis of mastitis caused by HPAI H5N1 virus in dairy cattle remains to be elucidated. The initial evaluation of IAV mastitis in dairy cattle identified strong epitheliotropism on the basis of on histologic, immunohistochemical, and FA evaluation. The intramacrophagic viral IAV-Np could be the result of phagocytosis or active infection with

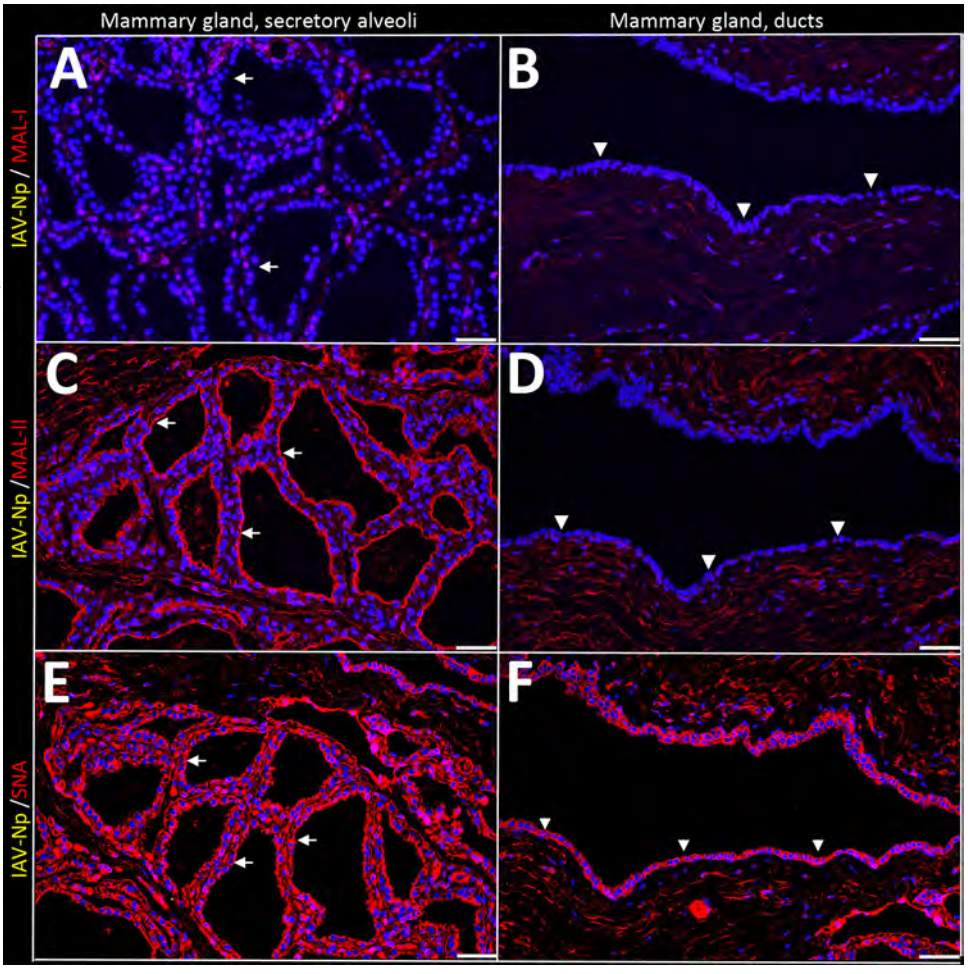

Figure 5. Unaffected region of the mammary gland from a US dairy cow infected with highly pathogenic avian influenza A(H5N1) virus, labeled with IAV-Np (yellow pseudocolor, DyLight 594), individually duplexed with MAL-I (red pseudocolor, Alexa Fluor 647), MAL-II (red pseudocolor, Alexa Fluor 647), and SNA (red pseudocolor, Alexa Fluor 647) using fluorescent staining. Representative merged images of IAV-Np/MAL-I (A, B), IAV-Np/MAL-II (C, D), and IAV-Np/SNA (E, F). IAV-Np labeling was not detected within unaffected mammary gland tissue sections. MAL-I labeling was neither observed in the epithelial cells (white arrows) lining the secretory alveoli (A) nor on the epithelial cells (white arrowheads) lining the interlobular ducts (B). Intense, apical, fibrillary MAL-II labeling was observed in the epithelial cells (white arrows) lining the secretory alveoli of unaffected mammary glands (C). MAL-II labeling was not observed in the epithelial cells (arrowheads) lining the interlobular ducts (D). Intense, apical, granular, membranous to cytoplasmic SNA labeling in the epithelial cells lining (white arrows) the secretory alveoli (E) and lining the interlobular ducts (arrowheads) (F) was observed. Scale bars indicate 50 μm. IAV-Np, influenza A virus nucleoprotein; MAL, *Maackia amurensis* lectin; SNA, *Sambucus nigra* lectin.

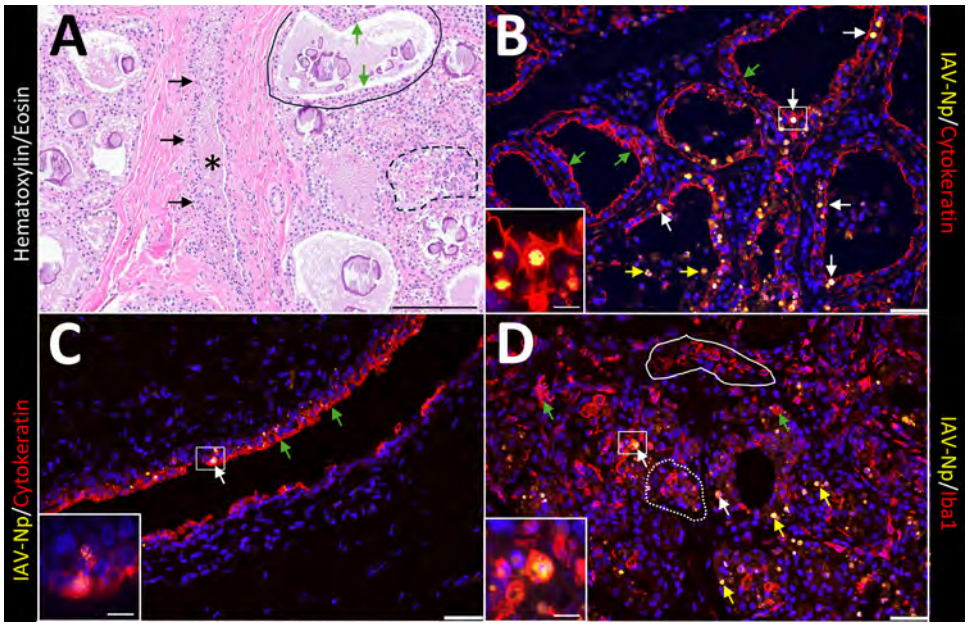

Figure 6. Infected region of the mammary gland from a US dairy cow infected with highly pathogenic avian influenza A(H5N1) virus, labeled with IAV-Np (yellow pseudocolor, DyLight 594), individually duplexed either with epithelial marker pan-cytokeratin (red pseudocolor, Alexa Fluor 647) (B, C) or macrophage or monocytic marker ionized calcium binding adaptor molecule 1 (Iba1) (red pseudocolor, Alexa Fluor 647) (D) using fluorescent labeling. A representative image from a hematoxylin and eosin stain section highlights the cellular architecture of the affected mammary gland (A). Unaffected secretory alveoli were observed in the section (solid black outline). Secretory alveoli variably contain eosinophilic proteinaceous material and corpora amylacea. The secretory alveoli were lined by cuboidal epithelial cells (green arrows) that were variably vacuolated. A few secretory alveoli were disrupted by inflammation (macrophages and neutrophils) and epithelial necrosis (dashed black outline). A single interlobular duct (black asterisk) lined by a bilayer of low cuboidal epithelial cells (black arrows) was observed. The duct contains eosinophilic proteinaceous fluids with scattered inflammatory cells (macrophages and neutrophils) and sloughed epithelium (A). Epithelial cells lining secretory alveoli (B) and interlobular ducts (C) were labeled with pancytokeratin as expected. IAV-Np intranuclear co-labeling (white arrows) in epithelial cells lining the secretory alveoli (B) and ducts (C). Intraluminal cells within secretory alveoli had intranuclear IAV-Np labeling (yellow arrows) that variably co-labeled with pan-cytokeratin. Likewise, Iba1 labeling (green arrows) was observed in the lumens of secretory alveoli or interlobular (alveolus labeling highlighted by white dotted outline) and interstitium (highlighted by the solid white outline) (D). Iba1 labeling was intense, diffuse, and cytoplasmic. IAV-Np intranuclear and intracytoplasmic labeling was less commonly co-labeled within Iba1 labeled cells (white arrows) (D). IAV-Np labeling was not observed in Iba1-labeled cells in the interstitium solid white outline). Insets highlight intranuclear labeling in panels C, B, and D, and the white boxes in the corresponding images represent the origin of the inset image. Scale bars indicate 200 μm (A), 50 μm (B, C, D), and 20 μm (insets). IAV-Np, influenza A virus nucleoprotein; Iba1, ionized calcium binding adaptor molecule 1.

virus replication. Intranuclear localization observed in this case may suggest viral replication in macrophages. Previous studies have shown that H5N1 virus replicates efficiently in human macrophages (*34*). Even in pigs, pulmonary alveolar macrophages expressing SA receptors have been shown to be susceptible to IAVs and undergo rapid apoptosis (*35*). Phagocytosis of viral antigen also is probably occurring given that only intraluminal macrophages mixed with inflammatory exudate contained viral antigen, whereas the interstitial macrophages did not. Overall, resident or infiltrating macrophages in the bovine mammary gland may be susceptible to infection, but further studies are required.

IAV infections are typically respiratory tract infections. Severe infections can result in a systemic inflammatory response, but the spread of IAV to tissues outside of the respiratory tract is rare (*36*). HPAI H5N1 and H5N8 viruses been reported to cause lesions outside of the respiratory tract, including encephalitis and myocarditis, in humans and wild mammals (*37*–*39*). The multifocal random pattern of viral distribution and lesion development in dairy cattle may suggest either a hematogenous spread (viremia or lymphohistiocytic trafficking) or ascending infection from the teat sinus. Although it is beyond the scope of this article, it will be interesting to explore other suspected routes of infection. The involvement of other organ systems (e.g., the gastrointestinal tract through pancreatic tropism), have been observed in naturally infected poultry and cats with systemic disease (*38*,*40*,*41*).

Virus attachment through hemagglutinin to host cell SA and the association between the attachment pattern, disease pathogenesis, and transmission efficiency is complex. Slight changes in the receptor-binding activity, as occurs with changes in pH, can influence the functional balance of the IAV infection process (*42*–*44*). The pH required for the fusion of many avian-adapted IAVs is less acidic than human IAVs (*42*,*44*). The pH of normal cow milk is mildly acidic (6.3–6.9), and the pH of mastitis milk often increases (*45*); however, pH was not

measured in the submitted milk sample. It is possible that the mildly acidic environment in the bovine mammary gland, coupled with the presence of SA receptors across the lacteal ducts, can be some of the predisposing factors for HPAI H5N1 virus infection in dairy cattle. As hypothesized earlier, imbalances in pH-associated hemagglutinin and neuraminidase conformational changes may lead to inefficient viral progeny release (*42*). However, those observations require additional studies, and the pH of milk from experimentally infected cows should be assessed temporally to assess how these imbalances may affect viral replication.

Sporadic human cases of H5N1 virus infection have occurred when humans are in close and prolonged contact with birds (*46*,*47*). Humans have some α2,3-linked SA receptors deep within their lungs (*14*), and prolonged close contact with infected birds is postulated to cause infection attributable to inhaling large amounts of virus from those birds with introduction into the deeper recesses of the lungs (*48*,*49*). Even in the current HPAI H5N1 outbreak, there was a reported case of a dairy farm worker who had direct and close exposure to dairy cows that had onset of bilateral conjunctivitis and was later confirmed positive for H5N1 clade 2.3.4.4b virus through rRT-PCR

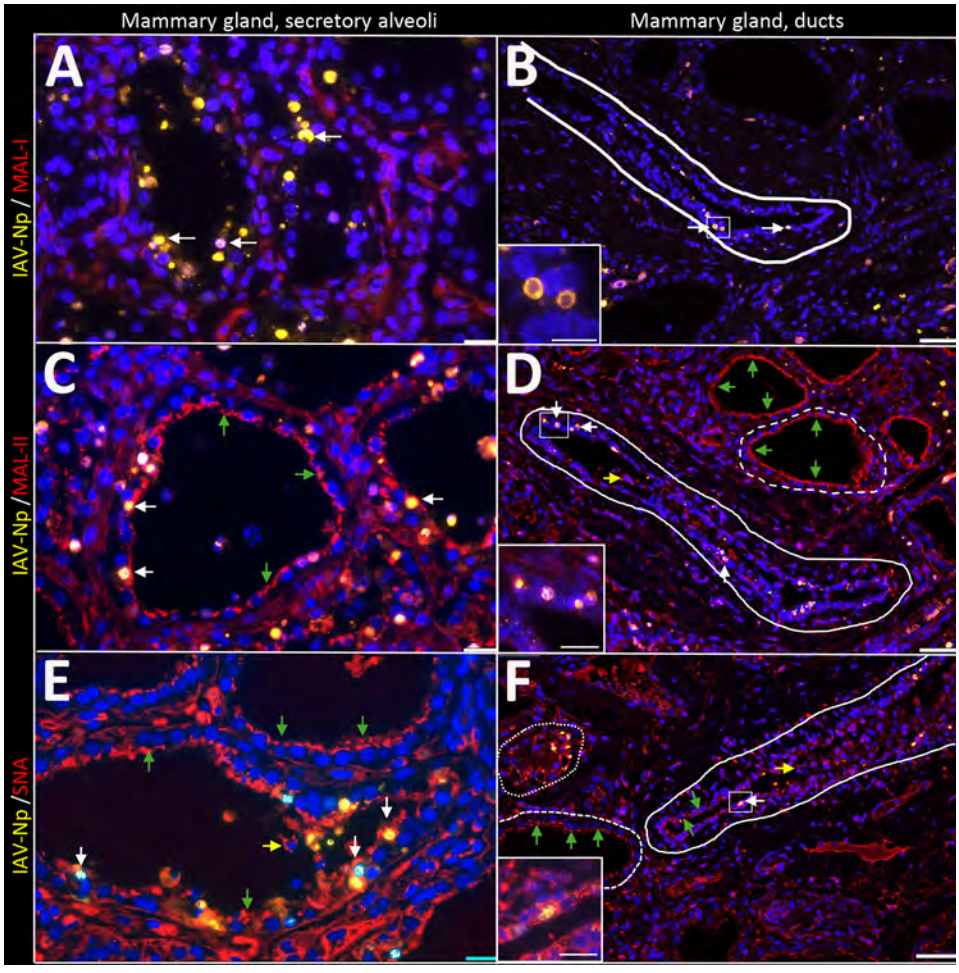

Figure 7. Infected region of the mammary gland from a US dairy cow infected with highly pathogenic avian influenza A(H5N1) virus, labeled with IAV-Np (yellow pseudocolor, DyLight 594), individually duplexed with MAL-I (red pseudocolor, Alexa Fluor 647), MAL-II (red pseudocolor, Alexa Fluor 647), and SNA (red pseudocolor, Alexa Fluor 647) using fluorescent staining. Representative merged images of IAV-Np/MAL-I (A, B), IAV-Np/MAL-II (C, D), and IAV-Np/SNA (E, F) are shown. Moderate to intense intranuclear and intracytoplasmic IAV-Np labeling (yellow, white arrows) was observed in epithelial cells lining the secretory alveolus of the mammary gland; however, no MAL-I labeling was detected (A). Rare, moderate intranuclear IAV-Np labeling (yellow, white arrows), but no MAL-I labeling was observed in epithelial cells lining the interlobular duct (solid white outline) (B). Intense, apical, fibrillary MAL-II labeling (green arrows) was observed in the epithelial cells lining the secretory alveoli of infected mammary glands (C). IAV-Np labeling was co-labeled with MAL-II in individual epithelial cells (white arrows). IAV-Np labeling (white arrows) was observed in epithelial cells of interlobular ducts (solid white outline) (D). MAL-II labeling was not observed in interlobular ducts but was detected in the unaffected secretory alveoli (dashed white outline) (D). Intraluminal cells with cytoplasmic MAL-II labeling were observed (yellow arrow) (D). Intense, apical, granular, membranous to cytoplasmic SNA labeling (green arrows) was observed in the epithelial cells lining the secretory alveoli of infected mammary glands (E). IAV-Np intranuclear labeling was co-labeled with SNA in individual epithelial cells (white arrows) in the secretory alveoli (E). SNA (green arrows) and IAV-Np (white arrows) were observed in epithelial cells of the interlobular ducts (dashed or solid white outline) and were co-labeled to individual ductal epithelial cells (F). Sloughed intraluminal cells had membranous SNA labeling (yellow arrows). Adjacent secretory alveoli had prominent SNA labeling (dashed white outline). The dotted white outline highlights a severely affected secretory gland (F). Insets highlight white boxed areas in panels B, D, and F. Scale bar indicate 20 μm (A, C, E), 50 μm (B, D, F), and 20 μm (insets). IAV-Np, influenza A virus nucleoprotein; MAL, *Maackia amurensis* lectin; SNA, *Sambucus nigra* lectin.

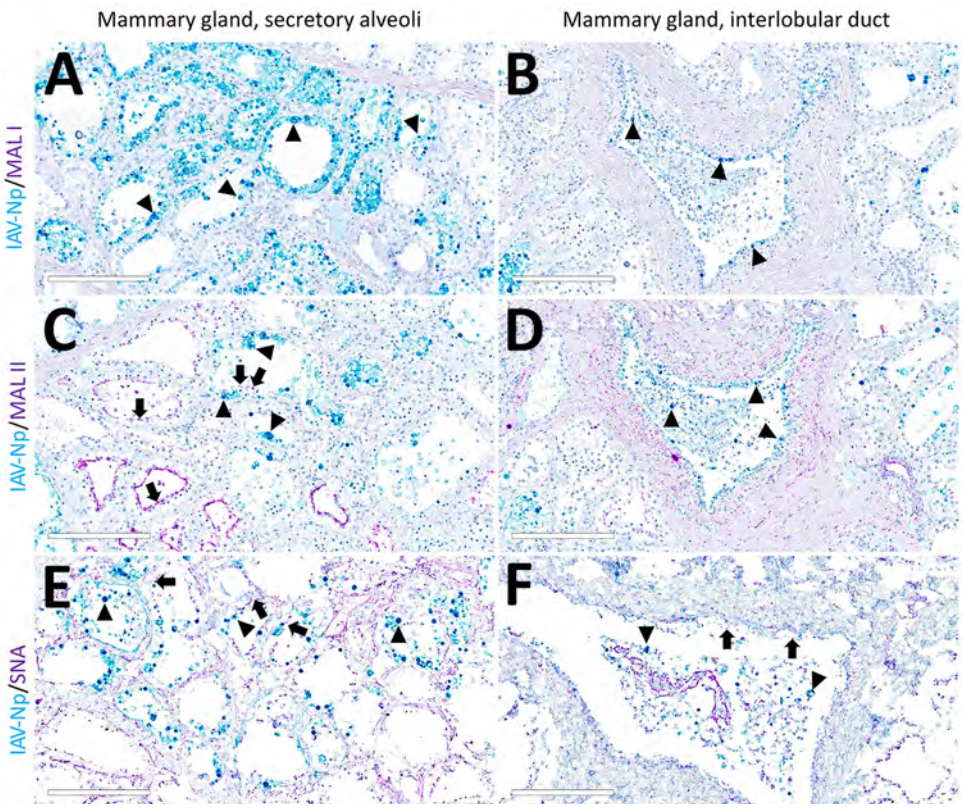

Figure 8. Infected region of the mammary gland from a US dairy cow infected with highly pathogenic avian influenza A(H5N1) virus, showing IAV-Np (teal chromogen), individually duplexed with MAL-I (magenta chromogen), MAL-II (magenta chromogen), and SNA (magenta chromogen) using chromogenic staining. Representative images IAV-Np/MAL-I (A, B), IAV-Np/MAL-II (C, D), and IAV-Np/SNA (E, F) in infected mammary gland and interlobular duct are shown. Strong intracytoplasmic and intranuclear immunoreactivity with IAV-Np was observed within the glandular epithelium of the mammary alveolus and interlobular ducts (arrowheads) with no substantial MAL-I labeling (A, B). Scant, multifocal, apical, punctate MAL-II labeling was observed in degenerative mammary gland epithelial cells (arrows) with strong, intranuclear, and intracytoplasmic immunoreactivity for IAV-Np (arrowheads) (C). Interlobular ductal epithelium exhibits strong, multifocal intranuclear and intracytoplasmic immunoreactivity to IAV-Np in attenuated and sloughed cells (arrowheads) with no substantial epithelial MAL-II detected (D). Strong, multifocal, punctate, apical labeling with SNA in attenuated or degenerative epithelial cells (arrows) with strong, intranuclear, and intracytoplasmic immunoreactivity for IAV-Np (arrows) was observed within mammary gland epithelium (E). Scant, multifocal, delicate, apical labeling for SNA (arrows) within ductal epithelium with strong, intranuclear, and intracytoplasmic immunoreactivity within sloughed, intraluminal epithelial cells for IAV-Np (arrowheads) was observed in an interlobular duct (F). Scale bars indicate 200 μm. IAV-Np, influenza A virus nucleoprotein; MAL, *Maackia amurensis* lectin; SNA, *Sambucus nigra* lectin.

and sequence analysis (*50*). Sequence analysis of the hemagglutinin gene in HPAI H5N1 virus samples from cattle and humans reportedly lacked changes in the receptor-binding affinity (i.e., the virus still preferentially binds to SA α2–3–linked receptors) (*50*). However, the sample size tested in both dairy cattle (2 cows) and humans (1 human) is relatively small. Continued sequence analysis of identified cases is important to assess viral mutations and potential adaptation to other species. This monitoring will assist preparedness and decision making.

From a public health standpoint, there is an urgent need to understand why these avian influenza viruses are now infecting so many mammal species. There is also a need to understand why and how often these viruses infect humans. Our study is an initial foray into answering those questions. Ongoing surveillance and sequence comparisons of HPAI viruses in various mammals are needed to better understand spillover events and the underlying pathogenic mechanisms. A better understanding of viral host range will help inform public health decisions and guide research to help prevent future influenza epidemics.

Acknowledgments

We are exceedingly grateful to Patrick Halbur, Patrick Gorden, and Rodger Main for their leadership, programmatic support, and guidance, and to the rest of the team in Iowa State University's Veterinary Diagnostic Laboratory and Department of Veterinary Diagnostic and Production Animal Medicine. We are also grateful to Amanda Fales-Williams for her leadership and programmatic support from the Veterinary Pathology Department and to the faculty and staff of that department for their help on this project. We also greatly appreciate the guidance, scientific advice, and support we received from Mark Ackermann and influenza experts Amy Vincent-Baker and Bailey Arruda. We are incredibly thankful to Margie Carter for helping us with confocal microscopic imaging.

Financial and programmatic support was provided by the College of Veterinary Medicine, Iowa State University.

About the Author

Dr. Nelli is a research assistant professor at Iowa State University. His research interests include evaluating innate and adaptive immune responses towards influenza and coronaviral infections. Dr. Bell is a professor of veterinary pathology at Iowa State University. His research focuses on high-consequence infectious diseases and the intersection of veterinary pathology and virology.

References

1. Burrough ER, Magstadt DR, Petersen B, Timmermans SJ, Gauger PC, Zhang J, et al. Highly pathogenic avian influenza A(H5N1) clade 2.3.4.4b virus infection in domestic dairy cattle and cats, United States, 2024. Emerg Infect Dis. 2024;30:30. https://doi.org/10.3201/eid3007.240508
2. US Department of Agriculture, Animal and Plant Health Inspection Service. Federal and state veterinary, public health agencies share update on HPAI detection in Kansas, Texas dairy herds. 2024 [cited 2024 May 5]. https://www.aphis.usda.gov/news/agency-announcements/federal-state-veterinary-public-health-agencies-share-update-hpai
3. Gilbertson B, Subbarao K. Mammalian infections with highly pathogenic avian influenza viruses renew concerns of pandemic potential. J Exp Med. 2023;220:e20230447. https://doi.org/10.1084/jem.20230447
4. US Department of Agriculture, US Department of Health and Human Services. USDA, HHS announce new actions to reduce impact and spread of H5N1. 2024 [cited 2024 May 5]. https://www.usda.gov/media/press-releases/2024/05/10/usda-hhs-announce-new-actions-reduce-impact-and-spread-h5n1
5. Bevins SN, Shriner SA, Cumbee JC Jr, Dilione KE, Douglass KE, Ellis JW, et al. Intercontinental movement of highly pathogenic avian influenza A(H5N1) clade 2.3.4.4 virus to the United States, 2021. Emerg Infect Dis. 2022;28:1006–11. https://doi.org/10.3201/eid2805.220318
6. Caliendo V, Lewis NS, Pohlmann A, Baillie SR, Banyard AC, Beer M, et al. Transatlantic spread of highly pathogenic avian influenza H5N1 by wild birds from Europe to North America in 2021. Sci Rep. 2022;12:11729. https://doi.org/10.1038/s41598-022-13447-z
7. Centers for Disease Control and Prevention. Emergence and evolution of H5N1 bird flu. 2024 [cited 2024 May 5]. https://www.cdc.gov/flu/avianflu/communication-resources/bird-flu-origin-infographic.html
8. Elsmo EJ, Wünschmann A, Beckmen KB, Broughton-Neiswanger LE, Buckles EL, Ellis J, et al. Highly pathogenic avian influenza A(H5N1) virus clade 2.3.4.4b infections in wild terrestrial mammals, United States, 2022. Emerg Infect Dis. 2023;29:2451–60. https://doi.org/10.3201/eid2912.230464
9. US Department of Agriculture, Animal and Plant Health Inspection Service, Wildlife Services. National Wildlife Disease Program: HPAI detections in mammals. 2024 [cited 2024 May 13]. https://www.aphis.usda.gov/livestock-poultry-disease/avian/avian-influenza/hpai-detections/mammals
10. Suzuki Y, Ito T, Suzuki T, Holland RE Jr, Chambers TM, Kiso M, et al. Sialic acid species as a determinant of the host range of influenza A viruses. J Virol. 2000;74:11825–31. https://doi.org/10.1128/JVI.74.24.11825-11831.2000
11. Arruda B, Baker ALV, Buckley A, Anderson TK, Torchetti M, Bergeson NH, et al. Divergent pathogenesis and transmission of highly pathogenic avian influenza A(H5N1) in swine. Emerg Infect Dis. 2024;30:738–51. https://doi.org/10.3201/eid3004.231141
12. Nicholls JM, Chan RWY, Russell RJ, Air GM, Peiris JSM. Evolving complexities of influenza virus and its receptors. Trends Microbiol. 2008;16:149–57. https://doi.org/10.1016/j.tim.2008.01.008
13. Venkatesh D, Anderson TK, Kimble JB, Chang J, Lopes S, Souza CK, et al. Antigenic characterization and pandemic risk assessment of North American H1 influenza a viruses circulating in swine. Microbiol Spectr. 2022;10:e0178122. https://doi.org/10.1128/spectrum.01781-22
14. Shinya K, Ebina M, Yamada S, Ono M, Kasai N, Kawaoka Y. Avian flu: influenza virus receptors in the human airway. Nature. 2006;440:435–6. https://doi.org/10.1038/440435a
15. Angata T, Varki A. Chemical diversity in the sialic acids and related alpha-keto acids: an evolutionary perspective. Chem Rev. 2002;102:439–69. https://doi.org/10.1021/cr000407m
16. Lin SJH, Helm ET, Gabler NK, Burrough ER. Acute infection with *Brachyspira hyodysenteriae* affects mucin expression, glycosylation, and fecal MUC5AC. Front Cell Infect Microbiol. 2023;12:1042815. https://doi.org/10.3389/fcimb.2022.1042815
17. Nelli RK, Kuchipudi SV, White GA, Perez BB, Dunham SP, Chang KC. Comparative distribution of human and avian type sialic acid influenza receptors in the pig. BMC Vet Res. 2010;6:4. https://doi.org/10.1186/1746-6148-6-4
18. Matrosovich M, Herrler G, Klenk HD. Sialic acid receptors of viruses. In: Gerardy-Schahn R, Delannoy P, Von Itzstein M, editors. SialoGlyco chemistry and biology II. Cham (Switzerland): Springer International Publishing; 2013. p. 1–28 [cited 2024 May 5]. http://link.springer.com/10.1007/128_2013_466
19. van Riel D, Munster VJ, de Wit E, Rimmelzwaan GF, Fouchier RA, Osterhaus AD, et al. Human and avian influenza viruses target different cells in the lower respiratory tract of humans and other mammals. Am J Pathol. 2007;171:1215–23. https://doi.org/10.2353/ajpath.2007.070248
20. Kuchipudi SV, Nelli R, White GA, Bain M, Chang KC, Dunham S. Differences in influenza virus receptors in chickens and ducks: implications for interspecies transmission. J Mol Genet Med. 2009;3:143–51. https://doi.org/10.4172/1747-0862.1000026
21. Costa T, Chaves AJ, Valle R, Darji A, van Riel D, Kuiken T, et al. Distribution patterns of influenza virus receptors and viral attachment patterns in the respiratory and intestinal tracts of seven avian species. Vet Res (Faisalabad). 2012;43:28. https://doi.org/10.1186/1297-9716-43-28
22. Kandeil A, Patton C, Jones JC, Jeevan T, Harrington WN, Trifkovic S, et al. Rapid evolution of A(H5N1) influenza viruses after intercontinental spread to North America. Nat Commun. 2023;14:3082. https://doi.org/10.1038/s41467-023-38415-7
23. Centers for Disease Control and Prevention. Technical report: highly pathogenic avian influenza A(H5N1) viruses. 2024 [cited 2024 May 5]. https://www.cdc.gov/flu/avianflu/spotlights/2023-2024/h5n1-technical-report_april-2024.htm
24. van Riel D, Munster VJ, de Wit E, Rimmelzwaan GF, Fouchier RA, Osterhaus AD, et al. H5N1 virus attachment to lower respiratory tract. Science. 2006;312:399. https://doi.org/10.1126/science.1125548

25. Gambaryan A, Yamnikova S, Lvov D, Tuzikov A, Chinarev A, Pazynina G, et al. Receptor specificity of influenza viruses from birds and mammals: new data on involvement of the inner fragments of the carbohydrate chain. Virology. 2005;334:276–83. https://doi.org/10.1016/j.virol.2005.02.003
26. Ghosh S. Sialic acid and biology of life: an introduction. In: sialic acids and sialoglycoconjugates in the biology of life, health and disease. Amsterdam: Elsevier; 2020. p. 1–61 [cited 2024 May 5]. https://linkinghub.elsevier.com/retrieve/pii/B9780128161265000019
27. Varki A, Schnaar RL, Schauer R. Sialic acids and other nonulosonic acids. In: Varki A, Cummings RD, Esko JD, Stanley P, Hart GW, Aebi M, et al., editors. Essentials of glycobiology. 3rd edition. Cold Spring Harbor (NY): Cold Spring Harbor Laboratory Press; 2015 [cited 2024 May 5]. http://www.ncbi.nlm.nih.gov/books/NBK453082
28. Kuchipudi SV, Nelli RK, Gontu A, Satyakumar R, Surendran Nair M, Subbiah M. Sialic acid receptors: the key to solving the enigma of zoonotic virus spillover. Viruses. 2021;13:262. https://doi.org/10.3390/v13020262
29. Spruit CM, Nemanichvili N, Okamatsu M, Takematsu H, Boons GJ, de Vries RP. N-glycolylneuraminic acid in animal models for human influenza A virus. Viruses. 2021;13:815. https://doi.org/10.3390/v13050815
30. Sharma R, Ahlawat S, Sharma H, Aggarwal RAK, Sharma V, Tantia MS. Variable sialic acid content in milk of Indian cattle and buffalo across different stages of lactation. J Dairy Res. 2019;86:98–101. https://doi.org/10.1017/S002202991800081X
31. De Sousa YRF, Da Silva Vasconcelos MA, Costa RG, De Azevedo Filho CA, De Paiva EP, Queiroga RDCRDE. Sialic acid content of goat milk during lactation. Livest Sci. 2015;177:175–80. https://doi.org/10.1016/j.livsci.2015.04.005
32. Puente R, Hueso P. Lactational changes in the N-glycoloylneuraminic acid content of bovine milk gangliosides. Biol Chem Hoppe Seyler. 1993;374:475–8. https://doi.org/10.1515/bchm3.1993.374.7-12.475
33. Sata T, Roth J, Zuber C, Stamm B, Heitz PU. Expression of α 2,6-linked sialic acid residues in neoplastic but not in normal human colonic mucosa. A lectin-gold cytochemical study with *Sambucus nigra* and *Maackia amurensis* lectins. Am J Pathol. 1991;139:1435–48.
34. Westenius V, Mäkelä SM, Julkunen I, Österlund P. Highly pathogenic H5N1 influenza A virus spreads efficiently in human primary monocyte-derived macrophages and dendritic cells. Front Immunol. 2018;9:1664. https://doi.org/10.3389/fimmu.2018.01664
35. Chang P, Kuchipudi SV, Mellits KH, Sebastian S, James J, Liu J, et al. Early apoptosis of porcine alveolar macrophages limits avian influenza virus replication and pro-inflammatory dysregulation. Sci Rep. 2015;5:17999. https://doi.org/10.1038/srep17999
36. Taubenberger JK, Morens DM. The pathology of influenza virus infections. Annu Rev Pathol. 2008;3:499–522. https://doi.org/10.1146/annurev.pathmechdis.3.121806.154316
37. Zhang Z, Zhang J, Huang K, Li KS, Yuen KY, Guan Y, et al. Systemic infection of avian influenza A virus H5N1 subtype in humans. Hum Pathol. 2009;40:735–9. https://doi.org/10.1016/j.humpath.2008.08.015
38. Reperant LA, van Amerongen G, van de Bildt MWG, Rimmelzwaan GF, Dobson AP, Osterhaus ADME, et al. Highly pathogenic avian influenza virus (H5N1) infection in red foxes fed infected bird carcasses. Emerg Infect Dis. 2008;14:1835–41. https://doi.org/10.3201/eid1412.080470
39. Floyd T, Banyard AC, Lean FZX, Byrne AMP, Fullick E, Whittard E, et al. Encephalitis and death in wild mammals at a rehabilitation center after infection with highly pathogenic avian influenza A(H5N8) virus, United Kingdom. Emerg Infect Dis. 2021;27:2856–63. https://doi.org/10.3201/eid2711.211225
40. Sillman SJ, Drozd M, Loy D, Harris SP. Naturally occurring highly pathogenic avian influenza virus H5N1 clade 2.3.4.4b infection in three domestic cats in North America during 2023. J Comp Pathol. 2023;205:17–23. https://doi.org/10.1016/j.jcpa.2023.07.001
41. Arruda PHE, Stevenson GW, Killian ML, Burrough ER, Gauger PC, Harmon KM, et al. Outbreak of H5N2 highly pathogenic avian influenza A virus infection in two commercial layer facilities: lesions and viral antigen distribution. J Vet Diagn Invest. 2016;28:568–73. https://doi.org/10.1177/1040638716658929
42. Wagner R, Matrosovich M, Klenk HD. Functional balance between haemagglutinin and neuraminidase in influenza virus infections. Rev Med Virol. 2002;12:159–66. https://doi.org/10.1002/rmv.352
43. Short KR, Richard M, Verhagen JH, van Riel D, Schrauwen EJA, van den Brand JMA, et al. One Health, multiple challenges: the inter-species transmission of influenza A virus. One Health. 2015;1:1–13. https://doi.org/10.1016/j.onehlt.2015.03.001
44. Galloway SE, Reed ML, Russell CJ, Steinhauer DA. Influenza HA subtypes demonstrate divergent phenotypes for cleavage activation and pH of fusion: implications for host range and adaptation. PLoS Pathog. 2013;9:e1003151. https://doi.org/10.1371/journal.ppat.1003151
45. Kandeel SA, Megahed AA, Ebeid MH, Constable PD. Ability of milk pH to predict subclinical mastitis and intramammary infection in quarters from lactating dairy cattle. J Dairy Sci. 2019;102:1417–27. https://doi.org/10.3168/jds.2018-14993
46. Van Kerkhove MD, Mumford E, Mounts AW, Bresee J, Ly S, Bridges CB, et al. Highly pathogenic avian influenza (H5N1): pathways of exposure at the animal–human interface, a systematic review. PLoS One. 2011;6:e14582.
47. Bertran K, Balzli C, Kwon YK, Tumpey TM, Clark A, Swayne DE. Airborne transmission of highly pathogenic influenza virus during processing of infected poultry. Emerg Infect Dis. 2017;23:1806–14. https://doi.org/10.3201/eid2311.170672
48. Kumlin U, Olofsson S, Dimock K, Arnberg N. Sialic acid tissue distribution and influenza virus tropism. Influenza Other Respir Viruses. 2008;2:147–54. https://doi.org/10.1111/j.1750-2659.2008.00051.x
49. Maginnis MS. Virus–receptor interactions: the key to cellular invasion. J Mol Biol. 2018;430:2590–611. https://doi.org/10.1016/j.jmb.2018.06.024
50. Uyeki TM, Milton S, Abdul Hamid C, Reinoso Webb C, Presley SM, Shetty V, et al. Highly pathogenic avian influenza A(H5N1) virus infection in a dairy farm worker. N Engl J Med. 2024 May 3:NEJMc2405371 [Epub ahead of print]. https://doi.org/10.1056/NEJMc2405371

Address for correspondence: Rahul Kumar Nelli, Department of Veterinary Diagnostic and Production Animal Medicine, College of Veterinary Medicine, 1907 ISU C Dr, VMRI #2, Iowa State University, Ames, IA 50011, USA; email: rknelli@iastate.edu; or Todd M. Bell, Department of Veterinary Pathology, College of Veterinary Medicine, Iowa State University, 1800 Christensen Dr, Ames, IA 50011, USA; email: toddbell@iastate.edu

Electronic Health Record Data for Lyme Disease Surveillance, Massachusetts, USA, 2017–2018

Kshema Nagavedu, Karen Eberhardt, Sarah Willis, Monica Morrison, Aileen Ochoa, Susan Soliva, Sarah Scotland, Noelle M. Cocoros, Myfanwy Callahan, Liisa M. Randall, Catherine M. Brown, Michael Klompas

Lyme disease surveillance based on provider and laboratory reports underestimates incidence. We developed an algorithm for automating surveillance using electronic health record data. We identified potential Lyme disease markers in electronic health record data (laboratory tests, diagnosis codes, prescriptions) from January 2017–December 2018 in 2 large practice groups in Massachusetts, USA. We calculated their sensitivities and positive predictive values (PPV), alone and in combination, relative to medical record review. Sensitivities ranged from 57% (95% CI 47%–69%) for immunoassays to 87% (95% CI 70%–100%) for diagnosis codes. PPVs ranged from 53% (95% CI 43%–61%) for diagnosis codes to 58% (95% CI 50%–66%) for immunoassays. The combination of a diagnosis code and antibiotics within 14 days or a positive Western blot had a sensitivity of 100% (95% CI 86%–100%) and PPV of 82% (95% CI 75%–89%). This algorithm could make Lyme disease surveillance more efficient and consistent.

Lyme disease, caused by infection with the bacterium *Borrelia burgdorferi*, is the most common vector-borne illness in the United States and is steadily affecting an expanding area of the country (*1*). In 2022, a total of 63,000 cases of Lyme disease were reported to US public health authorities (*2*). However, that case count was derived from provider-based and laboratory-based disease reports that likely underestimate the true burden of Lyme disease (*3*,*4*). Analysis of US insurance claims data suggests the true incidence of Lyme disease may be 6-fold to 8-fold higher than the number of cases reported to public health agencies (*4*).

Historically, the Massachusetts Department of Public Health (MDPH), as in most US states, required providers and laboratories to report information on suspected cases of Lyme disease. Laboratories sent positive test results, usually electronically, to MDPH, which then triggered MDPH to mail a request to providers for more information. Providers were asked to complete case report forms with the clinical information needed to classify each case in accordance with Council of State and Territorial Epidemiologists (CSTE) case definitions for Lyme disease (*5*). In 2016, given the high volume of positive Lyme disease–related laboratory tests in Massachusetts, the burden on public health staff to send case report forms to providers, the burden on clinicians to complete and return forms, and the burden on public health staff to abstract and compile case report forms, Massachusetts stopped mailing case report forms to providers after a positive laboratory result. In 2021, CSTE adopted an updated Lyme disease surveillance case definition that relies on laboratory criteria alone that does not require clinicians to complete supplementary case reports to classify suspected and probable cases in high-incidence states. This case definition went into effect nationally in January 2022 (*6*).

MDPH still receives electronic laboratory reports on Lyme disease, but they provide an incomplete picture of Lyme disease for several reasons: some cases of Lyme disease are treated empirically without testing; laboratory testing for early Lyme disease is insensitive; some Lyme disease laboratory tests are not specific; most laboratory tests do not differentiate between current active Lyme disease versus remote resolved Lyme disease; and electronic laboratory reporting does not include relevant contextual information, such as stage of disease and whether or what treatment was given. Those data could help provide

Author affiliations: Harvard Medical School and Pilgrim Health Care Institute, Boston, Massachusetts, USA (K. Nagavedu, S. Willis, A. Ochoa, N.M. Cocoros, M. Klompas); Massachusetts Department of Public Health, Boston (K. Nagavedu, M. Morrison, S. Soliva, S. Scotland, L.M. Randall, C.M. Brown); Commonwealth Informatics, Waltham, Massachusetts, USA (K. Eberhardt); Atrius Health, Boston (M. Callahan); Brigham and Women's Hospital, Boston (M. Klompas)

DOI: http://doi.org/10.3201/eid3007.230942

an expanded picture of Lyme disease epidemiology to inform state and local policies and priorities as they pertain to Lyme disease prevention and management.

Using electronic health record (EHR) data provides a potential complementary strategy for Lyme disease surveillance. EHRs contain a wealth of clinical information on patients, including demographic data, vital signs, pregnancy status, clinical manifestations of disease, laboratory test orders, laboratory test results, and medication prescriptions. Automated analyses of these data can result in more complete and clinically detailed case reporting than provider- or laboratory-based reporting alone (*7*). However, information on how best to detect Lyme disease using EHR data is limited (*8*).

We sought to develop an algorithm for automated surveillance of Lyme disease using structured clinical data routinely recorded in EHRs. Potential components of a Lyme disease algorithm available in EHRs include diagnosis codes, laboratory tests, and prescriptions for medications typically used to treat Lyme disease (*8*). Those elements can be used as standalone criteria or in combination and likely vary in their sensitivity and positive predictive value (PPV). We assessed the frequency of those potential Lyme disease markers using EHR data from 2 large clinical practice groups and calculated the sensitivity and PPV of each marker, both alone and in combination, relative to medical record review. We then proposed a combination surveillance algorithm designed to maximize sensitivity and PPV and validated its performance in a third, independent practice group. The Institutional Review Board of the Harvard Pilgrim Health Care Institute reviewed this study and deemed it public health operations.

Methods

Data Sources

We selected potential markers of Lyme disease in EHR data through consultation with MDPH epidemiologists and an infectious disease physician. Those markers included diagnosis codes from the International Classification of Diseases, 10th Revision, Clinical Modification (ICD-10-CM), as well as positive laboratory tests for Lyme disease and prescriptions for antibiotics typically used to treat Lyme disease, excluding postexposure prophylaxis after tick bites (Appendix 1 Tables 1–3, https://wwwnc.cdc.gov/EID/article/30/7/23-0942-App1.pdf).

We identified patients who had ≥1 potential Lyme disease marker during the study period of January 1, 2017–December 31, 2018, in 3 large clinical practice groups located in eastern Massachusetts using the Electronic Medical Record Support for Public Health Surveillance platform (ESP; https://www.esphealth.org) (*9*–*13*). ESP is an open-source public health surveillance platform that uses daily extracts of data from EHR systems to identify and report conditions of public health interest to health departments. ESP maps EHR data to common terms, analyzes the data for reportable diseases, and automatically submits case reports to health departments' electronic surveillance systems or generates aggregate summaries. At the time of our study, ESP captured ≈50% of the population of Massachusetts for reportable infectious disease cases and ≈20% of the population for chronic disease surveillance.

The 3 practice groups included in the evaluation were Boston Medical Center, Cambridge Health Alliance, and Atrius Health. Boston Medical Center is a 514-bed academic medical center in the city of Boston that provides inpatient, emergency, and outpatient care to ≈220,000 persons. Cambridge Health Alliance is a safety net system for vulnerable populations living in communities north of Boston and provides inpatient, emergency, and outpatient care for ≈200,000 persons. Atrius Health provides outpatient care to a generally well-insured population of ≈700,000 persons primarily in eastern Massachusetts. We used the data from Boston Medical Center and Cambridge Health Alliance to develop a surveillance algorithm and data from Atrius Health to validate results.

Algorithm Development

We calculated the sensitivities and positive predictive values of each EHR-based potential Lyme disease marker and combinations of these markers for 2017–2018 among patients seen at Boston Medical Center and Cambridge Health Alliance. We created 10 nonoverlapping strata with unique combinations of potential algorithm components (diagnosis codes, medications, positive enzyme immunoassays, and positive Western blots for both IgG and IgM) (Table 1). We then reviewed 209 randomly selected charts and arrayed them into the strata.

We conducted chart reviews in 2020 and 2021 using standardized forms to capture information in the EHR on erythema migrans; tick bite or exposure to ticks; signs and symptoms associated with Lyme disease; cardiovascular, musculoskeletal, or nervous system manifestations of Lyme disease; prescriptions for antibiotics used to treat Lyme disease; and results of Lyme disease–related laboratory tests (enzyme immunoassays and Western blots). Each case was adjudicated using the 2017 CSTE surveillance definition for Lyme disease and

Table 1. Sensitivity and positive predictive values of candidate criteria for a Lyme disease algorithm at 2 clinical practice groups in Massachusetts, USA, 2017–2018*

Strata	Algorithm components: ICD codes	+ EIA	+ WB	ABX	Charts reviewed/ flagged: Site 1	Site 2	No. Lyme disease cases†: C	P	S	Summary performance: PPV, % (95% CI)‡	No. projected Lyme disease cases§	Sensitivity, % (95% CI)#
1	1				18/90	20/52	3	1	0	10.5 (1.5–21.6)	14.9	6.5 (1.7–13.2)
2	1			1	20/53	20/105	22	3	0	62.5 (47.4−77.0)	98.8	43.1 (35.8–49.2)
3		1			12/12	19/65	0	0	1	3.2 (0.0–12.0)	2.5	1.1 (0.0–4.3)
4	1	1			0	1/3	0	0	0	0.0 (0.0–85.0)	0.0	0.0 (0.0 −1.3)
5		1		1	5/5	12/18	0	0	0	0.0 (0.0–10.4)	0.0	0.0 (0.0–1.2)
6	1	1		1	2/2	7/11	2	0	0	22.2 (0.0–51.8)	2.9	1.3 (0.0 −3.0)
7		1	1		9/9	15/15	2	6	16	100.0 (92.5–100.0)	24.0	10.5 (8.3–10.9)
8	1	1	1		6/6	3/5	1	3	5	100.0 (81.5–100.0)	11.0	4.8 (3.7–5.4)
9		1	1	1	12/15	5/9	1	9	7	100.0 (89.6–100.0)	24.0	10.5 (8.8–11.8)
10	1	1	1	1	8/29	15/22	14	5	4	100.0 (92.2–100.0)	51.0	22.3 (19.2–25.1)

*ABX, antibiotics; C, confirmed; EIA, enzyme immunoassay; ICD, International Classification of Diseases, 10th Revision, Clinical Modification; P, probable; PPV, positive predictive value; S, suspected; WB, Western blot.
†Based on criteria from the Council of State and Territorial Epidemiologists and Centers for Disease Control and Prevention.
‡PPV for each stratum was calculated by summing up the total number of confirmed, probable, and suspected cases for the stratum and then dividing by the total number of charts reviewed for the stratum.
§The total number of projected Lyme disease cases for each stratum was calculated by multiplying the total number of charts flagged in the stratum by the positive predictive value for the stratum.
#Sensitivity was calculated as the total number of projected Lyme disease cases for the criteria of interest divided by the total number of projected Lyme disease cases for the entire population. The total number of projected Lyme disease cases for the entire population is 229.1, which is the sum of the projected Lyme disease cases from each of the 10 unique strata in the top half of the table using unrounded numbers.

classified as confirmed, probable, or suspected Lyme disease, prophylaxis for Lyme disease, or not a case (5). MDPH personnel performed record review, data abstraction, and adjudication; they received training on the abstraction forms before their first medical record review. Records were single adjudicated.

We calculated the PPV for each stratum relative to 2017 CSTE criteria as the number of confirmed, probable, or suspected cases in the chart review sample for the stratum divided by the number of charts reviewed in the stratum. We multiplied the count of patients in each stratum by the stratum PPV to project the total number of patients with Lyme disease in that stratum. We then summed the projected number of patients with Lyme disease from each stratum to estimate the total number of Lyme disease patients in the study population. We used that estimate of the total number of Lyme disease patients as the denominator for calculating the sensitivity of each stratum and the sensitivities of all candidate Lyme disease surveillance criteria.

We estimated PPVs and sensitivities for all candidate criteria (e.g., ICD code, enzyme immunoassay, ICD code and antibiotics, etc.) by combining the counts of charts flagged, charts reviewed, and the number of patients with confirmed, probable, or suspected Lyme disease from each of the strata that included the candidate criteria of interest (Table 2). We calculated PPV as the number of persons with confirmed, probable, or suspected Lyme disease divided by the number of charts reviewed for each candidate criteria. We calculated sensitivity by multiplying the number of persons flagged by the candidate criteria PPV to project the total number of persons in the study population with the candidate criteria and then dividing by the estimated total number of Lyme disease patients in the total study population as described above.

We validated the final algorithm by applying it to 2017–2018 EHR data drawn from Atrius Health. To maximize the efficiency of chart reviews, we opted to review the charts of 25 randomly selected patients that met the final algorithm's diagnosis code and antibiotic criteria who did not have positive Western blots and then assumed all other patients flagged by the final algorithm who did have positive Western blots were true positive cases. We conducted data analyses using SAS version 9.4 (SAS Institute Inc., https://www.sas.com).

Results

Algorithm Validation

No single criterion had optimal sensitivity and positive predictive value (Table 2). Sensitivity ranged from 57.2% (95% CI 46.7%–68.8%) for Lyme disease enzyme immunoassay (EIA) to 86.6% (95% CI 69.8%–100%) for a Lyme disease diagnosis code. Conversely, PPVs ranged from 58.0% (95% CI 49.5%–66.4%) for

Lyme disease EIA to 52.5% (95% CI 43.6%–61.4%) for a Lyme disease diagnosis code. Combining criteria, however, improved performance. The combination of a Lyme disease diagnosis code and a prescription for an antibiotic of interest within 14 days had a sensitivity of 67.3% (95% CI 54.8%–81.7%) and PPV of 69.4% (95% CI 58.6%–79.8%). The combination of Lyme disease EIA and antibiotics had a sensitivity of 30.8% (95% CI 24.4%–38.2%) and a PPV of 63.6% (95% CI 51.9%–75.0%). A multicomponent algorithm composed of a Lyme disease diagnosis code and a prescription within 14 days or a positive Western blot had a sensitivity of 100% (95% CI 86.2%–100%) and PPV of 82.0% (95% CI 74.9%–88.5%).

We validated the multicomponent algorithm in Atrius Health. Chart reviews at Atrius focused on the combination of a Lyme disease diagnosis code and an antibiotic within 14 days. We otherwise assumed all patients with positive Western blots to have confirmed Lyme disease. On this basis, we estimated the PPV of the combination of a Lyme disease diagnosis code and antibiotics within 14 days, or a positive Lyme disease Western blot as 90.0% (95% CI 87.0%–93.0%).

We applied the algorithm to retrospective data within from 3 clinical practices that collectively provide care for >20% of the state population. For June–August 2022, we found that the prevalence of Lyme disease was 1 case/1,000 patients (*14*). Patients were 71% Caucasian and 53% male. Cases were clustered in neighborhoods to the south and north of Boston as well as on Cape Cod and the surrounding islands. Our results were consistent with historic data on the geographic distribution of Lyme disease in Massachusetts (*15*).

Discussion

In this analysis of EHR-based algorithm criteria for Lyme disease, we observed that a diagnosis code for Lyme disease and a prescription for a relevant antibiotic within 14 days, or a positive Western blot was associated with high sensitivity (100%) and PPV (82%) for chart review–confirmed Lyme disease in accordance with CSTE criteria.

A key challenge with Lyme disease surveillance using EHR data is that no 1 criterion is both sensitive and specific. Diagnosis codes are variably assigned to patients and do not reliably differentiate between current acute disease versus remote resolved disease. Combining this criterion with an antibiotic prescription, however, increased positive predictive value. Likewise, surveillance using Lyme disease test results alone is imperfect. A first-tier Lyme disease EIA is prone to false positives and misses infections diagnosed clinically and treated empirically without testing. Indeed, Lyme disease guidelines recommend treating patients in disease-endemic areas who have a classic erythema migrans rash without performing any laboratory tests (*16*).

Table 2. Summary performance rates for algorithm components and combinations calculated by summing the pertinent strata in study of electronic medical records for Lyme disease, Massachusetts, 2017–2018*

Strata used	Algorithm components	Charts reviewed/ flagged		No. Lyme disease cases†			Summary performance		
		Site 1	Site 2	C	P	S	PPV, % (95% CI)‡	No. projected Lyme disease cases§	Sensitivity, % (95% CI)#
1, 2, 4, 6, 8, 10	ICD code	54/180	66/198	42	12	9	52.5 (43.6–61.4)	198.5	86.6 (69.8–100)
3–10	Positive EIA	54/78	77/148	20	23	33	58.0 (49.5–66.4)	131.1	57.2 (46.7–68.8)
2, 6, 10	ICD code and antibiotics	30/84	42/138	38	8	4	69.4 (58.6–79.8)	154.2	67.3 (54.8–81.7)
5, 6, 9, 10	Positive EIA and antibiotics	27/51	39/60	17	14	11	63.6 (51.9–75.0)	70.6	30.8 (24.4–38.2)
5, 6, 7–10	(Positive EIA and antibiotics) or positive WB	42/66	57/80	20	23	32	75.8 (67.1–83.9)	110.6	48.3 (40.2–56.5)
2, 6, 7–10	(ICD and antibiotics) or positive WB	57/114	65/167	42	26	32	82.0 (74.9–88.5)	230.3	100 (86.2–100)

*Strata and algorithms are defined in Table 1. ABX, antibiotics; C, confirmed; EIA, enzyme immunoassay; ICD, International Classification of Diseases, 10th Revision, Clinical Modification; P, probable; PPV, positive predictive value; S, suspected; WB, Western blot.
†Based on criteria from the Council of State and Territorial Epidemiologists and Centers for Disease Control and Prevention.
‡PPV value for each stratum was calculated by summing up the total number of confirmed, probable, and suspected cases for the stratum and then dividing by the total number of charts reviewed for the stratum.
§The total number of projected Lyme disease cases for each stratum was calculated by multiplying the total number of charts flagged in the stratum by the positive predictive value for the stratum.
#Sensitivity was calculated as the total number of projected Lyme disease cases for the criteria of interest divided by the total number of projected Lyme disease cases for the entire population. The total number of projected Lyme disease cases for the entire population is 229.1, which is the sum of the projected Lyme disease cases from each of the 10 unique strata in the top half of the table using unrounded numbers.

Likewise, focusing surveillance on second-tier Western blots alone is specific but misses patients for whom the Western blot is not ordered.

At the time this work was done, participating practices exclusively used Western blots as second-tier tests after a positive or equivocal first-tier EIA. In July 2019, the US Food and Drug Administration approved Lyme disease assays that use an EIA rather than a Western blot as a second-tier test (*17*). Although our chart review did not assess this modified 2-tiered testing algorithm, 2 positive EIA results from a single collection date of an FDA-cleared assay is likely an acceptable alternative to a positive Western blot in a Lyme disease surveillance algorithm.

Strengths of our analysis include the use of detailed EHR data (such as diagnosis codes, test results, and antibiotic prescriptions) to enhance Lyme disease surveillance beyond what is possible using diagnosis codes or laboratory test results alone; the capacity to identify early cases of Lyme disease among persons who were untested or who had negative tests, as long as their clinicians assigned a diagnosis code for Lyme disease and prescribed antibiotics; the derivation of an algorithm using data from 2 independent practice groups and validation in an independent third group; and the use of structured chart reviews to apply CSTE Lyme disease criteria. Limitations of our analysis include limited sampling per criterion, which led to wide CIs per criterion; our dependence on retrospective chart reviews to apply CSTE criteria and thus the possibility of misclassification resulting from incomplete or inaccurate documentation; and our focus on 3 practice groups in 1 high-incidence state, which may limit the generalizability of our findings, particularly to areas with less endemic disease. Likewise, our medication criterion did not incorporate dose or duration, which may have decreased specificity.

In Massachusetts, Lyme disease is endemic; traditional surveillance methods have been burdensome and incomplete. The EHR-based algorithm for Lyme disease surveillance complemented traditional surveillance methods for tracking disease incidence. Updating and revalidating the surveillance algorithm to include the FDA-cleared modified 2-tier laboratory test type will further strengthen the algorithm (*14*). Adopting the algorithm for routine reporting through ESP will provide DPH with real-time data on the incidence, temporal change, geographic distribution, and demographic characteristics of Lyme disease in the state.

Our analysis demonstrates the potential value of EHR-based algorithms for public health surveillance relative to electronic laboratory reporting alone because of the capacity to integrate diagnosis codes and prescriptions along with diagnostic testing. The method can readily be extended to provide surveillance for other tickborne infections and co-infections, such as babesiosis and anaplasmosis. This method might also be usable for surveillance of other complex conditions without definitive diagnostic tests or biomarkers, such as myalgic encephalomyelitis or post-acute sequelae of COVID-19.

This work was supported with funding from the Massachusetts Department of Public Health.

About the Author

Ms. Nagavedu is a senior research analyst in the Department of Population Medicine at Harvard Pilgrim Health Care Institute and a member of the Therapeutics and Infectious Disease Epidemiology team. Her research interests include infectious disease epidemiology and utilizing distributed research networks for public health surveillance.

References

1. Schwartz AM, Hinckley AF, Mead PS, Hook SA, Kugeler KJ. Surveillance for Lyme disease—United States, 2008–2015. MMWR Surveill Summ. 2017;66:1–12. https://doi.org/10.15585/mmwr.ss6622a1
2. Centers for Disease Control and Prevention. Lyme disease surveillance and data. 2024 [cited 2024 Jun 7]. https://www.cdc.gov/lyme/data-research/facts-stats/index.html
3. Nelson CA, Saha S, Kugeler KJ, Delorey MJ, Shankar MB, Hinckley AF, et al. Incidence of clinician-diagnosed Lyme disease, United States, 2005–2010. Emerg Infect Dis. 2015;21:1625–31. https://doi.org/10.3201/eid2109.150417
4. Schwartz AM, Kugeler KJ, Nelson CA, Marx GE, Hinckley AF. Use of commercial claims data for evaluating trends in Lyme disease diagnoses, United States, 2010–2018. Emerg Infect Dis. 2021;27:499–507. https://doi.org/10.3201/eid2702.202728
5. Centers for Disease Control and Prevention. Lyme disease (*Borrelia burgdorferi*) 2017 case definition. 2022 [cited 2022 Nov 23]. https://ndc.services.cdc.gov/case-definitions/lyme-disease-2017/
6. Centers for Disease Control and Prevention. Lyme disease (*Borrelia burgdorferi*) 2022 case definition. 2022 [cited 2023 Mar 13]. https://ndc.services.cdc.gov/case-definitions/lyme-disease-2022/
7. Willis SJ, Cocoros NM, Randall LM, Ochoa AM, Haney G, Hsu KK, et al. Electronic health record use in public health infectious disease surveillance, USA, 2018–2019. Curr Infect Dis Rep. 2019;21:32. https://doi.org/10.1007/s11908-019-0694-5
8. Moon KA, Pollak J, Hirsch AG, Aucott JN, Nordberg C, Heaney CD, et al. Epidemiology of Lyme disease in Pennsylvania 2006–2014 using electronic health records. Ticks Tick Borne Dis. 2019;10:241–50. https://doi.org/10.1016/j.ttbdis.2018.10.010
9. Klompas M, Lazarus R, Platt R, Hou X, Campion FX, Kruskal B, et al. Automated detection and reporting of

notifiable diseases using electronic medical records versus passive surveillance—Massachusetts, June 2006–July 2007. MMWR Morb Mortal Wkly Rep. 2008;57:373–6.
10. Klompas M, McVetta J, Lazarus R, Eggleston E, Haney G, Kruskal BA, et al. Integrating clinical practice and public health surveillance using electronic medical record systems. Am J Prev Med. 2012;42(Suppl 2):S154–62. https://doi.org/10.1016/j.amepre.2012.04.005
11. Klompas M, Cocoros NM, Menchaca JT, Erani D, Hafer E, Herrick B, et al. State and local chronic disease surveillance using electronic health record systems. Am J Public Health. 2017;107:1406–12. https://doi.org/10.2105/AJPH.2017.303874
12. Lazarus R, Klompas M, Campion FX, McNabb SJ, Hou X, Daniel J, et al. Electronic support for public health: validated case finding and reporting for notifiable diseases using electronic medical data. J Am Med Inform Assoc. 2009;16:18–24. https://doi.org/10.1197/jamia.M2848
13. Vogel J, Brown JS, Land T, Platt R, Klompas M. MDPHnet: secure, distributed sharing of electronic health record data for public health surveillance, evaluation, and planning. Am J Public Health. 2014;104:2265–70. https://doi.org/10.2105/AJPH.2014.302103
14. Cocoros NM, Kirby C, Zambarano B, Ochoa A, Eberhardt K, Rocchio C, et al. RiskScape: a data visualization and aggregation platform for public health surveillance using routine electronic health record data. Am J Public Health. 2021;111:269–76. https://doi.org/10.2105/AJPH.2020.305963
15. Massachusetts Department of Public Health. Lyme disease surveillance in Massachusetts, 2014. 2014 [cited 2023 Mar 13]. https://www.mass.gov/lists/tick-borne-disease-surveillance-summaries-and-data#lyme-disease-surveillance-data-
16. Lantos PM, Rumbaugh J, Bockenstedt LK, Falck-Ytter YT, Aguero-Rosenfeld ME, Auwaerter PG, et al. Clinical practice guidelines by the Infectious Diseases Society of America (IDSA), American Academy of Neurology (AAN), and American College of Rheumatology (ACR): 2020 guidelines for the prevention, diagnosis and treatment of Lyme disease. Clin Infect Dis. 2021;72:e1–48. https://doi.org/10.1093/cid/ciaa1215
17. Mead P, Petersen J, Hinckley A. Updated CDC recommendation for serologic diagnosis of Lyme disease. MMWR Morb Mortal Wkly Rep. 2019;68:703. https://doi.org/10.15585/mmwr.mm6832a4

Address for correspondence: Michael Klompas, Harvard Pilgrim Health Care Institute, 401 Park Dr, Ste 401, East Boston, MA 02215, USA; mklompas@bwh.harvard.edu

etymologia revisited

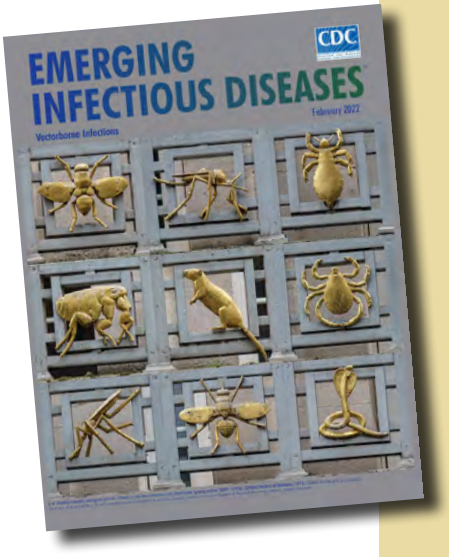

Originally published in February 2022

The Color Puce

For those with synesthesia, in whom stimulating one sensory pathway gives rise to a subjective sensation of a different character, the word plague may chromatically resonate with puce. In pre-revolutionary France, an era of "evocative color nomenclature," Marie Antoinette's reign was precipitating intense criticism. Her countrymen were experiencing severe socioeconomic stress, thus her sartorial self-indulgence was much resented.

After discovering the Queen wearing a new gown, her husband, Louis XVI, the King of France, chided her, describing the dress's unflattering purple–brown hue as "*couleur de puce*" (color of fleas). This admonishment had the unintended consequence of promoting puce as the exclusive color worn by the French court. Puce, the French word for flea, descends from *pulex* (Latin). Flea droppings leave puce colored "bloodstains" on bedsheets. The role of fleas, however, as a vector for bubonic plague was not proven until about 1895.

References:

1. Stedman's Medical Dictionary. 23rd ed. Baltimore: The Williams & Wilkins Company; 1976. p. 1392.
2. St. Clair K. The secret lives of color. New York: Penguin Books; 2017. p. 122–3.
3. Zietz BP, Dunkelberg H. The history of the plague and the research on the causative agent *Yersinia pestis.* Int J Hyg Environ Health. 2004;207:165–78. https://doi.org/10.1078/1438-4639-00259
4. Plague bacteria found in Arizona fleas, by Rachael Rettner, August 14, 2017 [cited 2021 Nov 4]. https://www.livescience.com/60130-plague-fleas-arizona.html)

https//wwwnc.cdc.gov/eid/article/28/2/et-2802_article

Prevalence of and Risk Factors for Post–COVID-19 Condition during Omicron BA.5–Dominant Wave, Japan

Arisa Iba, Mariko Hosozawa, Miyuki Hori, Yoko Muto, Isao Muraki, Rie Masuda, Nanako Tamiya, Hiroyasu Iso

The increased risk for post–COVID-19 condition after the Omicron-dominant wave remains unclear. This population-based study included 25,911 persons in Japan 20–69 years of age with confirmed SARS-CoV-2 infection enrolled in the established registry system during July–August 2022 and 25,911 age- and sex-matched noninfected controls who used a self-reported questionnaire in January–February 2023. We compared prevalence and age- and sex-adjusted odds ratios of persistent COVID-19 symptoms (lasting ≥2 months). We evaluated factors associated with post–COVID-19 condition by comparing cases with and without post–COVID-19 condition. We analyzed 14,710 (8,392 cases and 6,318 controls) of 18,183 respondents. Post–COVID-19 condition proportion among cases was 11.8%, higher by 6.3% than 5.5% persistent symptoms among controls. Female sex, underlying medical conditions, mild to moderate acute COVID-19, and vaccination were associated with post–COVID-19 condition. Approximately 12% had post–COVID-19 condition during the Omicron-dominant wave, indicating the need for longer follow-up.

COVID-19 has caused a significant global disease burden since it was first identified in December 2019; as of May 2024, ≥750 million cases had been confirmed, and ≈7.5 million deaths had occurred worldwide (*1*). In addition to acute illnesses, the prolonged or recurrent symptoms occurring after an initial infection SARS-CoV-2, referred to as post–COVID-19 condition (*2*), have also raised concerns.

More than 65 million persons worldwide have post–COVID-19 condition (*3*). On the basis of estimates of those infected during March 2020–November 2021, a total of 10%–30% of nonhospitalized case-patients and 50%–70% of hospitalized case-patients have had post–COVID-19 condition. Frequently reported symptoms included fatigue, dyspnea, neurocognitive impairment, and loss of smell in patients infected during January 2020–August 2021 (*4*–*8*). The risk of developing post–COVID-19 condition was higher in female patients, those with severe acute COVID-19, or those with a greater number of acute symptoms (*4*,*7*,*9*,*10*). We noted those results in patients infected with variants before the Omicron variant emerged.

The Omicron variant was identified in November 2021; the BA.5 lineage of that variant was detected in April 2022 and has since spread worldwide. The Omicron variant tends to cause less severe acute symptoms (*11*) and has a similar or lower risk for post–COVID-19 condition than the previous variants (*12*–*16*). However, most previous studies concerning post–COVID-19 condition in relation to the Omicron variant, except those that used electronic health record data (*17*), were hospital-based (*13*–*15*,*18*–*21*) or population-based without a control group (*12*,*16*,*22*,*23*). Longer sequelae and risks for post–COVID-19 condition in persons infected with the Omicron variant compared with noninfected populations remain unknown. As the number of COVID-19 cases has increased, with greater infectivity of the Omicron variant (*24*) in addition reductions in nonpharmaceutical interventions (e.g., lockdowns, social distancing, mask requirements), it is crucial to investigate the potential long-term consequences of infection with the Omicron variant. We conducted a population-based study of symptoms after acute COVID-19 using a self-reported questionnaire in a large city in Japan. Our objective was to examine the increased risk for persistent symptoms after SARS-CoV-2 infection

Author affiliations: National Center for Global Health and Medicine, Tokyo, Japan (A. Iba, M. Hosozawa, M. Hori, Y. Muto, H. Iso); Osaka University, Osaka, Japan (I. Muraki); University of Tsukuba, Ibaraki, Japan (R. Masuda, N. Tamiya)

DOI: http://doi.org/10.3201/eid3007.231723

compared with a noninfected population, focusing specifically on the Omicron variant (especially the BA.5 lineage). We also investigated the factors associated with post–COVID-19 condition.

Methods

Study Design and Participants

We conducted a population-based study of community-dwelling adults 20–69 years of age who had confirmed SARS-CoV-2 infection during July–August 2022. We extracted data from the Japan Health Center Real-time Information-sharing System on COVID-19 (HER-SYS), the established registry system, and age- and sex-matched controls using a self-reported web-based questionnaire in Shinagawa City, a metropolitan area located in the Tokyo area of Japan. The population of Shinagawa City is ≈400,000 and its population density is 17,700 persons/km^2.

Japan experienced the 7th wave of COVID-19 in July 2022, caused by the Omicron subvariant BA.5 lineage. The prevalence of the BA.5 lineage increased from 67% in epidemiologic week 27 (July 7–10, 2022) to 92% in epidemiologic week 30 (July 25–31, 2022), becoming dominant (*25*). When COVID-19 was diagnosed by a positive reverse transcription PCR or a lateral flow antigen test for SARS-CoV-2 or a clinical diagnosis (for symptomatic close contacts), the attending physician was required to document every case in HER-SYS until September 26, 2022. Patients needed to see a physician to undergo a test for SARS-CoV-2 until the Ministry of Health, Labour, and Welfare approved over-the-counter antigen test kits on August 24, 2022. However, most patients visited a physician even after the over-the-counter antigen test kits became available rather than testing themselves at home. Therefore, most of the infected persons were registered in HER-SYS during the study period.

We selected participants registered in the HER-SYS database who were 20–69 years of age and infected with SARS-CoV-2 during July 1–August 31, 2022. We excluded 3,365 of the 29,276 identified infected residents who had died or moved out of the area and selected the remaining 25,911 infected persons as study participants (infected group). We matched data from HER-SYS and the Basic Resident Registration system (the municipal residence record of the name, birthdate, sex, and address of all residents living in a municipality) to identify noninfected residents who had never been registered in the HER-SYS database during the participant selection. We selected 25,911 age- and sex-matched noninfected persons (noninfected group) from the matched dataset (Figure 1). The ethics committee of the National Center for Global Health and Medicine approved this study (NCGM-S-004571).

We sent research information and invitations to the online questionnaire to the selected participants

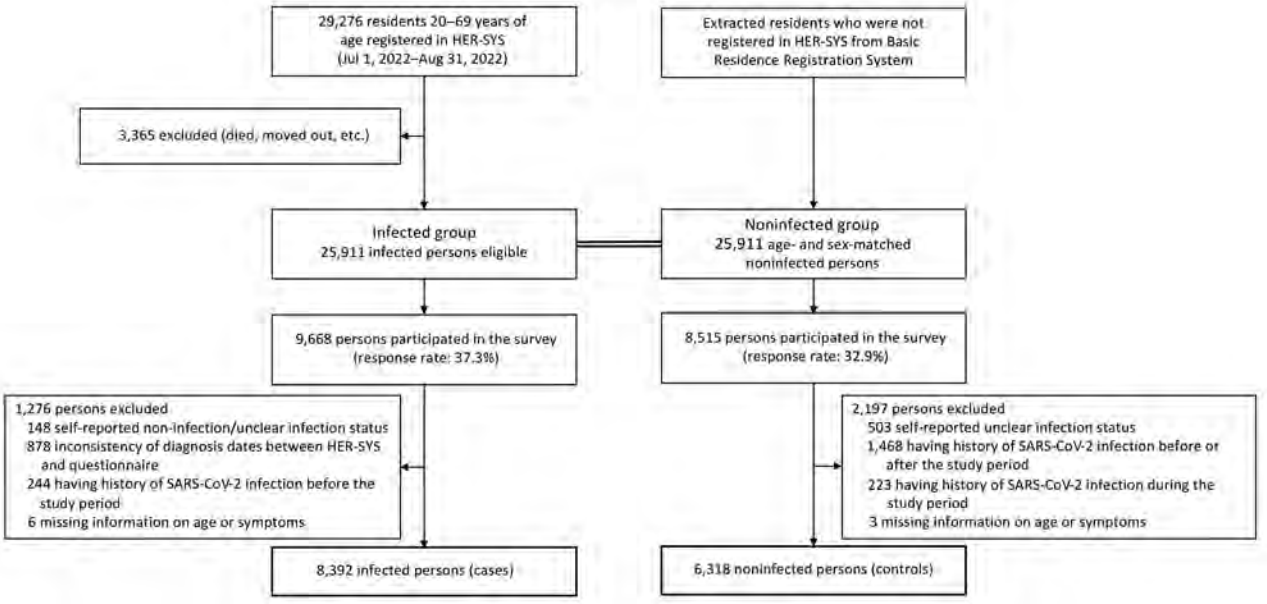

Figure 1. Flowchart of participant selection in study of prevalence and risk factors for post–COVID-19 condition during Omicron BA.5–dominant wave, Japan. Of 29,276 residents 20–69 years of age identified in the municipal HER-SYS database as infected with COVID-19, we selected a total of 25,911 participants; we extracted the same number of age- and sex-matched noninfected residents from the Basic Residence Registration System to serve as the control group. HER-SYS, Health Center Real-time Information-sharing System on COVID-19.

(25,911 each in the infected and noninfected group) by mail on January 11–13, 2023, approximately 6 months after infection for those who had COVID-19 (cases). Respondents were required to provide consent to participate in the study before accessing the website; those who agreed answered the questionnaire by February 13. At the beginning of the questionnaire, we asked participants if they had a diagnosis of COVID-19. If they answered "yes," they were directed to the questions for infected persons, which inquired about the number and date of infection episodes. If they answered "no," "I don't know," or "I prefer not to answer," they were directed to the questions for noninfected persons (Appendix, https://wwwnc.cdc.gov/EID/article/30/7/23-1723-App1.pdf). We included persons whose answers on infection status were consistent with HER-SYS data and whose first infection was within the study period.

Post–COVID-19 Condition (Cases) and Persistent Symptoms (Controls)

We asked the participants about the presence of 26 symptoms that emerged during or after the first SARS-CoV-2 infection for cases and in July 2022 for controls. The symptoms were selected from the International Severe Acute Respiratory and Emerging Infection Consortium COVID-19 questionnaire. Symptoms were fever, cough, fatigue, sore throat, chest pain, anorexia, brain fog, difficulty concentrating, anosmia, ageusia, shortness of breath, hair loss, muscle weakness, palpitations, sleep disorder, rhinorrhea, headache, joint pain and swelling, muscle aches, nausea/vomiting, abdominal pain, skin rash, eye-related symptoms, dizziness, erectile dysfunction (male only), and menstrual change (female only) (*26*). If a symptom was present, we asked about its timing and duration: whether they had the symptom at illness onset or 3 months after infection (infected group only), whether they had it at the time of the survey, and whether the symptom persisted for ≥2 months. For those who affirmed they had any symptoms, we asked the extent to which the symptoms hindered daily life at the time of response using an 11-point scale from 0 (no effect) to 10 (extreme hindrance) and categorized those responses into 4 levels: 0, no effect; 1–3, mild hindrance; 4–6, moderate hindrance; and 7–10, serious hindrance.

For cases, we defined post–COVID-19 condition based on the World Health Organization (WHO) definition (*27*): a symptom that persisted for ≥2 months after the acute phase. For brain fog, difficulty concentrating, hair loss, and muscle weakness, we defined post–COVID-19 condition as symptoms having lasted ≥2 months during the observation period regardless of the timing because those symptoms develop in the subacute phase (*17*,*28*). For controls, we defined persistent symptoms as symptoms lasting ≥2 months experienced between July 2022 and the date of the survey.

Variables

We asked infected persons about the severity of acute COVID-19 and categorized them into 4 groups according to the WHO clinical severity scale: asymptomatic, mild (symptomatic but not admitted to the hospital), moderate (admitted to the hospital, required supplemental oxygen, or both), and severe (received mechanical ventilation or intensive care admission) (*29*). We counted the number of infections because some participants had been infected >1 time during the observation period. We also asked participants about their demographics (i.e., age at the answering date, sex, height, and weight), underlying medical conditions before the infection (or before July 2022 in the noninfected group), lifestyle, and socioeconomic status (e.g., household income and educational level). We calculated equivalized household income by dividing household income by the square root of the household size. For vaccination status, we extracted the vaccination date, vaccination type, and number of vaccinations from the municipality's Vaccination Record System. We substituted the questionnaire responses for missing values for 1,589 (10%) respondents (e.g., those who had moved from the original municipality).

Statistical Analysis

We determined the participants' characteristics according to their infection status and compared using the *t*-test for continuous variables and χ^2 test for categorical variables. We calculated the proportions of overall and each post–COVID-19 condition (cases) and persistent symptoms (controls). Using multivariable logistic regression analysis, we calculated the age- and sex-adjusted odds ratios of each symptom in the cases compared with the persistent symptoms in the controls as a reference. We also investigated the risk factors associated with post–COVID-19 condition among cases using multivariate logistic regression models. Model 1 comprised age group and sex; model 2, underlying medical conditions, body mass index, severity, and vaccination status before infection; and model 3, household income and educational level. We conducted multiple imputations using chained equations to account for missing data in model 3; the proportion of missing values in household income

was 13.1%. We included all explanatory and outcome variables in the imputation model to create 50 imputed datasets. We also calculated the proportion of influence of post–COVID-19 condition on daily life. We defined statistical significance as a 2-sided p value <0.05. We used Stata version 17 MP software (StataCorp LLC, https://www.stata.com) for all analyses.

Results

A total of 51,822 persons were invited to participate in the study, of whom 18,183 responded to the questionnaire (response rate 35.1%). The response rate was higher in the infected group than in the noninfected group (37.3% vs. 32.9%, difference of 4.4% [95% CI 3.0%–5.8%]). The response rate was higher among female than male persons in all age groups of both infected and noninfected groups. Among male invitees, the difference in response rates between the infected and noninfected groups was large for age groups in their 50s (12.8% [95% CI 8.1%–17.5%]) and 60s (8.5% [95% CI 1.6%–15.4%]) (Table 1).

We excluded 3,473/18,183 respondents for responses of infectious status inconsistent with HER-SYS (answering different infection statuses or different diagnosis date) and reporting a prior infection and 9 because their records were missing data on age or symptoms. A total of 14,710 participants (8,392 cases and 6,318 controls) were eligible for the analysis (Figure 1). Mean age of all participants was 42.4 (SD 11.7) years; 8,502 (57.8%) participants were female and 6,087 (41.4%) male (Table 2). Mean age of case participants was 42.3 (SD 11.6) years; 4,802 (57.2%) case participants were female and 3,535 (42.1%) male. The mean follow-up period from SARS-CoV-2 infection to the response date was 167.9 (SD 14.5) days. Most cases (8,326 [99.2%] patients) demonstrated asymptomatic to mild disease, whereas 66 (0.8%) cases had moderate to severe disease.

The percentage of post–COVID-19 condition for cases was 11.8%, whereas the percentage of persistent symptoms among controls was 5.5% (Figure 2). The prevalence did not differ between cases under follow-up for <6 months (11.6%) and cases under follow-up for ≥6 months (12.6%). The most frequent post–COVID-19 condition was cough (3.7%), followed by difficulty concentrating (3.1%), hair loss (2.8%), fatigue (2.4%), and brain fog (2.2%). The most frequent persistent symptoms among the controls were sleep disorders (1.3%), followed by cough (0.9%), fatigue (0.7%), and rhinorrhea (0.7%). The age- and sex-adjusted odds ratio (OR) of any persistent symptoms for cases versus controls was 2.33 (95% CI 2.05–2.64). Symptoms with higher OR in cases than controls were ageusia (27.4 [95% CI 6.7–111.8]), muscle weakness (11.8 [95% CI 5.5–25.5]), anosmia (11.6 [95% CI 4.7–28.6]), hair loss (6.5 [95% CI 4.4–9.6]), and brain fog (5.9 [95% CI 3.8–9.0]).

We conducted multivariable logistic regression analysis to investigate the factors associated with post–COVID-19 condition among cases (Table 3, https://wwwnc.cdc.gov/EID/article/30/7/23-1723-T3.htm). In all 3 models, participants 40–49 years of age had higher odds of having post–COVID-19 condition than those 20–29 years (OR 1.26, 95% CI 1.01–1.57 for model 3); female participants had higher odds of having post–COVID-19 condition than male participants (OR 2.00, 95% CI 1.71–2.34). When models were further adjusted, 2 variables were

Table 1. Response rates of persons in study of prevalence and risk factors for post–COVID-19 condition during BA.5 Omicron-dominant wave, Japan*

	Infected persons				Noninfected persons				Difference in response rates (95% CI)
Age group, y	HER-SYS†	No. participants	No. responses	Response rate, %	BRRS‡	No. participants	No. responses	Response rate, %	
Male patients									
20–29	3,404	2,979	611	20.5	3,404	2,979	574	19.3	1.2 (–3.3 to 5.7)
30–39	3,806	3,328	1,120	33.7	3,806	3,328	896	26.9	6.8 (2.8–10.8)
40–49	3,461	3,058	1,061	34.7	3,461	3,058	943	30.8	3.9 (–0.2 to 8.0)
50–59	2,586	2,243	923	41.2	2,586	2,243	636	28.4	12.8 (8.1–17.5)
60–69	1,152	1,024	413	40.3	1,152	1,024	326	31.8	8.5 (1.6–15.4)
Subtotal	14,409	12,632	4,129	32.7	14,409	12,632	3,375	26.7	6.0 (3.9–8.1)
Female patients									
20–29	3,682	3,218	960	29.8	3,682	3,218	912	28.3	1.5 (–2.6 to 5.6)
30–39	4,028	3,582	1,565	43.7	4,028	3,582	1,491	41.6	2.1 (–1.4 to 5.6)
40–49	3,671	3,313	1,554	46.9	3,671	3,313	1,423	43.0	3.9 (3.2–7.5)
50–59	2,386	2,166	971	44.8	2,386	2,166	884	40.8	4.0 (–0.5 to 8.5)
60–69	1,100	1,000	402	40.2	1,100	1,000	333	33.3	6.9 (–0.1 to 13.9)
Subtotal	14,867	13,279	5,456	41.1	14,867	13,279	5,047	38.0	3.1 (1.2–5.0)
Total	29,276	25,911	9,668	37.3	29,276	25,911	8,515	32.9	4.4 (3.0–5.8)

*BRRS, Basic Resident Registration system; HER-SYS, Health Center Real-Time Information-Sharing System.
†Numbers of SARS-CoV-2–infected persons extracted from the HER-SYS database.
‡Numbers of age- and sex-adjusted noninfected persons extracted from the Basic Resident Registration system database.

Table 2. Characteristics of participants in study of prevalence and risk factors for post–COVID-19 condition during BA.5 Omicron-dominant wave, Japan*

Characteristic	Cases, n = 8,392	Controls, n = 6,318	p value
Mean age, y (±SD)	42.3 (±11.6)	42.4 (±11.8)	0.63
Age group, y			0.29
20–29	1,316 (15.7)	1,036 (16.4)	
30–39	2,340 (27.9)	1,674 (26.5)	
40–49	2,326 (27.7)	1,766 (28.0)	
50–59	1,695 (20.2)	1,270 (20.1)	
60–70†	715 (8.5)	572 (9.1)	
Patient sex			0.01
M	3,535 (42.1)	2,552 (40.4)	
F	4,802 (57.2)	3,700 (58.6)	
Prefer not to answer	55 (0.7)	66 (1.0)	
Mean BMI, kg/m^2 (±SD)	22.1 (±3.5)	22.3 (±3.8)	0.08
BMI, kg/m^2			0.001
<18.5	932 (11.1)	757 (12.0)	
18.5–25.0	5,902 (70.3)	4,271 (67.6)	
≥25.0	1,406 (16.8)	1,174 (18.6)	
Underlying medical conditions‡			0.01
0	6,445 (76.8)	4,752 (75.2)	
1	1,382 (16.5)	1,057 (16.7)	
≥2	565 (6.7)	509 (8.1)	
Hypertension	557 (6.6)	441 (7.0)	0.41
Dyslipidemia	396 (4.7)	362 (5.7)	0.01
Respiratory diseases	394 (4.7)	317 (5.0)	0.37
Depression/anxiety	272 (3.2)	243 (3.8)	0.05
Heart diseases	197 (2.3)	180 (2.8)	0.06
Malignancy	169 (2.0)	131 (2.1)	0.80
Diabetes	152 (1.8)	167 (2.6)	0.001
No. COVID-19 vaccinations§			<0.001
0	685 (8.2)	412 (6.5)	
1	49 (0.6)	28 (0.4)	
2	1,675 (20.0)	1,145 (18.1)	
≥3	5,983 (71.3)	4,733 (74.9)	
Household income, ¥			0.002
<4 million	2,520 (34.5)	2,022 (32.0)	
4–8 million	3,699 (50.7)	2,614 (41.4)	
≥8 million	1,077 (14.8)	858 (13.6)	
Education level			0.68
High school or lower	1,242 (14.8)	961 (15.2)	
Some college	1,710 (20.4)	1,259 (19.9)	
College or higher	5,299 (63.1)	4,004 (63.4)	
Mean follow-up, d (±SD)	167.9 (±14.5)	NA	
No. SARS-CoV-2 infections			
1	8,284 (98.7)	NA	
2	108 (1.3)	NA	
Severity of infection			
Asymptomatic	228 (2.7)	NA	
Mild	8,098 (96.5)	NA	
Moderate/severe	66 (0.8)	NA	

*Values are no. (%) except as indicated. Continuous variables were compared by using *t*-tests; categorical variables were compared by using χ^2 tests. BMI, body mass index; NA, not applicable.
†Includes patients who turned 70 years of age between the participant selection and survey periods.
‡Respiratory diseases included interstitial lung diseases, asthma, and chronic obstructive pulmonary diseases. Heart diseases included myocardial infarction, angina, heart failure, arrhythmia, myocarditis, and cardiomyopathy. Mental disorder included anxiety and depression.
§Number of vaccinations administered until 14 d before infection (cases) or before June 2022 (controls).

associated with having post–COVID-19 condition: having any underlying medical conditions (OR 1.36, 95% CI 1.16–1.59, compared with no underlying medical conditions), and severity of acute COVID-19 (mild, OR 2.07, 95% CI 1.18–3.66; moderate, OR 4.49, 95% CI 1.97–10.23, compared with asymptomatic). Those participants vaccinated before infection had lower odds of developing post–COVID-19 condition (OR 0.75, 95% CI 0.60–0.95, compared with unvaccinated). Socioeconomic status, including household income and educational level, was not associated with post–COVID-19 condition.

Among the 992 cases who had experienced any post–COVID-19 condition, 84 (8.5%) answered that the condition was a serious hindrance on their daily lives at the time of response. A total of 402 (40.5%)

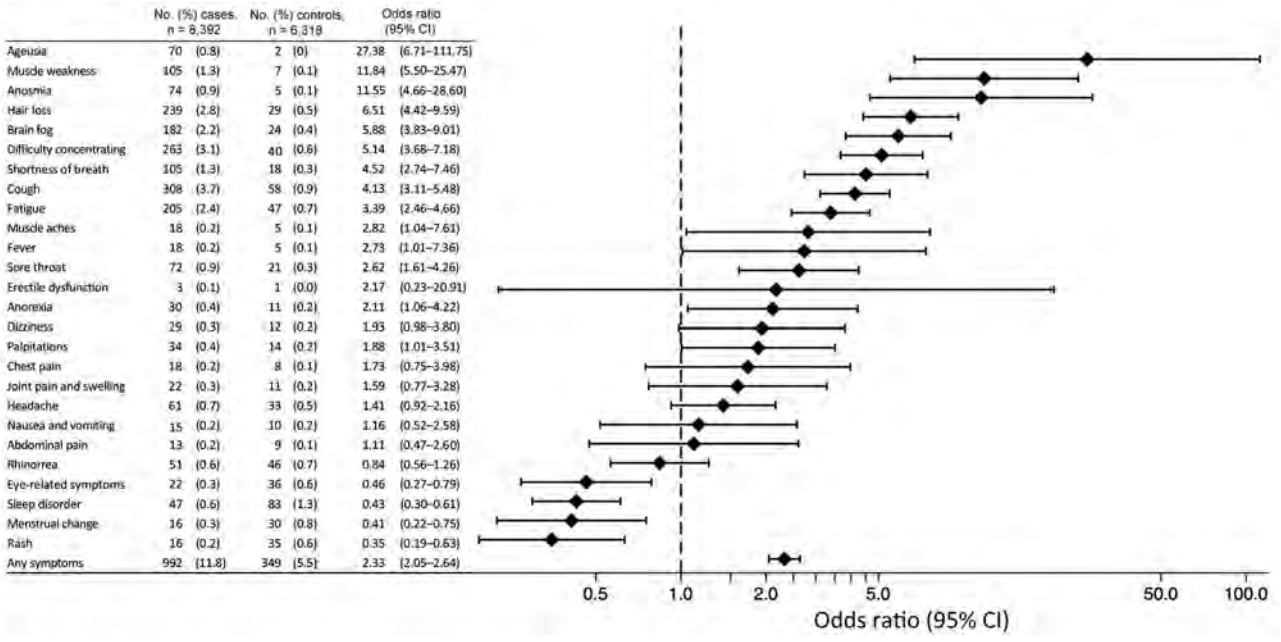

Figure 2. Prevalence and age- and sex-adjusted odds ratios of persistent symptoms in cases compared with controls in study of prevalence and risk factors for post–COVID-19 condition during Omicron BA.5–dominant wave, Japan. All cases and controls are included in the multivariable logistic regression analysis to estimate the odds ratio of developing post–COVID-19 condition among cases compared with controls adjusting for age (as a continuous variable) and sex.

noted that it was no hindrance, 362 (36.5%) mild hindrance, and 144 (14.5%) moderate hindrance.

Discussion

We conducted a population-based study using a self-reported questionnaire among adults in Japan who had confirmed SARS-CoV-2 infection during July–August 2022, when the Omicron BA.5 subvariant was dominant. We compared their post–COVID-19 condition with concordant persistent symptoms among noninfected controls. The percentage of post–COVID-19 condition was 11.8% for cases, which was 2.3 times higher than the 5.5% of persistent symptoms noted in controls. The cases had a 6.2% higher prevalence of post–COVID-19 condition than the controls, suggesting that their symptoms were likely associated with SARS-CoV-2 infection.

Population-based studies of infected persons in the United Kingdom (n = 56,003) and the United States (n = 1,480) using smartphone applications reported that the prevalence of post–COVID-19 condition associated with the Omicron variant, defined as symptoms lasting 4 weeks after the infection, was 4.5%–18.7% (*12*,*23*). Another population-based study of infected persons in the United States (n = 16,091) showed a prevalence of 11.2% (*16*) applying the WHO definition of the continuation or development of new symptoms 3 months after the initial SARS-CoV-2 infection, with those symptoms lasting for ≥2 months with no other explanation (*27*). Although the definition of post–COVID-19 condition varies among previous studies (*12*,*16*,*23*,*27*), the proportion shown in our study is consistent with previous results. In those reports, post–COVID-19 condition was less prevalent among those infected during the Omicron variant–dominant wave than those infected during the previous waves with the ancestral strain predominance (*16*,*23*). However, although a multicenter prospective cohort study showed a higher proportion of prolonged severe fatigue and multiple symptoms at 3 months during the pre-Delta wave than that during the Delta and Omicron waves, the differences disappeared after accounting for sociodemographics and vaccination status (*19*). Systematic reviews suggested that vaccination before infection was associated with a lower risk of experiencing post–COVID-19 condition (*30*,*31*). Similarly, we found that vaccination before infection was associated with lesser post–COVID-19 condition. An in-depth study would clarify whether the reduced risk for post–COVID-19 condition during the Omicron wave was a result of the differences in strains, the effect of vaccination, or both.

Population-based large cohort studies in the United Kingdom (n = 606,434 and n = 486,149) and Germany (n = 11,710) reported that patients infected with previous-variant SARS-CoV-2 frequently experienced persistent symptoms such as fatigue, shortness of breath, concentration difficulties, memory disturbance, hair loss, and anosmia (*5*,*7*,*32*). Studies

on patients infected with the Omicron variant, including a population-based study in the United States (n = 16,091) and hospital-based studies from China (n = 1,829) and India (n = 524), revealed that fatigue, brain fog, cough, and shortness of breath were frequently observed as post–COVID-19 condition (*13*,*16*,*33*). Our findings were comparable with previous results; we observed that post–COVID-19 condition after the Omicron-dominant epidemic frequently included neurologic symptoms such as difficulty concentrating, fatigue, and brain fog, in addition to cough and hair loss. In addition, those neurologic symptoms, as well as ageusia, anosmia, and muscle weakness, were distinctive symptoms among cases, who showed a higher OR than controls. Fatigue and neurocognitive impairment are reportedly related to impaired health recovery and reduced working capacity, even among young and middle-aged adults, after mild infection

Table 3. Factors associated with the prevalence and risk factors for post–COVID-19 condition during BA.5 Omicron-dominant wave, Japan*

Factor	No. at risk, n = 8,392	No. (%) cases,† n = 992	Model 1		Model 2		Model 3	
			OR (95% CI)	p value	OR (95% CI)	p value	OR (95% CI)	p value
Age group, y								
20–29	1,316	134 (10.2)	Referent	NA	Referent	NA	Referent	NA
30–39	2,340	289 (12.4)	1.31 (1.05–1.63)	0.02	1.23 (0.98–1.54)	0.07	1.22 (0.97–1.52)	0.08
40–49	2,326	307 (13.2)	1.40 (1.12–1.74)	0.003	1.32 (1.06–1.65)	0.01	1.26 (1.01–1.57)	0.05
50–59	1,695	206 (12.2)	1.33 (1.05–1.69)	0.02	1.23 (0.96–1.56)	0.10	1.16 (0.91–1.48)	0.24
60–70	715	56 (7.8)	0.83 (0.60–1.16)	0.28	0.75 (0.53–1.05)	0.10	0.70 (0.50–0.98)	0.04
Patient sex								
M	3,535	280 (7.9)	Referent	NA	Referent	NA	Referent	NA
F	4,802	703 (14.6)	1.98 (1.71–2.30)	<0.001	2.05 (1.76–2.39)	<0.001	2.00 (1.71–2.34)	<0.001
Underlying medical conditions								
Yes	1,947	263 (13.5)	NA	NA	1.36 (1.15–1.60)	<0.001	1.36 (1.16–1.59)	<0.001
No	6,445	729 (11.3)	NA	NA	Referent		Referent	NA
BMI, kg/m^2								
<18.5	932	119 (12.8)	NA	NA	0.94 (0.76–1.17)	0.59	0.94 (0.76–1.16)	0.58
18.5–25.0	5,902	686 (11.6)	NA	NA	Referent		Referent	NA
≥25.0	1,406	162 (11.5)	NA	NA	1.09 (0.90–1.32)	0.36	1.09 (0.90–1.31)	0.39
Severity of acute COVID-19								
Asymptomatic	228	13 (5.7)	NA	NA	Referent		Referent	NA
Mild	8,098	965 (11.9)	NA	NA	2.00 (1.13–3.52)	0.02	2.07 (1.18–3.66)	0.01
Moderate	64	14 (21.9)	NA	NA	4.00 (1.73–9.23)	0.001	4.49 (1.97–10.23)	<0.001
Severe	2	0	NA	NA	NA	NA	NA	NA
Vaccination before infection								
Yes	7,707	890 (11.5)	NA	NA	0.74 (0.59–0.92)	0.01	0.75 (0.60–0.95)	0.02
No	685	102 (14.9)	NA	NA	Referent	NA	Referent	NA
Household income, ¥								
<4 million	2,520	295 (11.7)	NA	NA	NA	NA	Referent	NA
4–8 million	3,699	433 (11.7)	NA	NA	NA	NA	1.05 (0.89–1.25)	0.54
≥8 million	1,077	128 (11.9)	NA	NA	NA	NA	1.10 (0.87–1.40)	0.43
Education level								
High school or lower	1,242	137 (11.0)	NA	NA	NA	NA	Referent	NA
Some college	1,710	252 (14.7)	NA	NA	NA	NA	1.20 (0.95–1.50)	0.12
College or higher	5,299	583 (11.0)	NA	NA	NA	NA	1.01 (0.82–1.25)	0.92

*Associations were determined by using multivariable logistic regression models for 8,392 infected persons (cases). Model 1 included age (as a categorical variable) and sex; model 2 added preexisting medical conditions (factor variable), BMI (categorical variable), severity of acute COVID-19 (categorical variable), and vaccination before infection (factor variable); model 3 added household income and education level (categorical variables). BMI, body mass index; NA, not applicable; OR, odds ratio.
†Number of cases who had post–COVID-19 condition.

(*7*). Our results showed that ≈10% of those who had post–COVID-19 condition had persistent difficulties in daily living 4.5–7 months after the Omicron-dominant wave, which may have led to a deterioration in economic conditions or work productivity. Although background socioeconomic status was not associated with developing post–COVID-19 condition in this study, further investigation is required to evaluate the effect of post–COVID-19 condition on changes in economic conditions, schooling, and employment.

Large-scale population-based cohort studies on infection before the Omicron wave found that post–COVID-19 condition was more common in female persons, smokers, persons with obesity, those with more severe acute COVID-19 symptoms, and those who were deprived or had lower household income (*5*,*7*,*32*). Moreover, hospital-based studies in China (n = 21,799) and South Africa (n = 4,685) showed that the female sex, concurrent conditions, and severe acute illnesses were associated with post–COVID-19 condition in association with the Omicron variant (*14*,*21*), which was consistent with our findings. Although the results regarding age are unclear, some studies on the Omicron variant have suggested that the population 18–50 years of age has a higher risk for post–COVID-19 condition (*21*,*34*). Our study showed that post–COVID-19 condition for those infected during the Omicron-dominant epidemic was also more prevalent in middle-aged persons. A substantial proportion of the working-age population might have been affected; of 9 million persons infected during July–August 2022 in Japan, 31.2% were in their 30s and 40s (*35*).

The strengths of this study are the large number of participants including noninfected controls, the population-based approach, and the inclusion of all infected residents registered in the HER-SYS database within a municipality. We compared the infected persons with noninfected persons as a control and assessed the proportion of post–COVID-19 condition after the Omicron-dominant wave.

The first limitation of this study is that the response rate was higher among the infected group than the noninfected group overall. The infected participants may have been more interested in the survey on COVID-19 and post–COVID-19 condition. However, because we did not specify the purpose of the survey to investigate the post–COVID-19 condition but rather informed the participants that we aimed to investigate the effect of the pandemic on their health and daily lives, we believe that the influence of interest in post–COVID-19 condition on the responses to the questionnaire was small. Moreover, the response rate was higher for infected and noninfected female participants and middle-aged infected male participants; this finding could have been because those persons were inherently willing to answer questionnaires more than other persons, or because patients with those attributes (such as female sex and middle age) suffered more from persistent symptoms and had a higher motivation to answer the questionnaire. The results could be biased in both ways; however, we believe the effect was small because the higher odds of having post–COVID-19 condition in our study were consistent with findings from previous studies. Second, although we excluded those who self-reported having SARS-CoV-2 infection, it is possible that some infected persons were included in the controls, causing an underestimation of the difference in persistent symptoms between the cases and controls. Third, because the study was retrospective, recall bias may have occurred. In addition, because we relied on self-reporting, we could not rule out the possibility that the participants' symptoms were caused by conditions other than COVID-19. However, we estimated the symptoms attributable to COVID-19 by comparing with a noninfected control group. Finally, although this study included all infected persons registered in the nationally established registry system, caution is needed to generalize the results of this single-city analysis to other populations in Japan.

In this population-based study, 11.8% of patients with COVID-19 had post–COVID-19 condition during the Omicron-dominant wave; this rate was 2.3 times higher than the persistent symptoms among noninfected controls. Among the cases, female sex, underlying medical conditions, and severity of acute COVID-19 were associated with having post–COVID-19 condition. We recommend a longer follow-up study of the effects on daily life and socioeconomic status after infection during the Omicron-dominant wave.

Acknowledgments

We thank Keiko Fukuuchi, Atsuko Abe, Shoji Sakano, and the staff of Shinagawa City Public Health Center for their cooperation in conducting this study.

This work was supported by MHLW Research on Emerging and Re-emerging Infectious Diseases and Immunization (program grant no. JPMH21HA2011).

About the Author

Dr. Iba is a senior research fellow at the Institute for Global Health Policy Research, Bureau of International Health Cooperation, National Center for Global Health and Medicine, Tokyo, Japan. Her research focuses on epidemiology and health services research.

References

1. World Health Organization. WHO COVID-19 dashboard [cited 2023 Aug 29]. https://covid19.who.int
2. Soriano JB, Murthy S, Marshall JC, Relan P, Diaz JV; WHO Clinical Case Definition Working Group on Post-COVID-19 Condition. A clinical case definition of post–COVID-19 condition by a Delphi consensus. Lancet Infect Dis. 2022; 22:e102–7. https://doi.org/10.1016/S1473-3099(21)00703-9
3. Davis HE, McCorkell L, Vogel JM, Topol EJ. Long COVID: major findings, mechanisms and recommendations. Nat Rev Microbiol. 2023;21:133–46. https://doi.org/10.1038/s41579-022-00846-2
4. Huang L, Li X, Gu X, Zhang H, Ren L, Guo L, et al. Health outcomes in people 2 years after surviving hospitalisation with COVID-19: a longitudinal cohort study. Lancet Respir Med. 2022;10:863–76. https://doi.org/10.1016/S2213-2600(22)00126-6
5. Whitaker M, Elliott J, Chadeau-Hyam M, Riley S, Darzi A, Cooke G, et al. Persistent COVID-19 symptoms in a community study of 606,434 people in England. Nat Commun. 2022;13:1957. https://doi.org/10.1038/s41467-022-29521-z
6. Ballering AV, van Zon SKR, Olde Hartman TC, Rosmalen JGM; Lifelines Corona Research Initiative. Persistence of somatic symptoms after COVID-19 in the Netherlands: an observational cohort study. Lancet. 2022;400:452–61. https://doi.org/10.1016/S0140-6736(22)01214-4
7. Peter RS, Nieters A, Kräusslich HG, Brockmann SO, Göpel S, Kindle G, et al.; EPILOC Phase 1 Study Group. Post-acute sequelae of covid-19 six to 12 months after infection: population based study. BMJ. 2022;379:e071050. https://doi.org/10.1136/bmj-2022-071050
8. Sudre CH, Murray B, Varsavsky T, Graham MS, Penfold RS, Bowyer RC, et al. Attributes and predictors of long COVID. Nat Med. 2021;27:626–31. https://doi.org/10.1038/s41591-021-01292-y
9. Menges D, Ballouz T, Anagnostopoulos A, Aschmann HE, Domenghino A, Fehr JS, et al. Burden of post-COVID-19 syndrome and implications for healthcare service planning: a population-based cohort study. PLoS One. 2021;16:e0254523. https://doi.org/10.1371/journal.pone.0254523
10. Sigfrid L, Drake TM, Pauley E, Jesudason EC, Olliaro P, Lim WS, et al.; ISARIC4C investigators. Long COVID in adults discharged from UK hospitals after COVID-19: a prospective, multicentre cohort study using the ISARIC WHO Clinical Characterisation Protocol. Lancet Reg Health Eur. 2021;8:100186. https://doi.org/10.1016/j.lanepe. 2021.100186
11. Menni C, Valdes AM, Polidori L, Antonelli M, Penamakuri S, Nogal A, et al. Symptom prevalence, duration, and risk of hospital admission in individuals infected with SARS-CoV-2 during periods of omicron and delta variant dominance: a prospective observational study from the ZOE COVID Study. Lancet. 2022;399:1618–24. https://doi.org/10.1016/S0140-6736(22)00327-0
12. Antonelli M, Pujol JC, Spector TD, Ourselin S, Steves CJ. Risk of long COVID associated with delta versus omicron variants of SARS-CoV-2. Lancet. 2022;399:2263–4. https://doi.org/10.1016/S0140-6736(22)00941-2
13. Arjun MC, Singh AK, Roy P, Ravichandran M, Mandal S, Pal D, et al. Long COVID following Omicron wave in Eastern India—a retrospective cohort study. J Med Virol. 2023;95:e28214. https://doi.org/10.1002/jmv.28214
14. Jassat W, Mudara C, Vika C, Welch R, Arendse T, Dryden M, et al. A cohort study of post–COVID-19 condition across the Beta, Delta and Omicron waves in South Africa: 6-month follow-up of hospitalized and nonhospitalized participants. Int J Infect Dis. 2023;128:102–11. https://doi.org/10.1016/j.ijid.2022.12.036
15. Morioka S, Tsuzuki S, Suzuki M, Terada M, Akashi M, Osanai Y, et al. Post–COVID-19 condition of the Omicron variant of SARS-CoV-2. J Infect Chemother. 2022;28:1546–51. https://doi.org/10.1016/j.jiac.2022.08.007
16. Perlis RH, Santillana M, Ognyanova K, Safarpour A, Lunz Trujillo K, Simonson MD, et al. Prevalence and correlates of long COVID symptoms among US adults. JAMA Netw Open. 2022;5:e2238804. https://doi.org/10.1001/jamanetworkopen.2022.38804
17. Taquet M, Sillett R, Zhu L, Mendel J, Camplisson I, Dercon Q, et al. Neurological and psychiatric risk trajectories after SARS-CoV-2 infection: an analysis of 2-year retrospective cohort studies including 1 284 437 patients. Lancet Psychiatry. 2022;9:815–27. https://doi.org/10.1016/S2215-0366(22)00260-7
18. Nehme M, Vetter P, Chappuis F, Kaiser L, Guessous I; CoviCare Study Team. Prevalence of post-COVID disease condition 12 weeks after Omicron infection compared with negative controls and association with vaccination status. Clin Infect Dis. 2023;76:1567–75. https://doi.org/10.1093/cid/ciac947
19. Gottlieb M, Wang RC, Yu H, Spatz ES, Montoy JCC, Rodriguez RM, et al. Severe fatigue and persistent symptoms at 3 months following severe acute respiratory syndrome coronavirus 2 infections during the pre-Delta, Delta, and Omicron time periods: a multicenter prospective cohort study. Clin Infect Dis. 2023;76:1930–41. https://doi.org/10.1093/cid/ciad045
20. Kahlert CR, Strahm C, Güsewell S, Cusini A, Brucher A, Goppel S, et al. Post-acute sequelae after severe acute respiratory syndrome coronavirus 2 infection by viral variant and vaccination status: a multicenter cross-sectional study. Clin Infect Dis. 2023;77:194–202. https://doi.org/10.1093/cid/ciad143
21. Cai J, Lin K, Zhang H, Xue Q, Zhu K, Yuan G, et al. A one-year follow-up study of systematic impact of long COVID symptoms among patients post SARS-CoV-2 Omicron variants infection in Shanghai, China. Emerg Microbes Infect. 2023;12:2220578. https://doi.org/10.1080/22221751.2023.2220578
22. Diexer S, Klee B, Gottschick C, Xu C, Broda A, Purschke O, et al. Association between virus variants, vaccination, previous infections, and post–COVID-19 risk. Int J Infect Dis. 2023;136:14–21. https://doi.org/10.1016/j.ijid.2023.08.019
23. Durstenfeld MS, Peluso MJ, Peyser ND, Lin F, Knight SJ, Djibo A, et al. Factors associated with long COVID symptoms in an online cohort study. Open Forum Infect Dis. 2023;10:ofad047. https://doi.org/10.1093/ofid/ofad047
24. Chen J, Wang R, Gilby NB, Wei GW. Omicron variant (B.1.1.529): infectivity, vaccine breakthrough, and antibody resistance. J Chem Inf Model. 2022;62:412–22. https://doi.org/10.1021/acs.jcim.1c01451
25. CoV-Spectrum. Detect and analyze variants of SARS-CoV-2. 2023 [cited 2023 Nov 24]. https://cov-spectrum.org
26. International Severe Acute Respiratory and Emerging Infection Consortium. COVID-19 long-term protocol. 2023 [cited 2023 Nov 24]. https://isaric.org/research/covid-19-clinical-research-resources/covid-19-long-term-follow-up-study
27. World Health Organization. A clinical case definition of post–COVID-19 condition by a Delphi consensus, 6 October 2021 [cited 2023 Nov 24]. https://www.who.int/

publications/i/item/WHO-2019-nCoV-Post_COVID-19_condition-Clinical_case_definition-2021.1
28. Miyazato Y, Morioka S, Tsuzuki S, Akashi M, Osanai Y, Tanaka K, et al. Prolonged and late-onset symptoms of coronavirus disease 2019. Open Forum Infect Dis. 2020;7:ofaa507. https://doi.org/10.1093/ofid/ofaa507
29. WHO Working Group on the Clinical Characterisation and Management of COVID-19 infection. A minimal common outcome measure set for COVID-19 clinical research. Lancet Infect Dis. 2020;20:e192–7. https://doi.org/10.1016/S1473-3099(20)30483-7
30. Watanabe A, Iwagami M, Yasuhara J, Takagi H, Kuno T. Protective effect of COVID-19 vaccination against long COVID syndrome: a systematic review and meta-analysis. Vaccine. 2023;41:1783–90. https://doi.org/10.1016/j.vaccine.2023.02.008
31. Byambasuren O, Stehlik P, Clark J, Alcorn K, Glasziou P. Effect of COVID-19 vaccination on long covid: systematic review. BMJ Med. 2023;2:e000385. https://doi.org/10.1136/bmjmed-2022-000385
32. Subramanian A, Nirantharakumar K, Hughes S, Myles P, Williams T, Gokhale KM, et al. Symptoms and risk factors for long COVID in non-hospitalized adults. Nat Med. 2022;28:1706–14. https://doi.org/10.1038/s41591-022-01909-w
33. Liao X, Guan Y, Liao Q, Ma Z, Zhang L, Dong J, et al. Long-term sequelae of different COVID-19 variants: the original strain versus the Omicron variant. Glob Health Med. 2022;4:322–6. https://doi.org/10.35772/ghm.2022.01069
34. Luo J, Zhang J, Tang HT, Wong HK, Lyu A, Cheung CH, et al. Prevalence and risk factors of long COVID 6–12 months after infection with the Omicron variant among nonhospitalized patients in Hong Kong. J Med Virol. 2023;95:e28862. https://doi.org/10.1002/jmv.28862
35. Japan Ministry of Health, Labour and Welfare. Visualizing the data: information on COVID-19 infections. 2023 [cited 2023 Sep 12]. https://covid19.mhlw.go.jp/en

Address for correspondence: Arisa Iba, Institute for Global Health Policy Research, Bureau of International Health Cooperation, National Center for Global Health and Medicine, 1-21-1 Toyama, Shinjuku, Tokyo, 162-8655, Japan; email: aiba@it.ncgm.go.jp

Engaging Communities in Emerging Infectious Disease Mitigation to Improve Public Health and Safety

Michàlle E. Mor Barak, Shinyi Wu, Gil Luria, Leslie P. Schnyder, Ruotong Liu, Anthony Nguyen, Charles D. Kaplan

The COVID-19 pandemic highlighted the need for potent community-based tools to improve preparedness. We developed a community health-safety climate (HSC) measure to assess readiness to adopt health behaviors during a pandemic. We conducted a mixed-methods study incorporating qualitative methods (e.g., focus groups) to generate items for the measure and quantitative data from a February 2021 national survey to test reliability, multilevel construct, and predictive and nomologic validities. The 20-item HSC measure is unidimensional (Cronbach $\alpha = 0.87$). All communities had strong health-safety climates but with significant differences between communities ($F = 10.65$; $p<0.001$), and HSC levels predicted readiness to adopt health-safety behaviors. HSC strength moderated relationships between HSC level and behavioral indicators; higher climate homogeneity demonstrated stronger correlations. The HSC measure can predict community readiness to adopt health-safety behaviors in communities to inform interventions before diseases spread, providing a valuable tool for public health authorities and policymakers during a pandemic.

The COVID-19 pandemic demonstrated the influence community attitudes have on the health behaviors of its residents (e.g., wearing facemasks, accepting vaccines). Evidence on COVID-19 spread indicates that within-community contexts affect individual perceptions regarding taking precautions and following government guidelines and policies vary (*1*–*3*). Because COVID-19 and other infectious diseases spread mainly among persons sharing a physical environment, behaviors of members of a geographic community can influence transmission.

Climate in the context of health-safety refers to shared perceptions within a community about the importance of maintaining and supporting behaviors that protect residents from infectious diseases. Climate theory postulates that individual persons perceive how others in their group expect them to behave and shape their behaviors accordingly (*4*). From a social psychology perspective, climate refers to the shared perceptions of members of an organization, group, or community concerning the procedures, practices, and kinds of behaviors that are rewarded and supported within the unit (*5*,*6*). Tests of climate theory related to community characteristics (e.g., service, productivity, innovation, inclusion) have demonstrated climate to be an effective predictor of behaviors (*7*,*8*). Previous research suggests that tools to measure community climate can help identify differences in levels of health-safety climate (HSC level) among communities and extent of agreement among residents within a community (climate strength) (*5*,*9*).

We defined communities as persons living in the same geographic area, having substantial interactive relations, and holding many attitudes in common (*10*). Data from the COVID-19 pandemic emphasize the central role of community dynamics in viral transmission (*11*,*12*). Community-based research demonstrates that interactions between persons within

Author affiliations: University of Southern California Marshall School of Business, Los Angeles, California, USA (M.E. Mor Barak); University of Southern California Suzanne Dworak-Peck School of Social Work, Los Angeles (M.E. Mor Barak, S. Wu, L.P. Schnyder, R. Liu); University of Southern California Viterbi School of Engineering, Los Angeles (S. Wu, A. Nguyen); University of Haifa Faculty of Social Welfare and Health Sciences, Haifa, Israel (G. Luria, C.D. Kaplan)

DOI: https://doi.org/10.3201/eid3007.230932

geographic communities enable both transmission of infectious diseases among residents and emergence of shared perceptions, which can be used in efforts to prevent and control spread of the disease. Studies have confirmed that shared norms, values, and behaviors exist in communities and influence the perceptions and behaviors of community members (*13*–*15*). However, other studies indicate that perceptions about the climate within a group may vary among individual persons (*7*,*9*).

Mischel's theoretical formulation of strong situations (i.e., communities with high HSC strength) explains the possible effects of climate strength (*16*). Degree of ambiguity about appropriate health-safety behaviors within communities differs on the basis of climate strength; strong situations demonstrate little ambiguity and weak situations greater ambiguity among members about perceptions and expectations regarding appropriate behavior. In strong-climate communities, individual responses vary little, whereas in weak-climate communities, variability is greater (*16*–*18*). Thus, climate strength may act as a moderator between climate level and behavioral outcomes. Members of communities with stronger climate levels will achieve greater consensus about the perceived necessity of community-related climate interventions (e.g., health-safety behaviors during a pandemic). Groups with greater consensus among members more consistently perceive the need to adopt health-safety behaviors, resulting in a stronger relationship between climate level and behaviors.

Community health-safety behaviors are critical for preventing transmission of infectious diseases and returning to normal life through mitigating disease spread depends heavily on community behaviors. Having a tool to measure community HSC is essential for informing decisions and strategies to limit the spread of disease and combat variants during a pandemic. Some efforts to develop that measure have been undertaken at the organizational level, but no measure has been available at the community level (*19*,*20*). To address this gap, we developed a measure of the strength of community climate levels for adopting health-safety behaviors. During phase I, we used qualitative data derived from community-based focus groups, and during phase II, we validated the measure with data from a nationally representative sample. To assess reliability, we hypothesized that the HSC measure would demonstrate high internal consistency. To assess multilevel construct validity (*21*,*22*), we hypothesized that a sufficient level of agreement in HSC perceptions will exist among members of geographic communities. To assess predictive validity (*23*,*24*), we hypothesized that HSC level will be positively related to health-safety behaviors. To assess nomologic validity (*25*) (Figure 1), we hypothesized that HSC strength will moderate the relationship between HSC levels and health behaviors. The full research protocol was approved by the institutional review board at the University of Southern California (Los Angeles, CA, USA).

Methods

Phase I—Generating the HSC Measure

Sample and Procedure

We conducted a series of focus groups from 4 diverse communities, each predominantly Asian, Latinx, Black, and White, across a large urban county in California. The groups resided in the same geographic area and had similar proportions of racial/ethnic composition; we tried to represent participants proportionally by age, sex, and socioeconomic status. With the help of community gatekeepers, social media, and messaging applications, we used purposive and snowball sampling to select participants and reduce bias. Ten focus groups (n = 39 persons) were organized; 12 (30.77%) participants were Latinx, 11 (28.21%) Chinese/Taiwanese, 9 (23.08%) White, and 7 (17.95%) Black. By age group, 17 (43.59%) participants were 18–39 years, 14 (35.90%) 40–59 years, and

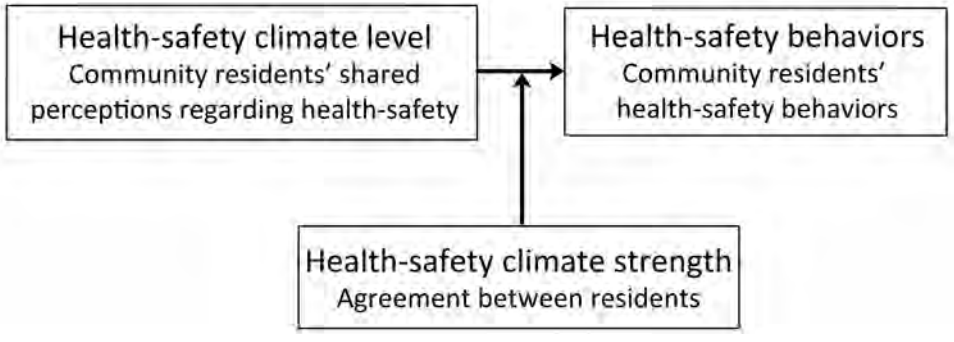

Figure 1. Diagram showing moderating effect of relationship health-safety climate strength on health-safety climate level leading to health-safety behaviors.

8 (20.51%) 60–79 years. Most (30; 76.92%) participants were women, 23 (58.97%) had children, 25 (64.1%) had a college degree, and 24 (61.54%) reported a religious affiliation (Protestant, Catholic, Buddhist, or Jewish).

Using climate theory as a theoretical background, we brainstormed potential topics for inclusion in the focus groups. Questions focused on participants' perceptions and observations of pandemic-related behaviors among the residents in their communities. Each focus group session lasted ≈75 minutes, was hosted on Zoom, and was video recorded.

Data Analysis

We used a 4-step approach to identify items for inclusion in the HSC measure (*26*). In step 1, focus group transcripts were generated automatically from the video recordings. One team member reviewed the transcripts for accuracy by comparing them to the recordings, and another member completed an additional review. All personally identifiable information was removed. All transcripts were uploaded into NVivo 12 (https://help-nv.qsrinternational.com/12/win/v12.1.115-d3ea61/Content/welcome.htm) for analysis. We used deductive thematic analysis during the initial coding process to generate a provisional codebook and coding framework (*27*,*28*). We used the codebook to enhance the accuracy and consistency of coding, as well as navigate the pragmatic demands of research (*28*). Examples of coded elements included behavioral expectations (e.g., behavioral cues), COVID-19–related policy (e.g., adherence, enforcement), and reasons persons do or do not follow guidelines. Four team members were trained as coders, and each focus group transcript was analyzed independently by 2 coders. The coders met in analytic seminars to discuss the coding hierarchical process and modify the codebook of parent (main) codes and related child (minor) subcodes. New parent and child codes emerged during data analysis, and we added them to the codebook. Finally, the coders identified overarching themes representative of core categories and storylines from the qualitative data.

In step 2, we used a top-down/bottom-up approach to guide generation of measure items (*6*). Items were statements about the measure that respondents were asked to endorse. These statements were validated and used to construct the final scale. Initial themes identified in step 1 guided further brainstorming of sample items representative of the final general themes. Examples for each item generated were drawn directly from focus group discussions to represent variation in context and topic. For example, 1 item generated was the statement "In my community, members are likely to tell someone to follow COVID health-safety guidelines (wearing masks, social distancing, vaccinations, etc.)." Another was "In my community, members make others feel uncomfortable (make fun of, sarcastic remarks, etc.) for following COVID health-safety guidelines (wearing masks, social distancing, vaccinations, etc.)." Next, we used a bottom-up approach to review examples related to the themes developed in step 1. We then reviewed each example to assess whether we needed to develop a new item. This process generated 62 items; we analyzed those items for overlap and removed duplicates.

In step 3, we developed checklist statements of items that unambiguously identified behaviors related to COVID-19 health-safety. We first rank-ordered checklist statements on the basis of our experience collecting and analyzing focus group data. Using the same checklist, we rank-ordered items on the basis of perceived relative importance. We discussed the adequacy of external referents and refined the wording of the final set of statements to ensure relevance and minimize response acquiescence bias. This process continued until we reached consensus.

In step 4, we finalized the HSC measure using Q-sort analysis by first clustering similar statements into piles and assigning names to each pile. This analysis provided a key for interpreting the underlying measurement construct and enhancing reliability of clustering. We then revised and finalized the measure for field testing (*29*).

Phase II—Validating the Measure

Sample and Procedure

Using qualitative data obtained from the focus groups in phase I, we developed a 20-item HSC measure. To validate the measure, we incorporated the items into the Understanding Coronavirus in America tracking survey, which is an expansion of the Understanding America Study (UAS) (*30*) that includes questions related to the COVID-19 pandemic. The UAS is an ongoing internet panel of ≈9,500 adult respondents who represent households across the United States. Beginning in 2020 and continuing throughout the pandemic, UAS sent out waves of the tracking surveys to inquire about personal behaviors and perceptions relevant to COVID-19.

We selected questions from the Understanding Coronavirus in America tracking survey relevant to behaviors during the COVID-19 pandemic to serve as a standard for the predictive validity of the HSC

measure. Questions included: "Which of the following have you done in the last seven days to keep yourself safe from coronavirus: 1) Avoid public spaces, gatherings, or crowds; 2) Avoid contact with high-risk persons; 3) Avoid eating at restaurants; 4) Wear a face mask or some other face coverings; 5) Remain in your residence except for essential activities or exercise; and 6) Wash hands with soap or used hand sanitizer several times a day." Potential responses for each question were yes, no, or unsure.

To enable reporting of the HSC measure in community subgroups, we selected all ZIP (postal) codes within the UAS that had ≥10 respondents, resulting in 153 postal codes. In February 2021, we distributed English- and Spanish-language versions of the HSC measure to all UAS participants residing in one of the 153 postal codes (n = 2,359). We received responses from 1,672 (70.9%) participants. We excluded from analysis 24 (1.4%) respondents with missing data (final n = 1,648).

To protect the identities of respondents and ensure a sufficient number of respondents from each geographic community, we created a community for each postal code, identified by the first 3 digits of the postal code. To mask respondent identifiers, the UAS survey team created a variable that provided respondents with an index number associated with their 3-digit postal-code community. Only postal-code communities with ≥10 respondents were included in the analyses. The final sample included 1,438 respondents who were nested in 49 communities. The average number of respondents from each community was 29.34 (range 10–319).

Data Analysis

We used an exploratory factor analysis (EFA) of the curated UAS data to determine construct validity. The EFA used principal components analysis with varimax rotation to uncover underlying factor structures for each of the 20 HSC items using data from the 1,438 respondents. We performed 2 tests for the fit of factor analysis to the data: Bartlett's test of sphericity, which yielded a significant test statistic of 8,961.302 ($p<0.001$), and the Kaiser-Meyer-Olim test, which yielded a test statistic of 0.924. Both tests indicated that factor analyses were appropriate. We calculated Cronbach α for the 20 identified items to determine internal consistency of the measure. To assess multilevel construct validity (*21*,*22*), we calculated an index for HSC strength at the community level using group-level interrater agreement measured by the ratio of within-group variance (r_{WG}) (*31*), which is the proportion of observed group variance relative to expected random variance (*32*). r_{WG} ≥0.70 indicates satisfactory group-level agreement (*31*).

We assessed predictive validity using a series of multilevel logistic regression analyses among the HSC measure and behavioral indicators while controlling for age and sex (*23*,*24*). We used behavioral indicators from the Understanding Coronavirus in America survey (*30*) and included avoiding public places and wearing a face mask. The dependent variable was whether the respondent had performed each behavioral indicator (yes = 1, no = 0). Because the number of unsure responses was relatively small (n = 8 for washing hands to n = 21 for avoiding public places), we excluded those responses from the analyses. Independent variables included the HSC measure, age, and sex (male = 0, female = 1).

We assessed nomologic validity using multilevel logistic regression analyses (*25*). We explored the moderating effects of climate strength on the relationship between HSC level and the same UAS behavioral indicators used in the predictive validity procedure. We selected behavioral indicators from Centers for Disease Control and Prevention recommendations: avoiding public places, avoiding contact with high-risk persons, avoiding eating at restaurants, washing hands, wearing a face mask, and remaining in one's own residence except for essential activities, including exercise. We performed multilevel modeling analyses with r_{WG} as a moderator between HSC and behavioral outcomes, controlling for age and sex; persons were nested within groups at the community level. We measured HSC and health-safety behaviors at the individual level and climate strength at the community level.

Results

Phase I

We generated a 20-item community HSC measure that included questions related to following health-safety behaviors, including community mask wearing, distancing guidelines, and the effects of community leadership, among others (Appendix). The HSC measure incorporated a 5-point Likert scale with responses ranging from 1 (strongly disagree) to 5 (strongly agree). To avoid response-set bias, we applied reverse wording to negative statements, when appropriate. For example, "In my community, members will socially distance themselves from someone who is not wearing a mask (keep away from someone)" and "In my community, persons believe that their freedom to decide what is right for them is more important than following COVID health-safety guidelines (wearing masks, social distancing, vaccinations, etc)." The HSC measure score was determined quantitatively by totaling Likert scale responses from each item and

dividing by 20. Because missing data were minimal (n = 14, 0.8%), we performed factor analysis only when respondents answered all 20 questions. HSC measure scores ranged from 1.3 to 4.7; higher scores indicated higher community HSC levels.

Phase II

Community HSC Level

Based on the scree plot and factor loadings, 2 factors accounted for most of the variance in the items proposed to measure community HSC: factor 1 had an eigenvalue of 6.38 and factor 2 a value of 2.05, explaining 42.12% of the variance (factor 1 = 31.88%, factor 2 = 10.24%). Review of the item content and their loadings indicated that all positive items loaded on factor 1, whereas all negative (reverse-coded) items loaded on factor 2. Because we could determine no other explanation for the formation or potential reversed-item biases, we concluded the measure was unidimensional (*33*). All 20 items were included in the final measure (reverse-coding the negative statements). A Cronbach α of 0.87 for the overall measure indicated strong internal consistency.

Community HSC Agreement Strength

High agreement was demonstrated in climate perception (strength of climate) levels (median r_{WG} = 0.9). All communities sampled in the study had strong climates (r_{WG} >0.73). Analysis of variance revealed significant differences among community climate levels (F = 10.65; p<0.001). Thus, members of a given community agreed on the climate level within their community, but communities had significantly different climate levels between one another.

HSC Relationships with Behavioral Indicators

Multilevel modeling analyses between the HSC measure and COVID-19 behavioral indicators demonstrated that the higher the HSC level, the more likely persons within the group were to avoid public places (b = 0.73; p<0.001), avoid contact with high-risk persons (b = 0.87; p<0.001), avoid eating at restaurants (b = 0.52; p<0.001), wash their hands frequently (b = 0.68; p<0.01), wear a face mask (b = 1.25; p<0.001), and remain in their own residence except for essential activities or to exercise (b = 0.66; p<0.001) (Table).

HSC as a Moderator

Multilevel modeling analyses with r_{WG} as moderator demonstrated that HSC strength moderated the relationship between HSC level and behavioral indicators, including avoiding public spaces (b = 11.12; p<0.01), avoiding contact with high-risk persons (b = 15.37; p<0.01), and washing hands frequently (b = 20.97; p<0.05) (Table; Figure 2). Moderation effects were not found for the other 3 indicators: avoiding restaurants, wearing a face mask, and remaining in own residence. Communities with higher climate homogeneity demonstrated a stronger correlation between HSC and behavioral outcomes than groups with lower climate homogeneity.

Discussion

We generated and validated an HSC measure as a tool to measure community climate level for health-safety. Using qualitative data from 4 distinct geographic communities, we generated 20 items to assess the level of community climate for health-safety behaviors. To validate the measure, we tested 4 hypotheses using nationally representative samples from the UAS.

Table. Multilevel logistic regression analysis of health-safety climate and behavioral outcomes, controlling for age and sex, as part of developing a community HSC measure to assess readiness to adopt health behaviors during a pandemic*

Category	Avoid public spaces, n = 1,048	Avoid contact with high-risk persons, n = 992	Avoid eating at restaurants, n = 1,048	Wash hands, n = 1,060	Wear a face mask, n = 1,061	Remain in residence except for essential activities, n = 1,064
Predictor variables						
HSC level†	0.73‡	0.87‡	0.52‡	0.68§	1.25‡	0.66‡
Age¶	0.01	0.02†	0.01	0.01	–0.01	0.02‡
Female sex#	0.27**	0.42**	0.04	0.82‡	0.15	0.24
Moderation analysis with HSC strength as moderator						
HSC level‡	–9.03**	–12.59§	–6.83	–17.74**	–1.42	–4.18
HSC strength††	–28.19**	–42.86§	–19.63	62.56**	–5.02	–11.71
HSC level × HSC strength	11.12§	15.37§	8.33	20.97**	3.01	5.49
Age¶	0.01	0.02‡	0.01	0.01	–0.01	0.02‡
Female sex#	0.25	0.039**	0.04	0.79§	0.17	0.24

*Five records were excluded from each regression model because of missing information. HSC, health-safety climate.
†HSC level ranged from 1.3 to 4.7 (mean 3.17, SD 0.49)
‡Statistical significance at p<0.001 level based on the Wald test.
§Statistical significance at p<0.01 level based on the Wald test.
¶Age ranged from 19 to 111 y (mean 47.42 y, SD 16.23 y).
#Sex: 890 participants (62.46%) were female and 535 (37.54%) were male.
**Statistical significance at p<0.05 level based on the Wald test.
††HSC strength (r_{WG}) ranged from 0.69 to 0.95 (mean 0.88, SD 0.03).

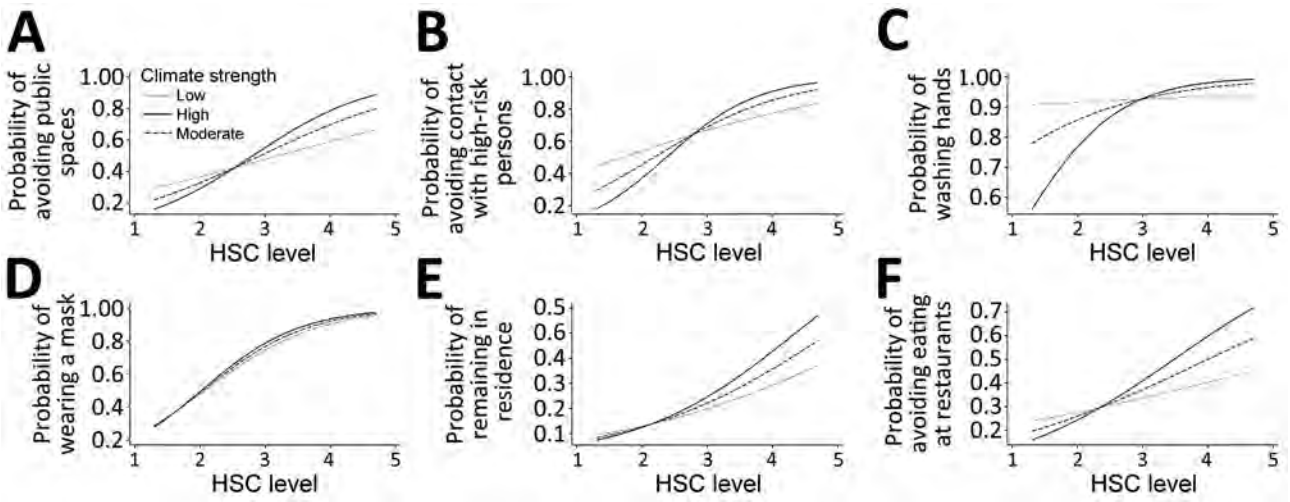

Figure 2. HSC and behavioral outcomes by HSC strength. Moderate HSC is represented by the mean of r_{WG}; low HSC is represented by 1 SD below and high by 1 SD above the mean of r_{WG}. HSC, health-safety climate.

The HSC measure demonstrated high internal consistency. We found strong agreement regarding HSC perceptions among members within single geographic communities and demonstrated that HSC level was positively related to health-safety behaviors. Finally, we demonstrated that HSC strength moderates the relationship between climate level and health behaviors. The multilevel modeling analyses supported HSC strength as a moderator between HSC level and behavioral indicators. Communities with higher climate homogeneity showed stronger correlation between HSC and behavioral outcomes. Overall, the HSC measure demonstrated internal consistency and strong predictive, multilevel, and nomologic validities. Of note, the HSC measure can be applied to a variety of infectious diseases and used in public health studies of current and future epidemics and pandemics.

Consistent with climate theory, the HSC measure clearly demonstrated that community HSC can predict behaviors in a variety of communities (*5*,*6*). Our study focused on persons who live in the same geographic area; members of geographically close communities tend to have substantive interactive relations and common attitudes, both of which are relevant to the transmission levels of infectious diseases (*10*). That dynamic was evident during the COVID-19 pandemic, in which infection rates differed between neighborhoods (*11*,*12*).

Our findings might clarify the general effect of normative social influence on decision-making, including community climate regarding informal health-safety mores and norms and formalized rules and procedures. Understanding underlying perceptions of social and health-related behaviors of community members is vital for mitigating disease spread during a pandemic (*34*), especially before vaccine availability and as variants emerge. During the COVID-19 pandemic, many communities over time exhibited reduced tolerance and growing resentment toward external controls and enforcement of behavioral guidelines by authorities (*35*). Given the diminishing returns of such formal enforcements over time, enlisting local communities and their leaders to create climates that encourage residents to voluntarily take health-safety actions is critical. Furthermore, the HSC measure can be especially useful given the heterodoxy of scientific opinions regarding the most effective mitigation strategies, guidelines, and policies at the community level (*3*). The HSC measure can also help democratize policymaking in public health pandemic control by systematically accounting for and addressing perspectives among community members.

Further analysis at the community level is needed. Of particular interest are studies examining the interrelationships of community HSC and health-safety decision-making during a pandemic with regard to competing social values, such as following government guidelines versus rights of individual determination. Similarly, differences in individual perceptions regarding the risk of infection, perceived risks in family and friend circles, and risks to the public should be assessed. Such assessments could inform future research on how trust of particular sources for providing information and personal preferences affect health-safety behaviors. Finally, future research should measure the relationship between community HSC and objective data (e.g., infection rates, number of persons hospitalized because of infection).

Among our study's strengths, we combined an in-depth qualitative process to generate measurable items

with data from diverse communities and use of a large national cohort for validation. Among limitations, we performed our analysis at the community level, but because of the nature of the large national sample used for validation and the need to protect participants' anonymity, the best proxy available was to designate communities based on postal codes. Analyses of smaller geographic communities may provide more accurate results; thus, future studies should sample smaller communities (e.g., neighborhoods). Although major racial/ethnic groups were represented in our focus groups, groups were not proportional with respect to sex, age, and family size. Because of countywide research regulations during the COVID-19 pandemic, we were unable to recruit participants in person or conduct face-to-face focus groups. Future research in this area should include more representative samples for recruiting focus groups to generate measurable items. Finally, reliance on self-reports from respondents may have introduced single-source bias.

In conclusion, during pandemics, shared perceptions within communities and the consequent behaviors of community members can affect transmission of infectious diseases (*13*–*15*). Building on climate research, our HSC measure can assist in assessing HSC level and strength in different communities and identifying communities in which risk for infection spread is high. The HSC measure can assist public health authorities and policymakers in preventing and controlling the spread of a pandemic by enabling focused interventions to improve health-safety climates before disease spread occurs or is amplified. Thus, the HSC measure can serve as a valuable tool for pandemic preparedness and response as well as for public health studies of current and future pandemics.

Acknowledgments

The authors thank the editor and the anonymous reviewers at EDI; Arie Kapteyn and the team at the Understanding America Study; Beatrice Martinez, Natalie Humber, Maya Neuenschwander, and Lily Shah.

The project described in this paper relies in part on data from a survey administered in the Understanding America Study probability panel, which is maintained by the Center for Economic and Social Research (CESR) at the University of Southern California.

USC Research and Innovation at the University of Southern California for the Zumberge Special Solicitation—Epidemic- and Virus-Related Research and Development Award provided support for this research project.

About the Author

Dr. Mor Barak is the Dean Endowed Professor at the University of Southern California School of Social Work with a joint appointment at the Marshall School of Business. Her research interests focus on diversity and inclusion in communities and organizations, with an emphasis on health and mental health outcomes.

References

1. Centers for Disease Control and Prevention. How to protect yourself and others [cited 2023 Feb 11]. https://www.cdc.gov/coronavirus/2019-ncov/prevent-getting-sick/prevention.html
2. Chu DK, Akl EA, Duda S, Solo K, Yaacoub S, Schünemann HJ; COVID-19 Systematic Urgent Review Group Effort (SURGE) study authors. Physical distancing, face masks, and eye protection to prevent person-to-person transmission of SARS-CoV-2 and COVID-19: a systematic review and meta-analysis. Lancet. 2020;395:1973–87. https://doi.org/10.1016/S0140-6736(20)31142-9
3. Shir-Raz Y, Elisha E, Martin B, Ronel N, Guetzkow J. Censorship and suppression of Covid-19 heterodoxy: tactics and counter-tactics. Minerva. 2022;3:1–27.
4. Zohar D. Safety climate in industrial organizations: theoretical and applied implications. J Appl Psychol. 1980;65:96–102. https://doi.org/10.1037/0021-9010.65.1.96
5. Luria G, Boehm A, Cnaan RA. Community climate: adapting climate theory to the study of communities. In: Serpe RT, editor. Handbook of community movements and local organizations in the 21st century. New York: Springer; 2018. p. 41–59.
6. Luria G, Boehm A, Mazor T. Conceptualizing and measuring community road-safety climate. Saf Sci. 2014;70:288–94. https://doi.org/10.1016/j.ssci.2014.07.003
7. Luria G. Climate as a group level phenomenon: theoretical assumptions and methodological considerations. J Organ Behav. 2019;40:1055–66. https://doi.org/10.1002/job.2417
8. Patterson M, Warr P, West M. Organizational climate and company productivity: the role of employee affect and employee level. J Occup Organ Psychol. 2004;77:193–216.
9. Luria G. Climate strength–how leaders form consensus. Leadersh Q. 2008;19:42–53. https://doi.org/10.1016/j.leaqua.2007.12.004
10. Rubin HJ, Rubin I. Community organizing and development. 4th ed. London: Pearson; 2008.
11. Thomas LJ, Huang P, Yin F, Xu J, Almquist ZW, Hipp JR, et al. Geographical patterns of social cohesion drive disparities in early COVID infection hazard. Proc Natl Acad Sci U S A. 2022;119:e2121675119. https://doi.org/10.1073/pnas.2121675119
12. Jackson SL, Derakhshan S, Blackwood L, Lee L, Huang Q, Habets M, et al. Spatial disparities of COVID-19 cases and fatalities in United States counties. Int J Environ Res Public Health. 2021;18:8259. https://doi.org/10.3390/ijerph18168259
13. Hill JM, Jobling R, Pollet TV, Nettle D. Social capital across urban neighborhoods: a comparison of self-report and observational data. Evol Behav Sci. 2014;8:59–66. https://doi.org/10.1037/h0099131
14. Colombo M, Mosso C, De Piccoli N. Sense of community and participation in urban contexts. J Community Appl Soc Psychol. 2001;11:457–64. https://doi.org/10.1002/casp.645

15. Agarwal R, Dugas M, Ramaprasad J, Luo J, Li G, Gao GG. Socioeconomic privilege and political ideology are associated with racial disparity in COVID-19 vaccination. Proc Natl Acad Sci U S A. 2021;118:e2107873118. https://doi.org/10.1073/pnas.2107873118
16. Mischel W. Towards a cognitive social-learning model reconceptualization of personality. In: Endler DM, Magnusson D, editors. Interactional psychology and personality. New York: Wiley; 1976. p. 166–207.
17. González-Romá V, Peiró JM, Tordera N. An examination of the antecedents and moderator influences of climate strength. J Appl Psychol. 2002;87:465–73. https://doi.org/10.1037/0021-9010.87.3.465
18. Schneider B, Salvaggio AN, Subirats M. Climate strength: a new direction for climate research. J Appl Psychol. 2002;87:220–9. https://doi.org/10.1037/0021-9010.87.2.220
19. Bazzoli A, Probst TM. COVID-19 moral disengagement and prevention behaviors: the impact of perceived workplace COVID-19 safety climate and employee job insecurity. Saf Sci. 2022;150:105703. https://doi.org/10.1016/j.ssci.2022.105703
20. Probst TM, Lee HJ, Bazzoli A, Jenkins MR, Bettac EL. Work and non-work sickness presenteeism: the role of workplace COVID-19 climate. J Occup Environ Med. 2021;63:713–8. https://doi.org/10.1097/JOM.0000000000002240
21. Meade AW, Eby LT. Using indices of group agreement in multilevel construct validation. Organ Res Methods. 2007;10:75–96. https://doi.org/10.1177/1094428106289390
22. Chen G, Mathieu JE, Bliese PD. A framework for conducting multi-level construct validation. In: Yammarino FJ, Dansereau F, editors. Multi-level issues in organizational behavior and processes. Vol. 3. Bingley (UK): Emerald Group Publishing Limited; 2005. p. 273–303.
23. Cronbach LJ, Meehl PE. Construct validity in psychological tests. Psychol Bull. 1955;52:281–302. https://doi.org/10.1037/h0040957
24. American Psychological Association. Standards for educational and psychological tests. Washington: The Association; 1974.
25. Bagozzi RP. An examination of the validity of two models of attitude. Multivariate Behav Res. 1981;16:323–59. https://doi.org/10.1207/s15327906mbr1603_4
26. Judge TA, Kammeyer-Mueller JD. Job attitudes. Annu Rev Psychol. 2012;63:341–67. https://doi.org/10.1146/annurev-psych-120710-100511
27. Braun V, Clarke V. Using thematic analysis in psychology. Qual Res Psychol. 2006;3:77–101. https://doi.org/10.1191/1478088706qp063oa
28. Braun V, Clarke V. One size fits all? What counts as quality practice in (reflexive) thematic analysis? Qual Res Psychol. 2021;18:328–52. https://doi.org/10.1080/14780887.2020.1769238
29. Rost F. Q-sort methodology: bridging the divide between qualitative and quantitative. An introduction to an innovative method for psychotherapy research. Couns Psychother Res. 2021;21:98–106. https://doi.org/10.1002/capr.12367
30. University of Southern California Dornsife Center for Economic and Social Research. Understanding America study 2022 [cited 2023 Feb 11]. https://uasdata.usc.edu/index.php
31. James LR, Demaree RG, Wolf G. r_{WG}: an assessment of within-group interrater agreement. J Appl Psychol. 1993;78:306–9. https://doi.org/10.1037/0021-9010.78.2.306
32. Cohen A, Doveh E, Eick U. Statistical properties of the r_{WG} (J) index of agreement. Psychol Methods. 2001;6:297–310. https://doi.org/10.1037/1082-989X.6.3.297
33. Weijters B, Baumgartner H, Schillewaert N. Reversed item bias: an integrative model. Psychol Methods. 2013;18:320–34. https://doi.org/10.1037/a0032121
34. Holmes EA, O'Connor RC, Perry VH, Tracey I, Wessely S, Arseneault L, et al. Multidisciplinary research priorities for the COVID-19 pandemic: a call for action for mental health science. Lancet Psychiatry. 2020;7:547–60. https://doi.org/10.1016/S2215-0366(20)30168-1
35. Gadarian SK, Goodman SW, Pepinsky TB. Partisanship, health behavior, and policy attitudes in the early stages of the COVID-19 pandemic. PLoS One. 2021;16:e0249596. https://doi.org/10.1371/journal.pone.0249596

Address for correspondence: Michàlle E. Mor Barak, Suzanne Dworak-Peck School of Social Work, University of Southern California, University Park, MRF Bldg, Rm 341, Los Angeles, CA 90089-0411, USA; email: morbarak@usc.edu

Wuchereria bancrofti Lymphatic Filariasis, Barrancabermeja, Colombia, 2023

José A. Suárez, Jose A. Vargas-Soler, Laura Isabel Manosalva-Arciniegas, Stephanie Becerra-González, Angie L. Ramirez, Tatiana Cáceres, Nicolas Luna, Juan David Ramírez, Alberto Paniz-Mondolfi

We describe a recent case of lymphatic filariasis in Colombia caused by *Wuchereria bancrofti* nematodes. Our study combines clinical-epidemiologic findings with phylogenetic data. Resurgence of lymphatic filariasis may be linked to increasing urbanization trends and migration from previously endemic regions. Fieldwork can be a beneficial tool for screening and containing transmission.

"…could not avoid a spasm of horror at the sight of men with ruptures sitting in their doorways on hot afternoons, fanning their enormous testicle as if it were a child sleeping between their legs […] well-carried rupture was, more than anything else, a display of masculine honor."

"For a long time and with great pride, the scrotal hernia that many men in the city endured was attributed to the water from the cisterns, not only without shame but even with a certain patriotic insolence."

—Gabriel García Márquez,
Love in the Time of Cholera

Lymphatic filariasis (LF) is caused by an infection with the mosquitoborne filarial nematodes *Wuchereria bancrofti*, *Brugia malayi*, and *Brugia timori* (*1*). Transmission has occurred in various regions, including Africa, Southeast Asia, and the Pacific basin (*1*). In addition, cases have been documented in specific areas across the Middle East, Caribbean, and South America (*1*,*2*). Historically, LF was endemic in 24 countries within the Americas (*1*,*3*); currently, 4 countries remain endemic for LF (Brazil, Haiti, Guyana, and the Dominican Republic), and 13.4 million persons are at risk for infection (*2*). Aside from Guyana, little is known about the occurrence and endemicity of LF caused by the *W. bancrofti* nematodes in northern South America, particularly in Colombia and Venezuela, where no recent cases were reported. We describe an LF case in Colombia caused by *W. bancrofti* infection.

Author affiliations: Universidad Internacional Sek Quito, Quito, Ecuador (J.A. Suárez); Sistema Nacional de Investigación, Senacyt, Panama (J.A. Suárez); Universidad de Panamá, Panama City, Panama (J.A. Suárez); Universidad Industrial de Santander, Bucaramanga, Colombia (J.A. Vargas-Soler); Fundación Cardiovascular de Colombia, Bucaramanga (J.A. Vargas-Soler, L.I. Manosalva-Arciniegas, S. Becerra-González); Universidad del Rosario, Bogotá, Colombia (A.L. Ramirez, T. Cáceres, N. Luna, J.D. Ramirez); Icahn School of Medicine at Mount Sinai, New York, NY, USA (J.D. Ramirez, A. Paniz-Mondolfi).

DOI: https://doi.org/10.3201/eid3007.231363

The Study

A 14-year-old boy residing in an urban area of Barrancabermeja, Santander, Colombia, located to the east bank of the Magdalena River, sought care for a history of progressive lymphedema lasting for 3 years. His symptoms began after a hunting trip to the San Rafael plateau, a forest area situated in the foothills of the eastern mountain range, ≈37 km west of Barrancabermeja. He was referred to Fundación Cardiovascular de Colombia because of progressive enlargement of both testicles, which had become painful over the previous few weeks, and recurrent episodes of fever, erythema, urticarial-like lesions, itching, and pain in the left lower limb. The patient had previously been under outpatient care with a vascular surgery team, who had considered a diagnosis of arteriovenous malformation. Of note, the patient did not experience symptom onset until age 11.

Physical examination of the patient showed extensive lymphedema of the left lower limb, extending from the foot to the genital region, along with areas of induration in the left thigh and painful bilateral inguinal lymphadenopathy (Figure 1, panel A). We also found severe scrotal edema (Figure 1, panel B). Complete blood count results showed leukocytosis with 87.4% neutrophils, indicating neutrophilia (reference

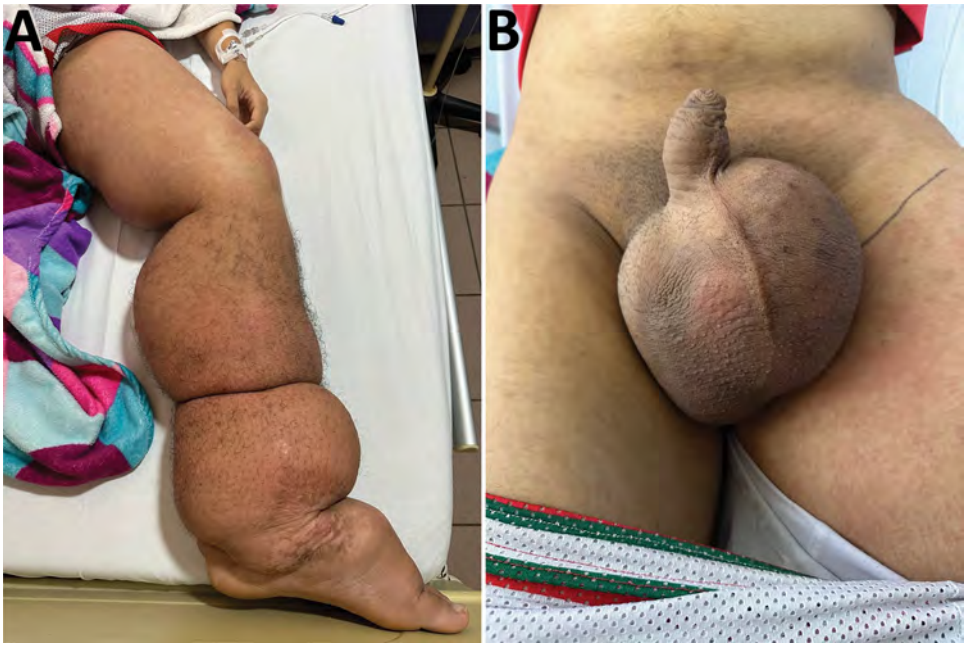

Figure 1. Images of a 14-year-old patient from Colombia experiencing severe progressive lymphedema caused by a *Wuchereria bancrofti* nematode infection. A) Patient's left lower limb, showing generalized lymphedema extending from the foot to the genital region along with erythematous areas involving the left thigh and areas of perimaleolar hypocromia and hypercromia reflective of post-inflammatory trophic skin changes. B) Severe scrotal edema (hydrocele).

range 45%–70%). All other laboratory test results were unremarkable, including no eosinophilia. Doppler ultrasound revealed bilateral giant scrotal hydrocele. A computed tomography scan of the abdomen and pelvis, performed 3 months earlier, had demonstrated bilateral hydrocele along with left para-aortic, right iliac, and bilateral inguinal lymphadenopathy.

Our suspicion of chronic filariasis prompted nocturnal direct examination by using the Knott concentration method, which yielded inconclusive results (Appendix, https://wwwnc.cdc.gov/EID/article/30/7/23-1363-App1.pdf). We then pursued molecular characterization. We extracted DNA from the patient's blood sample and conducted a PCR-based filarial detection by using specific primers for *W. bancrofti* nematodes. Those primers targeted the cytochrome c oxidase subunit I, along with short and long fragments of the 18S gene (Appendix).

We identified the species by using the MinION Sequencing System (Oxford Nanopore, https://nanoporetech.com) for the 3 gene fragments, as described previously (*4*,*5*). We evaluated phylogenetic relationships of the sequenced isolate by comparison against other filarial species, confirming its taxonomic assignment as *W. bancrofti* (Figure 2; Appendix Figure 1). We started the patient on treatment consisting of clindamycin (600 mg intravenously every 8 h for 7 d) and single doses of ivermectin (100 µg/kg) and albendazole (400 mg) while awaiting diethylcarbamazine (DEC), which is currently unavailable in Colombia.

LF was a prevalent clinical condition in Colombia from the 16th Century until the mid-20th Century, prominent in the Caribbean city of Cartagena de Indias, where the initial cases were documented (*6*). However, it was not until 1930 that its endemicity was identified in communities residing along the Magdalena River, specifically in the oil city of Barrancabermeja, where the last case was reported in the late 1940s (*7*). The estimated incidence in that area was ≈16 cases/1000 oil-workers annually, making it one of the country's major endemic regions (*7*). The incidence of the disease markedly declined during the 1960s and 1970s, resulting in only sporadic and subclinical cases, eventually leading to the apparent disappearance of the disease foci for reasons that remain undetermined. Since that time, no new cases were reported in Colombia until 2016, when a case of giant penile and scrotal lymphedema was documented in a 33-year-old patient in the city of Cali, Valle del Cauca (*8*). However, there was no confirmation of parasite presence or verification of a travel history or residency in endemic areas (*8*).

This case shows the potential for reemergence of LF in Colombia and highlights the clinical characteristics associated with LF. The patient was a 14-year-old boy with chronic manifestations of the disease, including lymphedema and hydrocele, typically observed in the adult population (*9*). The case features dermatolymphangioadenitis attacks characteristic of the acute phase (*9*,*10*). Studies of LF in children suggest advanced stages of lymphedema and the presence of hydrocele, although rare, tend to be more prevalent in male children during puberty or older, which aligns with the observations in our case (*10*,*11*).

DEC is the drug of choice for *W. bancrofti*–caused LF, because of its dual action; primary microfilaricidal and partial macrofilaricidal effects typically result in a 50% reduction in adult filaria (*12*). Because DEC is unavailable in Colombia, we made the decision to initiate treatment with ivermectin in combination with albendazole, leveraging the microfilaricidal properties of ivermectin (*10*). Clindamycin therapy was started to mitigate the risk of secondary bacterial infection because of the patient's acute dermatolymphangioadenitis. While awaiting DEC availability, initiating doxycycline treatment is being considered, because of its potential for controlling the adult parasite forms (*13*).

Because the patient's medical history did not indicate travel, we believe the resurgence of LF may be associated with increasing urbanization trends, leading to the breakthrough of new ecologic niches and migration from previously known endemic regions such as Venezuela. From an epidemiologic perspective, it is important to highlight that *W. bancrofti* filaria exhibit a nocturnal periodicity of microfilaremia, which coincides with the peak activity hours of its main vector, *Culex quinquefasciatus* mosquitoes (*14*). *C. quinquefasciatus* mosquitoes demonstrate anthropodomestic habits, which are determining factors in the focal transmission of *W. bancrofti* infection in the vicinity of human dwellings (*14*). The patient's

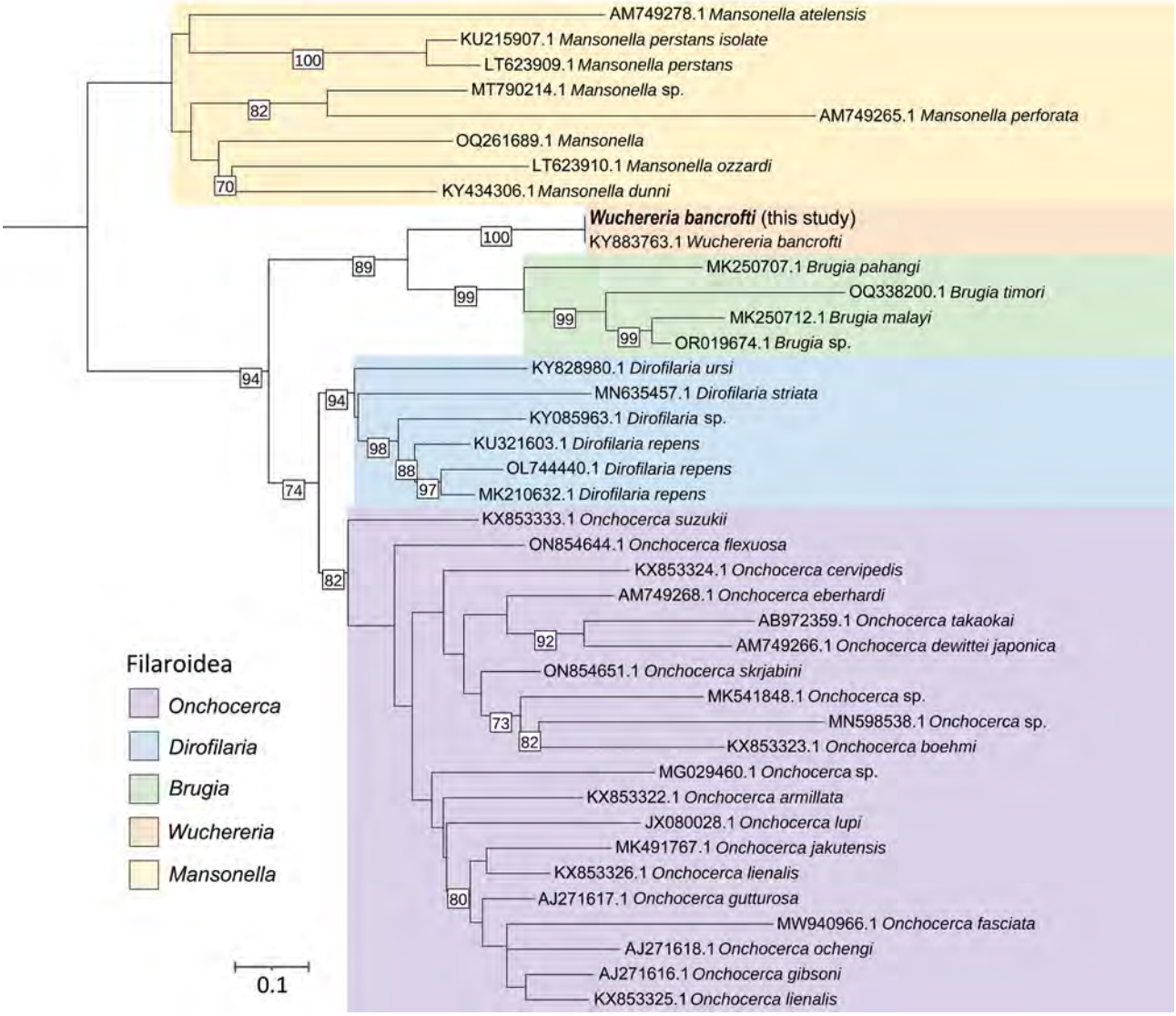

Figure 2. Phylogenetic reconstruction of consensus sequences of filaria, generated from a sample collected from a 14-year-old patient in Colombia (bold text). Cytochrome c oxidase I (COI) gene marker was used for this reconstruction. GenBank accession numbers are provided for reference sequences. Numbers along branch lengths indicate measures of support. Scale bar indicates the distance scale.

place of residence (Barrancabermeja) is an endemic area not only for *Culex* spp. mosquitoes but also for other vectors involved in the urban transmission of *W. bancrofti* filaria, such as *Aedes* spp. mosquitoes.

Conclusions

As previously reported, exposure to the LF infection within households appears to be a major contributor to childhood LF infection (*10*,*14*). Investigating familial clustering in this case is warranted. Despite renewed control efforts led by the Global Programme for the Elimination of LF, *W. bancrofti* infection foci persist in the region. Vigilance is crucial to prevent the reactivation of former endemic foci or a resurgence of cases in hypoendemic regions, which is potentially the scenario in this case. Parasite and entomologic surveillance should be promptly established to help develop and implement targeted interventions, including mass drug administration, vector control measures, and other strategic approaches. Such measures are essential for preventing the potential emergence of additional cases of LF within this geographic region of Colombia.

About the Author

Dr. Suárez is a clinician research scientist in the Panamanian Investigation System and CIDES, Panama City, Panama, and a professor at the International University SEK-Ecuador, Quito, Ecuador, and the University of Panama, Panama City, Panama. His primary research interests are tropical medicine, and fungal and parasitic diseases.

References

1. Cromwell EA, Schmidt CA, Kwong KT, Pigott DM, Mupfasoni D, Biswas G, et al.; Local Burden of Disease 2019 Neglected Tropical Diseases Collaborators. The global distribution of lymphatic filariasis, 2000-18: a geospatial analysis. Lancet Glob Health. 2020;8:e1186–94. https://doi.org/10.1016/S2214-109X(20)30286-2
2. Pan American Health Organization, World Health Organization. Lymphatic filariasis [cited 2023 Oct 4]. https://www.paho.org/en/topics/lymphatic-filariasis
3. Fontes G, da Rocha EMM, Scholte RGC, Nicholls RS. Progress towards elimination of lymphatic filariasis in the Americas region. Int Health. 2020;13(Suppl 1):S33–8. https://doi.org/10.1093/inthealth/ihaa048
4. Davidov K, Iankelevich-Kounio E, Yakovenko I, Koucherov Y, Rubin-Blum M, Oren M. Identification of plastic-associated species in the Mediterranean Sea using DNA metabarcoding with Nanopore MinION. Sci Rep. 2020;10:17533. https://doi.org/10.1038/s41598-020-74180-z
5. Knot IE, Zouganelis GD, Weedall GD, Wich SA, Rae R. DNA barcoding of nematodes using the MinION. 2020. [cited 2023 Sep 27]. https://www.frontiersin.org/articles/10.3389/fevo.2020.00100/full
6. Sotomayor Tribin, H.A. Medical and literary annotations of the history of *Wuchereria bancrofti* filariasis in Cartagena and Colombia [in Spanish]. Rev Cinc Biomed. 2014;5:374–81.
7. Paterson JC. Observations on filariasis in Colombia. 1932 [cited 2023 Oct 4]. https://academic.oup.com/trstmh/article/26/2/169/1907303
8. Vives F, García-Perdomo HA, Ocampo-Flórez GM. Giant lymphedema of the penis and scrotum: a case report. Autops Case Rep. 2016;6:57–61. https://doi.org/10.4322/acr.2016.026
9. Pani SP, Balakrishnan N, Srividya A, Bundy DA, Grenfell BT. Clinical epidemiology of bancroftian filariasis: effect of age and gender. Trans R Soc Trop Med Hyg. 1991;85:260–4. https://doi.org/10.1016/0035-9203(91)90048-4
10. Shenoy RK, Bockarie MJ. Lymphatic filariasis in children: clinical features, infection burdens and future prospects for elimination. Parasitology. 2011;138:1559–68. https://doi.org/10.1017/S003118201100117X
11. Witt C, Ottesen EA. Lymphatic filariasis: an infection of childhood. Trop Med Int Health. 2001;6:582–606. https://doi.org/10.1046/j.1365-3156.2001.00765.x
12. Gyapong JO, Kumaraswami V, Biswas G, Ottesen EA. Treatment strategies underpinning the global programme to eliminate lymphatic filariasis. Expert Opin Pharmacother. 2005;6:179–200. https://doi.org/10.1517/14656566.6.2.179
13. Mand S, Debrah AY, Klarmann U, Batsa L, Marfo-Debrekyei Y, Kwarteng A, et al. Doxycycline improves filarial lymphedema independent of active filarial infection: a randomized controlled trial. Clin Infect Dis. 2012;55:621–30. https://doi.org/10.1093/cid/cis486
14. Simonsen PE, Mwakitalu ME. Urban lymphatic filariasis. Parasitol Res. 2013;112:35–44. https://doi.org/10.1007/s00436-012-3226-x

Address for correspondence: Alberto Paniz Mondolfi, Icahn School of Medicine at Mount Sinai, 1428 Madison Ave, Atran Bldg, 2nd Fl, New York, NY 10029, USA; email: alberto.paniz-mondolfi@mountsinai.org

Treatment Outcomes for Tuberculosis Infection and Disease Among Persons Deprived of Liberty, Uganda, 2020

Deus Lukoye, Julius N. Kalamya, Anna Colletar Awor, Gail Gustavson, Joseph Kabanda, Odile Ferroussier-Davis, Charles Kajoba, Azaria Kanyamibwa, Leonard Marungu, Stavia Turyahabwe, Simon Muchuro, Lisa Mills, Emilio Dirlikov, Lisa J. Nelson

We report that unsuccessful treatment outcomes were 11.8% for tuberculosis (TB) disease and 21.8% for TB infection among persons deprived of liberty in Uganda Prisons Service facilities. Remedial efforts should include enhancing referral networks to ensure treatment continuity, strengthening data systems for complete outcome documentation, and prioritizing short-course treatment regimens.

Tuberculosis (TB) remains a major public health challenge and the most frequent cause of illness and death among persons living with HIV (PLHIV) (*1*). Globally, TB occurs in congregate settings marked by malnutrition, overcrowding, underlying illnesses or conditions such as HIV, and poor ventilation, which include correctional facilities (*2*–*4*). High TB prevalence in prisons contributes to illness and death not only among persons deprived of liberty (PDLs; e.g., persons who are incarcerated or otherwise being held in detention facilities) but also among the general population who interact with PDLs in prison or after a PDL's release (*3*).

In 2020, the Uganda Prisons Service housed ≈65,000 PDLs across 259 facilities. The average stay was 19.1 months for capital offenders and 3.6 months for petty offenders. In Uganda, TB incidence was estimated to be 2,071/100,000 persons in prisons in 2019 (*5*). All PDLs are screened at entry into Uganda Prisons Service facilities for TB disease and HIV status to establish eligibility for TB preventive treatment (TPT). Case finding during incarceration is determined from symptom self-reporting. Since 2016, the treatment regimens recommended by the Uganda Ministry of Health have been isoniazid, rifampin, ethambutol, and pyrazinamide for 2 months, followed by isoniazid/rifampin for 2 months for TB disease and 6 months of isoniazid for TB infection (TBI). However, 2019–2021 Uganda Prisons Service data indicated suboptimal treatment outcomes for those regimens; the TB disease treatment success rate was 89% and cure rate was 65%, and TPT completion rate was 75% (*6*). To inform remedial interventions, we conducted a cross-sectional study to evaluate correlates of unsuccessful treatment outcomes for TB disease and TBI among PDLs in Uganda.

The Study

In December 2021, we extracted data on PDLs who received TB disease or TBI treatment during January–December 2020 at 27 prisons that were selected according to availability of TB and HIV services at those sites (Appendix Figure, https://wwwnc.cdc.gov/EID/article/30/7/23-0611-App1.pdf). We abstracted sociodemographic and clinical information (age, sex, HIV status, incarceration stay, treatment initiation date, and outcome) from prison entry, TPT, and unit TB registers. TB disease data collected from unit TB registers were TB treatment history (new, previously treated), diagnosis (laboratory confirmed, clinical), and site (pulmonary, extrapulmonary) (*7*).

Author affiliations: US Centers for Disease Control and Prevention, Kampala, Uganda (D. Lukoye, J.N. Kalamya, A.C. Awor, G. Gustavson, J. Kabanda, L. Mills, E. Dirlikov, L.J. Nelson); Centers for Disease Control and Prevention, Atlanta, Georgia, USA (O. Ferroussier-Davis); Uganda Prisons Service, Kampala (C. Kajoba, A. Kanyamibwa, L. Marungu); Uganda Ministry of Health, Kampala (S. Turyahabwe, S. Muchuro)

DOI: https://doi.org/10.3201/eid3007.230611

We calculated the duration of prison stays before initiation of TB disease or TBI treatments. For TB disease treatment, we defined successful outcomes as cured or treatment completion (treatment was completed but no bacteriologic proof of cure) and unsuccessful outcomes as lost to follow-up (LTFU), death, treatment failure, or no documented outcome (*7*). For TBI treatment, we defined successful outcomes as treatment completed and unsuccessful outcomes as LTFU, death, or treatment stopped. When the outcome was treatment stopped, we collected data on reported reasons (*8*).

We calculated descriptive statistics and conducted bivariate analyses to determine associations between exposure and outcome variables. We used χ^2 tests for categorical variables and *t*-tests for continuous variables to identify associations between independent and outcome variables. We considered variables with a p value of <0.05 and an estimate range within a 95% CI to be significant. We included all variables with a p value of ≤0.2 from bivariate analysis in the multivariate analysis. We used logistic regression to control for effect modification and confounders with dichotomous outcomes. We conducted analyses by using SAS version 9.4 (SAS Institute Inc., https://www.sas.com).

PDLs residing in the 27 selected prisons comprised 62.5% (38,005/60,771) of the total prison population in Uganda during December 2020; the median number of PDLs was 953 (range 79–5,998). During the study period, 1,117 PDLs were treated for TB disease; median age was 34 (interquartile range [IQR] 26–43) years, and most (1,098 [98.3%]) were men. The median number of TB patients per prison was 28 (IQR 6–68). Among the 1,116 with TB disease who had documented HIV status, 340 (30.5%) were HIV-positive. Only 7.3% (82/1,117) of PDLs were previously treated for TB disease (80 relapses and 2 returns after LTFU). Among the 985 (88.1%) PDLs who had successful outcomes, 446 (45.3%) were cured and 539 (54.7%) completed treatment. Among the 132 PDLs who had unsuccessful outcomes, 36 (27.2%) were LTFU, 35 (26.5%) died, 5 (3.7%) failed treatment, and 56 (42.4%) had no documented outcome (54 transferred out, 1 had multidrug resistant TB treatment, and 1 was not evaluated). The death rate among PDLs treated for TB disease was 3.1% (35/1,117). PDLs with laboratory-confirmed pulmonary TB (adjusted odds ratio [aOR] 2.2, 95% CI 1.03–4.81; p = 0.04) and extrapulmonary TB (aOR 1.7, 95% CI 1.11–2.54; p = 0.014) had higher odds of unsuccessful treatment outcomes than those with clinically diagnosed pulmonary TB (Table 1). PDLs whose prison stays were <6 months had higher odds of unsuccessful outcomes (aOR 3.1, 95% CI 1.60–6.11; p = 0.0008) than those who stayed ≥6 months.

A total of 2,672 PDLs were treated for TBI; the median age was 30 (IQR 26–38) years, and most of those treated (2,337 [87.5%]) were men. Of 2,668 PDLs with documentedHIV status, 2,468 (92.5%) were

Table 1. Characteristics and treatment outcomes among persons deprived of liberty who had TB disease in Uganda prisons, January–December 2020*

Variable	Total, no. (%)	Successful treatment, no. (%)	Unsuccessful treatment, no. (%)	Crude OR (95% CI)	p value	aOR (95% CI)	p value
Patient sex							
F	19 (1.7)	18 (94.7)	1 (5.2)	0.4 (0.06–3.12)	0.39	0.5 (0.07–3.88)	0.51
M	1,098 (98.3)	967 (88.2)	131 (11.8)	Referent		Referent	
Age, y							
≤35	858 (76.8)	784 (91.4)	74 (8.6)	1.2 (0.83–1.73)	0.34	1.1 (0.76–1.63)	0.58
>35	259 (23.2)	202 (78.0)	57 (22.0)	Referent		Referent	
Patient category							
New	1,035 (92.7)	912 (88.1)	123 (11.9)	1.2 (0.57–2.58)	0.61	1.5 (0.66–3.54)	0.32
Previously treated	82 (7.3)	74 (90.2)	8 (9.8)	Referent		Referent	
TB form							
Pulmonary, laboratory confirmed†	631 (56.5)	548 (86.8)	83 (13.2)	1.6 (1.06–2.40)	0.03	2.2 (1.03–4.81)	0.04
Extrapulmonary	56 (5.0)	46 (82.1)	10 (17.9)	2.3 (1.07–4.92)	0.02	1.7 (1.11–2.54)	0.014
Pulmonary, clinical diagnosis	428 (38.5)	391 (91.7)	37 (8.6)	Referent		Referent	
HIV status, n = 1,116‡							
Negative	776 (69.7)	683 (88.0)	93 (11.9)	0.9 (0.62–1.39)	0.72	0.9 (0.57–1.46)	0.703
Positive	338 (30.3)	300 (88.8)	38 (11.2)	Referent		Referent	
Length of incarceration before treatment							
<6 mo	908 (81.4)	787 (86.7)	121 (13.3)	3.0 (1.58–5.91)	0.0010	3.1 (1.60–6.11)	0.0008
≥6 mo	208 (18.6)	198 (95.2)	10 (4.8)	Referent		Referent	

*aOR, adjusted odds ratio; TB, tuberculosis.
†Pulmonary TB was confirmed by bacteriologic laboratory tests.
‡Data are for a total of 1,116 patients with TB disease who had documented HIV status.

Table 2. Characteristics and treatment outcomes among persons deprived of liberty who had TB infections in Uganda prisons, January–December 2020*

Variable	Total, no. (%)	Successful treatment, no. (%)	Unsuccessful treatment, no. (%)	Crude OR (95% CI)	p value	aOR (95% CI)	p value
Patient sex							
M	2,337 (87.5)	1,829 (78.2)	508 (21.8)	1.7 (1.23–2.36)	0.0012	1.6 (1.10–2.27)	0.014
F	335 (12.5)	288 (86.0)	47 (14.0)	Referent		Referent	
Age, y							
≤35	1,720 (64.5)	1,359 (79.0)	361 (21.0)	1.0 (0.85–1.26)	0.7495	1.1 (0.88–1.37)	0.44
>35	948 (35.5)	754 (79.5)	194 (20.5)	Referent		Referent	
HIV status							
Negative	200 (7.5)	166 (83.0)	34 (17.0)	Referent		Referent	
Positive	2,468 (92.5)	1,947 (78.9)	521 (21.1)	1.3 (0.89–1.91)	0.1684	2.1 (1.42–3.21)	0.00
Length of incarceration before treatment							
<6 mo	2,212 (84.6)	1,714 (77.5)	498 (22.5)	1.8 (1.34–2.43)	<0.0001	1.8 (1.28–2.48)	0.0006
≥6 mo	403 (15.4)	347 (86.1)	56 (13.9)	Referent		Referent	

*aOR, adjusted odds ratio; TB, tuberculosis.

HIV-positive. The median number of PDLs treated for TBI per prison was 70 (IQR 44–126). Overall, 79.1% (2,113/2,672) completed TBI treatment. Among 555 PDLs who had unsuccessful outcomes, 245 (44.1%) transferred out, 207 (37.3%) were LTFU, 98 (17.7%) stopped treatment (31 experienced adverse events, 11 had TB disease and appropriate treatment was started, and 56 did not have reported reasons), 5 (0.9%) died (including 4 PLHIVs), and 4 had missing data. The death rate among PDLs treated for TBI was 0.2% (5/2,672). Higher risk for unsuccessful TBI treatment outcomes was associated with PDLs who stayed <6 months (aOR 1.8, 95% CI 1.28–2.48; p = 0.0006), were men (aOR 1.60, 95% CI 1.10–2.27; p = 0.014), and were PLHIVs (aOR 2.13, 95% CI 1.42–3.21; p = 0.0003) (Table 2).

TB is common in Uganda Prisons Service facilities and, despite improvements among the general population, treatment outcomes among PDLs remain suboptimal (*6*). Renewed efforts are needed to improve treatment outcomes, especially for PDLs who have extrapulmonary infection or laboratory-confirmed pulmonary TB or who are PLHIVs (*9*,*10*). Because of transmission risks within this congregate setting, TPT could be further expanded, including among HIV-negative persons. Unsuccessful outcomes did not differ markedly according to HIV status among patients with TB disease. Reported deaths among PLHIV treated for TBI might be attributed to opportunistic infections or missed TB disease diagnoses (*11*).

Short prison stays are challenging for successful TB treatment (*12*). Enhanced referral networks could ensure treatment continuity, including during prison transfers and after release. Strengthened data systems are needed to properly document and report treatment outcomes regardless of release or transfer status. Finally, World Health Organization–recommended short-course treatment regimens for TB disease and TBI could be prioritized for prisons to improve treatment completion (*13*,*14*) and documentation, given the frequent transfers, short average stay, and suboptimal continuity of care after release.

The first limitation of our study is that we could not evaluate outcomes among PDLs who transferred out or those without documented outcomes, which could negatively skew results. Second, data limitations precluded analysis of other known risk factors for unsuccessful treatment outcomes (e.g., homelessness, substance abuse, previous imprisonment, presence of cavitary disease) (*15*). Finally, the concurrent COVID-19 outbreak during the study period, which disturbed health service provisions, could have affected treatment outcomes, limiting generalizability of findings to the years before and after the outbreak.

Conclusions

We found suboptimal treatment outcomes for PDLs with TB disease and TBI in Uganda Prisons Service facilities. Remedial efforts are needed to enhance referral networks to ensure treatment continuity, strengthen data systems for complete outcome documentation, and prioritize short-course treatment regimens.

This activity was covered by a certificate of confidentiality from the US Centers for Disease Control and Prevention and approved by the Uganda National Council of Science and Technology. The Uganda Ministry of Health, Uganda Prisons Service, and US Centers for Disease Control and Prevention provided oversight for data sharing and management.

This study was supported by the President's Emergency Plan for AIDS Relief through the US Centers for Disease Control and Prevention (cooperative agreement no. NU2GGH001605). Findings and conclusions in are those of the authors and do not necessarily represent the official position of the funding agencies.

About the Author

Dr. Lukoye is an epidemiologist in the Division of Global HIV and TB, Center for Global Health, US Centers for Disease Control and Prevention, Uganda. He serves as the public health expert for TB prevention, TB/HIV co-infections, and multidrug-resistant TB and supports the Uganda Ministry of Health and implementing partners to achieve TB elimination.

References

1. World Health Organization. Global tuberculosis report 2021 [cited 2021 Oct 14]. https://www.who.int/publications/i/item/9789240037021
2. Baussano I, Williams BG, Nunn P, Beggiato M, Fedeli U, Scano F. Tuberculosis incidence in prisons: a systematic review. PLoS Med. 2010;7:e1000381. https://doi.org/10.1371/journal.pmed.1000381
3. MacNeil JR, Lobato MN, Moore M. An unanswered health disparity: tuberculosis among correctional inmates, 1993 through 2003. Am J Public Health. 2005;95:1800–5. https://doi.org/10.2105/AJPH.2004.055442
4. World Health Organization. Regional Office for Europe. Status paper on prisons and tuberculosis. 2007 [cited 2007 May 8]. https://iris.who.int/handle/10665/107818
5. Martinez L, Warren JL, Harries AD, Croda J, Espinal MA, Olarte RAL, et al. Global, regional, and national estimates of tuberculosis incidence and case detection among incarcerated individuals from 2000 to 2019: a systematic analysis. Lancet Public Health. 2023;8:e511–9. https://doi.org/10.1016/S2468-2667(23)00097-X
6. Ministry of Health, Government of Uganda. National strategic plan for tuberculosis and leprosy control 2020/21–2024/25 [cited 2020 Nov 24]. https://www.health.go.ug/cause/national-strategic-plan-for-tuberculosis-and-leprosy-control-2020-21-2024-25
7. Ministry of Health, Government of Uganda. Uganda national tuberculosis and leprosy control programme: manual for management and control of tuberculosis and leprosy. 2017 March [cited 2020 Nov 20]. https://www.health.go.ug/wp-content/uploads/2019/12/NTLP-Manual-3rd-edition_17th-Aug_final.pdf
8. World Health Organization. WHO consolidated guidelines on tuberculosis: module 1: prevention: tuberculosis preventive treatment. February 2020 [cited 2020 Feb 25]. https://www.who.int/publications/i/item/9789240001503
9. Ribeiro Macedo L, Reis-Santos B, Riley LW, Maciel EL. Treatment outcomes of tuberculosis patients in Brazilian prisons: a polytomous regression analysis. Int J Tuberc Lung Dis. 2013;17:1427–34. https://doi.org/10.5588/ijtld.12.0918
10. Ministry of Health, Government of Uganda. The Uganda national tuberculosis prevalence survey, 2014–2015 survey report. 2015 [cited 2017 Aug 23]. https://www.health.go.ug/wp-content/uploads/2019/11/Uganda-National-TB-Prevalence-Survey-2014-2015_final-23rd-Aug17_0.pdf
11. Dhana A, Hamada Y, Kengne AP, Kerkhoff AD, Rangaka MX, Kredo T, et al. Tuberculosis screening among ambulatory people living with HIV: a systematic review and individual participant data meta-analysis. Lancet Infect Dis. 2022;22:507–18. https://doi.org/10.1016/S1473-3099(21)00387-X
12. Schwitters A, Kaggwa M, Omiel P, Nagadya G, Kisa N, Dalal S. Tuberculosis incidence and treatment completion among Ugandan prison inmates. Int J Tuberc Lung Dis. 2014;18:781–6. https://doi.org/10.5588/ijtld.13.0934
13. Juarez-Reyes M, Gallivan M, Chyorny A, O'Keeffe L, Shah NS. Completion rate and side-effect profile of three-month isoniazid and rifapentine treatment for latent tuberculosis infection in an urban county jail. Open Forum Infect Dis. 2016;3:ofv220. https://doi.org/10.1093/ofid/ofv220
14. Wheeler C, Mohle-Boetani J. Completion rates, adverse effects, and costs of a 3-month and 9-month treatment regimen for latent tuberculosis infection in California inmates, 2011–2014. Public Health Rep. 2019;134:71S–9S. https://doi.org/10.1177/0033354919826557
15. Kozhoyarova A, Sargsyan A, Goncharova O, Kadyrov A. Who is doing worse? Retrospective cross-sectional study of TB key population treatment outcomes in Kyrgyzstan (2015–2017). J Infect Dev Ctries. 2020;14:101S–8S. https://doi.org/10.3855/jidc.11897

Address for correspondence: Deus Lukoye, US Centers for Disease Control and Prevention, Uganda, US Embassy, 1577 Ggaba Rd, Nsambya, PO Box 7007, Kampala, Uganda; email: oju0@cdc.gov

Relapsed Mpox Keratitis, St. Louis, Missouri, USA

Cinthia Pi, Osasu Adah, Preetam A. Cholli, Roosecelis Martines, Getahun Abate, Lori Hainaut, Erich Seipel, T. Scott Isbell, Roddy Frankel, Nongnooch Poowanawittayakom

We describe a case of a 46-year-old man in Missouri, USA, with newly diagnosed advanced HIV and PCR-confirmed mpox keratitis. The keratitis initially resolved after intravenous tecovirimat and penicillin for suspected ocular syphilis coinfection. Despite a confirmatory negative PCR, he developed relapsed, ipsilateral PCR-positive keratitis and severe ocular mpox requiring corneal transplant.

Ocular mpox, caused by monkeypox virus (MPXV), can threaten eyesight and requires prompt ophthalmologic consultation. Understanding of the disease course, treatments, and treatment durations is limited. We describe a case of relapsed mpox keratitis after an initial PCR-confirmed resolution. The patient provided informed consent for this report's publication.

The Case Study

A 46-year-old man sought care at St. Louis University Hospital in St. Louis, Missouri, USA, after 1 month of ulcerating skin lesions and a painful right corneal ulcer. He reported changing his monthly soft contact lenses every 2–3 months and having unprotected sex with multiple male partners. An eye examination showed diminished right eye visual acuity (20/70; baseline unknown), and the right cornea had a large (8.5 × 7.3mm) ovoid ring extending onto the nasal bulbar conjunctiva with central infiltrate and an overlying epithelial defect (Figure 1). Laboratory testing for HIV-1 antibody was reactive; viral load was 1.1 million copies/mL and absolute CD4 count 75 cells/μL (reference range 430–1,800 cells/μL). We conducted PCR testing from biopsies of the patient's skin lesions and corneal swabs and detected nonvariola orthopoxvirus DNA consistent with MPXV. Laboratory testing for other sexually transmitted infections returned *Treponema pallidum* antibody and particle agglutination positive, rapid plasma reagin nonreactive. Hepatitis C, B, and urine gonorrhea/chlamydia tests were negative. Treatment for possible ocular syphilis was deferred because of discordant syphilis test results and the positive orthopoxvirus PCR.

We started the patient on oral tecovirimat and bictegravir/emtricitabine/tenofovir alafenamide for HIV. The patient's vision and examination results remained unchanged, but he reported improved eye pain. He was discharged on day 7 of hospitalization with a regimen of bictegravir/emtricitabine/tenofovir, trimethoprim/sulfamethoxazole, and oral tecovirimat for 2 weeks.

Two weeks after completing oral tecovirimat (29 days after the initial visit), the patient returned for recurrent right eye pain. His skin lesions had fully resolved. An eye examination showed unchanged visual acuity and epithelial defect (8.5 × 7.3mm). The patient was readmitted, and the Center for Disease Control and Prevention's mpox clinical consultations team was contacted.

We initiated treatment with intravenous (IV) tecovirimat, topical trifluridine eye drops, antibiotic eye drops, 2% cyclopentolate, and oral analgesics. Laboratory testing showed improved CD4 count (336 cells/μL) and decreased HIV viral load (430 copies/mL). Repeat corneal PCR of the right eye remained orthopoxvirus positive. Ocular herpes simplex virus 1 and 2 PCR and varicella zoster virus PCR results were negative. Serum cytomegalovirus PCR showed low-level detection (<50 IU/mL).

Despite treatment, the patient's keratopathy worsened. We began empiric treatment for ocular syphilitic scleritis with a 14-day course of IV penicillin. The patient reported significant pain improvement, and examination of his eye showed a decreasing corneal ulcer (5 × 5 mm) with completely healed

Author affiliations: St. Louis University, St. Louis, Missouri, USA (C. Pi, O. Adah, G. Abate, L. Hainaut, E. Seipel, T.S. Isbell, R. Frankel, N. Poowanawittayakom); CDC, Atlanta, Georgia, USA (P.A. Cholli, R. Martines)

DOI: https://doi.org/10.3201/eid3007.240388

conjunctival epithelium, suggesting the patient possibly had ocular syphilis. We transitioned the patient to oral tecovirimat on day 8 and discharged him on day 12 of readmission with a 1-week course of prednisolone acetate eye drops (4×/d) and a 14-day course of oral tecovirimat.

At 1-week follow-up, the patient's visual acuity had improved to 20/30, and all ocular symptoms resolved except for a 1.7 × 4.5 mm epithelial defect. Results of repeat MPXV PCR of the right eye lesion were negative. Repeat absolute CD4 was 365 cells/μL and HIV viral load was 191 copies/mL.

Eighty-five days after the patient initially sought care, he returned with relapsed right eye pain. Examination revealed worsening visual acuity to 20/300 with a new right corneal ulcer overlapping the site of a previous fully healed scarred lesion. We ordered a repeat MPXV PCR that was positive. The patient denied interval sexual partners, known mpox exposures, or other mpox symptoms; we interpreted findings as evidence of relapsed mpox keratitis.

The patient declined brincidofovir or additional tecovirimat to avoid side effects, including dry skin with prior tecovirimat, but was amenable to monthly ophthalmology follow-up. His eye pain and keratitis resolved over serial visits, but he had residual corneal infiltrates requiring corneal transplant. Surgery was performed, and his postoperative course was uneventful.

We conducted a corneal biopsy and found stromal scarring with vascular proliferation and mixed inflammatory infiltrate with lymphocytes, plasma cells, and rare neutrophils. No cytoplasmic inclusion bodies were observed. We conducted an immunohistochemistry assay by using a MPXV polyclonal rabbit antibody and orthopoxviral antigens were identified in the stromal mononuclear cells (Figure 2 panels A, B). The patient had a dense cataract in the same eye (previously obscured by the corneal opacity) and underwent cataract surgery 4 months after the corneal transplant; results of orthopoxvirus PCR of the aspirated lens material were negative.

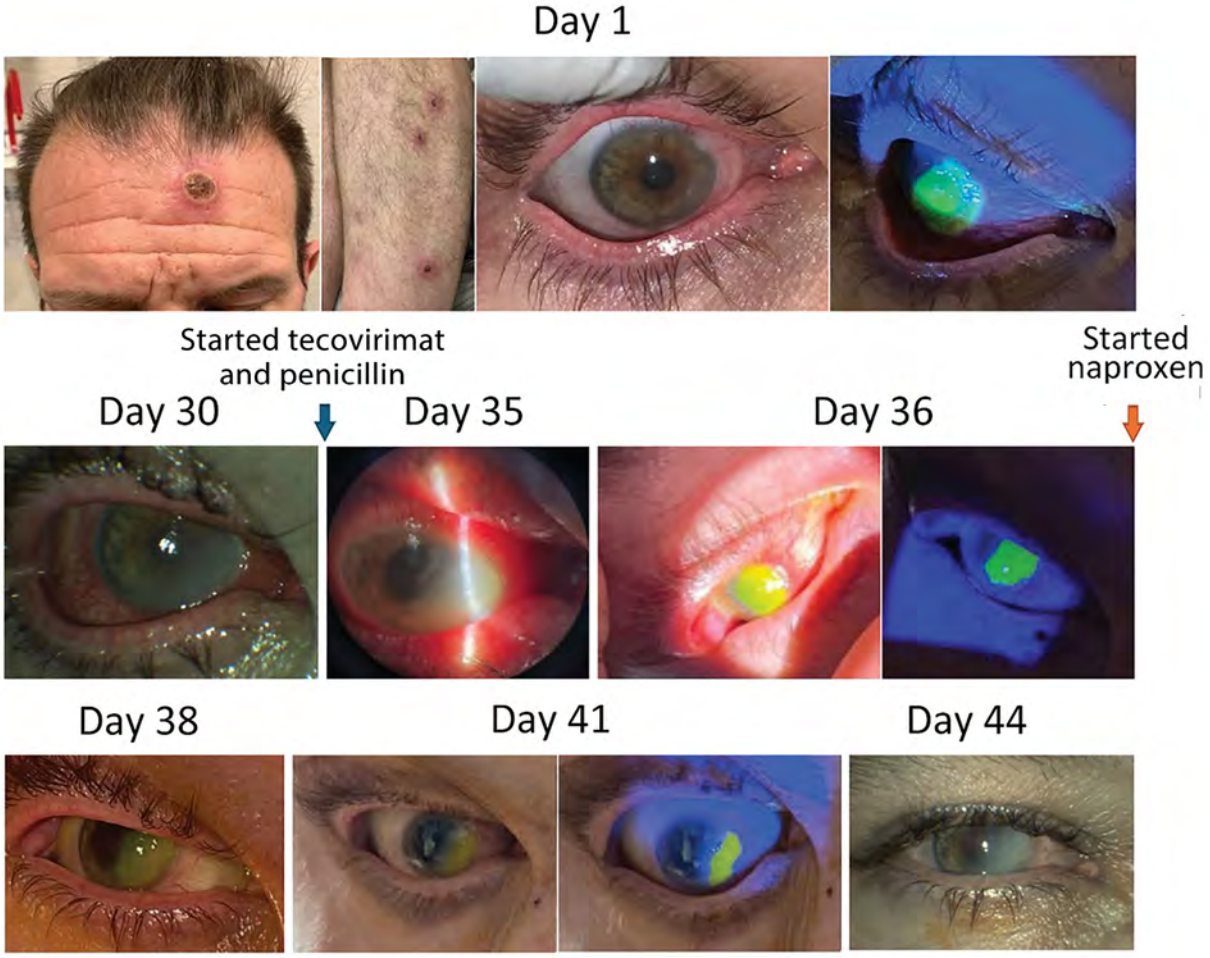

Figure 1. Physical and ophthalmologic examination results over time of a 46-year-old patient in St. Louis, Missouri, USA, after receiving mpox and HIV diagnoses. The exam remained unchanged after day 44 despite treatment. IV, intravenous.

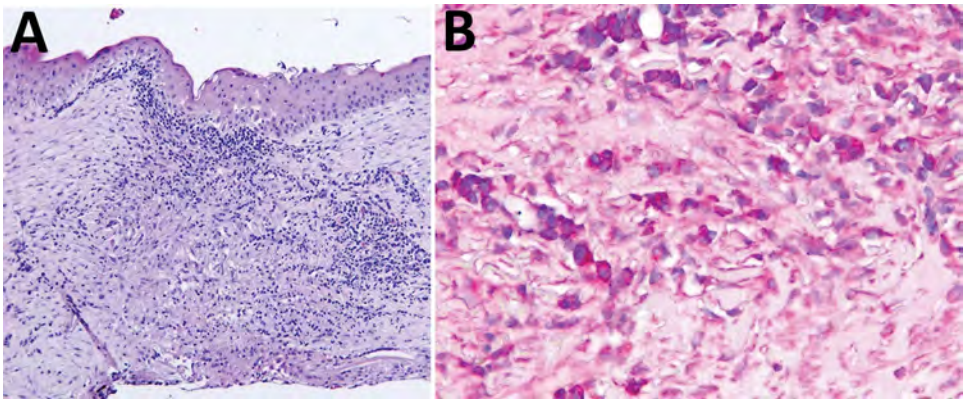

Figure 2. Right eye cornea histopathology from a 46-year-old patient in St. Louis, Missouri, USA, with ocular mpox diagnosis. Sample was collected on day 217 after the patient initially sought care. A) Corneal epithelium is intact. Stromal lesion shows focal scarring with inflammation composed of lymphocytes, plasma cells, and rare neutrophils. B) Orthopoxvirus antigens detected by immunohistochemistry in area of stromal lesion.

PCR is highly sensitive for detecting MPXV in conjunctival and corneal samples (*1*–*4*). Surface PCR tests of this patient's corneal ulcer remained positive after 1 round of antiviral treatment, despite restored immunity and ongoing antiretroviral therapy. His protracted PCR positivity could have been be because of residual mpox DNA rather than active viral replication. Treatment decisions were based on his corneal lesions and pain symptoms. However, PCR results correlated well with his symptoms. His PCR results became negative 2 weeks after resolution of his initial keratitis.

Our patient developed PCR-confirmed mpox keratitis over his healed lesion ≥40 days after his initial episode resolved. The identical location and lack of systemic mpox symptoms raised concerns for possible recrudescence from a persistent subclinical viral reservoir. Whereas the negative PCR could have been a false negative, PCR samples were all obtained in the same manner, and specimen collection was not considered to have been a factor in the test results. PCR testing was positive from corneal ulcer swab samples and from within the patient's excised cornea but not from within aspirated lens material from his subsequent cataract surgery. This result suggests the infection was restricted to the ocular surface and did not penetrate the anterior chamber or lens.

There is 1 reported case of recrudescent corneal erosion from cowpox (a related orthopoxvirus), attributed to viral persistence in the presence of systemic immunosuppressants and steroid eye drops (*5*). In the case we report, the patient's steroid drops were discontinued ≥1 month before his relapsed keratitis. An external viral reservoir could have been a source for reinfection, although our patient's relapse occurred beyond the windows in which MPXV persists on surfaces at ambient temperatures in environmental and experimental contexts (*6*–*8*).

Prevalence of HIV and STI co-infection in the recent mpox outbreak has been high; an international case series found 41% concurrent HIV and 9% concurrent syphilis infections in confirmed cases of mpox (*9*). The patient we report had newly diagnosed advanced HIV, and his first corneal ulcer resolved after he began empiric penicillin for possible ocular syphilis. It remains unclear if his initial keratitis resolved due to the natural course of illness, restored native immunity from antiretroviral therapy, transitioning from oral to IV tecovirimat that may have enabled more reliable tecovirimat absorption, or cotreatment for syphilitic sclerokeratitis.

Conclusions

This case highlights the importance of considering ocular co-infections, particularly in cases of persistent or prolonged mpox. Systemic treatment should be considered for all ocular mpox cases (*10*). However, the efficacy of options remains unclear (*10*), and there are no data regarding ocular penetration of oral versus IV tecovirimat. Our understanding of ocular mpox treatment comes only from case reports. Patients with ocular infections need close follow-up. Immunocompromised patients may have more frequent and unusual complications than normal hosts and may require prolonged (≥14 days) courses of tecovirimat until native immunity is restored (*11*).

About the Author

Dr. Pi is an ophthalmology resident at St. Louis University. Her research interests include cataracts and glaucoma.

References

1. Nogueira Filho PA, Lazari CDS, Granato CFH, Shiroma MARDV, Santos ALD, Campos MSQ, et al. Ocular manifestations of monkeypox: a case report. Arq Bras Oftalmol. 2022;85:632–5. https://doi.org/10.5935/0004-2749.2022-0281
2. Mazzotta V, Mondi A, Carletti F, Baldini F, Santoro R, Meschi S, et al. Ocular involvement in monkeypox: description of an unusual presentation during the current

outbreak. J Infect. 2022;85:573–607. https://doi.org/10.1016/j.jinf.2022.08.011
3. Alexis J, Hohnen H, Kenworthy M, Host BKJ. Ocular manifestation of monkeypox virus in a 38-year old Australian male. IDCases. 2022;30:e01625. https://doi.org/10.1016/j.idcr.2022.e01625
4. Meduri E, Malclès A, Kecik M. Conjunctivitis with monkeypox virus positive conjunctival swabs. Ophthalmology. 2022;129:1095. https://doi.org/10.1016/j.ophtha.2022.07.017
5. Graef S, Kurth A, Auw-Haedrich C, Plange N, Kern WV, Nitsche A, et al. Clinicopathological findings in persistent corneal cowpox infection. JAMA Ophthalmol. 2013;131:1089–91. https://doi.org/10.1001/jamaophthalmol.2013.264
6. Morgan CN, Whitehill F, Doty JB, Schulte J, Matheny A, Stringer J, et al. Environmental persistence of monkeypox virus on surfaces in household of person with travel-associated infection, Dallas, Texas, USA, 2021. Emerg Infect Dis. 2022;28:1982–9. https://doi.org/10.3201/eid2810.221047
7. Li F, Shen X, Zhang H, Jin H, Zhang L, Lv B, et al. Stability of mpox virus on different commonly contacted surfaces. J Med Virol. 2023;95:e29296. https://doi.org/10.1002/jmv.29296
8. Meister TL, Brüggemann Y, Todt D, Tao R, Müller L, Steinmann J, et al. Stability and inactivation of monkeypox virus on inanimate surfaces. J Infect Dis. 2023;228:1227–30. https://doi.org/10.1093/infdis/jiad127
9. Thornhill JP, Barkati S, Walmsley S, Rockstroh J, Antinori A, Harrison LB, et al.; SHARE-net Clinical Group. Monkeypox virus infection in humans across 16 countries—April–June 2022. N Engl J Med. 2022;387:679–91. https://doi.org/10.1056/NEJMoa2207323
10. Centers for Disease Control and Prevention. Interim clinical considerations for management of ocular mpox virus infection. 2023 Mar 27 [cited 2023 Aug 15]. https://www.cdc.gov/poxvirus/mpox/clinicians/ocular-infection.html
11. Centers for Disease Control and Prevention. Update on managing monkeypox in patients receiving therapeutics. 2022 Nov 17 [cited 2022 Dec 19] https://emergency.cdc.gov/han/2022/han00481.asp

Address for correspondence: Nongnooch Poowanawittayakom, Internal Medicine Department, St. Louis University, 1201 S Grand Blvd, St. Louis, MO 63104, USA; email: nongnooch.poowanawittayakom@health.slu.edu

Multicountry Spread of Influenza A(H1N1)pdm09 Viruses with Reduced Oseltamivir Inhibition, May 2023–February 2024

Mira C. Patel,[1] Ha T. Nguyen,[1] Philippe Noriel Q. Pascua, Rongyuan Gao, John Steel, Rebecca J. Kondor, Larisa V. Gubareva

Since May 2023, a novel combination of neuraminidase mutations, I223V + S247N, has been detected in influenza A(H1N1)pdm09 viruses collected in countries spanning 5 continents, mostly in Europe (67/101). The viruses belong to 2 phylogenetically distinct groups and display ≈13-fold reduced inhibition by oseltamivir while retaining normal susceptibility to other antiviral drugs.

Three classes of direct-acting antivirals targeting the influenza virus matrix protein 2 (M2) ion channel, neuraminidase (NA), or polymerase cap-dependent endonuclease (CEN) are approved to treat influenza in many countries (*1*). Although most seasonal influenza viruses are susceptible to NA and CEN inhibitors, emergence of antiviral-resistant variants is a public health concern because of widespread resistance to M2 inhibitors and possibilities of similar resistance developing for other antiviral drugs (*2*). Oseltamivir, an NA inhibitor, is the drug most prescribed for influenza (*2*). The NA amino acid substitution H275Y, acquired spontaneously or after drug exposure, confers resistance to oseltamivir. Oseltamivir-resistant influenza A(H1N1) viruses with H275Y emerged first in Europe during 2007–2008 and rapidly spread worldwide (*3*). However, they were displaced by influenza A(H1N1)pdm09 (pH1N1), the swine-origin virus that caused the 2009 pandemic (*4*).

Monitoring oseltamivir susceptibility is a priority for the World Health Organization Global Influenza Surveillance and Response System (WHO-GISRS). In addition to H275Y, many NA substitutions in N1 subtype viruses are suspected of reducing oseltamivir susceptibility (*5*). Although there are no established criteria for determining clinically relevant oseltamivir resistance based on phenotypic testing, for surveillance purposes, influenza A viruses tested in NA inhibition assays are classified as displaying reduced inhibition if they have a 50% inhibitory concentration (IC_{50}) 10-100–fold higher or as highly reduced inhibition if IC_{50} >100-fold higher than that of a reference (*6*).

The Study

The Centers for Disease Control and Prevention (CDC) monitors antiviral susceptibility of viruses submitted to the national surveillance system and those collected in other countries. Nearly all influenza-positive samples undergo next-generation sequencing. We analyzed NA sequences of submitted viruses for substitutions previously associated with reduced susceptibility (*5*), tested the viruses in an NA inhibition assay, and compared IC_{50}s with a reference IC_{50} to determine inhibition levels (*7*).

During May 2023–February 2024, we analyzed 2,039 pH1N1 viruses from the United States (n = 1,274) and 38 other countries (n = 765). Four had the H275Y substitution, indicating low frequency of oseltamivir resistance. Analysis revealed NA substitution I223V in 18 and S247N in 15 viruses; those substitutions confer mildly elevated oseltamivir IC_{50} (<10-fold). We also detected 17 viruses carrying both substitutions, I223V + S247N (Table 1; Appendix Table 1, https://wwwnc.cdc.gov/EID/article/30/7/24-0480-App1.pdf). As expected, single mutants exhibited normal inhibition by oseltamivir and other NA inhibitors in NA inhibition assay (Table 2). The 6 viruses with I223V + S247N displayed 13- to 16-fold

Author affiliation: Centers for Disease Control and Prevention, Atlanta, Georgia, USA

DOI: https://doi.org/10.3201/eid3007.240480

[1]These authors contributed equally to this article.

Table 1. Influenza A(H1N1)pdm09 viruses with amino acid substitutions in neuraminidase that may affect inhibition by oseltamivir*

NA substitution†	No. viruses with NA substitution	Viruses collected from countries (no. in each)
H275Y	4	Argentina (1),‡ Panama (1), USA (2)
I223V	18	Abu Dhabi (5), Bangladesh (5), Bahrain (2), Canada (1), Costa Rica (1), USA (4)
S247N	15	Abu Dhabi (2), Bhutan (3), Brazil (1), Canada (1), Hong Kong (1), Oman (1), USA (6)
I223V + S247N§	17	Bangladesh (11), Hong Kong (1), Maldives (1), Niger (3), USA (1)

*Next-generation sequencing–based virologic surveillance conducted at the Centers for Disease Control and Prevention, May 2023–February 2024. Summary of NA amino acid substitutions assessed for their effects on inhibition by NA inhibitors prepared by members of the World Health Organization Antiviral Working Group (*5*) was used as a reference for NA sequence analysis. A total of 2,039 NA sequences of influenza A(H1N1)pdm09 viruses (duplicate sequences excluded; n = 1,274 viruses collected from the United States and n = 765 from 38 other countries) were analyzed to screen for previously listed or suspected NA amino acid substitutions. Detailed information about those viruses is provided in Appendix Table 1 (https://wwwnc.cdc.gov/EID/article/30/7/24-0480-App1.pdf). NA, neuraminidase.
†According to a subtype-specific NA amino acid numbering system.
‡This virus also contains NA-S247N. Virus was not recovered in cell culture.
§Combination of I223V + S247N was not reported previously.

reduced inhibition for oseltamivir and normal inhibition (≤4-fold) for other NA inhibitors (Table 2; Appendix Table 2). Both single and dual mutants remained susceptible to the CEN inhibitor baloxavir (Table 2).

The dual mutants were collected in the United States and 4 other countries during August–November 2023 (Table 1; Appendix Table 1), which prompted us to explore when dual mutants emerged and how broadly single or dual mutants were circulating worldwide. Analysis of available NA sequences from the GISAID EpiFlu database (https://www.gisaid.org) revealed that pH1N1 viruses with single mutation I223V (n = 110) or S247N (n = 203) were found in many countries (Figure 1, panel A). In addition to the 17 viruses we sequenced, 84 additional dual mutants were identified (total n = 101). Together, they were collected in 15 countries spanning 5 continents (Africa, Asia, Europe, North America, and Oceania) (Figure 1, panel B). The first dual mutant was collected from Canada in May 2023, and the latest were collected from 4 countries (France, the Netherlands, Spain, and the United Kingdom) during January–February 2024. Most dual mutants were detected in the Netherlands (n = 30), France (n = 24), Bangladesh (n = 11), Oman (n = 9), and the United Kingdom (n = 9); fewer were found in Hong Kong (n = 4), Niger (n = 3), Australia (n = 2), Spain (n = 2), and the United States (n = 2). One dual mutant each was detected in Canada, Ethiopia, Maldives, Norway, and Sweden (Figure 1, panel B; Appendix Tables 1, 3).

On the basis of NA phylogenetic analysis, we determined that most single S247N mutants belonged to either subclade C.5 (16%) or the most abundantly sequenced subclade, C.5.3 (80%) (*8*). All subclade C.5.3 viruses share substitution S200N located at the antibody binding family site VI (Figure 1, panel A). Most single I223V mutants (92%) also belonged to subclade C.5.3 and formed a distinct branch with substitution S366N located at the antibody binding family site III. Within that branch, 2 separate introductions of S247N have occurred, giving rise to dual I223V + S247N mutants that could be divided into distinct groups 1 and

Table 2. Antiviral susceptibility of available influenza A(H1N1)pdm09 virus isolates with NA-I223V or NA-S247N or NA-I223V + S247N substitutions*

NA substitution†	No. virus isolates tested	NA inhibitors IC_{50}, nM, average ± SD (fold)‡				CEN inhibitor baloxavir EC_{50}, nM, average ± SD (fold)§
		Oseltamivir	Zanamivir	Peramivir	Laninamivir	
Test viruses						
I223V	9	0.71 ± 0.17 (3)	0.23 ± 0.03 (1)	0.08 ± 0.01 (1)	0.25 ± 0.01 (1)	1.15 ± 0.15 (2)
S247N	6	0.82 ± 0.16 (4)	0.34 ± 0.05 (2)	0.19 ± 0.01 (3)	0.55 ± 0.03 (3)	1.46 ± 0.62 (2)
I223V + S247N	6	2.71 ± 0.20 (13)	0.49 ±0.02 (3)	0.29 ± 0.01 (4)	0.64 ± 0.02 (3)	0.67 ± 0.14 (1)
Reference						
Median IC_{50}/EC_{50} 2022–2023	253	0.21	0.19	0.07	0.21	0.70

*Next-generation sequencing–flagged influenza A(H1N1)pdm09 viruses were propagated in MDCK-SIAT1 cells, followed by sequence confirmation of virus isolates. Susceptibility of available virus isolates with indicated single or dual NA substitution(s) were tested for NA inhibitors (oseltamivir, zanamivir, peramivir, and laninamivir) by using Centers for Disease Control and Prevention–standardized fluorescence-based NA inhibition assay and baloxavir by using a cell-based Influenza replication inhibition neuraminidase-based assay. Virus isolates were tested against each antiviral in at least 2–3 independent tests, and average ± SD of IC_{50}s/EC_{50}s is shown. Fold changes in IC_{50}s/EC_{50}s of test viruses were calculated compared with median IC_{50}s/EC_{50}s of influenza A(H1N1)pdm09 viruses tested during the 2022–23 influenza season (October 1, 2022–September 30, 2023). CEN, cap-dependent endonuclease; EC_{50}, 50% effective concentration; IC_{50}, 50% inhibitory concentration; NA, neuraminidase.
†According to a subtype-specific NA amino acid numbering system.
‡Fold changes were interpreted according to World Health Organization classification criteria for type A: <10-fold, normal inhibition; 10–100-fold, reduced inhibition; >100-fold, highly reduced inhibition.
§Fold changes were interpreted according to arbitrary criteria, according to which ≥3-fold increase in EC_{50} of test virus compared with reference EC_{50} is defined as reduced susceptibility to baloxavir.

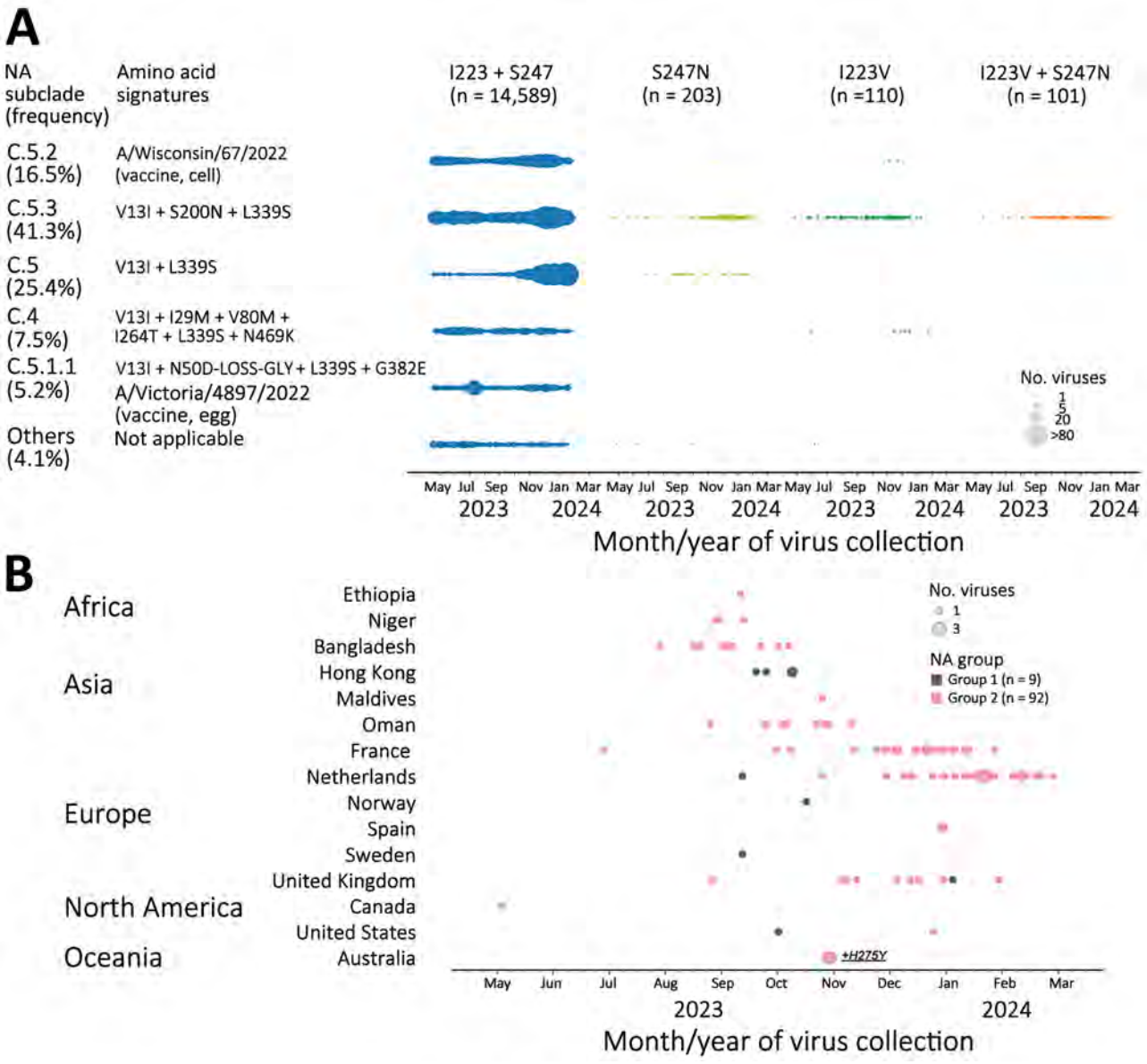

Figure 1. Detection of influenza A(H1N1)pdm09 viruses with dual NA-I223V + S247N substitutions through NA inhibitors susceptibility surveillance conducted by the Centers for Disease Control and Prevention and analysis of available sequences (GISAID EpiFlu, https://www.gisaid.org, accessed March 11, 2024), May 2023–February 2024. A total of 15,003 NA sequences of pH1N1 viruses (duplicate sequences excluded: 2,039 from Centers for Disease Control and Prevention and the remaining 12,964 from GISAID EpiFlu) were analyzed to screen for amino acid substitutions at residues 223 and 247. A) Introduction of single substitution (I223V or S247N) or dual substitutions (I223V + S247N) across NA subclades of pH1N1 viruses circulating during May 2023–February 2024. Amino acid signatures of NA subclades are shown in comparison to A/Wisconsin/67/2022, the Northern Hemisphere 2023–2024 vaccine cell prototype virus for the pH1N1 component. Vaccine viruses, A/Wisconsin/67/2022 and A/Victoria/4897/2022 (Northern Hemisphere 2023–2024 vaccine egg prototype virus), represented NA subclades C.5.2 and C.5.1.1, respectively. C.5.3 was the subclade most abundantly sequenced (41.3% frequency), followed by other minor subclades: C.5 (25.4%), C.5.2 (16.5%), C.4 (7.5%), C.5.1.1 (5.2%), and others (4.1%). Most viruses with single S247N substitution belonged to dominant NA subclade C.5.3 and minor subclade C.5. Conversely, most viruses with single I223V substitution and all viruses with dual I223V + S247N substitutions belonged to NA subclade C.5.3. B) Spatiotemporal distribution of dual mutant viruses. Dual mutants were divided into 2 groups based on their NA sequence difference. Group 1 shared additional substitution R257K not found in group 2. The small group 1 had 9 dual mutants, and the large group 2 had 92 dual mutants. The first dual mutant belonging to group 2 was collected in Canada at the end of May 2023, and most dual mutants were collected between September 2023 and February 2024. Two dual mutant viruses collected in Australia also contained NA-H275Y. NA, neuraminidase.

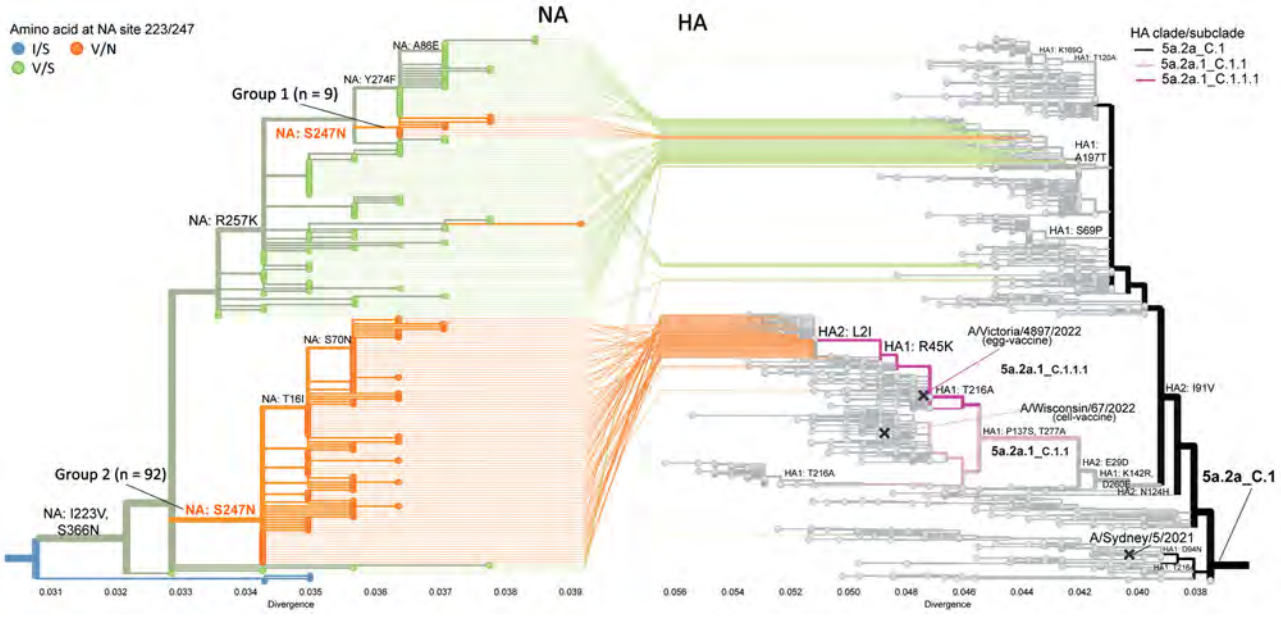

Figure 2. Tanglegram showing influenza A(H1N1)pdm09 phylogenies for NA gene (left) and HA gene (right) from susceptibility surveillance conducted by the Centers for Disease Control and Prevention and analysis of available sequences (GISAID EpiFlu, https://www.gisaid.org, accessed March 11, 2024), May 2023–February 2024. The NA-HA tangle tree was constructed by using Nextclade (*8*) and visualized by Auspice (https://auspice.us). NA phylogenetic tree is zoomed to show only subclade C.5.3 with 2 groups of dual I223V + S247N mutants. All dual mutant viruses shared ≥6 NA amino acid substitutions (V13I, S200N, I223V, S247N, L339S, S366N) compared with vaccine prototype virus A/Wisconsin/67/2022. Group 1 shared an additional substitution R257K not observed in group 2. Tree tips colored in blue indicate viruses with wild type amino acids at residues 223 and 247 (i.e., I223 and S247); green shows single I223V mutants; and orange shows dual mutants. Small group 1 with 9 dual mutants and large group 2 with 92 dual mutants are indicated. The NA sequence and corresponding HA of each virus are connected by lines. Group 1 dual mutants have HA 5a.2a_C.1. Only 2 group 2 dual mutants (A/British Columbia/PHL1108/2023 collected in May 2023 and A/France/IDF-RELAB-IPP24993/2023 collected in October 2023) have HA 5a.2a_C.1; remaining group 2 dual mutants shared HA 5a.2a.1_C.1.1.1. HA 5a.2a_C.1 is represented by A/Sydney/5/2021, the Southern Hemisphere 2023 vaccine egg/cell prototype virus. HA 5a.2a.1_C.1.1.1 is represented by A/Victoria/4897/2022, the Northern Hemisphere 2023–2024 vaccine egg prototype virus. The Northern Hemisphere 2023–2024 vaccine cell prototype virus, A/Wisconsin/67/2022, represents HA 5a.2a.1_C.1.1. HA, hemagglutinin; NA, neuraminidase.

2 (Figure 2). Only 9 dual mutants collected in 6 countries belonged to group 1 and shared an additional substitution R257K. Group 2 encompassed 92 dual mutants from countries with multiple detections (i.e., France, Netherlands, Bangladesh, the United Kingdom, Oman, and Niger) (Figure 1, panel B).

To further characterize the dual mutants, we performed hemagglutinin (HA) phylogenetic analysis. Two major HA clades, 6B.1A.5a.2a (5a.2a) and 6B.1A.5a.2a.1 (5a.2a.1), were seen globally during this period (*8*,*9*). Viruses belonging to HA subclades 5a.2a_C.1 (55%–61%) and 5a.2a.1_C.1.1.1 (13%–39%) predominated. Of note, all group 1 dual mutants had HA from 5a.2a_C.1, represented by the previous vaccine prototype virus A/Sydney/5/2021 (Figure 2). Conversely, most group 2 dual mutants had HA from 5a.2a.1_C.1.1.1, represented by the current vaccine prototype virus A/Victoria/4897/2022, and most shared 2 HA changes: R45K in HA1 and L2I in HA2 (Figure 2).

Conclusions

We report the emergence and intercontinental spread of pH1N1 viruses displaying reduced susceptibility to oseltamivir resulting from acquisition of NA-I223V + S247N mutations. Emergence of the dual mutants was also recently noticed by researchers in Hong Kong (*10*). The dual mutants that we tested retained susceptibility to other approved influenza antiviral drugs, including baloxavir. Analysis of available sequence data revealed that dual mutants have been in global circulation since May 2023; overall detection frequency was low (0.67%, 101/15,003). However, those data may not necessarily represent the actual proportion of what was in circulation because of differences in surveillance and sequencing strategies in each country.

Substitutions at residues 223 or 247 were previously reported and occurred spontaneously in circulating viruses (*5*,*11*,*12*). pH1N1 viruses with S247N circulated in several countries during 2009–2011

(*11*), and influenza B viruses with I223V (I221V in B numbering) were found in several US states during 2010–2011 (*12*). Isoleucine at 223 is a highly conserved framework residue in the NA active site. The S247N substitution may alter the hydrogen bonding network of the active site and the conformation of the residue E277 side chain, thereby weakening oseltamivir binding (*11*). Changes at 223 or 247 are monitored because they can enhance drug resistance by combining with mutations at other residues (*11*,*13*,*14*).

Rapid spread of dual mutants to countries on different continents suggests no substantial loss in their replicative fitness and transmissibility. I223V was shown to alter NA activity (*14*), and change at 247 may produce a similar effect, which warrants the question whether signature substitution(s) of NA subclade C.5.3 and of the branch to which the dual mutants belong (i.e., S200N, S366N) could serve as prerequisites for emergence of dual mutants. All group 1 dual mutants had an additional substitution R257K, which was previously associated with restoring NA activity of viruses with the H275Y substitution (*15*). Conversely, most group 2 viruses acquired HA from subclade 5a.2a.1_C.1.1.1 by reassortment, which may have helped to restore the functional HA and NA balance. Acquisition of the antigenically distinct HA could further enhance the spread of group 2 dual mutants. Our study highlights the need to closely monitor evolution of dual mutants because additional changes may further affect susceptibility to antiviral drugs or provide a competitive advantage over circulating wild-type viruses.

Acknowledgments

We are grateful to the US public health laboratories and other laboratories participating in the WHO-GISRS for productive collaboration with the CDC National Center for Immunization and Respiratory Diseases Influenza Division and their timely submission of influenza viruses. We acknowledge the efforts and contributions of WHO-GISRS laboratories and other laboratories that have performed genetic sequencing and submitted influenza sequence data to GISAID EpiFlu. We also acknowledge the valuable contributions of colleagues from the Virology, Surveillance and Diagnosis Branch of the CDC Influenza Division.

This study was supported by the CDC Influenza Division.

About the Author

Dr. Patel and Dr. Nguyen are scientists in the Influenza Division, National Center for Immunization and Respiratory Diseases, CDC, Atlanta. Their research interests are respiratory viruses and antiviral therapeutics targeting viral or host proteins, and their research focuses on influenza viruses, molecular characterization of antiviral resistance mechanisms, and development of in vitro assays for monitoring drug susceptibility.

References

1. Holmes EC, Hurt AC, Dobbie Z, Clinch B, Oxford JS, Piedra PA. Understanding the impact of resistance to influenza antivirals. Clin Microbiol Rev. 2021;34:e00224-20. https://doi.org/10.1128/CMR.00224-20
2. Centers for Disease Control and Prevention. Influenza antiviral drug resistance [cited 2024 Mar 18]. https://www.cdc.gov/flu/treatment/antiviralresistance.htm
3. Meijer A, Lackenby A, Hungnes O, Lina B, van-der-Werf S, Schweiger B, et al.; European Influenza Surveillance Scheme. Oseltamivir-resistant influenza virus A (H1N1), Europe, 2007–08 season. Emerg Infect Dis. 2009;15:552–60. https://doi.org/10.3201/eid1504.181280
4. Garten RJ, Davis CT, Russell CA, Shu B, Lindstrom S, Balish A, et al. Antigenic and genetic characteristics of swine-origin 2009 A(H1N1) influenza viruses circulating in humans. Science. 2009;325:197–201. https://doi.org/10.1126/science.1176225
5. World Health Organization-Antiviral Working Group. Summary of neuraminidase (NA) amino acid substitutions assessed for their effects on inhibition by neuraminidase inhibitors (NAIs). 2023 Mar 7 [cited 2024 Mar 18]. https://cdn.who.int/media/docs/default-source/global-influenza-programme/1.-nai_human_reduced-susceptibility-marker-table-(who)_07.03.23_update.pdf
6. Meetings of the WHO working group on surveillance of influenza antiviral susceptibility—Geneva, November 2011 and June 2012. Wkly Epidemiol Rec. 2012;87:369–74.
7. Okomo-Adhiambo M, Mishin VP, Sleeman K, Saguar E, Guevara H, Reisdorf E, et al. Standardizing the influenza neuraminidase inhibition assay among United States public health laboratories conducting virological surveillance. Antiviral Res. 2016;128:28–35. https://doi.org/10.1016/j.antiviral.2016.01.009
8. Aksamentov I, Roemer C, Hodcroft EB, Neher RA. Nextclade: clade assignment, mutation calling and quality control for viral genomes. J Open Source Softw. 2021;6:3773. https://doi.org/10.21105/joss.03773
9. Nextstrain. Real-time tracking of influenza A/H1N1pdm evolution [cited 2024 Mar 18]. https://nextstrain.org/flu/seasonal/h1n1pdm/ha/2y
10. Leung RC, Ip JD, Chen LL, Chan WM, To KK. Global emergence of neuraminidase inhibitor-resistant influenza A(H1N1)pdm09 viruses with I223V and S247N mutations: implications for antiviral resistance monitoring. Lancet Microbe. 2024;S2666-5247(24)00037-5. https://doi.org/10.1016/S2666-5247(24)00037-5
11. Hurt AC, Lee RT, Leang SK, Cui L, Deng YM, Phuah SP, et al. Increased detection in Australia and Singapore of a novel influenza A(H1N1)2009 variant with reduced oseltamivir and zanamivir sensitivity due to a S247N neuraminidase mutation. Euro Surveill. 2011;16:19884. https://doi.org/10.2807/ese.16.23.19884-en
12. Garg S, Moore Z, Lee N, McKenna J, Bishop A, Fleischauer A, et al. A cluster of patients infected with I221V influenza B virus variants with reduced oseltamivir susceptibility—North Carolina and South Carolina, 2010-2011. J Infect Dis. 2013;207:966–73. https://doi.org/10.1093/infdis/jis776

13. Centers for Disease Control and Prevention. Oseltamivir-resistant 2009 pandemic influenza A (H1N1) virus infection in two summer campers receiving prophylaxis—North Carolina, 2009. MMWR Morb Mortal Wkly Rep. 2009; 58:969–72.
14. Pizzorno A, Bouhy X, Abed Y, Boivin G. Generation and characterization of recombinant pandemic influenza A(H1N1) viruses resistant to neuraminidase inhibitors. J Infect Dis. 2011;203:25–31. https://doi.org/10.1093/infdis/jiq010
15. Bloom JD, Nayak JS, Baltimore D. A computational-experimental approach identifies mutations that enhance surface expression of an oseltamivir-resistant influenza neuraminidase. PLoS One. 2011;6:e22201. https://doi.org/10.1371/journal.pone.0022201

Address for correspondence: Larisa V. Gubareva, Centers for Disease Control and Prevention 1600 Clifton Rd NE, Mailstop H17-5, Atlanta, GA 30329-4018, USA; email: lgubareva@cdc.gov

Reemergence of Clade IIb–Associated Mpox, Germany, July–December 2023

Patrick E. Obermeier, Clarissa F. Plinke, Annika Brinkmann, Raskit Lachmann, Julia Melchert, Victor M. Corman, Andreas Nitsche, Ulrich Marcus, Axel J. Schmidt, Klaus Jansen, Susanne C. Buder

In July 2023, clade IIb–associated mpox reemerged in Germany at low levels, mainly affecting men who have sex with men. We report a representative case and phylogeny of available genome sequences. Our findings underscore the need for standardized surveillance and indication-based vaccination to limit transmission and help prevent endemicity.

Mpox is caused by infection with monkeypox virus (MPXV). Phylogenomically and clinically, clades I and II can be distinguished; clade II has 2 subclades, IIa and IIb (*1*). In July 2022, the World Health Organization (WHO) declared a global clade IIb–associated mpox outbreak a Public Health Emergency of International Concern (*2*). Worldwide, >87,000 laboratory-confirmed cases were reported by the time the emergency was declared over in May 2023 after a marked decline in case reporting. Overall, the WHO Region of the Americas had the highest number of mpox cases (≈59,000), followed by the European Region (≈26,000), particularly Spain (≈7,600), France (≈4,100), the United Kingdom, and Germany (≈3,700, each). Since 2023, only sporadic cases have been reported across Europe, and no cases were notified in Germany during February–July 2023 (*3*,*4*).

The Study

In September 2023, a man in his 40s visited a tertiary-care, dermatologic emergency department in Berlin after his general practitioner, a urologist, and a dermatologist could not explain his 1-week history of penile rash, tender lymph nodes, sore throat, cough, malaise, and fever. Signs and symptoms had severely affected his life, as reflected by a Dermatology Life Quality Index (*5*) score of 20 out of 30. Examination revealed the man to be in a reduced general condition, with inguinal lymphadenopathy, a bright red enanthem, and multiple umbilicated penile papules (Figure 1). The man reported a steady female partner but also anal intercourse with an anonymous male partner in a Berlin nightclub 28 days before symptom onset. The man denied any further sexual contact since that encounter and confirmed no mpox or smallpox vaccination nor recent travels abroad.

Testing revealed MPXV-positive results (LightMix Modular Monkeypox Virus; TIB MOLBIOL, https://www.tib-molbiol.de) obtained by penile papule swab sample (cycle threshold value 27.47) and by urine sample (cycle threshold value 35.34). The patient received antipyretic and analgetic medications. Symptoms resolved, and MPXV PCR results were negative 26 days after disease onset. Further tests revealed negative results for hepatitis B and C viruses, HIV, *Chlamydia trachomatis*, *Mycoplasma genitalium*, *Neisseria gonorrhoeae*, and *Treponema pallidum*.

We considered the case-patient significant because few mpox cases were being reported in Germany at the time and he had been misdiagnosed by 3 different healthcare experts despite typical manifestations. An examination of national surveillance data revealed 110 laboratory-confirmed mpox cases during July–December 2023, after 25 weeks without case reports (*4*). Men accounted for all but 1 patient; median age was 36 years (range 17–80 years). Reported cases originated from 12 of 16 federal states, but most notifications came from the federal state of Berlin (62/110) (Figure 2). Of the 90 cases with information

Author affiliations: Vaccine Safety Initiative, Berlin, Germany (P.E. Obermeier); Vivantes Hospital Neukölln, Berlin (C.F. Plinke, S.C. Buder); Robert Koch-Institute, Berlin (A. Brinkmann, R. Lachmann, A. Nitsche, U. Marcus, K. Jansen); Charité–Universitätsmedizin Berlin and Berlin Institute of Health, Berlin (J. Melchert, V.M. Corman); London School of Hygiene and Tropical Medicine, London, UK (A.J. Schmidt)

DOI: http://doi.org/10.3201/eid3007.240092

on the probable route of transmission, 89 were men who have sex with men. Most cases with information on the place of infection (n = 88) traced acquisition to Berlin (59/88), and 10 cases were imported (2 cases each from the United States, Spain, and the Netherlands and 1 case each from Egypt, Greece, Saudi Arabia, and Thailand).

Investigators performed a phylogenetic analysis of 29 available sequences from the reemergence of mpox in Germany, generated by using native Illumina NextSeq (Illumina, https://www.illumina.com) or amplicon-based Oxford Nanopore MinION (Oxford Nanopore Technologies, https://nanoporetech.com) sequencing (A. Brinkmann et al., unpub data, https://doi.org/10.1101/2022.10.20.512862). We used those sequences and a selection of 58 publicly available MPXV sequences from GISAID (https://www.gisaid.org) for an alignment of the central conserved region (≙vaccinia virus genes F9L-A24R) by using Mafft version 7.307 with default parameters (https://mafft.cbrc.jp). We performed phylogenetic analysis by using IQ-TREE v1.6.12 (http://www.iqtree.org) with the maximum-likelihood method, general time reversible plus gamma distribution plus invariate sites model, and 1,000 bootstrap replicates, which showed that all available Germany genome sequences belonged to clade IIb. Most genome sequences (n = 17) were B.1 lineage sequences, followed by C.1 (n = 10) and B.1.20 (n = 2). The MPXV genome of the case-patient we describe (GenBank accession no. PP002089) could be assigned to lineage B.1 (Appendix Figure 1, https://wwwnc.cdc.gov/EID/article/30/7/24-0092-App1.pdf), with highest identity to other genomes from Berlin during October 2023. A second cluster of sequences from Berlin, separated by >10 mutations, circulated simultaneously. Three C.1 sequences from Berlin showed 100% identity, and the sequences were also identical to a genome from Portugal. However, C.1 strains from Berlin also clustered with genomes from China in July 2023. Three C.1 genomes from Berlin showed 3 unique mutations to cocirculating C.1 genomes from China, Japan, and Portugal.

We ascertained information on mpox vaccination from available data for 96 of 110 cases: 54 case-patients (56%) were vaccinated, and 30 had received 2 doses, 16 received 1 dose, and 8 received an

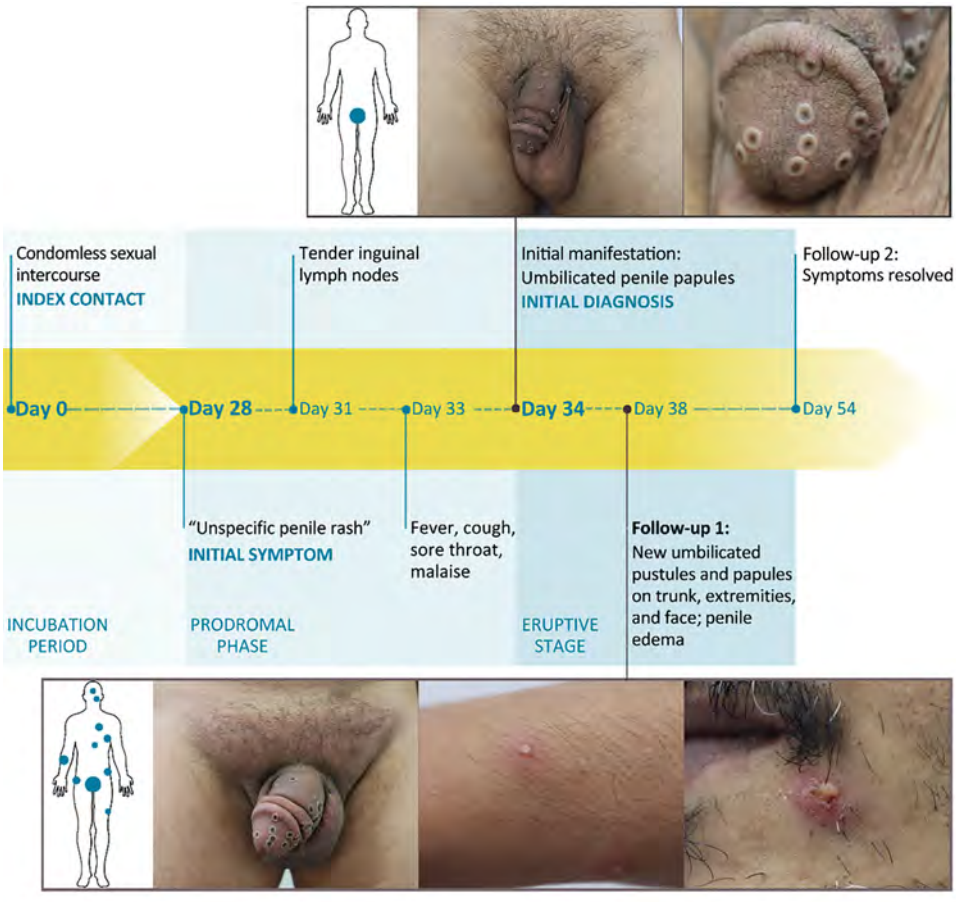

Figure 1. Clinical features and chronology of events in an instructive case from clade IIb–associated reemergence of mpox in Germany, July–December 2023.

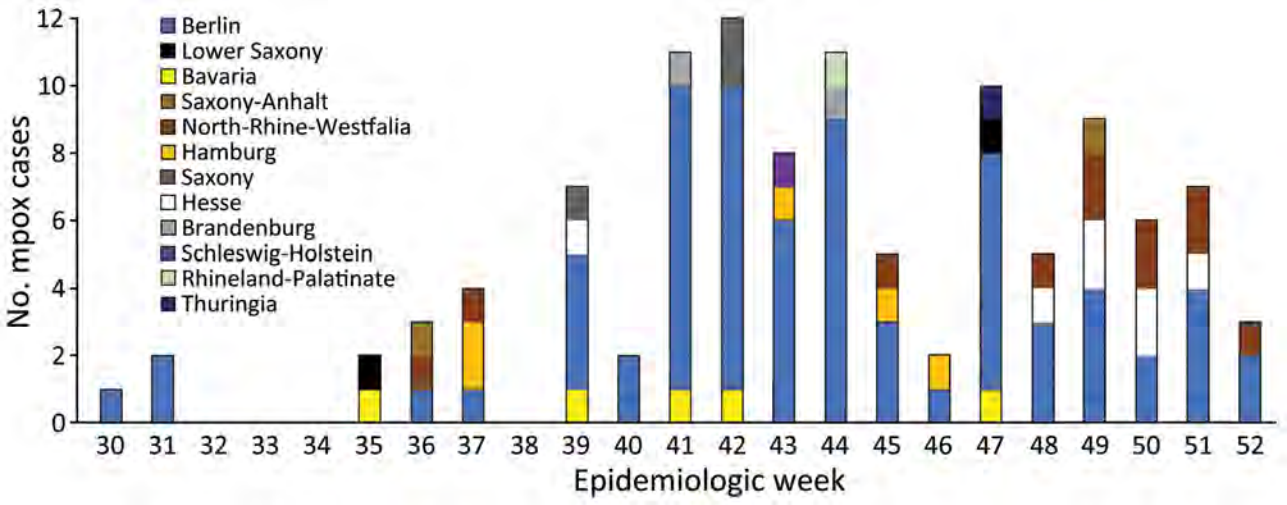

Figure 2. Number of clade II–associated mpox cases in Germany, July–December 2023, by federal state and reporting week (weeks 30–52). Total number of cases was 110.

undisclosed number of doses. In Germany, ≥47,537 persons were vaccinated with ≥1 dose of mpox vaccine since its approval in July 2022 through the end of November 2023, according to the framework of voluntary national vaccination monitoring (*6*). On the basis of sexual behavior data from representative population surveys in Germany (*7*) and the European MSM Internet Survey (EMIS-2017) (*8*), we estimated the denominator of the German population likely to be at high risk for mpox—that is, self-identified gay men reporting >5 anal intercourse partners within the previous 12 months—to be ≈90,000 persons (*9*,*10*) (Appendix Figure 2). When adding the reported number of mpox cases and the reported number of vaccinations for the numerator, we assumed a maximum proportion of 58% of self-identified gay men at high risk for mpox to be immunized.

Conclusions

We report re-emergence of mpox in Germany, mainly in Berlin, since July 2023, after 6 months without a single case in the German notification system. Transmission remained at a relatively stable, low level until December 2023 and mainly affected men who have sex with men. A thorough, sensitive assessment of a patient's sexual history remains essential in the diagnostic workup, and a reported long incubation period of >21 days (*11*) does not rule out mpox. Prior vaccination also does not automatically exclude mpox.

The phylogenomic analysis supports low-level transmission of clade IIb MPXV in Germany, particularly in Berlin, and intra-lineage diversity indicates ≥1 origin. Genome sequence similarity among strains from several countries in Europe, the Americas, and Asia underscores the status of mpox as an international concern. Our investigation supports the need for genomic surveillance to monitor transmission and the circulation and cocirculation of lineages and clades, particularly because of the increase of clade I–associated mpox in Africa (*12*,*13*).

We have based this study on data from national passive surveillance and our data likely underestimates the true number of case-patients because of such factors as ascertainment bias (as was the case with our case-patient) and omission of paucisymptomatic or clinically inapparent infections. We also concede that it is not possible to understand all transmission chains, given the often incomplete data in the notification system. We would require additional study data to assess disease severity or vaccine effectiveness.

The persistence of MPXV transmission worldwide, combined with vaccination monitoring and surveillance data, indicates that herd immunity has not yet been achieved, particularly in the indication group. Of note, official surveillance data offer an unclear picture of whether all vaccinated persons actually met the criteria for vaccination (or the narrower definition used for the denominator calculation in our study). Persons who were not, strictly speaking, at risk for mpox might have been vaccinated, and some persons at risk likely did not get vaccinated.

Our study elucidates the need for increased awareness of mpox among healthcare professionals and at-risk persons to reduce further spread and endemicity. We advocate indication-based vaccination, including healthcare professionals at risk, and improved vaccine communication and education to increase vaccine uptake as a public health measure.

Sequence data generated in this study have been deposited in GenBank and are publicly available (Appendix).

This study was conducted using aggregated, anonymized data from the German mandatory surveillance system within the framework of the Protection against Infection Act (IfSG). The analysis and publication of this data is mandated by law (§4 (2) IfSG). The study was conducted according to the Ethical Principles for Medical Research, version of the 64th General Assembly, Fortaleza, 2013. The case-patient provided written informed consent for the publication of his anonymized data. The Ethics Committee of the Berlin Medical Association (Ärztekammer Berlin) has exempted our description of patient data from formal review by the Ethics Committee because it does not involve biomedical research on humans or identifiable patient data (reference number ETH KB-2024/0001).

About the Author

Dr. Obermeier is a physician scientist at the Vaccine Safety Initiative in Berlin, Germany. His primary research interests are precision medicine approaches in the surveillance of (re)emerging infectious diseases.

References

1. Zhu J, Yu J, Qin H, Chen X, Wu C, Hong X, et al. Exploring the key genomic variation in monkeypox virus during the 2022 outbreak. BMC Genom Data. 2023;24:67. https://doi.org/10.1186/s12863-023-01171-0
2. Wenham C, Eccleston-Turner M. Monkeypox as a PHEIC: implications for global health governance. Lancet. 2022;400:2169–71. https://doi.org/10.1016/S0140-6736(22)01437-4
3. World Health Organization. Multi-country outbreak of mpox, External situation report #22—11 May 2023 [cited 2024 Jan 7]. https://www.who.int/publications/m/item/multi-country-outbreak-of-mpox--external-situation-report--22---11-may-2023
4. Robert Koch-Institut. SurvStat@RKI 2.0 [cited 2023 Nov 11] https://survstat.rki.de
5. Finlay AY, Khan GK. Dermatology Life Quality Index (DLQI)—a simple practical measure for routine clinical use. Clin Exp Dermatol. 1994;19:210–6.https://doi.org/10.1111/j.1365-2230.1994.tb01167.x
6. Robert Koch-Institut. Mpox vaccination monitoring June 2022–December 2023 [cited 2023 Dec 22]. https://www.rki.de/DE/Content/Infekt/Impfen/ImpfungenAZ/Affenpocken/Affenpocken-Impfmonitoring.pdf
7. Von Rüden U. AIDS in the public consciousness of the Federal Republic of Germany 2016: knowledge, attitudes and behaviour for protection against HIV/AIDS and other sexually transmitted infections (STIs). BZgA research report. Cologne: Federal Centre for Health. Aufklarung (Hambg). 2017 [cited 2024 Apr 23]. https://www.bzga.de/fileadmin/user_upload/PDF/studien/aioeb_2016_kurzbericht--a344710f2ec9af0c39b1d0bfe2ce140d.pdf
8. Weatherburn P, Hickson F, Reid DS, Marcus U, Schmidt AJ. European men-who-have-sex-with-men internet survey (EMIS-2017): design and methods. Sex Res Soc Policy. 2020;17:543–57. https://doi.org/10.1007/s13178-019-00413-0
9. Koch J, Vygen-Bonnet S, Bogdan C, Burchard G, Garbe E, Heininger U, et al. Scientific justification of the STIKO for the recommendation to vaccinate against monkeypox with *Imvanex* (MVA-Impfstoff). Epidemiologisches Bulletin: Current Data and Information on Infectious Diseases and Public Health. 2022;25-26:5–17 [cited 2023 Nov 26]. https://edoc.rki.de/bitstream/handle/176904/9878/EB-25-26-2022-Begr%c3%bcndung-Affenpocken.pdf
10. Standing Committee on Vaccination (STIKO). Recommendations of the Standing Committee on Vaccination (STIKO) at the Robert Koch Institute–2023. Epidemiologisches Bulletin: Current Data and Information on Infectious Diseases and Public Health. 2023;4:3–68 [cited 2024 Apr 27] https://www.rki.de/EN/Content/infections/Vaccination/recommandations/04_23_englisch.pdf
11. McFarland SE, Marcus U, Hemmers L, Miura F, Iñigo Martínez J, Martínez FM, et al. Estimated incubation period distributions of mpox using cases from two international European festivals and outbreaks in a club in Berlin, May to June 2022. Euro Surveill. 2023;28:2200806. https://doi.org/10.2807/1560-7917.ES.2023.28.27.2200806
12. Kibungu EM, Vakaniaki EH, Kinganda-Lusamaki E, Kalonji-Mukendi T, Pukuta E, Hoff NA, et al.; International Mpox Research Consortium. Clade I–associated mpox cases associated with sexual contact, the Democratic Republic of the Congo. Emerg Infect Dis. 2024;30:172–6. https://doi.org/10.3201/eid3001.231164
13. European Centre for Disease Prevention and Control. Implications of the EU/EEA of the outbreak of mpox caused by monkeypox virus clade I in the Democratic Republic of the Congo. Stockholm: European Centre for Disease Prevention and Control; 2023 [cited 2024 Apr 27]. https://www.ecdc.europa.eu/sites/default/files/documents/Implications-mpox-drc-TAB-erratum.pdf

Address for correspondence: Patrick E. Obermeier, Vaccine Safety Initiative, Kienberger Allee 4, 12529 Berlin-Schoenefeld, Germany; email: p.e.obermeier@gmail.com

Risk for Donor-Derived Syphilis after Kidney Transplantation, China, 2007–2022

Saifu Yin,[1] Lijuan Wu,[1] Congke Liu,[1] Zihao Jia,[1] Jiapei Wu, Fan Zhang, Xianding Wang, Turun Song, Tao Lin

To evaluate the risk of acquiring syphilis from a donated kidney, we evaluated kidney transplantation pairs from West China Hospital, Sichuan, China, during 2007–2022. Donor-derived syphilis was rare. Risk may be higher if donors have active syphilis and may be reduced if recipients receive ceftriaxone.

Syphilis transmission remains a public health challenge; ≈7.1 million new cases were reported in 2020 (*1*). Despite its relatively low incidence, if left untreated, syphilis results in substantial disease and death. Although the causative organism of syphilis, *Treponema pallidum*, is primarily transmitted sexually and vertically, transmission through solid organ transplantation is theoretically possible (*2*).

Kidneys are the most commonly and successfully transplanted solid organs. According to the Chinese National Renal Data System (http://www.cnrds.net), in 2022, 177,445 persons began dialysis, bringing the total undergoing dialysis to 984,809. However, according to the China Scientific Registry of Kidney Transplantation (https://www.csrkt.org.cn), the total number of kidney transplants in mainland China was only 12,712 in the same year, highlighting a challenge posed by organ shortages. Consequently, considerable efforts have been dedicated to expanding the donor pool, including accepting donors with syphilis. According to Chadban et al. (*3*) and the American Society of Transplantation Infectious Diseases Community of Practice (*4*), donors with syphilis might be considered after treatment, with recipient-informed consent and posttransplant prophylactic treatment.

Although several cases have documented no syphilis transmission from donors with treated syphilis (*2*,*5*,*6*), syphilis events were reported if the donors had active syphilis infection (*2*,*7*). Clinical guidelines recommend syphilis screening before donation (*3*,*4*). However, because of the urgency of organ procurement and the limited time for organ preservation, transplantation may occur before serologic testing results (*8*). Consequently, surgeons have learned only after transplantation that they had transplanted a kidney from a donor with syphilis. Moreover, large transplant centers may expand their donor eligibility criteria to encompass persons with syphilis because doing so improves transplant accessibility and substantially reduces time on the waiting list (*3*). However, even those proactive approaches increase the risk for donor-derived infection. We evaluated the risk of acquiring syphilis infection from a donated kidney among transplant pairs in western China. The study was approved by the Ethics Committee of West China Hospital, Sichuan University (2023SHEN354).

The Study

We enrolled kidney transplantation pairs from West China Hospital, a national medical center in Sichuan, China, during 2007–2022. The reverse sequence algorithm was used for syphilis screening before donation and transplantation (Appendix Figure 1, https://wwwnc.cdc.gov/EID/article/30/7/24-0009-App1.pdf) (*9*). Donors and recipients initially underwent chemiluminescence immunoassay (CLIA, treponemal testing); if positive, testing with the toluidine red unheated serum test (TRUST, nontreponemal testing) and *Treponema pallidum* particle agglutination (TPPA, treponemal testing) were performed. Among 5,521 kidney transplants, 102 (1.8%) pairs had risk for donor-derived infection when donors tested positive for CLIA and recipients were CLIA negative (Appendix Figure 2). The 102 pairs were from western China, predominantly Sichuan Province (44.1%), followed by Chongqing (15.7%), Tibet (9.80%), Qinghai (8.8%), Gansu (5.9%), Guizhou (5.9%), Yunnan (3.9%), Guangxi (2.9%),

Author affiliation: West China Hospital, Sichuan University, Chengdu, China

DOI: https://doi.org/10.3201/eid3007.240009

[1]These authors contributed equally to this article.

Shanxi (2.0%), and Xinjiang (1.0%) Provinces (Appendix Figure 3, panel C). The mean age of donors was 48.7 years and recipients 33.5 years; 52.0% of donors were male and 48.0% female, and 71.6% of recipients were male and 28.4% female (Table 1). Living-donor kidney transplantation involved 3 pairs of spouses, 12 pairs of siblings, and 35 pairs of parent–child relationships.

The kidney transplant pairs were divided according to donors' serologic testing results: 13 were CLIA+/TPPA–/TRUST–, 45 were CLIA+/TPPA+/TRUST–, and 44 were CLIA+/TPPA+/TRUST+. More male than female recipients (69/89 [77.5%]) received kidneys from donors with confirmed syphilis (p = 0.001). More living donors in the CLIA+/TPPA+/TRUST– group received penicillin treatment before donation (13/21 [61.9%]) (p<0.001) compared with the other 2 groups. A total of 47 (46.1%) recipients received cefmetazole, followed by ceftriaxone

Table. Baseline characteristics of 102 kidney transplantation pairs, western China, 2007–2022*

Characteristics	No. (%) patients				p value
	Overall, n = 102	CLIA+/TPPA–/TRUST–, n = 13	CLIA+/TPPA+/TRUST–, n = 45	CLIA+/TPPA+/TRUST+, n = 44	
Donor					
Type					0.848†
Deceased	52 (51.0)	7 (53.8)	24 (53.3)	21 (47.7)	
Living	50 (49.0)	6 (46.2)	21 (46.7)	23 (52.3)	
Living donor-recipient relationship					0.799‡
Spouses	3 (6.0)	0	1 (4.8)	2 (8.7)	
Parent-Child	35 (70.0)	4 (66.7)	14 (66.7)	17 (73.9)	
Siblings	12 (24.0)	2 (33.3)	6 (28.6)	4 (17.4)	
Sex					0.390‡
M	53 (52.0)	9 (69.2)	23 (51.1)	21 (47.7)	
F	49 (48.0)	4 (30.8)	22 (48.9)	23 (52.3)	
Mean age, y (± SD)	48.7 (8.9)	54.3 (6.2)	47.7 (6.7)	48.0 (10.8)	0.047§
Syphilis treatment of the living donor before donation					<0.001‡
Penicillin	16 (32.0)	0	13 (61.9)	3 (13.0)	
None	34 (68.0)	6 (100)	8 (38.1)	20 (87.0)	
Recipient					
Sex					0.001‡
M	73 (71.6)	4 (30.8)	37 (82.2)	32 (72.7)	
F	29 (28.4)	9 (69.2)	8 (17.8)	12 (27.3)	
Mean age, y (± SD)	33.5 (9.8)	37.7 (9.6)	32.4 (10.0)	33.5 (9.4)	0.224§
Hemodialysis					0.648‡
No	17 (16.7)	1 (7.7)	8 (17.8)	8 (18.2)	
Yes	85 (83.3)	12 (92.3)	37 (82.2)	36 (81.8)	
Peritoneal dialysis					0.892‡
No	92 (90.2)	12 (92.3)	41 (91.1)	39 (88.6)	
Yes	10 (9.8)	1 (7.7)	4 (8.9)	5 (11.4)	
Mean duration dialysis, mo, (± SD)	12.8 (16.0)	19.8 (26.8)	11.8 (14.6)	11.7 (13.0)	0.243¶
Induction therapy					0.534‡
Anti-thymocyte globulin	26 (25.5)	3 (23.1)	12 (26.7)	11 (25.0)	
Basiliximab	66 (64.7)	7 (53.8)	30 (66.7)	29 (65.9)	
None	10 (9.8)	3 (23.1)	3 (6.7)	4 (9.1)	
Maintenance immunosuppressive therapy					0.022‡
Cyclosporine	3 (2.9)	2 (15.4)	0 (0.0)	1 (2.3)	
Tacrolimus	99 (97.1)	11 (84.6)	45 (100.0)	43 (97.7)	
Antimicrobial use					0.016‡
Aztreonam	3 (2.9)	0	2 (4.4)	1 (2.3)	
Cefmetazole	47 (46.1)	7 (53.8)	23 (51.1)	17 (38.6)	
Cefoperazone	4 (3.9)	0	4 (8.9)	0	
Ceftriaxone	32 (31.4)	2 (15.4)	9 (20.0)	21 (47.7)	
Cefoxitin	2 (2.0)	0	2 (4.4)	0	
Ceftizoxime	10 (9.8)	4 (30.8)	2 (4.4)	4 (9.1)	
Imipenem–cilastatin	4 (3.9)	0	3 (6.7)	1 (2.3)	

*Persons were from Sichuan, Chongqing, Tibet, Qinghai, Gansu, Guizhou, Yunnan, Guangxi, Shanxi, and Xinjiang Province, China. CLIA, chemiluminescence immunoassay; mNGS, metagenomic next-generation sequencing; TPPA, *Treponema pallidum* particle agglutination; TRUST, toluidine red unheated serum test.
†By χ^2 test.
‡By Fisher exact test.
§By Student *t*-test.
¶By Wilcoxon–Mann–Whitney U-test.

(32 [31.4%]), ceftizoxime (10 [9.8%]), and aztreonam (3 [2.9%]). More recipients in the CLIA+/TPPA+/TRUST+ group received ceftriaxone (21/44 [47.7%]; p = 0.016) compared with the other 2 groups.

After transplantation, 7 recipients had confirmed syphilis (1 in the CLIA+/TPPA+/TRUST– group; 6 in the CLIA+/TPPA+/TRUST+ group), suggesting a rare risk for donor-derived syphilis (7/5521 [0.1%]). Incidence of CLIA+ was higher for persons in the CLIA+/TPPA+/TRUST+ group (16/44 [36.4%]) than in the CLIA+/TPPA+/TRUST– (5/45 [11.1%]) and CLIA+/TPPA–/TRUST– (1/13 [7.7%]) groups (p = 0.006). Incidence of TPPA+ was marginally higher for persons in the CLIA+/TPPA+/TRUST+ group (6/44 [13.6%]), than in the CLIA+/TPPA+/TRUST– (1/45 [2.2%]), and CLIA+/TPPA–/TRUST– (0/13 [0%]) groups (p = 0.060). Incidence of TRUST+ was numerically higher for persons in the CLIA+/TPPA+/TRUST+ group (3/44 [6.8%]) than in the CLIA+/TPPA+/TRUST– (0/45 [0%]) and CLIA+/TPPA+/TRUST+ (0/13 [0%]) groups (p = 0.130) (Figure 1). Specifically, 2 recipients received kidneys from CLIA+/TPPA+/TRUST+ spouses, and 1 was infected after transplantation despite the use of aztreonam. The three groups had similar kidney function, graft, and patient survival rates (Appendix Figure 4).

In the CLIA+/TPPA+/TRUST+ group, use of ceftriaxone was associated with a lower incidence of TPPA+ (6/23 [26.1%] with vs. 0/21 [0%] without; p = 0.022) and with a numerically lower incidence of TRUST+ (3/23 [13.0%] with vs. 0/21 [0%] without; p = 0.234) compared with no use (Figure 2, panel A). In addition, receiving kidneys from deceased donors was associated with a numerically higher incidence of TPPA+ (4/21 [19.0%] deceased donor vs. 2/23 [8.7%] living donor; p = 0.403) and a numerically higher incidence of TRUST+ (3/21 [14.3%] vs. 0/23 [0.0%]; p = 0.100) compared with receiving kidneys from living donors (Figure 2, panel B).

Through systematic searching, we identified 9 publications (1987–2023) with sample sizes of 1–28 participants (Appendix Table). Of 65 transplant pairs, 6 recipients were CLIA+ and 4 were TPPA+ after transplantation, despite differences in donor syphilis status and recipient antimicrobial prophylaxis.

Conclusions

We detected 7 potential donor-derived syphilis infection events among >5,000 kidney transplantations. The reverse sequence algorithm we used for syphilis screening is more sensitive than the traditional algorithm for detecting early or late latent syphilis (*10*). The extremely low incidence of syphilis transmission can be attributed to several factors: donors with syphilis were uncommon, accounting for <2% in the large cohort; living donors had the opportunity to receive treatment before donation; and after transplantation, antimicrobial prophylaxis was administered to recipients. Similarly, in a large-scale cohort study enrolling 1,460 liver recipients and 3,072 kidney recipients, 6 diagnoses of syphilis were new (*11*).

T. pallidum can persist in various tissues and organs at different stages of infection, in untreated and treated persons (*12*). Our findings suggest that using donors with treated syphilis poses a lower risk for infection among recipients than using donors with active syphilis. Despite the relatively low transmission risk from donors with treated syphilis, our study reported 1 infected recipient who received the kidney from his mother. Although uncommon, a possible reason could be false-negative TRUST result for persons with secondary syphilis and early latent syphilis. A similar case was reported after liver transplantation, in which a recipient received a TPPA+/Venereal Disease Research Laboratory test–negative liver graft (*13*), which clinically emphasized the role of syphilis treatment before donation, particularly in living-donor kidney transplantation.

In our study, 3 recipients received kidneys from their spouses. By chance, 1 recipient was infected after receiving a kidney from his spouse with active syphilis infection even when prophylactic measures were implemented. In the nationwide cohort study

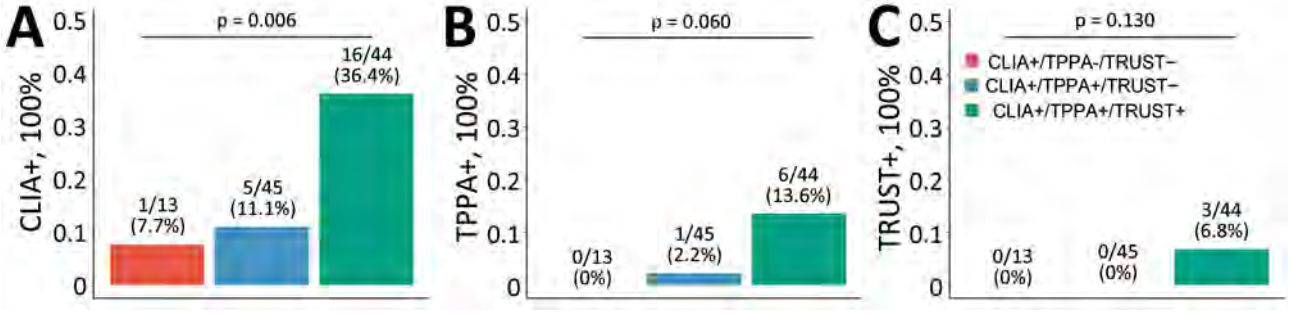

Figure 1. Incidence of donor-derived syphilis, China, 2007–2022. Percentage of CLIA+ (A), TPPA+ (B), and TRUST+ (C) after transplantation were determined by χ^2 or Fisher exact test, as appropriate. CLIA+, positive by chemiluminescence immunoassay; TPPA+, positive by *Treponema pallidum* particle agglutination test; TRUST+, positive by toluidine red unheated serum test.

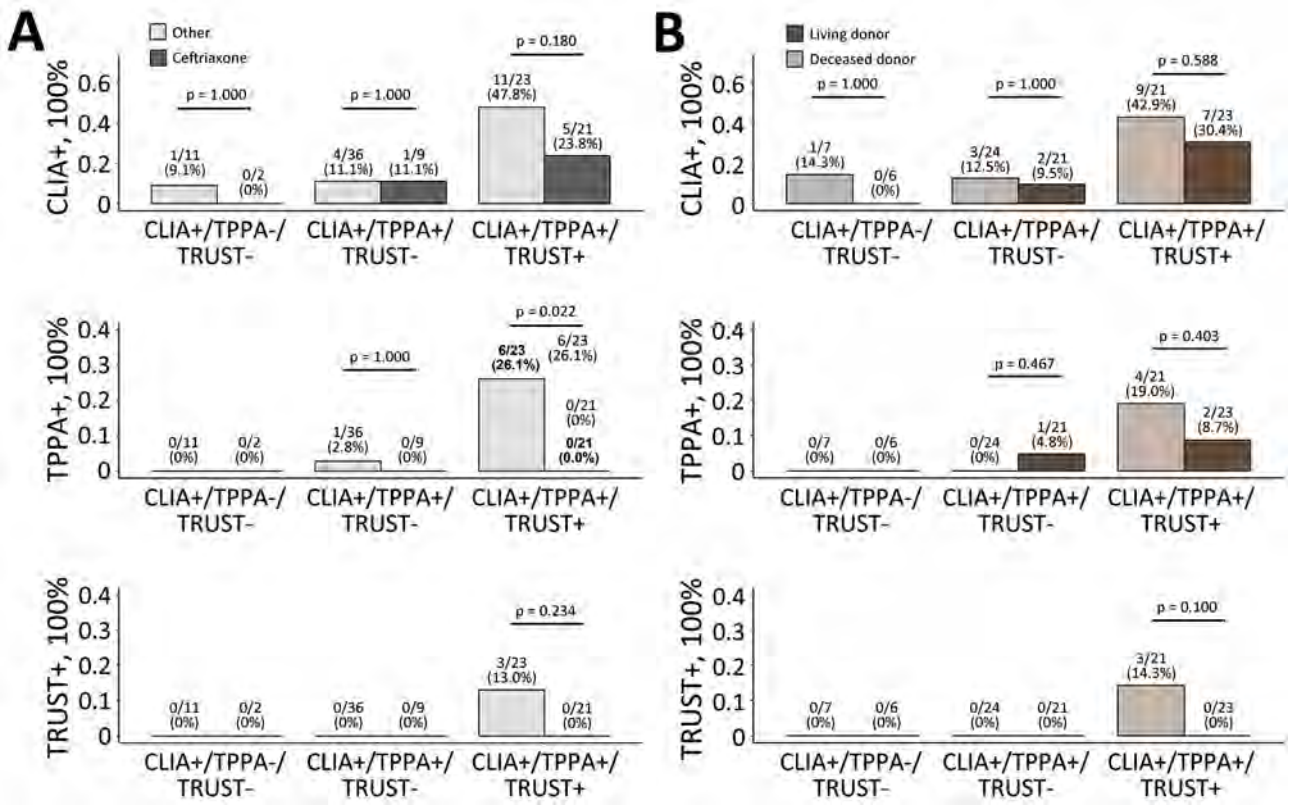

Figure 2. Subgroup analyses of the incidence of donor-derived syphilis, China, 2007–2022, determined by χ^2 or Fisher exact test, as appropriate. A) Percentage of CLIA+, TPPA+, and TRUST+ after transplantation based on the use of ceftriaxone versus other antimicrobial drugs. B) Percentage of CLIA+, TPPA+, and TRUST+ after transplantation based on donor type. CLIA+, positive by chemiluminescence immunoassay; TPPA+, positive by *Treponema pallidum* particle agglutination test; TRUST+, positive by toluidine red unheated serum test.

evaluating the burden of sexually transmitted infections after transplantation, 25 of 3,612 recipients were confirmed to have acquired infections, including 1 case of syphilis (*14*). Those findings underscore the imperative for recipients and their spouses to undergo treatment.

A limitation of our study is its retrospective design. In addition, the number of kidney transplants from serologically positive donors was small, potentially limiting our ability to estimate the overall risk for donor-derived syphilis. Last, antimicrobial prophylaxis against syphilis infection varied in our study.

In summary, donor-derived syphilis transmission was rare after kidney transplantation. Risk was increased if the donor had active syphilis and decreased if the recipient received prophylactic ceftriaxone.

This work was supported by the Natural Science Foundation of China (81870513, 82370753) and the Sichuan Science and Technology Program (2023NSFSC0599). The funders had no role in study design, data collection or analysis, preparation of the manuscript, or the decision to publish.

After publication, data are available upon reasonable request of the authors. A proposal with a detailed description of study objectives and statistical analysis plan will be needed for evaluation of the reasonability of requests. Additional materials might also be required during the process of evaluation. Participant data will be provided after approval from the corresponding author.

T.L. had full access to all data in the study and takes responsibility for the integrity of the data and the accuracy of the data analysis. T.L., T.S., and S.Y. were responsible for concept and design; S.Y., C.L., L.W., and Z.J. for data acquisition; S.Y., L.W., J.W., F.Z., and X.W. for statistical analysis and data interpretation; S.Y. and L.W. for drafting the manuscript; T.L. and T.S. for critical revision of the manuscript for intellectual content; and T.L. and T.S. for supervision.

About the Author

Mr. Yin is a doctoral student at the Department of Urology/Kidney Transplantation Center, West China Hospital, Sichuan University, Chengdu, China. His research interests are primarily focused on kidney transplantation.

References

1. World Health Organization. Syphilis [cited 2023 Nov 3]. https://www.who.int/news-room/fact-sheets/detail/syphilis
2. Caballero F, Domingo P, Rabella N, López-Navidad A. Successful transplantation of organs retrieved from a donor with syphilis. Transplantation. 1998;65:598–9. https://doi.org/10.1097/00007890-199802270-00029
3. Chadban SJ, Ahn C, Axelrod DA, Foster BJ, Kasiske BL, Kher V, et al. KDIGO clinical practice guideline on the evaluation and management of candidates for kidney transplantation. Transplantation. 2020;104:S11–S103. https://doi.org/10.1097/TP.0000000000003136
4. Malinis M, Boucher HW; AST Infectious Diseases Community of Practice. Screening of donor and candidate prior to solid organ transplantation—guidelines from the American Society of Transplantation Infectious Diseases Community of Practice. Clin Transplant. 2019;33:e13548. PubMed https://doi.org/10.1111/ctr.13548
5. Gibel LJ, Sterling W, Hoy W, Harford A. Is serological evidence of infection with syphilis a contraindication to kidney donation? Case report and review of the literature. J Urol. 1987;138:1226–7. PubMed https://doi.org/10.1016/S0022-5347(17)43558-0
6. Ko WJ, Chu SH, Lee YH, Lee PH, Lee CJ, Chao SH, et al. Successful prevention of syphilis transmission from a multiple organ donor with serological evidence of syphilis. Transplant Proc. 1998;30:3667–8. https://doi.org/10.1016/S0041-1345(98)01185-3
7. Cortes NJ, Afzali B, MacLean D, Goldsmith DJ, O'Sullivan H, Bingham J, et al. Transmission of syphilis by solid organ transplantation. Am J Transplant. 2006;6:2497–9. https://doi.org/10.1111/j.1600-6143.2006.01461.x
8. Gov.UK. Advisory Committee on the Safety of Blood Tissues and Organs (SaBTO) [cited 2023 Nov 5]. https://www.gov.uk/government/groups/advisory-committee-on-the-safety-of-blood-tissues-and-organs
9. Papp JR, Park IU, Fakile Y, Pereira L, Pillay A, Bolan GA. CDC laboratory recommendations for syphilis testing, United States, 2024 [cited 2024 Apr 4]. https://www.cdc.gov/mmwr/volumes/73/rr/rr7301a1.htm
10. Binnicker MJ, Jespersen DJ, Rollins LO. Direct comparison of the traditional and reverse syphilis screening algorithms in a population with a low prevalence of syphilis. J Clin Microbiol. 2012;50:148–50. https://doi.org/10.1128/JCM.05636-11
11. Cleveland H, Kothari R, Niemann C, Chin-Hong P, Fung M. Syphilis in liver and kidney recipients. Am J Transplant. 2022;22:1064.
12. Peeling RW, Mabey D, Chen XS, Garcia PJ. Syphilis. Lancet. 2023;402:336–46. https://doi.org/10.1016/S0140-6736(22)02348-0
13. Tariciotti L, Das I, Dori L, Perera MT, Bramhall SR. Asymptomatic transmission of *Treponema pallidum* (syphilis) through deceased donor liver transplantation. Transpl Infect Dis. 2012;14:321–5. https://doi.org/10.1111/j.1399-3062.2012.00745.x
14. Helanterä I, Gissler M, Kanerva M, Rimhanen-Finne R, Lempinen M, Finne P. Incidence of sexually transmitted infections is lower among kidney transplant recipients compared to the general population—a nationwide cohort study. Transpl Infect Dis. 2022;24:e13814. https://doi.org/10.1111/tid.13814

Address for correspondence: Turun Song or Tao Lin, Guoxue alley 37#, Wuhou District, Chengdu, Sichuan, China; email: songturun1986@scu.edu.cn or kidney1234@163.com

Avian Influenza A(H5N1) Virus among Dairy Cattle, Texas, USA

Judith U. Oguzie,[1] Lyudmyla V. Marushchak,[1] Ismaila Shittu, John A. Lednicky, Aaron L. Miller, Haiping Hao, Martha I. Nelson, Gregory C. Gray

During March and April 2024, we studied dairy cattle specimens from a single farm in Texas, USA, using multiple molecular, cell culture, and next-generation sequencing pathogen detection techniques. Here, we report evidence that highly pathogenic avian influenza A(H5N1) virus strains of clade 2.3.4.4b were the sole cause of this epizootic.

Since the arrival of clade 2.3.4.4b avian influenza A(H5N1) in North America in late 2021, frequent mammal spillover events have occurred in a diverse range of species, including 1 human infection, but those strains have not affected cattle. Cattle are known to be permissive but resilient to infection with influenza A, B, and C viruses (*1*); however, they are susceptible to influenza D virus, which is thought to have near-worldwide distribution (*2*). Influenza D virus is thought to move from cow-to-cow through direct contact or short-distance aerosol respiratory transmission (*2*), and possible occasional influenza D virus spillover to humans is a concern (*3*,*4*). Even so, influenza viruses are not the first pathogens veterinarians or veterinary diagnostic laboratories search for in studying cattle respiratory epizootics. We report results of an investigation into influenza virus infections among dairy cattle on a farm in Texas, USA.

The Study

On March 18, 2024, we were notified of epidemics of illness among Texas dairy cattle. The cattle had transient respiratory and gastrointestinal signs (*5*). Veterinary diagnostic laboratory results were largely unremarkable except for rumors among cattle veterinarians of possible influenza A virus detection among cattle and conjunctivitis among dairy farm workers. The University of Texas Medical Branch (UTMB) research team offered diagnostic support owing to the team's novel pathogen detection capabilities (*6*–*9*) and having recognized that conjunctivitis among workers handling animals had been previously noted in association with highly pathogenic avian influenza (HPAI) epizootics (*10*–*13*). On March 19, we were invited to investigate the outbreak by a farm owner. We provided the farm with sampling supplies and instructions. UTMB's Institutional Animal Care and Use Committee has viewed such diagnostic work to be exempt from formal ethics review.

To determine the etiology of cattle illnesses, we used molecular screening and, in some cases, cell culture and metagenomics, to examine cattle swab specimens (Appendix 1, https://wwwnc.cdc.gov/EID/article/30/7/24-0717-App1.pdf). We targeted 6 viral groups, adenoviruses, coronaviruses, enteroviruses, influenza viruses, paramyxoviruses, and pneumoviruses, using previously published techniques (*8*).

At our request, on March 21, dairy farm management collected and shipped swab specimens from the nasal passages of 14 cows with signs of illness and 6 cows with no sign of illness in a shipping container with ice packs. We received the samples and completed questionnaires on March 22. To determine whether pathogens were enteric, we requested additional samples from the dairy farm on March 28. Nasal and rectal swab specimens were taken from 10 additional ill cows on April 1; we received those 20 additional swab specimens on April 3.

Author affiliations: University of Texas Medical Branch, Galveston, Texas, USA (J.U. Oguzie, L.V. Marushchak, I. Shittu, A.L. Miller, H. Hao, G.C. Gray); University of Florida, Gainesville, Florida, USA (J.A. Lednicky); National Center for Biotechnology Information, National Library of Medicine, National Institutes of Health, Bethesda, Maryland, USA (M.I. Nelson)

DOI: https://doi.org/10.3201/eid3007.240717

[1]These first authors contributed equally to this article.

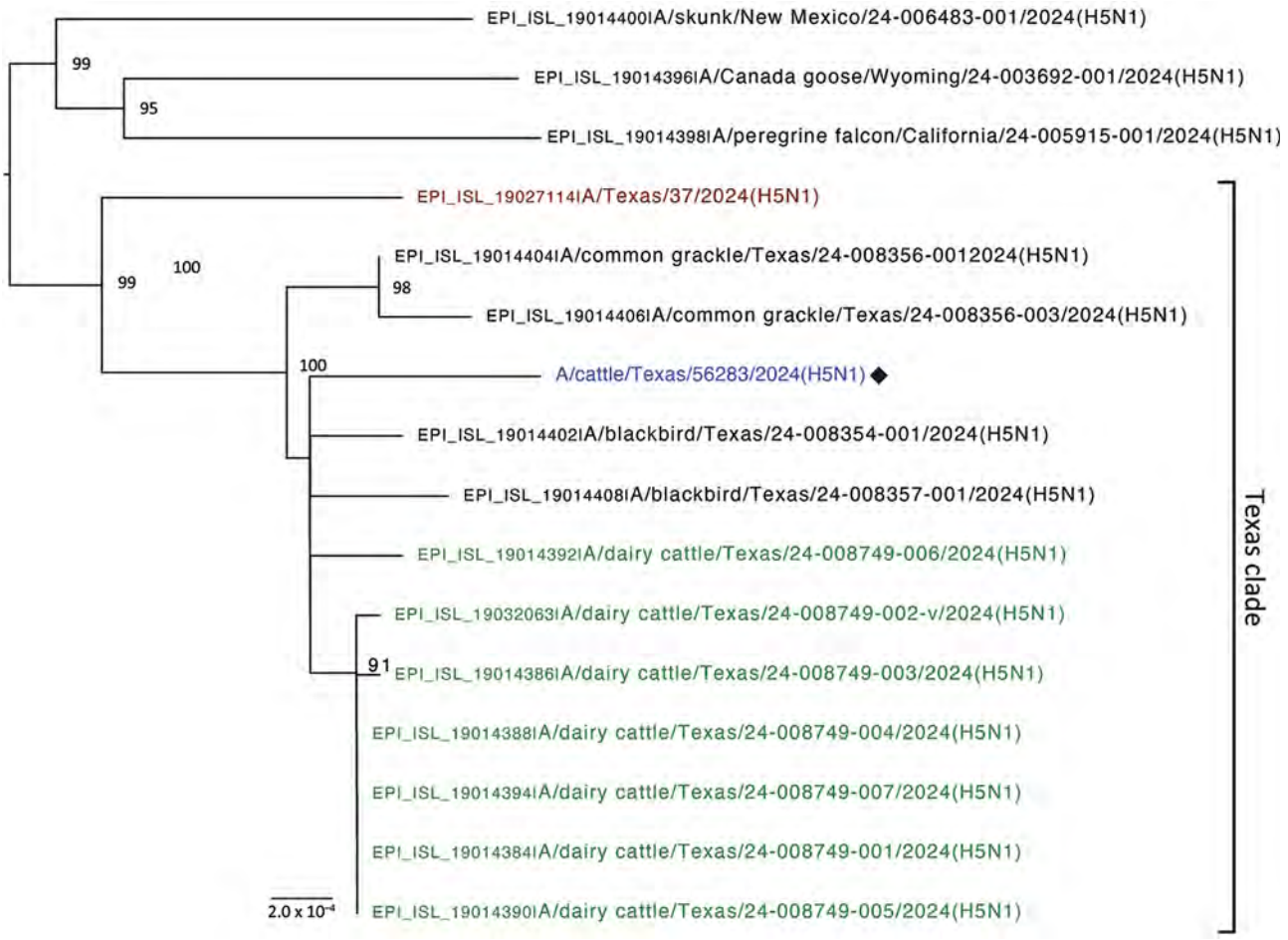

Figure 1. Phylogenetic tree of the concatenated genome in study of avian influenza A(H5N1) virus among dairy cattle, Texas, USA. Maximum-likelihood phylogenetic tree inferred for the A/cattle/Texas/5628356283/2024 (H5N1) virus isolated in this study (blue text) and 15 other closely related HPAI H5N1 viruses downloaded from GISAID (https://www.gisaid.org). Bootstrap values are provided for key nodes. The clade of 13 Texas viruses collected during March 2024 is labeled. Red text indicates human case (A/Texas/37/2024) and green text indicates cattle viruses collected from other farm(s) in Texas. Branch lengths are drawn to scale. Scale bar indicates number of substitutions per site.

The 40 swab specimens were obtained from 30 different cows (24 sick and 6 healthy) from the same dairy farm (Appendix 1 Table 1); specific farm location, name, and cattle breed are withheld for privacy purposes. Sampled cattle ranged from 2 years 3 months of age to 7 years 10 months of age.

Farm staff first observed illnesses in cattle on March 6. Cattle with otherwise healthy records showed signs of decreased appetite, lethargy, increased respiratory secretions, high temperatures (up to 105°F or 40.56°C), abnormal bowel movements, and decreased milk production. During March 10–12, >4.75% of the herd had clinical signs of influenza-like illness and were being treated in the hospital pens. No dead birds, dead cats, or other deceased wildlife were observed. At the time of specimen collections, cattle illnesses were on the wane.

Several workers experienced influenza-like symptoms and missed work during March 4–6. A maternity worker visited a local clinic and received treatment for influenza-like symptoms; 2 milkers also experienced influenza-like symptoms and stayed home. No cases of conjunctivitis, severe illness, or hospitalizations were reported among workers.

Multiple cattle swab specimens demonstrated molecular evidence of H5 avian influenza A virus (Appendix 1 Table 1). Of the first 20 cattle swab samples received, none had evidence of adenovirus, coronavirus, enterovirus, or influenza D. Of those first 20 specimens, 3 (2 healthy cows, 1 sick cow) demonstrated molecular evidence of a Paramyxoviridae or Pneumoviridae virus (Appendix 1 Table 1). Multiple swab cultures in MDBK, Vero E6, and MDCK cells also had molecular evidence of H5 avian influenza A virus. Molecular study of the HA cleavage site demonstrated that those viruses were highly pathogenic. Next-generation sequencing (NGS)

corroborated these findings; 1 cultured cattle nasal swab specimen yielded a complete genome A/cattle/Texas/56283/2024 (H5N1) (GenBank accession nos. PP600140–7 for the 8 viral segments), confirmed to be HPAI and of clade 2.3.4.4b. We performed phylogenetic comparisons of related viruses in GenBank and GISAID (https://www.gisaid.org) for the entire genome (Figure 1) and the virus's 8 gene segments (Figure 2), which documented similarity to 13 other viruses in the Texas epizootic clade. A/cattle/Texas/56283/2024 (H5N1) had several novel mutations in comparison to related viruses (Table). One mutation (PB2-M631L) increases the capability of H5N1 to replicate in human cells by enhancing the polymerase activity of the viruses in human cells. Pathogenicity studies in animal models will be necessary to better understand such viruses. NGS analyses suggested that the sick cow in which a nasal swab specimen tested positive for Paramyxoviridae or Pneumoviridae virus (cattle identification [ID] 49869) (Appendix 1 Table 1) had a bovine viral diarrhea virus (BVDV), indicating a possible cause of illness.

Conclusions

This preliminary study of a single Texas dairy farm affected by what is now a multistate epizootic of HPAI H5N1 documents several key observations. H5N1 virus detections were made solely in the sick cows without apparent co-infecting viruses (5 other viral families examined). HPAI H5N1 virus was more prevalent among nasal swab samples than rectal swab samples, supporting the notion that the respiratory tract of cattle could be involved in cow-to-cow transmission.

Although 1 sick cow (cattle ID 49869; Appendix 1 Table 1) was found by NGS to have evidence of a BVDV in its nasal swab specimen, 2 other healthy cows also had panspecies evidence of such a virus (cattle IDs 74061 and 54972; Appendix 1 Table 1);

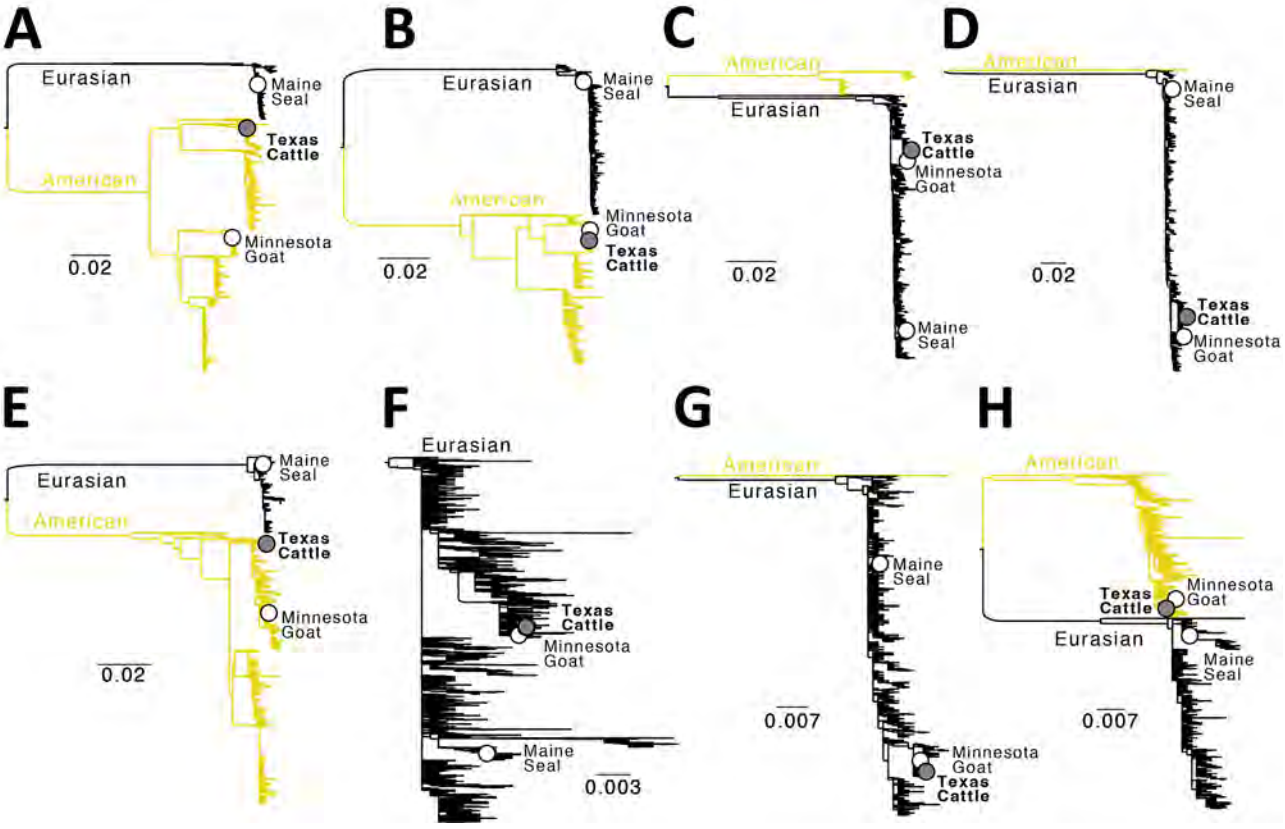

Figure 2. Phylogenetic trees for 8 genome segments in study of avian influenza A(H5N1) virus among dairy cattle, Texas, USA. Maximum-likelihood phylogenetic trees inferred for each of the 8 segments of the influenza A virus genome, including A/cattle/Texas/56283/2024(H5N1) isolated in this study (positioned in the Texas Cattle clade defined in Figure 1) and 3516–3644 H5N1 sequences (depending on the segment) from North America and South America, collected December 21, 2021–March 28, 2024, that were downloaded from GISAID (https://www.gisaid.org) on April 10, 2024. A) Polymerase basic 1; B) polymerase basic 2; C) polymerase acidic; D) hemagglutinin; E) nucleoprotein; F) neuraminidase; G) matrix; H) nonstructural. Outbreaks in Maine harbor seals and gray seals (June 2022), Minnesota goats (March 2024), and Texas cattle/humans (March 2024) are labeled. The American and Eurasian avian influenza lineage are labeled. All branch lengths drawn to scale. Scale bars indicate number of substitutions per site.

Table. Identified mutations, by gene segment, in avian influenza A(H5N1) strain A/cattle/Texas/56283/2024 (H5N1) detected in cattle on a dairy farm, Texas, USA*

Mutation region	All mutations	Red mutation	Orange mutations	Reference strain
HA	K3N, G16S, N110S, L120M, L131Q, T139P, T156A, Q185R, V194I, A201E, T211I, V226A, N252D, E284G, M285V, I298V, K492E, I526V, V538A, I547M, V548M		N110S, L131Q, T139P, V226A	A/Sichuan/26221/2014 (H5N6)
M1	N82S, N85S, N87T, T140A, F144L, M165I, V166A, A200V, A227T, K230R, M248L			A/duck/Guangdong/E1/2012 (H10N8)
M2	R12K, K18N, V27A, I51V, R61G, D88N	V27A		A/mallard/Astrakhan/263/1982 (H14N5)
NA	I8T, V17I, I20V, H44Y, A46P, V67I, N71S, T76A, K78Q, A81T, V99I, H100Y, H155Y, T188I, M258I, L269M, E287D, T289M, V321I, G336S, V338M, S339P, P340S, N366S, G382E, A395E, I418M, S434N, D460G			A/goose/Guangdong/1/1996 (H5N1)
NP	Y52H, S482N			A/chicken/BCFAV8//2014 (H5N2)
NS1	S7L, R21Q, S87P, C116S, D139N, A223E, V226I		A223E, V226I	A/duck/Guangdong/E1/2012 (H10N8)
NS2	E67G		E67G	A/quail/Italy/1117/1965 (H10N8)
PA	A36T, I61M, T85A, K113R, L219I, S277P, A404S, M441V, K497R, Y535H, I543L, S558L, T608S		A36T, A404S	A/Netherlands/219/2003 (H7N7)
PB1	T59S, E75D, I114V, I171V, M179I, S384T, V401A, A587P			A/Singapore/1/1957 (H2N2)
PB2	T58A, V109I, V139I, E362G, K389R, D441N, V478I, V495I, M631L, V649I, M676A			A/duck/Guangdong/E1/2012 (H10N8)

*As listed in FluSurver (http://flusurver.bii.a-star.edu.sg), red mutations alter viral virulence, cause strong drug resistance, or reverse the effects of the premature STOP codon. These have an assigned warning level of 3 (most significant); Orange mutations are those at drug binding sites or sites that alter host-cell specificity. These have a warning level 2 (significant). In addition, mutations at sites known to result in antigenic shifts or cause mild drug resistance are in this group. HA, hemagglutinin; M, matrix; NA, neuraminidase; NP, nucleoprotein; NS, nonstructural; PA, polymerase acidic; PB, polymerase basic.

however, we did not perform NGS on their specimens. BVDVs are frequently associated with mild respiratory disease on cattle farms; because this farm routinely administers a vaccine with live BVDV components, we doubt that the BVDV explains the unusual illness seen in this farm's dairy cattle herd.

The complete genome of the H5N1 virus isolated from 1 sick cow's nasal swab specimen suggests that this H5N1 strain is very similar to the H5N1 strains characterized from dead birds, other cattle (*14*), and 1 cattle worker (*15*). The high genetic similarity of A/cattle/Texas/56283/2024 (H5N1) and other avian, human, and cattle strains in the Texas clade suggests a single interconnected multispecies outbreak in Texas, the precise directions of transmission still to be determined.

A limitation of our study is that we only examined specimens sent to us. We did not collect milk, study animal workers, or collect environmental specimens, nor did we immediately visit the farm for a comprehensive outbreak investigation. However, many barriers to performing a more traditional outbreak investigation on HPAI-infected farms currently exist.

The ongoing multispecies HPAI H5N1 outbreak involving birds, cattle, goats, alpacas, humans, cats, and other species epitomizes why interdisciplinary cooperation under a One Health framework is required. If we wish to resolve complex problems such as this epizootic, finding ways to assure farm owners that necessary epidemiological investigations will not harm their businesses will be imperative.

Acknowledgments

We thank Diego Silva and Claudia Trijillo for their administrative and laboratory support of this work. We thank Robert H. Carpenter and Kay Russo for their education regarding livestock farming. We thank the dairy farm owners for engaging us in research collaboration. We gratefully acknowledge all data contributors (i.e., the authors and their originating laboratories responsible for obtaining the specimens and their submitting laboratories for generating the genetic sequence and metadata and sharing via the GISAID Initiative) on which this research is based (Appendix 2, https://wwwnc.cdc.gov/EID/article/30/7/24-0717-App2.xlsx).

Data needed to evaluate the conclusions in the paper are present in the paper and the Appendices. Researchers with BSL3Ag-approved laboratories may request A/cattle/Texas/56283/2024 (H5N1) by contacting Kenneth Plante (ksplante@utmb.edu) of UTMB's World Reference Center for Emerging Viruses and Arboviruses (https://www.utmb.edu/wrceva). Additional data or specimens may be requested from the corresponding author. The sharing of additional data or specimens will require the signing of a materials transfer agreement.

This work was supported by G.C.G.'s startup funding from the University of Texas Medical Branch and in support of M.I.N.'s work, by the Intramural Research Program at the National Library of Medicine at the National Institutes of Health and the Centers of Excellence for Influenza Research and Surveillance, National Institute of Allergy and Infectious Diseases, National Institutes of Health, Department of Health and Human Services (contract HHSN272201400006C).

G.C.G. conceptualized the study. J.U.O., L.V.M., I.S., A.L.M., J.A.L., H.H., and G.C.G. constructed the methodology. Investigation was carried out by G.C.G., J.U.O., L.V.M., I.S., A.L.M., J.A.L., and H.H. M.I.N. and J.U.O. performed data analysis. Visualization was performed by J.U.O. and H.H. Funding was acquired by G.C.G., and the project was administered by G.C.G. and L.V.M. G.C.G. and L.V.M. supervised the study. J.U.O. and G.C.G. wrote the original draft, and all authors contributed to the review and editing of the final manuscript.

About the Author

Dr. Oguzie is a veterinarian, molecular biologist, and current postdoctoral fellow at the University of Texas Medical Branch in Galveston, Texas. Her primary research interests are molecular surveillance and genomic characterization of novel pathogens. Dr. Marushchak is a veterinary scientist and postdoctoral fellow at the University of Texas Medical Branch in Galveston, Texas. Her primary research interest is conducting molecular surveillance for emerging pathogens at the human-animal interface.

References

1. Sreenivasan CC, Sheng Z, Wang D, Li F. Host range, biology, and species specificity of seven-segmented influenza viruses—a comparative review on influenza C and D. Pathogens. 2021;10:1583. https://doi.org/10.3390/pathogens10121583
2. Ruiz M, Puig A, Bassols M, Fraile L, Armengol R, Influenza D. Influenza D virus: a review and update of its role in bovine respiratory syndrome. Viruses. 2022;14:2717. https://doi.org/10.3390/v14122717
3. White SK, Ma W, McDaniel CJ, Gray GC, Lednicky JA. Serologic evidence of exposure to influenza D virus among persons with occupational contact with cattle. J Clin Virol. 2016;81:31–3. https://doi.org/10.1016/j.jcv.2016.05.017
4. Leibler JH, Abdelgadir A, Seidel J, White RF, Johnson WE, Reynolds SJ, et al. Influenza D virus exposure among US cattle workers: a call for surveillance. Zoonoses Public Health. 2023;70:166–70. https://doi.org/10.1111/zph.13008
5. American Association of Bovine Practitioners. AABP statement on Texas cattle outbreak. 2024 Mar 18 [cited 2024 Mar 18]. https://agpartners.net/2024/03/18/aabp-statement-on-texas-cattle-outbreak
6. Ramesh A, Bailey ES, Ahyong VLC, Phelps M, Neff N, Sit R, et al. Microbial diversity in a North American swine farm operation. Sci Rep. 2021;11:16994. https://doi.org/10.1038/s41598-021-95804-y
7. Xiu L, Binder RA, Alarja NA, Kochek K, Coleman KK, Than ST, et al. A RT-PCR assay for the detection of coronaviruses from four genera. J Clin Virol. 2020;128:104391. https://doi.org/10.1016/j.jcv.2020.104391
8. Gray GC, Robie ER, Studstill CJ, Nunn CL. Mitigating future respiratory virus pandemics: new threats and approaches to consider. Viruses. 2021;13:637. https://doi.org/10.3390/v13040637
9. Vlasova AN, Diaz A, Damtie D, Xiu L, Toh TH, Lee JS, et al. Novel canine coronavirus isolated from a hospitalized patient with pneumonia in east Malaysia. Clin Infect Dis. 2022;74:446–54. https://doi.org/10.1093/cid/ciab456
10. Arzey GG, Kirkland PD, Arzey KE, Frost M, Maywood P, Conaty S, et al. Influenza virus A (H10N7) in chickens and poultry abattoir workers, Australia. Emerg Infect Dis. 2012;18:814–6. https://doi.org/10.3201/eid1805.111852
11. Liu Q, Liu DY, Yang ZQ. Characteristics of human infection with avian influenza viruses and development of new antiviral agents. Acta Pharmacol Sin. 2013;34:1257–69. https://doi.org/10.1038/aps.2013.121
12. Belser JA, Creager HM, Zeng H, Maines TR, Tumpey TM. Pathogenesis, transmissibility, and tropism of a highly pathogenic avian influenza A(H7N7) virus associated with human conjunctivitis in Italy, 2013. J Infect Dis. 2017;216(suppl_4):S508–11. https://doi.org/10.1093/infdis/jiw559
13. Creager HM, Kumar A, Zeng H, Maines TR, Tumpey TM, Belser JA. Infection and replication of influenza virus at the ocular surface. J Virol. 2018;92:e02192-17. https://doi.org/10.1128/JVI.02192-17
14. Burrough ER, Magstadt DR, Petersen B, Timmermans SJ, Gauger PC, Zhang J, et al. Highly pathogenic avian influenza A(H5N1) clade 2.3.4.4b virus infection in domestic dairy cattle and cats, United States, 2024. Emerg Infect Dis. 2024;30. https://doi.org/10.3201/eid3007.240508
15. Uyeki TM, Milton S, Abdul Hamid C, Reinoso Webb C, Presley SM, Shetty V, et al. Highly pathogenic avian influenza A(H5N1) virus infection in a dairy farm worker. N Engl J Med. 2024;NEJMc2405371. https://doi.org/10.1056/NEJMc2405371

Address for correspondence: Gregory C. Gray, Infectious Disease Epidemiology, Departments of Internal Medicine (Infectious Diseases), Microbiology and Immunology, and Global Health, University of Texas Medical Branch, 301 University Blvd, Rte 0435, Galveston, TX 77555, USA; email: gcgray@utmb.edu

Vaccine Effectiveness against SARS-CoV-2 among Household Contacts during Omicron BA.2–Dominant Period, Japan

Tsuyoshi Ogata, Hideo Tanaka, Akemi Kon, Noriko Sakaibori, Emiko Tanaka

We calculated attack rates for household contacts of COVID-19 patients during the SARS-CoV-2 Omicron BA.2–dominant period in Japan. Attack rates among household contacts without recent (≤3 months) vaccination was lower for contacts of index patients with complete vaccination than for contacts of index patients without complete vaccination, demonstrating indirect vaccine effectiveness.

BA.2 is a subvariant of the SARS-CoV-2 Omicron variant. XBB.1.5 and XBB.1.16, recombinants of the BA.2.10.1 and BA.2.75 sublineages, were circulating SARS-CoV-2 variants of interest in July 2023 (*1*,*2*), but few estimates of vaccine effectiveness (VE) against infectiousness of those variants were available.

On April 20, 2022, the government of Japan required local public health centers (PHCs) to be notified of all COVID-19 patients and to implement contact tracing (*3*). By that date, the jurisdiction of the Itako PHC (population ≈265,000) in Ibaraki Prefecture had 13,555 confirmed COVID-19 patients (5.1% of the population) (*4*). Among patients with confirmed COVID-19, a total of 2.0% were hospitalized during April–May 2022.

In our previous study of the Omicron BA.1 dominant period in Itako (*5*), the household contact attack rate (HCAR) was lower for household contacts of index patients who were completely vaccinated than for household contacts of other index patients. However, the vaccination status of household contacts was associated with the vaccination status of the associated index patient (*5*). Therefore, adjustment, such as stratification for confounding by the contacts' vaccination status, was needed for adequate evaluation of VE against infectiousness. This study aimed to assess VE against the infectiousness of the SARS-CoV-2 Omicron BA.2 variant among household contacts.

The Study

We obtained information on COVID-19 patients and household contacts reported in the jurisdiction of the Itako PHC in Ibaraki Prefecture, Japan, during April 21–30, 2022. The epidemiologic investigation and data collection procedure on COVID-19 index patients was almost the same as that described in our previous study (*5*). The study design was approved by the Ibaraki Prefecture Epidemiologic Research Joint Ethics Review Committee (protocol no. R3-10). We performed statistical analyses by using R version 4.4.1 (The R Foundation for Statistical Computing, https://www.r-project.org).

Genomic sequencing surveillance showed that 90% of 5,630 variants of concern sampled in Japan during April 18–May 1 were BA.2 (*6*). In Ibaraki, sequencing of 69 samples collected during April 23–May 13 demonstrated that 65 (94%) samples were BA.2 and 4 (6%) were BA.1.

Itako PHC undertook or requested SARS-CoV-2 testing of household contacts who had any symptoms during their 5-day observational and quarantine period of a COVID-19 patient (*5*,*7*,*8*). Asymptomatic household contacts were not tested. During the study period, the PHC jurisdiction identified 729 confirmed COVID-19 cases (*4*) (Figure). After excluding 112 index cases without household members, we identified 617 infected household members, and a total of 1,575 household members, including cases and contacts. We deemed patients with the earliest symptom

Author Affiliations: Itako Public Health Center of Ibaraki Prefectural Government, Itako, Japan (T. Ogata, A. Kon, N. Sakaibori, E. Tanaka); Public Health Center of Neyagawa City, Neyagawa, Osaka, Japan (H. Tanaka)

DOI: https://doi.org/10.3201/eid3007.230968

onset date as index cases in the household, which comprised 388 patients. Of 1,187 household contacts of the 388 index patients, we included 952 who had available data and no history of previous infection in the study. Of the 235 excluded household contacts, we excluded 7 because of a history of infection before the study period. Of the 952 contacts, 395 were infected; the overall HCAR was 41.5%.

Excluding health professionals, 82.5% of residents in Ibaraki had completed 2 COVID-19 vaccine doses, and 56.3% had received a booster dose by April 20, 2022 (*9*). Among initial vaccinations in Ibaraki, 81% were BNT162b2 vaccine (Pfizer-BioNTech, https://www.pfizer.com) and 19% mRNA-1273 vaccine (Moderna, https://www.modernatx.com) (*5*).

We stratified vaccination status on the basis of vaccination doses or recent vaccination, which we defined as receiving the last vaccine dose within 3 months. HCAR was 30.9% for contacts with 3-dose vaccination and 32.4% for contacts with recent vaccination, substantially lower than the 49.6% for contacts without complete vaccination (0–1 doses) and 46.0%, without recent vaccination (Table 1). Of the 307 contacts with 3-dose vaccination status, 272 had been vaccinated within the previous 3 months.

The HCAR for contacts of an index patient who had a 2-dose vaccination status was 37.2% and HCAR was 33.1% for contacts of index cases with a 3-dose status. Those results were substantially lower than the 46.2% for contacts of an index patient without complete vaccination status. However, the HCAR for contacts of an index patient with recent vaccination was not substantially lower than that for contacts of an index patient without recent vaccination (Table 1).

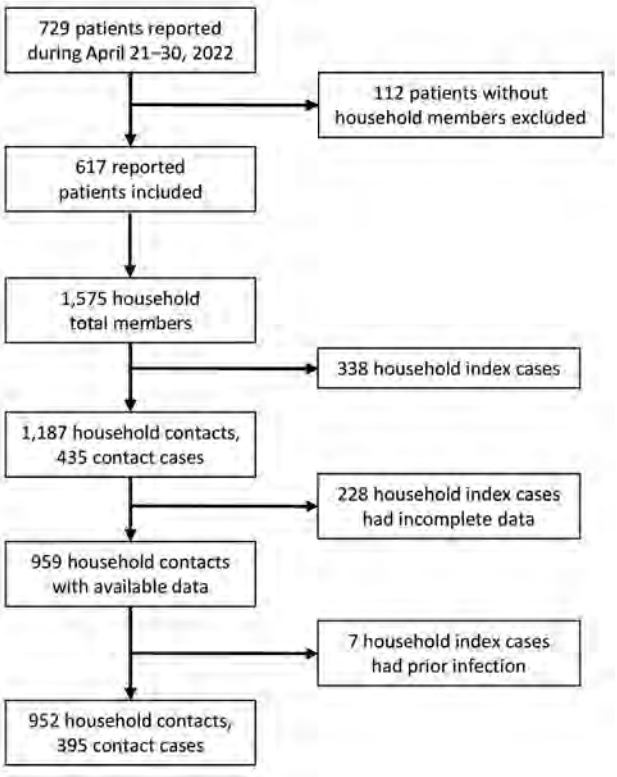

Figure. Flowchart of enrollment of index patients and household contacts in study of vaccine effectiveness against SARS-CoV-2 among household contacts during Omicron BA.2–dominant period, Japan.

Among household contacts who had a 2-dose vaccination status, HCAR was 34.8% for contacts of index patients with complete vaccination but was 49.5% for contacts of index patients without complete vaccination status. However, among household

Table 1. Attack rates among household contacts of index patients with SARS-CoV-2 Omicron BA.2 infection in study of vaccine effectiveness against SARS-CoV-2 among household contacts during Omicron BA.2–dominant period, Japan*

Variables	No. household contacts, n = 952	Infected contacts, n = 395	Contact attack rate, %	Risk ratio (95% CI)†
Household contacts				
No. vaccination doses				
0–1	399	198	49.6	Referent
2	246	102	41.5	0.84 (0.70–0.999)
3	307	95	30.9	0.62 (0.51–0.76)
Recent vaccination				
N	637	293	46.0	Referent
Y	315	102	32.4	0.70 (0.59–0.84)
Index patients				
No. vaccination doses				
0–1	515	238	46.2	Referent
2	301	112	37.2	0.81 (0.68–0.96)
3	136	45	33.1	0.72 (0.55–0.93)
Recent vaccination‡				
N	802	343	42.8	Referent
Y	150	52	34.7	0.81 (0.64–1.01)

*Attack rates are stratified by vaccination doses or recent vaccination for household contacts or index patients.
†Monovariate analyses.
‡Recent vaccination indicates last vaccine dose <3 months.

Table 2. Household contact attack rates by vaccination status in a study of vaccine effectiveness against SARS-CoV-2 among household contacts during Omicron BA.2–dominant period, Japan*

Vaccination status of household contacts	Vaccination status of index patients	Total no. household contacts	No. infected contacts	Contact attack rate, %	Risk ratio (95% CI)
No. vaccine doses					
0–1	0–1	256	136	53.1	Referent
	2	105	45	42.9	0.81 (0.63–1.03)
	3	38	17	44.7	0.84 (0.58–1.22)
	2–3	143	62	43.4	0.82 (0.66–1.02)
2	0–1	111	55	49.5	Referent
	2	108	39	36.1	0.73 (0.53–0.997)
	3	27	8	29.6	0.60 (0.32–1.10)
	2–3	135	47	34.8	0.70 (0.52–0.95)
3	0–1	148	47	31.8	Referent
	2	88	28	31.8	1.00 (0.68–1.47)
	3	71	20	28.2	0.90 (0.57–1.38)
	2–3	159	48	30.2	0.95 (0.68–1.33)
Vaccination status†					
No recent vaccination	0–1	365	190	52.1	Referent
	2	213	81	38.0	0.73 (0.60–0.89)
	3	59	22	37.3	0.71 (0.51–1.01)
	2–3	272	103	37.9	0.73 (0.61–0.87)
Recent vaccination	0–1	150	48	32.0	Referent
	2	88	31	35.2	1.10 (0.76–1.59)
	3	77	23	29.9	0.93 (0.62–1.41)
	2–3	165	54	32.7	1.02 (0.74–1.41)

*Risk rates are stratified by vaccination doses or recent vaccination for household contacts or index patients.
†Recent vaccination indicates last vaccine dose ≤3 months before illness.

contacts with 3-dose vaccination and without complete vaccination, the HCAR was not much lower for contacts of index patients with complete vaccination than for contacts of index patients without complete vaccination status (Table 2). The HCAR among household contacts without recent vaccination was 37.9% for contacts of index patients with complete vaccination, compared with 52.1% for contacts of index patients without complete vaccination (relative risk 0.73 [95% CI 0.61–0.87]); VE 0.27 [95% CI 0.13–0.39]) (Table 2). We obtained similar results in multivariate analyses (Appendix Table, https://wwwnc.cdc.gov/EID/article/30/7/23-0968-App1.pdf). Among household contacts with recent vaccination, HCAR was not substantially different for contacts of index patients with complete vaccination status and contacts of patients without complete vaccination status (Table 2).

Conclusions

Our study found the HCAR among household contacts of index SARS-CoV-2 Omicron BA.2 patients with complete vaccination was substantially lower than that among contacts of index patients without complete vaccination. In our previous study on the Omicron BA.1 variant–dominant period, the VE was 0.43 against infectiousness (*5*). Several other previous studies also reported VE against Omicron infectiousness (*10*–*12*); however, the vaccination doses of index patients in those studies might have been associated with the vaccination doses of their household contacts.

Among household contacts without recent vaccination in our study, HCAR was lower for contacts of index patients with complete vaccination status than for contacts of index patients without complete vaccination, a VE of 0.27. However, among household contacts with recent vaccination, we noted no major effect of vaccination completeness for index patients.

VE was greatly affected by vaccination completeness for index patients among household contacts with 2-dose vaccination but not among household contacts with 3-dose vaccination. Another study in Japan also showed relatively low VE against infectiousness among contacts with 3-dose vaccination compared with VE against infectiousness among other contacts (*13*).

In this study, the HCAR for contacts of an index patient with recent vaccination was not much lower than for contacts of an index patient without recent vaccination. Previous studies have reported relatively stable VE against infectiousness compared with VE against susceptibility (*12*,*14*).

The first limitation of this study is that we did not adjust for confounding factors, such as demographic data, for analyses on all household contacts. The second limitation is that we did not confirm specific variant types with genomic sequencing and different variants might have had different infection rates. Finally, our assessment of risk factors and potential confounders might be limited to the data reported to the PHCs.

In summary, our results indicate that the SARS-CoV-2 Omicron BA.2 attack rate among household contacts without recent vaccination was lower for household contacts of vaccinated index patients than for contacts of unvaccinated index patients. These results strengthen data on indirect effectiveness of COVID-19 vaccines and the value of continued vaccine campaigns to prevent severe illness among index cases and household contacts.

Acknowledgments

We thank the staff of the Itako Public Health Center, Ibaraki Prefectural Institute of Public Health, and the Ibaraki Prefectural Government for their contributions to our study. We thank Editage (http://www.editage.com) for editing and reviewing this manuscript for English language.

About the Author

Dr. Ogata is the director of the Itako Public Health Center and works to evaluate data on and respond to epidemics in the center's jurisdiction. His primary research interest is strengthening infectious disease epidemiology among public health professionals in public health centers throughout Japan.

References

1. World Health Organization. Tracking SARS-CoV-2 variants. [cited 2023 Jul 17]. https://www.who.int/en/activities/tracking-SARS-CoV-2-variants
2. National Institute of Infectious Diseases. Current situation of infection. 2023 Apr 19 [cited 2023 Jul 17]. https://www.niid.go.jp/niid/en/2019-ncov-e/12009-covid19-ab121st-en.html
3. National Institute of Infectious Diseases, Infectious Disease Epidemiology Center. Manual for conducting active epidemiological surveillance of patients with novel coronavirus infection [cited 2023 Jul 17]. https://www.niid.go.jp/niid/en/2019-ncov-e/2484-idsc/9472-2019-ncov-02-en.html
4. Ibaraki Prefectural Government. Current situation of COVID-19 patients in the prefecture [in Japanese] [cited 2023 Jul 17]. https://www.pref.ibaraki.jp/1saigai/2019-ncov/shiryouteikyou.html
5. Ogata T, Tanaka H, Tanaka E, Osaki N, Noguchi E, Osaki Y, et al. Increased secondary attack rates among the household contacts of patients with the Omicron variant of the coronavirus disease 2019 in Japan. Int J Environ Res Public Health. 2022;19:8068. https://doi.org/10.3390/ijerph19138068
6. Advisory Board of the Ministry of Health, Labour and Welfare. COVID-19: current situation of infection and others [in Japanese] [cited 2023 Jul 17]. https://www.mhlw.go.jp/stf/seisakunitsuite/bunya/0000121431_00348.html
7. Ministry of Health, Labour and Welfare. Handling of admission, discharge, and close contacts, and disclosure regarding the patients confirmed infection with B.1.1.529 strain (Omicron variant) [in Japanese] [cited 2023 Jul 17]. https://www.niph.go.jp/h-crisis/wp-content/uploads/2022/01/20220120103933_content_000881572.pdf
8. Ministry of Health, Labour and Welfare. The identification of close contacts, restrictions of behavior, and implementation of contact tracing by each transmission setting based on the characteristics of the B.1.1.529 (Omicron variant) while it is the mainstream [in Japanese] [cited 2023 Jul 17]. https://www.mhlw.go.jp/content/000968056.pdf
9. Ibaraki Prefectural Government. Vaccination status [in Japanese] [cited 2023 Jul 17]. https://ibaraki.stopcovid19.jp
10. Lyngse FP, Kirkeby CT, Denwood M, Christiansen LE, Mølbak K, Møller CH, et al. Household transmission of SARS-CoV-2 Omicron variant of concern subvariants BA.1 and BA.2 in Denmark. Nat Commun. 2022;13:5760. https://doi.org/10.1038/s41467-022-33498-0
11. Tan ST, Kwan AT, Rodríguez-Barraquer I, Singer BJ, Park HJ, Lewnard JA, et al. Infectiousness of SARS-CoV-2 breakthrough infections and reinfections during the Omicron wave. Nat Med. 2023;29:358–65. https://doi.org/10.1038/s41591-022-02138-x
12. Mongin D, Bürgisser N, Laurie G, Schimmel G, Vu DL, Cullati S, et al.; Covid-SMC Study Group. Effect of SARS-CoV-2 prior infection and mRNA vaccination on contagiousness and susceptibility to infection. Nat Commun. 2023;14:5452. https://doi.org/10.1038/s41467-023-41109-9
13. Maeda M, Murata F, Fukuda H. Effect of COVID-19 vaccination on household transmission of SARS-CoV-2 in the Omicron era: the Vaccine Effectiveness, Networking, and Universal Safety (VENUS) study. Int J Infect Dis. 2023;134:200–6. https://doi.org/10.1016/j.ijid.2023.06.017
14. Braeye T, Catteau L, Brondeel R, van Loenhout JAF, Proesmans K, Cornelissen L, et al. Vaccine effectiveness against transmission of Alpha, Delta and Omicron SARS-COV-2-infection, Belgian contact tracing, 2021–2022. Vaccine. 2023;41:3292–300. https://doi.org/10.1016/j.vaccine.2023.03.069

Address for correspondence: Tsuyoshi Ogata, Itako Public Health Center of Ibaraki Prefectural Government, Osu 1446-1, Itako, Ibaraki, 311-2422, Japan; email: kenkoukikikanri@gmail.plala.or.jp

Alongshan Virus Infection in *Rangifer tarandus* Reindeer, Northeastern China

Wenbo Xu,[1] Wei Wang,[1] Liang Li,[1] Nan Li, Ziyan Liu, Lihe Che, Guanyu Wang, Kaiyu Zhang, Xianmin Feng, Wen-Jing Wang, Quan Liu, Zedong Wang

We investigated Alongshan virus infection in reindeer in northeastern China. We found that 4.8% of the animals were viral RNA–positive, 33.3% tested positive for IgG, and 19.1% displayed neutralizing antibodies. These findings suggest reindeer could serve as sentinel animal species for the epidemiologic surveillance of Alongshan virus infection.

The novel tickborne virus Alongshan virus (ALSV) belongs to the Jingmenvirus group of the *Flaviviridae* family and is associated with human febrile illness (*1*). Initially identified in tick-bitten patients and *Ixodes persulcatus* ticks in the Greater Khingan Mountains of northeastern China (*1*), ALSV has since been identified in *I. persulcatus* and *I. ricinus* ticks in various locations, including Russia (*2*), Finland (*3*), Switzerland (*4*), and Germany (*5*). ALSV-specific antibodies have been detected in game animals, such as roe deer and red deer, as well as in domestic animals such as cattle, sheep, goats, and horses (*5*,*6*).

Semidomesticated reindeer, primarily raised by the Ewenki people in the northern Greater Khingan Mountains of China, are the predominant animals in this region (*7*). The reindeer serve as blood meals for ticks and could potentially act as reservoir hosts for tickborne pathogens. However, the extent of ALSV infection in reindeer remains largely unexplored. In this study, we investigated the RNA viromes of reindeer and their parasitic ticks, offering molecular and serologic evidence for ALSV infection in tick-exposed reindeer. The research protocol for this study was approved by the Animal Administration and Ethics Committee of the First Hospital of Jilin University (Changchun, China).

The Study

In July 2022, we collected a total of 21 reindeer serum samples from Genhe in the Greater Khingan Mountains in northeastern China (Figure 1, panel A). In addition, we collected 93 bloodsucking ticks from the reindeer, morphologically identified them as *I. persulcatus* ticks, and grouped them into 13 pools on the basis of tick sex and size (Figure 1, panel B) (*8*). We pooled the reindeer serum samples and tick lysate supernatants separately, treated them with micrococcal nuclease (New England Biolabs, https://www.neb.com), and extracted viral RNA using the TIANamp Virus RNA kit (TIANGEN, https://en.tiangen.com). We sent the samples to Tanpu Biologic Technology in Shanghai, China, for metatranscriptomic analysis as previously described (*8*).

The sequencing process resulted in 5.2 GB of clean data and 38.5 million non-rRNA reads for the reindeer serum library, as well as 6.0 GB of clean data and 45.0 million non-rRNA reads for the tick library. From the reindeer serum library, we identified only 1 contig sequence related to ALSV. In contrast, the tick library revealed a total of 64 tickborne viral contigs. Those viral contigs were further annotated, revealing their association with 7 distinct viruses across 5 viral families. The identified viruses consisted of ALSV and tickborne encephalitis virus (TBEV) from the *Flaviviridae* family, Beiji nairovirus (BJNV) from

Author affiliations: Department of Infectious Diseases and Center of Infectious Diseases and Pathogen Biology, First Hospital of Jilin University, Changchun, China (W. Xu, Z. Liu, L. Che, K. Zhang, Q. Liu, Z. Wang); Gansu Agricultural University, Lanzhou, China (W. Wang); Hulunbuir Animal Disease Control Center, Hailar, China (W. Wang, G. Wang); Changchun Veterinary Research Institute, Chinese Academy of Agricultural Sciences, Changchun (L. Li, N. Li, Q. Liu, Z. Wang); Jilin Medical University, Jilin, China (X. Feng); Beijing YouAn Hospital, Capital Medical University, Beijing, China (W.-J. Wang)

DOI: https://doi.org/10.3201/eid3007.231219

[1]These authors contributed equally to this article.

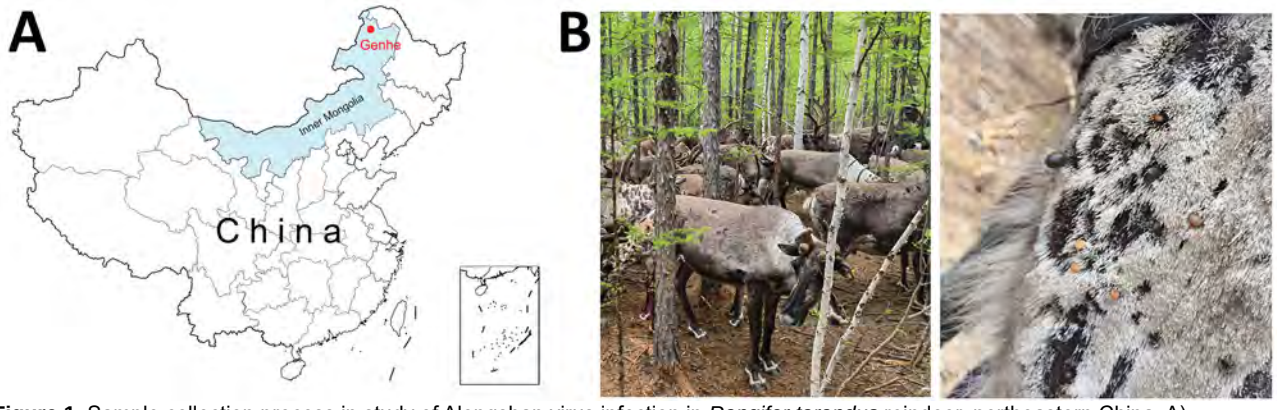

Figure 1. Sample collection process in study of Alongshan virus infection in *Rangifer tarandus* reindeer, northeastern China. A) Collection site of reindeer serum samples and their parasitic ticks. B) Sampled reindeer group and the presence of ticks on a reindeer.

the *Nairoviridae* family, Sara tick phlebovirus (STPV) and Onega tick phlebovirus (OTPV) from the *Phenuiviridae* family, and Nuomin virus (NUMV) from *Chuviridae*, and Jilin luteo-like virus 2 (JLLV2) from the *Solemoviridae* family (Table 1).

Among the tickborne viruses identified in the tick library, ALSV showed the highest mean depth at 80.8×, followed by JLLV2 with a mean depth of 12.7×, BJNV at 10.3×, and TBEV at 7.1×. In contrast, NUMV, OTPV, and STPV displayed the lowest mean depths, measuring 4.9× (NUMV), 1.8× (OTPV), and 1.9× (STPV). Of note, ALSV in the reindeer serum library had a low mean depth of 1.8× (Figure 2, panel B; Appendix Figure 1, https://wwwnc.cdc.gov/EID/article/30/7/23-1219-App1.pdf).

We subsequently confirmed all tickborne viruses identified in this study through seminested reverse transcription PCR (Appendix Table 1). Among the 21 serum samples analyzed, only 1 tested positive for ALSV (4.8%). For the 13 tick pools, each pool exhibited the presence of 3–6 viral species (Figure 2, panel A). Specifically, we consistently detected NUMV, OTPV, and STPV in all tick pools, whereas BJNV was found in 12 pools and ALSV in 9 pools; prevalence rates were 29.5% for BJNV and 16.3% for ALSV. In contrast, JLLV2 and TBEV were only identified in 3 and 2 tick pools, accounting for a prevalence of 3.5% for JLLV2 and 2.2% for TBEV (Appendix Table 2).

Phylogenetic analysis on the basis of the RNA-dependent RNA polymerase gene revealed that all ALSV strains in the Greater Khingan Mountains region clustered together; nucleotide identities ranged from 95.4% to 99.8% (Appendix Figures 2, 3). For the detection of ALSV antibodies, we subjected reindeer serum samples to an indirect ELISA (*2*). Among the 21 samples tested, 7 (33.3%) were positive for ALSV IgG. Of note, 4 of these samples achieved endpoint titers of 320 (Table 2). To further assess neutralizing antibodies against ALSV, we conducted a plaque-reduction neutralization test (*6*) and identified 4 serum samples as ALSV-positive, representing a prevalence of 19.1%; the highest endpoint titer was recorded at 40 (Table 2).

Conclusions

The Greater Khingan Mountains, located in northeast China and sharing borders with Russia and Mongolia, boast abundant forest resources, covering as much as 74% of the region (*9*). Over time, the area

Table 1. Tickborne viruses identified in study of Alongshan virus infection in *Rangifer tarandus* reindeer, northeastern China

Classification	Virus species	Closest relative strain (% nt identity)
Flaviviridae		
Jingmenvirus	Alongshan virus	NE-TH4 (96.9–98.7)
Orthoflavivirus	Tick-borne encephalitis virus	HLB-T74 (96.6–98.4)
Nairoviridae		
Norwavirus	Beiji nairovirus	NE-SL3 (99.6)
Phenuiviridae		
Ixovirus	Sara tick phlebovirus	NE-SL3 (99.3)
	Onega tick phlebovirus	NE-SL3 (99.1)
Chuviridae		
Mivirus	Nuomin virus	SL4 (99.6)
Solemoviridae		
Sobemo-like	Jilin luteo–like virus 2	DH3 (98.5)

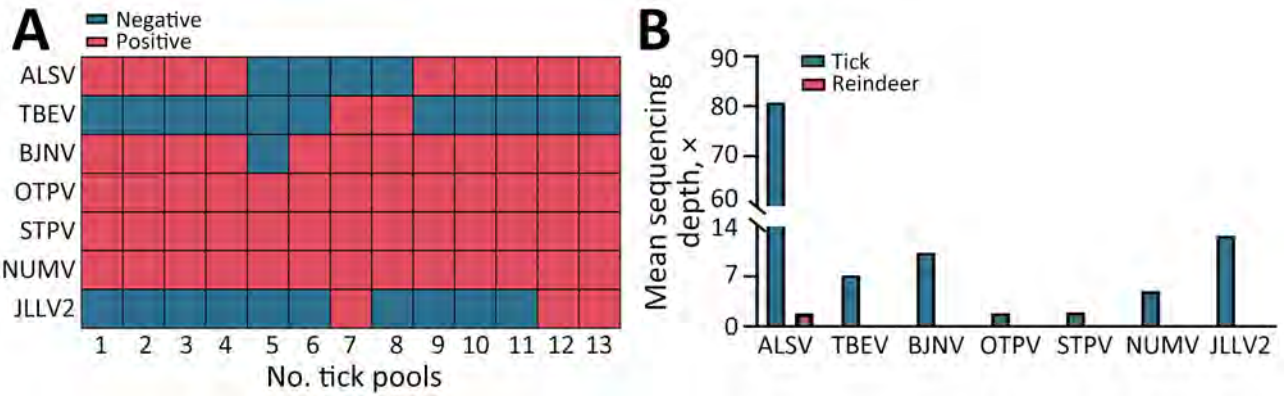

Figure 2. Identified tickborne viruses in study of Alongshan virus infection in *Rangifer tarandus* reindeer, northeastern China. A) Composition of tickborne viruses in tick pools. B) Mean sequencing depth of identified tickborne viruses in libraries. ALSV, Alongshan virus; BJNV, Beiji nairovirus; JLLV2, Jilin luteo-like virus 2; NUMV, Nuomin virus; OTPV, Onega tick phlebovirus; STPV, Sara tick phlebovirus; TBEV, tick-borne encephalitis virus.

has gradually transformed into a popular tourist destination during the summer months. Reindeer, serving as a unique and captivating attraction for tourists, increasingly come into close contact with humans. This study detected 3 tickborne viral species (TBEV, ALSV, and BJNV) in ticks that are pathogenic to humans, highlighting the spillover risk for tick-borne viruses to humans (*1*,*10*,*11*).

Large wild cervids, such as roe deer, red deer, and reindeer, play a crucial role in the epidemiology of TBEV. In Europe, those cervids are regarded as sentinel species for TBEV because they contribute substantially to tick breeding and activity (*12*). ALSV, an emerging segmented flavivirus, shares several key characteristics with TBEV, including the tick vectors (*I. persulcatus* and *I. ricinus*) and natural foci in China and Europe (*1*–*4*,*6*,*13*).

In this study, ALSV viremia was detected in only 1 reindeer. Conversely, high prevalences of ALSV IgG (33.3%) and neutralizing antibodies (19.1%) were seen (Table 2). This serologic pattern is consistent with observations in animals infected with TBEV, in which seroconversion occurs after a brief viremia after TBEV infection and specific antibodies are rapidly induced and persist for an extended period (*14*). Of note, the study revealed no TBEV viremia in the reindeer, yet a high prevalence of TBEV antibodies (67.7%) was detected (Table 2). Although ALSV and TBEV were not found co-infected in tick pools, neutralizing antibodies to both viruses were detected in 1 reindeer

Table 2. Serologic detection of Alongshan virus and tickborne encephalitis virus in reindeer, northeastern China*

Sample ID	Reindeer age, y	Reindeer sex	Alongshan virus		Tickborne encephalitis virus	
			ELISA†	PRNT	ELISA†	PRNT
1	≥3	M	<20	<20	<20	<20
2	1	M	<20	<20	<20	<20
3	1	M	160	<20	<20	<20
4	2	F	<20	<20	320	80
5	0.5	F	320	20	<20	<20
6	≥3	M	320	20	<20	<20
7	1	M	<20	<20	320	80
8	2	M	<20	<20	320	<20
9	2	F	<20	<20	<20	<20
10	≥3	M	<20	<20	<20	<20
11	≥3	F	20	<20	160	40
12	0.5	F	<20	<20	320	40
13	1	F	<20	<20	320	80
14	2	M	320	20	320	160
15	2	M	80	<20	320	40
16	0.5	M	<20	<20	320	40
17	≥3	M	<20	<20	160	<20
18	2	F	<20	<20	20	<20
19	2	F	<20	<20	80	<20
20	1	M	<20	<20	40	<20
21	1	F	320	40	20	<20

*Antibody titer ≥20 was considered ELISA- or PRNT-positive. PRNT, plaque-reduction neutralization test.
†The ELISA used in our study was specifically targeted against the Alongshan virus VP2 protein.

(no. 14) (Table 2; Figure 2, panel A). This finding suggests potential cross-reactivity or exposure to both viruses in this particular reindeer.

Our findings underscore the need to use serologic testing alongside molecular detection in epidemiologic studies concerning ALSV and TBEV in reindeer populations. Moreover, given the substantial reindeer population in the Greater Khingan Mountains and the established practice of monitoring TBEV in reindeer in Europe, this study advocates designating reindeers as wildlife sentinel species for ALSV and TBEV in the Greater Khingan Mountains of northeastern China. Their unique role in tickborne virus epidemiology and close interaction with humans make them invaluable subjects for ongoing surveillance and research efforts in this region.

In conclusion, our study unveiled a diverse array of tickborne viruses in ticks collected from reindeer, substantiating ALSV infection in those animals through both molecular and serologic methods. These findings contribute to our understanding of the tickborne viral ecosystem in northeastern China, highlighting the potential role of reindeer as sentinel animals for the epidemiologic monitoring of ALSV and other emerging tickborne viruses in this region.

All sequence reads have been deposited in the National Center for Biotechnology Information Short Read Archive under BioProjects PRJNA1083014 (reindeer) and PRJNA1082896 (tick). The viral genomes have been submitted to GenBank (Appendix Table 4).

This study was supported by the National Key Research and Development Program of China (2022YFC2601900), the National Natural Science Foundation of China (82002165 and 32072887), the Natural Science Foundation of Jilin Province (YDZJ202101ZYTS094), the Outstanding Young Scholars Cultivating Plan of the First Hospital of Jilin University (2021-YQ-01), and the Medical Innovation Team Project of Jilin University (2022JBGS02).

About the Author

Dr. Xu is a physician at the Department of Infectious Diseases and Center of Infectious Diseases and Pathogen Biology, First Hospital of Jilin University, Changchun, China. His primary research interest is emerging tickborne diseases.

References

1. Wang ZD, Wang B, Wei F, Han SZ, Zhang L, Yang ZT, et al. A new segmented virus associated with human febrile illness in China. N Engl J Med. 2019;380:2116–25. 10.1056/NEJMoa1805068 https://doi.org/10.1056/NEJMoa1805068
2. Kholodilov IS, Belova OA, Morozkin ES, Litov AG, Ivannikova AY, Makenov MT, et al. Geographical and tick-dependent distribution of flavi-like Alongshan and Yanggou tick viruses in Russia. Viruses. 2021;13:458. https://doi.org/10.3390/v13030458
3. Kuivanen S, Levanov L, Kareinen L, Sironen T, Jääskeläinen AJ, Plyusnin I, et al. Detection of novel tick-borne pathogen, Alongshan virus, in *Ixodes ricinus* ticks, south-eastern Finland, 2019. Euro Surveill. 2019;24:1900394. https://doi.org/10.2807/1560-7917.ES.2019.24.27.1900394
4. Stegmüller S, Fraefel C, Kubacki J. Genome sequence of alongshan virus from *Ixodes ricinus* ticks collected in Switzerland. Microbiol Resour Announc. 2023;12:e0128722. https://doi.org/10.1128/mra.01287-22
5. Ebert CL, Söder L, Kubinski M, Glanz J, Gregersen E, Dümmer K, et al. Detection and characterization of Alongshan virus in ticks and tick saliva from Lower Saxony, Germany with serological evidence for viral transmission to game and domestic animals. Microorganisms. 2023;11:543. https://doi.org/10.3390/microorganisms11030543
6. Wang ZD, Wang W, Wang NN, Qiu K, Zhang X, Tana G, et al. Prevalence of the emerging novel Alongshan virus infection in sheep and cattle in Inner Mongolia, northeastern China. Parasit Vectors. 2019;12:450. https://doi.org/10.1186/s13071-019-3707-1
7. Wang SN, Zhai JC, Liu WS, Xia YL, Han L, Li HP. Origins of Chinese reindeer (*Rangifer tarandus*) based on mitochondrial DNA analyses. PLoS One. 2019;14:e0225037. https://doi.org/10.1371/journal.pone.0225037
8. Liu Z, Li L, Xu W, Yuan Y, Liang X, Zhang L, et al. Extensive diversity of RNA viruses in ticks revealed by metagenomics in northeastern China. PLoS Negl Trop Dis. 2022;16:e0011017. https://doi.org/10.1371/journal.pntd.0011017
9. Meng F, Ding M, Tan Z, Zhao Z, Xu L, Wu J, et al. Virome analysis of tick-borne viruses in Heilongjiang Province, China. Ticks Tick Borne Dis. 2019;10:412–20. https://doi.org/10.1016/j.ttbdis.2018.12.002
10. Lu Z, Bröker M, Liang G. Tick-borne encephalitis in mainland China. Vector Borne Zoonotic Dis. 2008;8:713–20. https://doi.org/10.1089/vbz.2008.0028
11. Wang YC, Wei Z, Lv X, Han S, Wang Z, Fan C, et al. A new nairo-like virus associated with human febrile illness in China. Emerg Microbes Infect. 2021;10:1200–8. https://doi.org/10.1080/22221751.2021.1936197
12. Michelitsch A, Wernike K, Klaus C, Dobler G, Beer M. Exploring the reservoir hosts of tick-borne encephalitis virus. Viruses. 2019;11:669. https://doi.org/10.3390/v11070669
13. Kholodilov IS, Litov AG, Klimentov AS, Belova OA, Polienko AE, Nikitin NA, et al. Isolation and characterization of Alongshan virus in Russia. Viruses. 2020;12:362. https://doi.org/10.3390/v12040362
14. Klaus C, Ziegler U, Kalthoff D, Hoffmann B, Beer M. Tick-borne encephalitis virus (TBEV)—findings on cross reactivity and longevity of TBEV antibodies in animal sera. BMC Vet Res. 2014;10:78. https://doi.org/10.1186/1746-6148-10-78

Address for correspondence: Quan Liu, Department of Infectious Diseases and Center of Infectious Diseases and Pathogen Biology, State Key Laboratory for Diagnosis and Treatment of Severe Zoonotic Infectious Diseases, First Hospital of Jilin University, Changchun 130122, Jilin, China; email: liuquan1973@hotmail.com

Bluetongue Virus Serotype 3 and Schmallenberg Virus in *Culicoides* Biting Midges, Western Germany, 2023

Anja Voigt, Helge Kampen, Elisa Heuser, Sophie Zeiske, Bernd Hoffmann, Dirk Höper, Mark Holsteg, Franziska Sick, Sophia Ziegler, Kerstin Wernike, Martin Beer, Doreen Werner

In October 2023, bluetongue virus serotype 3 (BTV-3) emerged in Germany, where Schmallenberg virus is enzootic. We detected BTV-3 in 1 pool of *Culicoides* biting midges collected at the time ruminant infections were reported. Schmallenberg virus was found in many vector pools. Vector trapping and analysis could elucidate viral spread.

Biting midge–borne bluetongue virus (BTV), an orbivirus of the *Sedoreoviridae* family, can cause epizootic disease in domestic and wild ruminants (*1*). Bluetongue (BT) is a World Organisation for Animal Health–listed disease and is regulated within the European Union (EU) in accordance with Regulation (EU) 2016/429 and its delegated regulations (*2*). Under those regulations, BT outbreaks require trade restrictions in EU member states to prevent the etiologic agent from spreading.

BTV serotype 3 (BTV-3) emerged in continental Europe in early September 2023, when clinical disease was observed on 4 sheep farms in the Netherlands (M. Holwerda et al., unpub. data, https://doi.org/10.1101/2023.09.29.560138). By mid-October, >1,000 outbreaks had been detected throughout the Netherlands, increasing to 5,884 by mid-December 2023 (*3*). At the same time, BTV-3 reached Belgium and was detected in the United Kingdom in November 2023 (*4*,*5*).

Author affiliations: Leibniz-Centre for Agricultural Landscape Research, Muencheberg, Germany (A. Voigt, D. Werner); Friedrich-Loeffler-Institut, Greifswald–Insel Riems, Germany (H. Kampen, E. Heuser, S. Zeiske, B. Hoffmann, D. Höper, F. Sick, S. Ziegler, K. Wernike, M. Beer); Chamber of Agriculture for North Rhine-Westphalia, Bad Sassendorf, Germany (M. Holsteg)

DOI: https://doi.org/10.3201/eid3007.240275

In contrast to emerging BTV-3, the orthobunyavirus Schmallenberg virus (SBV) is enzootic in continental Europe; it was initially detected in 2011 near the border between Germany and the Netherlands (*6*). Another biting midge–borne virus, epizootic hemorrhagic disease virus (EHDV), emerged in Europe in 2022 (*7*). Those 3 viruses share major epidemiologic characteristics; all 3 are transmitted by *Culicoides* biting midges (Diptera: Ceratopogonidae) and affect mainly ruminants (*1*,*6*). Germany was declared free of BTV-8 in June 2023 (*8*), but on October 12, 2023, a case of BTV-3 was confirmed in a sheep in the Kleve district, close to the border with the Netherlands. By April 18, 2024, a total of 55 additional BTV-3 cases were reported from sheep and cattle farms in the federal states of North Rhine-Westphalia and Lower Saxony, Germany (Figure). We collected biting midges from those 2 states to evaluate the extent of vectorborne viruses in the region.

The Study

After BTV-3 emerged in the Netherlands, and before any clinically suspicion cases had been announced in ruminants in Germany, we installed biting midge traps in animal stables in western Germany to collect putative BTV-3 vectors and test them for virus infection. Traps were equipped with a UV light but no CO_2 source (Biogents, https://eu.biogents.com). During September 24–26, we set 1 trap each on 18 cattle, sheep, and goat farms in North Rhine-Westphalia and Lower Saxony, along the border with the Netherlands. We placed the traps close to the animals at sites protected from wind and rain. Traps operated continuously, and we recovered collected insects every day until November 9 or 11, depending on the location.

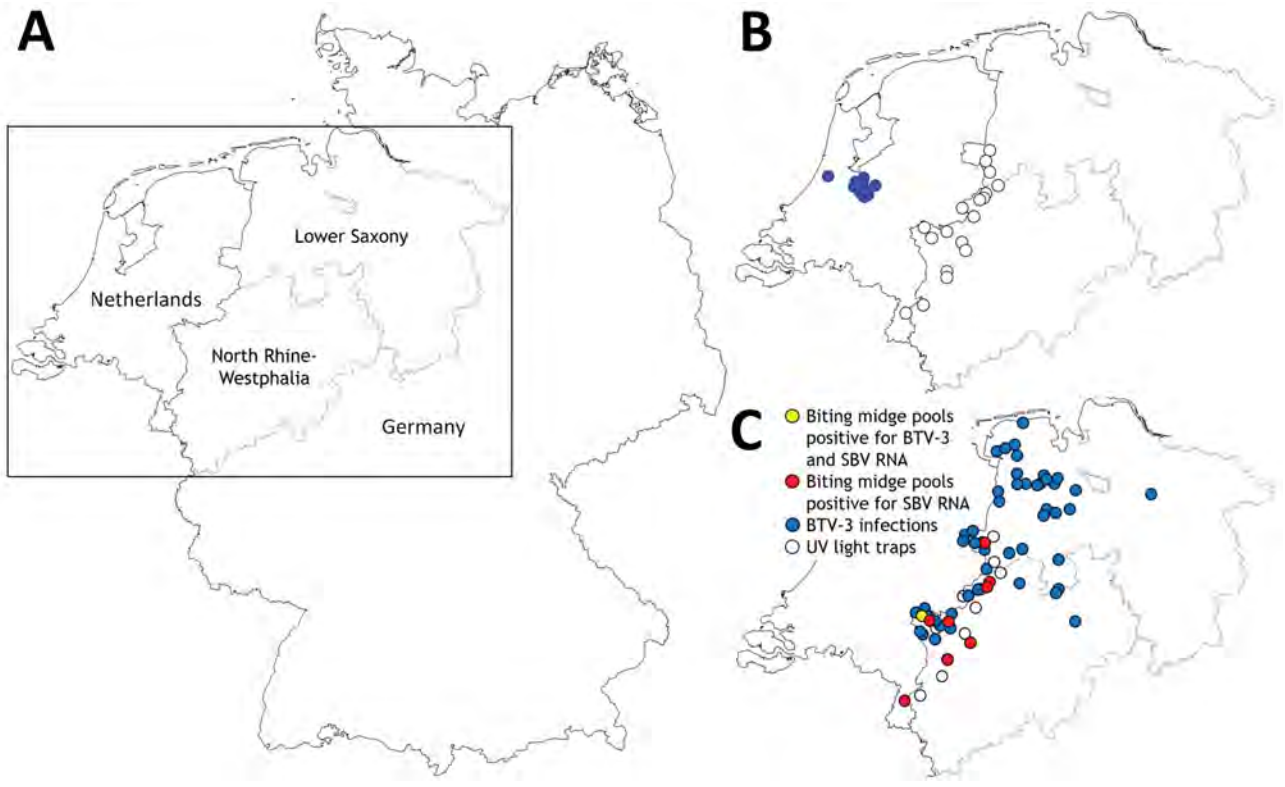

Figure. Sampling locations and infection sites in study of BTV-3 and SBV in *Culicoides* biting midges, western Germany, 2023. A) Overview map of Germany and the Netherlands showing North Rhine-Westphalia and Lower Saxony study areas. B) BTV-3 cases in the Netherlands (blue dots) as of September 8, 2023, and locations of UV light traps (white dots) along the border between Germany and the Netherlands. C) BTV-3 infections in ruminants (blue dots) reported to the animal disease reporting system in Germany as of April 18, 2024, and geographic assignment of farms with biting midge pools that tested positive for BTV-3 and SBV RNA (yellow dot) and those with pools only positive for SBV RNA (red dots). BTV-3, bluetongue virus serotype 3; SBV, Schmallenberg virus.

After those dates, the traps were only activated for 24 hours per week and samples were collected that day.

We collected biting midges and placed them in 80% ethanol, and stored them at room temperature in the dark until processing. A few days, but not >4 weeks, after collection, we morphologically identified midges as *C. obsoletus* group, *C. pulicaris* complex, and other *Culicoides*. *C. obsoletus* group and *C. pulicaris* complex-midges are considered the main BTV and SBV vectors in Europe (*9*). We used a multiplex quantitative reverse transcription PCR (qRT-PCR) to screen pools of ≤50 *C. obsoletus* group and *C. pulicaris* complex midges for BTV and EHDV RNA (*10*). EHDV only recently emerged in southern and western Europe (*7*) and might be the next biting midge–borne virus to spread to central Europe. We also tested midge pools for SBV RNA because that virus is enzootic in the ruminant population in the region and expected to be detectable in insect vectors (*11*). We subsequently analyzed pools that tested BTV-positive by using a BTV-3–specific qRT-PCR (*12*). We retrospectively examined BTV-3–positive pools to determine the specific biting midge species (*13*,*14*).

During September 26–November 9, we collected 1,603 biting midge pools at 9 sites. The number of pools per site ranged from 27–466, depending on the number of midges collected. We tested those pools for viral RNA; 1 pool of *C. obsoletus* group midges collected in Kleve (Figure, panel C) on October 12 tested positive for BTV RNA (quantification cycle [Cq] value 35.6). We subsequently confirmed that pool as BTV-3–positive (Cq 37.5). The pool consisted of a mixture of *C. obsoletus* clade O1 (or *C. montanus*, which cannot be reliably differentiated from *C. obsolestus* clade O1 with the test system used but is not supposed to occur in Central Europe), *C. scoticus*, and *C. chiopterus*. Another pool of *C. obsoletus* group midges captured on the same day and at the same site tested SBV RNA–positive. In addition, we detected SBV in 534 midge pools collected during the 6.5-week period from all 9 locations: 1 site in Lower Saxony in the Grafschaft-Bentheim district, and 8 sites in North Rhine-Westphalia (3 in Kleve district, 2 in Wesel district, 2 in Borken district, and 1 in Heinsberg district) (Figure; Appendix, https://wwwnc.cdc.gov/EID/

article/30/7/24-0275-App1.pdf). Except for 2 *C. pulicaris* complex pools, all SBV RNA–positive pools belonged to the *C. obsoletus* group (Appendix). No pools were positive for both BTV and SBV RNA, and all tested pools were EHDV-negative.

We calculated the minimum infection rates (MIR; i.e., number of positive pools divided by number of tested pools, multiplied by 1,000) for each virus (*15*). We found an MIR of 333.13 for SBV, indicating high circulation, and an MIR of 0.62 for BTV-3, indicating low circulation. However, MIR can be affected by pool size; the more specimens in a pool, the higher the possibility that ≥1 positive biting midge would be included, but that effect would not become evident when pools are examined. Conversely, the sensitivity of detection decreases with increasing pool size if only 1 positive biting midge was in the pool.

Using an isolate obtained from a BTV-3–positive sheep blood sample and further characterized on both *Culicoides* cells and baby hamster kidney cells, we produced a nearly complete genome sequence (International Nucleotide Sequence Database Collaboration, http://www.insdc.org; project no. PRJEB72862). The obtained genome was 99.94% identical to the sequence of a recent BTV-3 isolate from the Netherlands (GenBank accession nos. OR603992–4001) at the nucleotide level and 99.95% at the amino acid level. The genome segments of the strain from Germany were 83.24%–97.67% identical to the BTV-3 SAR2018 strain isolated from a sheep in Italy in 2018 (GenBank accession nos. MK348537–46) and 81.26%–97.89% identical to the TUN2016 strain isolated from a sheep in Tunisia in 2016 (GenBank accession nos. KY432369–78).

Conclusions

BTV-3 was confirmed in an infected sheep in Germany on October 12, 2023, and viral spread was detected in 2 federal states by winter 2023–2024. The isolated BTV-3 is nearly identical to virus strains from outbreaks in the Netherlands. A pool of *C. obsoletus* group biting midges collected on a cattle farm in the same district on the same day BTV-3 was confirmed in Germany tested positive for BTV-3 RNA. Detecting BTV-3 in its putative vectors confirms an ongoing transmission cycle, albeit circulating at a low level; only 1 insect pool tested positive, and only a few animals were BTV-3–positive on affected farms. In contrast, we found SBV RNA in numerous *Culicoides* pools, reflecting its intense circulation in ruminant populations; SBV-infected cattle, sheep, and goats have been reported in Germany since 2011, although prevalence between years varies (*6*). The Cq values of the SBV qRT-PCR in some of the investigated *Culicoides* pools indicate substantial virus loads, reflecting extensive regional SBV circulation in autumn 2023 (Appendix).

In conclusion, circulation of BTV-3 in Germany is likely to continue, intensify, and spread with the onset of seasonal biting midge activity in spring 2024. Large-scale biting midge monitoring combined with rapid analysis for viruses could contribute to an early warning system for emerging biting midge–borne diseases.

This article was preprinted at https://doi.org/10.1101/2024.02.26.582175.

Acknowledgments

We thank all farmers who supported the study and volunteered to tend biting midge traps.

The study was funded by the German Federal Ministry of Food and Agriculture (BMEL) through the Federal Office for Agriculture and Food (BLE), grant nos. 28N207601 and 28N207602, and EU Horizon 2020 program project Versatile Emerging infectious disease Observatory (VEO), grant no. 874735.

About the Author

Ms. Voigt is a PhD student at the Leibniz-Centre for Agricultural Landscape Research, Muencheberg, Germany. Her research interests include behavior and habitat binding of biting midge vectors.

References

1. MacLachlan NJ, Mayo CE, Daniels PW, Savini G, Zientara S, Gibbs EP. Bluetongue. Rev Sci Tech. 2015;34:329–40. https://doi.org/10.20506/rst.34.2.2360
2. European Commission. Regulation (EU) No. 2016/429 of 9 March 2016 on transmissible animal diseases and amending and repealing certain acts in the area of animal health ('Animal Health Law'). Off J EU. 2016; L84:1–208.
3. Leis P. Bluetongue (BTV-3). Presented: PAFF Animal Health and Welfare committee meeting; the Netherlands: December 14, 2023 [cited 24 Apr 2024]. https://food.ec.europa.eu/system/files/2023-12/reg-com_ahw_20231214123_pres-07.pdf
4. World Animal Health Information System. Belgium—Bluetongue virus (Inf. with), event 5265, report ID 163218 [cited 2024 Apr 24]. https://wahis.woah.org/#/in-event/5265/dashboard
5. World Animal Health Information System. United Kingdom—Bluetongue virus (Inf. with), event 5330, report ID 163824 [cited 2024 Apr 24]. https://wahis.woah.org/#/in-event/5330/dashboard
6. Wernike K, Beer M. Schmallenberg virus: a novel virus of veterinary importance. Adv Virus Res. 2017;99:39–60. https://doi.org/10.1016/bs.aivir.2017.07.001
7. Lorusso A, Cappai S, Loi F, Pinna L, Ruiu A, Puggioni G, et al. Epizootic hemorrhagic disease virus serotype 8, Italy, 2022. Emerg Infect Dis. 2023;29:1063–5. https://doi.org/10.3201/eid2905.221773
8. European Commission. Commission implementing regulation (EU) 2021/620. Off J EU. 2021;131:78.

9. Mellor PS, Boorman J, Baylis M. *Culicoides* biting midges: their role as arbovirus vectors. Annu Rev Entomol. 2000; 45:307–40. https://doi.org/10.1146/annurev.ento. 45.1.307
10. Wernike K, Hoffmann B, Beer M. Simultaneous detection of five notifiable viral diseases of cattle by single-tube multiplex real-time RT-PCR. J Virol Methods. 2015;217:28–35. https://doi.org/10.1016/j.jviromet.2015.02.023
11. Bilk S, Schulze C, Fischer M, Beer M, Hlinak A, Hoffmann B. Organ distribution of Schmallenberg virus RNA in malformed newborns. Vet Microbiol. 2012;159:236–8. https://doi.org/10.1016/j.vetmic.2012.03.035
12. Lorusso A, Sghaier S, Di Domenico M, Barbria ME, Zaccaria G, Megdich A, et al. Analysis of bluetongue serotype 3 spread in Tunisia and discovery of a novel strain related to the bluetongue virus isolated from a commercial sheep pox vaccine. Infect Genet Evol. 2018;59:63–71. https://doi.org/10.1016/j.meegid.2018.01.025
13. Dähn O, Werner D, Mathieu B, Kampen H. Development of conventional multiplex PCR assays for the identification of 21 West Palaearctic biting midge taxa (Diptera: Ceratopogonidae) belonging to the *Culicoides* subgenus *Culicoides*, including recently discovered species and genetic variants. Diversity (Basel). 2023;15:699. https://doi.org/10.3390/d15060699
14. Dähn O, Werner D, Mathieu B, Kampen H. Large-scale cytochrome c oxidase subunit I gene data analysis for the development of a multiplex polymerase chain reaction test capable of identifying biting midge vector species and haplotypes (Diptera: Ceratopogonidae) of the *Culicoides* subgenus *Avaritia* Fox, 1955. Genes (Basel). 2024;15:323. https://doi.org/10.3390/genes15030323
15. Walter SD, Hildreth SW, Beaty BJ. Estimation of infection rates in population of organisms using pools of variable size. Am J Epidemiol. 1980;112:124–8. https://doi.org/10.1093/oxfordjournals.aje.a112961

Address for correspondence: Martin Beer, Friedrich-Loeffler-Institut, Federal Research Institute for Animal Health, Suedufer 10, 17493 Greifswald–Insel Riems, Germany; email: martin.beer@fli.de

Evidence of *Orientia* spp. Endemicity among Severe Infectious Disease Cohorts, Uganda

Paul W. Blair, Kenneth Kobba, Stephen Okello, Sultanah Alharthi, Prossy Naluyima, Emily Clemens, Hannah Kibuuka, Danielle V. Clark, Francis Kakooza, Mohammed Lamorde, Yukari C. Manabe, J. Stephen Dumler; Acute Febrile Illness and Sepsis in Uganda study teams[1]

At 3 severe infection cohort sites in Uganda, *Orientia* seropositivity was common. We identified 4 seroconversion cases and 1 PCR-positive case. These results provide serologic and molecular support for *Orientia* spp. circulating in sub-Saharan Africa, possibly expanding its endemic range. *Orientia* infections could cause severe illness and hospitalizations in this region.

Scrub typhus is a leading cause of nonmalarial febrile illness in Southeast Asia (*1*). Scrub typhus is caused by miteborne *Orentia tsutsugamushi* infections, which until recently were thought to be limited to South and Southeast Asia. Molecular identification of different *Orientia* species in clinical cases from Chile (*2*) and the United Arab Emirates (*3*) has suggested a broader epidemiology. *Orientia* spp. were found in mites in Kenya (*4*), and descriptions of *Orientia* seroconversion in patients from sub-Saharan Africa have slowly accrued, suggesting the possibility of *Orientia* spp. transmission in Africa (*5*). We used archived samples collected in 2 severe infection prospective cohorts in western, central, and northwest Uganda to assess *Orientia* endemicity in the country.

The Study

Using archived samples, we measured serial *Orientia* immunofluorescence assay (IFA) IgG titers and performed reflex *Orientia* spp. reverse transcription PCR (RT-PCR). Samples were collected as part of 2 severe infection prospective cohorts and had undergone broad microbiologic testing. In both cohorts, adult patients ≥18 years of age who fulfilled acute febrile illness (AFI; hospitals in Mubende and Arua, Uganda) or sepsis-specific (hospital in Fort Portal, Uganda) eligibility criteria were evaluated for enrollment at admission in the outpatient or emergency department, or on medical wards (Appendix, https://wwwnc.cdc.gov/EID/article/30/7/23-1040-App1.pdf) (*6*). Matched acute and convalescent serum samples were available from 269 of 310 participants enrolled in the sepsis cohort and 67 of 132 participants in the AFI cohort.

In brief, across both prospective cohorts, study teams collected demographic and symptom information, examination findings, and laboratory data on standardized forms during hospitalization and at 1 month after enrollment. Clinical tests were routinely performed, including complete blood counts and chemistries. Microbiologic testing included blood culture with antimicrobial sensitivity testing, HIV testing, malaria smears, and rapid diagnostic tests, as previously described (*6*) (Appendix).

We performed IgG IFAs by using *Orientia tsutsugamushi* Karp strain antigen slides (BIOCELL Diagnostics Inc., https://biocelldx.com). Baseline (acute) and 1-month follow-up (convalescent) serum samples were screened at a titer of 1:64 and titrated up to 1:65,000. We considered a sample seropositive at a threshold titer of ≥128. We performed IgG IFAs by using commercial slides to evaluate for cross-reactivity

Author affiliations: Uniformed Services University, Bethesda, Maryland, USA (P.W. Blair, S. Alharthi, E. Clemens, J.S. Dumler); Henry M. Jackson Foundation for the Advancement of Military Medicine, Inc., Bethesda (P.W. Blair, S. Alharthi, D.V. Clark); Johns Hopkins University School of Medicine, Baltimore, Maryland, USA (P.W. Blair, Y.C. Manabe); Infectious Diseases Institute, Makerere University, Kampala, Uganda (K. Kobba, F. Kakooza, M. Lamorde); Makerere University Walter Reed Project, Kampala (S. Okello, P. Naluyima, H. Kibuuka)

DOI: https://doi.org/10.3201/eid3007.231040

[1]Members of the Acute Febrile Illness and Sepsis in Uganda study teams are listed at the end of this article.

to spotted fever group rickettsia (SFGR), *Rickettsia conorii* Molish 7 strain, typhus group rickettsia (TGR), and *Rickettsia typhi* Wilmington strain (BIOCELL Diagnostics, Inc.). We performed a Kruskal-Wallis test to evaluate for differences between *Orientia* IFA IgG titers between those with and without available matched samples. We used a titer of 32 to calculate -fold increase if the screen was negative at a titer of 1:64. We had a blind second reader review ≤5% of each batch.

Because no prior estimates of *Orientia* seroprevalence were available for Uganda, we used stringent criteria to define probable cases (Appendix Figure 1). To evaluate the specificity of IFA results, we used a subset of high titer samples to corroborate evidence of antibody binding by using a dot blot, Western blot, and Gilliam strain IFA (Appendix Methods, Figure 2). To optimize sensitivity for RT-PCR, we targeted mRNA and rRNA from serum from both cohorts (*7*), whole blood from the AFI cohort, or buffy coat from the sepsis cohort. We used QIAamp RNA Mini Kit (QIAGEN, https://www.qiagen.com) to extract RNA. We performed RT-PCR targeting *Orientia* spp. 16S rRNA, Orien16S and *rrs* by using previously published methods (*3*,*8*), and mRNA from *Orientia* spp. 56-kDa antigen gene, SFGR OmpA (*sca0*) gene, and TGR kDa (*9*) outer membrane protein gene. We only called positives that were in duplicate.

We found that 33.9% (148/436) of acute samples and 38.4% (129/336) of convalescent samples were seropositive (≥128) for *Orientia* spp. Among acute samples, 25.5% (111/436) were positive at ≥256 titer and 19.0% (85/436) were positive at ≥512 (Figure 1). We observed no difference in acute IFA titers between patients with and without a convalescent blood samples (p = 0.33). Among samples with a positive 1:64 titer screen, the median acute titer was 128 (up to 8,192; interquartile range [IQR] 64–512) and median convalescent titer was 256 (up to 4,096; IQR 64–1,024). Seropositivity was highest (acute, 38.7% [120/310]; convalescent, 41.6% [112/269]) in Fort Portal, but was also high in Arua (acute, 26.5% [9/34]; convalescent, 30.0% [6/20]) and Mubende (acute, 20.7% [19/92]; convalescent, 23.4% [11/47]). The overall geometric mean titers were 90.8 (95% CI 80.2–102.8) for acute samples and 100.3 (95% CI 86.1–116.9) for convalescent samples.

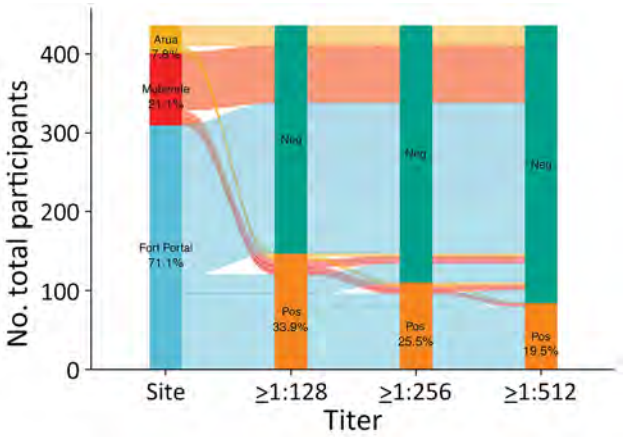

Figure 1. Alluvial diagram of serology from acute serum samples used in a study of *Orientia* genus endemicity among severe infectious disease cohorts, Uganda. The diagram represents *Orientia* spp.–positive immunofluorescent assay IgG at ≥128, ≥256, and ≥512 from 3 sites in Uganda. Colored lines indicate total participants from each site with positive or negative serology at 3 different titer cutoffs. Neg, negative; pos, positive.

Four participants met our case definition for *Orientia* spp. seroconversion (Table 1). Participants meeting the case definition were 24–56 years of age; 3 were female and 1 was male, and 3 had HIV (Table 2). Leukocyte counts ranged from 5–10 × 10^3 cells/μL, platelet counts were 56–220 × 10^3 cells/μL, and aspartate transaminase was 21–136 U/L. Three patients survived, but a 34-year-old woman with HIV in whom a papular rash developed died of unknown causes 8 months after follow-up. Three participants with seroconversion had negative malaria smears, blood cultures, and rapid antigen and molecular diagnostic tests for nonrickettsial pathogens (Table 2).

We used molecular methods to confirm *Orientia* spp. infection. The acute serum sample from participant D was repeatedly *rrs*-positive with RT-PCR (mean

Table 1. Rickettsia IgG results from participants with *Orientia spp.* seroconversion in a study of *Orientia* genus endemicity among severe infectious disease cohorts, Uganda*

	Days after illness onset†		*Orientia* spp.–positive titer‡			Spotted fever group titer			Typhus group titer		
Participant	Acute	Conv.	Fold change	Acute	Conv.	Fold change	Acute	Conv.	Fold change	Acute	Conv.
Mubende											
A	7	34	4	256	1,024	1	32	32	1	32	32
Fort Portal											
B	2	32	8	64	512	1	32	32	1	32	32
C	14	36	4	128	512	1	32	32	1	32	32
D	1	38	4	128	512	1	32	32	1	32	32

*Conv., convalescent; IFA, immunofluorescent assay.
†Sample collection after illness onset.
‡Karp strain IFA. Gilliam strain IFA seroconversion also observed in Fort Portal participant D (acute titers 1:512 and convalescent titers 1:2,048) but not among participants A-C.

Table 2. Clinical characteristics of participants with *Orientia spp.* seroconversion in a study of *Orientia* genus endemicity among severe infectious disease cohorts, Uganda*

Characteristics	Patient identification			
	A	B	C	D
Age, y/sex	24/M	34/F	23/F	56/F
Occupation	Mine worker	Business or trade	Fuel attendant	Farmer
Rash, type	Y, pustular and eschar	Y, papular	N	N
Clinical laboratory parameters				
WBC, x 10^3 cells/μL	7	10	5	8
Platelet count, x 10^3 cells/μL	56	220	128	177
AST, U/L	21	62	136	26
Microbiologic results†				
HIV (CD4)	+ (603)	+ (NA)	+ (NA)	–
Malaria smear	+, 126 parasites/μL	–	–	–
TB				
PCR	NA	NA	NA	–
Urine LAM	+	–	–	NA
Clinical diagnosis	TB	Urinary tract infection	Unidentified	Abdominal source
Inpatient treatment	ACT	CIP, CTX, MTZ	CTX, cefixime	CIP, MTZ
Outcome	Survived	Died, 8.2 mo.	Survived	Survived

*ACT, artemisinin-based combination therapy; AST, aspartate transaminase; CIP, ciprofloxacin; CTX, ceftriaxone; LAM, lipoarabinomman; MTZ, metronidazole; NA, not available; NG, no growth; TB, tuberculosis; WBC, white blood cells; –, negative; +, positive.
†All had negative blood cultures and negative multiplex PCR results.

cycle threshold 34.1, SD 0.4) and was confirmed by Sanger sequencing of the amplicon. A BLAST analysis (https://blast.ncbi.nlm.nih.gov) of a 96-bp sequenced fragment of the amplicon revealed 96%–100% homology with *Orientia* spp., and a single polymorphism aligned with *Candidatus* O. chuto (Figure 2). RT-PCR was negative using other primers for *Orientia* spp. (Orien16S 56-kDa) targets, SFGR (*sca0* [*ompA*] targets, and TGR (17-kDa antigen gene) targets.

Conclusions

We identified *Orientia* seroconversion among 4 participants hospitalized with severe infection in sub-Saharan Africa. We demonstrated that *Orientia* seropositivity was common among patients admitted for severe infection at 3 hospitals in Uganda. Our findings of highly prevalent seropositivity at 3 sites, identification of seroconversion, and molecular confirmation of a case with otherwise negative broad microbiologic testing support *Orientia* circulation and raise suspicion for infections extending to East Africa.

Prior clinical evidence of suspected scrub typhus in Africa relied on case reports of returning travelers with *Orientia* seroconversion (*5*). In addition to seroconversion identified in this study, seroconversions were observed in a pediatric cohort in Kenya (3.6%; n = 10) (*10*), and in 1 case among 49 abattoir workers in Djibouti (*11*). Our well-characterized multisite results supplement the limited literature suggesting *Orientia* spp. infections in sub-Saharan Africa.

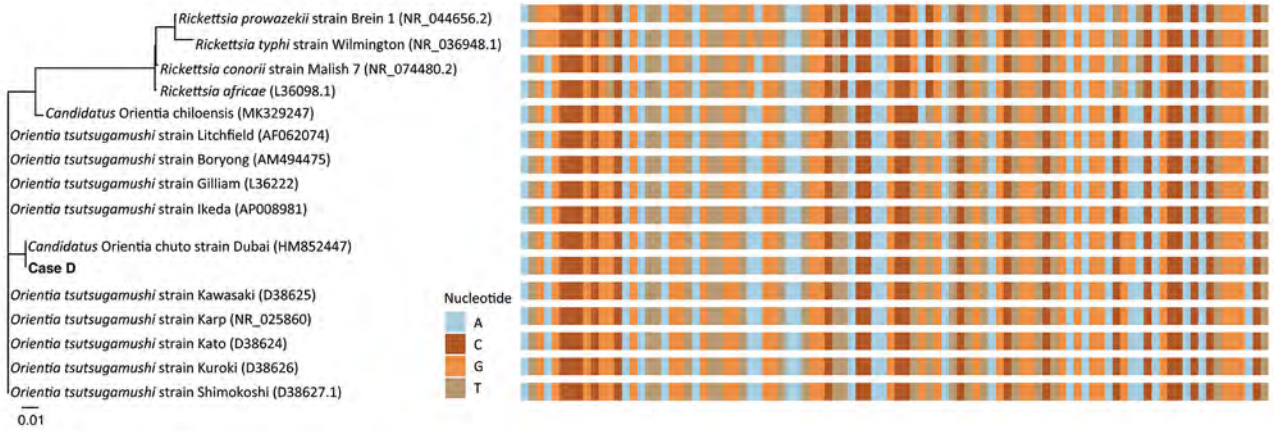

Figure 2. Phylogenetic tree (left) and aligned sequences (right) of *Orientia* spp. and locally endemic *Rickettsia* spp. in a study of *Orientia* genus endemicity among severe infectious disease cohorts, Uganda. We compared the 16S rRNA gene with an *Orientia* infection (case D) in Uganda. We aligned the 96-bp amplicon region and created the tree by using the neighbor-joining algorithm in R (The R Foundation for Statistical Computing, https://www.r-project.org). GenBank accession numbers of reference sequences are in parentheses. A single polymorphism aligned with *Candidatus* O. chuto, possibly differentiating case D from other *Orientia* spp. Scale bar indicates nucleotide substitutions per site.

In addition to prior suggestive evidence, our results build on a shift in understanding of worldwide *Orientia* spp. clinical infections. SFGR and TGR test results were negative in our cohorts, decreasing the likelihood of cross-reactivity. Despite IFA being the preferred method for rickettsial diagnosis, intrinsic interobserver variability limitations exist (*12*); we aimed to reduce those limitations through our reading approach and seroconversion criteria. Although we were able to confirm an infection by using real-time RT-PCR, sequence results were limited to a small fragment of the abundant 16S rRNA. The clinical relevance requires further confirmation with *Orientia* culture growth and extended genome sequencing. Because we relied on convalescent serology, we might have missed early fatal cases, which could skew our results toward less severe illness. Research efforts are needed to characterize the circulating species, incidence, pathogenic potential, and clinical relevance of *Orientia* infections in East Africa.

In summary, our findings suggest *Orientia* spp. circulation within the human–environment interface in Uganda and suggest novel *Orientia* infections within severe infection cohorts in Uganda. After excluding common causes of infections, our findings provide evidence of locally acquired *Orientia* infections among adults in sub-Saharan Africa.

Acute Febrile Illness and Sepsis in Uganda Study Team members: Nehkonti Adams, Rodgers R. Ayebare, Helen Badu, Melissa Gregory, Francis Kakooza, Mubaraka Kayiira, Willy Kayondo, Stacy M. Kemigisha Hannah Kibuuka, Abraham Khandathil, Prossy Naluyima, Edgar C. Ndawula, David F. Olebo, Matthew Robinson, Abdullah Wailagala, and Peter Waitt.

This study was conducted in compliance with the Declaration of Helsinki and Good Clinical Practice Guidelines. All participants signed written informed consent prior to study procedures. The investigators have adhered to the policies for protection of human subjects as prescribed in 45 CFR 46. Parent acute febrile illness cohort: The study and informed consent process were reviewed and approved by the Joint Clinical Research Centre (JCRC) Research Ethics Committee (JC1518) and the Uganda National Council for Science and Technology (UNCST), HS 371ES, and Johns Hopkins University School of Medicine Internal Review Board (IRB no. 00176961). Parent sepsis cohort: This protocol and informed consent were approved by the US Army Medical Research and Development Command Institutional Review (approval no. M-10573) and Makerere University School of Public Health (IRB no. 490). *Secondary use protocol:* this laboratory work was reviewed and received an exempt determination by Uniformed Services University (IRB no. DBS.2020.174).

Pathogen testing was supported by cooperative agreement with the Naval Medical Logistics Command (NMLC; agreement no. N626451920001) and by the Congressionally Directed Medical Research Program (agreement no. W81XWH-19-2-0057).

The opinions and assertions expressed herein are those of the authors and do not reflect the official policy or position of the Uniformed Services University of the Health Sciences, US Department of Defense, Henry M. Jackson Foundation for the Advancement of Military Medicine, Inc., or any other government or agency. Mention of trade names, commercial products, or organizations does not imply endorsement by the US government. Some of the authors of this work are employees of the US government. This work was prepared as part of their official duties. Title 17 U.S.C. x105 provides that "Copyright protection under this title is not available for any work of the United States government." Title 17 U.S.C. x101 defines a US government work as a work prepared by a military service member or employee of the US government as part of that person's official duties.

Y.C.M. receives research funding from Becton Dickinson, Quanterix, and Hologic, and receives funding support from miDiagnostics to Johns Hopkins University. Y.C.M. receives research funding from Becton Dickinson, Quanterix, and Hologic, and receives funding support from miDiagnostics to Johns Hopkins University. M.L. receives research funding support from Pfizer Inc. to Infectious Diseases Institute.

About the Author

Dr. Blair is an infectious diseases physician-scientist at Uniformed Services University, Bethesda, Maryland, USA. His research interests include molecular and imaging approaches to clinically detect emerging infectious diseases.

References

1. Bonell A, Lubell Y, Newton PN, Crump JA, Paris DH. Estimating the burden of scrub typhus: a systematic review. PLoS Negl Trop Dis. 2017;11:e0005838. https://doi.org/10.1371/journal.pntd.0005838
2. Weitzel T, Dittrich S, López J, Phuklia W, Martinez-Valdebenito C, Velásquez K, et al. Endemic scrub typhus in South America. N Engl J Med. 2016;375:954–61. https://doi.org/10.1056/NEJMoa1603657
3. Izzard L, Fuller A, Blacksell SD, Paris DH, Richards AL, Aukkanit N, et al. Isolation of a novel *Orientia* species (*O. chuto* sp. nov.) from a patient infected in Dubai. J Clin Microbiol. 2010;48:4404–9. https://doi.org/10.1128/JCM.01526-10
4. Masakhwe C, Linsuwanon P, Kimita G, Mutai B, Leepitakrat S, Yalwala S, et al. Identification and characterization of *Orientia chuto* in trombiculid chigger

mites collected from wild rodents in Kenya. J Clin Microbiol. 2018;56:e01124-18. https://doi.org/10.1128/JCM.01124-18
5. Richards AL, Jiang J. Scrub typhus: historic perspective and current status of the worldwide presence of *Orientia* species. Trop Med Infect Dis. 2020;5:49. https://doi.org/10.3390/tropicalmed5020049
6. Blair PW, Kobba K, Kakooza F, Robinson ML, Candia E, Mayito J, et al. Aetiology of hospitalized fever and risk of death at Arua and Mubende tertiary care hospitals in Uganda from August 2019 to August 2020. BMC Infect Dis. 2022;22:869. https://doi.org/10.1186/s12879-022-07877-3
7. Yun NR, Kim CM, Kim DY, Seo JW, Kim DM. Clinical usefulness of 16S ribosomal RNA real-time PCR for the diagnosis of scrub typhus. Sci Rep. 2021;11:14299. https://doi.org/10.1038/s41598-021-93541-w
8. Jiang J, Martínez-Valdebenito C, Weitzel T, Farris CM, Acosta-Jamett G, Abarca K, et al. Development of a new genus-specific quantitative real-time PCR assay for the diagnosis of scrub typhus in South America. Front Med (Lausanne). 2022;9:831045. https://doi.org/10.3389/fmed.2022.831045
9. Reller ME, Dumler JS. Optimization and evaluation of a multiplex quantitative PCR assay for detection of nucleic acids in human blood samples from patients with spotted fever rickettsiosis, typhus rickettsiosis, scrub typhus, monocytic ehrlichiosis, and granulocytic anaplasmosis. J Clin Microbiol. 2020;58:e01802-19. https://doi.org/10.1128/JCM.01802-19
10. Maina AN, Farris CM, Odhiambo A, Jiang J, Laktabai J, Armstrong J, et al. Q fever, scrub typhus, and rickettsial diseases in children, Kenya, 2011–2012. Emerg Infect Dis. 2016;22:883–6. https://doi.org/10.3201/eid2205.150953
11. Horton KC, Jiang J, Maina A, Dueger E, Zayed A, Ahmed AA, et al. Evidence of rickettsia and *Orientia* infections among abattoir workers in Djibouti. Am J Trop Med Hyg. 2016;95:462–5. https://doi.org/10.4269/ajtmh.15-0775
12. Phetsouvanh R, Thojaikong T, Phoumin P, Sibounheuang B, Phommasone K, Chansamouth V, et al. Inter- and intra-operator variability in the reading of indirect immunofluorescence assays for the serological diagnosis of scrub typhus and murine typhus. Am J Trop Med Hyg. 2013;88:932–6. https://doi.org/10.4269/ajtmh.12-0325

Address for correspondence: Paul W. Blair, Uniformed Services University, 4301 Jones Bridge Rd, Bethesda, MD 20814, USA; email: paul.blair.ctr@usuhs.edu

Effect of Rodent Control Program on Incidence of Zoonotic Cutaneous Leishmaniasis, Iran

Amir Abdoli, Samaneh Mazaherifar, Kavous Solhjoo, Mohsen Farhang Zargar, Hayedeh Parvin Jahromi, Ali Taghipour, Mohammad Darayesh, Milad Badri, Majid Pirestani, Shahab Falahi, Azra Kenarkoohi

We report the effect of a rodent control program on the incidence of zoonotic cutaneous leishmaniasis in an endemic region of Iran. A 1-year interruption in rodent control led to 2 years of increased incidence of zoonotic cutaneous leishmaniasis. Restarting rodent control led to a decline of zoonotic cutaneous leishmaniasis.

Leishmaniasis is a neglected tropical disease that is prevalent worldwide (*1*). Cutaneous leishmaniasis (CL) is endemic in different regions of Iran and has an approximate incidence rate of 1.18 cases/100,000 population and a difference of 5.7 disability-adjusted life-years (*2*). Zoonotic cutaneous leishmaniasis (ZCL), caused by the parasite *Leishmania major*, is the primary cause of CL in Iran, where anthroponotic cutaneous leishmaniasis, caused by *Leishmania tropica*, is less prevalent (*2*,*3*). Because rodents are the main reservoirs of ZCL, the rodent control program (RCP) is an important intervention for the control of ZCL in endemic areas (*1*). ZCL is endemic in Jahrom county in Fars Province, Iran (Appendix Figure 1, https://wwwnc.cdc.gov/EID/article/30/7/23-1404-App1.pdf). We report the effects of an RCP on incidence of ZCL in this region. This study was approved by the Research and Ethics Committee of Jahrom University of Medical Sciences, Jahrom, Iran (ethics code IR.JUMS.REC.1402.067).

The Study

The RCP is conducted in rural areas of Jahrom county 5 times a year, beginning with the destruction of rodent nests in early April (*4*). Once a month in April, May, June, and September, rodent nest baiting is performed by using a mixture of wheat with 2.5% zinc phosphide (*4*) (Appendix Figure 3). The rodent nest baiting is conducted in a 500-m circle around houses within the intervention area (*4*).

The RCP was completely ceased during the first year of the COVID-19 pandemic in Jahrom county because of a lack of equipment and personnel. The program was resumed routinely in early April 2021 (*5*). The outcome of the 1-year interruption in the RCP was a mild increase in the incidence of ZCL in 2020 and a high increase in ZCL in 2021 (Appendix Figure 2). Incidence rates for the period before the pandemic were stable: 103.7 cases/100,000 population in 2016, 95.1 cases/100,000 population in 2017, 99.7 cases/100,000 population in 2018, and 99.6 cases/100,000 population in 2019 (Figure). After the RCP stopped because of the COVID-19 pandemic, ZCL incidence rates increased to 129.4 cases/100,000 population in 2020 and 321.5 cases/100,000 population in 2021, (Table; Figure). Of interest, the outcome of restarting the RCP in 2021 was not apparent until 2022 and 2023, when the incidence rate of ZCL decreased to 72.1 cases/100,000 population in 2022 and 19.2 cases/100,000 population in 2023 (Table; Figure; Appendix Figure 2).

Jahrom county has an agricultural environment that provides suitable conditions for both the rodent reservoirs and sand fly vectors of *L. major*. Although different studies have demonstrated the effectiveness of the RCP for control of ZCL (*4*,*6*,*7*), little is known about the impact of a short-term interruption of the RCP on the incidence of ZCL in an endemic region. The unplanned interruption of the RCP in Jahrom county because of the COVID-19 pandemic gave us the opportunity to evaluate the impact of the RCP on the incidence of ZCL in an endemic area. Although the RCP was paused for only 1 year and resumed routinely in early April

Author affiliations: Jahrom University of Medical Sciences, Jahrom, Iran (A. Abdoli, S. Mazaherifar, K. Solhjoo, M. Farhang Zargar, H.P. Jahromi, A. Taghipour, M. Darayesh); Qazvin University of Medical Sciences, Qazvin, Iran (M. Badri); Tarbiat Modares University, Tehran, Iran (M. Pirestani); Ilam University of Medical Sciences, Ilam, Iran (S. Falahi, A. Kenarkoohi)

DOI: https://doi.org/10.3201/eid3007.231404

Table. Annual incidence rate of zoonotic cutaneous leishmaniasis cases/100,000 people in Jahrom county, Iran, between 2016 and 2023.

Year	Total population	No. patients	Incidence rate (per 100,000)
2016	228,443	237	103.7
2017	231,256	220	95.1
2018	233,592	233	99.7
2019	235,825	235	99.6
2020	237,194	307	129.4
2021	239,829	771	321.5
2022	242,852	175	72.1
2023	244,458	47	19.2

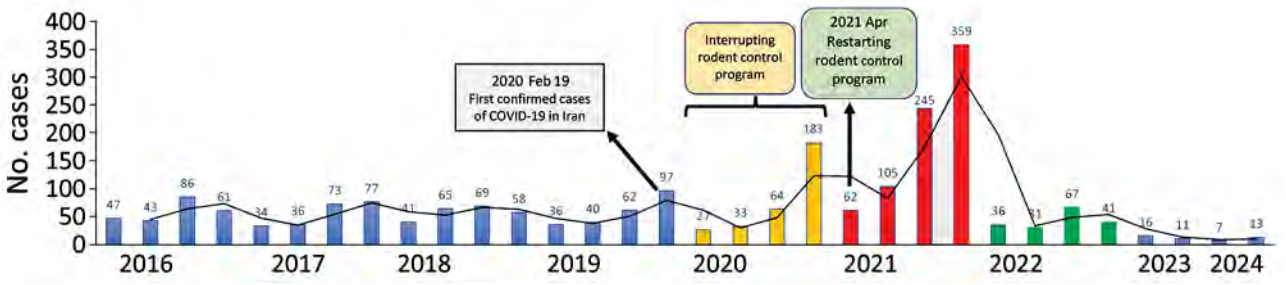

Figure. Trends of cutaneous leishmaniasis from 2016 to the beginning of 2024 in Jahrom county, Iran, highlighting the period during the COVID-19 pandemic in which the rodent control program was interrupted in 2020 and restarted in 2021.

2021, a slight increase in the incidence of ZCL was observed (129.4 cases/100,000 population in 2020) and a marked increase in ZCL the following year (321.5 cases/100,000 population in 2021). However, because of the COVID-19 lockdown, the diagnosis and treatment of CL patients were interrupted during the first year of the pandemic (2020), so those factors could be involved in the increase in the incidence of ZCL in 2020 and 2021. Of interest, a sharp decline in the incidence rates was observed in 2022 and 2023 (72.1 cases/100,000 population in 2022 and 19.2 cases/100,000 population in 2023). However, comparing the incidences of ZCL in 2022 and 2023 with the incidences before 2020 has shown that factors other than the RCP could be contributing to the decline of ZCL because the incidence rates of 2022 and 2023 were much lower than the incidence rates before 2020 (Table; Figure; Appendix Figure 2). Other factors, such as climate conditions and rainfall, which are involved in the propagations of rodents and sand flies, could also contribute to the decline of ZCL observed in 2022 and 2023.

The emergence of COVID-19 has a considerable influence on the burden of noncommunicable and communicable diseases throughout the world and in Iran (*8*,*9*). In Brazil, the COVID-19 pandemic seems to have contributed to an increase in the incidence of tegumentary leishmaniasis in 2020 (*10*). A decreasing incidence of CL was reported in an endemic region in western Iran during the COVID-19 pandemic (2020–2021), possibly because of the disruption of CL diagnosis and treatment follow-up (*11*).

Conclusions

Our study showed a 1-year interruption to the RCP contributed to 2 years of increased incidence of ZCL in an endemic region of Iran. Restarting the RCP led to the decline of ZCL after 2 years of program activity. However, additional factors, such as environmental conditions (e.g., climate conditions and rainfall) that have an influence on vector and reservoir propagation, and diagnosis and treatment follow-up, could influence the incidence of ZCL (*12*, *13*). In the absence of a vaccine for ZCL, an RCP is an effective strategy for ZCL control in endemic regions.

This study was supported by Jahrom University of Medical Sciences, Jahrom, Iran (grant nos. 402000084 and 99000159) and the National Institute for Medical Research Development (grant no. 978507).

About the Author

Dr. Abdoli is associate professor of medical parasitology at Jahrom University of Medical Sciences. His research interests include parasitology and zoonotic infections.

References

1. Reithinger R, Dujardin JC, Louzir H, Pirmez C, Alexander B, Brooker S. Cutaneous leishmaniasis. Lancet Infect Dis. 2007;7:581–96. https://doi.org/10.1016/S1473-3099(07)70209-8
2. Piroozi B, Moradi G, Alinia C, Mohamadi P, Gouya MM, Nabavi M, et al. Incidence, burden, and trend of cutaneous leishmaniasis over four decades in Iran. Iran J Public Health. 2019;48(Supple 1):28–35.

3. Mazaherifar S, Solhjoo K, Rasti S, Heidarnejadi SM, Abdoli A. Patterns of cutaneous leishmaniasis during the COVID-19 pandemic in four endemic regions of Iran. Trans R Soc Trop Med Hyg. 2023;117:38–44. https://doi.org/10.1093/trstmh/trac081
4. Ershadi MR, Zahraei-Ramazani A-R, Akhavan A-A, Jalali-Zand A-R, Abdoli H, Nadim A. Rodent control operations against zoonotic cutaneous leishmaniasis in rural Iran. Ann Saudi Med. 2005;25:309–12. https://doi.org/10.5144/0256-4947.2005.309
5. Mazaherifar S, Solhjoo K, Abdoli A. Outbreak of cutaneous leishmaniasis before and during the COVID-19 pandemic in Jahrom, an endemic region in the southwest of Iran. Emerg Microbes Infect. 2022;11:2218–21. https://doi.org/10.1080/22221751.2022.2117099
6. Rezaei F, Saghafipour A, Rassi Y, Abai MR. Effect of rodents' management plan on controlling cutaneous leishmaniasis in endemic centers of Gom province in 2012. Hormozgan Med J. 2015;19:219–25.
7. Kalteh EA, Sofizadeh A, Yapng Gharavi AH, Ozbaki GM, Kamalinia HR, Bagheri A, et al. Effect of wild rodents control in reduction of zoonotic cutaneous leishmaniasis in Golestan province, north of Iran (2016). Majallah-i Danishgah-i Ulum-i Pizishki-i Gurgan. 2019;21:94–100.
8. Lim MA, Huang I, Yonas E, Vania R, Pranata R. A wave of non-communicable diseases following the COVID-19 pandemic. Diabetes Metab Syndr. 2020;14:979–80. https://doi.org/10.1016/j.dsx.2020.06.050
9. Abdoli A, Falahi S, Kenarkoohi A. COVID-19-associated opportunistic infections: a snapshot on the current reports. Clin Exp Med. 2022;22:327–46. https://doi.org/10.1007/s10238-021-00751-7
10. Andrade MC, Ferreti Bonan PR, Hilan E, Marques NP, Guimarães-Carvalho SF, Martelli H. COVID-19 pandemic causes increased clinic visits with diagnosis of tegumentary leishmaniasis in Brazil in 2020. Int J Infect Dis. 2021;113:87–9. https://doi.org/10.1016/j.ijid.2021.10.003
11. Shams M, Rashidi A, Mohamadi J, Moradi M, Pakzad R, Naserifar R, et al. Real-time impact of COVID-19 pandemic on cutaneous leishmaniasis case finding and strategic planning, preventive interventions, control and epidemiology in a region with a high burden of cutaneous leishmaniasis and COVID-19: a cross-sectional descriptive study based on registry data in Ilam-Iran. Health Sci Rep. 2023;6:1489. https://doi.org/10.1002/hsr2.1489
12. Abdolahnejad A, Mousavi SH, Sofizadeh A, Jafari N, Shiravand B. Climate change and distribution of zoonotic cutaneous leishmaniasis (ZCL) reservoir and vector species in central Iran. Model Earth Syst Environ. 2021;7:105–15. https://doi.org/10.1007/s40808-020-00860-4
13. Charrahy Z, Yaghoobi-Ershadi MR, Shirzadi MR, Akhavan AA, Rassi Y, Hosseini SZ, et al. Climate change and its effect on the vulnerability to zoonotic cutaneous leishmaniasis in Iran. Transbound Emerg Dis. 2022;69:1506–20. https://doi.org/10.1111/tbed.14115

Address for correspondence: Amir Abdoli, Jahrom University of Medical Sciences, PO Box 74148-46199, Ostad Motahari Ave, Jahrom, Iran; email: a.abdoli25@gmail.com

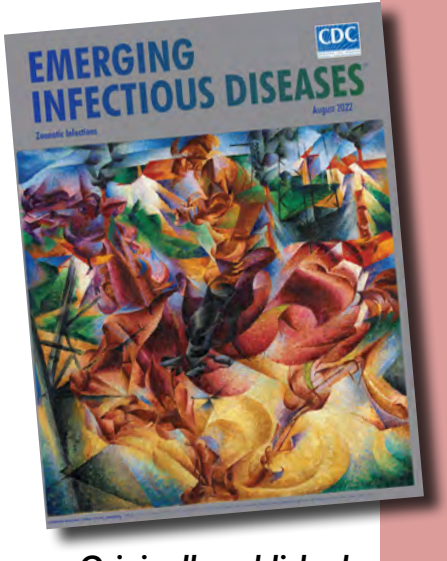

Originally published in August 2022

etymologia revisited

Dermatophilus congolensis

[dur"mə-tof'-s con-gō-len'sis]

Dermatophilus congolensis From the Greek *derma* (skin) + *philos* (loving), *Dermatophilus congolensis* is a Gram-positive, aerobic actinomycete, and facultatively anaerobic bacteria. D. congolensis infects the epidermis and produces exudative dermatitis termed dermatophilosis that was previously known as rain rot, rain scald, streptotrichosis, and mycotic dermatitis.

In 1915, René Van Saceghem, a Belgian military veterinarian stationed at a veterinary laboratory in the former Belgian Congo (thus, the species name *congolensis*), reported *D. congolensis* from exudative dermatitis in cattle. Local breeders and veterinarians had observed the disease since 1910, but the causal agent was not identified.

Dermatophilosis affects animals, mainly cattle, and more rarely humans. Outbreaks of *D. congolensis* infection have severe economic implications in the livestock and leather industries.

Sources

1. Amor A, Enríquez A, Corcuera MT, Toro C, Herrero D, Baquero M. Is infection by *Dermatophilus congolensis* underdiagnosed? J Clin Microbiol. 2011;49:449–51. https://doi.org/10.1128/JCM.01117-10
2. Branford I, Johnson S, Chapwanya A, Zayas S, Boyen F, Mielcarska MB, et al. Comprehensive molecular dissection of *Dermatophilus congolensis* genome and first observation of *tet*(z) tetracycline resistance. Int J Mol Sci. 2021;22:7128. https://doi.org/10.3390/ijms22137128
3. Dorland's illustrated medical dictionary. 32nd ed. Philadelphia: Elsevier Saunders; 2012.
4. Van Saceghem R. Contagious skin disease (contagious impetigo) [in French]. Bull Soc Pathol Exot. 1915;8:354–9.

https//wwwnc.cdc.gov/eid/article/28/8/et-2808_article

Body Louse Pathogen Surveillance among Persons Experiencing Homelessness, Canada, 2020–2021

Carl Boodman, Leslie R. Lindsay, Antonia Dibernardo, Kathy Kisil, Heather Coatsworth, Chris Huynh, Amila Heendeniya, John Schellenberg, Yoav Keynan

We analyzed body lice collected from persons experiencing homelessness in Winnipeg, Manitoba, Canada, during 2020–2021 to confirm vector species and ecotype and to identify louseborne pathogens. Of 556 lice analyzed from 7 persons, 17 louse pools (218 lice) from 1 person were positive for the louseborne bacterium *Bartonella quintana*.

In 2020, Canada's largest cluster of *Bartonella quintana* endocarditis, an infection caused by a louseborne bacterium, was detected among persons experiencing homelessness in Winnipeg, Manitoba, Canada (*1*). Over a 6-month period, 4 people required hospitalization for *B. quintana* endocarditis (*1*). The outbreak triggered a retrospective analysis revealing 11 cases of *B. quintana* in Manitoba in the preceding decade (*2*). In 2022, the first pediatric case of *B. quintana* endocarditis acquired in a high-income country was reported from Manitoba (*3*). Prior to the Manitoba outbreak, only 3 cases of *B. quintana* infection were detected in Canada (*4*).

B. quintana is a fastidious gram-negative bacillus transmitted through the feces of infected body lice, *Pediculus humanus humanus* (*5*). The bacterium was first detected during World War I as the cause of trench fever and was later determined to cause bacteremia, endocarditis, and bacillary angiomatosis (*5*). *B. quintana* enters the bloodstream through broken skin (*5*).

Body lice and head lice are morphotypes of a single species, *Pediculus humanus* (*6*). Unlike head lice, body lice live in clothing, intermittently moving to the skin to feed on blood (*5*). Body lice are traditionally known to transmit 3 pathogens: *B. quintana, Rickettsia prowazekii* (epidemic typhus), and *Borrelia recurrentis* (louseborne relapsing fever) (*5*). Whereas they are not typically louseborne, *Coxiella burnetii* and *Acinetobacter* spp. have been detected in body lice (*7*). Body louse infestation is associated with poverty, experiencing homelessness, and an inability to wash and change clothing.

The possibility that body lice–infested persons from Winnipeg could be exposed to louseborne pathogens is unknown. In this article, we discuss what louseborne pathogens were found in Winnipeg body lice and the difference in pathogen real-time PCR cycle threshold (Ct) values according to louse instar and sex. This study was approved by the University of Manitoba and multiple other institutional ethics review boards (Appendix, https://wwwnc.cdc.gov/EID/article/30/7/23-1660-App1.pdf).

The Study

We collected ectoparasites from the clothing of participants in inner city Winnipeg. We separated ectoparasites from the same person into pools based on instar and sex. We pooled ectoparasites from the first and second instars but tested those from the third and fourth instars separately. We tested ectoparasites positive for *B. quintana* from the fourth instar in separate pools of male and female parasites. We decontaminated ectoparasite pools by using 70% ethanol and homogenized them by using a copper clad bead beater. We then extracted DNA by using the DNeasy 96 kit (QIAGEN, https://www.qiagen.com). We identified vector species, louse morphotype, and pathogens by using real-time PCR (Appendix). We used cytochrome b genes to identify louse species and Phum_PHUM540560 genes to identify ecotype

Author affiliations: Institute of Tropical Medicine, Antwerp, Belgium (C. Boodman), University of Antwerp, Belgium (C. Boodman); University of Manitoba, Winnipeg, Manitoba, Canada (C. Boodman, A. Heendeniya, J. Schellenberg, Y. Keynan); Public Health Agency of Canada, Winnipeg (L.R. Lindsay, A. Dibernardo, H. Coatsworth, C. Huynh); Access Downtown, Winnipeg (K. Kisil)

DOI: https://doi.org/10.3201/eid3007.231660

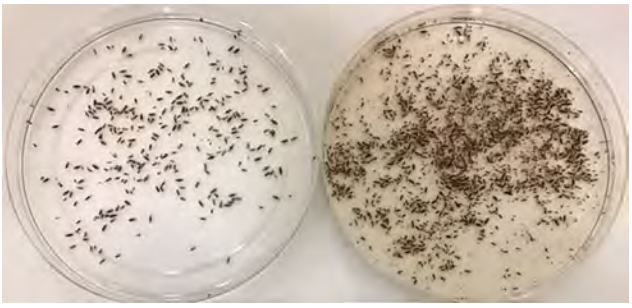

Figure 1. Body lice collected from a person experiencing homelessness in inner city Winnipeg, Manitoba, Canada. Not all ectoparasites from this person were analyzed.

(*8*). We identified pathogens by using the following targets: ITS3, *Bartonella* genus; *yopP* and *fabB*, *B. quintana*; *ompB*, *Rickettsia prowazekii*; IS1111a, *Coxiella burnetii*; and *rpoB*, *Acinetobacter* spp. We conducted statistical analysis by using Mann-Whitney U and Kruskal-Wallis tests (Bonferroni correction, post-hoc Dunn test) to compare groups of Ct values (Appendix). We considered values of $p<0.05$ significant.

Seven persons submitted ectoparasites, 2 in 2020, and 5 in 2021 (Appendix). We analyzed 556 ectoparasites. The range of ectoparasites tested per participant was 5–218 and per pool was 5–48. We confirmed all ectoparasite pools were *P. humanus humanus* lice by using PCR positivity on louse and body lice targets and morphology (*9*) (Figures 1, 2). All louse pools from 1 participant (1/7 = 14%, 218 lice) demonstrated positivity on all *Bartonella* and *B. quintana* targets (Table 1). Of the 7 louse pools positive for *B. quintana*, 4 also demonstrated molecular positivity for *Acinetobacter* spp. Ectoparasites from all participants were negative for *R. prowazekii* and *C. burnetii*.

When analyzing *B. quintana*–positive louse pools, we found Ct values were similar between ITS3, *yopP*, and *fabB* genes (test statistic H = 0.54; p = 0.76). The average ITS3 Ct values decreased from the first and second instar pools (34.6) to the third instar pools (28.9) by 5.7, and from the third instar pools to the fourth instar pool (21.8) by 7.1. Pools from female lice demonstrated lower ITS3 Ct values than male lice pools (p = 0.0214) (Table 2).

Figure 2. Two female body lice, *Pediculus humanus humanus*, collected from a person experiencing homelessness in inner city Winnipeg, Manitoba, Canada (*9*).

Conclusions

We determined by molecular testing that body lice collected from a person experiencing homelessness in Winnipeg were positive for *B. quintana* bacteria. This finding complements the recent Manitoba cluster of *B. quintana* cases, suggesting a poorly described burden of infection (*1*,*2*,*4*). The hidden presence of *B. quintana* bacteria in Canada was recently highlighted in an outbreak of transplant-derived *B. quintana* infection in cities that had not previously reported transmission: 5 cases of bacillary angiomatosis were linked to 3 deceased donors from 2 cities in Alberta (Health Canada, pers. comm., email, 2023 Nov 4). All cases

Table 1. Testing of lice to determine species and infection with *Bartonella quintana* and *Acinetobacter* spp. from a person experiencing homelessness in inner city Winnipeg, Manitoba, Canada*

			Ct values				
Pool	No. lice/pool	Instar	Body louse gene	*Bartonella* ITS3	*B. quintana yopP* gene	*B. quintana fabB* gene	*Acinetobacter rpoB*
1	48	1st and 2nd	31.2	33.6	30.8	30.8	40
2	7	1st and 2nd	29.8	35.6	36.2	35.4	40
3	26	3rd	30.6	25.6	26.2	26.0	36.2
4	26	3rd	30.4	23.0	27.0	26.7	38.5
5	5	3rd	29.9	33.6	34	34.2	40
6	6	3rd	30.5	33.3	34.2	33.8	37.4
7	30	4th	29.3	21.8	23.1	22.9	29.6

*Ct ≥40 indicates a negative result. Genes used to determine species identities: PHUM540560, body lice gene distinguishing body lice from head lice; ITS3, internal transcribed spacer 3, identifies *Bartonella* to genus level; *yopP*, hypothetical intracellular effector gene, identifies *B. quintana* to species; *fabB*, 3-oxoacyl-synthase gene, identifies *B. quintana* to species; *rpoB*, RNA polymerase β subunit gene, identifies *Acinetobacter* spp. Ct, cycle threshold.

Table 2. Testing of fourth instar body lice pools, divided by sex and associated C) for 3 *Bartonella* genes, from a person experiencing homelessness in Winnipeg, Manitoba, Canada*

Pool	No. lice/pool	Sex	Ct values		
			Bartonella ITS3 gene	*B. quintana yopP* gene	*B. quintana fabB* gene
8	6	Female	21.5	23.1	22.7
9	7	Female	24.2	25.2	24.9
10	7	Female	24.6	25.8	25.4
11	7	Female	24.8	25.7	25.5
12	7	Female	25.6	26.6	26.3
13	7	Male	27.2	28.1	27.6
14	7	Male	27.6	27.4	27.2
15	7	Male	25.2	26.1	25.7
16	7	Male	27.6	28.6	28.2
17	8	Male	28.1	29.1	28.6

*Genes used to determine species identities: PHUM540560, body lice gene distinguishing body lice from head lice; ITS3, internal transcribed spacer, identifies *Bartonella* to genus level; *yopP*, hypothetical intracellular effector gene, identifies *B. quintana* to species; *fabB*, 3-oxoacyl-synthase gene, identifies *B. quintana* to species; *rpoB*, RNA polymerase β subunit gene, identifies *Acinetobacter* spp.

were confirmed to be *B. quintana* bacteria with donors experiencing homelessness as the common risk factor (Health Canada, pers. comm., email, 2023 Nov 4).

Our study suggests a minority of body lice cases from Winnipeg are positive for pathogens, including *B. quintana* bacteria. We did not collect epidemiologic data for this study, but all participants were persons who experienced homelessness in inner city Winnipeg. Because of Winnipeg's harsh winters and few homeless shelters, it is possible the participant with *B. quintana*–positive lice lives in close proximity to others and other persons with *B. quintana* infection remain undocumented. Only 1/7 persons with body lice had *B. quintana*–positive lice, which may be because of the small number of participants and that 3 participants submitted few ectoparasites. Nationwide body lice studies to compare *B. quintana* bacterial prevalence across different areas are needed to identify locations of infection.

The absence of other pathogens likely reflects differences in transmission dynamics and ecology (*10*,*11*). Unlike *B. quintana* bacteria, which does not alter louse survival, lice infected with *R. prowazekii* bacteria die within a week of infection, limiting transmission (*11*). The urban setting of our study diminishes the chance of replicating the occasional documentation of *C. burnetii* bacteria in lice. Whereas *Acinetobacter* spp. bacteria are commonly identified in body lice, no proven cases of *Acinetobacter* disease caused by body lice have been confirmed (*11*,*12*).

The lower *Bartonella* Ct values (stronger signal) with advancing louse instar and female sex may indicate larger blood meals of those subpopulations. *B. quintana* bacteria replicate in the louse intestine but are not known to be transmitted transovarially, indicating the person with *B. quintana*–positive lice from all instars likely had sustained bacteremia for at least 1 month (body lice lifespan). This study highlights the usefulness of identifying ectoparasites by using molecular methods when arthropod taxonomic expertise is not accessible.

B. quintana bacteria is excreted in louse feces continuously for weeks in quantities up to 10^7 bacteria/louse each day (*13*,*14*). The explosive replication, coupled with *B. quintana* bacteria remaining infectious in biofilm-like structures for up to 1 year, suggests even a single case of *B. quintana* infection may indicate a hidden burden of infected persons (*5*,*14*).

Our study is limited by a small sample size, the heterogenous number of ectoparasites submitted per person, the focus on urban populations from 1 jurisdiction, and the lack of DNA quantity normalization. Active case finding, contact tracing, and public health engagement are needed to clarify the epidemiology of *B. quintana* infection in Canada. Manitoba residents with body lice should be evaluated for *B. quintana* infection. Sampling of ectoparasites may provide an effective way to perform surveillance for emerging pathogens in marginalized settings.

About the Author

Dr. Boodman is an infectious disease doctor and medical microbiologist who is currently a PhD candidate at the Institute of Tropical Medicine (Belgium) and the University of Antwerp (Belgium), supported by University of Manitoba's Clinical Investigator Program (Canada). His interests include neglected infections linked to poverty and vectorborne intracellular bacteria.

References

1. Boodman C, Wuerz T, Lagacé-Wiens P. Endocarditis due to *Bartonella quintana*, the etiological agent of trench fever. Can Med Assoc J. 2020;192:E1723–E1726. https://doi.org/10.1503/cmaj.201170
2. Boodman C, Wuerz T, Lagacé-Wiens P, Lindsay R, Dibernardo A, Bullard J, et al. Serologic testing for *Bartonella* in Manitoba, Canada, 2010–2020: a retrospective case series. CMAJ Open. 2022;10:E476 LP–E482. https://doi.org/10.9778/cmajo.20210180
3. Boodman C, MacDougall W, Hawkes M, Tyrrell G, Fanella S. *Bartonella quintana* endocarditis in a child from North-

ern Manitoba, Canada. PLoS Negl Trop Dis. 2022;16:e0010399. https://doi.org/10.1371/journal.pntd.0010399
4. Lam JC, Fonseca K, Pabbaraju K, Meatherall BL. Case report: *Bartonella quintana* endocarditis outside of the Europe-African gradient: comprehensive review of cases within North America. Am J Trop Med Hyg. 2019;100:1125–9. https://doi.org/10.4269/ajtmh.18-0929
5. Foucault C, Brouqui P, Raoult D. *Bartonella quintana* characteristics and clinical management. Emerg Infect Dis. 2006;12:217–23. https://doi.org/10.3201/eid1202.050874
6. Light JE, Toups MA, Reed DL. What's in a name: the taxonomic status of human head and body lice. Mol Phylogenet Evol. 2008;47:1203–16. https://doi.org/10.1016/j.ympev.2008.03.014
7. Amanzougaghene N, Fenollar F, Raoult D, Mediannikov O. Where are we with human lice? A review of the current state of knowledge. Front Cell Infect Microbiol. 2020;9:474. https://doi.org/10.3389/fcimb.2019.00474
8. Drali R, Boutellis A, Raoult D, Rolain JM, Brouqui P. Distinguishing body lice from head lice by multiplex real-time PCR analysis of the Phum_PHUM540560 gene. PLoS One. 2013;8:e58088. https://doi.org/10.1371/journal.pone.0058088
9. Bonilla DL, Durden LA, Eremeeva ME, Dasch GA. The biology and taxonomy of head and body lice—implications for louse-borne disease prevention. PLoS Pathog. 2013;9:e1003724. https://doi.org/10.1371/journal.ppat.1003724
10. Bonilla DL, Kabeya H, Henn J, Kramer VL, Kosoy MY. *Bartonella quintana* in body lice and head lice from homeless persons, San Francisco, California, USA. Emerg Infect Dis. 2009;15:912–5. https://doi.org/10.3201/eid1506.090054
11. Badiaga S, Raoult D, Brouqui P. Preventing and controlling emerging and reemerging transmissible diseases in the homeless. Emerg Infect Dis. 2008;14:1353–9. https://doi.org/10.3201/eid1409.080204
12. La Scola B, Raoult D. *Acinetobacter baumannii* in human body louse. Emerg Infect Dis. 2004;10:1671–3. https://doi.org/10.3201/eid1009.040242
13. Chomel BB, Boulouis H-J, Breitschwerdt EB, Kasten RW, Vayssier-Taussat M, Birtles RJ, et al. Ecological fitness and strategies of adaptation of *Bartonella* species to their hosts and vectors. Vet Res. 2009;40:29. https://doi.org/10.1051/vetres/2009011
14. Seki N, Kasai S, Saito N, Komagata O, Mihara M, Sasaki T, et al. Quantitative analysis of proliferation and excretion of *Bartonella quintana* in body lice, *Pediculus humanus* L. Am J Trop Med Hyg. 2007;77:562–6. https://doi.org/10.4269/ajtmh.2007.77.562

Address for correspondence: Carl Boodman, Max Rady College of Medicine, University of Manitoba, Rm 543 Basic Medical Sciences Bdg, 745 Bannatyne Ave, Winnipeg, MN R3E 0J9, Canada; email: boodmanc@myumanitoba.ca

etymologia revisited

Mycobacterium chimaera

[mi'ko-bak-tēr'e-əm ki-mēr'ə]

Formerly an unnamed *Mycobacterium* sequevar within the *M. avium–M. intracellulare–M. scrofulaceum* group (MAIS), *M. chimaera* is an emerging opportunistic pathogen that can cause infections of heart valve prostheses, vascular grafts, and disseminated infections after open-heart surgery. Heater–cooler units used to regulate blood temperature during cardiopulmonary bypass have been implicated, although most isolates are respiratory. In 2004, Tortoli et al. proposed the name M. chimaera for strains that a reverse hybridization–based line probe assay suggested belonged to MAIS but were different from *M. avium, M. intracellulare*, or *M. scrofulaceum*.The new species name comes from the chimera, a mythological being made up of parts of 3 different animals.

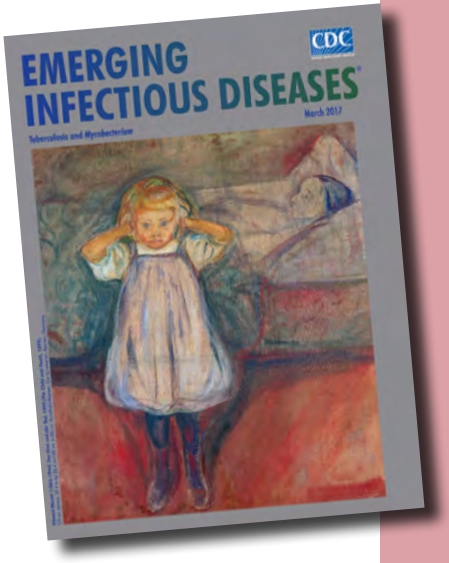

Originally published in March 2017

References:

1. Schreiber PW, Kuster SP, Hasse B, Bayard C, Rüegg C, Kohler P, et al. Reemergence of *Mycobacterium chimaera* in heater–cooler units despite intensified cleaning and disinfection protocol. Emerg Infect Dis. 2016;22:1830–3.
2. Struelens MJ, Plachouras D. *Mycobacterium chimaer*a infections associated with heater-cooler units (HCU): closing another loophole in patient safety. Euro Surveill. 2016;21:1–3.
3. Tortoli E, Rindi L, Garcia MJ, Chiaradonna P, Dei R, Garzelli C, et al. Proposal to elevate the genetic variant MAC-A, included in the *Mycobacterium avium* complex, to species rank as *Mycobacterium chimaera* sp. nov. Int J Syst Evol Microbiol. 2004;54:1277–85.

https://wwwnc.cdc.gov/eid/article/23/3/et-2303_article

Orthohantaviruses in Misiones Province, Northeastern Argentina

María Victoria Vadell, Eliana Florencia Burgos, Daniela Lamattina, Carla Bellomo, Valeria Martínez, Rocío Coelho, Cecilia Lanzone, Carolina Alicia Labaroni, Laura Tauro, Oscar Daniel Salomón, Isabel Elisa Gómez Villafañe

Few cases of hantavirus pulmonary syndrome have been reported in northeastern Argentina. However, neighboring areas show a higher incidence, suggesting underreporting. We evaluated the presence of antibodies against orthohantavirus in small rodents throughout Misiones province. Infected *Akodon* affinis *montensis* and *Oligoryzomys nigripes* native rodents were found in protected areas of Misiones.

Orthohantavirus is a genus of globally distributed RNA viruses in the family *Hantaviridae*. In the Americas, the viruses are hosted by native rodent species within the Cricetidae family (*1*). Although not all orthohantaviruses cause disease in humans, some genotypes are etiologic agents of hantavirus cardiopulmonary syndrome (HCPS), a serious emerging disease (*1*). Along with Brazil and Chile, Argentina is among the countries in South America with the highest incidence of HCPS (*1*). HCPS cases in the country are distributed in 4 epidemiologic regions; incidence is lowest in the northeast. HCPS cases in that region were first registered in 2003 in the south of Misiones province (*2*). Those cases led to the identification of Lechiguanas virus and Juquitiba virus, 2 *Orthohantavirus andesense*–like genotypes, as etiologic agents, and of *Oligoryzomys nigripes* (black-footed pygmy rice rats) as a reservoir of Juquitiba virus, whereas the host of Lechiguanas virus (presumably *O. flavescens* yellow pygmy rice rats) was not confirmed (*2*). Almost 15 years later, infected montane grass mice (*Akodon montensis*) were detected in north Misiones, implicating this species as a new reservoir for orthohantavirus in Argentina (*3*).

Since 2003, <10 orthohantavirus cases have been diagnosed in Misiones (*4*,*5*). However, the circulation of >1 pathogenic genotype and the presence of 3 known orthohantavirus reservoirs, together with a higher incidence of human cases in neighboring states of Brazil, suggest that HCPS might be underreported in this province (*2*,*3*,*6*). Underreporting is likely a result of the high rates of poverty, rurality, and lack of access to healthcare in Misiones (*7*,*8*), factors that are known to contribute to underreporting of diseases (*9*). To identify areas with a potential for higher risk for HCPS, identifying areas where pathogenic orthohantavirus circulates within the rodent community is crucial. In this study, we sought to estimate the seroprevalence of orthohantavirus (as a proxy for infection) and identify the main hosts in protected areas of Misiones. This research was reviewed and approved by the institutional animal care and use committee of the University of Buenos Aires (Faculty of Natural and Exact Sciences).

The Study

We conducted 24 trapping sessions spanning 2–4 consecutive nights in 10 protected areas throughout Misiones Province: Iguazú National Park and Urugua-í Provincial Park in the north; Cruce Caballero, Piñalito, Caá Yarí, and Moconá provincial parks and Forestal Belga protected area in the central part of the province; and Osununú Natural Reserve, Campo San Juan Federal Park, and De las Sierras Provincial Park in the south (Figure 1). We live-trapped rodents during October 2019–February

Author affiliations: Consejo Nacional de Investigaciones Científicas y Técnicas (CONICET), Buenos Aires, Argentina (M.V. Vadell, E.F. Burgos, D. Lamattina, L. Tauro, O.D. Salomón, I.E. Gómez Villafañe); Instituto Nacional de Medicina Tropical, ANLIS Dr. C.G. Malbrán, Puerto Iguazú, Argentina (M.V. Vadell, E.F. Burgos, D. Lamattina, O.D. Salomón); Instituto Nacional de Enfermedades Infecciosas, ANLIS Dr. C.G. Malbrán, Buenos Aires (C. Bellomo, V. Martínez, R. Coelho); Instituto de Biología Subtropical (UNaM–CONICET), Misiones, Argentina (C. Lanzone, C.A. Labaroni, L. Tauro); Instituto de Ecología, Genética y Evolución de Buenos Aires (CONICET-UBA), Facultad de Ciencias Exactas y Naturales, Universidad de Buenos Aires, Buenos Aires (I.E. Gómez Villafañe)

DOI: https://doi.org/10.3201/eid3007.240183

Figure 1. Study areas (green dots) in Misiones Province and part of Corrientes Province (first-level subnational administrative division) in study of orthohantavirus, northeastern Argentina. The Selva Paranaense (Alto Paraná Atlantic Forest) ecoregion is shown in green and Campos y Malezales (savanna-like ecoregion) is shown in yellow. Mouse icons indicate the sites where seropositive *Oligoryzomys* sp. rodents (in orange) and *Akodon* affinis *montensis* mice (in blue) were detected.

2023. In each area, we set 60–200 Sherman traps, plus 90 cage traps in some areas, along tracks in the woods. We baited Sherman traps using a mixture of peanut butter, fat, and rolled oats (plus bananas and sardines in most trapping sessions), whereas we baited cage traps with chicken meat and carrots. We identified captured animals up to the last taxonomic level possible according to external morphology. We recorded sex and reproductive conditions of individual rodents. We obtained a blood sample from a small cut on the tip of the tail and later used that sample to analyze the presence of antibodies against orthohantaviruses by using ELISA (*10*). To estimate the diversity of the small rodent community in each study area, we calculated richness, Shannon-Wiener diversity index ($-\Sigma p_i \times \ln(p_i)$, where p_i is the relative proportion of species i in the community), evenness (H/H_{max}, where $H_{max} = \ln[S]$), and Simpson diversity index ($1 - \Sigma p_i^2$) using the overall data per trapping area.

A total of 12,424 trap nights yielded 765 rodents of 9 species, resulting in an overall trap success of 6.16%. Species consisted of *A.* affinis *montensis* mice (656), *Oligoryzomys* sp. rodents (28, 1 confirmed as *O. nigripes*), *Sooretamys angouya* (rat-headed rice rat) (23), *Thaptomys nigrita* (blackish grass mouse) (17), *Nectomys squamipes* (scaly-footed water rat) (14), *Euryoryzomys russatus* (big-headed rice rat) (11), *Brucepattersonius iheringi* (Ihering's akodont) (9), *Oxymycterus quaestor* (quaestor hocicudo) (2), and *Rattus rattus* (black rat) (5) (Table 1).

We detected antibodies against orthohantavirus in *A.* aff. *montensis* mice with an overall seroprevalence of 0.007; overall seroprevalence in *Oligoryzomys* sp. rodents was 0.083 (Table 2). Seropositive rodents were captured in 4 natural areas, Urugua-í, Cruce Caballero, Iguazú, and Forestal Belga; Urugua-í was the only area in which antibodies were found in both species (Table 2; Figure 1). Because of its relevance to this research, the seropositive *Oligoryzomys* sp. rodent captured in Iguazú National Park was identified at the species level through molecular characterization. We amplified a fragment of the cytochrome b gene (1073 bp) by PCR using primers Mus 14095 and Mus 15398 (*11*). We used BLAST (http://blast.ncbi.nlm.nih.gov) to compare the sequence obtained (GenBank accession no. PP372564) with reference GenBank sequences and identified it as *O. nigripes* (98.71% BLAST identity and 100% coverage).

All seropositive rodents were active males (the sex of 1 seropositive *Oligoryzomys* sp. rodent was

Table 1. Number of captures per species and values of diversity indices in each trapping session and for each area in study of orthohantavirus in Misiones Province, northeastern Argentina*

Study area	Trapping session	Species									Index			
		Am	*Tn*	*O*	*Sa*	*Er*	*Bi*	*Oq*	*Ns*	*Rr*	S	H	E	D
Iguazú	2021 Apr	20	0	0	0	0	0	0	0	0	1	0.00	NA	0.00
	2021 Nov	3	0	2	0	0	0	0	0	0	2	0.67	0.97	0.48
	2022 Apr	7	0	0	0	0	0	0	0	0	1	0.00	NA	0.00
	Overall	30	0	2	0	0	0	0	0	0	2	0.23	0.34	0.12
Urugua-í	2021 Jun	24	1	0	0	0	0	0	0	0	2	0.17	0.24	0.08
	2021 Dec	47	1	4	7	0	1	0	0	0	5	0.76	0.47	0.37
	2022 Feb	82	10	2	0	0	0	0	0	0	3	0.44	0.40	0.23
	2022 Jun	62	2	1	0	1	0	0	0	0	4	0.29	0.21	0.12
	Overall	215	14	7	7	1	1	0	0	0	6	0.53	0.29	0.22
Piñalito	2021 Apr	56	0	0	0	0	0	0	0	0	1	0.00	NA	0.00
	2021 Nov†	4	0	2	3	0	0	0	0	0	3	1.06	0.97	0.64
	2022 Apr†	40	1	0	0	0	0	0	0	0	2	0.11	0.17	0.05
	Overall	100	1	2	3	0	0	0	0	0	4	0.27	0.20	0.11
Forestal Belga	2019 Oct†	19	1	2	0	4	1	0	3	0	6	1.20	0.67	0.56
	2021 Oct†	2	0	0	4	0	0	0	0	0	2	0.64	0.92	0.44
	Overall	21	1	2	4	4	1	0	3	0	7	1.37	0.70	0.62
Cruce Caballero	2021 Apr	31	0	0	0	1	1	0	0	0	3	0.27	0.25	0.12
	2021 Nov†	19	1	0	4	1	1	0	0	0	5	0.89	0.55	0.44
	2022 Apr†	54	0	0	0	1	1	0	0	0	3	0.18	0.16	0.07
	Overall	104	1	0	4	3	3	0	0	0	5	0.44	0.27	0.18
Caá Yarí	2021 Aug	6	0	2	0	0	0	0	4	0	3	1.01	0.92	0.61
Moconá	2022 Apr	23	0	3	0	3	4	2	0	0	5	1.11	0.69	0.54
Osununú	2021 Aug	12	0	0	0	0	0	0	0	0	1	0.00	NA	0.00
	2021 Oct	7	0	0	1	0	0	0	0	0	2	0.38	0.54	0.22
	2022 Jan	22	0	0	0	0	0	0	0	0	1	0.00	NA	0.00
	Overall	41	0	0	1	0	0	0	0	0	2	0.11	0.16	0.05
Campo San Juan	2021 Aug	13	0	7	0	0	0	0	5	0	3	1.02	0.93	0.61
	2022 Nov†	40	0	0	0	0	0	0	0	5	2	0.35	0.50	0.20
	2023 Feb†	55	0	1	0	0	0	0	0	0	2	0.09	0.13	0.04
	Overall	108	0	8	0	0	0	0	5	5	4	0.56	0.41	0.26
De las Sierras	2021 Oct	8		2	4		0	0	2	0	4	1.21	0.88	0.66

*_Am_, _Akodon_ affinis _montensis_; _Bi_, _Brucepattersonius iheringi_; D, Simpson index; E, evenness index; _Er_, _Euryoryzomys russatus;_ H, Shannon-Wiener index; NA, not applicable; _Ns_, _Nectomys squamipes_; _O_, _Oligoryzomys_ sp.; _Oq_, _Oxymycterus quaestor_; _Rr_, _Rattus rattus_; S, richness index; _Sa_, _Sooretamys angouya_; _Tn_, _Thaptomys nigrita_.
†Both cage and Sherman traps were used in these trapping sessions (more Sherman traps than cage traps)

not recorded). Overall male-to-female ratio by species was 1.7:1 for *A.* aff. *montensis* and 2.3:1 for *Oligoryzomys* sp.

Overall seroprevalence in *A.* aff. *montensis* mice was significantly correlated (Spearman test) with richness ($\rho = 0.775$, $p = 0.008$) but not with the Shannon-Wiener diversity index ($\rho = 0.261$, $p = 0.466$), evenness index ($\rho = -0.052$, $p = 0.886$), or Simpson diversity index ($\rho = 0.172$, $p = 0.636$) (Figure 2). Overall seroprevalence of *Oligoryzomys* sp. rodents was not significantly correlated with any of the diversity measures (richness, $\rho = -0.110$, $p = 0.762$; Shannon-Wiener diversity, $\rho = -0.372$, $p = 0.290$; evenness, $\rho = -0.164$, $p = 0.65$; Simpson diversity, $\rho = -0.277$, $p = 0.439$) (Figure 2).

Conclusions

Our findings not only expand the known distribution of orthohantavirus in Misiones, Argentina, but also provide evidence of orthohantavirus infection in *O. nigripes* rodents in the north of this province, suggesting the presence of a pathogenic genotype in an area without known human cases. This information is relevant, particularly considering that Iguazú National Park, where 1 seropositive *O. nigripes* rat was captured, is visited by >1 million tourists every year.

Several pathogenic orthohantavirus have been associated with *O. nigripes* rodents and other *Oligoryzomys* spp. rodents in eastern Paraguay, southern Brazil, and northeastern Argentina (*1*,*2*,*12*), suggesting the seropositive animals detected in this study are probably hosts of a pathogenic genotype. However, the possibility of a spillover event from infected *A.* aff. *montensis* mice cannot be ruled out because this species is an orthohantavirus host in north Misiones (*3*). In fact, *Oligoryzomys* spp. rodents and *A.* aff. *montensis* mice were found in sympatry in all but 2 areas, suggesting the high potential for genetic reassortment and host-switching events (*13*), particularly in Urugua-í, where both species were found seropositive. Future studies should aim to identify the orthohantavirus genotypes in these hosts.

Although the male-to-female ratio was close to 2:1 for both species, the fact that all seropositive

Table 2. Number of trap nights, total captures (xcluding same-session recaptures) and seroprevalence of orthohantavirus in *Akodon* affinis *montensis* and *Oligoryzomys* sp. rodents in each trapping session and overall in each study area in study of orthohantavirus in Misiones Province, northeastern Argentina

Location	Trapping session	Trap nights	Total captures	*A.* aff. *montensis* seroprevalence	*Oligoryzomys* sp. seroprevalence
Iguazú	2021 Apr	300	20	0 (0/20)	0 (0/0)
	2021 Nov	800	5	0 (0/3)	0.5 (1/2)
	2022 Apr	534	7	0 (0/7)	0 (0/0)
Urugua-í	2021 Jun	792	25	0 (0/22)	0 (0/0)
	2021 Dec	800	60	0.021 (1/47)	0.25 (1/4)
	2022 Feb	540	94	0 (0/82)	0 (0/0)
	2022 Jun	800	66	0 (0/57)	0 (0/1)
Piñalito	2021 Apr	400	56	0 (0/54)	0 (0/0)
	2021 Nov*	920	9	0 (0/4)	0 (0/2)
	2022 Apr*	400	41	0 (0/14)	0 (0/0)
Forestal Belga	2019 Oct*	750	30	0 (0/19)	0 (0/2)
	2021 Oct*	720	6	1.0 (1/1)	0 (0/0)
Cruce Caballero	2021 Apr	300	33	0.032 (1/31)	0 (0/0)
	2021 Nov*	920	26	0.071 (1/19)	0 (0/0)
	2022 Apr*	720	56	0 (0/54)	0 (0/0)
Caá Yarí	2021 Aug	390	12	0 (0/5)	0 (0/2)
Moconá	2022 Apr	680	35	0 (0/20)	0 (0/2)
Osununú	2021 Aug	648	12	0 (0/9)	0 (0/0)
	2021 Oct	656	8	0 (0/5)	0 (0/0)
	2022 Jan	776	22	0 (0/21)	0 (0/0)
Campo San Juan	2021 Aug	360	25	0 (0/8)	0 (0/7)
	2022 Nov*	720	45	0 (0/34)	0 (0/0)
	2023 Feb*	720	56	0 (0/47)	0 (0/0)
De las Sierras	2021 Oct	438	16	0 (0/8)	0 (0/2)

*Both cage and Sherman traps were used in this trapping session (more Sherman traps than cage traps).

rodents were reproductively active males supports the role of sex in orthohantavirus transmission (*1*,*3*,*14*). Seroprevalence in *A.* aff. *montensis* mice was positively correlated with richness. However, that evidence is weak because of the low number of sites with seropositive rodents and was not supported by any other diversity measure.

The low overall seroprevalence detected in this study suggests HCPS risk is low in Misiones Province. However, the capacity of cricetid populations to peak unexpectedly under certain conditions (*14*,*15*), in addition to the evidence of orthohantavirus circulation in northern and central Misiones, highlight the potential risk and the need to continue surveillance.

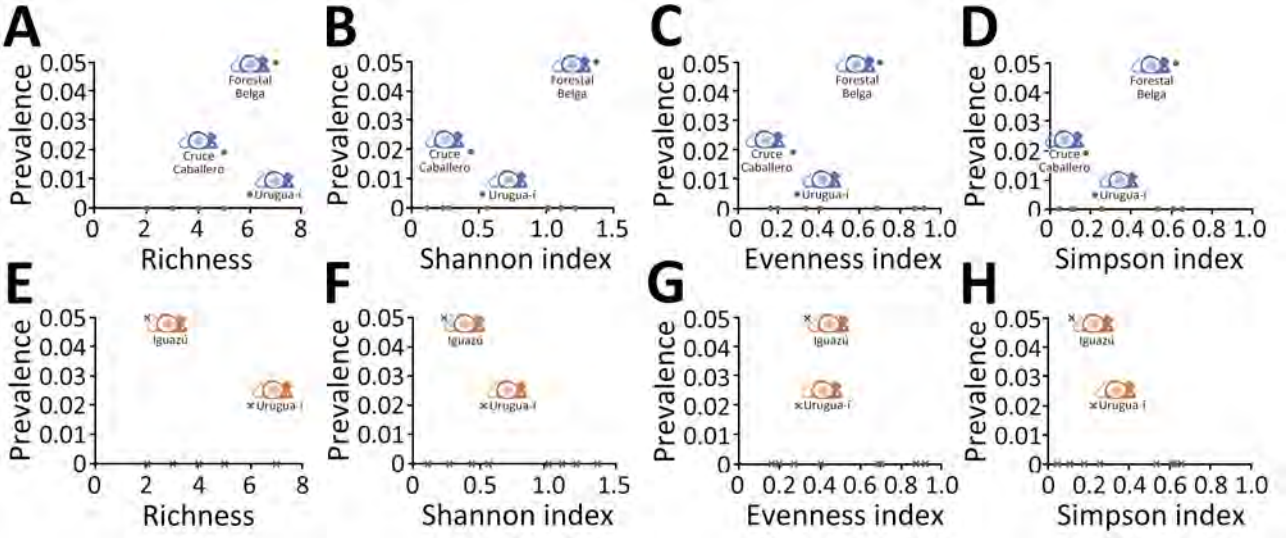

Figure 2. Orthohantavirus seroprevalence in *Akodon* affinis *montensis* mice (green dots) and in *Oligoryzomys* sp. rodents (blue crosses) as a function of richness and Shannon-Wiener, evenness, and Simpson indices in study of orthohantavirus in Misiones Province, northeastern Argentina. Mouse icons indicate presence of seropositive *A.* aff. *montensis* (in blue) and *Oligoryzomys* sp. (in orange) rodents.

Acknowledgments

We are thankful to all park guards and employees in the study areas for their hospitality and collaboration and to all field assistants who helped us in fieldwork, particularly Nilso Molina, Ramón Sosa, Santiago Carrizo, and Milagros Galotta. We would also like to thank Administración de Parques Nacionales (National Parks Administration) and Ministerio de Ecología y Recursos Renovables de Misiones (Ecology and Renewable Resources Ministry of Misiones Province) for granting us support and authorization to work in the field. We also thank Laurie Bonneville for her help with English grammar. We are grateful for the dedicated comments and suggestions of the anonymous reviewers, which helped us to enrich this manuscript.

We dedicate this article to the memory of our coauthor, Laura Tauro, who died May 23, 2023.

Organizations and institutions that provided funding for this research: Agencia Nacional de Promoción Científica y Tecnología (PICT 2018-#1652, PICT-2020-#01910, PICT 2019-#02710), Universidad de Buenos Aires (UBACyT 2018-#20-20020170100171BA), Consejo Nacional de Investigaciones Científicas y Técnicas (PIP 2015-#11220150100536CO; PIBAA 2022-2023 #2872021 0101231), Ministerio de Salud de la Nación Argentina (FOCANLIS 2019 - NRU 1907), Instituto Nacional de Medicina Tropical, and Fundación Temaikèn.

About the Author

Dr. Vadell is a CONICET research biologist at the Instituto Nacional de Medicina Tropical in Misiones, Argentina. Her interests focus on wildlife ecology and understanding pathogen-host interactions, particularly rodent and bat-borne viruses.

References

1. Vadell MV. Hantaviruses—a concise review of a neglected virus. In: Ahmad SI, editor. Human viruses: diseases, treatments and vaccines. Cham (Switzerland): Springer; 2021. p. 387–407.
2. Padula P, Martinez VP, Bellomo C, Maidana S, San Juan J, Tagliaferri P, et al. Pathogenic hantaviruses, northeastern Argentina and eastern Paraguay. Emerg Infect Dis. 2007;13:1211–4. https://doi.org/10.3201/eid1308.061090
3. Burgos EF, Vadell MV, Bellomo CM, Martinez VP, Salomon OD, Gómez Villafañe IE. First evidence of *Akodon*-borne orthohantavirus in northeastern Argentina. EcoHealth. 2021;18:429–39. https://doi.org/10.1007/s10393-021-01564-6
4. Chesini F, Brunstein L, Perrone M, Orman M, Gazia M, Gómez A, et al. Climate and health in Argentina: diagnosis of the situation 2018 [in Spanish] [cited 2023 Nov 22]. https://repositorio.smn.gob.ar/handle/20.500.12160/1223
5. National Health Ministry of Argentina. Integrated Surveillance Report No. 106. Epi-week no 4 January 2012 [in Spanish] [cited 2023 Sep 12]. https://bancos.salud.gob.ar/sites/default/files/2020-01/boletinintegradodevigilanciaversion_n106-se04.pdf
6. Pinto Junior VL, Hamidad AM, Albuquerque Filho DdO, Santos VMd. Twenty years of hantavirus pulmonary syndrome in Brazil: a review of epidemiological and clinical aspects. J Infect Dev Ctries. 2014;8:137–42.
7. World Bank, Demombynes G, Verner D. The invisible poor: a portrait of rural poverty in Argentina. Washington: World Bank Publications; 2010.
8. National Health Ministry of Argentina. Basic indicators. 26th edition [in Spanish]. Buenos Aires: Ministerio de Salud y Organización Panamericana de la Salud; 2022.
9. Gibbons CL, Mangen M-JJ, Plass D, Havelaar AH, Brooke RJ, Kramarz P, et al.; Burden of Communicable diseases in Europe (BCoDE) consortium. Measuring underreporting and under-ascertainment in infectious disease datasets: a comparison of methods. BMC Public Health. 2014;14:147. https://doi.org/10.1186/1471-2458-14-147
10. Padula PJ, Rossi CM, Valle MOD, Martínez PV, Colavecchia SB, Edelstein A, et al. Development and evaluation of a solid-phase enzyme immunoassay based on Andes hantavirus recombinant nucleoprotein. J Med Microbiol. 2000;49:149–55. https://doi.org/10.1099/0022-1317-49-2-149
11. Anderson S, Yates TL. A new genus and species of phyllotine rodent from Bolivia. J Mammal. 2000;81:18–36. https://doi.org/10.1644/1545-1542(2000)081<0018:ANGASO>2.0.CO;2
12. Eastwood G, Camp JV, Chu YK, Sawyer AM, Owen RD, Cao X, et al. Habitat, species richness and hantaviruses of sigmodontine rodents within the Interior Atlantic Forest, Paraguay. PLoS One. 2018;13:e0201307. https://doi.org/10.1371/journal.pone.0201307
13. Klempa B. Reassortment events in the evolution of hantaviruses. Virus Genes. 2018;54:638–46. https://doi.org/10.1007/s11262-018-1590-z
14. de Oliveira RC, Guterres A, Fernandes J, D'Andrea PS, Bonvicino CR, de Lemos ER. Hantavirus reservoirs: current status with an emphasis on data from Brazil. Viruses. 2014;6:1929–73. https://doi.org/10.3390/v6051929
15. Douglass RJ, Vadell MV. How much effort is required to accurately describe the complex ecology of a rodent-borne viral disease? Ecosphere. 2016;7:e01368. https://doi.org/10.1002/ecs2.1368

Address for correspondence: María Victoria Vadell, Instituto Nacional de Medicina Tropical, Puerto Iguazú, Misiones, 3370, Argentina; email: toyavadell@gmail.com or victoria.vadell@conicet.gov.ar

Rickettsia parkeri Rickettsiosis in Kidney Transplant Recipient, North Carolina, USA, 2023

Gautam M. Phadke, Kiran Gajurel, Jennifer Kasten, Marlene DeLeon-Carnes, Carmen Ramos, Sandor E. Karpathy, Arlyn N. Gleaton, Sydney N. Adams, Pallavi D. Annambhotla, Sridhar V. Basavaraju, Carl Williams, Christopher D. Paddock

Spotted fever rickettsiosis is rarely observed in solid organ transplant recipients, and all previously reported cases have been associated with tick bite months to years after transplantation. We describe a kidney transplant recipient in North Carolina, USA, who had a moderately severe *Rickettsia parkeri* infection develop during the immediate posttransplant period.

Spotted fever rickettsiosis in solid organ transplant recipients is rarely described, and all reports document disease acquired months to years after the transplant, after recognized tick bites or exposures to tick-infested habitats (*1*–*4*). In the United States, *Rickettsia parkeri* rickettsiosis is a tickborne infection transmitted by the Gulf Coast tick (*Amblyomma maculatum*) that results in a disease similar to but milder than Rocky Mountain spotted fever. Human infection with *R. parkeri* was first described in 2004 (*5*). We report a case of *R. parkeri* rickettsiosis in a kidney transplant recipient in North Carolina, USA, during the immediate posttransplant period.

The Case

In July 2023, a 56-year-old woman in central North Carolina who had end-stage renal disease from autosomal dominant Alport syndrome received a living unrelated kidney transplant from a 52-year-old woman, also a resident of central North Carolina (Figure 1). The recipient received alemtuzumab and methylprednisolone for induction immunosuppression and tacrolimus and mycophenolate for maintenance immunosuppression. She received 2 units of packed red blood cells from 2 blood donors, from central North Carolina and western South Carolina, on the first day after transplantation. Five days later, fever developed (101°F), along with a diffuse rash involving her chest and upper and lower extremities and arthralgia involving her ankles, knees, and hips. Seven days after transplantation, arthralgia extended to her elbows, wrists, and metacarpophalangeal joints, and additional rash lesions appeared on her extremities and chest. She was readmitted the next day with pain in the left knee and left elbow. A tender maculopapular rash, comprising ≈30 lesions of 0.2–3 cm in greatest dimension, was identified on her chest and extremities (Figure 2, panels A, B). No eschars were identified.

At admission, laboratory results were notable for elevated erythrocyte sedimentation rate (26 mm/h; reference ≤20 mm/h) and C-reactive protein (3.2 mg/dL; reference <0.5 mg/dL). Peripheral leukocyte and platelet counts remained within reference limits during her hospitalization. Because of a history of gout, empiric methylprednisolone (100 mg/d for 3 d) was initiated. The patient subsequently had intermittent low-grade fever to 100.9°F, mild elevations in hepatic transaminases (peak aspartate aminotransferase 75 U/L [reference 13–39 U/L], peak alanine aminotransferase 109 U/L [reference 7–52 U/L]), additional rash lesions on her extremities and chest, and 2-mm tender ulcerated lesions on her inner lip. Nine days after transplantation, a biopsy from a rash lesion showed multifocal perivascular neutrophilic infiltrates. A plasma specimen

Author affiliations: Metrolina Nephrology Associates, Charlotte, North Carolina, USA (G. Phadke), Carolinas Medical Center, Atrium Health, Charlotte (G. Phadke, K. Gajurel); Centers for Disease Control and Prevention, Atlanta, Georgia, USA (J. Kasten, M. DeLeon-Carnes, C. Ramos, S. Karpathy, A.N. Gleaton, S.N. Adams, P.D. Annambhotla, S.V. Basavaraju, C.D. Paddock); Oak Ridge Institute for Science and Education, Oak Ridge, Tennessee, USA (S.N. Adams); North Carolina Department of Health and Human Services, Raleigh, North Carolina, USA (C. Williams)

DOI: https://doi.org/10.3201/eid3007.240217

was obtained 12 days after transplantation and evaluated by a microbial cell-free DNA test (Karius, https://kariusdx.com) that identified *R. parkeri* (88 DNA molecules/μL, reference <10 DNA molecules/μL). Therapy with oral doxycycline (100 mg 2×/d) was initiated ≈2 weeks after transplantation. Her arthralgias improved within 2 days, and rash resolved within 5 days. Approximately 3 weeks after completing a 14-day course of doxycycline, she reported mild arthralgia involving hand, ankle and hip joints, and a few macular lesions recurred on her extremities. Doxycycline was administered for an additional 2 weeks, and complete resolution of disease ensued.

The transplant recipient denied recent tick bite or exposure to tick-infested habitats during the 2 weeks before transplantation and remained indoors from the time of hospital discharge until readmission. Neither blood donor reported a tick bite in the 2 weeks preceding their donations in late June and early July or an illness during the 2 weeks after donation. The blood collection establishment identified no similar illnesses in other recipients who received other blood products from those donors. The kidney donor recalled a bite from a large brown tick with white markings ≈2 weeks before transplantation; however, the donor had no illness in the subsequent weeks.

The Centers for Disease Control and Prevention tested residual pretransplant and posttransplant serum samples from the kidney donor and the recipient and samples from each blood donor at the time of donation by using indirect immunofluorescence antibody assays to detect IgG reactive with *R. rickettsii* and *R. parkeri* antigens (*5*). Titers ≥64 were considered positive. DNA extracted from residual whole blood, serum, or plasma samples from the recipient, kidney donor, and blood donors was tested by using a real-time PCR targeting a segment of the 23S rRNA gene of *Rickettsia* spp. (*6*) and by an *R. parkeri*–specific real-time PCR (*7*). The Centers for Disease Control and Prevention also evaluated the skin biopsy specimen, stained by an immunoalkaline phosphatase technique for multiple species of spotted fever group *Rickettsia*, including *R. parkeri*; DNA was extracted and evaluated by a multiplex real-time PCR to detect *R. parkeri* (*8*). Cycle threshold values <40 were considered positive for each PCR.

The 4 serum specimens from the kidney recipient collected 2 weeks pretransplant through 7 weeks posttransplant showed titers ≤32 against both antigens (Figure 1). Serum specimens obtained from the kidney donor on the day of transplant through 7 weeks posttransplant revealed a stationary titer of 64 to antigens of *R. rickettsii* and titers ≤32 to those of *R. parkeri*. Aliquots obtained from both samples of residual transfused blood revealed titers <32 to *R. parkeri* and *R. rickettsii* antigens. No *R. parkeri* DNA was detected in pretransplant or posttransplant whole blood, serum, or plasma specimens from the recipient or from the organ or blood donors.

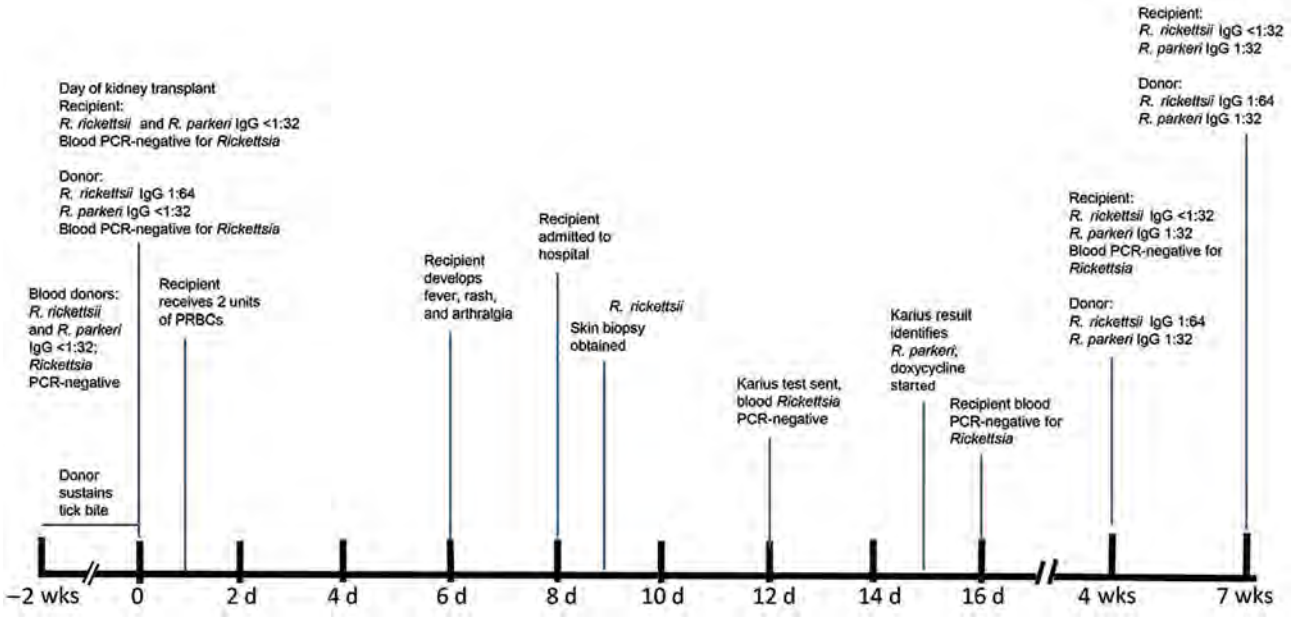

Figure 1. Transmission and testing timeline for case of *Rickettsia parkeri* rickettsiosis in a kidney transplant receipient, North Carolina, USA, 2023. Pretransplant samples were tested retrospectively to determine possible transmission risk from 2 blood donors and the kidney donor. PRBCs, packed red blood cells.

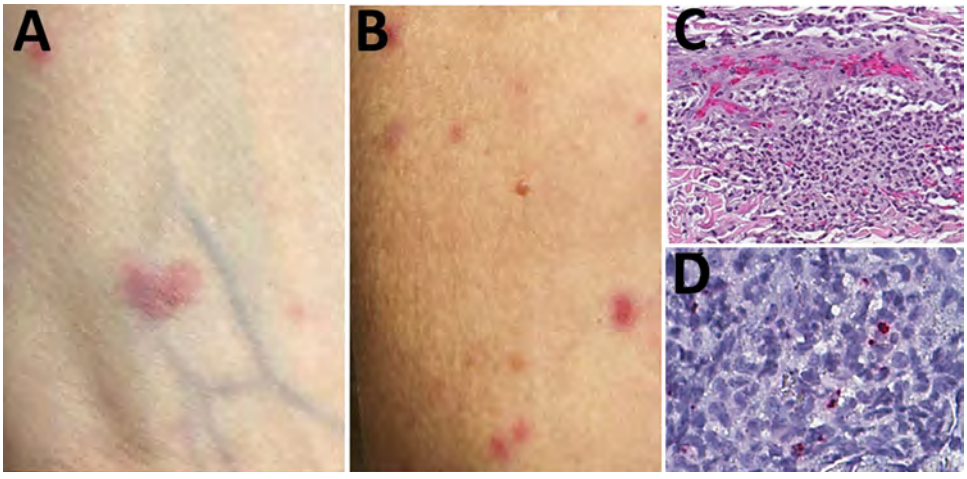

Figure 2. Skin lesions and testing results for a kidney transplant receipient diagnosed with *Rickettsia parkeri* rickettsiosis, North Carolina, USA, 2023. A, B) Sparse maculopapular rash involving forearms. Lesions ranged from 0.2 to 3 cm in greatest dimension and were tender and erythematous. C) Histopathologic appearance of rash lesion demonstrating perivascular collections of mixed inflammatory cell infiltrates in the mid-dermis comprising predominantly neutrophils and macrophages. Hematoxylin and eosin stain; original magnification ×50. D) Immunohistochemical detection of antigens of *R. parkeri* (red) in dermal inflammatory cell infiltrates. Immunoalkaline phosphatase with naphthol-fast red and hematoxylin counterstain; original magnification ×100.

Histologic evaluation of the skin biopsy specimen revealed small vessel vasculitis with thrombi, perivascular inflammatory cell infiltrates comprising neutrophils, lymphocytes, and macrophages; and periadnexal fibrinoid necrosis (Figure 2, panel C). An immunohistochemical stain for spotted fever group *Rickettsia* spp. identified rickettsial antigens in the inflammatory cell infiltrates (Figure 2, panel D), and real-time PCR detected *R. parkeri* DNA in the tissue.

Conclusions

We identified *R. parkeri* rickettsiosis in a kidney transplant recipient in the immediate posttransplant period. The organ donor, 1 of the blood donors, and the recipient resided in the Piedmont region of North Carolina, where *R. parkeri*–infected Gulf Coast ticks have been identified repeatedly (*9*,*10*). The mode of acquisition of *R. parkeri* remains undetermined, although evidence indicates this infection was possibly acquired through transplantation (*11*), including absence of tick bite or exposure to tick-infested habitat by the recipient during the 2 weeks before transplantation; absence of an inoculation eschar in the recipient; and documented tick bite of the donor by an adult tick morphologically compatible with *A. maculatum* 2 weeks before organ procurement. Neither an illness compatible with a rickettsioisis nor a seroconversion to antigens of spotted fever group *Rickettsia* were identified for the donor; nonetheless, recent surveys suggest that up to 30%–40% of adult *A. maculatum* ticks are infected with *R. parkeri* in the Piedmont region of North Carolina where the donor resided (*9*,*10*). The donor reported frequent tick bites during her lifetime, suggesting the possibility of an asymptomatic infection after repeated past exposures to *R. parkeri* (*12*). Transfusion-associated transmission of *R. rickettsii*, the agent of Rocky Mountain spotted fever, has been described (*13*); however, we believe that transmission route was less likely because of the composite histories, negative serologic and molecular test results of residual blood from each transfused unit, and absence of illness compatible with rickettsiosis in the blood donors or other recipients of blood products from the blood donors. Lack of a serologic response in the recipient was likely related to an intensive immunosuppresive regimen that included alemtuzumab during the postoperative period.

This case highlights the utility of increasingly sensitive and commercially available molecular methods to detect otherwise unsuspected or difficult-to-diagnose infectious diseases, including rickettsioses, in solid organ transplant recipients (*14*). Although tickborne pathogens constitute a small proportion of infections transmitted by solid organ transplants (*15*), enhanced awareness of their potential occurrence, coupled with increasingly sensitive methods of pathogen-diagnostic laboratory detection, will reveal additional cases of rickettsial diseases in this patient cohort.

Acknowledgments

We thank Diane Derkowski, Lorie Lockwood, and Christina Maguire for helping gather data and samples.

About the Author

Dr. Phadke is a consultant nephrologist with Metrolina Nephrology Associates and Atrium Health, Charlotte, North Carolina. His research interests are kidney transplantation, glomerular diseases, and hypertension.

References

1. Rallis TM, Kriesel JD, Dumler JS, Wagoner LE, Wright ED, Spruance SL. Rocky Mountain spotted fever following cardiac transplantation. West J Med. 1993;158:625–8.
2. Barrio J, de Diego A, Ripoll C, Perez-Calle JL, Núñez O, Salcedo M, et al. Mediterranean spotted fever in liver transplantation: a case report. Transplant Proc. 2002;34:1255–6. https://doi.org/10.1016/S0041-1345(02)02807-5
3. Schmulewitz L, Moumile K, Patey-Mariaud de Serre N, Poirée S, Gouin E, Mechaï F, et al. Splenic rupture and malignant Mediterranean spotted fever. Emerg Infect Dis. 2008;14:995–7. https://doi.org/10.3201/eid1406.071295
4. Kondo M, Nishikawa K, Iida S, Nakanishi T, Habe K, Yamanaka K. Japanese spotted fever and irreversible renal dysfunction during immunosuppressive therapy after a living-donor kidney transplant. Trop Med Infect Dis. 2022;7:175. https://doi.org/10.3390/tropicalmed7080175
5. Paddock CD, Finley RW, Wright CS, Robinson HN, Schrodt BJ, Lane CC, et al. *Rickettsia parkeri* rickettsiosis and its clinical distinction from Rocky Mountain spotted fever. Clin Infect Dis. 2008;47:1188–96. https://doi.org/10.1086/592254
6. Kato CY, Chung IH, Robinson LK, Austin AL, Dasch GA, Massung RF. Assessment of real-time PCR assay for detection of *Rickettsia* spp. and *Rickettsia rickettsii* in banked clinical samples. J Clin Microbiol. 2013;51:314–7. https://doi.org/10.1128/JCM.01723-12
7. Jiang J, Stromdahl EY, Richards AL. Detection of *Rickettsia parkeri* and *Candidatus* Rickettsia andeanae in *Amblyomma maculatum* Gulf Coast ticks collected from humans in the United States. Vector Borne Zoonotic Dis. 2012;12:175–82. https://doi.org/10.1089/vbz.2011.0614
8. Denison AM, Amin BD, Nicholson WL, Paddock CD. Detection of *Rickettsia rickettsii, Rickettsia parkeri*, and *Rickettsia akari* in skin biopsy specimens using a multiplex real-time polymerase chain reaction assay. Clin Infect Dis. 2014;59:635–42. https://doi.org/10.1093/cid/ciu358
9. Varela-Stokes AS, Paddock CD, Engber B, Toliver M. *Rickettsia parkeri* in *Amblyomma maculatum* ticks, North Carolina, USA, 2009-2010. Emerg Infect Dis. 2011;17:2350–3. https://doi.org/10.3201/eid1712.110789
10. Johnson CR, Ponnusamy L, Richards AL, Apperson CS. Analyses of bloodmeal hosts and prevalencce of *Rickettsia parkeri* in the Gulf Coast tick *Amblyomma maculatum* (Acari: Ixodidae) from a reconstructed Piedmont prairie ecosytem, North Carolina. J Med Entomol. 2022;59:1382–93. https://doi.org/10.1093/jme/tjac033
11. Green M, Covington S, Taranto S, Wolfe C, Bell W, Biggins SW, et al. Donor-derived transmission events in 2013: a report of the Organ Procurement Transplant Network Ad Hoc Disease Transmission Advisory Committee. Transplantation. 2015;99:282–7. https://doi.org/10.1097/TP.0000000000000584
12. Herrick KL, Pena SA, Yaglom HD, Layton BJ, Moors A, Loftis AD, et al. *Rickettsia parkeri* rickettsiosis, Arizona, USA. Emerg Infect Dis. 2016;22:780–5. https://doi.org/10.3201/eid2205.151824
13. Wells GM, Woodward TE, Fiset P, Hornick RB. Rocky Mountain spotted fever caused by blood transfusion. JAMA. 1978;239:2763–5. https://doi.org/10.1001/jama.1978.03280530027015
14. Park SY, Chang EJ, Ledeboer N, Messacar K, Lindner MS, Venkatasubrahmanyam S, et al. Plasma microbial cell-free DNA sequencing from over 15,000 patients identified a broad spectrum of pathogens. J Clin Microbiol. 2023;61:e0185522. https://doi.org/10.1128/jcm.01855-22
15. Saha A, Browning C, Dandamudi R, Barton K, Graepel K, Cullity M, et al. Donor-derived ehrlichiosis: 2 clusters following solid organ transplantation. Clin Infect Dis. 2022;74:918–23. https://doi.org/10.1093/cid/ciab667

Address for correspondence: Gautam Phadke, Metrolina Nephrology Associates and Carolinas Medical Center, Atrium Health, Division of Transplantation, Charlotte, NC 28204, USA; email: gautam.phadke@atriumhealth.org

Rocky Mountain Spotted Fever Mimicking Multisystem Inflammatory Syndrome in Hospitalized Children, Sonora, Mexico

Gerardo Álvarez-Hernández, Cristian N. Rivera-Rosas, J.R. Tadeo Calleja-López, David W. McCormick, Christopher D. Paddock, Jehan Bonizú Álvarez-Meza, Fabián Correa-Morales

We describe 5 children who had Rocky Mountain spotted fever (RMSF) and manifested clinical symptoms similar to multisystem inflammatory syndrome in Sonora, Mexico, where RMSF is hyperendemic. Physicians should consider RMSF in differential diagnoses of hospitalized patients with multisystem inflammatory syndrome to prevent illness and death caused by rickettsial disease.

Rocky Mountain spotted fever (RMSF), a tickborne disease caused by *Rickettsia rickettsii*, is the leading cause of death from rickettsial infections in the Western Hemisphere (*1*). The disease can progress rapidly to death or severe illness in persons who do not receive appropriate antimicrobial drug therapy within the first 5 days after illness onset (*1*–*3*).

Hyperendemic RMSF levels are present in several communities in the southwestern United States and multiple states across northern Mexico (*4*). Case-fatality rates in northern Mexico are 27%–33% (*5*,*6*). A total of 2,176 RMSF cases were identified in Mexico during 2015–2023, of which 933 (42.9%) patients were children and adolescents 1 month–19 years of age (*7*). Sonora, in northwestern Mexico, has the greatest RMSF burden within the country; 222 pediatric cases were identified during 2015–2022, comprising ≈50% of the state's total RMSF incidence during that period (*6*).

During March 2020–December 31, 2022, a total of 16,207 pediatric cases of COVID-19 occurred in Sonora, of which 434 (2.7%) case-patients were hospitalized and 36 died (case-fatality rate 0.22%) (*8*). However, national- or state-level data are not available for cases of multisystem inflammatory syndrome in children (MIS-C). The early signs and symptoms of RMSF are nonspecific and include fever, headache, rash, nausea, vomiting, arthralgia, and myalgia. Early manifestations of RMSF often resemble other common pediatric febrile illnesses, such as Kawasaki disease and toxic shock syndrome (*1*–*3*). As RMSF progresses, abdominal pain, extremity edema, dyspnea, tachycardia, hypotension, organ edema, hemorrhages, septic shock, distal necrosis of the extremities, and death can occur (*3*,*9*). The clinical profile of MIS-C (*10*,*11*) overlaps with that of severe rickettsioses, particularly during the later stages of RMSF infections, and this clinical similarity might lead to critical gaps in prompt diagnosis and treatment of both diseases in endemic regions. We describe 5 pediatric patients with RMSF admitted to a hospital in Sonora who were initially suspected of having MIS-C.

The Study

We identified patients after reviewing 8,432 inpatient admissions at the Sonora Children's Hospital in Hermosillo, Mexico, during September 30, 2020–December 31, 2022. During the study period, RMSF was diagnosed in 61 patients, COVID-19 in 27 patients, and MIS-C in 13/27 (48%) patients who had COVID-19 (*12*). We retrieved sociodemographic and clinical

Author affiliations: University of Sonora, Hermosillo, Mexico (G. Álvarez-Hernández, C.N. Rivera-Rosas, J.R.T. Calleja-López); Centers for Disease Control and Prevention, Atlanta, Georgia, USA (D.W. McCormick, C.D. Paddock); Sonora Children's Hospital, Hermosillo (J.B. Álvarez-Meza); Centro Nacional de Programas Preventivos y Control de Enfermedades, Mexico City, Mexico (F. Correa-Morales)

DOI: https://doi.org/10.3201/eid3007.240033

characteristics from medical charts. The study was approved by the Sonora Children's Hospital Institutional Review Board.

We used the World Health Organization case definition to identify patients with MIS-C (*13*); we defined evidence of COVID-19 as detectable SARS-CoV-2 antibodies in serum samples or a positive antigen test from a nasopharyngeal swab sample. We defined an RMSF case as a patient who had ≥2 acute clinical manifestations within 7 days, such as fever, headache, malaise, rash, diarrhea, vomiting, and a history of tick exposure, along with a single positive *Rickettsia* confirmatory test. Confirmatory tests included detection of *R. rickettsii* or *Rickettsia* spp. DNA in whole-blood specimens by using quantitative PCR (qPCR) or detection of *R. rickettsia*–specific IgG at a titer of ≥1:256 in a single serum specimen by using an indirect immunofluorescence assay.

We identified 5 patients with RMSF who also met World Health Organization criteria for MIS-C. The median patient age was 8 (range 6–17) years; 4 were male and 1 female (Table 1). The median duration from illness onset to hospital admission was 10 (range 4–10) days. All patients had a fever and rash; other common symptoms were abdominal pain in 3 (60%) patients and edema of the hands and feet in 3 (60%) patients. The rash preceded hospital admission in 4 (80%) patients. All patients reported a history of tick exposure and received corticosteroids; 3 received intravenous immunoglobulin for treatment of suspected MIS-C.

R. rickettsii infection was confirmed by IFA for 2 patients whose blood samples were drawn on the 6th and 13th days after onset of symptoms. Two patients were positive for *R. rickettsii* by qPCR, and qPCR detected *Rickettsia* spp. in 1 case. Although all patients received their first medical consultation within 1–3 days after onset of symptoms, a delay in clinical suspicion of RMSF beyond day 5 was found in 4 (80%) cases; the median delay in prescribing specific antimicrobial drugs for RMSF was 10 (range 3–13) days after symptom onset (Table 2). Doxycycline treatment was belatedly initiated in all 5 patients, in 4 at the time of hospital admission and in 1 patient 3 days after hospitalization.

Laboratory test abnormalities seen in the 5 patients included thrombocytopenia; elevated inflammatory markers such as C-reactive protein, procalcitonin, D-dimer, ferritin, and aminotransferases; and leukocytosis (Table 1). Four patients were admitted to the hospital's intensive care unit and required vasopressor support. Echocardiography was performed for 3 patients: 1 patient had no abnormal findings, 1 patient had trace pericardial effusion, and 1 patient had a 0.5 cm pericardial effusion and tricuspid regurgitation. The median duration of hospitalization was 13 (range 3–15) days. No patients died, and severe sequelae were not reported.

Conclusions

RMSF and MIS-C share clinical and laboratory test abnormalities and distinguishing between those 2

Table 1. Demographic, clinical, and laboratory test characteristics of patients at hospital admission in study of Rocky Mountain spotted fever mimicking multisystem inflammatory syndrome in hospitalized children, Sonora, Mexico*

Variable	Reference range	Case 1	Case 2	Case 3	Case 4	Case 5
Age, y		6.2	17.9	11.0	7.1	8.7
Sex		M	M	F	M	M
BMI Z-score†		0–1	1–2	1–2	1–2	>2
Laboratory confirmation of SARS-CoV-2 infection‡		Antigen+, IgM+	IgG+	IgG+, IgM+	IgG+	IgG+
Laboratory confirmation of *Rickettsia rickettsii* infection		IFA IgG 1:256	PCR	PCR	IFA IgG 1:2,048	PCR, *Rickettsia* spp.
Leukocyte count, × 10^3/μL	4.6–10.2	4.3	6.8	15.7	10.5	19.9
Platelet count, × 10^3/μL	150–450	72.0	57.0	45.0	22.0	317.0
Procalcitonin, ng/mL	0–0.5	10.8	2.6	75.4	6.6	0.8
C-Reactive protein, mg/dL	<0.5	10.8	17.1	10.2	6.6	NA
D-dimer, μg/mL	0–0.5	17.6	NA	7.9	3.6	NA
Ferritin, ng/mL	21–274	1,099.8	NA	5,474.4	3,229.2	1,260.30
Prothrombin time, s	11.1–14.1	14.7	16.0	14.0	17.6	16.3
Fibrinogen, mg/dL	200–400	215.0	NA	134.0	329.0	379.0
ESR, mm/h	3–10	35.0	26.0	20.0	65.0	40.0
LDH, U/L	240–480	NA	738.0	754.0	880.0	569.0
AST, U/L	5–34	91.0	186.0	111.0	121.0	69.0
ALT, U/L	0–55	44.0	76.0	47.0	54.0	77.0

*ALT, alanine aminotransferase; AST, aspartate aminotransferase; BMI, body mass index; ESR, erythrocyte sedimentation rate; IFA, indirect immunofluorescence assay; LDH, lactate dehydrogenase; NA, not available; ; +, positive.
†Calculated by using data from the World Health Organization (https://www.who.int/tools/growth-reference-data-for-5to19-years/indicators/bmi-for-age). According to those data, a normal BMI is defined as a Z-score of −1 to 1, an overweight BMI is defined as a Z-score of 1–2, and an obese BMI is defined as a Z-score of >2.
‡Confirmed by presence of SARS-CoV-2–specific IgG or IgM in serum samples or a positive antigen test from a nasopharyngeal swab sample.

Table 2. Medical therapies and selected characteristics of patients in study of Rocky Mountain spotted fever mimicking multisystem inflammatory syndrome in hospitalized children, Sonora, Mexico*

Case no.	IVIg	Corticosteroid	Anticoagulation prophylaxis	Vasopressor or inotrope	First outpatient medical consultation, d†	Treatment delay, d‡	Hospital care, d
1	1 g/kg, day 1; 2 g/kg, day 2	Methylprednisolone IV, 30 mg/kg/dose; dexamethasone IV, 8 mg/d	Enoxaparin, 0.5 mg/kg/dose	Dobutamine, 5 μg/kg/min; norepinephrine, 0.05 μg/kg/min	1	13	15
2	NA	Hydrocortisone IV, 4 mg/kg/d; methylprednisolone IV, 1 g/d	NA	Dobutamine, 5 μg/kg/min; norepinephrine, 0.1 μg/kg/min	1	6	4
3	1 g/kg/day for 2 d	Methylprednisolone IV, 1 mg/kg/d; dexamethasone IV, 0.2 mg/kg/dose; hydrocortisone IV, 2 mg/kg/dose	Enoxaparin SC, 0.5 mg/kg/dose; aspirin by mouth, 60 mg/kg/d	Norepinephrine, 0.22 μg/kg/min	3	3	15
4	NA	Hydrocortisone IV, 1 mg/kg/dose	NA	Norepinephrine, 0.22 μg/kg/min; dobutamine, 8.3 μg/kg/min	1	10	13
5	1 g/kg/day for 2 d	Methylprednisolone IV, 1 mg/kg/d; prednisone PO, 1 mg/kg/d	Enoxaparin SC, 0.5 mg/kg/dose	NA	3	10	4

*IV, intravenous; IVIg, intravenous immunoglobulin; NA, not applicable; SC, subcutaneous.
†Number of days until first outpatient medical consultation after symptom onset.
‡Delay in doxycycline treatment after symptom onset; doxycycline was initiated at the time RMSF was clinically suspected during the hospital stay.

conditions can be challenging for clinicians in endemic regions. We describe 5 children who had clinical and laboratory evidence of both RMSF and MIS-C. Those patients improved with doxycycline treatment, highlighting the importance of timely recognition and treatment of RMSF, even when clinicians suspect SARS-CoV-2 infections. Because those infections can co-exist, a high degree of clinical suspicion is necessary. A history of tick exposure should prompt clinicians to consider RMSF, although tick bites are recognized in <50% of RMSF cases.

Clinical suspicion of MIS-C should not preclude consideration of RMSF and other rickettsial diseases (*12*,*13*). Fever, rash, gastrointestinal manifestations, and abdominal pain are among the most frequent clinical features in hospitalized children with MIS-C (*10*) or RMSF (*2*,*3*,*9*). Although ≈90% of patients with MIS-C or RMSF manifest fever, a rash is present in up to 90% of RMSF patients (*6*), compared with ≈50% of children with MIS-C (*10*,*14*). Patients with RMSF and MIS-C have similar laboratory test abnormalities that include thrombocytopenia, hyponatremia, and elevated inflammatory markers (i.e., procalcitonin and C-reactive protein) (*6*,*9*,*10*,*14*), probably because both diseases are characterized by a generalized inflammatory response, endothelial damage, and increased vascular permeability (*1*,*10*).

Doxycycline is the recommended antimicrobial drug treatment for all patients who have suspected RMSF and should be empirically initiated to reduce fatal outcomes and severe sequelae (*1*,*3*,*9*), particularly in vulnerable children living with social disadvantages (*1*,*14*). Physicians and other health personnel practicing in RMSF-endemic areas should systematically consider RMSF in the differential diagnosis of hospitalized patients who have MIS-C to reduce delays in therapy and prevent death and severe sequelae caused by this rickettsial disease.

About the Author

Dr. Álvarez-Hernández is a professor in the Department of Medicine and Health Sciences at the Universidad de Sonora, Mexico. His primary research interests are focused on epidemiology of infectious diseases, particularly tick-borne diseases, as well as public health policies.

References

1. Biggs HM, Behravesh CB, Bradley KK, Dahlgren FS, Drexler NA, Dumler JS, et al. Diagnosis and management of tickborne rickettsial diseases: Rocky Mountain spotted fever and other spotted fever group rickettsioses, ehrlichioses, and anaplasmosis—United States. MMWR Recomm Rep. 2016;65:1–44. https://doi.org/10.15585/mmwr.rr6502a1
2. Kirkland KB, Wilkinson WE, Sexton DJ. Therapeutic delay and mortality in cases of Rocky Mountain spotted fever. Clin Infect Dis. 1995;20:1118–21. https://doi.org/10.1093/clinids/20.5.1118
3. Buckingham SC, Marshall GS, Schutze GE, Woods CR, Jackson MA, Patterson LER, et al. Clinical and laboratory features, hospital course, and outcome of Rocky Mountain spotted fever in children. J Pediatr. 2007;150:180–4.e1. https://doi.org/10.1016/j.jpeds.2006.11.023

4. Foley J, Álvarez-Hernández G, Backus LH, Kjemtrup A, Lopéz-Pérez AM, Paddock CD, et al. The emergence of Rocky Mountain spotted fever in the southwestern United States and northern Mexico requires a binational One Health approach. J Am Vet Med Assoc. 2024;262:698–704. https://doi.org/10.2460/javma.23.07.0377
5. Zazueta OE, Armstrong PA, Márquez-Elguea A, Hernández Milán NS, Peterson AE, Ovalle-Marroquín DF, et al. Rocky Mountain spotted fever in a large metropolitan center, Mexico–United States border, 2009–2019. Emerg Infect Dis. 2021;27:1567–76. https://doi.org/10.3201/eid2706.191662
6. Álvarez-López DI, Ochoa-Mora E, Nichols Heitman K, Binder AM, Álvarez-Hernández G, Armstrong PA. Epidemiology and clinical features of Rocky Mountain spotted fever from enhanced surveillance, Sonora, Mexico: 2015–2018. Am J Trop Med Hyg. 2021;104:190–7. https://doi.org/10.4269/ajtmh.20-0854
7. Government of Mexico. Ministry of Health, General Director of Epidemiology. Morbidity yearbooks 1984–2022 [in Spanish] [cited 2023 Nov 13]. https://www.gob.mx/salud/acciones-y-programas/anuarios-de-morbilidad-1984- a-2022
8. Government of Mexico, National Council of Humanities, Science and Technology. COVID-19 dashboard Mexico [in Spanish] [cited 2023 Nov 13]. https://datos.covid-19.conacyt.mx
9. Alvarez-Hernandez G, Murillo-Benitez C, Candia-Plata MC, Moro M. Clinical profile and predictors of fatal Rocky Mountain spotted fever in children from Sonora, Mexico. Pediatr Infect Dis J. 2015;34:125–30. https://doi.org/10.1097/INF.0000000000000496
10. Kundu A, Maji S, Kumar S, Bhattacharya S, Chakraborty P, Sarkar J. Clinical aspects and presumed etiology of multisystem inflammatory syndrome in children (MIS-C): a review. Clin Epidemiol Glob Health. 2022;14:100966. https://doi.org/10.1016/j.cegh.2022.100966
11. Jiang L, Tang K, Irfan O, Li X, Zhang E, Bhutta Z. Epidemiology, clinical features, and outcomes of multisystem inflammatory syndrome in children (MIS-C) and adolescents—a live systematic review and meta-analysis. Curr Pediatr Rep. 2022;10:19–30. https://doi.org/10.1007/s40124-022-00264-1
12. Government of Mexico. Ministry of Health, General Director of Health Information. SINBA. National System of Basic Health Information [in Spanish] [cited 2023 Nov 13]. https://sinba.salud.gob.mx
13. World Health Organization. Multisystem inflammatory syndrome in children and adolescents with COVID-19. Scientific brief, May 15, 2020 [cited 2024 May 4]. https://www.who.int/publications/i/item/multisystem-inflammatory-syndrome-in-children-and-adolescents-with-covid-19
14. Álvarez-Hernández G, Roldán JFG, Milan NSH, Lash RR, Behravesh CB, Paddock CD. Rocky Mountain spotted fever in Mexico: past, present, and future. Lancet Infect Dis. 2017;17:e189–96. https://doi.org/10.1016/S1473-3099(17)30173-1

Address for correspondence: Gerardo Álvarez-Hernández, University of Sonora, Blvd Luis D. Colosio SN, col. Centro, Hermosillo, CP 83000, Mexico; email: gerardo.alvarez@unison.mx

etymologia revisited

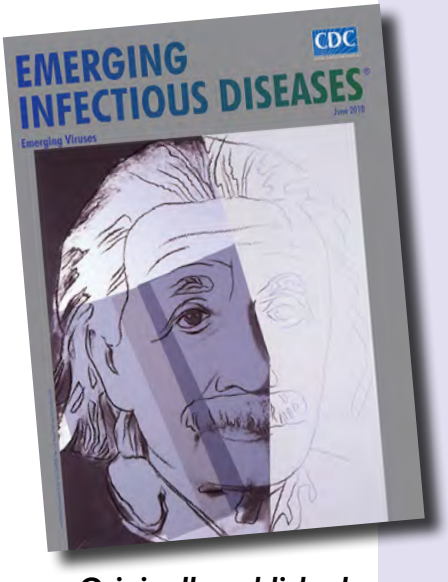

Originally published in June 2010

Lassa Virus

[lah sə] virus

This virus was named after the town of Lassa at the southern end of Lake Chad in northeastern Nigeria, where the first known patient, a nurse in a mission hospital, had lived and worked when she contracted this infection in 1969. The virus was discovered as part of a plan to identify unknown viruses from Africa by collecting serum specimens from patients with fevers of unknown origin. Lassa virus, transmitted by field rats, is endemic in West Africa, where it causes up to 300,000 infections and 5,000 deaths each year.

References:

1 Frame JD, Baldwin JM Jr, Gocke DJ, Troup JM. Lassa fever, a new virus disease of man from West Africa. I. Clinical description and pathological findings. Am J Trop Med Hyg. 1970;19:670–6
2. Mahy BW. The dictionary of virology, 4th ed. Burlington (MA): E lsevier; 2009.

https://wwwnc.cdc.gov/eid/article/16/6/et-1606_article

Molecular Confirmation of *Anopheles stephensi* Mosquitoes in the Al Hudaydah Governorate, Yemen, 2021 and 2022

Methaq Assada, Mohammed Al-Hadi, Mohammed A. Esmail, Jamil Al-Jurban, Abdulsamad Alkawri, Arif Shamsan, Payton Terreri, Jeanne N. Samake, Adel Aljasari, Abdullah A. Awash, Samira M. Al Eryani, Tamar E. Carter

We detected malaria vector *Anopheles stephensi* mosquitoes in the Al Hudaydah governorate in Yemen by using DNA sequencing. We report 2 cytochrome *c* oxidase subunit I haplotypes, 1 previously found in Ethiopia, Somalia, Djibouti, and Yemen. These findings provide insight into invasive *An. stephensi* mosquitoes in Yemen and their connection to East Africa.

Malaria remains a major threat to global health with ≈247 million cases reported in 2021 (*1*). An invasive malaria vector, *Anopheles stephensi* mosquito, has emerged in Africa; the first detection was in Djibouti in 2012 and was followed by detections in Ethiopia, Somalia, Sudan, Nigeria, Ghana, Kenya, and Eritrea (*2*) (Appendix, https://wwwnc.cdc.gov/EID/article/30/7/24-0331-App1.pdf). With growing evidence of *An. stephensi* mosquito resistance to multiple classes of insecticides (*3*,*4*), its association with a recent malaria outbreak (*5*), and genomic evidence that outbreak sites may also be central locations for *An. stephensi* mosquito travel to new areas (*6*), concerns are growing about the status and spread of this mosquito species in the Mediterranean region.

In the Arabian Peninsula, the geographic distribution of *An. stephensi* mosquitoes is unclear. Previous field investigations and predictive modeling indicate native populations exist in the northeastern coastal region along the Persian Gulf and inland in countries including Saudi Arabia (*7*,*8*). The status of *An. stephensi* mosquitoes is important in Yemen, where an increase in malaria cases was reported in the city of Aden beginning in 2017, although a link to *An. stephensi* mosquitoes has not been investigated (*9*). The first report of *An. stephensi* mosquitoes in Yemen occurred in Aden in 2021 and was confirmed with molecular analysis in 2023 (*2*,*10*). Recent retrieval of an unpublished entomological survey report indicated *An. stephensi* mosquitoes were present within the Al Zuhra district in the Al-Hudaydah governorate in 2000 (World Health Organization Yemen, unpub. data). No documentation of *An. stephensi* mosquitoes before 2000 or in later entomological surveys was found until the recent detection in 2021. Little is known about the distribution and characteristics of this vector in western governorates where the highest prevalence of malaria in Yemen is documented (*9*). *An. stephensi* mosquitoes were reported for the first time in the Ad Dahi district in December 2021 and in the Zabid district in March 2022, both within the Al Hudaydah governorate (*2*). *An. stephensi* mosquitoes have recently been found in multiple suburban areas in the Tehama coastal plain region (*11*). In this study, we characterize the genetic diversity of *An. stephensi* mosquitoes found during vector surveillance in the Al Hudaydah governorate.

Author affiliations: Ministry of Health, Sana'a, Yemen (M. Assada, M. Al-Hadi, M.A. Esmail, J. Al-Jurban, A. Alkawri, A. Shamsan); Baylor University, Waco, Texas, USA (P. Terreri, J.N. Samake, T.E. Carter); World Health Organization Country Office, Sana'a (A. Aljasari, A.A. Awash); World Health Organization, Cairo, Egypt (S.M. Al Eryani)

DOI: https://doi.org/10.3201/eid3007.240331

The Study

We analyzed immature mosquitoes collected from 2 semiurban locations, Ad Dahi and Zabid districts (Figure 1,). We collected the Ad Dahi district specimens over the course of a single day in December 2021 while conducting *Aedes* surveillance during a dengue fever

Figure 1. Locations in Yemen where invasive *Anopheles stephensi* mosquitoes were detected in 2021 and 2022 (yellow diamonds). Map was created by using MapChart (https://www.mapchart.net).

outbreak. The Zabid district specimens were collected during monthlong *Anopheles* surveillance in March 2022. Potential breeding containers surveyed included open concrete ponds and cement water tanks near block factories, washing basins in mosques, and car washing sites. Mosquitos used in this study were collected as immature specimens by using the dipping method. We reared them to adults in field insectaries and then identified them by using updated morphological keys (*12*). The specimens we morphologically identified as *An. stephensi* mosquitoes were preserved with silica gel. We sent a subsample of specimens to Baylor University (Waco, Texas, USA) for molecular analysis.

For species identification, we analyzed 2 loci, cytochrome *c* oxidase subunit 1 (COI) and internal transcribed spacer 2 (ITS2), by using previously described protocols (*13*). We used an *An. stephensi*–specific endpoint PCR as previously described (*14*). We conducted ITS2- and COI-targeted DNA sequencing, then used BLAST (https://blast.ncbi.nlm.nih.gov) and conducted phylogenetic analysis to determine species identification and evaluate the level of genetic diversity (Appendix).

Most of the *Anopheles* larvae were collected from cement water tanks found outside of homes, which were like other invasive settings found in eastern Ethiopia and Aden (*4*,*10*). We identified 41 mosquitoes morphologically as *An. stephensi*, 7 from Ad Dahi and 34 from Zabid City. Of the 41 specimens, all 7 Ad Dahi and 32 of the Zabid City specimens were confirmed to be *An. stephensi* mosquitoes by ITS2 endpoint assay and by COI and ITS2 targeted DNA sequence analysis (Appendix). We observed no discrepancy between the endpoint assay and sequencing assay for species identification. We did not report any discrepancies with the ITS2 endpoint assay results when compared with the DNA sequence results, but incorrect identification with the endpoint assay for other populations with unreported ITS2 variation is possible. Sequencing should accompany initial implementation of an endpoint assay in newly surveyed populations to evaluate both false negatives and false positives.

Two non–*An. stephensi* mosquitoes were recovered; 1 was identified as *Anopheles culicifacies* and 1 as *Aedes aegypti* on the basis of ITS2 and COI sequence BLAST analysis. This change from the initial morphological identification could be the result of sorting the *Anopheles* and *Aedes* mosquitoes from the same habitat or from the selection of specimens for molecular analysis in the laboratory. Phylogenetic analysis confirmed the species identification of the *An. stephensi* mosquito specimens (bootstrap = 100 for COI, bootstrap = 100 for ITS2) (Figures 2, 3).

ITS2 sequences were all identical for the *An. stephensi* mosquito specimens and BLAST analysis

revealed a 100% sequence identification in GenBank. Sequence analysis of COI revealed 2 haplotypes. One haplotype (n=35) was previously reported throughout the Horn of Africa (HoA) (COIHap 3) with the highest frequency in northeastern Ethiopia, Somaliland, and Djibouti (*15*). This haplotype was also noted in a recent report on the detection of *An. stephensi* mosquitoes in Aden, Yemen (*10*). The second haplotype (n=4), differing by a single nucleotide from COIHap3, has not previously been reported (designated COIHapYem1).

These findings demonstrate the successful use of ongoing vector surveillance activities for the initial detection of *An. stephensi* mosquitoes. The detection of a common HoA COI haplotype raises questions about the relationship between the invasive *An. stephensi* mosquitoes in northern HoA and Yemen. It is possible they share a common origin or that movement of *An. stephensi* mosquitoes has occurred between the 2 regions. Sequencing of additional loci could assist with delineating their relationship. Our findings provide information about the relative timing of the Yemen introduction of *An. stephensi* mosquitoes relative to the HoA detection on the basis of several observations. Fewer haplotypes were observed in the Al Hudaydah region in comparison to northeastern Ethiopia, Somalia, and Djibouti, which may indicate a recent introduction into the Al Hudaydah region. COIHap3 has a limited geographic range in comparison to the HoA-wide Hap2, which suggests the haplotype from our study could be associated with a later introduction in HoA and potentially Yemen. As for the HoA specimens and the study in Aden, no Saudi Arabian haplotypes were detected. Unlike the HoA specimens, no South Asia haplotypes were detected. Further genomic analysis and extensive *An. stephensi* mosquito sampling in Yemen, Saudi Arabia, and other parts of the Arabian Peninsula are needed to evaluate the hypothesis of a recent introduction in Yemen relative to the HoA.

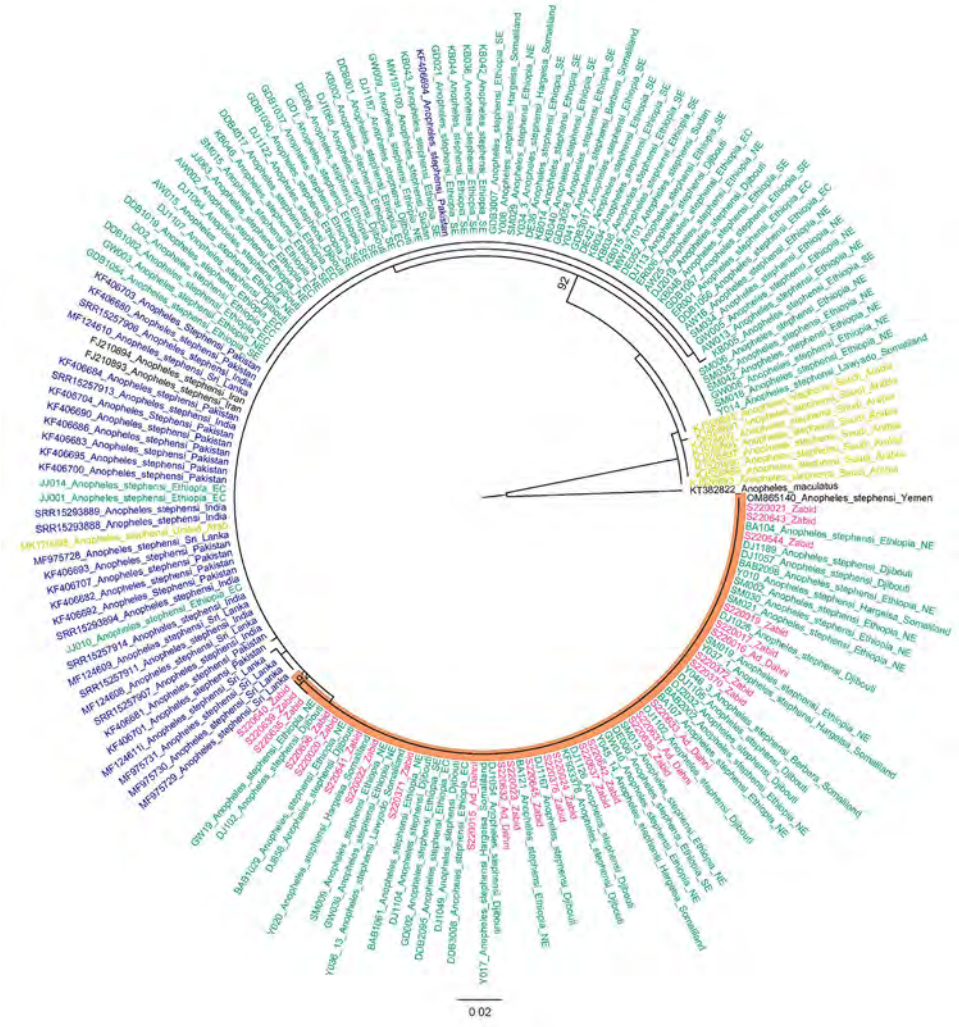

Figure 2. Maximum-likelihood phylogenetic analysis of cytochrome *c* oxidase subunit 1 gene sequences for *Anopheles stephensi* mosquitoes collected in Yemen. Pink indicates sequences from Yemen, blue indicates sequences from South Asia, green indicates sequences from the Horn of Africa and yellow-green indicates sequences from the Arabian Peninsula. Orange shading indicates branch containing Yemen and Horn of Africa specimens only. Numbers along branches indicate bootstrap values. Only values ≥70 are shown. Scale bar indicates the number of nucleotide substitutions per site.

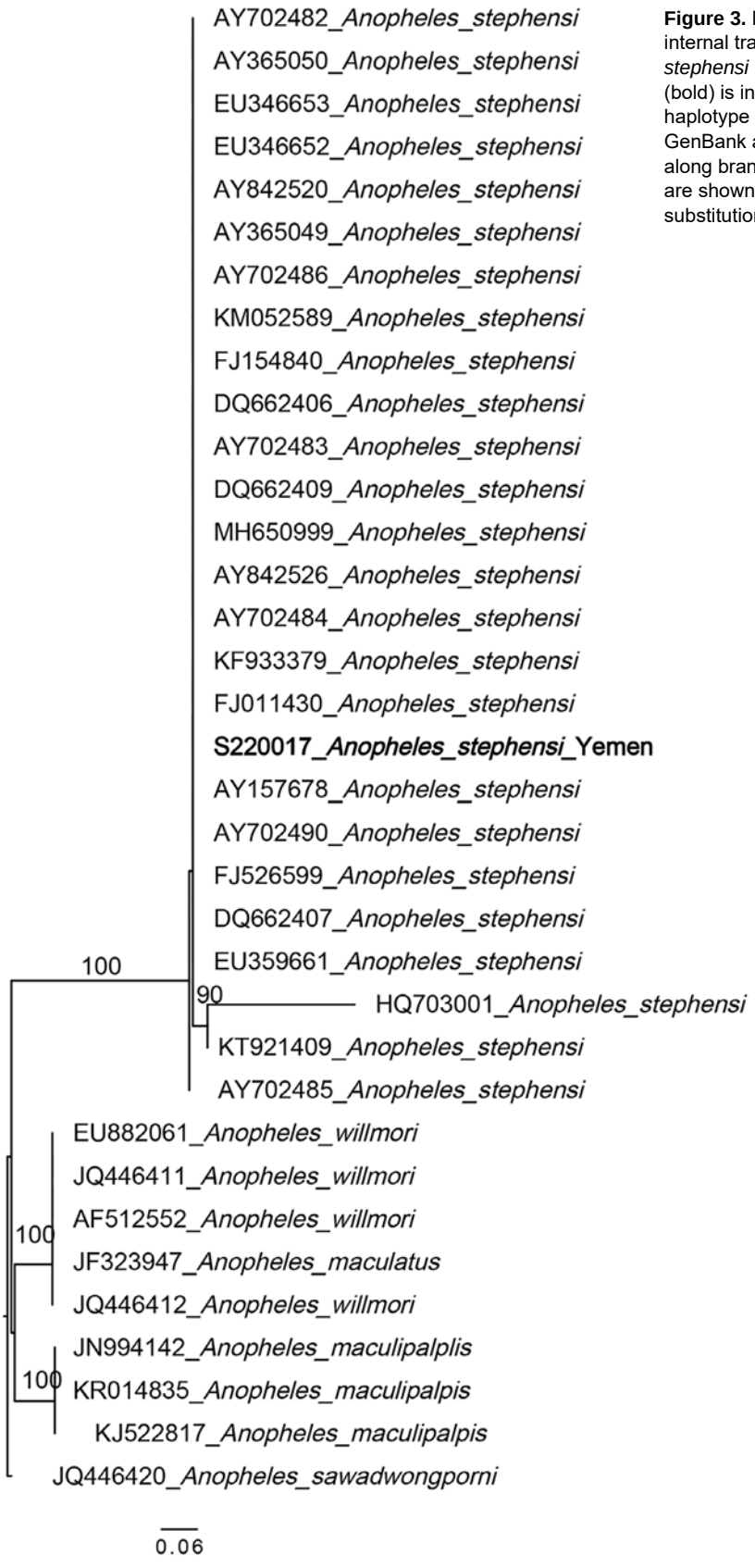

Figure 3. Maximum-likelihood phylogenetic analysis of internal transcribed spacer 2 DNA sequences for *Anopheles stephensi* mosquitoes collected in Yemen. Only 1 sequence (bold) is included as a representative of the single haplotype observed in the Yemen *An. stephensi* specimens. GenBank accession numbers are provided. Numbers along branches indicate bootstrap values. Only values ≥70 are shown. Scale bar indicates the number of nucleotide substitutions per site.

Conclusions

Our findings provide insight into the genetic diversity of *An. stephensi* mosquito populations in Al Hudaydah governorate, Yemen. The findings also provide support for the need of long-term entomological and epidemiologic surveillance of *An. stephensi* mosquitoes on malaria transmission in the region. With the detection of *An. stephensi* mosquitoes in Yemen, concerns remain related to the status of these mosquitoes in other areas of Yemen and their relationship with the HoA *An. stephensi* mosquitoes. Additional genomic analysis should be conducted to further examine the relative timing of the introduction of *An. stephensi* mosquitoes to Yemen.

Acknowledgments

We would like to thank Dr. Ghasem Zamani for his contribution to the conceptualization of the project, technical support for implementation of surveillance, and review of the manuscript. We would also like to thank Yamaan Foundation for Health and Social Development for their support of this work.

This research was funded by a NIH Research Enhancement Award (1R15AI151766) awarded to Tamar E. Carter and Baylor University.

Author contributions: Conception and project design (T.E.C., M.A., and S.A.E.); specimen collection and organization (M.A., M.A.H., M.A.E., J.A.J., and A.S.); data generation (T.E.C., P.A., and J.S.); data analysis (T.E.C. and P.A.); first draft (T.E.C.). All authors read and approved the final version of this manuscript.

About the Author

Dr. Methaq is an epidemiologist and director of the National Malaria Control Program, Ministry of Health, Sana'a, Yemen. His interests include the species composition and bionomics of mosquito vectors in Yemen.

References

1. World Health Organization. World malaria report 2023. [cited 2024 Feb 1]. https://www.who.int/teams/global-malaria-programme/reports/world-malaria-report-2023
2. World Health Organization. Malaria Threats Map. [cited 2021 Sep 1]. https://apps.who.int/malaria/maps/threats
3. Yared S, Gebressielasie A, Damodaran L, Bonnell V, Lopez K, Janies D, et al. Insecticide resistance in *Anopheles stephensi* in Somali region, eastern Ethiopia. Malar J. 2020;19:180. https://doi.org/10.1186/s12936-020-03252-2
4. Balkew M, Mumba P, Yohannes G, Abiy E, Getachew D, Yared S, et al. An update on the distribution, bionomics, and insecticide susceptibility of *Anopheles stephensi* in Ethiopia, 2018-2020. Malar J. 2021;20:263. https://doi.org/10.1186/s12936-021-03801-3
5. Emiru T, Getachew D, Murphy M, Sedda L, Ejigu LA, Bulto MG, et al. Evidence for a role of *Anopheles stephensi* in the spread of drug- and diagnosis-resistant malaria in Africa. Nat Med. 2023;29:3203–11. https://doi.org/10.1038/s41591-023-02641-9
6. Samake JN, Lavretsky P, Gunarathna I, Follis M, Brown JI, Ali S, et al. Population genomic analyses reveal population structure and major hubs of invasive *Anopheles stephensi* in the Horn of Africa. Mol Ecol. 2023;32:5695–708. https://doi.org/10.1111/mec.17136
7. Sinka ME, Bangs MJ, Manguin S, Chareonviriyaphap T, Patil AP, Temperley WH, et al. The dominant *Anopheles* vectors of human malaria in the Asia-Pacific region: occurrence data, distribution maps and bionomic précis. Parasit Vectors. 2011;4:89. https://doi.org/10.1186/1756-3305-4-89
8. Munawar K, Saleh A, Afzal M, Qasim M, Khan KA, Zafar MI, et al. Molecular characterization and phylogenetic analysis of anopheline (*Anophelinae*: *Culicidae*) mosquitoes of the Oriental and Afrotropical zoogeographic zones in Saudi Arabia. Acta Trop. 2020;207:105494. https://doi.org/10.1016/j.actatropica.2020.105494
9. Al-Eryani SM, Irish SR, Carter TE, Lenhart A, Aljasari A, Montoya LF, et al. Public health impact of the spread of *Anopheles stephensi* in the WHO Eastern Mediterranean region countries in Horn of Africa and Yemen: need for integrated vector surveillance and control. Malar J. 2023;22:187. https://doi.org/10.1186/s12936-023-04545-y
10. Allan R, Weetman D, Sauskojus H, Budge S, Hawail TB, Baheshm Y. Confirmation of the presence of *Anopheles stephensi* among internally displaced people's camps and host communities in Aden city, Yemen. Malar J. 2023;22:1. https://doi.org/10.1186/s12936-022-04427-9
11. Entomological Report NMCP. National Malaria Control Programme MoPHaP. 2022.
12. Coetzee M. Key to the females of afrotropical *Anopheles* mosquitoes (*Diptera*: *Culicidae*). Malar J. 2020;19:70. https://doi.org/10.1186/s12936-020-3144-9
13. Waymire E, Samake JN, Gunarathna I, Carter TE. A decade of invasive *Anopheles stephensi* sequence-based identification: toward a global standard. Trends Parasitol. 2024;40:477–86. https://doi.org/10.1016/j.pt.2024.04.012
14. Djadid ND, Gholizadeh S, Aghajari M, Zehi AH, Raeisi A, Zakeri S. Genetic analysis of rDNA-ITS2 and RAPD loci in field populations of the malaria vector, *Anopheles stephensi* (*Diptera*: *Culicidae*): implications for the control program in Iran. Acta Trop. 2006;97:65–74. https://doi.org/10.1016/j.actatropica.2005.08.003
15. Carter TE, Yared S, Getachew D, Spear J, Choi SH, Samake JN, et al. Genetic diversity of *Anopheles stephensi* in Ethiopia provides insight into patterns of spread. Parasit Vectors. 2021;14:602. https://doi.org/10.1186/s13071-021-05097-3

Address for correspondence: Tamar E. Carter 101 Bagby Ave Rm A124, Waco, TX, USA, 76706; email: tamar_carter@baylor.edu

Acute Meningoencephalitis Associated with *Borrelia miyamotoi*, Minnesota, USA

Jeffrey M. Kubiak, Michael Klevay, Evann E. Hilt, Patricia Ferrieri

Borrelia miyamotoi is an emerging tickborne pathogen that has been associated with central nervous system infections in immunocompromised patients, albeit infrequently. We describe a case-patient in Minnesota, USA, who had meningeal symptoms of 1 month duration. *B. miyamotoi* infection was diagnosed by Gram staining on cerebrospinal fluid and confirmed by sequencing.

Borrelia miyamotoi is an emerging tickborne pathogen initially discovered in Japan in 1995 but not recognized as a human pathogen until described in a case series from Russia in 2011 (*1*). The bacterium has a geographic distribution across northern Europe and Asia, as well as in the northeastern and midwestern United States; the first case of *B. miyamotoi* in Minnesota, USA, was reported in 2016 (*2*). *B. miyamotoi* is spread by many species of the deer tick, including *Ixodes scapularis* in North America and *I. ricinus* in Europe and Asia. *B. miyamotoi* is classified within the relapsing-fever group of spirochetes; infection typically manifests as a nonspecific febrile illness with headaches, chills, myalgia, and arthralgia and is likely underdiagnosed because of its rarity and lack of specific symptoms (*3*,*4*).

B. miyamotoi has been associated with cases of neuroborreliosis in which spirochetes proliferate in the cerebrospinal fluid (CSF) to cause disease ranging from acute meningitis symptoms to prolonged encephalitis with altered mentation and cranial nerve deficits (*5*–*8*). Here, we report a case of acute meningoencephalitis associated with *B. miyamotoi* in the midwestern United States that was diagnosed on CSF Gram stain and confirmed by sequencing.

Author affiliations: M Health Fairview University of Minnesota Medical Center, Minneapolis, Minnesota, USA (J.M. Kubiak, E.E. Hilt, P. Ferrieri); St. Paul Infectious Disease Associates, M Health Fairview, Saint Paul, Minnesota, USA (M. Klevay)

DOI: https://doi.org/10.3201/eid3007.231611

The Study

A 68-year-old man with immunosuppression from rituximab, in remission from mantle cell lymphoma involving the right eye, sought treatment at an emergency department in Minnesota in late summer. He had a 5-week history of headaches of increasing severity, worsened by positional changes and physical activity, as well as double vision, hearing difficulties, and some altered mentation. The patient was afebrile and had no nuchal rigidity. Cranial nerves exhibited no dysfunction other than subjective hearing loss, and physical examination results were otherwise unremarkable. He was an avid outdoorsman who had hiked frequently in the woodlands of Minnesota and Wisconsin over the months before seeking treatment, and he recalled identifying an engorged tick among several tick bites on his body during this time. He reported no travel history outside of the midwestern United States. The patient had been treated ≈1 year earlier with doxycycline for clinically diagnosed Lyme disease with fever and erythema migrans, but serologic *B. burgdorferi* testing at the time was negative.

We performed a magnetic resonance imaging scan of the brain and orbits with and without contrast, which showed bilateral abnormal cranial nerve enhancement of the oculomotor, trigeminal, facial, and vestibulocochlear nerves compared with a magnetic resonance image from 2 months earlier. Results of a lumbar puncture included a neutrophil-predominant pleocytosis (177 leukocytes/μL, 73% neutrophils). CSF flow cytometry results were unremarkable. A Biofire FilmArray (bioMérieux, https://www.biomerieux.com) meningitis/encephalitis multiplex PCR panel was negative. The patient had an elevated C-reactive protein (19.5 mg/L). Serologic results for *B. burgdorferi* in both the blood and CSF samples were negative, as were results of antitreponemal testing. Blood culture results were negative, and routine laboratory values were otherwise unremarkable.

A direct CSF Gram stain was performed in the University of Minnesota Medical Center Infectious Diseases Diagnostic Laboratory (Minneapolis, MN, USA) (Figure). The CSF specimen showed numerous gram-negative bacteria that measured 10–20 μm long with a tight coil, consistent with spirochetes. The CSF specimen was sent to the University of Washington Molecular Diagnosis Microbiology Section (Seattle, WA, USA) for bacterial 16S ribosomal RNA (rRNA) sequencing and fungal 28S rRNA sequencing.

The patient was admitted and treated with 2 g intravenous ceftriaxone daily for presumed neuroborreliosis, pending identification of the organism. After administering the initial antimicrobial treatment, we sent a plasma sample for a tickborne relapsing fever PCR panel, which broadly detects *Borrelia* species including *B. hermsii, B. parkeri, B. turicatae*, and *B. miyamotoi*; the test result was negative. Within 24 hours, the patient's condition improved on antimicrobial therapy, and on day 3 of hospitalization, we discharged him; he reported no headaches and some improvement in his cognition, hearing, and vision. Six days after we discharged the patient from the hospital, his 16S ribosomal sequencing result returned positive results for *B. miyamotoi*. We administered daily outpatient infusion therapy with ceftriaxone for 4 weeks, during which time he reported mild residual subjective memory loss, hearing loss, and loss of visual acuity from baseline, although double vision resolved. We advised him on appropriate tick-prevention methods because his history of outdoor activity indicated increased risk for future tick bites.

Conclusions

In cases of *B. miyamotoi* with neurologic manifestations, clinical symptoms have ranged from acute meningeal symptoms, including headache, vomiting, and dizziness (*5*,*9*), to prolonged neurologic disease, in some cases involving several months of progressive mental decline, confusion, gait instability, and hearing difficulty (*6*,*7*). Typically, in acute meningoencephalitis cases, spirochetes cannot be visualized in direct CSF specimen Gram or Giemsa stains (*5*). Diagnosis in those cases has relied on either broad-based 16S sequencing of bacteria rRNA, targeted PCR identification of the GlpQ or flagellin genes, darkfield microscopy, or acridine orange stain (*5*,*6*,*9*,*10*). In contrast, in 1 case, spirochetes were visualized on direct specimen Giemsa and Gram stains in the presence of prolonged neuroborreliosis of ≈4 months duration (*7*). Although literature on the subject remains lacking because of the relative rarity of this disease manifestation, those cases suggest that, in immunocompromised patients, spirochetes may proliferate in CSF over time, leading to an increased likelihood of detecting spirochetes on direct specimen examination in patients with prolonged symptoms. It is notable that DNA from *B. miyamotoi* was not detected in our patient's plasma, suggesting a neurologic tropism that enabled continued spirochetal proliferation even after the organisms were cleared from the patient's bloodstream.

This patient had abnormal MRI findings, including abnormal cranial nerve enhancement of the oculomotor, trigeminal, facial, and vestibulocochlear cranial nerves. Those findings were initially worrisome for leptomeningeal progression of the patient's ocular lymphoma, but flow cytometry of his CSF did not demonstrate abnormal proliferation of B cells. Although previous case reports have shown no abnormalities on cranial MRI (*5*–*7*), given this patient's constellation of symptoms, we believe that these MRI findings were attributable to this infection and the proliferation of spirochetes in the CSF.

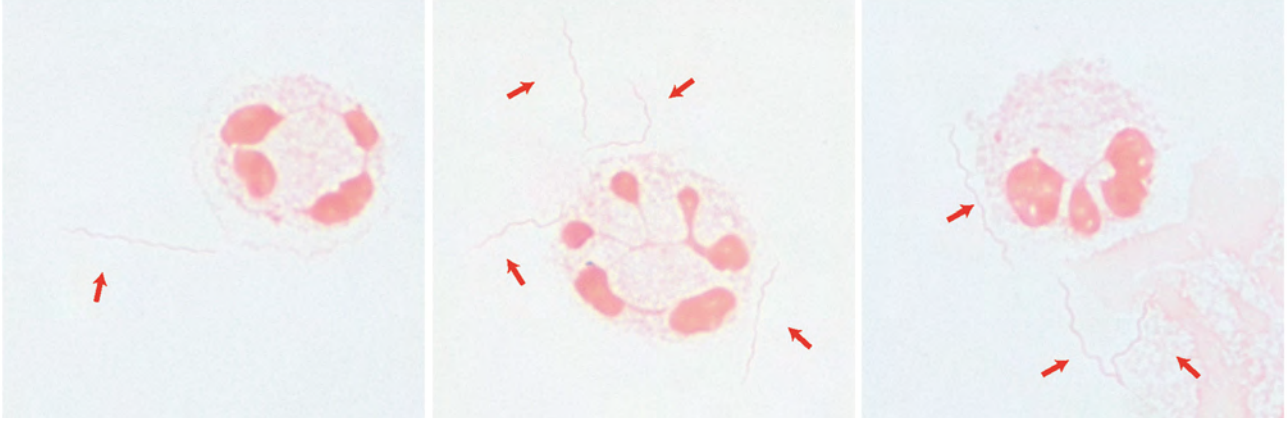

Figure. Spirochetes (red arrows) visualized on Gram stain in a cerebrospinal fluid sample from a 68-year-old man with immunosuppression from rituximab, Minnesota, USA. Visualization was done after concentration using cytospin (original magnification ×1,000 with oil immersion). The spirochetes were later identified as *Borrelia miyamotoi* by 16S ribosomal sequencing.

Differential diagnosis of spirochetes visualized on CSF Gram stain is limited. We found 1 other published case report with this finding, also for *B. miyamotoi* (*7*). Although other spirochetes, such as *B. burgdorferi* and *Treponema pallidum*, are known to cause neurologic manifestations ranging from acute meningoencephalitis to chronic encephalitis, those organisms are not visualized with Gram stain; diagnoses require darkfield microscopy, PCR, or serologic evidence of disease (*10*–*13*). We posit that finding spirochetes on CSF Gram stain is highly suggestive of *B. miyamotoi*, and patients should be empirically treated for neuroborreliosis pending definitive identification, particularly patients active in geographic areas with known tick exposure who have rituximab-caused immunosuppression.

Of note, most reported cases of neuroborreliosis caused by *B. miyamotoi* have been found in older patients on rituximab therapy with B-cell depletion, as in this case-patient, although there are rare reports of neuroborreliosis in immunocompetent persons (*9*). The adaptive immune system is considered key in controlling *B. miyamotoi* infection; *B. miyamotoi* activates dendritic cells, phagocytizing the bacteria and stimulating release of several cytokines (*14*). Furthermore, studies in related species, such as *B. hermsii*, have shown that clearance of spirochetes is mediated by antibodies (*15*). Further research into the pathogenesis of *B. miyamotoi* meningoencephalitis, with an emphasis on the regulators of proliferation of these organisms in CSF and disease progression in immunocompromised patients, are certainly warranted. Greater awareness of this manifestation of *B. miyamotoi* disease is needed to increase diagnostic accuracy and antimicrobial treatment to enable improved patient outcomes.

Acknowledgments

We thank the patient for agreeing to the publication of this report. In addition, we thank the technical staff of the Infectious Diseases Diagnostic Laboratory for considering the spirochetal possibility on the CSF direct Gram stain.

About the Author

Dr. Kubiak is the assistant medical director of the Infectious Diseases Diagnostic Laboratory at the M Health Fairview University of Minnesota Medical Center, where he is an assistant professor in the Department of Laboratory Medicine and Pathology. His primary research interests are in new laboratory diagnostics and laboratory informatics.

References

1. Platonov AE, Karan LS, Kolyasnikova NM, Makhneva NA, Toporkova MG, Maleev VV, et al. Humans infected with relapsing fever spirochete *Borrelia miyamotoi*, Russia. Emerg Infect Dis. 2011;17:1816–23. https://doi.org/10.3201/eid1710.101474
2. Minnesota Department of Health. About *Borrelia miyamotoi* disease [cited 2023 Nov 21]. https://www.health.state.mn.us/diseases/bmiyamotoi/basics.html
3. Cleveland DW, Anderson CC, Brissette CA. *Borrelia miyamotoi*: a comprehensive review. Pathogens. 2023;12:267. https://doi.org/10.3390/pathogens12020267
4. McCormick DW, Brown CM, Bjork J, Cervantes K, Esponda-Morrison B, Garrett J, et al. Characteristics of hard tick relapsing fever caused by *Borrelia miyamotoi*, United States, 2013–2019. Emerg Infect Dis. 2023;29:1719–29. https://doi.org/10.3201/eid2909.221912
5. Boden K, Lobenstein S, Hermann B, Margos G, Fingerle V. *Borrelia miyamotoi*–associated neuroborreliosis in immunocompromised person. Emerg Infect Dis. 2016; 22:1617–20. https://doi.org/10.3201/eid2209.152034
6. Hovius JWR, de Wever B, Sohne M, Brouwer MC, Coumou J, Wagemakers A, et al. A case of meningoencephalitis by the relapsing fever spirochaete *Borrelia miyamotoi* in Europe. Lancet. 2013;382:658. https://doi.org/10.1016/S0140-6736(13)61644-X
7. Gugliotta JL, Goethert HK, Berardi VP, Telford SR III. Meningoencephalitis from *Borrelia miyamotoi* in an immunocompromised patient. N Engl J Med. 2013;368:240–5. https://doi.org/10.1056/NEJMoa1209039
8. Kubiak K, Szczotko M, Dmitryjuk M. *Borrelia miyamotoi*—an emerging human tick-borne pathogen in Europe. Microorganisms. 2021;9:154. https://doi.org/10.3390/microorganisms9010154
9. Henningsson AJ, Asgeirsson H, Hammas B, Karlsson E, Parke Å, Hoornstra D, et al. Two cases of *Borrelia miyamotoi* meningitis, Sweden, 2018. Emerg Infect Dis. 2019;25:1965–8. https://doi.org/10.3201/eid2510.190416
10. Gyllemark P, Wilhelmsson P, Elm C, Hoornstra D, Hovius JW, Johansson M, et al. Are other tick-borne infections overlooked in patients investigated for Lyme neuroborreliosis? A large retrospective study from South-eastern Sweden. Ticks Tick Borne Dis. 2021;12:101759. https://doi.org/10.1016/j.ttbdis.2021.101759
11. Cutler SJ. Relapsing fever *Borreliae*. Clin Lab Med. 2015;35:847–65. https://doi.org/10.1016/j.cll.2015.07.001
12. Madison-Antenucci S, Kramer LD, Gebhardt LL, Kauffman E. Emerging tick-borne diseases. Clin Microbiol Rev. 2020;33:e00083–18. https://doi.org/10.1128/CMR.00083-18
13. Ramchandani MS, Cannon CA, Marra CM. Syphilis: a modern resurgence. Infect Dis Clin North Am. 2023;37:195–222. https://doi.org/10.1016/j.idc.2023.02.006
14. Mason LMK, Koetsveld J, Trentelman JJA, Kaptein TM, Hoornstra D, Wagemakers A, et al. *Borrelia miyamotoi* activates human dendritic cells and elicits T cell responses. J Immunol. 2020;204:386–93. https://doi.org/10.4049/jimmunol.1801589
15. Crowder CD, Ghalyanchi Langeroudi A, Shojaee Estabragh A, Lewis ERG, Marcsisin RA, Barbour AG. Pathogen and host response dynamics in a mouse model of *Borrelia hermsii* relapsing fever. Vet Sci. 2016;3:19. https://doi.org/10.3390/vetsci3030019

Address for correspondence: Jeffrey M. Kubiak, Department of Laboratory Medicine and Pathology, University of Minnesota Medical Center, 420 Delaware St SE, Minneapolis, MN 55455, USA; email: kubia046@umn.edu

Pasteurella bettyae Infections in Men Who Have Sex with Men, France

Andy Li, Florian Herms, Dominique Pataut, Jean-Baptiste Louison, Charles Cassius, Manel Merimèche, Jean David Bouaziz, Béatrice Berçot,[1] Sébastien Fouéré[1]

Author affiliations: Hôpital Saint-Louis Centre for Genital and Sexually Transmitted Diseases, Paris, France (A. Li, F. Herms, D. Pataut, J.-B. Louison, C. Cassius, J.D. Bouaziz, S. Fouéré); Hôpital Saint Louis National Reference Centre for Bacterial Sexually Transmitted Infections, Paris (M. Merimèche, B. Berçot); French Institute for Medical Research (INSERM) Joint Research Unit 1137, Paris (M. Merimèche, B. Berçot)

DOI: https://doi.org/10.3201/eid3007.240352

Pasteurella bettyae is a gram-negative bacillus sporadically involved in human infections; its main reservoirs are cats and dogs. A recent publication suggests the possibility of sexual transmission leading to genital infections in men who have sex with men. We report 9 cases in France of genital infection among this population.

Pasteurella bettyae is a gram-negative bacillus for which main reservoirs are cats, dogs, other mammals, and birds. *P. bettyae* has caused infections of the human genitourinary tract (*1*) and lungs (*2*) and can be transmitted through neonatal sepsis (*3*). A recent publication from Spain suggested possible sexual transmission in 2 men who have sex with men (MSM) (*4*). We describe 9 cases of *P. bettyae* genital infections in MSM in France during 2018–2022. As required by national ethics regulations, all patients received written information concerning the retrospective use of anonymized data; none expressed opposition to use and publication of those data.

We extracted clinical and biologic data from medical and bacteriology laboratory records. All 9 patients were MSM who sought care at the Hôpital Saint-Louis Center for Genital and Sexually Transmitted Diseases in Paris, France. Patients were 22–58 (mean 41.33) years of age. Seven patients were living in Paris, 1 in a northern suburb of Paris, and 1 in the region north of Paris closest to the city. The average number of sexual partners was 10.4; 2 patients were in monogamous relationships. Six patients did not use protection; 3 used condoms except for oral sex. No patients were HIV-positive, but 1 was immunosuppressed because of a kidney transplant. Two were receiving preexposure prophylaxis (PrEP) for HIV (Table 1).

One patient had a cat, another acknowledged contact with cows 2 weeks before clinical signs appeared, and 2 reported no contact with animals; data were missing for the other 4 patients. The main clinical manifestations were balanitis (4/9, 44.4%) and balanoposthitis (2/9, 22.2%). Balano-preputial sulcus ulcers in 2 patients were ultimately diagnosed as lymphogranuloma venereum and syphilis and urethral discharge in 1 patient was diagnosed as gonorrhea. No other signs or symptoms, including fever or lymphadenopathy, were reported (Table 1).

According to national guidelines, we presumptively treated patients with antimicrobial drugs; those with ulcers received benzathine benzylpenicillin plus doxycycline and the patient with urethral discharge received ceftriaxone plus doxycycline. We targeted co-pathogens when detected by nucleic acid amplification tests. One patient who had not received antimicrobial drugs attended a review visit and recovered after receiving specific treatment (cefixime) (Table 1).

We obtained *P. bettyae* colonies after 24-hour culture on polyvitex agar (bioMérieux, https://www.biomerieux.com) at <5% CO_2 and 35°C–37°C. We identified *P. bettyae* using Vitek MS matrix-assisted laser desorption/ionization time-of-flight mass spectrometry (bioMérieux). We used disk diffusion (Bio-Rad Laboratories, https://www.bio-rad.com) on polyvitex agar to test antimicrobial susceptibility and interpreted results according to European Committee on Antimicrobial Susceptibility Testing recommendations (*5*). All *P. bettyae* isolates showed susceptibility to amoxicillin/clavulanic acid, ceftriaxone, tetracycline, and fluoroquinolones, as is usually observed for this genus. One isolate from patient 9 exhibited resistance to amoxicillin and penicillin G (penicillin G MIC of 0.75 mg/L), 1 from patient 4 to penicillin G only, and 1 from patient 8 to trimethoprim/sulfamethoxazole (Table 1).

We performed whole-genome sequencing and bioinformatics analysis of 6/9 available *P. bettyae* isolates (BioProject accession no. PRJNA1039245) as described elsewhere (*6*). We developed the distance matrix of *Pasteurella* clinical isolates and rooted it by comparison with the genome reference sequence of *P. bettyae* strain CCUG 2042 (National Center for Biotechnology Information Reference Sequence database accession no. NZ_AJSX01000007.1). We observed relatedness between all *P. bettyae* isolates (Table 2), highlighting that 4 isolates, from patients 1, 3, 5, and 6, were closely related, varying among them by only 12–270 single-nucleotide polymorphisms and by

[1]These authors contributed equally to this article.

Table 1. Demographic and behavioral characteristics, bacteriological data, clinical manifestations, and evolution of *Pasteurella bettyae* infection among 9 men who have sex with men, France*

Pt no.	Year pos	Age	Partners/ y	Animal contact	Condom use	PrEP	Clinical manifestation	Culture site	Other pathogens retrieved	*P. bettyae* AMR	Antimicrobial treatment (follow-up)
1	2018	52	10	N	Y, exc oral	N	Balanitis	Coronal sulcus	None	None	None (healing)
2	2018	34	8	N	Y, exc oral	N	Balanitis	Coronal sulcus	*Haemophilus parainfluenzae*, *Finegoldia magna*	None	Cefixime (none)
3	2019	46	Unk	Unk	Occ	Y	Balanitis	First void urine + urethra	*H. parainfluenzae*	None	None (none)
4	2020	22	1	N	N	N	Balanoposthitis	Coronal sulcus	None	Penicillin G	None (none)
5	2020	27	10	Unk	Occ	N	Urethritis	Urethra	*Neisseria gonorrhoeae*	None	Ceftriaxone/ doxycycline (none)
6	2021	22	8	Unk	Y, exc oral	N	Balanitis	Glans penis	*Streptococcus dysgalactiae*	None	None (none)
7	2021	54	35	Cat	N	Y	Genital ulcer	Coronal sulcus	*C. trachomatis*	None	Penicillin G benzathine/ doxycycline (ulcer healing)
8	2021	56	10	Cows	Occ	N	Punctuate balanoposthitis	Coronal sulcus	*S. agalactiae*, *F. magna*	TMP/SMX	None (partial healing on zinc oxide paste)
9	2022	58	1	Unk	N	N	Persistent genital ulcer 2 wk after primary syphilis treatment	Coronal sulcus	None	Penicillin G/ ampicillin	Amoxicillin/ clavulanate (healing with indurated scar)

*AMR, antimicrobial resistance; exc, except; occ, occasional; pos, positive; PrEP, preexposure HIV prophylaxis; pt, patient; TMP/SMX, trimethoprim/sulfamethoxazole; unk, unknown.

587–628 SNPs from the *P. bettyae* CCUG 2042 strain described in 2012 in the United States. Isolates from patients 4 and 7 were more distant but had ribosomal identification and 16S rRNA of *P. bettyae.*

The 9 cases of genital *P. bettyae* infection exclusively in MSM we describe clustered within a 4-year period; no case was registered at our hospital before 2018. Fewer than 50 cases (mainly genital) have been reported worldwide across the previous 60 years, in male and female patients. In this series, the most specific clinical manifestation was balanitis/balanoposthitis. Because only 1 patient received targeted treatment, we could not deduce that *P. bettyae* was solely responsible for his symptoms or treatment responsible for his recovery. In case-patients with ulcers and urethritis, *P. bettyae* superinfection was more likely. Only half of patients for whom information was available had contact with animals, which provides insufficient support to determine direct anthropozoonotic transmission. Two thirds of patients reported not using condoms and the remaining third not using them for oral sex, which is not enough evidence to determine the transmission route and preventive efficacy of using condoms. However, if balanitis is indeed the main clinical manifestation, condoms provide an obvious physical barrier. Of note, the first case in this cluster occurred 2 years after PrEP policy implementation in France, but

Table 2. Differences in single-nucleotide polymorphisms among 6 *Pasteurella bettyae* isolates from 9 men who have sex with men, France, and a reference strain*

Isolate source	CCUG 2042	Patient 7	Patient 4	Patient 6	Patient 5	Patient 1	Patient 3
CCUG 2042	0	4,551	4,729	587	587	628	587
Patient 7	4,551	0	1,714	4,665	4,665	4,540	4,595
Patient 4	4,729	1,714	0	4,913	4,915	4,766	4,823
Patient 6	587	4,665	4,913	0	12	179	270
Patient 5	587	4,665	4,915	12	0	181	270
Patient 1	628	4,540	4,766	179	181	0	97
Patient 3	587	4,595	4,823	270	270	97	0

*Reference *P. bettyae* strain CCUG 2042 from National Center for Biotechnology Information Reference Sequence database (accession no. NZ_AJSX01000007.1). Numbers in cells indicate distances in SNPs.

whether receding usage of condoms by PrEP users had any part in this emergence remains speculative.

P. bettyae appears to be an emerging cause of sexually transmitted genital infection among MSM in Europe (*3*). More case descriptions are needed to delineate its clinical spectrum and appropriate handling. We encourage physicians to test bacterial swab samples when managing similar genital symptoms, especially balanitis.

About the Author

Mr. Li is a medical resident at Hôpital Saint-Louis Centre for Genital and Sexually Transmitted Diseases, Paris, France, specializing in dermatology and venereology.

References

1. Gómez-Camarasa C, Foronda-García-Hidalgo C, Borrego Jiménez J, Fernández-Parra J, Gutierrez-Fernández J. Emerging presence of *Pasteurella bettyae* in the genital tract of a woman [in Spanish]. Rev Investig Vet Peru. 2020;31:e16028. https://doi.org/10.15381/rivep.v31i1.16028
2. Moritz F, Martin E, Lemeland JF, Bonmarchand G, Leroy J, Escande F. Fatal *Pasteurella bettyae* pleuropneumonia in a patient infected with human immunodeficiency virus. Clin Infect Dis. 1996;22:591–2. https://doi.org/10.1093/clinids/22.3.591
3. Shapiro DS, Brooks PE, Coffey DM, Browne KF. Peripartum bacteremia with CDC group HB-5 (*Pasteurella bettyae*). Clin Infect Dis. 1996;22:1125–6. https://doi.org/10.1093/clinids/22.6.1125
4. Rosales-Castillo A, Hidalgo-Tenorio C, Navarro-Marí JM, Gutiérrez-Fernández J. Emerging presence of urethritis and balanitis by *Pasteurella bettyae.* Infect Dis Now. 2021;51:492–4. https://doi.org/10.1016/j.idnow.2020.10.006
5. European Committee on Antimicrobial Susceptibility Testing (EUCAST). Breakpoint tables for interpretation of MICs and zone diameters, version 12.0 [cited 2024 May 14]. https://www.eucast.org/clinical_breakpoints
6. Caméléna F, Morel F, Merimèche M, Decousser JW, Jacquier H, Clermont O, et al.; IAME Resistance Group. Genomic characterization of 16S rRNA methyltransferase-producing *Escherichia coli* isolates from the Parisian area, France. J Antimicrob Chemother. 2020;75:1726–35. https://doi.org/10.1093/jac/dkaa105

Address for correspondence: Sebastien Fouéré, Centre for Genital and Sexually Transmitted Diseases, Dermatology department, Hôpital Saint Louis, 1 Avenue Claude Vellefaux, Paris 75010, France; email: sebastien.fouere@aphp.fr

Plasmodium vivax Infections among Immigrants from China Traveling to the United States

Paloma Khamly, Nahel Kapadia, Minette Umali-Wilcox, Susan M. Butler-Wu, Kusha Davar

Author affiliations: Los Angeles General Medical Center, Los Angeles, California, USA (P. Khamly, N. Kapadia, M. Umali-Wilcox, S.M. Butler-Wu, K. Davar); Keck School of Medicine of University of Southern California/Los Angeles, Los Angeles (S.M. Butler-Wu)

DOI: https://doi.org/10.3201/eid3007.240177

Beginning in 2023, we observed increased *Plasmodium vivax* malaria cases at an institution in Los Angeles, California, USA. Most cases were among migrants from China who traveled to the United States through South and Central America. US clinicians should be aware of possible *P. vivax* malaria among immigrants from China.

Plasmodium vivax, the most widely geographically distributed species of the *Plasmodium* genus, causes malaria in humans and is transmitted through the bite of infectious *Anopheles* mosquitoes. *P. vivax* is the second most prevalent cause of malaria globally and constitutes a large portion of the annual malaria cases in the Western Hemisphere; ≈397,000 cases of *P. vivax* malaria were reported in the Americas in 2022 (*1*). Conversely, *P. vivax* malaria is relatively infrequently encountered at most institutions in the United States because most cases are travel-associated. The Centers for Disease Control and Prevention (CDC) reported 72% of all *P. vivax* cases in the United States in 2018 were imported from malaria-endemic countries (*2*). A central epidemiologic factor of *P. vivax* is its ability to establish a dormant liver stage that can later reactivate, leading to episodic parasitemia. This latent stage poses a potential risk for transmission to another human through a mosquito vector if appropriate treatment is not administered (*3*).

Since early 2023, Los Angeles General Medical Center in Los Angeles, California, USA, has observed a concerning rise in *P. vivax* cases, specifically among immigrants from China entering the United States via the southern US border. We diagnosed 10 cases of *P. vivax* malaria, 9 of which were among immigrants from China who came to the United States by land via South and Central America. In contrast, we only saw 2 cases of *P. vivax* at our institution during 2016–2022, one patient in 2017 and another in 2018, neither of whom were of

Table. Characteristics and treatment regimens of patients with diagnosed *Plasmodium vivax* infections among immigrants from China traveling to the United States via Central and South America, Los Angeles, California, USA, January 2023–April 2024*

Case no.	Date diagnosed	Clinical signs and symptoms	Duration of symptoms	% Parasitemia	Outpatient vs. inpatient	Treatment	Antirelapse treatment
Case 1	Mar 2023	Fever, chills, myalgias, shortness of breath	2 mo	0.10%	Inpatient	HCQ	Primaquine
Case 2	Mar 2023	Fever, diaphoresis, nausea	1.5 mo	0.30%	Inpatient	AP	Primaquine
Case 3	May 2023	Fever, fatigue, myalgias	9 d	<0.20%	Outpatient	AP	Primaquine
Case 4	Jun 2023	Fever, chills	1 wk	0.13%	Outpatient	Chloroquine	Primaquine
Case 5	Sept 2023	Fever, headache, diarrhea, nausea, vomiting	1 wk	0.05%	Outpatient	AP	Primaquine
Case 6	Jan 2024	Fever, cough	10 d	<0.20%	Outpatient	AP	Primaquine
Case 7	Jan 2024	Fever, chills, myalgias, nausea	10 d	<0.20%	Inpatient	AP	Primaquine
Case 8	Jan 2024	Fever, chills, myalgias	10 d	0.20%–1.0%	Inpatient	AP	Primaquine
Case 9	Jan 2024	Fever, chills, fatigue, cough	4 d	0.20%–1.0%	Inpatient	Chloroquine	Primaquine

*All patients met criteria for uncomplicated malaria. AP, atovaquone/proguanil; HCQ, hydroxychloroquine.

Asian descent. In addition, we saw 1 case of non–*P. vivax* malaria during that timeframe. All cases were diagnosed by thick and thin blood smear microscopy and the BinaxNOW Malaria test (Abbott Laboratories, https://www.abbott.com).

Whether any of the 9 immigrants from China traveled together is unknown because they sought care individually at our institution. They all met criteria for uncomplicated malaria and were treated with either hydroxychloroquine, chloroquine, or atovaquone/proguanil, followed by antirelapse treatment with primaquine (Table). Upon further correspondence with nearby microbiology laboratory directors, similar findings of dramatic increases in *P. vivax* cases since 2023 have also been observed in at least 1 local hospital that serves as a catchment area in the San Gabriel Valley, California, with a majority Asian American population. All cases were acquired by travel, and we noted no evidence of local transmission.

Of note, the United States Border Patrol reported a 1,000% increase in the number of immigrants from China arriving at the southern border during 2023 compared with previous years (*4*). The immigrants are primarily following a well-traveled route that begins in Ecuador, a country that does not require visas for citizens of China. From there, they traverse the jungle terrain of Panama's Darién Gap, proceeding into Central America and Mexico before arriving at the southern US border.

Hospitals serving newly arrived immigrants should be cognizant of this new emigration route from China via South and Central America and the associated risk of acquiring *P. vivax* malaria. All patients should be screened for malaria when they have compatible symptoms, and a detailed travel history should always be obtained. A vital detail to consider with travel history is that patients with prior *P. vivax* infection can relapse weeks, months, or years after initial diagnosis because the parasites can lay dormant in the liver as hypnozoites (*5*). Persons with diagnosed malaria should be assessed for severe symptoms, such as impaired consciousness, severe anemia, acute kidney injury, acute respiratory distress, or shock. For severe *P. vivax* malaria, patients typically are treated with intravenous artesunate. For uncomplicated *P. vivax* malaria, providers can prescribe chloroquine, hydroxychloroquine, artemether/lumefantrine, or atovaquone/proguanil, depending on endemic country-specific resistance factors and institutional formulary supply. Primaquine or tafenoquine are used afterwards as antirelapse treatment. Full treatment recommendations can be found on the CDC website (*6*). In addition, the CDC malaria hotline provides for immediate assistance (*7*).

Of note, China was declared malaria-free by the World Health Organization in 2021, and no indigenous cases of malaria had been reported since 2016, suggesting that travel from China is not an epidemiologic risk factor itself (*8*). If feasible, persons embarking on travel via the South and Central America route should consider taking malaria prophylaxis.

In conclusion, clinical microbiology laboratories, particularly those in border states, should consider implementing rapid antigen testing for malaria to improve turnaround time for case detection but should be aware of the potential for false-negative results in patients with low parasitemia levels (*9*). Clinicians also should be aware of the possibility for an increase in *P. vivax* malaria cases among immigrants from China arriving via the southern US border.

About the Author

Dr. Khamly is a first-year fellow at the University of Southern California/Los Angeles General Medical Center Infectious Diseases Program. Her primary research interest is in antimicrobial stewardship and infection prevention.

References

1. World Health Organization. World malaria report 2023. Geneva: The Organization; 2023.
2. Mace KE, Lucchi NW, Tan KR. Malaria surveillance—United States, 2018. MMWR Surveill Summ. 2022;71:1–35. https://doi.org/10.15585/mmwr.ss7108a1
3. Centers for Diseases Control and Prevention. DPDx—laboratory identification of parasites of public health concern: malaria [cited 2023 Dec 12]. https://www.cdc.gov/dpdx/malaria/index.html
4. US Customs and Border Protection. FY20–FY23 nationwide encounters by state [cited 2024 Apr 10]. https://www.cbp.gov/document/stats/nationwide-encounters
5. Flannery EL, Kangwanrangsan N, Chuenchob V, Roobsoong W, Fishbaugher M, Zhou K, et al. *Plasmodium vivax* latent liver infection is characterized by persistent hypnozoites, hypnozoite-derived schizonts, and time-dependent efficacy of primaquine. Mol Ther Methods Clin Dev. 2022;26:427–40. https://doi.org/10.1016/j.omtm.2022.07.016
6. Centers for Diseases Control and Prevention. Malaria treatment (United States) [cited 2024 Apr 10]. https://www.cdc.gov/malaria/diagnosis_treatment/treatment.html
7. Centers for Diseases Control and Prevention. Division of Parasitic Diseases and Malaria: contact us [cited 2024 Apr 10]. https://www.cdc.gov/parasites/contact.html
8. World Health Organization, Global Malaria Programme. Countries and territories certified malaria-free by WHO [cited 2024 Apr 10]. https://www.who.int/teams/global-malaria-programme/elimination/countries-and-territories-certified-malaria-free-by-who
9. Centers for Diseases Control and Prevention. DPDx—laboratory identification of parasites of public health concern: blood specimens, detection of parasite antigens [cited 2024 Apr 25]. https://www.cdc.gov/dpdx/diagnosticprocedures/blood/antigendetection.html

Address for correspondence: Paloma Khamly, Division of Infectious Diseases, Los Angeles General Medical Center, 1100 N State St, Clinic Tower, A6E, Los Angeles, CA 90033, USA: email: pkhamly@dhs.lacounty.gov

Emergence of Indigenous Dengue Fever, Niger, October 2023

Habibatou Idé Amadou, Saada Moussa, Ibrahim Issa Arzika, Hadiza Ousmane, Soumana Amadou, Balki Aoula, Abdoulaye Ousmane, Ibrahim Maman Laminou, Adamou Lagare

Author affiliations: Centre de Recherche Medicale et Sanitaire, Niamey, Niger (H. Idé Amadou, I.I. Arzika, H. Ousmane, S. Amadou, B. Aoula, I.M. Laminou, A. Lagare); Hopital National de Niamey, Niger (S. Moussa); Universite Dan Dicko Dankoulodo, Maradi, Niger (A. Ousmane)

DOI: https://doi.org/10.3201/eid3007.240301

Dengue fever is a growing worldwide public health concern. In mid-October 2023, multiple cases of uncommon febrile illness were reported among patients in Niamey, Niger. Fifteen samples were tested by using molecular methods, from which 7 (46.66%) were confirmed positive for mosquitoborne dengue virus belonging to serotypes 1 and 3.

Dengue fever is a mosquitoborne arbovirus infection, mainly reported in tropical and subtropical regions. Dengue fever is caused by the 4 types of dengue virus (DENV), 1–4 (*1*). Patients with DENV infection have onset of high and abrupt fevers that are often accompanied by redness of the face, cutaneous erythema, myalgia, arthralgia, and headaches (*2*,*3*). In severe cases, healthcare workers will find evidence of hemorrhagic manifestations and signs of shock. The most common laboratory findings from a complete blood count are leukopenia, thrombocytopenia, and increased hematocrit (hemoconcentration) (*4*).

In recent years, DENV infection has progressed worldwide and become a major public health concern (*5*). Annually, ≥390 million infections are reported across the globe, of which 96 million have clinical manifestations and ≥25,152 result in death (*6*,*7*). DENV is now endemic in ≥34 countries in Africa (*7*). In 2023, a total of 171,991 suspected cases of dengue fever, including 70,223 confirmed cases and 753 deaths, were reported from 15 countries in West Africa. Burkina Faso is the most affected by dengue fever, accounting for 85% of reported cases and 91% of recorded fatalities (*8*). In Niger, there was a lack of data related to DENV infection until the recent confirmation of an imported case in November 2022 (*9*). In this report, we describe findings from 7 indigenous confirmed DENV cases in Niger. The Niger National

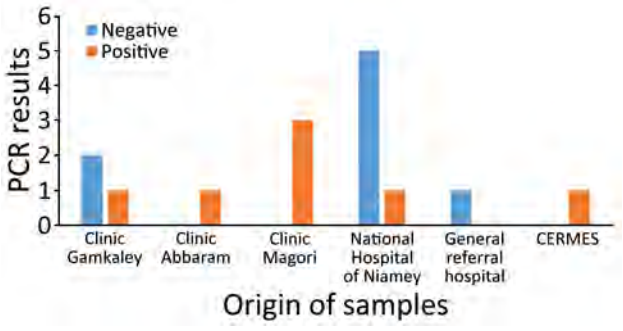

Figure. Distribution and results of dengue fever testing of suspected cases according to hospital or clinical origin in Niamey, Niger, October 2023. CERMES, Centre de Recherche Medicale et Sanitaire.

Ethical Committee at the Ministry of Health approved the surveillance protocol as minimal risk research, and written consent forms were not required. Oral consent was obtained from the patients. All methods, including the use of human samples, were conducted in accordance with the Declaration of Helsinki.

During October 25–27, 2023, several public and private hospitals in Niamey reported cases of febrile syndrome including fever (>38°C), persistence of headaches despite administration of analgesics, muscle pain, and vomiting (Figure). None of the patient complaints included a body rash or hemorrhage, and the initial provider assessment was otherwise unremarkable. We conducted microscopic blood smear examinations of 15 patient samples; all were negative for malarial parasites. Our clinical management of the patients (hospitalized and ambulatory) consisted of symptom treatment. We observed thrombocytopenia and leukopenia an average of 72 hours after the initial examination. Of note, we tested all 15 patients for DENV infection within 7 days of symptom onset.

Because of the suggestive symptomatology of our cases and the ongoing DENV epidemic in neighboring countries, particularly Burkina Faso, we collected blood samples and sent them to the National Reference Laboratory for arboviruses at the Centre de Recherche Medicale et Sanitaire for virological confirmation. Testing was conducted by using qRT-PCR with specific primers and probes for the detection of the 3 main arboviruses, DENV, chikungunya, and Zika virus (*10*). Differentiation of DENV serotypes 1, 2, 3, and 4 was conducted by using the Dengue Real-TMGenotype kit (Sacace Biotechnology, https://sacace.com).

A total of 15 samples were tested for all 3 viruses, of which 7 (46.66%) were positive for DENV. No detection of chikungunya or Zika virus was confirmed. Among the patients tested, 8 (53%) were male and 7 (47%) female; mean age was 34 (range 13–76) years. In the confirmed cases of DENV, the average age was 36 (range 13–51) years, 4 (57%) were male, and 3 (43%) were female (Table). The 7 confirmed DENV cases were linked to residents from Niamey, the capital city of Niger, and had no reported travel history outside the county. The detection of DENV serotypes was successful in 4 of the positive samples; 2 were DENV-1 and 2 DENV-3. Serotyping was not possible for the other 3 samples because of low viral levels (Table). The 7 cases, both hospitalized and ambulatory, recovered from the DENV infection without any severe complications.

After the official notification to the National Health Authorities, public health actions were implemented to contain the spread of the virus. An investigation team was dispatched by the Ministry of Health to investigate all confirmed cases of dengue fever. Prevention and control measures were put into place, namely awareness raising at the community level and awareness raising and training of healthcare personnel on the diagnosis and management of dengue fever. An entomologic survey was also conducted around patients' residences and hospitalization facilities, but 2 *Aedes* spp. mosquitoes captured and tested yielded no positive results for dengue, chikungunya, or Zika viruses.

Table. Clinical and paraclinical characteristics of indigenous dengue-confirmed patients in Niamey, Niger, October 2023*

Variables	Case 1	Case 2	Case 3	Case 4	Case 5	Case 6	Case 7
Sex	M	M	F	F	M	F	M
Age, y	40	13	47	28	51	45	16
Signs/symptoms	Fever, headache, muscle pain	Fever, headache, muscle pain	Fever, headache, muscle pain	Fever, headache, muscle pain, vomiting, vertigo	Fever, headache, muscle pain, vomiting, asthenia	Fever, headache, muscle pain	Fever, muscle pain
Mode of care	Hospitalized	Hospitalized	Hospitalized	Ambulatory	Hospitalized	Hospitalized	Hospitalized
Fever onset date	2023 Oct 10	2023 Oct 19	2023 Oct 22	2023 Oct 21	2023 Oct 20	2023 Oct 23	2023 Oct 20
Sampling date	2023 Oct 25	2023 Oct 25	2023 Oct 25	2023 Oct 27	2023 Oct 27	2023 Oct 27	2023 Oct 27
Dengue typing	Positive	Positive	Positive	Positive	Positive	Positive	Positive
Dengue serotyping	DENV-3	DENV-3	ND	DENV-1	ND	ND	DENV-1

*DENV, dengue virus; ND, serotyping not done because of low viral load.

In conclusion, we describe 7 indigenous cases of dengue fever in Niger. Dengue fever cases are underreported in Africa, where it is often misdiagnosed as malaria (*1*). Misdiagnosis and underreporting highlights the need to train healthcare staff on the recognition and diagnosis of dengue fever. Strong vector control measures are also beneficial for containing the spread of dengue fever (*4*).

Acknowledgments

We thank the medical staff who were engaged in patient care and the patients for participation in this study.

Author contributions: conceptualization (H.I.A., S.M., I.M.L., and A.L.); experiments and testing (I.I.A., S.A., B.A., and A.L.); field investigations (H.I.A. and S.M.); formal analysis (H.I.A., A.O., I.M.L., and A.L.); writing (H.I.A., S.M., and A.L.); review and editing (H.I.A., S.M., I.I.A., A.O., I.M.L., and A.L.). All authors read and approved the final version of the manuscript.

About the Author

Dr. Idé Amadou works as a researcher with the Centre de Recherche Medicale et Sanitaire. Her interests include field epidemiology, pediatrics, and health emergencies.

References

1. World Health Organization. Aide-memoire: dengue et dengue severe. 2014 [cited 2023 Nov 27]. https://applications.emro.who.int/docs/Fact_Sheet_WHD_2014_FR_15260.pdf
2. Institut Pasteur. Dengue fever. 2016 [cited 2024 Feb 16]. https://www.pasteur.fr/fr/centre-medical/fiches-maladies/dengue
3. Zatta M, Brichler S, Vindrios W, Melica G, Gallien S. Autochthonous dengue outbreak, Paris region, France, September–October 2023. Emerg Infect Dis. 2023;29:2538–40. https://doi.org/10.3201/eid2912.231472
4. World Health Organization. Dengue guidelines, for diagnosis, treatment, prevention and control [cited 2024 Feb 16]. https://www.who.int/publications-detail-redirect/9789241547871
5. Guzman MG, Harris E. Dengue. Lancet. 2015;385:453–65. https://doi.org/10.1016/S0140-6736(14)60572-9
6. World Health Organization. Dengue and severe dengue fever. 2023 [cited 2024 Feb 16]. https://www.who.int/fr/news-room/fact-sheets/detail/dengue-and-severe-dengue
7. Tinto B, Kania D, Samdapawindé Kagone T, Dicko A, Traore I, de Rekeneire N, et al. Circulation du virus de la dengue en Afrique de l'Ouest—une problématique émergente de santé publique. Med Sci (Paris). 2022;38:152–8. https://doi.org/10.1051/medsci/2022007
8. World Health Organization. Dengue in the WHO African region. Situation report 01: 19 December 2023 [cited 2024 Apr 2]. https://www.afro.who.int/countries/burkina-faso/publication/dengue-who-african-region-situation-report-01-19-december-2023
9. Lagare A, Faye M, Fintan G, Fall G, Ousmane H, Ibrahim ET, et al. First introduction of dengue virus type 3 in Niger, 2022. IJID Reg. 2023;7:230–2. https://doi.org/10.1016/j.ijregi.2023.04.001
10. Álvarez-Díaz DA, Valencia-Álvarez E, Rivera JA, Rengifo AC, Usme-Ciro JA, Peláez-Carvajal D, et al. An updated RT-qPCR assay for the simultaneous detection and quantification of chikungunya, dengue and zika viruses. Infect Genet Evol. 2021;93:104967. https://doi.org/10.1016/j.meegid.2021.104967

Address for correspondence: Habibatou Idé Amadou, Centre de Recherche Medicale et Sanitaire, 634 Bld de la Nation Niamey BP, 10887, Niger; email: ide.habibatou@yahoo.fr

Large-Scale Outbreak of *Mycoplasma pneumoniae* Infection, Marseille, France, 2023–2024

Sophie Edouard, Housni Boughammoura, Philippe Colson, Bernard La Scola, Pierre-Edouard Fournier, Florence Fenollar

Author affiliations: IHU–Méditerranée Infection, Marseille, France (S. Edouard, H. Boughammoura, P. Colson, B. La Scola, P.-E. Fournier, F. Fenollar); Aix-Marseille Université, Marseille (S. Edouard, P. Colson, B. La Scola, P.-E. Fournier, F. Fenollar)

DOI: https://doi.org/10.3201/eid3007.240315

We report a large-scale outbreak of *Mycoplasma pneumoniae* respiratory infections encompassing 218 cases (0.8% of 26,449 patients tested) during 2023–2024 in Marseille, France. The bacterium is currently circulating and primarily affects children ≤15 years of age. High prevalence of co-infections warrants the use of a syndromic diagnostic strategy.

Mycoplasma pneumoniae is known to cause upper respiratory tract infections and pneumonia, especially in children 5–15 years of age (*1*). Although mostly sporadic, *M. pneumoniae* infections may occur as successive epidemics every few years (*1*). The precedent outbreak was observed during

the 2019–2020 cold season, simultaneously in several countries, just before onset the COVID-19 pandemic (*2*). Then, the number of cases observed worldwide decreased markedly during this pandemic. However, although the resurgence of most respiratory pathogens was gradually observed from 2021, incidence of *M. pneumoniae* remained particularly low until June 2023, when a major resurgence of cases was reported worldwide (*2*–*3*).

We describe *M. pneumoniae* respiratory infections diagnosed in Marseille, France, university hospitals during January 1, 2014–February 15, 2024. We analyzed retrospectively all respiratory samples tested with 1 of the following specific quantitative PCRs (qPCRs) for *M. pneumoniae*: qPCR carried out by point-of-care laboratories using the Biofire FilmArray Respiratory Panel 2 Plus Assay (bioMérieux, https://www.biomerieux.com); qPCR performed routinely at the core laboratory using the FTD Respiratory Pathogens 21 Assay (Siemens Healthineers, https://www.siemens-healthineers.com); or an in-house specific qPCR (*4*). We used OpenEpi version 3.01 (https://www.openepi.com) for statistical analyses and considered differences significant at $p \leq 0.05$.

Overall, 98,401 samples from 74,355 patients were tested for *M. pneumoniae* as part of the diagnosis of respiratory infections during 2014–2024. Median patient age was 30 years (range 0–108 years); 52% were male and 48% female. *M. pneumoniae* was detected in 449 patients (0.6%). Median age of positive patients was 10 years (range 0–101 years); 57% were male and 43% female.

We observed a few *M. pneumoniae* outbreaks in Marseille during 2014–2020, with a peak in early 2020 (Figure). Incidence then declined until a resurgence was observed beginning in 2023. Initially, 9 cases were observed in January 2023, followed by 6 cases during February–May. Then, a major increase in diagnoses was observed during June 1, 2023–February 15, 2024 (203 total with a peak of 48 cases in December 2023). From January 2023 through mid-February 2024, we diagnosed 218 *M. pneumoniae* infections (0.8% of 26,449 patients tested), compared with 231 cases (0.3% of 71,952 patients tested) during January 2014–December 2022 ($p<0.0001$). Median age was significantly lower for patients diagnosed since 2023 than for previous years (8 vs. 15 years; $p<0.0001$) (Table). Concurrent presence of ≥1 respiratory viruses was found for 114/316 (36%) *M. pneumoniae*–positive patients. The prevalence of co-infections was significantly higher in children <5 years of age than in other age groups ($p<0.0001$). The most common co-infections were with rhinovirus (n = 49), influenza A virus (n = 13), respiratory syncytial virus (n = 12), human coronavirus OC43 (n = 10), influenza B virus (n = 9) and metapneumovirus (n = 9) (Appendix Figure 1, https://wwwnc.cdc.gov/EID/article/30/7/24-0315-App1.pdf). Co-infections were significantly less frequent in patients diagnosed during 2014–2022 (45/164 [27%]) compared with those diagnosed since 2023 (69/152 [45.4%]; p = 0.0008).

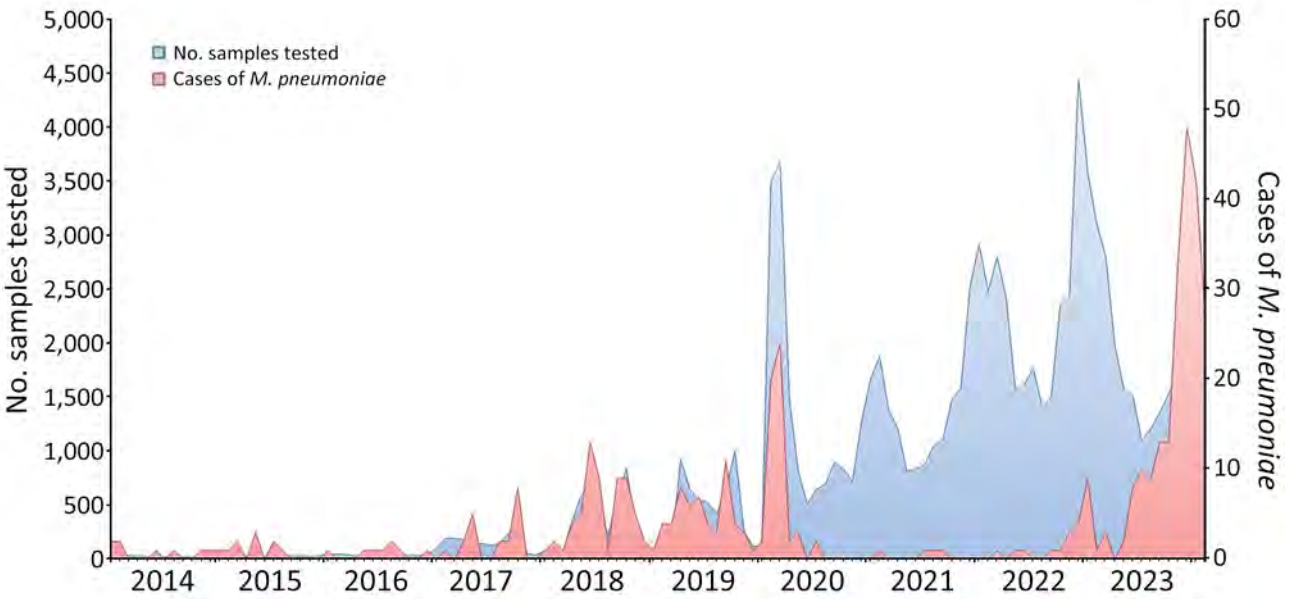

Figure. Monthly number of *Mycoplasma pneumoniae*–specific quantitative PCR tests performed and positive cases at a university hospital, Marseilles, France, January 1, 2014–February 15, 2024. Scales for the y-axes differ substantially to underscore patterns but do not permit direct comparisons.

Table. Demographic characteristics of 449 patients who had *Mycoplasma pneumoniae* infection diagnosed using quantitative PCR, Marseille, France, 2014–2022 versus 2023–2024*

Characteristic	Total	2014–2022	2023–2024	p value
No. patients	449	231	218	
Sex				
M	258 (57)	137 (59)	121 (56)	0.41
F	191 (43)	94 (41)	97 (44)	
Median age, y (range)	10 (0–101)	15 (0–93)	8 (0–101)	<0.001
Age group, y				
0–4	117 (26)	50 (22)	67 (31)	0.028
5–14	146 (32)	63 (27)	83 (38)	0.015
15–44	106 (24)	67 (29)	39 (18)	0.006
45–64	40 (9)	29 (13)	11 (5)	0.005
≥65	40 (9)	22 (9)	18 (8)	0.638
Co-infections				
No. patients tested	316	164	152	
No. patients with co-infection	114 (36)	45 (27)	69 (45)	0.0008
With 1 pathogen	94 (82)	41 (91)	53 (77)	0.049
With ≥2 pathogens	20 (17)	4 (9)	16 (23)	
Median age, y (range)	4 (0–101)	7 (0–86)	3 (0–101)	0.012
Age group, y				
0–4	58 (51)	18 (40)	40 (58)	<0.001
5–14	27 (24)	7 (16)	20 (29)	0.005
15–44	13 (11)	10 (22)	3 (4)	0.089
45–64	8 (7)	6 (13)	2 (3)	0.286
≥65	8 (7)	4 (9)	4 (6)	1

*Values are no. (%) except as indicated.

The increase of *M. pneumoniae* infection cases observed in our center are in line with observations from surveillance networks in France and throughout Europe (i.e., detection of the first epidemic sign in June 2023 until a peak reaching in December 2023) (*2*). High percentages of positivity (up to 50%) have been reported in China (*5*). In Marseille, we observed a lower percentage (1.8%), similar to the 0.89% observed in the United States since September 2023 (*9*). Most previous studies reported an increased incidence of *M. pneumoniae* infection particularly in school-age children and young adults (*3*,*7*). In Marseille, children ≤15 years were more affected during 2023–2024 than in previous seasons. However, we observed a switch regarding the population affected by the epidemic; adults became more affected beginning in January 2024 (Appendix Figure 2), possibly because of a massive transmission of the bacterium from infected children. We also observed a high rate of co-infections (≈50%), compared with 18% in the Netherlands (*3*). A high rate of co-infection with *M. pneumoniae* and other pathogens has also been previously reported in 65% of children and 34% of adults with acute respiratory infections in the United States (*8*). *M. pneumoniae* carriage ranging from 21% to 56% has also been reported in asymptomatic children (*9*). Interactions during co-detected microorganisms are complex, making it difficult to clearly define the contribution of each to respiratory infection. A high rate of asymptomatic carriers suggests a critical role for the nasopharyngeal microbiota in the clinical expression of respiratory infection.

There are several hypotheses for this re-emergence of *M. pneumoniae*, including the emergence of a new strain or a decline in individual and collective immunity. The current outbreak could be the usual periodic recurrence marked by an exacerbation resulting from a period of low exposure linked to restrictive measures during the COVID-19 pandemic. We did not investigate macrolide resistance, but reported resistance is low in Europe (*10*), and most studies described favorable outcomes after macrolide treatment (*7*). The number of *M. pneumoniae* infection cases is probably underestimated, particularly because patients with mild symptoms are not systematically tested. The high prevalence of co-infections with respiratory viruses justifies the use of a syndromic diagnostic strategy.

Acknowledgments

We thank Didier Stoupan for his technical support.

Data are available from the corresponding author upon reasonable request.

About the Author

Dr. Edouard is a medical bacteriologist at the Microbiological Laboratory at IHU–Méditerranée Infection in Marseille, France. Her research interests focus on infectious diseases and microbiology including intracellular bacteria and emerging pathogens.

References

1. Waites KB, Talkington DF. *Mycoplasma pneumoniae* and its role as a human pathogen. Clin Microbiol Rev. 2004;17:697–728. https://doi.org/10.1128/CMR.17.4.697-728.2004
2. Meyer Sauteur PM, Beeton ML; European Society of Clinical Microbiology and Infectious Diseases (ESCMID) Study Group for *Mycoplasma* and *Chlamydia* Infections (ESGMAC), and the ESGMAC *Mycoplasma pneumoniae* Surveillance (MAPS) Study Group. *Mycoplasma pneumoniae*: delayed re-emergence after COVID-19 pandemic restrictions. Lancet Microbe. 2024;5:e100-e101.
3. Nordholm AC, Søborg B, Jokelainen P, Lauenborg Møller K, Flink Sørensen L, Grove Krause T, et al. *Mycoplasma pneumoniae* epidemic in Denmark, October to December, 2023. Euro Surveill. 2024;29:2300707. https://doi.org/10.2807/1560-7917.ES.2024.29.2.2300707
4. Morel AS, Dubourg G, Prudent E, Edouard S, Gouriet F, Casalta JP, et al. Complementarity between targeted real-time specific PCR and conventional broad-range 16S rDNA PCR in the syndrome-driven diagnosis of infectious diseases. Eur J Clin Microbiol Infect Dis. 2015;34:561–70. https://doi.org/10.1007/s10096-014-2263-z
5. Li H, Li S, Yang H, Chen Z, Zhou Z. Resurgence of *Mycoplasma pneumoniae* by macrolide-resistant epidemic clones in China. Lancet Microbe. 2024:S2666-5247(23)00405-6.
6. Edens C, Clopper BR, DeVies J, Benitez A, McKeever ER, Johns D, et al. Notes from the field: reemergence of *Mycoplasma pneumoniae* infections in children and adolescents after the COVID-19 pandemic, United States, 2018–2024. MMWR Morb Mortal Wkly Rep. 2024;73:149–51. https://doi.org/10.15585/mmwr.mm7307a3
7. Zayet S, Poloni S, Plantin J, Hamani A, Meckert Y, Lavoignet CE, et al. Outbreak of *Mycoplasma pneumoniae* pneumonia in hospitalized patients: who is concerned? Nord Franche-Comté Hospital, France, 2023–2024. Epidemiol Infect. 2024;152:e46. https://doi.org/10.1017/S0950268824000281
8. Diaz MH, Cross KE, Benitez AJ, Hicks LA, Kutty P, Bramley AM, et al. Identification of bacterial and viral codetections with *Mycoplasma pneumoniae* using the TaqMan array card in patients hospitalized with community-acquired pneumonia. Open Forum Infect Dis. 2016;3:ofw071. https://doi.org/10.1093/ofid/ofw071
9. Koenen MH, de Groot RCA, de Steenhuijsen Piters WAA, Chu MLJN, Arp K, Hasrat R, et al. *Mycoplasma pneumoniae* carriage in children with recurrent respiratory tract infections is associated with a less diverse and altered microbiota. EBioMedicine. 2023;98:104868. https://doi.org/10.1016/j.ebiom.2023.104868
10. Kim K, Jung S, Kim M, Park S, Yang HJ, Lee E. Global trends in the proportion of macrolide-resistant *Mycoplasma pneumoniae* infections: a systematic review and meta-analysis. JAMA Netw Open. 2022;5:e2220949. https://doi.org/10.1001/jamanetworkopen.2022.20949

Address for correspondence: Florence Fenollar, IHU–Méditerranée Infection, 19-21 boulevard Jean Moulin, 13005 Marseille, France; email: florence.fenollar@univ-amu.fr

Fatal Infection in Ferrets after Ocular Inoculation with Highly Pathogenic Avian Influenza A(H5N1) Virus

Jessica A. Belser, Xiangjie Sun, Joanna A. Pulit-Penaloza, Taronna R. Maines

Author affiliation: Centers for Disease Control and Prevention, Atlanta, Georgia, USA

DOI: https://doi.org/10.3201/eid3007.240520

Ocular inoculation of a clade 2.3.4.4b highly pathogenic avian influenza A(H5N1) virus caused severe and fatal infection in ferrets. Virus was transmitted to ferrets in direct contact. The results highlight the potential capacity of these viruses to cause human disease after either respiratory or ocular exposure.

In recent years, clade 2.3.4.4b highly pathogenic avian influenza A(H5N1) viruses have exhibited substantial host expansion, geographic spread, and reassortment with other circulating influenza A viruses (IAVs) in birds, resulting in epornitics on all continents and virus detection in an expanding group of mammals (*1*). Human cases of H5N1 clade 2.3.4.4b virus infection have been reported, typically following direct exposure to infected animals, contaminated environments, or both (*2*). A 2.3.4.4b highly pathogenic avian influenza A(H5N1) virus was isolated from a human patient in Chile during 2023 (A/Chile/25945/2023 [Chile/25945]) (*3*) and caused severe and fatal disease in ferrets intranasally inoculated with 10^6 PFU of virus. Transmission of virus to animals housed in close contact was also reported (*3*), highlighting the pandemic potential of clade 2.3.4.4b viruses.

Although the eyes represent a secondary mucosal surface that is susceptible to respiratory virus exposure (*4*), as evidenced by recent reports of conjunctivitis in 2 dairy workers exposed to clade 2.3.4.4b H5N1 virus (*5*), risk assessment approaches for clade 2.3.4.4b H5N1 viruses to date have been limited to standard intranasal inoculation (*3*,*6*) and have not evaluated the capacity of those viruses to cause disease after alternative portals of entry. To investigate relative similarities between ocular and respiratory exposure to H5N1 virus, we assessed the severity and kinetics of disease after ocular exposure of ferrets to Chile/25945 virus and compared our findings with a previously published assessment of animals intranasally inoculated with

this virus at the Centers for Disease Control and Prevention in 2023 (*3*).

To assess disease severity and transmissibility under different exposure concentrations, we inoculated ferrets by the ocular route with either a high (10^6 PFU) or low (10^3 PFU) dose of Chile/25945 virus (*7*). At either challenge dose, all ferrets inoculated by the ocular route became productively infected, reaching mean maximum weight loss of 12.7% (high dose) and 13.2% (low dose) and mean maximum rises in temperature of 2.4°C (high dose) and 2.0°C (low dose). Humane endpoints were reached on postinoculation days 5–7 in 3/3 (high dose) and 2/3 (low dose) animals (Figure 1, panel A). During necropsy, we detected infectious virus throughout the respiratory tract and in several extrapulmonary tissues (including from the gastrointestinal tract, central nervous system, and ocular system) (Figure 1, panel C), consistent with the highly virulent phenotype observed after high-dose intranasal inoculation of ferrets (*3*). One ferret survived the challenge with a serologic titer of 160.

To assess if ferrets inoculated by the ocular route were as capable as intranasally inoculated ferrets to transmit Chile/25945 virus in a direct contact setting (*3*), we cohoused a serologically naive ferret with each inoculated ferret 24 hours after inoculation. To assess virus replication within and beyond the respiratory tract, we collected nasal wash, conjunctival wash/swab, and rectal swab samples from inoculated and contact animals. All ferrets inoculated by the ocular route with a high dose of virus had detectable infectious virus in nasal wash (mean peak titer 5.3 ± 0.2 $\log_{10}$ PFU/mL), conjunctival wash/swab (4.4 ± 0.9 $\log_{10}$ PFU/mL), and rectal swab (3.6 ± 0.3 $\log_{10}$ PFU/mL) samples (Figure 2, panel A). The magnitude and frequency of viral titers in these specimens was reduced, but still present, in animals inoculated with a low dose of virus (Figure 2, panel B). Infectious virus was detected in either nasal or rectal wash samples in all contact animals on at least

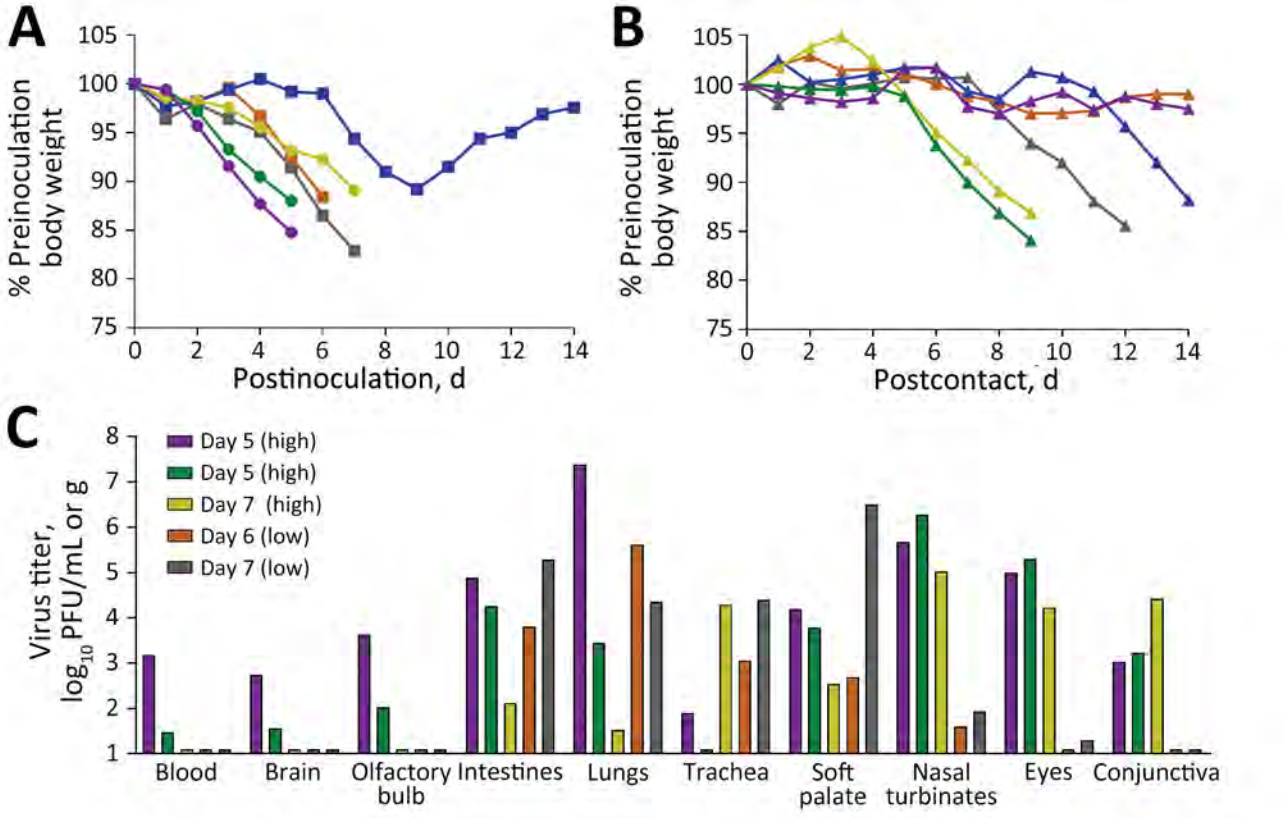

Figure 1. Disease severity and systemic spread of Chile/25945 influenza virus after ocular inoculation of ferrets. Ferrets were inoculated by the ocular route as previously described (*7*) with a high (10^6 PFU, circles) or low (10^3 PFU, squares) dose of Chile/25945 virus (100 μL volume), and each was cohoused with a serologically naive ferret 24 hours after inoculation (triangles). A, B) Inoculated (A) and contact (B) animals were weighed daily and humanely euthanized after reaching previously described endpoints (*3*). Ferret inoculated:contact pairs are indicated with shared colors. C) Systemic tissues were collected from inoculated animals that reached humane endpoints and titered for the presence of infectious virus as previously described (*7*). Bars represent individual ferrets with the postinoculation day on which humane endpoints were reached and tissues were collected specified per inoculation dose (bar color is linked with ferret morbidity data shown in panel A). Limit of detection was 10 PFU.

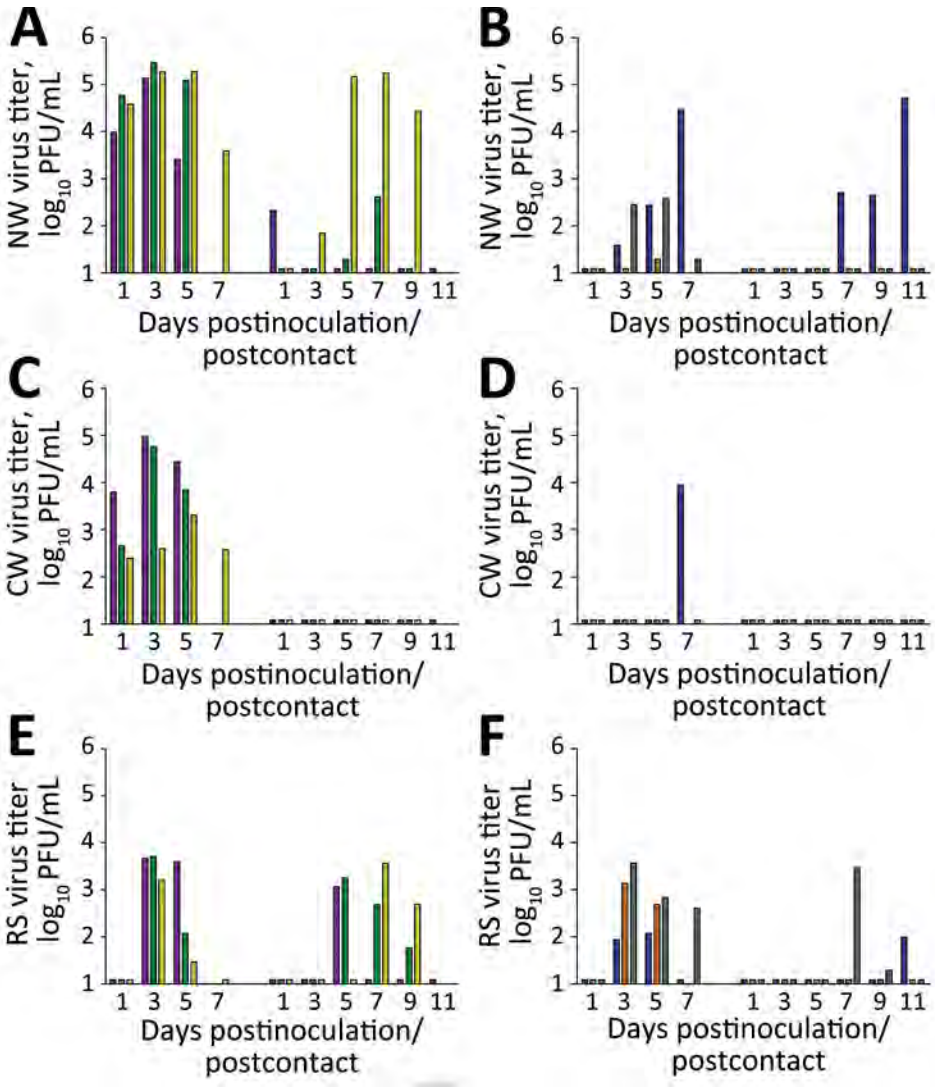

Figure 2. Transmission of Chile/25945 virus after ocular inoculation of ferrets. Ferrets were inoculated by the ocular route as previously described (*7*) with a high (10^6 PFU) or low (10^3 PFU) dose of Chile/25945 virus (100 μL), and each was cohoused with a serologically naive ferret 24 hours after inoculation. Specimens were collected from all ferrets as previously described (*7*) on alternate days after contact. A) NW specimen after ferret inoculation with 10^6 PFU challenge dose; B) NW specimen after inoculation with 10^3 PFU challenge dose; C) CW specimen after ferret inoculation with 10^6 PFU challenge dose; D) CW specimen after ferret inoculation with 10^3 PFU challenge dose; E) RS specimen after ferret inoculation with 10^6 PFU challenge dose; F) RS specimen after ferret inoculation with 10^3 PFU challenge dose. On each graph, left-hand bars indicate inoculated ferrets and right-hand bars indicate contact ferrets. Absence of a bar indicates an animal was humanely euthanized and no specimen was collected. Bar colors are linked with ferret morbidity data shown in Figure 1, panels A, B. Limit of detection was 10 PFU. CW, conjunctival wash/ swab sample; NW, nasal wash sample; RS, rectal swab sample.

1 day; infectious virus was not detected in conjunctival wash samples from any contact animal, possibly resulting from less overall virus shedding than in inoculated animals. Humane euthanasia because of severe disease was warranted for 4/6 contact animals (Figure 1, panel B); the other 2 survived, 1 of which exhibited a low level of seroconversion (hemagglutination inhibition titer 20).

Our finding that a clade 2.3.4.4b H5N1 virus isolated from a human can exhibit a virulent and transmissible phenotype after nontraditional inoculation, even with a low dose of inoculum, underscores the public health threat posed by those IAVs. The ocular surfaces may be exposed to infectious virus from the environment by several means (e.g., airborne particles, physical transfer from contact with fomites, and splashing liquids). Furthermore, circulation of tear fluid between ocular and nasopharyngeal tissues via the lacrimal duct offers an opportunity for infectious virus to spread from the respiratory tract to the ocular system (*8*), in agreement with successful H5N1 viral isolation from both conjunctival and nasopharyngeal swab specimens from a human with conjunctivitis (*5*). Conjunctivae may be exposed to virus by direct contact (e.g., virus-contaminated hands), indirect contact (e.g., virus-contaminated fomites), or after deposition of virus-laden droplets or aerosols onto the ocular surface (*4*), permitting opportunities for H5N1 virus to establish a productive infection in humans even in the absence of an ocular tropism. Considering the myriad ways humans may be exposed to IAVs, our study supports the need to consider nontraditional inoculation modalities in risk assessment activities and supports consideration of using eye protection in potentially contaminated environments (*9*).

About the Author

Dr. Belser is a microbiologist in the Influenza Division, National Center for Immunization and Respiratory Diseases, Centers for Disease Control and Prevention, Atlanta, GA. Her research interests include the pathogenicity, transmissibility, and tropism of influenza viruses, with an emphasis on ocular tropism and ocular exposure.

References

1. Xie R, Edwards KM, Wille M, Wei X, Wong SS, Zanin M, et al. The episodic resurgence of highly pathogenic avian influenza H5 virus. Nature. 2023;622:810–7. https://doi.org/10.1038/s41586-023-06631-2
2. Centers for Disease Control and Prevention. Technical report: highly pathogenic avian influenza A(H5N1) viruses [cited 2024 Jun 2]. https://www.cdc.gov/flu/avianflu/spotlights/2023-2024/h5n1-technical-report_april-2024.htm
3. Pulit-Penaloza JA, Brock N, Belser JA, Sun X, Pappas C, Kieran TJ, et al. Highly pathogenic avian influenza A(H5N1) virus of clade 2.3.4.4b isolated from a human case in Chile causes fatal disease and transmits between co-housed ferrets. Emerg Microbes Infect. 2024 Mar 17:2332667. https://doi.org/10.1080/22221751.2024.2332667
4. Belser JA, Lash RR, Garg S, Tumpey TM, Maines TR. The eyes have it: influenza virus infection beyond the respiratory tract. Lancet Infect Dis. 2018;18:e220–7. https://doi.org/10.1016/S1473-3099(18)30102-6
5. Uyeki TM, Milton S, Abdul Hamid C, Reinoso Webb C, Presley SM, Shetty V, et al. Highly pathogenic avian influenza A(H5N1) virus infection in a dairy farm worker. N Engl J Med. 2024;NEJMc2405371. https://doi.org/10.1056/NEJMc2405371
6. Kandeil A, Patton C, Jones JC, Jeevan T, Harrington WN, Trifkovic S, et al. Rapid evolution of A(H5N1) influenza viruses after intercontinental spread to North America. Nat Commun. 2023;14:3082. https://doi.org/10.1038/s41467-023-38415-7
7. Belser JA, Gustin KM, Maines TR, Pantin-Jackwood MJ, Katz JM, Tumpey TM. Influenza virus respiratory infection and transmission following ocular inoculation in ferrets. PLoS Pathog. 2012;8:e1002569. https://doi.org/10.1371/journal.ppat.1002569
8. Olofsson S, Kumlin U, Dimock K, Arnberg N. Avian influenza and sialic acid receptors: more than meets the eye? Lancet Infect Dis. 2005;5:184–8. https://doi.org/10.1016/S1473-3099(05)70026-8
9. Centers for Disease Control and Prevention. Prevention and antiviral treatment of bird flu viruses in people [cited 2024 Jun 2]. https://www.cdc.gov/flu/avianflu/prevention.htm

Address for correspondence: Jessica A. Belser, Centers for Disease Control and Prevention, Mailstop H17-5, 1600 Clifton Rd NE, Atlanta, GA 30329-4018, USA; email: jbelser@cdc.gov

Genomic Epidemiology of Large Blastomycosis Outbreak, Ontario, Canada, 2021

Lisa R. McTaggart, Nobish Varghese, Karthikeyan Sivaraman, Samir N. Patel, Julianne V. Kus

Author affiliations: Ontario Agency of Health Protection and Promotion (Public Health Ontario), Toronto, Ontario, Canada (L.R. McTaggart, N. Varghese, K. Sivaraman, S.N. Patel, J.V. Kus); University of Toronto, Toronto (S.N. Patel, J.V. Kus)

DOI: http://doi.org/10.3201/eid3007.231594

Using phylogenomic analysis, we provide genomic epidemiology analysis of a large blastomycosis outbreak in Ontario, Canada, caused by *Blastomyces gilchristii*. The outbreak occurred in a locale where blastomycosis is rarely diagnosed, signaling a possible shift in geographically associated incidence patterns. Results elucidated fungal population genetic structure, enhancing understanding of the outbreak.

North American blastomycosis is an infection most commonly caused by environmental dimorphic fungi *Blastomyces dermatitidis* and *B. gilchristii*. Infections range from asymptomatic to severe, typically presenting as respiratory illness, with possible systemic dissemination (*1*,*2*). The geographic range of *B. dermatitidis* and *B. gilchristii* fungi spans the eastern half of North America, including Ontario, Canada (*2*,*3*). Although overall incidence rates are low, isolated cases of blastomycosis are diagnosed regularly among populations in endemic areas (*2*,*3*), and clusters and outbreaks occur due to common environmental exposures (*1*,*4*–*7*).

We describe a large genomic epidemiology investigation of a blastomycosis outbreak in Constance Lake First Nation, a small community (population <2,000) in northeastern Ontario, Canada, in a locale where blastomycosis has rarely been encountered (*2*). We studied samples from 181 patients that were received by the Public Health Ontario Laboratory during November 2021–May 2022. By August 2022, we identified *B. gilchristii* fungus, by using multilocus sequence typing (*8*), in cultures from 40 persons linked to the outbreak (37 community residents and 3 persons [deemed travel A, B, and C] who visited the community during the possible exposure window). We observed that most positive cultures (35/40) were derived from specimens collected during a 7-week period—mid-November 2021 through December

2021—and most (39/40) were obtained from respiratory specimens (Table). Patients spanned all age groups; 55% were male and 45% female (Table).

We performed whole genome short-read sequencing (Illumina, https://www.illumina.com) on outbreak isolates and 21 other randomly selected *B. gilchristii* isolates (Appendix, https://wwwnc.cdc.gov/EID/article/30/7/23-1594-App1.pdf) cultured from specimens of patients from northern and eastern Ontario in July 2019–July 2022 (BioProject no. PRJNA890593). This collection of sequenced isolates contributes substantially to the number of *B. gilchristii* genomes available to advance research on this important pathogen. We conducted single-nucleotide variant (SNV) analysis to determine genetic diversity and relatedness between the 61 Ontario isolates plus 4 isolates from patients in Minnesota, USA (BioProject no. PRJNA786864), by using MycoSNP v0.22 (https://github.com/CDCgov/mycosnp-nf) with reference genome *B. gilchristii* SLH14081 (GenBank accession no. GCA_000003855.2) and conducted phylogenomic analysis (neighbor-joining method) using MEGA11 (https://www.megasoftware.net) (*1*).

Phylogenomic analysis of SNVs suggested that 39 of the 40 outbreak isolates were genetically highly similar, including isolates from 2 nonresidents who had traveled to the impacted community (travel A and B) (Figure). By contrast, the isolate from travel C was genetically dissimilar from the other outbreak isolates and likely represents a sporadic case acquired elsewhere (Figure). High genetic similarity between outbreak isolates and the brief 7-week timeframe for symptom onset for 90% of cases suggests a shared discrete exposure window. The overall analysis depicts multiple genetically distinct populations of *B. gilchristii* fungi separated by thousands of SNVs, correlated with different geographic regions.

Table. Clinical characteristics of culture-confirmed outbreak cases from a large blastomycosis outbreak, Ontario, Canada, 2021

Characteristic	Culture-confirmed cases, no.
Patient age, y	
0–19	13
20–34	7
35–49	13
50–69	7
Patient sex	
M	22
F	18
Date collected	
2021 Nov	23
2021 Dec	12
2022 Jan–Aug	5
Specimen type	
Sputum	37
Other	3

To validate the number of SNV differences between isolates, we separately investigated 9 pairs of biologic replicates (isolates from separate specimens from the same person) and 3 technical replicates from 2 other randomly selected isolates (Appendix). We found that 8 of 9 biologic replicates and all technical replicates averaged 12 (range 5–20) SNVs between corresponding isolates. In contrast, the number of SNVs between 39 outbreak isolates (excluding travel C) averaged 380 (range 96–778); 1 pair of biologic replicates differed by 192 SNVs. By comparison, 5 other clusters of isolates, including 2 clusters from Minnesota patients, had <100 SNVs between isolates. Taken together with the timing of the outbreak, the SNV differences between isolates suggests a shared exposure to a genetically similar yet heterogeneous fungal population, rather than a genetically identical point source. We theorize that the pair of biologic replicates differing by 192 SNVs might represent infection by 2 different strains of the fungal population. Of note, the outbreak locale possesses several environmental niches considered suitable reservoirs for *Blastomyces* spp. fungi, namely waterway-adjacent and forested areas, with coniferous trees supplying acidic soil rich in decaying organic material (*7*).

During the past 40 years, reports have documented several outbreaks and case clusters of North American blastomycosis (*1*,*4*–*7*). Most ascribe exposure to a discrete time and environmental locale, although that presumption is challenging to confirm because of the variable incubation time (1–6 months) (*6*) and patient travel. Recently, genomic epidemiologic information gleaned from whole-genome bioinformatics analysis has enhanced the description of outbreaks and case clusters of fungal pathogens (*9*,*10*), including *B. gilchristii* (*1*), enabling a more fulsome understanding of disease acquisition. In this study, we have interpreted the genomic epidemiology of a large outbreak of *B. gilchristii* within the context of several contemporaneous, genetically unrelated isolates to describe pathogen population genetic structure. We consider such genomic epidemiologic analyses useful in identifying cases caused by genetically related strains and, when combined with other epidemiologic factors including patient travel, pinpointing the timing and location of exposure. Epidemiologic investigation combined with pathogen phylogenomic analyses enables improved understanding of blastomycosis outbreaks and disease dynamics. This detailed information might help elucidate ecologic variables (possibly altered by climate change or modified land-use patterns) that influence disease acquisition (*3*). We believe that increased awareness of pathogen range and risk can aid prompt future case diagnoses.

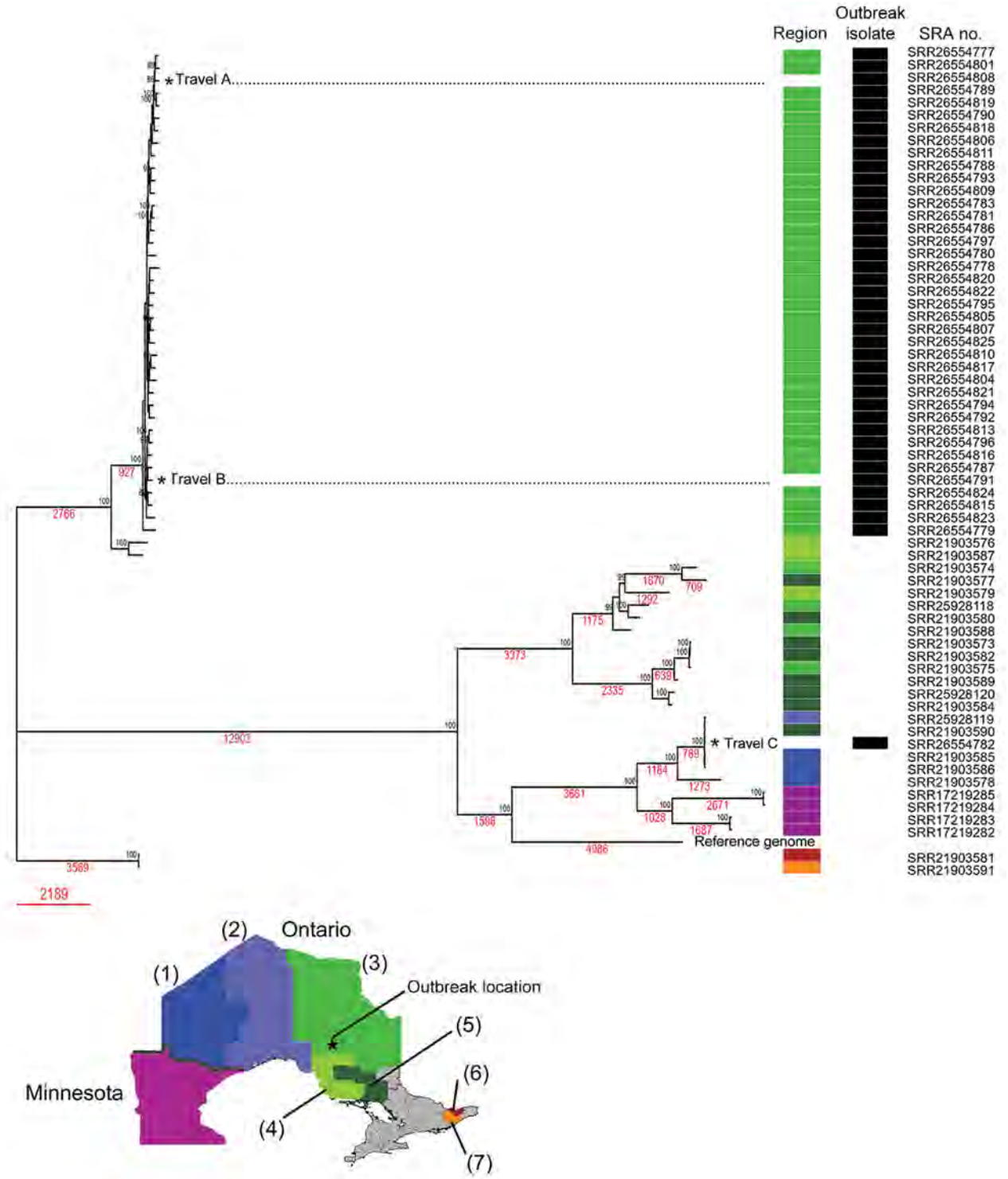

Figure. Phylogenomic analysis of whole-genome single-nucleotide variants by neighbor-joining method of *Blastomyces gilchristii* isolates from a large blastomycosis outbreak, Ontario, Canada, 2021. Percentage of trees of 500 bootstrap replications in which the associated taxa clustered together is shown next to the nodes. The tree is drawn to scale, with branch lengths measured in number of substitutions per site (red text). There were 45,321 positions in the final dataset. Outbreak isolates are designated with black bars. Colors indicate geographic region in which the patient resided is as shown on map, including cases from Minnesota, USA; numbers indicate regions: (1) Northwest, (2) Thunder Bay District, (3) Porcupine, (4) Algoma, (5) Sudbury, (6) Ottawa, (7) Leeds/Grenville/Lanark. The geographic regions of residence for the travel cases were not available. SRA, National Center for Biotechnology Information Sequence Read Archive.

Acknowledgments

We respectfully acknowledge the devastating impact this outbreak has had on the Constance Lake First Nation community and beyond. We are grateful for the permission granted by the community to share these findings to enhance our collective understanding of blastomycosis to help mitigate illness. We also acknowledge the support from Public Health Ontario staff, Indigenous Services Canada, and Porcupine Health Unit, especially Jo Ann Majerovich and Lianne Catton.

About the Author

Dr. McTaggart is a research technician at Public Health Ontario, Toronto, Ontario, Canada. Her research interests include mycology, infectious disease epidemiology, and the application of genomic analysis to pathogens of public health significance.

References

1. Bagal UR, Ireland M, Gross A, Fischer J, Bentz M, Berkow EL, et al. Molecular epidemiology of *Blastomyces gilchristii* clusters, Minnesota, USA. Emerg Infect Dis. 2022;28:1924–6. https://doi.org/10.3201/eid2809.220392
2. Brown EM, McTaggart LR, Dunn D, Pszczolko E, Tsui KG, Morris SK, et al. Epidemiology and geographic distribution of blastomycosis, histoplasmosis, and coccidioidomycosis, Ontario, Canada, 1990–2015. Emerg Infect Dis. 2018;24:1257–66. https://doi.org/10.3201/eid2407.172063
3. Ashraf N, Kubat RC, Poplin V, Adenis AA, Denning DW, Wright L, et al. Re-drawing the maps for endemic mycoses. Mycopathologia. 2020;185:843–65. https://doi.org/10.1007/s11046-020-00431-2
4. Roy M, Benedict K, Deak E, Kirby MA, McNiel JT, Sickler CJ, et al. A large community outbreak of blastomycosis in Wisconsin with geographic and ethnic clustering. Clin Infect Dis. 2013;57:655–62. https://doi.org/10.1093/cid/cit366
5. Dwight PJ, Naus M, Sarsfield P, Limerick B. An outbreak of human blastomycosis: the epidemiology of blastomycosis in the Kenora catchment region of Ontario, Canada. Can Commun Dis Rep. 2000;26:82–91.
6. Klein BS, Vergeront JM, Weeks RJ, Kumar UN, Mathai G, Varkey B, et al. Isolation of *Blastomyces dermatitidis* in soil associated with a large outbreak of blastomycosis in Wisconsin. N Engl J Med. 1986;314:529–34. https://doi.org/10.1056/NEJM198602273140901
7. Pfister JR, Archer JR, Hersil S, Boers T, Reed KD, Meece JK, et al. Non-rural point source blastomycosis outbreak near a yard waste collection site. Clin Med Res. 2011;9:57–65. https://doi.org/10.3121/cmr.2010.958
8. Brown EM, McTaggart LR, Zhang SX, Low DE, Stevens DA, Richardson SE. Phylogenetic analysis reveals a cryptic species *Blastomyces gilchristii*, sp. nov. within the human pathogenic fungus *Blastomyces dermatitidis*. PLoS One. 2013;8:e59237. https://doi.org/10.1371/journal.pone.0059237
9. Chow NA, Gade L, Tsay SV, Forsberg K, Greenko JA, Southwick KL, et al.; US Candida auris Investigation Team. Multiple introductions and subsequent transmission of multidrug-resistant *Candida auris* in the USA: a molecular epidemiological survey. Lancet Infect Dis. 2018;18:1377–84. https://doi.org/10.1016/S1473-3099(18)30597-8
10. Oltean HN, Springer M, Bowers JR, Barnes R, Reid G, Valentine M, et al. Suspected locally acquired coccidioidomycosis in human, Spokane, Washington, USA. Emerg Infect Dis. 2020;26:606–9. https://doi.org/10.3201/eid2603.191536

Address for correspondence: Julianne V. Kus, Public Health Ontario, 661 University Ave, Toronto, ON M5G 1M1, Canada; email: julianne.kus@oahpp.ca

Serosurvey of Chikungunya Virus in Old World Fruit Bats, Senegal, 2020–2022

William M. de Souza,[1] Alioune Gaye,[1] El Hadji Ndiaye, Angelica L. Morgan, El Hadji Daouda Sylla, Faty Amadou SY, Mawlouth Diallo,[1] Scott C. Weaver[1]

Author affiliations: University of Kentucky, Lexington, Kentucky, USA (W.M. de Souza); University of Texas Medical Branch, Galveston, Texas, USA (W.M. de Souza, A.L. Morgan, S.C. Weaver); Institut Pasteur de Dakar, Dakar, Senegal (A. Gaye, E.H. Ndiaye, F. Amadou SY, M. Diallo); Institut de Recherche pour le Développement, Dakar (E.H. Daouda Sylla)

DOI: http://doi.org/10.3201/eid3007.240055

We conducted a cross-sectional serosurvey for chikungunya virus (CHIKV) exposure in fruit bats in Senegal during 2020–2023. We found that 13.3% (89/671) of bats had CHIKV IgG; highest prevalence was in *Eidolon helvum* (18.3%, 15/82) and *Epomophorus gambianus* (13.7%, 63/461) bats. Our results suggest these bats are naturally exposed to CHIKV.

Chikungunya virus (CHIKV) is a mosquitoborne alphavirus that has caused >10 million cases in >125 countries and territories in the past 2 decades. Chikungunya disease is characterized by acute and chronic signs and symptoms in humans and can sometimes lead to neurologic complications and fatal outcomes (*1*). CHIKV is transmitted among humans mainly by *Aedes aegypti* and *Ae. albopictus* mosquitoes

[1]These authors contributed equally to this work.

in a human-amplified urban cycle (2). The virus is also transmitted in ancestral African enzootic cycles involving several species of arboreal mosquito vectors that transmit among diverse, nonhuman primates and possibly other amplifying hosts (2,3). The role of Old World fruit bats (Pteropodidae) in CHIKV transmission in West Africa remains understudied. We investigated CHIKV exposure of these bats in the Kédougou region in Senegal, a CHIKV-enzootic region with a history of spillover epidemics but not human-amplified, *Ae. aegypti*–borne outbreaks (A. Padane et al., unpub. data).

During October 23, 2020–March 4, 2022, we collected blood samples from fruit bats in 5 locations in the Kédougou region of southeastern Senegal (Figure, panel A). All bats were identified by external morphology. We tested all serum samples (dilution 1:100) in duplicate by an in-house ELISA for detection of IgG against CHIKV by using a recombinant envelope 2 protein and an anti-bat secondary antibody. We defined the cutoff value for positive results as the mean of negative controls (uninfected mice) plus 3 SDs (Appendix, https://wwwnc.cdc.gov/EID/article/30/7/24-0055-App1.pdf). All animals collected were adults and apparently healthy at the time of sampling. All procedures followed the approval of the National Ethical Committee for Research of Senegal and the University of Texas Medical Branch Institutional Animal Care and Use Committee.

We analyzed blood samples from 671 bats belonging to 13 species across 6 families. *Epomophorus gambianus* bats represented 68.7% (461/671) of captured specimens, followed by *Micropteropus pusillus* (13.1%) and *Eidolon helvum* (12.1%) bats. We detected IgG against CHIKV envelope 2 protein in 13.3% (89/671) of bats tested (Figure, panel B; Appendix Table). Testing revealed the bat species most frequently seropositive in 4 of 5 sites analyzed to be *E. helvum* (18.3%, 15/82), *E. gambianus* (13.7%, 63/461), and *M. pusillus* (8%, 7/88) (Figure, panel B; Appendix Figure). The locations with the highest seroprevalence were Ndebou (20.9%, 18/86) and Samecouta (18.4%, 58/316) (Figure, panel B). CHIKV seropositivity was consistent in bats collected in 2020 (13.7%, 17/124) and 2021 (13.2%, 72/325). Also, CHIKV seropositivity rates were similar between male (14.2%, 69/485) and female (13.2%, 19/144) bats.

We identified IgG specific for CHIKV in 5 species of fruit bats in several rural areas within the Kédougou region of southeastern Senegal before a 2023 outbreak (A. Padane et al., unpub. data). Bats are recognized to traverse wild, rural, and urban zones and possess favorable biologic features for hosting and amplifying several emerging viruses, including viral spread across large geographic areas linked to migration (4). CHIKV has been previously isolated from *Scotophilus* spp. bats in Senegal (5). Experimental infection of *Eptesicus fuscus* bats with CHIKV demonstrated persistent viremia, followed by neutralizing antibody production without apparent clinical signs (6), compatible features for enzootic amplifying and reservoir host status. Of note, other domestic and wild animals (e.g., birds and livestock) appear unlikely to amplify CHIKV effectively (6). One study revealed that 36% (15/42) of fruit bats captured near human settlements tested positive for CHIKV after an initial outbreak in Grenada Island (7), suggesting that CHIKV can infect

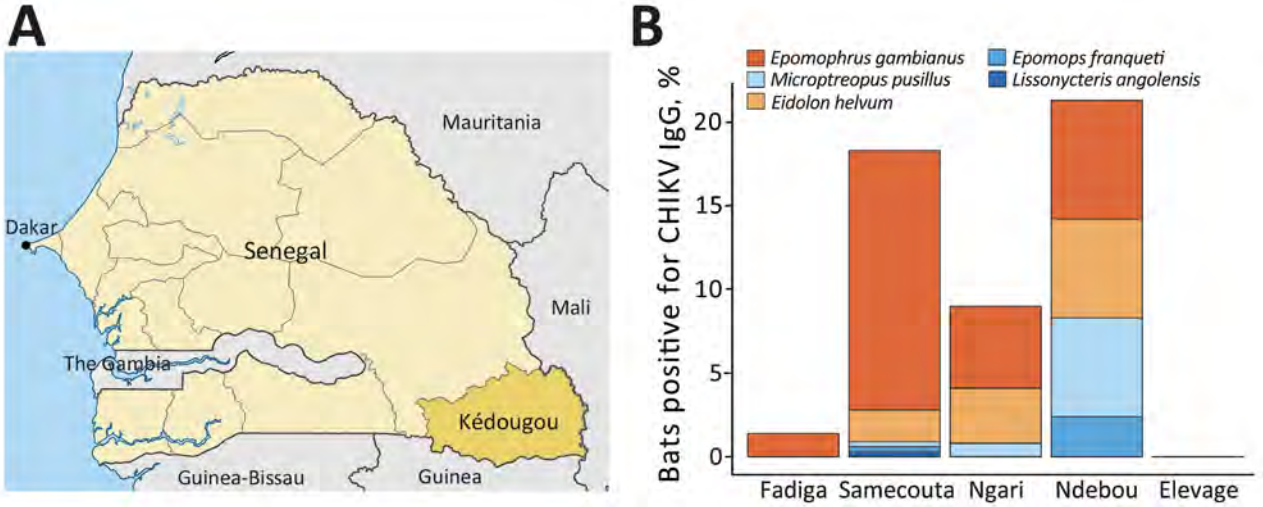

Figure. Serosurvey of CHIKV in the Kédougou region, Senegal. A) Location of Kédougou region (dark yellow) within Senegal (light yellow). B) Colored bars show the proportion of bats testing positive for CHIKV IgG at each capture site. Each color corresponds to a specific bat species, as indicated in the key above the graph. CHIKV, chikungunya virus.

bats during human-amplified outbreaks. Another study found that 0.7% (2/303) of *Rousettus aegyptiacus* bats in Uganda have neutralizing antibodies against CHIKV (*8*).

Collectively, our findings suggest that *E. gambianus*, *E. helvum*, and *M. pusillus* bats are exposed to CHIKV infection in the enzootic cycle in West Africa. Limitations of our study include the absence of more specific neutralizing antibody tests in bat samples because of limited volumes of blood collected and the need for testing for antibodies against several other viruses. Thus, we recognize that some CHIKV-positive samples could have resulted from cross-reactions with other alphaviruses circulating in the region, particularly o'nyong-nyong virus (Appendix) (*9*). Nonetheless, *E. gambianus* bats, unlike highly migratory *E. helvum* bats, are rarely observed to migrate or disperse long distances. This fact suggests that the high seropositivity we noted is unlikely due to cross-reaction with o'nyong-nyong virus, a virus rarely detected in West Africa. Limited blood sample volumes also prevented molecular testing (e.g., reverse transcription PCR) to identify active CHIKV infections. Future investigations should prioritize direct virus detection and isolation from bats. In addition, although our serologic data indicate past exposure, we could not ascertain the timing of CHIKV infection in the bats we studied. Re-capturing bats, particularly during interepidemic periods, would offer valuable insights into infection dynamics and reservoir potential. Finally, experimental infection of the high-seropositive bat species is needed to determine if they develop viremia of adequate magnitude to participate in mosquito transmission. In conclusion, our study strengthens evidence for natural CHIKV exposure in some Old World fruit bat species in West Africa.

W.M. de Souza was supported by a Global Virus Network fellowship, Burroughs Wellcome Fund (#1022448), and Wellcome Trust–Digital Technology Development award (Climate Sensitive Infectious Disease Modelling; 226075/Z/22/Z). S.C. Weaver was supported by National Institutes of Health grants AI12094, U01AI151801, and AI121452.

About the Author

Dr. de Souza is an assistant professor at the University of Kentucky. His research is focused on transmission dynamics of emerging and reemerging RNA viruses and arboviruses.

References

1. de Souza WM, de Lima STS, Simões Mello LM, Candido DS, Buss L, Whittaker C, et al. Spatiotemporal dynamics and recurrence of chikungunya virus in Brazil: an epidemiological study. Lancet Microbe. 2023;4:e319–29. https://doi.org/10.1016/S2666-5247(23)00033-2
2. Weaver SC, Chen R, Diallo M. Chikungunya virus: role of vectors in emergence from enzootic cycles. Annu Rev Entomol. 2020;65:313–32. https://doi.org/10.1146/annurev-ento-011019-025207
3. Althouse BM, Guerbois M, Cummings DAT, Diop OM, Faye O, Faye A, et al. Role of monkeys in the sylvatic cycle of chikungunya virus in Senegal. Nat Commun. 2018;9:1046. https://doi.org/10.1038/s41467-018-03332-7
4. Calisher CH, Childs JE, Field HE, Holmes KV, Schountz T. Bats: important reservoir hosts of emerging viruses. Clin Microbiol Rev. 2006;19:531–45. https://doi.org/10.1128/CMR.00017-06
5. Diallo D, Dia I, Diagne CT, Gaye A, Diallo M. Chapter 4: Emergences of chikungunya and Zika in Africa. In: Higgs S, Vanlandingham DL, Powers AM, editors. Chikungunya and Zika viruses. New York: Academic Press (Elsevier Inc); 2018. p. 87–133 [cited 2024 Jan 8]. https://www.sciencedirect.com/book/9780128118658/chikungunya-and-zika-viruses
6. Bosco-Lauth AM, Bowen RA, Nemeth NM, Kohler DJ. Viremia in North American mammals and birds after experimental infection with Chikungunya viruses. Am J Trop Med Hyg. 2016;94:504–6. https://doi.org/10.4269/ajtmh.15-0696
7. Stone D, Lyons AC, Huang YS, Vanlandingham DL, Higgs S, Blitvich BJ, et al. Serological evidence of widespread exposure of Grenada fruit bats to chikungunya virus. Zoonoses Public Health. 2018;65:505–11. https://doi.org/10.1111/zph.12460
8. Kading RC, Borland EM, Mossel EC, Nakayiki T, Nalikka B, Ledermann JP, et al. Exposure of Egyptian rousette bats (*Rousettus aegyptiacus*) and a little free-tailed bat (*Chaerephon pumilus*) to alphaviruses in Uganda. Diseases. 2022;10:121. https://doi.org/10.3390/diseases10040121
9. Powers AM, Brault AC, Tesh RB, Weaver SC. Re-emergence of Chikungunya and o'nyong-nyong viruses: evidence for distinct geographical lineages and distant evolutionary relationships. J Gen Virol. 2000;81:471–9.

Address for correspondence: Scott C Weaver, University of Texas Medical Branch, 301 University Blvd, Galveston, TX 77550, USA; email: sweaver@utmb.edu

World Health Organization Enhanced Gonococcal Antimicrobial Surveillance Programme, Cambodia, 2023

Vichea Ouk, Heng Lon Say, Mot Virak, Serakea Deng, Rebekah Frankson, Robert McDonald, Ellen N. Kersh, Teodora Wi, Ismael Maatouk, Sebastiaan van Hal, Monica M. Lahra; for the EGASP Cambodia working group[1]

Author affiliations: National Center for HIV/AIDS, Dermatology and Sexually Transmitted Diseases, Phnom Penh, Cambodia (V. Ouk, H.L. Say); Laboratory of the National Institute of Public Health, Phnom Penh (M. Virak); World Health Organization Office of Cambodia, Phnom Penh (S. Deng); Centers for Disease Control and Prevention, Atlanta, Georgia, USA (R. Frankson, R. McDonald, E.N. Kersh); World Health Organization, Geneva, Switzerland (T. Wi, I. Maatouk); The University of Sydney, Sydney, New South Wales, Australia (S.J. van Hal); The Prince of Wales Hospital, Randwick, New South Wales, Australia (M.M. Lahra); The University of New South Wales, Sydney (M.M. Lahra)

DOI: https://doi.org/10.3201/eid3007.240354

To determine antimicrobial susceptibility of *Neisseria gonorrhoeae*, we analyzed phenotypes and genomes of 72 isolates collected in Cambodia in 2023. Of those, 9/72 (12.5%) were extensively drug resistant, a 3-fold increase from 2022. Genomic analysis confirmed expansion of newly emerging resistant clones and ongoing resistance emergence across new phylogenetic backbones.

The World Health Organization (WHO) Enhanced Gonococcal Antimicrobial Surveillance Programme (EGASP) was established in Cambodia in 2020. The program is led by the National Center for HIV/AIDS, Dermatology and Sexually Transmitted Diseases, Cambodia, in partnership with the WHO headquarters, regional and country offices, and WHO Collaborating Centres based in the US Centers for Disease Control and Prevention (Atlanta, GA, USA) and New South Wales Health Pathology (Sydney, NSW, Australia). The WHO Collaborating Centre for Sexually Transmitted Infections and Antimicrobial Resistance in Australia provides technical support for the surveillance, including whole-genome sequencing of isolates. As part of the EGASP protocol, *Neisseria gonorrhoeae* isolates were collected from men with urethral discharge seen at 6 sentinel clinics in Phnom Penh and 4 sentinel clinics in neighboring provinces. EGASP protocols are set to alert public health authorities of strains approaching resistance. EGASP sets *N. gonorrhoeae* MIC alerts for ceftriaxone, cefixime, gentamicin, and azithromycin (*1*) (Table).

The first report from EGASP (*2*) detailed findings from 76 *N. gonorrhoeae* isolates collected by EGASP in Cambodia in 2022 and tested at the WHO Collaborating Centre for Sexually Transmitted Infections (STIs) and Antimicrobial Resistance in Australia. Of those, 29/76 (38%) isolates had alert level MICs for ceftriaxone (MIC ≥0.125 μg/mL) and cefixime (MIC ≥0.25 μg/mL) (*1*) and were also resistant to penicillin and ciprofloxacin. Almost all isolates harbored the mosaic *penA*-60.001 allele (n = 27) across 9 multilocus sequence types (MLSTs), determined by in silico typing. Those findings suggested that *penA*-60.001 allele carriage is more extensive than previously reported and indicated that widespread dissemination across the region might have already occurred (*2*). Furthermore, 3 *penA*-60.001–containing isolates (3/76; 4%) had an extensively drug resistant (XDR) phenotype (*3*), all from a single sequence type (ST), ST-16406, and similar to previously reported XDR *N. gonorrhoeae* isolates with links to the region (*3*).

We present data from an additional 72 gonococcal isolates collected in 2023 by the Cambodia EGASP team and referred to the WHO Collaborating Centre in Australia for phenotypic and genomic analysis. All 72 isolates underwent antimicrobial susceptibility testing. EGASP alert MICs for ceftriaxone and cefixime were detected in 22/72 (31%), a proportion similar to that reported in 2022 (38%) (*2*) (Table). In 2023, a total of 9 (12.5%) isolates had the XDR phenotype and the same MLST, ST-16406, a 3-fold increase from 4% of isolates with the same phenotype reported in 2022 (3/76). The percentage of isolates with resistance or elevated MICs to ciprofloxacin and penicillin remained high (82%–97%, Table).

Genomic analysis (*2*) showed that, of the 54 isolates with ceftriaxone alert MICs in 2022 and 2023, a total of 50 harbored the *penA*-60.001 allele and 3 harbored the recently described mosaic *penA*-273.001 allele (*4*). The remaining isolate harbored a novel allele classified as *penA*-60.003, which differed from *penA*-60.001 by a single-nucleotide polymorphism. Compared with 2022, the 2023 *penA*-60.001 allele was seen across 5 similar MLSTs (ST-1587, ST-7363, ST-8130, ST-11368, and ST-16406) and 3 other MLSTs (ST-7827, ST-14950, novel ST). Critically, across the 2 years of the EGASP study, sequences from only 8 isolates from Cambodia clustered with the widely disseminated FC428 clone (*5*), confirming both expansion of newly

[1]Members are listed at the end of this article.

Table. Antimicrobial susceptibility of *Neisseria gonorrhoeae* isolates from the World Health Organization EGASP, Cambodia, 2022–2023*

Antimicrobial drug	2022, n = 76, no. (%) (*2*)	2023, n = 72, no. (%)
Ceftriaxone ≥0.125 μg/mL†	29 (38)	22 (31)
Cefixime ≥0.25 μg/mL†	29 (38)	22 (31)
Azithromycin ≥2.0 μg/mL†	0	1 (1.4)
Azithromycin ≥256 μg/mL†	3 (4)	9 (12.5)
Ciprofloxacin resistant ≥1 μg/mL‡	74 (97)	70 (97)
Penicillin resistant ≥2 μg/mL‡	71 (93)	59 (82)
Spectinomycin resistant ≥128 μg/mL‡	0	0

*EGASP, Enhanced Gonococcal Antimicrobial Surveillance Programme.
†The Clinical Laboratory Standards Institute criteria for resistance to ceftriaxone, cefixime, and azithromycin have not been established. The EGASP MIC alert value criteria were ceftriaxone, MIC ≥0.125 μg/mL; cefixime, MIC ≥0.25 μg/mL; azithromycin, MIC ≥2.0 μg/mL; and azithromycin, MIC ≥256 μg/mL.
‡Antimicrobial susceptibility criteria established by the Clinical Laboratory Standards Institute (https://www.clsi.org) were used to determine resistance to the antibiotics tested in the EGASP for ciprofloxacin, penicillin, and spectinomycin.

emerging resistant clones and ongoing emerging resistance across new phylogenetic backbones (Figure). Moreover, all *N. gonorrhoeae* isolates with azithromycin MICs ≥256 μg/mL were found to possess the 23S rRNA gene mutation (A2509G). All 12 isolates with an XDR phenotype detected during 2022–2023 belonged to a single ST (ST-16406), recently reported in Europe and the United Kingdom (*3*). Sequence reads are available from the National Center for Biotechnology Information (BioProject no. PRJNA909328).

Our data provide further evidence for sustained transmission of *N. gonorrhoeae* strains with elevated MICs for ceftriaxone and increased expansion of isolates with elevated MICs to ceftriaxone and azithromycin

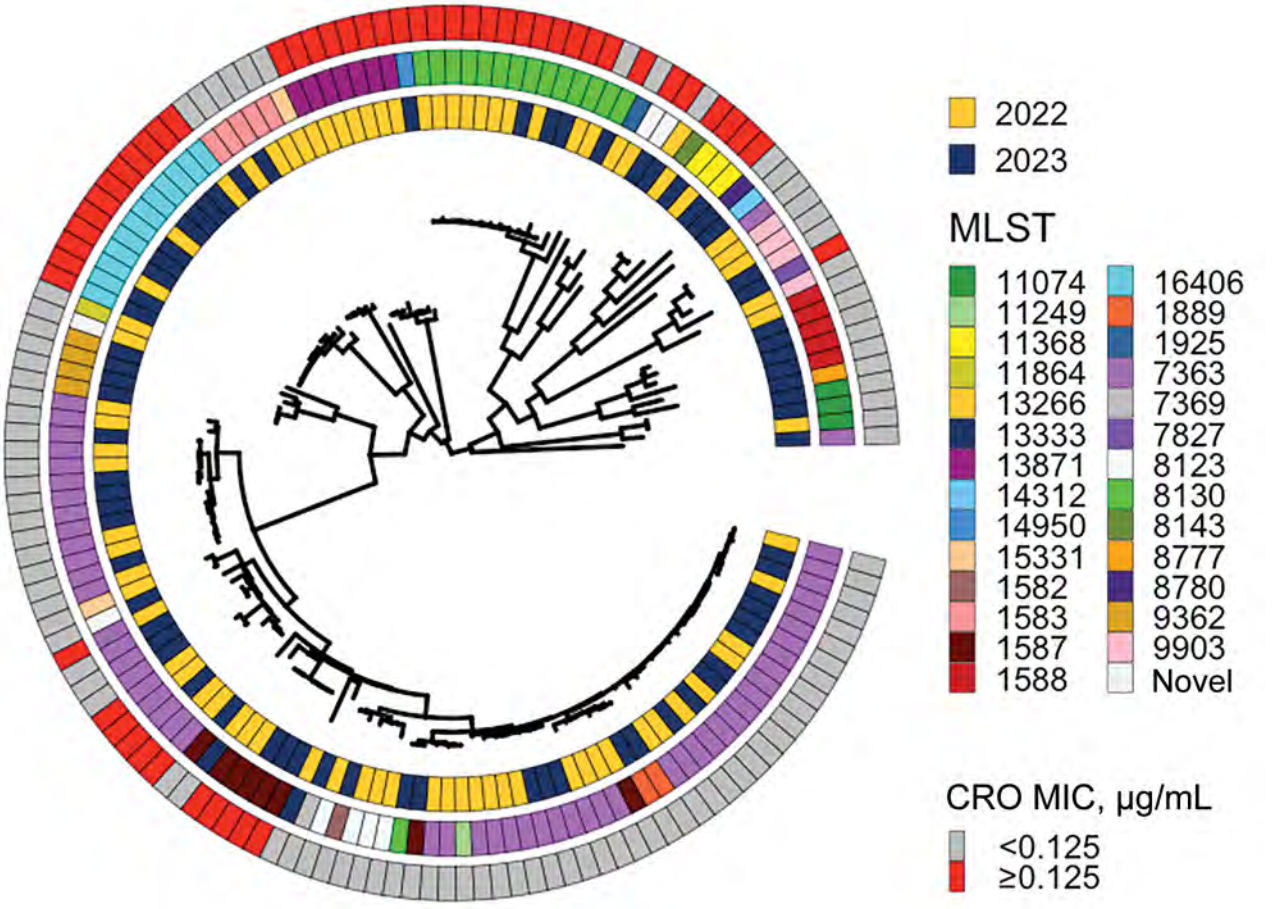

Figure. Circular midpoint rooted phylogeny of sequences from *Neisseria gonorrhoeae* isolates collected by the World Health Organization Enhanced Gonococcal Antimicrobial Surveillance Programme, Cambodia, 2022–2023. Associated metadata, year of isolation, MLST, and presence or absence of elevated MICs for CRO are depicted in concentric rings. White cells in the 3 rings correspond with the tree tip belonging to isolate FC428, the first *penA*-60.001-containing ceftriaxone-resistant isolate documented in Japan in 2015 (*6*). CRO, ceftriaxone; MLST, multilocus sequence type.

that genomically cluster with the XDR *N. gonorrhoeae* phenotype. Furthermore, strains with elevated MICs for ceftriaxone continue to emerge across different phylogenetic backbones separate from the previously described FC428 clone, confirming concerns that biological fitness is not compromised by that allele (*5*) and consequently poses a substantial threat for gonococcal disease control.

The proportion of alert-level isolates detected across the 2 years (2022–2023) of WHO EGASP Cambodia is of considerable concern, given the implications for future empirical therapy. Moreover, 2 recent publications from China report rates of *N. gonorrhoeae* with ceftriaxone MICs ≥0.125 μg/mL at or beyond 9%, most associated with the mosaic *penA*-60.001 allele (*7.8*), suggesting a far wider regional problem. That gonococcal antimicrobial resistance surveillance across the Asia–Pacific region is largely unmapped (*9*) reinforces high-level concerns regarding this priority pathogen. There is an urgent need to prioritize surveillance and data reporting to inform local and regional disease prevention and control strategies.

Members of the EGASP Cambodia Working Group: Phal Kun Mom (National Center for HIV/AIDS, Dermatology and Sexually Transmitted Diseases, Phnom Penh, Cambodia), Vivian Fensham (Integrated Quality Laboratory Services, Villeurbanne, France), Kristen M. Kreisel (Centers for Disease Control and Prevention, Atlanta, GA, USA), Martina Escher (WHO Global HIV, Hepatitis and STI Programmes, Geneva, Switzerland), Kiyohiko Izumi, Takeshi Nishijima (WHO Regional Office for the Western Pacific, Manila, the Philippines), Magnus Unemo (WHO Collaborating Centre for Gonorrhoea and other Sexually Transmitted Infections, Örebro, Sweden), Ratan L. Kundu, Sanghamitra Ray, Tiffany R. Hogan (WHO Collaborating Centre for Sexually Transmitted Infections and Antimicrobial Resistance, New South Wales Health Pathology, Microbiology, The Prince of Wales Hospital, Randwick, NSW, Australia).

Our study, as for most other WHO EGASP work, was funded by grants from the Global Antimicrobial Resistance Laboratory and Response Network.

The authors alone are responsible for the views expressed in this article and they do not necessarily represent the views, decisions, or policies of the institutions with which they are affiliated.

About the Author

Dr. Ouk is the director of the National Center for HIV/AIDS, Dermatology and Sexually Transmitted Diseases, Phnom Penh, Cambodia. His research interests include human immunodeficiency virus and sexually transmitted infections.

References

1. World Health Organization. Enhanced Gonococcal Surveillance Programme general protocol [cited 2022 Jan 20]. https://www.who.int/publications/i/item/9789240021341
2. Ouk V, Pham CD, Wi T, van Hal SJ, Lahra MM. EGASP Cambodia working group. The Enhanced Gonococcal Surveillance Programme, Cambodia. Lancet Infect Dis. 2023;23:e332–3. https://doi.org/10.1016/S1473-3099(23)00479-6
3. Maubaret C, Caméléna F, Mrimèche M, Braille A, Liberge M, Mainardis M, et al. Two cases of extensively drug-resistant (XDR) *Neisseria gonorrhoeae* infection combining ceftriaxone-resistance and high-level azithromycin resistance, France, November 2022 and May 2023. Euro Surveill. 2023;28:2300456. https://doi.org/10.2807/1560-7917.ES.2023.28.37.2300456
4. Berçot B, Caméléna F, Mérimèche M, Jacobsson S, Sbaa G, Mainardis M, et al. Ceftriaxone-resistant, multidrug-resistant *Neisseria gonorrhoeae* with a novel mosaic *penA-237.001* gene, France, June 2022. Euro Surveill. 2022;27:2200899. https://doi.org/10.2807/1560-7917.ES.2022.27.50.2200899
5. van der Veen S. Global transmission of the *penA* allele 60.001–containing high-level ceftriaxone-resistant gonococcal fc428 clone and antimicrobial therapy of associated cases: a review. Infectious Microbes & Diseases. 2023; 5:13–20. https://doi.org/10.1097/IM9.0000000000000113
6. Nakayama S, Shimuta K, Furubayashi K, Kawahata T, Unemo M, Ohnishi M. New ceftriaxone- and multidrug-resistant *Neisseria gonorrhoeae* strain with a novel mosaic pena gene isolated in Japan. Antimicrob Agents Chemother. 2016;60:4339–41. https://doi.org/10.1128/AAC.00504-16
7. Tang Y, Liu X, Chen W, Luo X, Zhuang P, Li R, et al. antimicrobial resistance profiling and genome analysis of the *penA*-60.001 *Neisseria gonorrhoeae* clinical isolates in China in 2021. J Infect Dis. 2023;228:792–9. https://doi.org/10.1093/infdis/jiad258
8. Liao Y, Xie Q, Yin X, Li X, Xie J, Wu X, et al. *penA* profile of *Neisseria gon*orrhoeae in Guangdong, China: novel *penA* alleles are related to decreased susceptibility to ceftriaxone or cefixime. Int J Antimicrob Agents. 2024;63:107101. https://doi.org/10.1016/j.ijantimicag.2024.107101
9. Unemo M, Lahra MM, Escher M, Eremin S, Cole MJ, Galarza P, et al. WHO global antimicrobial resistance surveillance for *Neisseria gonorrhoeae* 2017–18: a retrospective observational study. Lancet Microbe. 2021;2:e627–36. https://doi.org/10.1016/S2666-5247(21)00171-3

Address for correspondence: Monica Lahra, The Prince of Wales Hospital, NSWHP Microbiology, Randwick, NSW 2031, Australia; email: monica.lahra@health.nsw.gov.au

Serosurvey of Blood Donors to Assess West Nile Virus Exposure, South-Central Spain

Mario Frías, Javier Caballero-Gómez, Ana Vázquez, Elena Madrigal, Francisco Ruiz-Fons, Marina Gallo, Laura Herrero, María Jarilla, Ignacio García-Bocanegra, Antonio Rivero-Juárez Antonio Rivero

Author affiliations: CIBERINFEC, Madrid, Spain (M. Frías, J. Caballero-Gómez, M. Gallo, L. Herrero, I. García-Bocanegra, A. Rivero-Juárez, A. Rivero); Universidad de Córdoba, Córdoba, Spain (M. Frías, J. Caballero-Gómez, M. Gallo, I. García-Bocanegra, A. Rivero-Juárez, A. Rivero); CIBERESP, Madrid (A. Vázquez); Instituto de Salud Carlos III, Madrid (A. Vázquez, L. Herrero); Hospital General Universitario de Ciudad Real, Ciudad Real, Spain (E. Madrigal); Instituto de Investigación en Recursos Cinegéticos, Ciudad Real (F. Ruiz-Fons); Hospital Universitario Reina Sofía, Córdoba (M. Jarilla)

DOI: https://doi.org/10.3201/eid3007.240450

We analyzed West Nile Virus (WNV) exposure from 1,222 blood donors during 2017–2018 from an area of south-central Spain. Results revealed WNV seroprevalence of 0.08% (95% CI 0.004%–0.4%) in this population. Our findings underscore the need for continued surveillance and research to manage WNV infection in this region.

West Nile virus (WNV), a member of the family Flaviviridae, genus *Orthoflavivirus*, is classified within the Japanese encephalitis virus (JEV) serocomplex (*1*). It is the most widespread arbovirus globally, primarily because of the abundance and broad distribution of its main competent vector, mosquitoes belonging to the genus *Culex* (*2*). During the past 2 decades, WNV has led to epidemic outbreaks with a substantial proportion of severe cases in Europe, emerging as a considerable threat to public and animal health in these regions. Nonetheless, very limited information exists on seroprevalence in the general population, hindering a comprehensive understanding of the virus' epidemiologic landscape.

In Spain, WNV is considered endemic because of conducive conditions for virus maintenance and circulation, including diverse bird reservoirs, geographic characteristics such as migratory bird routes, and specific climatic conditions. Since a notable outbreak reported in 2020, the virus has produced human cases annually (*3*), demonstrating the spread of the virus in the country (*4*). Therefore, vigilant surveillance in new risk areas is imperative to anticipate potential human health emergencies. Studies in vectors and animal hosts in south-central Spain have underscored the region's potential as a hotspot zone (*5*–*7*). Within this area, the province of Ciudad Real, where no human WNV cases have been reported to date, serves as an ideal scenario for assessing circulation of the virus in the general population. We conducted a serosurvey in blood donors to investigate WNV exposure in the general population of this region in Spain, shedding light on the transmission dynamics of this emergent virus.

We conducted a retrospective cross-sectional study to analyze the seroprevalence of WNV in serum samples collected from blood donors at the Transfusion Center of the Hospital General Universitario de Ciudad Real (south-central Spain) (Figure) during 2017–2018 (Appendix, https://wwwnc.cdc.gov/EID/article/30/7/24-0450-App1.pdf). We selected and analyzed blood from 1,222 donors (Appendix Table 1). Sex and age data were not available for 129 (10.5%) donors. Of the 1,093 donors for whom information was available, 571 (52.2%) were men and 522 (47.8%) women. The age of the donors was categorized into 3 classes: <30 years (21.8% of samples), 30–50 years (34.8%), and >50 years (32.7%). Nineteen (1.6%) of the samples reacted positively to the IgG WNV ELISA. We administered an epidemiologic survey to the 19 ELISA-positive donors; 16 donors responded (Appendix Table 2).

We analyzed all ELISA-positive samples by using a virus neutralization test (VNT) (Appendix Table 2). Regarding WNV, ELISA reactivity was only confirmed by VNT in 1 donor who showed a titer of 1/256, which indicated a seroprevalence of 0.08% (95% CI 0.04%–0.4%) for WNV. This donor declared that he had not traveled outside of Spain and therefore did not receive any vaccine against yellow fever virus, tick-borne encephalitis virus, or Japanese encephalitis virus.

In Europe, no seroepidemiologic studies have been conducted since 2013; therefore, our study would provide valuable insights into the current status of WNV exposure. Our study encompasses a vast region of south-central Spain and marks initial identification of seropositivity in humans in this specific region of Spain, indicating a broad spread of the virus. In Spain, recent serosurveys are lacking; 2 studies were conducted in Catalonia in 2001 (0.2%) (*8*) and 2011 (0.12%) (*9*), and another was conducted in the province of Sevilla in 2006 (0.6%)

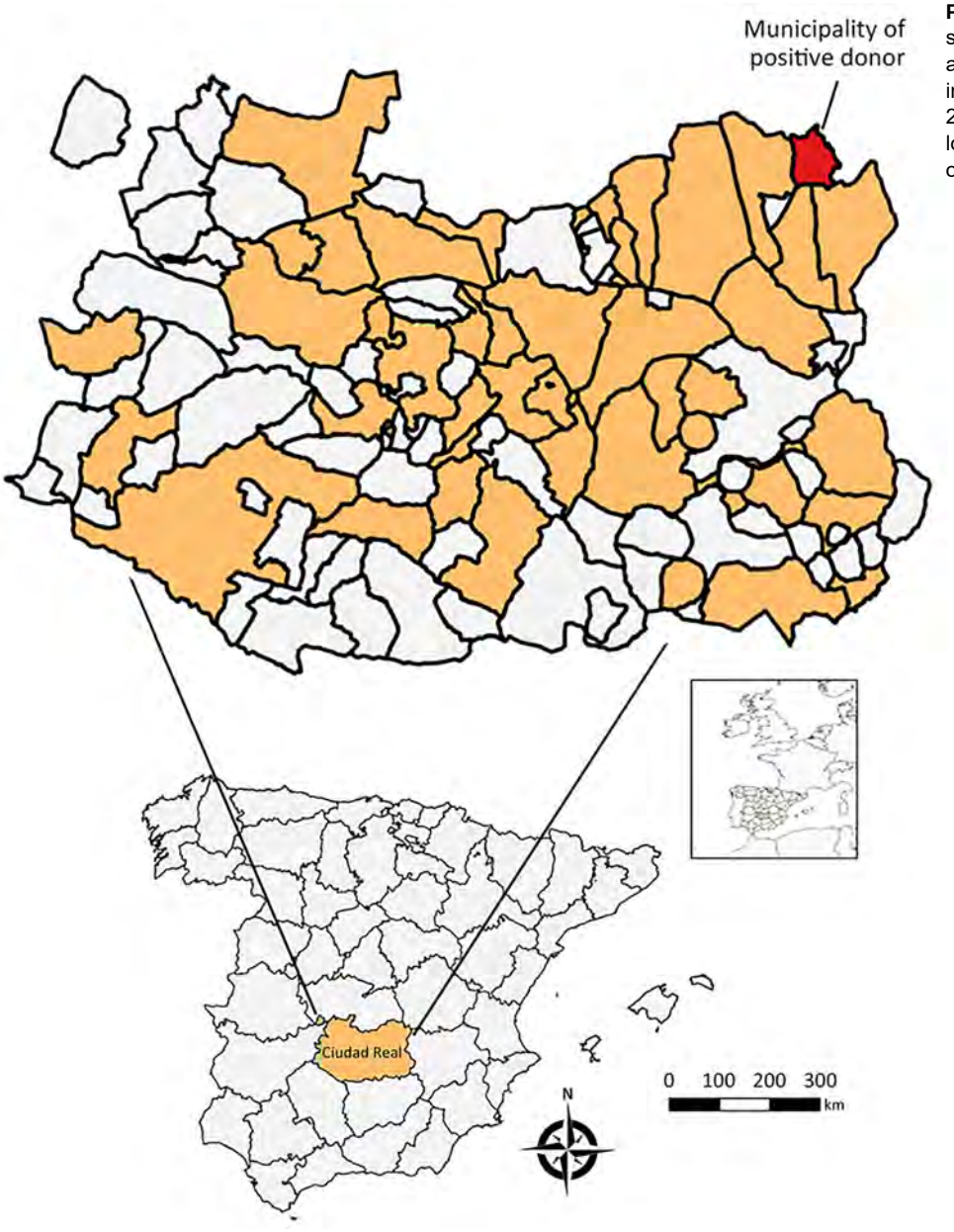

Figure. Locations sampled in serosurvey of blood donors to assess West Nile virus exposure in the general population, Spain, 2017–2018. Inset maps show location of study area in Spain and of Spain in Europe.

(*10*). In the past 3 years, the regions of those studies have experienced large WNV outbreaks, similar to that which occurred in summer of 2020 (*3*) or the first description of clinical cases in Catalonia in 2022 and 2023 (*4*). This development suggests greater exposure to the virus than in the previous decade and highlights the need to carry out new serosurveys in the general population that enable collection of updated data.

The observed seroprevalence among blood donors from south-central Spain in our study suggests a low exposure (0.08%) to WNV in the general population within this spatiotemporal context. Of note, the number of WNV cases in Spain has been on the rise in recent years, being detected even in areas where previously no evidence of WNV circulation existed, suggesting that WNV has been expanding during recent years and that outbreaks can be expected in areas not currently considered endemic for WNV.

In our study, and in line with other studies (*9*), a high percentage (94.7%) of ELISA-positive WNV samples could not be confirmed as positive for specific antibodies. This finding highlights the need to perform additional neutralization tests against other flaviviruses in the serosurvey studies. The absence

of an ELISA test with high sensitivity and, more crucially, specificity for WNV, limits the design of large-scale population serosurvey studies. Urgent efforts are required to address this limitation.

In conclusion, our study indicated seropositivity in the south-central region of Spain. In this way, reporting cases in Spain may be plausible even in areas not at high risk, highlighting the importance of ongoing surveillance and research to manage WNV infection in this region.

Acknowledgments

We gratefully acknowledge Laura Ruiz Torres and Ismael Zafra Soto for their technical support in sample processing.

This work was supported by Secretaría General de Investigación, Desarrollo e Innovación en Salud (grant no. PI-0287-2019) for grants for the financing of Investigación, Desarrollo e Innovación Biomédica y en Ciencias de la Salud en Andalucía; the Ministerio de Sanidad (grant no. RD12/0017/0012) integrated into the Plan Nacional de I+D+I and co-financed by the ISCIII-Subdirección General de Evaluación and the Fondo Europeo de Desarrollo Regional. A.R.J. is supported by a contract from the Spanish Junta de Andalucia (Nicolas Monardes program, grant no. C1-0001-2023). J.C.G. is supported by the CIBER Consorcio Centro de Investigación Biomédica en Red (grant no. CB21/13/00083), Instituto de Salud Carlos III, Ministerio de Ciencia e Innovación and Unión Europea–NextGenerationEU.

About the Author

Dr. Frías is a postdoctoral researcher at the Animal Health and Zoonosis Research Group at the University of Cordoba and the Clinical Virology and Zoonoses Group at the Maimonides Biomedical Research Institute of Cordoba. His primary research interests are emerging zoonotic diseases.

References

1. Kramer LD, Li J, Shi PY. West Nile virus. Lancet Neurol. 2007;6:171–81. https://doi.org/10.1016/S1474-4422(07)70030-3
2. Kramer LD, Styer LM, Ebel GD. A global perspective on the epidemiology of West Nile virus. Annu Rev Entomol. 2008; 53:61–81. https://doi.org/10.1146/annurev.ento.53.103106.093258
3. García San Miguel Rodríguez-Alarcón L, Fernández-Martínez B, Sierra Moros MJ, Vázquez A, Julián Pachés P, García Villacieros E, et al. Unprecedented increase of West Nile virus neuroinvasive disease, Spain, summer 2020. Euro Surveill. 2021;26:19. https://doi.org/10.2807/1560-7917.ES.2021.26.19.2002010
4. Ministerio de Agricultura. Pesca y Alimentación. Update on the epidemiological situation of West Nile [cited 2024 May 14]. https://www.mapa.gob.es/es/ganaderia/temas/sanidad-animal-higiene-ganadera/informefno_tcm30-435293.pdf
5. Durán-Martínez M. Distribución, Abundancia y Composición de la Comunidad de Dípteros Hematófagos Vectores de Enfermedades en Castilla-La Mancha: Riesgos para la Salud Pública y la Sanidad Animal. 2012 [cited 2024 Jan 25]. https://digital.csic.es/handle/10261/147173.
6. García-Carrasco JM, Muñoz AR, Olivero J, Segura M, García-Bocanegra I, Real R. West Nile virus in the Iberian Peninsula: using equine cases to identify high-risk areas for humans. Euro Surveill. 2023;28:2200844. https://doi.org/10.2807/1560-7917.ES.2023.28.40.2200844
7. Casades-Martí L, Cuadrado-Matías R, Peralbo-Moreno A, Baz-Flores S, Fierro Y, Ruiz-Fons F. Insights into the spatiotemporal dynamics of West Nile virus transmission in emerging scenarios. One Health. 2023;16:100557. https://doi.org/10.1016/j.onehlt.2023.100557
8. Bofill D, Domingo C, Cardeñosa N, Zaragoza J, de Ory F, Minguell S, et al. Human West Nile virus infection, Catalonia, Spain. Emerg Infect Dis. 2006;12:1163–4. https://doi.org/10.3201/eid1207.060164
9. Piron M, Plasencia A, Fleta-Soriano E, Martinez A, Martinez JP, Torner N, et al. Low seroprevalence of West Nile virus in blood donors from Catalonia, Spain. Vector Borne Zoonotic Dis. 2015;15:782–4. https://doi.org/10.1089/vbz.2015.1787
10. Bernabeu-Wittel M, Ruiz-Pérez M, del Toro MD, Aznar J, Muniain A, de Ory F, et al. West Nile virus past infections in the general population of Southern Spain. Enferm Infecc Microbiol Clin. 2007;25:561–5. https://doi.org/10.1157/13111181

Address for correspondence: Antonio Rivero-Juárez, Virología Clínica y Zoonosis, Instituto Maimonides de Investigación Biomédica de Córdoba (IMIBIC), Avenida Menedez Pidal, s/n. 14004, Córdoba, Spain; email: arjvet@gmail.com

Correction: Vol. 29, No. 7

Funding information was missing in Novel Highly Pathogenic Avian Influenza A(H5N1) Clade 2.3.4.4b Virus in Wild Birds, South Korea (S.-h. Lee et al.). The article has been corrected online (https://wwwnc.cdc.gov/eid/article/29/7/22-1893_article).

Correction: Vol. 28, No. 6

An affiliation for the first author was missing in Lyme Disease, Anaplasmosis, and Babesiosis, Atlantic Canada (Z.O. Allehebi et al.). The article has been corrected online (https://wwwnc.cdc.gov/eid/article/28/6/22-0443_article).

Germ Theory: Medical Pioneers in Infectious Diseases, 2nd Edition

Robert P. Gaynes, American Society for Microbiology and John Wiley & Sons, Inc., Hoboken, NJ, USA, 2023 ISBN-10: 168367376X; ISBN-13: 978-1683673767 Pages: 384; Price: US $69.95 (paperback)

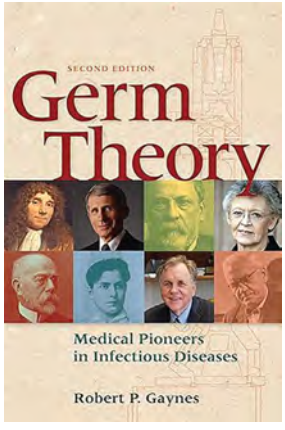

Robert P. Gaynes, professor at Emory University School of Medicine, has produced a second edition of *Germ Theory: Medical Pioneers in Infectious Diseases*, a chronicle of the evolution of germ theory told through stories of pioneers in science and medicine. The second edition adds new perspectives by expanding upon accounts of pioneers from the first edition of *Germ Theory*, such as Antony van Leeuwenhoek, Louis Pasteur, and Robert Koch. In addition, he introduces 3 pioneers of germ theory in the 20th Century, all personally interviewed by Gaynes. New chapters discuss the discoveries of HIV by Françoise Barré-Sinoussi and the connection between *Helicobacter pylori* and peptic ulcers by Barry Marshall. In addition, the book recounts the efforts of Anthony Fauci, from his early work in creating the President's Emergency Plan for AIDS Relief in 2003 to more recently becoming the face of COVID-19 information in the United States during the pandemic.

Gaynes marvelously uses intersections between key historic figures and disease epidemics as guidestones on a walk through the history and evolution of germ theory, explaining current prevailing understandings among the general public, scientific community, or both, and reasons behind advancements and regressions over time in medicine and science. In each chapter, Gaynes dives deeply into the personality qualities, early influences, and lesser-known contributions of a prominent pioneer better known for a higher-profile contribution to medical science. Those accounts provide fresh context for familiar histories of medical landmarks. Gaynes also expands the context and breadth of discoveries by introducing persons who provided mentoring or otherwise supported the pioneering scientists, contradicted their work, or concurrently came to the same conclusions.

Gaynes shares the frequent initial resistance of scientific and medical communities to discoveries. For example, he describes the persistence of the humoral theory of diseases into the early 18th Century because of the reputation of Galen of Pergamon, a 2nd Century Greek physician key to the foundation of Western medical education, who espoused that theory. Gaynes eloquently comments on this conflicted dynamic, stating that "major shifts in thinking often are products not just of the discovery but also of the age and culture." In addition, by describing Fauci's experiences working through 7 different presidencies, including during the COVID-19 pandemic, Gaynes provides insight into the connection between public health and politics at the highest levels of government.

Gaynes weaves scientific concepts across chapters, effectively connecting historic events to modern-day challenges and guiding the reader through the effects and implications of the evolution of germ theory in a contemporary context. By making *Germ Theory* pertinent and understandable to readers in fields across science and medicine, Gaynes provides a wonderful tool to engage the next generation of public health professionals and reinvigorate those currently in the field, especially when public health workers are recovering from the challenges of the COVID-19 pandemic. Gaynes concludes the book with a call to future action to address emerging threats from antimicrobial resistance, vaccination hesitancy, and the effects of ongoing social vulnerabilities.

Rachel N. Wofford

Author affiliation: Tennessee Department of Health, Nashville, Tennessee, USA

DOI: https://doi.org/10.3201/eid3007.231631

Address for correspondence: Rachel N Wofford, Tennessee Department of Health–CEDEP, 710 James Robertson Pkwy, Nashville, TN 37243, USA; email: rachel.wofford@tn.gov

Possibly Agnolo Bronzino (1503–1572). ***Allegorical Portrait of Dante*** (late 16th Century) (detail). Oil on panel, 49 15/16 in × 47 1/4 in/126.9 cm × 120 cm. National Gallery of Art, Washington, DC, USA. Open access image.

Poet, Politician, Exile, and Probable Malaria Victim

Byron Breedlove

Poet, politician, and exile all describe Durante di Alighiero degli Alighieri (1265–1321), who is best remembered as the author of *The Divine Comedy*. The epic poem chronicles his imagined journey from death to heaven across three realms of the afterlife: *Inferno, Purgatorio,* and *Paradiso*. In 1265, Dante Alighieri was born in Florence, Italy, and details about his early years are scare. He lived in Florence for 35 years, though his political affiliation eventually led to his exile.

During Dante's lifetime, the Guelphs and the Ghibellines, two rival political factions, vied for control of Florence. The Guelphs backed the papacy; the Ghibellines, the Holy Roman Emperor. Internal squabbles caused the Guelphs to split into the Black Guelphs and the White Guelphs. Professor of Italian Studies Guy P. Raffa explains, "Dante climbed the ladder of Florentine governance as a White Guelph, reaching its highest rung when he was elected to the city's six-member Council of Priors for a two-month term beginning on June 15, 1300. His triumph could not have come at a worse time. 'All my woes and all my misfortunes,' he reflected in a letter, 'had their cause and origin in my ill-omened election to the priorate.'" Because of trumped-up charges that the Black Guelphs leveled against a number of prominent White Guelphs, Dante was banished from Florence and sentenced to death should he return.

Allegorical Portrait of Dante, this month's cover image, has been credited to different artists. The National

Author affiliation: Centers for Disease Control and Prevention, Atlanta, Georgia, USA

DOI: https://doi.org/10.3201/eid3007.AC3007

Gallery of Art in Washington, DC, which houses the painting, ascribes it to an unknown 16th-century Florentine painter. Others, including art scholar Fiammetta Campagnoli, attribute the portrait to Agnolo Bronzino, a Florentine Mannerist painter. Campagnoli says, "Dante is immediately recognizable from his profile, traditional red clothing and the laurel wreath. Bronzino depicted his subject in front of a landscape background, with a striking turn of the body and as if the viewer is looking up at the figure from below."

Campagnoli adds that Dante's right hand "indicates Florence, which is shrouded in darkness, while he himself has turned towards the rising sun that is illuminating the very top of Purgatory and the spheres of Heavenly Paradise." A small boat visible on the Styx River flows around the tapering tower of Purgatory, and a golden streak from the right corner illuminates the darkened sky. Dante holds *The Divine Comedy*, opened to the first 48 lines from Canto XXV of *Paradiso.* Here, as Campagnoli observes, "it is possible to read the lines that speak of the great poet's desire to return to his homeland":

> then, with another voice and other fleece
> a Poet I'll return, and at the font
> of mine own baptism take the laurel crown…

Supported by sympathetic patrons, Dante moved about Italy but never returned to Florence to address corruption charges. Guido Novello da Polenta, lord of Ravenna from 1316 until 1322, was Dante's final benefactor and provided him, as Raffa explains, "a measure of stability and independence. The poet had his own house in Ravenna, the city in which he found the resources, inspiration, and ambiance conducive to writing the final cantos of the *Divine Comedy*."

In August 1321, as Ravenna where Dante resided was on the verge of war with the Republic of Venice, Dante was dispatched on a diplomatic mission. Raffa notes, "The land route between Venice and Ravenna posed risks of its own, more so during the time of year when Dante traveled. With the first rains of the season wetting the marshlands, parched after the hot summer months, conditions were ripe for contracting malaria. The rivers, canals, swamps, and lagunas of the region have always made it a fertile haven for mosquito-borne illnesses. By the time Dante returned to Ravenna in early September, the recurring bouts of fever had so weakened him that he died within days." It is plausible that the fevers Dante experienced were caused by malaria contracted during his travels—especially given the short incubation period (weeks) for malaria. Raffa added, "Although early chroniclers and biographers say precious little about Dante's final days, their accounts, supplemented by contextual documentation, allow for a plausible representation of his illness, death, and burial."

Pathologist Luigi Papi offers a similar perspective: "Concerning Dante Alighieri, however, it should be highlighted that there is no historical document which confirms the fact that his death was actually due to malaria, so this hypothesis is probably based only on the fact that at any rate, he died a few days after his long journey by land, through the marshes of the Venetian lagoon where the *Plasmodium* was particularly widespread." According to the World Health Organization, malaria is caused by 5 species of the *Plasmodium* parasites that Papi refers to, notably *Plasmodium falciparum* and *Plasmodium vivax,* and the vectors for transmission are infected *Anopheles* mosquitoes.

Dante was aware of malaria (which means "bad air" in Italian and comes from *malum aeris* in Latin). Paleopathologist Rafaella Bianucci et al. observe that Dante refers to malaria in several passages of the *Inferno*, including lines 85–90 from Canto XVII:

> Like one with quartan-fever's chill so near,
> that pale already are his fingernails, and that,
> but looking at the shade, he shudders;
> such at the words he uttered I became;
> but that shame made its threats to me,
> which renders,
> a servant strong when in a good lord's presence.

At this point in the poem, Dante has mounted Geryon— often described as a mythological monster with three heads—that will transport him and Virgil to the next level of hell. Bianucci et al. note that "Dante is afraid and compares himself to a man in a shivering fit of quartan fever. Dante expresses himself using terms that are very close to those used in medical treatises to exemplify the quartan fever, which reoccurs at regular intervals, oppresses the sick in the fear of the recurring attack."

More than 700 years after Dante's death, malaria is preventable and treatable yet kills more people than any other vectorborne disease. Despite gains in controlling malaria in *Plasmodium*-endemic regions, progress is hindered by interlinked factors, including international travel and migration, climate change, and antimalarial drug resistance. Improved surveillance, detection, prevention, and treatment may yield promise not just for controlling outbreaks of malaria but also for dealing with outbreaks of other vectorborne illnesses such as dengue, Crimean-Congo hemorrhagic fever, chikungunya, yellow fever, and Zika, which have also killed thousands of people and taxed systems since the start of this century.

Bibliography

1. Alighieri D. The Divine Comedy, 3 volumes. Langdon C, translation and commentary. Cambridge: Harvard University Press; 1918, 1920, 1921.
2. Anastasi L. Guelphs and Ghibellines: medieval feud [cited 2024 June 11]. https://historymedieval.com/guelphs-and-ghibellines-florentine-feud
3. Bianucci R, Charlier P, Perciaccante A, Appenzeller O, Lippi D. Malarial fevers in the fourteenth century Divine Comedy. Intern Emerg Med. 2018;13:1135–6. https://doi.org/10.1007/s11739-018-1903-1
4. Boccassini D. Why Dante Alighieri still matters today, 700 years after his death [cited 2024 May 23] https://fhis.ubc.ca/news/700-years-since-dante-alighieris-death-why-he-still-matters-today
5. Campagnoli F. Exposition: Agnolo di Bronzino. A portrait of Dante, Saint-Pétersbourg, Musée de l'Ermitage, jusqu'au 16 janvier 2022 [cited 2024 May 23]. https://char.hypotheses.org/22357
6. Etymologia: malaria. Emerg Infect Dis. 2006;12:1138. https://doi.org/10.3201/eid1207.ET1207
7. Papi L. The story of Dante Alighieri's human remains and their anthropological analysis in the past centuries. Med Hist. 2021;5:e2021017 https://mattioli1885journals.com/index.php/MedHistor/article/view/10846.
8. Raffa GP. Dante's exile: the struggle to memorialize the poet began in Ravenna [cited 2024 May 23]. https://www.laphamsquarterly.org/roundtable/dantes-exile
9. Rocklöv J, Dubrow R. Climate change: an enduring challenge for vector-borne disease prevention and control. Nat Immunol. 2020;21:479–83. https://doi.org/10.1038/s41590-020-0648-y
10. World Health Organization. Malaria [cited 2024 May 30]. https://www.who.int/news-room/fact-sheets/detail/malaria
11. World Health Organization. World malaria report 2023 [cited 2024 May 30]. https://www.who.int/teams/global-malaria-programme/reports/world-malaria-report-2023

Address for correspondence: Byron Breedlove, EID Journal, Centers for Disease Control and Prevention, 1600 Clifton Rd NE, Mailstop H16-2, Atlanta, GA 30329-4018, USA; email: wbb1@cdc.gov

etymologia revisited

Malaria

[mə-lar'e-ə]

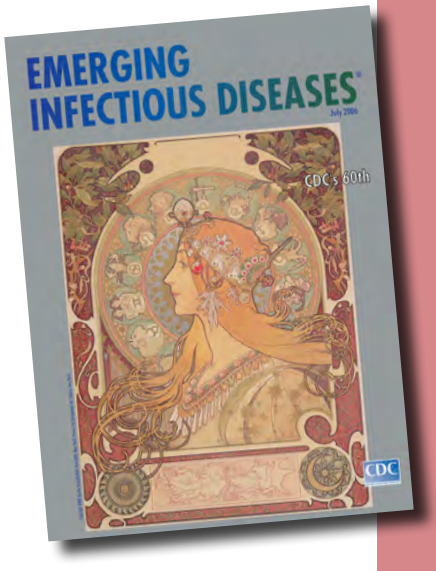

Originally published in July 2006

Malaria, "bad air" in Italian, was blamed for the deaths of >1,000 workers digging the Erie Canal in 1819. Work on the canal continued in winter, when the swamp was frozen over (and, although the vector was not known at the time, mosquitoes were dormant). Malaria, caused by parasites of the genus *Plasmodium* and usually transmitted by the bite of infected *Anopheles* mosquitoes, is endemic in many warm regions. Charles Louis Alphonse Laveran discovered the protozoan cause of malaria in 1880. The Office of Malaria Control in War Areas, which was established in 1942 to control malaria and other vectorborne diseases in the southern United States, evolved into what is today the Centers for Disease Control and Prevention.

Source:

Dorland's illustrated medical dictionary. 30th ed. Philadelphia: Saunders; 2003; cdc.gov; and wikipedia.org

https://wwwnc.cdc.gov/eid/article/12/7/ET-1207_article

EMERGING INFECTIOUS DISEASES®

Upcoming Issue

- Outbreak of Intermediate Species *Leptospira venezuelensis* Spread by Rodents to Cows and Humans in *Leptospira interrogans*–Endemic Region, Venezuela
- Systematic Review of Prevalence of *Histoplasma Antigenuria* in Persons with HIV in Latin America and Africa
- Retrospective Study of Infections by *Corynebacteria* of *diphtheriae* Species Complex, French Guiana, 2016–2021
- SARS-CoV-2 Seropositivity in Urban Population of Wild Fallow Deer, Dublin, Ireland, 2020–2022
- Detection of Rustrela Virus in Wild Mountain Lion (*Puma concolor*) with Staggering Disease, Colorado, USA
- Scrapie versus Chronic Wasting Disease in White-Tailed Deer
- *Emayella augustorita,* New Member of Pasteurellaceae, Isolated from Blood Cultures of Septic Patient
- Emergence of Bluetongue Virus Serotype 3, the Netherlands, September 2023
- Environmental Hotspots and Resistance-Related Application Practices for Azole-Resistant *Aspergillus fumigatus*, Denmark, 2020–2023
- Fatal SARS-CoV-2 Infection Among Children, Japan, January–September 2022
- Detection of Nucleocapsid Antibodies Associated with Primary SARS-CoV-2 Infection in Unvaccinated and Vaccinated Blood Donors
- Fecal Microbiota Transplantation for Severe Infant Botulism

Complete list of articles in the August issue at https://wwwnc.cdc.gov/eid/#issue-312

Earning CME Credit

To obtain credit, you should first read the journal article. After reading the article, you should be able to answer the following, related, multiple-choice questions. To complete the questions (with a minimum 75% passing score) and earn continuing medical education (CME) credit, please go to http://www.medscape.org/journal/eid. Credit cannot be obtained for tests completed on paper, although you may use the worksheet below to keep a record of your answers.

You must be a registered user on http://www.medscape.org. If you are not registered on http://www.medscape.org, please click on the "Register" link on the right hand side of the website.

Only one answer is correct for each question. Once you successfully answer all post-test questions, you will be able to view and/or print your certificate. For questions regarding this activity, contact the accredited provider, CME@medscape.net. For technical assistance, contact CME@medscape.net. American Medical Association's Physician's Recognition Award (AMA PRA) credits are accepted in the US as evidence of participation in CME activities. For further information on this award, please go to https://www.ama-assn.org. The AMA has determined that physicians not licensed in the US who participate in this CME activity are eligible for *AMA PRA Category 1 Credits*™. Through agreements that the AMA has made with agencies in some countries, AMA PRA credit may be acceptable as evidence of participation in CME activities. If you are not licensed in the US, please complete the questions online, print the AMA PRA CME credit certificate, and present it to your national medical association for review.

Article Title

Infectious Diseases and Clinical Xenotransplantation

CME Questions

1. Which of the following statements regarding the development of swine as source animals for clinical xenotransplantation is most accurate?

A. An international protocol for screening for source animals was developed in 2023
B. Specific pathogen-free animals receive regular preventive therapy with antibiotics
C. Specific pathogen-free animals no longer need to be contained in biosecure facilities
D. Pigs are rescreened at the time of organ procurement for both known pathogens and unknown organisms

2. In a study describing pathogens infecting swine that could affect humans as well, what was the most common organism encountered?

A. Bacteria
B. Viruses
C. Fungi
D. Parasites

3. Which of the following viruses are specific to swine and do not infect human cells?

A. Porcine circovirus
B. Porcine adenovirus
C. Porcine parvovirus 1
D. Porcine hepatitis E virus

4. Which of the following statements regarding prophylaxis and treatment of porcine viruses is most accurate?

A. Porcine cytomegalovirus (PCMV) may promote graft dysfunction even though it does not infect human cells
B. Porcine cytomegalovirus responds well to treatment with ganciclovir
C. Cidofovir has no role in the treatment of PCMV
D. There are no effective treatments or vaccination for PCMVs